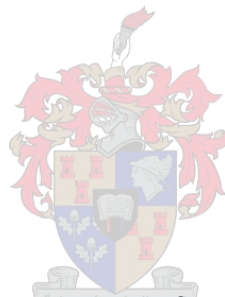


Non-destructive assessment of leaf composition as related to growth of the grapevine (*Vitis vinifera* L. cv. Shiraz)

by

AE Strever



Dissertation presented for the degree of
Doctor of Philosophy
(Agricultural Sciences)

at

Stellenbosch University

Department of Viticulture and Oenology, Faculty of AgriSciences

Supervisor: Prof JJ Hunter

Co-supervisor: Dr PR Young

March 2012

DECLARATION

By submitting this dissertation electronically, I declare that the entirety of the work contained therein is my own, original work, that I am the sole author thereof (save to the extent explicitly otherwise stated), that reproduction and publication thereof by Stellenbosch University will not infringe any third party rights and that I have not previously in its entirety or in part submitted it for obtaining any qualification.

Date: March 2012

SUMMARY

Field spectroscopy was used to study leaf composition and selected factors (including canopy growth manipulation and water status changes) that may impact on it in a *Vitis vinifera* cv. Shiraz vineyard, showing considerable variability in vigour. Temporal and spatial variability in leaf composition were incorporated into measurements by analysing leaves in different shoot positions and at different developmental stages during three different growing seasons. Irrigation and canopy manipulation treatments were also imposed in order to provide new insights into assessing the grapevine leaf and possibly also the canopy growth and ageing dynamics as well as pigment content, as a basis of executing a generally non-destructive measurement approach.

Despite large climatic differences between the seasons, canopy size seemed of crucial importance in determining grapevine water relations in the grapevines from the different canopy manipulation treatments. Drastic compensation effects in terms of secondary shoot growth also followed the canopy reduction treatment. Despite this, canopy microclimate was apparently improved, considering the results from light measurements as well as the ripening dynamics in the reduced canopies. Reduced canopies also seemed to display a different canopy composition, in favour of secondary growth. This could have impacted positively on water use efficiency as well as ripening, due to higher photosynthetic efficiency of these leaves during the ripening stages. The reduced canopy treatments offered the possibility of attaining technological ripeness at an earlier stage and at comparatively lower potential alcohol levels.

This study illustrated the relevance of considering the vegetative development of the grapevine, along with leaf ageing in the canopy, when conducting calibrated non-destructive measurements of leaf pigments, structure and water content. The relevance of using multivariate techniques in leaf spectroscopy was shown. This can be applied and simplified to aid in non-destructive leaf pigment, structure and water content estimation in future studies. Even with the general variation encountered in this vineyard, predictions of the major pigments in grapevine leaves were within acceptable error margins. Further work is required to improve the modelling of xanthophylls, which may require non-linear multivariate techniques.

Logistical shoot growth modelling was used in leaf age estimation and classification, which made it possible to simplify statistical analysis of the leaf parameters mentioned. Practical application of the modelled and predicted parameters was shown for a specific period in season two by comparing the reaction of different treatments to developing water deficits. The results indicated that several parameters, with special mention of the carotenoid:chlorophyll ratio and chlorophyll *a*:*b* ratio, can be monitored on young and old leaves in the canopy in order to monitor developing water deficit stress. The modelled parameters, however, did not seem to be sensitive enough to allow specific prediction of predawn leaf water potential values. Specific leaf mass, equivalent water thickness, total specific leaf mass as well as leaf chronological age were successfully predicted from leaf spectral absorbance data, and this may be useful in future work on quantifying leaf adaptation to the micro-environment within the canopy.

OPSOMMING

Veldspektroskopie is gebruik om blaarsamestelling en spesifieke faktore (insluitend lowergroei manipulasie en waterstatus veranderinge) wat 'n impak kan hê in 'n *Vitis vinifera* cv. Shiraz wingerd, met beduidende variasie in groeikrag, te ondersoek. Ruimtelike, asook tydsgebonde, variasie in blaarsamestelling is geïnkorporeer in die metings deur blare van verskillende lootposisies en vir verskillende ontwikkelingstadia gedurende drie verskillende groeiseisoene te meet. Besproeiings- en lowermanipulasie behandelings is ook uitgevoer om die dinamiek van blaar- en lowergroei, veroudering, asook pigmentinhoud te bestudeer binne die konteks van die uitvoering van 'n nie-destruktiwe meetstrategie.

Ondanks groot klimaatsverskille tussen die seisoene, blyk lowergrootteverskille belangrik te wees in die bepaling van wingerdstok-waterverhoudings in die verskillende lowermanipulasie behandelings. Drastiese kompensasiereaksies ten opsigte van sylootgroei is waargeneem in reaksie op die gereduseerde lowerbehandeling. Indien die resultate van ligmetings en druifrypwording in die gereduseerde lowerbehandeling in ag geneem word, is lowermikroklimaat egter steeds verbeter. Hierdie behandeling het oënskynlik ook veranderde lowersamestelling gehad, tot voordeel van sylootgroei. Dit kon moontlik 'n positiewe invloed gehad het op waterverbruikseffektiwiteit asook druifrypwording, as gevolg van moontlike hoër fotosintetiese effektiwiteit van die blare gedurende die rypwordingstadia. Die gereduseerde lowerbehandeling het die moontlikheid gebied om tegnologiese rypheid by 'n vroeër datum te bereik, met moontlike laer alkoholvlakke in die wyn.

Hierdie studie het die belangrikheid beklemtoon om die vegetatiewe ontwikkeling van die wingerdstok in ag te neem wanneer gekalibreerde nie-destruktiwe metings van blaarpigmente, blaarstruktuur asook waterinhoud onderneem word. Die belang van multi-variant meettegnieke in blaarspektroskopie is aangetoon. Dit kan verder vereenvoudig word ter ondersteuning van nie-destruktiwe meting van blaarpigment, -struktuur en -waterinhoudsbepaling in toekomstige studies. Selfs met die variasie wat in die wingerd voorgekom het, was die voorspellings van die vlakke van die belangrikste pigmente wat in wingerdblare aangetref word binne aanvaanbare foutgrense. Opvolgwerk is nodig om die modellering van xanthofil te verbeter, aangesien dit moontlik nie-lineêre multi-variant analise mag benodig.

Logistiese groeimodellering is gebruik om blaarouderdom te bepaal en te klassifiseer, wat dit moontlik gemaak het om statistiese analise te vereenvoudig vir die genoemde blaarparameters. Die praktiese toepassing van die gemodelleerde en voorspelde parameters is aangetoon vir 'n spesifieke gedeelte in seisoen twee, deur die reaksie van verskillende behandelings op toenemende watertekorte te bestudeer. Resultate het aangetoon dat verskeie parameters, met spesifieke klem op die karotenoïed:chlorofil verhouding, asook die chlorofil *a:b* verhouding, gemoniteer kan word op jong en ouer blare in die lower ten einde ontwikkelende waterstrestoestande te identifiseer. Die gemodelleerde parameters was egter klaarblyklik nie sensitief genoeg vir akkurate voorspelling van voorsonsoptkoms-waterpotensiaalvlakke nie. Spesifieke blaarmassa, ekwivalente waterdikte, totale spesifieke blaarmassa, sowel as blaarouderdom kon suksesvol voorspel word deur gebruik te maak van absorpsie-blaarspektroskopie, wat nuttig kan wees in toekomstige studies wat handel oor die kwantifisering van blaaraanpassing by die mikro-omgewing binne 'n wingerdlower.

This dissertation is dedicated to my wife, Elana, and daughter, Lisa.

¹ “I am the true vine, and my Father is the gardener. ² He cuts off every branch in me that bears no fruit, while every branch that does bear fruit he prunes so that it will be even more fruitful. ³ You are already clean because of the word I have spoken to you. ⁴ Remain in me, as I also remain in you. No branch can bear fruit by itself; it must remain in the vine. Neither can you bear fruit unless you remain in me.

⁵ “I am the vine; you are the branches. If you remain in me and I in you, you will bear much fruit; apart from me you can do nothing. ⁶ If you do not remain in me, you are like a branch that is thrown away and withers; such branches are picked up, thrown into the fire and burned. ⁷ If you remain in me and my words remain in you, ask whatever you wish, and it will be done for you. ⁸ This is to my Father’s glory, that you bear much fruit, showing yourselves to be my disciples. (John 15:1-5)

BIOGRAPHICAL SKETCH

Albert Strever matriculated from Groblershoop High School in 1995. He studied BScAgric (Viticulture and Oenology) at Stellenbosch University from 1997, graduating in 2000. He completed his MScAgric (Viticulture) degree *cum laude* in 2002 on the topic “A study of within-vineyard variability with conventional and remote sensing technology”. He started teaching in 2002 at the Cape Technikon (Wellington-campus) as a lecturer in viticulture and oenology, and has been employed as a lecturer in viticulture at the Department of Viticulture and Oenology, Stellenbosch University, since 2004.

ACKNOWLEDGEMENTS

I wish to express my sincere gratitude and appreciation to the following persons and institutions:

- To my mother and late father for their love and support during my upbringing and study years, and also my wife Elana, for her love, support and understanding.
- My supervisor, prof JJ Hunter for his support, expertise, mentorship and guidance throughout. It was a privilege to learn from a master in his discipline!
- To my colleagues for their support and understanding during my study years
- Winetech, NRF, THRIP and the ALT committee for funding
- Tara Mehmel, Ewan Potgieter, Albertus van Zyl, Federica Gaiotti and Anouck Delaere for technical assistance
- Justin Lashbrooke for collaboration on HPLC method development
- Co-supervisor Dr Philip Young for his guidance in the laboratory and collaboration on HPLC method development
- Prof Melane Vivier for acquiring ALT funding to purchase the field spectrometer and for guidance in preceding studies
- Prof Eben Archer and Prof PG Goussard who both acted as mentors in my viticultural career
- Prof H Boshoff, Dr M Kidd and Marieta van der Ryst who assisted in statistical analysis

PREFACE

This dissertation is presented as a compilation of eight chapters. Each chapter is introduced separately and is written according to the style of the South African Journal of Enology and Viticulture.

Chapter I **GENERAL INTRODUCTION AND PROJECT AIMS**

Chapter II **LITERATURE REVIEW**

A review of grapevine leaf biochemical composition: physiological relevance as related to spectral analysis.

Chapter III **RESEARCH RESULTS**

Interactive effects of growth manipulation and water deficit in grapevine (*Vitis vinifera* L.) cv. Shiraz.

Chapter IV **RESEARCH RESULTS**

Response of *Vitis vinifera* L. cv. Shiraz leaves to canopy manipulation and water deficit, with specific reference to leaf age.

Chapter V **RESEARCH RESULTS**

Leaf chlorophyll and carotenoid profiles during growth of *Vitis vinifera* L. cv. Shiraz.

Chapter VI **RESEARCH RESULTS**

Leaf structural components and water content during growth of *Vitis vinifera* L. cv. Shiraz.

Chapter VII **RESEARCH RESULTS**

Non-destructive assessment of leaf pigment content, specific leaf mass and water content during growth of *Vitis vinifera* L. cv. Shiraz.

Chapter VIII **GENERAL DISCUSSION AND CONCLUSIONS**

CONTENTS

1. CHAPTER I: INTRODUCTION AND PROJECT AIMS	2
1.1 INTRODUCTION	2
1.2 PROJECT AIMS	3
1.3 LITERATURE CITED	4
2. CHAPTER II: A REVIEW OF GRAPEVINE LEAF BIOCHEMICAL COMPOSITION: PHYSIOLOGICAL RELEVANCE AS RELATED TO SPECTRAL ANALYSIS	8
2.1 INTRODUCTION	8
2.2 LEAF MORPHOLOGY, BIOCHEMICAL COMPOSITION AND PHENOLOGY	8
2.3 LEAF STRUCTURE AND WATER CONTENT	9
2.4 LEAF PHYSIOLOGY AND PIGMENT CONTENT	10
2.4.1 <i>Photosynthesis and the role of pigments</i>	10
2.4.2 <i>Chlorophyll and carotenoid localisation</i>	12
2.4.3 <i>Chlorophyll structure</i>	14
2.4.4 <i>Carotenoid structure</i>	14
2.4.5 <i>Chlorophyll biosynthesis</i>	14
2.4.6 <i>Carotenoid biosynthesis</i>	14
2.4.7 <i>Chlorophyll functions</i>	15
2.4.8 <i>Carotenoid functions</i>	15
2.4.8.1 Light harvesting	15
2.4.8.2 Photoprotection	16
2.4.8.3 Structural roles of carotenoids	17
2.4.8.4 Precursors of biochemical compounds	17
2.4.9 <i>General physiological considerations (photo-protection)</i>	18
2.4.10 <i>Chlorophyll a:b ratio and light interception</i>	18
2.5 LEAF PIGMENT CONTENT AND INTERRELATIONS	19
2.5.1 <i>Chlorophyll content and pigment ratios in grapevine leaves</i>	19
2.5.2 <i>Carotenoid and xanthophyll pigment relations in leaves</i>	19
2.6 VITICULTURAL AND ECOPHYSIOLOGICAL EFFECTS ON LEAF PIGMENTS	22
2.6.1 <i>Grapevine leaf ageing and physiology</i>	22
2.6.1.1 Leaf age and pigment content/ratios	22
2.6.1.2 Leaf senescence and pigment degradation	24
2.6.2 <i>Microclimate effects on leaf structure/physiology</i>	25
2.6.3 <i>Leaf/canopy microclimate effects on pigments</i>	25
2.6.4 <i>Plant water status/disease</i>	28
2.6.4.1 Physiological effects	28
2.6.4.2 Effect on pigments	29
2.7 DESTRUCTIVE ANALYSIS OF LEAF PIGMENTS	29
2.8 NON-DESTRUCTIVE ANALYSIS OF LEAF COMPOSITION	30
2.8.1 <i>General leaf spectral properties</i>	30
2.8.1.1 Leaf interception of total radiation	30
2.8.2 <i>Factors that affect leaf interaction with radiation</i>	32
2.8.2.1 Leaf microclimate	32
2.8.2.2 Leaf surface properties (such as cuticle thickness or leaf hair coverage)	34

2.8.2.3	General leaf age effects	34
2.8.2.4	Leaf age and structural changes	34
2.8.2.5	Leaf age and visible radiation	34
2.8.2.6	Leaf age and NIR radiation	35
2.8.2.7	Leaf water content	35
2.9	GENERAL INDICES FOR DETECTING VEGETATION CONDITION	37
2.10	NON-DESTRUCTIVE ANALYSIS OF LEAF PIGMENT CONTENT/PROFILES	38
2.10.1	<i>Chlorophyll content</i>	39
2.10.2	<i>Carotenoid content</i>	39
2.10.3	<i>Carotenoid:chlorophyll ratio</i>	41
2.10.4	<i>Anthocyanin content and senescence detection</i>	42
2.10.5	<i>Model approaches to determine pigments from spectra</i>	42
2.11	NON-DESTRUCTIVE ESTIMATION OF LEAF STRUCTURAL COMPONENTS	42
2.12	CONCLUSIONS	43
2.13	LITERATURE CITED	44
3.	CHAPTER III: INTERACTIVE EFFECTS OF GROWTH MANIPULATION AND WATER DEFICIT IN GRAPEVINE (<i>VITIS VINIFERA</i> L.) CV. SHIRAZ	53
3.1	INTRODUCTION	53
3.2	MATERIALS AND METHODS	55
3.2.1	<i>Vineyard</i>	55
3.2.2	<i>Experiment layout and treatments</i>	55
3.2.3	<i>Climate measurements</i>	55
3.2.4	<i>Soil and plant water status</i>	56
3.2.5	<i>Light measurements</i>	56
3.2.6	<i>Vegetative measurements</i>	57
3.2.6.1	Pruning measurements	57
3.2.6.2	Shoot growth, leaf length and leaf plastochron index (LPI) measurements	57
3.2.6.3	Leaf area	58
3.2.7	<i>Reproductive measurements</i>	58
3.2.7.1	Berry sampling and analyses	58
3.2.8	<i>Statistical analysis</i>	58
3.3	RESULTS AND DISCUSSION	59
3.3.1	<i>Climatic data</i>	59
3.3.2	<i>Soil water status</i>	60
3.3.3	<i>Plant water status</i>	62
3.3.4	<i>Light measurements</i>	66
3.3.5	<i>Vegetative measurements</i>	67
3.3.5.1	Shoot growth	67
3.3.5.2	Leaf area	73
3.3.5.3	Pruning measurements	77
3.3.6	<i>Reproductive measurements</i>	79
3.3.6.1	Yield per vine and bunch mass results	79
3.3.6.2	Yield:pruning mass ratios	79
3.3.6.3	Berry growth	80
3.3.6.4	Berry total soluble solids accumulation	81
3.3.6.5	Titrateable acidity and pH	88

3.3.6.6	Ratio of total soluble solids to titratable acidity	95
3.4	CONCLUSIONS	98
3.5	LITERATURE CITED	99
3.6	ADDENDUM A - EXPERIMENT LAYOUT	104
3.7	ADDENDUM A - PHENOLOGY	106
3.8	ADDENDUM B - RAINFALL / ET	108
3.9	ADDENDUM B - IRRIGATION	109
3.10	ADDENDUM C - PRUNING AND YIELD DATA RESULTS	111
4.	CHAPTER IV: RESPONSE OF <i>VITIS VINIFERA</i> L. CV. SHIRAZ LEAVES TO CANOPY MANIPULATION AND WATER DEFICIT, WITH SPECIFIC REFERENCE TO LEAF AGE	118
4.1	INTRODUCTION	118
4.2	MATERIALS AND METHODS	119
4.2.1	<i>Plastochron measurements</i>	119
4.2.2	<i>Statistical analysis</i>	120
4.3	RESULTS AND DISCUSSION	120
4.3.1	<i>Plastochron development on shoots for the measurement seasons</i>	120
4.3.2	<i>Relationships between shoot growth parameters</i>	123
4.3.3	<i>Plastochron development on shoots from different treatments</i>	124
4.3.4	<i>Chronological leaf age estimation</i>	127
4.3.5	<i>Leaf age classification according to LPI</i>	128
4.3.6	<i>Canopy age</i>	129
4.4	CONCLUSIONS	131
4.5	LITERATURE CITED	132
5.	CHAPTER V: LEAF CHLOROPHYLL AND CAROTENOID PROFILES DURING GROWTH OF <i>VITIS VINIFERA</i> L. CV. SHIRAZ	135
5.1	INTRODUCTION	135
5.1	MATERIALS AND METHODS	135
5.1.1	<i>Experiment layout</i>	135
5.1.2	<i>Destructive pigment determination (HPLC)</i>	136
5.1.3	<i>Leaf age classification</i>	140
5.1.4	<i>Statistic and chemometric analysis</i>	140
5.2	RESULTS AND DISCUSSION	140
5.2.1	<i>Light measurements</i>	140
5.2.2	<i>Leaf water potential (pre-dawn)</i>	140
5.2.3	<i>Leaf age on the measuring dates</i>	141
5.2.4	<i>Range of measured pigments</i>	142
5.2.5	<i>Results from destructive pigment measurements</i>	142
5.2.5.1	Leaf total chlorophyll content	142
5.2.5.2	Total carotenoids	146
5.2.5.3	Carotenoid:chlorophyll ratios	147
5.2.5.4	Chlorophyll <i>a</i> : <i>b</i> ratios	148
5.2.5.5	De-epoxidation state of the xanthophylls	149
5.2.5.6	Xanthophyll pool size:chlorophyll ratio	152
5.2.5.7	Lutein:chlorophyll ratio	153
5.3	CONCLUSIONS	154

5.4	LITERATURE CITED	155
5.5	ADDENDUM A	157
6.	CHAPTER VI: LEAF STRUCTURAL COMPONENTS AND WATER CONTENT DURING GROWTH OF <i>VITIS VINIFERA</i> L. CV. SHIRAZ	161
6.1	INTRODUCTION	161
6.2	MATERIALS AND METHODS	162
6.2.1	<i>Vineyard</i>	162
6.2.2	<i>Experiment layout</i>	162
6.2.3	<i>Leaf sampling</i>	162
6.2.4	<i>Statistical analysis</i>	163
6.2.5	<i>Leaf age determination/classification</i>	163
6.2.6	<i>Leaf water potential measurements</i>	163
6.3	RESULTS AND DISCUSSION	163
6.3.1	<i>Results from Dataset 2011A</i>	163
6.3.1.1	Total specific leaf mass (TSLM) and specific leaf mass (SLM)	164
6.3.1.2	Mean leaf thickness measurements	167
6.3.1.3	Leaf mass density (LMD)	168
6.3.1.4	Leaf water content on a mass (LWC_d and LWC_f) and area basis (equivalent water thickness, EWT)	170
6.3.2	<i>Results from dataset 2011B</i>	172
6.3.3	<i>Results from Dataset 2010A</i>	174
6.3.4	<i>Results from Dataset 2010B</i>	177
6.4	CONCLUSIONS	180
6.5	LITERATURE CITED	180
7.	CHAPTER VII: NON-DESTRUCTIVE ASSESSMENT OF LEAF PIGMENT CONTENT, SPECIFIC LEAF MASS AND WATER CONTENT DURING GROWTH OF <i>VITIS VINIFERA</i> L. CV. SHIRAZ	184
7.1	INTRODUCTION	184
7.2	MATERIALS AND METHODS	185
7.2.1	<i>Vineyard, experiment layout and leaf sampling</i>	185
7.2.2	<i>Non-destructive measurements</i>	185
7.2.3	<i>Statistical analysis</i>	186
7.2.4	<i>Leaf radiation transfer modelling</i>	187
7.2.5	<i>Leaf age determination/classification</i>	187
7.2.6	<i>Leaf water potential measurements</i>	187
7.3	RESULTS AND DISCUSSION	187
7.3.1	<i>General spectral properties of leaves</i>	187
7.3.1.1	Leaf absorption of visible (400-700 nm) radiation	188
7.3.1.2	Leaf absorption of infrared (700-1400 nm) radiation	193
7.3.2	<i>Multivariate calibration and prediction of leaf structure and water content</i>	197
7.3.3	<i>Univariate regressions of leaf pigments</i>	202
7.3.4	<i>Multivariate calibration and prediction of leaf pigment content</i>	204
7.3.5	<i>"Photochemical reflectance index" performance</i>	210
7.3.6	<i>PROSPECT inversion</i>	211
7.3.7	<i>Results from spectral predictions of TSLM, SLM and EWT</i>	212
7.3.8	<i>Leaf age prediction from spectra</i>	214
7.3.9	<i>Non-destructive prediction evaluation</i>	215

7.3.10	<i>Prediction application</i>	225
7.4	CONCLUSIONS	226
7.5	LITERATURE CITED	227
8.	CHAPTER VIII: GENERAL DISCUSSION AND CONCLUSIONS	231
8.1	BRIEF OVERVIEW	231
8.2	GENERAL DISCUSSION OF FINDINGS ACCORDING TO ORIGINAL OBJECTIVES	231
8.2.1	<i>Objective I: Interactive effects of growth manipulation and water deficits</i>	231
8.2.2	<i>Objective II: Logistic growth models to determine leaf age and its response to canopy manipulation and water deficit</i>	232
8.2.3	<i>Objective III: Leaf age determination/classification for further studies</i>	232
8.2.4	<i>Objective IV: Analysis of leaf chlorophyll and carotenoid profiles during growth</i>	233
8.2.5	<i>Objective V: Leaf structural components and water content during growth</i>	233
8.2.6	<i>Objective VI: Non-destructive assessment of leaf pigment content, specific leaf mass and water content during growth</i>	233
8.3	MAJOR FINDINGS: LIMITATIONS AND NOVELTY VALUE – IMPLICATIONS	234
8.3.1	<i>Limitations</i>	234
8.3.2	<i>Novelty value</i>	234
8.4	PERSPECTIVES FOR FUTURE RESEARCH	235
8.5	FINAL REMARKS	235
8.6	LITERATURE CITED	236

List of abbreviations

ABA	Abscisic acid
ALA	5- aminolevulinate
ANOVA	Analysis of variance
ARI	Anthocyanin reflectance index
ASD	Analytical spectral devices
ATP	Adenosine triphosphate
BCH	β -carotene hydroxylase
BHT	Butylated hydroxytoluene
CPI	P700 chlorophyll a protein complex
CPII	P680 chlorophyll a protein complex
CPS	Carotenoid pool size
CR	Neutron count ratio
CRI	Carotenoid reflectance index
CV	Coefficient of variation
DAB	Days after budburst
DAB _{LE}	Days after budburst when leaf emerged
DAD	Diode array detector
DEPS	De-epoxidation state of the xanthophyll cycle
DLM	Dorsiventral leaf model
DM	Dry mass
DMAPP	Dimethylallyl diphosphate
EL	Eichhorn-Lorenz code
EPS	Epoxidation state
ET	Evapotranspiration
EWT	Equivalent water thickness
FM	Fresh mass
FR	Far-red
FWHM	Full-width at half-maximum
GDD	Growing degree days
GGPP	Geranylgeranyl pyrophosphate
HPLC	High-performance liquid chromatography
IPP	Isopentyl diphosphate
IS	Internal standard
KPa	Kilopascal
LA	Leaf area

LAI	Leaf area index
LBCY	Lycopene β - cyclase
LD	Leaf density
LECY	Lycopene ϵ -cyclase
LHC	Light harvesting complex
LMD	Leaf mass density
LPI	Leaf plastochron index
LSD	Least significant difference
LT	Leaf thickness
LUE	Light use efficiency
LWC	Leaf water content (LWC _d – dry mass based or LWC _f –fresh mass based)
LWP	Leaf water potential
mARI	Modified anthocyanin reflectance index
MLR	Multiple linear regression
mND	Modified normalised difference index
mSR	Modified simple ratio
NADPH	Nicotinamide adenine dinucleotide phosphate
NDPI	Normalised difference pigment index
NDVI	Normalised difference vegetation index
NED	N-ethyl-di-isopropylamine
NIR	Near-infrared
NPQ	Non-photochemical quenching
NPQI	Normalized pheophytinisation index
NS	Non-stressed treatment
NSF	Non-stressed full canopy treatment
NSR	Non-stressed reduced canopy treatment
NTF	Non-topped full canopy treatment shoots/canes
NTR	Non-topped reduced canopy treatment shoots/canes
PAR	Photosynthetically active radiation
PC	Principal component
PCA	Principal component analysis
PCR	Principal component regression

Ψ_{PD}	Pre-dawn leaf water potential
PD	Plastochron duration
PDR	Plastochron development rate
3PG	3-phosphoglyceric acid
Phe	Pheophytin
PI	Plastochron index
PI_{LE}	PI value of the shoot when the leaf in question emerged
PLS	Partial least-squares
PM	Pruning mass
PQ/PQH	Plastoquinone pool
PRI	Photochemical reflectance index
PSI	Photosystem I
PSII	Photosystem II
PSRI	Plant senescence reflectance index
QA / QB	Electron acceptor quinones
RC	Reaction centre
RE	Red edge
REIP	Red edge inflexion point
RMSECV	Root-mean square error of cross-validation
RMSEP	Root-mean square error of prediction
R_{NIR}	NIR reflectance
RP-HPLC	Reverse-phase HPLC
R_{REF}	Reference reflectance
RuBP	Ribulose bisphosphate
RWC	Relative water content
SD	Standard deviation
SF	Stressed full canopy treatment

SIPI	Structure-insensitive pigment index
SLA	Specific leaf area
SLM	Specific leaf mass
SR	Stressed reduced canopy treatment
SRPI	Simple-ratio pigment index
SWIR	Short-wave infrared
TA	Titrateable acidity
TBME	<i>Tert</i> -butyl methyl ether
TD	Tissue density
TEA	Tri-ethylamine
TF	Topped full canopy treatment shoots/canes
TM	Turgid mass
TR	Topped reduced canopy treatment shoots/canes
TSLM	Total specific leaf mass
TSS	Total soluble solids
TT	Thermal time
UPLC	Ultra-performance liquid chromatography
UV	Ultraviolet
VAZ	Violaxanthin, antheraxanthin and zeaxanthin
VDE	Violaxanthin de-epoxidase
VIS	Visible spectral region
WI	Water index (a vegetation index)
WUE	Water use efficiency
XPS	Xanthophyll pool size
ZEP	Zeaxanthin epoxidase

Chapter I

Introduction and project aims

Chapter I: Introduction and project aims

1.1 Introduction

Several remote sensing platforms, sensor types and resolution levels are available today and these technologies have also received significant attention in viticultural applications during the past few decades (Hall *et al.*, 2002). In viticulture, several studies utilised field spectroscopy techniques in order to study leaf or canopy reaction to different conditions. Lang *et al.* (2000) studied the effect of ultraviolet light and water deficit stress in leaves of *Vitis labrusca* cv. Concord. Blanchfield *et al.* (2006) studied the possibility of detecting phylloxera (*Daktulosphaira vitifoliae*) in Pinot noir and Cabernet Sauvignon using high-performance liquid chromatography (HPLC) measurements along with leaf spectral measurements. Leaf and canopy reflectance measurements were also used by Rodríguez-Pérez *et al.* (2007) to investigate the potential of detecting grapevine leaf water status and leaf water content changes. Different canopy zones were also included in this study, indicating that leaf water content and dry matter content were affected drastically depending on the position of the leaf within the canopy. Apart from reflectance-based approaches, radiometric surface temperature measurements also hold promise to detect grapevine water status (Leinonen & Jones, 2004; Grant *et al.*, 2007; Jones *et al.*, 2009).

All of these studies acknowledge, albeit to different degrees, that the vineyard canopy is complex, integrating different elements, such as canopy size, density, leaf age, pigment content, nutrient content and water status, which are then also subject to severe manipulation in the form of different types of trellising, canopy manipulation and pruning (Hunter & Archer, 2002). In addition to this, soil features that form the background of the canopy signal may also differ considerably, depending on factors such as slope, soil type and cover crop establishment, which need to be accounted for when using *scaling-up* approaches in remote sensing to assess vineyard condition (Zarco-Tejada *et al.*, 2005; Meggio *et al.*, 2010). Add to this the variability that may exist in a vineyard due to soil differences, soil preparation mistakes, irrigation system problems, plant material quality considerations, planting practices, badly performed young vine development, and different general managing practices during the season, and it becomes difficult to imagine that it could be possible to detect small changes in for instance pigment content from a space-borne platform. The extensive study by Zarco-Tejada *et al.* (2005) showed that it is possible to successfully use a *scaling-up* approach to estimate total chlorophyll from discontinuous vineyard canopies using a combination of radiative transfer modelling and canopy reflectance modelling. This study, however, did not incorporate different elements of the canopy in the calibration of the models, as leaves were only sampled from the top parts of the canopy.

Different statistical approaches exist for evaluating relationships between the interaction of spectral radiation with the leaf and canopy and the biochemical and biophysical composition of the targets. Spectral indices are very popular due to its relative simplicity and in some studies large numbers of different types of indices are evaluated and/or reviewed (Le Maire *et al.*, 2004; Zarco-Tejada *et al.*, 2005; Rodríguez-Pérez *et al.*, 2007; Serrano, 2008). In other studies, radiative transfer modelling is used with different variations of pre-processing or optimisation algorithms to estimate leaf pigment, dry matter or water content (Jacquemoud & Baret, 1990; Jacquemoud *et al.*, 2000; Ceccato *et al.*, 2001; Feret *et al.*, 2008). Surprisingly, there are very few studies that use multivariate calibration techniques to predict leaf or canopy constituents from spectral measurements, despite its wide application in spectroscopy in other fields. One example of such a study in viticulture was conducted by De Bei *et al.* (2011), with the goal of estimating leaf water potential in Cabernet

Sauvignon and Shiraz grapevines using multivariate techniques (principal component analysis and partial least squares regression), yielding very good prediction ability of the models.

The grapevine shoot follows a sigmoidal (logistic) growth pattern, even where severe defoliation has been performed (Hunter & Visser, 1990a). With shoot growth monitoring it is therefore necessary to account for delayed initial shoot growth after budburst, as well as declining shoot growth later in the season. This is not often done in viticultural studies when accounting for shoot growth in logistic models. Related to this, and considering the relation between internode and leaf growth (Schultz & Matthews, 1988), it seems logical to integrate limitations on shoot growth into a leaf ageing model. In previous studies, leaf age was determined by marking and monitoring individual leaves or by measuring and calculating the leaf plastochron index (Kriedemann *et al.*, 1970; Freeman & Kliwer, 1984; Schultz, 1992; Schultz, 1993; Poni & Giachino, 2000). The best solution to keep monitoring leaf age after shoot growth cessation was to adapt the age of leaves chronologically. The development of leaf area on shoots is also dynamic and could be linked to shoot development using logistic growth models (Schultz, 1992).

Leaf total chlorophyll and in some cases also total carotenoid content have been measured in many viticultural studies focused on different topics such as leaf thinning (Hunter & Visser, 1989), leaf ageing (Kriedemann *et al.*, 1970; Poni *et al.*, 1994b), canopy shading (Cartechini & Palliotti, 1995), and shoot development (Cloete *et al.*, 2008) or for validating non-destructive determination (Fanizza *et al.*, 1991). Some studies also used HPLC methods to determine chlorophyll, carotenoids or xanthophylls (Medrano *et al.*, 2002; Bertamini & Nedunchezian, 2004; Hendrickson *et al.*, 2004b; Blanchfield *et al.*, 2006), but none of these studies supplied complete chromatograms of the HPLC runs to prove that degradation components did not affect the results. Similarly, spectrophotometric techniques may also include undetected degradation components and in addition the use of the Arnon (1949) and Mackinney (1941) spectrophotometric equations may lead to underestimation of pigments and erratic chlorophyll a:b ratio estimation as shown by Porra (2002).

Even though the analysis of pigments or other leaf constituents on a canopy/shoot zone basis or relative to the leaf plastochron index, give an indication of how these parameters react to leaf age, these approaches do not account for changing plastochron duration through the season. As an example, the apical shoot zone could be erratically considered as a zone harbouring young leaves, especially after shoot growth cessation or topping of shoots. Studies such as those by Hunter & Visser (1989) accounted for this by providing information on pigment change in these zones at different times of the season, but other studies neglected this important factor, which is extremely relevant in remote sensing studies, as this is the part of the canopy that may dominate the signal at least in the visible spectral domain right through the growing season.

It is important in plant physiological studies where leaf pigment or nutrient content are measured to consider changes in leaf structure and water content. Specific leaf mass changes can lead to changes in area based pigment values without the pigment concentration actually changing. Conversely, if pigment content is expressed relative to leaf fresh mass, changes in leaf water content could affect the result. Not many studies assessing grapevine pigments combine these measurements on the same leaves.

1.2 Project aims

The goal of this study was not to suggest a spectral index or other analysis method that would apply globally to all vineyards for prediction of leaf structural, water or pigment content. The

diversity of growing conditions, cultivars and microclimate around the leaf would always require the necessary calibration and validation techniques before any generalisations are to be made with respect to a cultivar or site. This being said, the study aimed to provide some new insights into different ways to assess the grapevine leaf and possibly also the canopy growth and ageing dynamics as well as pigment content as the basis of validating a generally non-destructive measurement approach.

The main aim of this study was therefore to use field spectroscopy to study leaf composition and some factors that may affect it (including canopy growth manipulation and water status changes) within a vineyard showing considerable variability in vigour.

In order to achieve this aim, a field experiment was designed in order to reach six different objectives:

- I. To assess the interactive effects of growth manipulation and water deficits on pruning mass, shoot characteristics, grape ripening and harvest parameters in Shiraz, laying the foundation for determining the interactions between age, structure and pigment content of leaves in reaction to the modified conditions.
- II. To evaluate the use of logistic growth modelling to aid in leaf age determination of Shiraz, assess the relationships between shoot growth parameters (shoot length, node number and the plastochron index) and finally to assess the reaction of Shiraz leaf age to canopy manipulation and irrigation treatments.
- III. To establish a basis for leaf age determination as well as classification for further work on leaf structure, and leaf water and pigment content in the same vineyard.
- IV. To assess chlorophyll and carotenoid contents of leaves during grapevine growth by, firstly, establishing a reliable method for chlorophyll and carotenoid analyses using high-performance liquid chromatography (HPLC) and, secondly, to analyse leaf chlorophyll and carotenoids for specified leaf age categories throughout the growing season and in reaction to canopy manipulation and changing water deficit conditions.
- V. To assess leaf structure and water content during canopy growth and for different leaf age and canopy light conditions as well as selected canopy management and irrigation treatments during two growing seasons. The datasets generated will also be used to calibrate non-destructive field spectroscopy models.
- VI. To evaluate spectral techniques to determine leaf chlorophyll and carotenoid contents or interrelations, specific leaf mass, water content and leaf chronological age non-destructively.

This study aimed to make a novel contribution to viticulture by showing the relevance of integrating plant growth and leaf age monitoring throughout the growing season along with measurements of pigments, leaf structure and water content as a basis for non-destructive monitoring at leaf level and in future, at canopy level. The application of multivariate techniques in leaf spectroscopy was also investigated with the goal of simplifying non-destructive leaf pigment, structure and water content estimation in future studies.

1.3 Literature cited

- Arnon, D.I., 1949. Copper enzymes in isolated chloroplasts. Polyphenoloxidase in *Beta vulgaris*. *PLANT PHYSIOLOGY* 24, 1.
- Bertamini, M. & Nedunchezian, N., 2004. Photosynthetic responses for *Vitis vinifera* plants grown at different photon flux densities under field conditions. *Biologia Plantarum* 48, 149-152.

- Blanchfield, A.L., Robinson, S.A., Renzullo, L.J. & Powell, K.S., 2006. Phylloxera-infested grapevines have reduced chlorophyll and increased photoprotective pigment content—can leaf pigment composition aid pest detection? *Functional plant biology* 33, 507-514.
- Cartechini, A. & Palliotti, A., 1995. Effect of Shading on Vine Morphology and Productivity and Leaf Gas Exchange Characteristics in Grapevines in the Field. *American Journal of Enology and Viticulture* 46, 227-234.
- Ceccato, P., Flasseb, S., Tarantolac, S., Jacquemoud, S. & Gregoirea, J.-M., 2001. Detecting vegetation leaf water content using reflectance in the optical domain. *Rem. Sens. Environ.* 77, 22-33.
- Cloete, H., Archer, E., Novello, V. & Hunter, J.J., 2008. Shoot heterogeneity effects on Shiraz/Richter 99 grapevines. III, Leaf chlorophyll content.
- De Bei, R., Cozzolino, D., Sullivan, W., Cynkar, W., Fuentes, S., Dambergs, R., Pech, J. & Tyerman, S., 2011. Non-destructive measurement of grapevine water potential using near infrared spectroscopy. *Australian Journal of Grape and Wine Research* 17, 62-71.
- Fanizza, G., Della Gatta, C. & Bagnulo, C., 1991. A non-destructive determination of leaf chlorophyll in *Vitis vinifera*. *Annals of Applied Biology* 119, 203-205.
- Feret, J.-B., François, C., Asner, G.P., Gitelson, A.A., Martin, R.E., Bidet, L.P.R., Ustin, S.L., le Maire, G. & Jacquemoud, S., 2008. PROSPECT-4 and 5: Advances in the leaf optical properties model separating photosynthetic pigments. *Remote Sensing of Environment* 112, 3030-3043.
- Freeman, B.M. & Kliewer, W.M., 1984. Grapevine leaf development in relationship to potassium concentration and leaf dry weight density. *Am. J. Bot.* 3, 294-300.
- Grant, O.M., Tronina, Á.u., Jones, H.G. & Chaves, M.M., 2007. Exploring thermal imaging variables for the detection of stress responses in grapevine under different irrigation regimes. *Journal of Experimental Botany* 58, 815-825.
- Hall, A., Lamb, D.W., Holzappel, B. & Louis, J., 2002. Optical remote sensing applications in viticulture—a review. *Australian Journal of Grape and Wine Research* 8, 36-47.
- Hendrickson, L., Forster, B., Furbank, R.T. & Chow, W.S., 2004. Processes contributing to photoprotection of grapevine leaves illuminated at low temperature. *Physiologia Plantarum* 121, 272–281.
- Hunter, J.J. & Visser, J.H., 1990. The effect of partial defoliation on growth characteristics of *Vitis vinifera* L. cv. Cabernet Sauvignon I. Vegetative growth. *South African Journal of Enology and Viticulture* 11, 18-25.
- Hunter, J.J. & Archer, E., 2002. Status of grapevine canopy management and future prospects (Papel actual y perspectivas futuras de la gestión del follaje). *In ACE Revista de Enología*, May 2002, pp.
- Hunter, J.J. & Visser, J.H., 1989. The effect of partial defoliation, leaf position and developmental stage of the vine on leaf chlorophyll concentration in relation to the photosynthetic activity and light intensity in the canopy of *Vitis vinifera* L. cv. Cabernet Sauvignon. *S. Afr. J. Enol. Vitic.* 10, 67-73.
- Jacquemoud, S., Bacour, C., Poilve, H. & Frangi, J.P., 2000. Comparison of Four Radiative Transfer Models to Simulate Plant Canopies Reflectance:: Direct and Inverse Mode. *Remote Sensing of Environment* 74, 471-481.
- Jacquemoud, S. & Baret, F., 1990. PROSPECT: A model of leaf optical properties spectra. *Remote Sensing of Environment* 34, 75-91.
- Jones, H.G., Serraj, R., Loveys, B.R., Xiong, L., Wheaton, A. & Price, A.H., 2009. Thermal infrared imaging of crop canopies for the remote diagnosis and quantification of plant responses to water stress in the field. *Functional Plant Biology* 36, 978-989.
- Kriedemann, P.E., Kliewer, W.M. & Harris, J.M., 1970. Leaf age and photosynthesis in *Vitis vinifera* L. *Vitis* 9, 97-104.
- Lang, N.S., Mills, L., Wample, R.L., Silbernagel, J., Perry, E.M. & Smithyman, R., 2000. Remote image and leaf reflectance analysis to evaluate the impact of environmental stress on grape canopy metabolism. *HortTechnology* 10, 468-474.

- Le Maire, G., François, C. & Dufrêne, E., 2004. Towards universal broad leaf chlorophyll indices using PROSPECT simulated database and hyperspectral reflectance measurements. *Rem. Sens. Environ.* 89, 1-28.
- Leinonen, I. & Jones, H.G., 2004. Combining thermal and visible imagery for estimating canopy temperature and identifying plant stress. *Journal of Experimental Botany* 55, 1423-1431.
- Mackinney, G., 1941. Absorption of light by chlorophyll solutions. *Journal of Biological Chemistry* 140, 315-322.
- Medrano, H., Bota, J., Abadia, A., Sampol, B., Escalona, J. & Flexas, J., 2002. Effects of drought on light-energy dissipation mechanisms in high-light acclimated, field-grown grapevines *Functional Plant Biology* 29, 1197-1207.
- Meggio, F., Zarco-Tejada, P.J., Núñez, L.C., Sepulcre-Cantó, G., González, M.R. & Martín, P., 2010. Grape quality assessment in vineyards affected by iron deficiency chlorosis using narrow-band physiological remote sensing indices. *Remote Sensing of Environment* 114, 1968-1986.
- Poni, S. & Giachino, E., 2000. Growth, photosynthesis and cropping of potted grapevines (*Vitis vinifera* L. cv. Cabernet Sauvignon) in relation to shoot trimming. *Australian Journal of Grape and Wine Research* 6, 216-226.
- Poni, S., Intrieri, C. & Silvestroni, O., 1994. Interactions of LeafAge, Fruiting, and Exogenous Cytokinins in Sangiovese Grapevines Under Non-Irrigated Conditions. II. Chlorophyll and Nitrogen Content. *Am. J. Enol. Vitic.* 45, 278-284.
- Porra, R.J., 2002. The chequered history of the development and use of simultaneous equations for the accurate determination of chlorophylls a and b. *Photosynth. Res.* 73, 149-156.
- Rodríguez-Pérez, J.R., Riaño, D., Carlisle, E., Ustin, S. & Smart, D.R., 2007. Evaluation of Hyperspectral Reflectance Indexes to Detect Grapevine Water Status in Vineyards. *Am. J. Enol. Vitic.* 58, 302-317.
- Schultz, H.R., 1992. An empirical model for the simulation of leaf appearance and leaf area development of primary shoots of several grapevine (*Vitis vinifera* L.) canopy-systems. *Scientia Horticulturae* 52, 179-200.
- Schultz, H.R., 1993. Photosynthesis of sun and shade leaves of field-grown grapevine (*Vitis vinifera* L.) in relation to leaf age. Suitability of the plastochron concept for the expression of physiological age. *Vitis* 32, 197-205.
- Schultz, H.R. & Matthews, M.A., 1988. Vegetative Growth Distribution during Water Deficits in *Vitis vinifera* L. *Aust. J. Plant Physiol.* 15, 641-656.
- Serrano, L., 2008. Effects of leaf structure on reflectance estimates of chlorophyll content. *International Journal of Remote Sensing* 29, 5265-5274.
- Zarco-Tejada, P.J., Berjón, A., López-Lozano, R., Miller, J.R., Martín, P., Cachorro, V., González, M.R. & De Frutos, A., 2005. Assessing vineyard condition with hyperspectral indices: Leaf and canopy reflectance simulation in a row-structured discontinuous canopy. *Remote Sensing of Environment* 99, 271-287.

Chapter II

Literature review

A review of grapevine leaf biochemical composition: physiological relevance as related to spectral analysis

Chapter II: A review of grapevine leaf biochemical composition: physiological relevance as related to spectral analysis

2.1 Introduction

Assessment of grapevine leaf pigment composition utilising spectral non-destructive methods is relevant due to its non-obtrusive nature and the possibility of rapid determination of changes in the plant. One challenge of these techniques is that differences in scattering properties among or within leaves may produce additive offsets (baseline shifts) or multiplication effects in spectra, which may then affect the estimation of leaf pigments as well as other spectral features (Serrano, 2008). This is also the reason why many reflectance-based spectral indices used to estimate leaf pigments incorporate a region of the spectrum where reflectance is mainly affected by leaf internal structure, typically also where reflectance is much higher compared to the pigment reflectance area in the visible spectral region (Chappelle *et al.*, 1992; Sims & Gamon, 2002).

The spectral signatures of leaves are affected by, amongst others, its internal and external structure or texture, age, water status, mineral deficiency/toxicity, disease incidence and pigment content, which all complicates spectral feature extraction from leaves and also from canopies.

2.2 Leaf morphology, biochemical composition and phenology

The leaves of the grapevine are regarded as extremely valuable because of their role in photosynthesis, but also for their importance in ampelographic differentiation of cultivars. It consists of the petiole, by which it is attached to the shoot and at the basis of which two stipula occur that virtually encircle the shoot, and the leaf-blade, which is intersected by a network of veins (vascular bundles). The lamina is generally intersected by five main veins which arise together from the point of attachment of the petiole (Figure 1) (Goussard & Orffer, 2011).

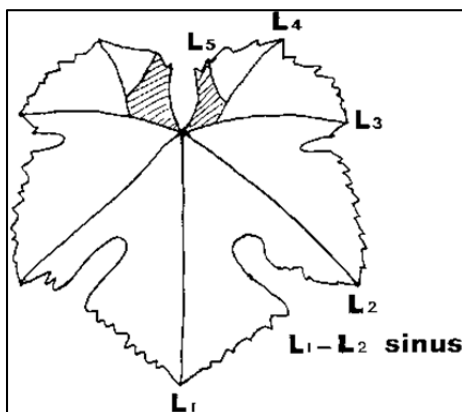


Figure 1 Tracing of a grapevine leaf indicating the position of the main veins, L1 to L5, as well as the L1 - L2 sinus; the L2 - L3 sinus and the petiole sinus tissue (striped) (Goussard & Orffer, 2011).

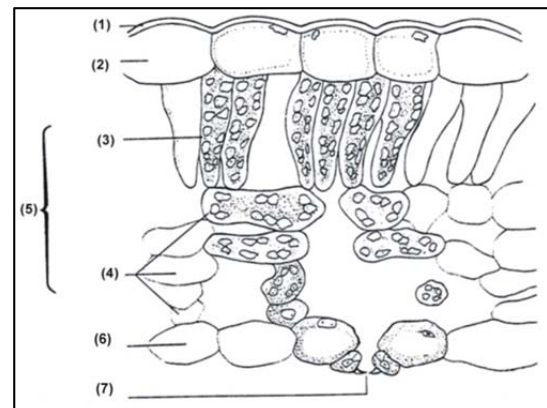


Figure 2 Cross-section of a mature grapevine leaf (1 – cuticle; 2 – adaxial epidermis; 3 – palisade parenchyma; 4 – spongy parenchyma; 5 – mesophyll; 6 – abaxial epidermis; 7 – stomatal opening) (Archer, 1981).

The upper surface of the leaf-blade (adaxial side) usually has no hairs, is relatively smooth and has very few or no stomata, while the underside (abaxial side) appears hairy and has a large number of stomata, depending on the cultivar (Pratt, 1974). The leaf cuticula is a waxy layer on the outer walls of the epidermis cells, which provides resistance to penetration by water. It gives the impression of small, overlapping scales and consists of carbohydrates, esters, aldehydes, alcohols as well as unknown acids.

Grapevine leaves have a dorsiventral leaf structure with the adaxial epidermis occurring as an uninterrupted single cell layer and the mesophyll consisting of a palisade and spongy parenchyma directly underneath the adaxial epidermis (Figure 2) (Archer, 1981). It consists of thin-walled, oblong or cylindrical cells that contain the majority of chloroplasts. The spongy parenchyma (four to six layers) is situated directly underneath the palisade parenchyma (single layer) and the cells are iso-diametrical with exceptionally large intercellular spaces, which is important to note when leaf radiative transfer properties are considered (Pratt, 1974). Mesophyll cells stop growing before the epidermis as leaves expand, causing the formation of intercellular spaces important for gas diffusion in the leaf (Van Volkenburgh, 1999).

The grapevine leaf is considered hypo-stomatal (stomata almost exclusively found abaxially) and the abaxial epidermis normally hairy (for instance in Clairette blanche). The hairs consist of one or more cells and can be dead or alive. Trichomes, which can also occur on leaves, are unicellular and originate from the epidermis cells (Pratt, 1974).

The abscission layer at the base of the petiole, by means of which normal leaf fall occurs, does not have a special cell structure. When leaf fall occurs, the cell walls of the epidermis and the cortex in the abscission layer dissolve and the vascular bundles are mechanically broken down. A protective cell layer is formed just below this break so that suberin and wound resin can be laid down in the cell walls and intercellular spaces of the remaining cells. A periderm is formed beneath this protective layer and this finally seals the abscission point (Pratt, 1974).

Water represented on average more than 66% of leaf fresh mass (FM), with the remaining part being cellulose, hemicellulose, lignin, protein, starch and minerals as well as lipids, soluble sugars, amino acids and other secondary metabolites (Jacquemoud *et al.*, 1996). Grapevine leaves also contain monoterpenes (Gholami *et al.*, 1996), with total chlorophyll and total carotenoid content (mainly β -carotene and lutein) ranging from 0.7 to 2.5 mg.g⁻¹ fresh mass and 0.3 to 1.0 mg.g⁻¹ fresh mass respectively (Hunter & Visser, 1989; Blanchfield *et al.*, 2006; Lashbrooke *et al.*, 2010).

According to Kriedemann (1968) the principal organic acid in leaves was malic acid, irrespective of leaf age, with tartaric acid originating from young leaves (16 - 20 days) of age. In Kriedemann *et al.* (1970) the biochemical composition of leaves was compared between leaves of differing ages. According to Jacquemoud *et al.* (1996), leaf carbon constituents are globally very stable and average about 47 g.g⁻¹ of dry matter.

Leaves normally reach their full size 30 - 40 days after unfolding (Kriedemann *et al.*, 1970). The first two leaves on a shoot mostly also develop as bracts and they are separated by a shorter internode (Keller, 2010). Leaves developing as large and thin as possible, is an adaptation to maximise gas exchange in shade conditions, but also brings vulnerability to dehydration and photodamage (Tsukaya, 2006). Leaf cells require about two weeks to expand to full size, allowing the leaf time to adapt to the environment in terms of leaf size or thickness, even though cell number is also important, with cell division ending when the leaf is about half its final size (Tsukaya, 2006; Keller, 2010). Environmental limitations during cell division and expansion would therefore limit leaf size considerably. The unproductive stage, followed by abscission, begins about four to five months after unfolding.

2.3 Leaf structure and water content

Several leaf structural and water indices are shown in Table 1. Leaf thickness can vary with leaf shape, number of layers and length of palisade cells as well as placements of veins, while leaf density can vary due to variations in thickness and density of the cuticle and cell walls, cell

inclusions (starch grains, crystals) as well as the amount of air spaces, crypts, hairs, sclereids, fibre caps and vascular bundles (Witkowski & Byron, 1991). Leaf thickness and density are relatively easy to determine, and in addition to specific leaf mass (SLM) should help to provide a better understanding of the relationship between physiological processes, leaf structure and environmental conditions (Witkowski & Byron, 1991). The equivalent water thickness (EWT) corresponds to a hypothetical thickness of a single layer of water averaged over the whole leaf area (Danson *et al.*, 1992). Results from Ceccato *et al.* (2001) showed that a unique leaf water content relative to fresh mass (LWCf) value may correspond to different EWT values. Conversely, a unique EWT value may correspond to different LWCf values. These examples showed that EWT and LWCf are two different ways to define vegetation water content and that they are not directly related.

Jacquemoud *et al.* (1996) found some correlations between biochemical constituents and leaf parameters, such as between leaf thickness and equivalent water thickness (EWT), and protein content and specific leaf area (SLA) relative to total chlorophyll. They showed that $1/\text{SLA}$, which is similar to specific leaf mass (SLM), varied inversely with the mass-based measure of leaf protein.

Poni *et al.* (1994b) showed that there is a general seasonal trend for SLM to increase steadily until a few weeks post-harvest, declining slightly afterward. This increase also confirms previous findings by Williams (1987), and it was also subsequently shown by Cartechini & Palliotti (1995). Regression analysis of photosynthesis *versus* SLM resulted in a quadratic fit with the highest photosynthetic rates at SLM of 6 - 7 $\text{mg}\cdot\text{cm}^{-2}$ and a sharp decrease after a threshold value of 7 $\text{mg}\cdot\text{cm}^{-2}$, corresponding to leaves older than 60 days. This decrease was not seen in Cartechini & Palliotti (1995), where fully irradiated vines showed a positive linear correlation ($r^2 = 0.84$) between photosynthesis and SLM. The difference in the last-mentioned study was that only middle-canopy leaves were measured at flowering and véraison, which may be a reason why the photosynthesis limitation was not similar to that measured in Poni *et al.* (1994b).

Poni *et al.* (1994b) also demonstrated a relation between SLM and leaf age measured according to the leaf plastochron index (LPI) (refer to Chapter IV). The SLM trend reported in Poni *et al.* (1994b), which suggested an increase until the post-harvest period, up to leaf chronological ages of almost 160 days, shows that probably leaf carbohydrate allocation (in the form of leaf thickening) takes place over a much longer period than the time needed for completing lamina expansion (completed at between 30 and 40 days after unfolding). Considering the experimental procedure, where shoots were drastically thinned light exposure probably had a minimal effect on SLM values of expanding leaves. Very similar SLM values were also reported for leaves similar in chronological age, but that were situated in different canopy zones, confirming a slight influence of the environment on this parameter. It was found by Cartechini & Palliotti (1995) that whole-vine shading using shade netting, significantly reduced the SLM during the entire growing season, and a positive and significant relationship was also confirmed between the SLM and photosynthesis.

Water stress may reduce turgor pressure and hence cell expansion, resulting in approximately the same dry mass being contained within a smaller leaf area, therefore raising leaf density (Witkowski & Byron, 1991).

2.4 Leaf physiology and pigment content

2.4.1 Photosynthesis and the role of pigments

In the grapevine, photosynthesis occurs mainly in leaves. Carbon dioxide enters leaves through the stomata by diffusion. The processes involved in photosynthesis can be separated into light and

dark reactions. Light energy is converted into chemical energy in the form of adenosine triphosphate (ATP) and nicotinamide adenine dinucleotide phosphate (NADPH). In chloroplasts, light energy is harvested by the photosystems, which mediate the transfer of electrons through a series of compounds connecting Photosystem II (PSII) (called P680, as the centre of maximum absorption is at 680 nm) with Photosystem I (PSI) (P700) in a series of redox reactions. A flow of electrons between the two photosystems results in the formation of ATP and NADPH. The electrons come from the splitting of H₂O in PSII and O₂ is a by-product of this reaction.

Table 1 Leaf structural parameters and formulae often used in literature.

Parameter	Abbreviation	Formulae*	Reference(s)
Specific leaf mass (density x thickness)	SLM (mg.cm ⁻²)	DM/LA	Witkowski & Byron (1991) Niinemets (1999) Garnier <i>et al.</i> (2001) Serrano (2008)
Total specific leaf mass (leaf thickness)	TSLM (mg.cm ⁻²)	FM/LA	Rodríguez-Pérez <i>et al.</i> (2007)
Leaf density / leaf mass density	LD / LMD (mg.cm ⁻³)	$\frac{DM}{Unit\ volume} = \frac{DM}{LA \times LT} = \frac{SLM}{LT}$	Niinemets (1999) Serrano (2008)
Leaf tissue density / leaf dry matter content	TD	DM/TM x 1000	Garnier <i>et al.</i> (2001)
Specific leaf area (density x thickness)	SLA (cm ⁻² .mg)	LA/DM	Garnier <i>et al.</i> (2001)
Leaf water content relative to dry mass	LWCd (%)	(FM-DM)/DM x 100	Ceccato <i>et al.</i> (2001) Rodríguez-Pérez <i>et al.</i> (2007)
Leaf water content relative to fresh mass	LWCf (%)	(FM-DM)/FM x 100	Ceccato <i>et al.</i> (2001) Rodríguez-Pérez <i>et al.</i> (2007)
Leaf relative water content	RWC	(FM-DM)/(TM-DM) x 100	Palliotti <i>et al.</i> (2000)
Leaf water content relative to leaf area (Equivalent water thickness)	EWT (mg.cm ⁻²)	(FM-DM)/LA	Danson <i>et al.</i> (1992) Ceccato <i>et al.</i> (2001) Rodríguez-Pérez <i>et al.</i> (2007) Serrano (2008)

* FM – leaf fresh mass (determined in a saturated environment)

DM – leaf dry mass (determined after desiccation, normally for up to 48 hours at 60°C)

TM – leaf turgid mass (determined after rehydration with distilled water for up to 10 hours)

LA – one-sided leaf area or area of disc for which mass were also determined.

LT – Leaf thickness measured using an electronic calliper.

The electron transport chain and chlorophyll molecules are imbedded in the thylakoid membrane of the chloroplast. Pairs of hydrogen ions are pumped across the thylakoid membrane into the stroma of the chloroplast, creating an electrochemical gradient. The hydrogen ions move back into the lumen of the thylakoid via ATPase complexes, generating ATP. Electrons are passed onto PSI and energised further, after which they are accepted by a further electron transport chain and used to create NADPH.

Chlorophylls and carotenoids are molecules adapted to light absorption, energy transfer, and electron transfer between the two photoreaction centres, with PSI preferentially absorbing far-red light (between 700 nm and 740 nm) and PSII absorbing red light (+/- 680 nm), while being driven inefficiently by far-red light (Taiz & Zeiger, 1998). It is notable that PSI absorbs radiation at 700 nm and PSII at 680 nm, but both photosystems can also absorb light at shorter wavelengths (Salisbury & Ross, 1978).

The light-absorbing pigments transfer their energy to the reaction centres by a sequence of pigments with absorption maxima that are progressively shifted toward longer red wavelengths: carotenoids transfer the photons to chlorophyll *b*, with absorption maximum at 650 nm, and then the photon is transferred to chlorophyll *a*, with absorption maximum at 670 nm, losing energy as heat in the process. Photons are therefore transported from higher to lower energy levels (Figure 3 and Figure 4). This energy-trapping process ensures that the energy transfer is always in a direction towards longer wavelengths while the photosystems receive energy for photochemical reactions (Taiz & Zeiger, 1998).

The Calvin cycle (Figure 4) uses chemical energy generated by the light reactions to reduce CO₂ to carbohydrates. The immediate by-product of CO₂ fixation with RuBP (Ribulose bisphosphate) is extremely unstable and splits almost instantaneously into two molecules of 3-phosphoglyceric acid (3PG). Intermediates of the cycle are directed towards the synthesis of sucrose and other organic compounds. The Calvin cycle passes through the processes of carboxylation, reduction and regeneration of ribulose 1,5 –bisphosphate. It relies on ATP and NADPH and is therefore light dependent. Grapevines are C₃ plants, as the first step in the Calvin cycle is the production of two molecules of 3PG. Various enzymes are necessary for the reactions involved in this cycle, most of them dependent on phosphates for their functioning. Several enzymes are regulated by light, as well as the pH and magnesium concentration in the stroma.

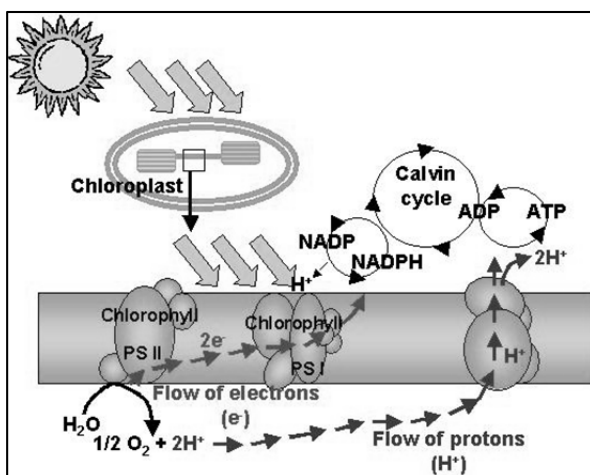


Figure 3 Simplified diagram of the light reactions of grapevine photosynthesis (Huglin & Schneider, 1998).

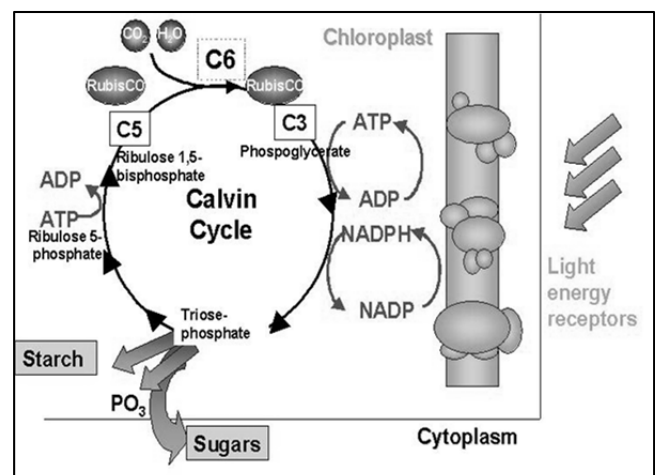


Figure 4 Simplified diagram of the dark reactions of grapevine photosynthesis (Huglin & Schneider, 1998).

2.4.2 Chlorophyll and carotenoid localisation

There are substantial differences between the pigments that absorb light in PSI and PSII. Chlorophylls and carotenoids are situated in the thylakoid membranes within the chloroplast (Figure 5 and Figure 6) and carotenoids are bound to specific chlorophyll/carotenoid-binding protein complexes of the two photosystems (PSI and PSII) (Demmig-Adams *et al.*, 1996), with some carotenoids also localised in the chloroplast envelope (Britton, 1982).

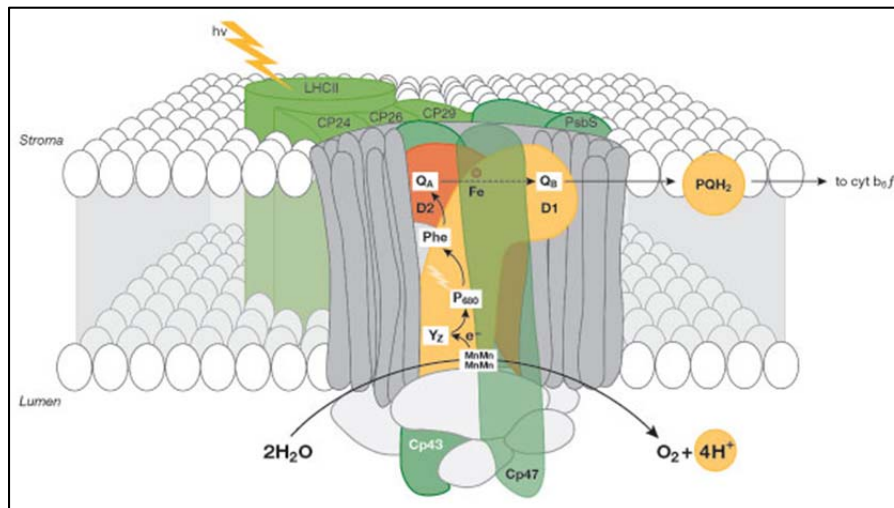


Figure 5 Simplified organization of photosystem II and light-harvesting complex II in the thylakoid membrane. Cp43, Cp47: internal antenna chlorophyll–protein complexes. D1, D2: main components of reaction centres (RCs) with binding sites for electron acceptor quinones (QB, QA). P680: chlorophyll special pair. Other cofactors associated with D1/D2: pheophytin (Phe), non-haem iron (Fe), Mn-cluster. Accessory chlorophylls and β -carotene are not shown. Chl, chlorophyll; PQH₂, plastoquinone pool; cytb₆f, cytochrome b₆f complex; YZ, D1-Tyr161. (Szabó *et al.*, 2005)

Carotenoids are unevenly distributed between PSI, PSII and among different protein complexes, with β -carotene mostly associated with the P700 chlorophyll a protein complex (CPI) and lutein with PSII, but also with all chlorophyll proteins (Eskins *et al.*, 1982; Demmig-Adams *et al.*, 1996). Most of the β -carotene that is present in PSII can be found in the core complexes surrounding the reaction centre. The rest of the carotenoids can be found in the remaining light harvesting antennae that include several functional components (Demmig-Adams *et al.*, 1996). Although lutein have been found to be the dominant carotenoid in higher plant leaves, it has also been shown that it may not be essential for photosynthesis in *Arabidopsis*, and that its structural and physiological function can be substituted by β -carotene (Pogson *et al.*, 1996).

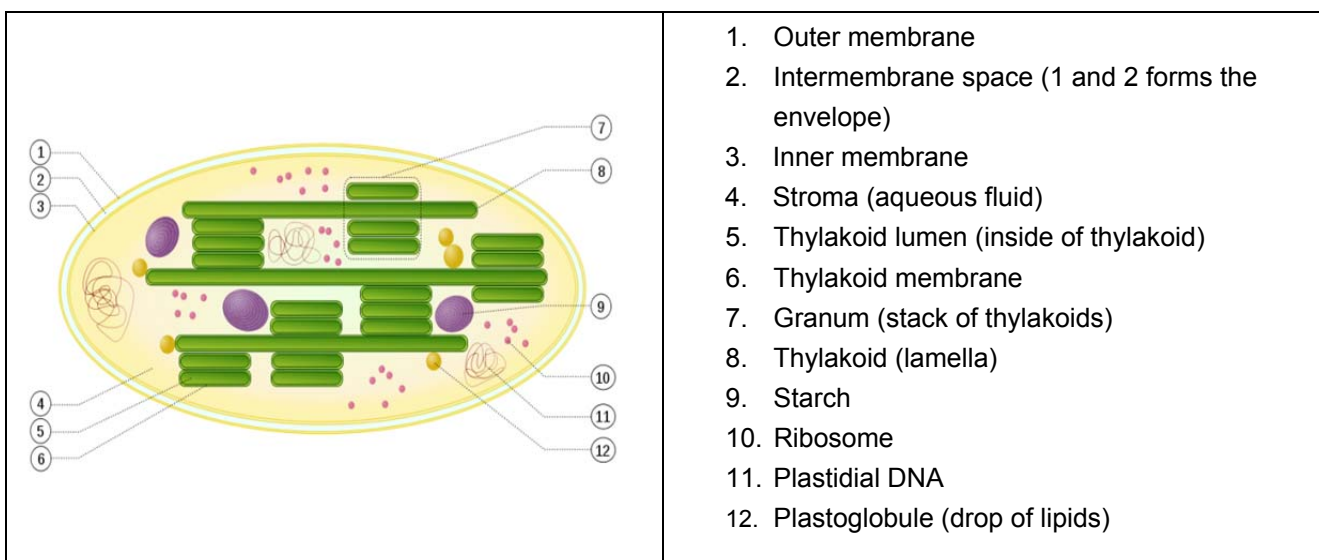


Figure 6 Simplified ultrastructure of a chloroplast showing the location of carotenoids and chlorophylls (from <http://en.wikipedia.org/wiki/Chloroplast>).

An analysis of the structure of the PSII light-harvesting complex has shown that it contains three different carotenoids in stoichiometric proportions, namely lutein, neoxanthin and violaxanthin, replaced by zeaxanthin in non-photochemical quenching (NPQ) energy dissipation. They have a

defined arrangement within PSII, with neoxanthin located in a highly selective binding site, localised between the helix C and helix A/B domains in light harvesting complex II (Croce *et al.*, 1999; North *et al.*, 2007).

2.4.3 Chlorophyll structure

Chlorophyll is a cyclic tetrapyrrole (porphyrin) with a central magnesium ion (Figure 7). Although several types of chlorophylls exist, chlorophyll a is the major light harvesting pigment and chlorophyll b an accessory pigment. These pigments normally exist in a ratio of between 2:1 and 4:1 in higher plants. Chlorophyll a differs structurally from chlorophyll b due to a methyl side-chain in chlorophyll a, and an aldehyde group in chlorophyll b (Fleming, 1967). This small difference makes chlorophyll b absorb light with wavelengths between 400 nm and 500 nm more efficiently. The structure of the tetrapyrrole ring is responsible for the green colour of these pigments, and the loss of structure (i.e. during degradation) can lead to formation of a colourless molecule (i.e. pheophytin).

2.4.4 Carotenoid structure

Carotenoids consist of a system of long, aliphatic conjugated double bonds, responsible for the various physical, biochemical and chemical properties they exhibit. They are mostly deeply red/orange or yellow lipophilic pigments with absorption maxima of between 400 nm and 500 nm depending on the amount of conjugated double bonds. There are two classes of carotenoids based on their structure, namely carotenes and xanthophylls (Figure 8). Xanthophylls are oxygenated carotenes, which can have various combinations of hydroxyl-, epoxy-, alcohol-, aldehyde-, keto-, lactone-, carboxylic acid-, ester or phenolic groups associated with its structure (Sajilata *et al.*, 2008). In grapevine leaves, as well as grapes, the most common carotenes are β -carotene and lutein, representing almost 85% of the total carotenoid content. They are accompanied by xanthophylls such as neoxanthin, violaxanthin, antheraxanthin, zeaxanthin, neochrome, flavoxanthin and luteoxanthin (Britton, 1979).

2.4.5 Chlorophyll biosynthesis

Chlorophyll synthesis is a light-induced/stimulated process as it is needed to reduce protochlorophyllide a (PCa) (Schoefs & Franck, 2003). Even though ALA (5-aminolevulinic acid) can be converted to PCa in darkness, ALA cannot be formed in darkness (Salisbury & Ross, 1978).

2.4.6 Carotenoid biosynthesis

Most carotenoids are synthesised in photosynthetic tissues. Biosynthesis follows the non-mevalonate pathway (Britton, 1979) via isopentenyl diphosphate (IPP) as a precursor, obtained by condensation of pyruvate and glyceraldehyde-3-phosphate via 1-deoxy-D-xylulose-5-phosphate (Figure 9). It is not yet certain whether the plastids can synthesise carotenoids from IPP or whether it is imported to the chloroplast after being synthesised elsewhere, but it does appear that the site of synthesis of the early precursors depends upon the development stage of the chloroplast (Goodwin & Lester, 1993; Lichtenthaler, 1999). The final steps highlighted in Figure 9 are known as the xanthophyll cycle and entail the de-epoxidation and epoxidation of the xanthophylls: zeaxanthin, antheraxanthin and violaxanthin (Demmig-Adams, 1990). These interconversions are catalysed by the enzymes zeaxanthin epoxidase and violaxanthin de-epoxidase localised at opposite sides of the thylakoid membrane. The xanthophyll cycle is involved in the quenching of excess radiation, and changes in the pH within the thylakoid membrane facilitate these interconversions in the course of minutes, or days (Demmig-Adams & Adams, 1996).

2.4.7 Chlorophyll functions

The chlorophylls are the main photoreceptors in photosynthesis, absorbing blue and red light in the 430 - 660 nm region (Taiz & Zeiger, 1998). The absorption of electromagnetic radiation by these pigments varies with wavelength, with strong absorption in the blue (400 - 500 nm) and red (600 - 700 nm) portions of the visible spectrum and less absorption in the green (500 - 600 nm) portion. Chlorophyll *a* shows shifts in the red spectral region as a consequence of dimer and trimer formation of the molecule and due to its association with thylakoid proteins.

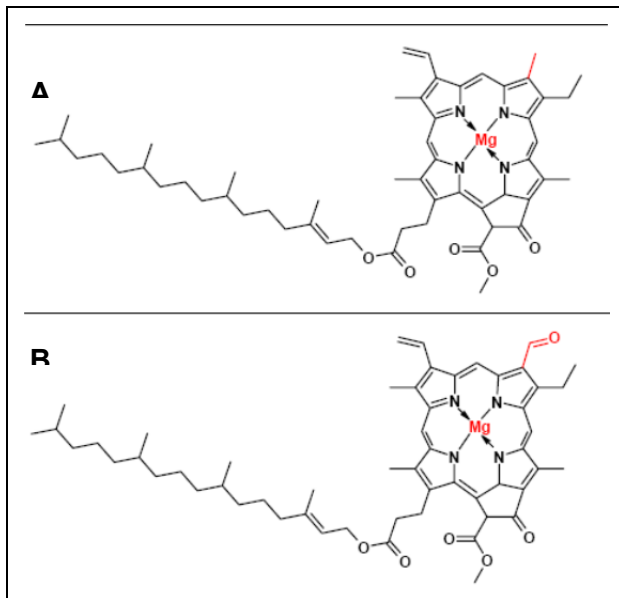


Figure 7 The structure of chlorophyll *a* and chlorophyll *b* (Schoefs & Franck, 2003).

2.4.8 Carotenoid functions

Carotenoids represent about 25% of the total photosynthetic pigment pool in leaves (Demmig-Adams, 1990) and are red, orange, and yellow lipid-soluble pigments embedded in the membranes of chloroplasts and chromoplasts. Initially, their colours are masked by chlorophyll, but in late stages of plant phenology (senescence) they contribute to the bright colours of many leaves, flowers, fruits and roots.

Carotenoids have the main functions of light harvesting, photoprotection, maintaining structural integrity in pigment-protein complexes, as well as acting as precursors to biochemical constituents important to plants.

2.4.8.1 Light harvesting

Carotenoids can contribute to light harvesting in the blue-green (380 - 500 nm) region of the electromagnetic spectrum, with most photosynthesis at 510 nm resulting from absorption by certain carotenoids (Havaux *et al.*, 1998). Light energy absorbed by the carotenoids is transferred to the chlorophylls (Gradinaru *et al.*, 2000). During photosynthesis the xanthophylls namely lutein, violaxanthin, neoxanthin and to a lesser extent β -carotene operates as accessory light harvesting pigments. The function of light harvesting by carotenes have however been questioned by (Demmig-Adams *et al.*, 1996), noting the low levels of β -carotene and lutein when chlorophyll concentrations are low in shaded leaves, which is not expected from light collecting pigments. Zeaxanthin is primarily responsible for the dissipation of excess light energy in the form of heat *via* the xanthophyll cycle, whereas β -carotene is an important antioxidant. At low light intensity when

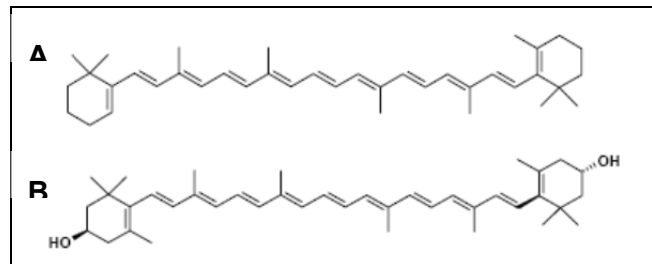


Figure 8 The structure of **A**: β -carotene **B**: Zeaxanthin (Sajilata *et al.*, 2008).

all photons are captured by photosynthesis, no zeaxanthin will be formed in leaves (Demmig-Adams & Adams, 1992).

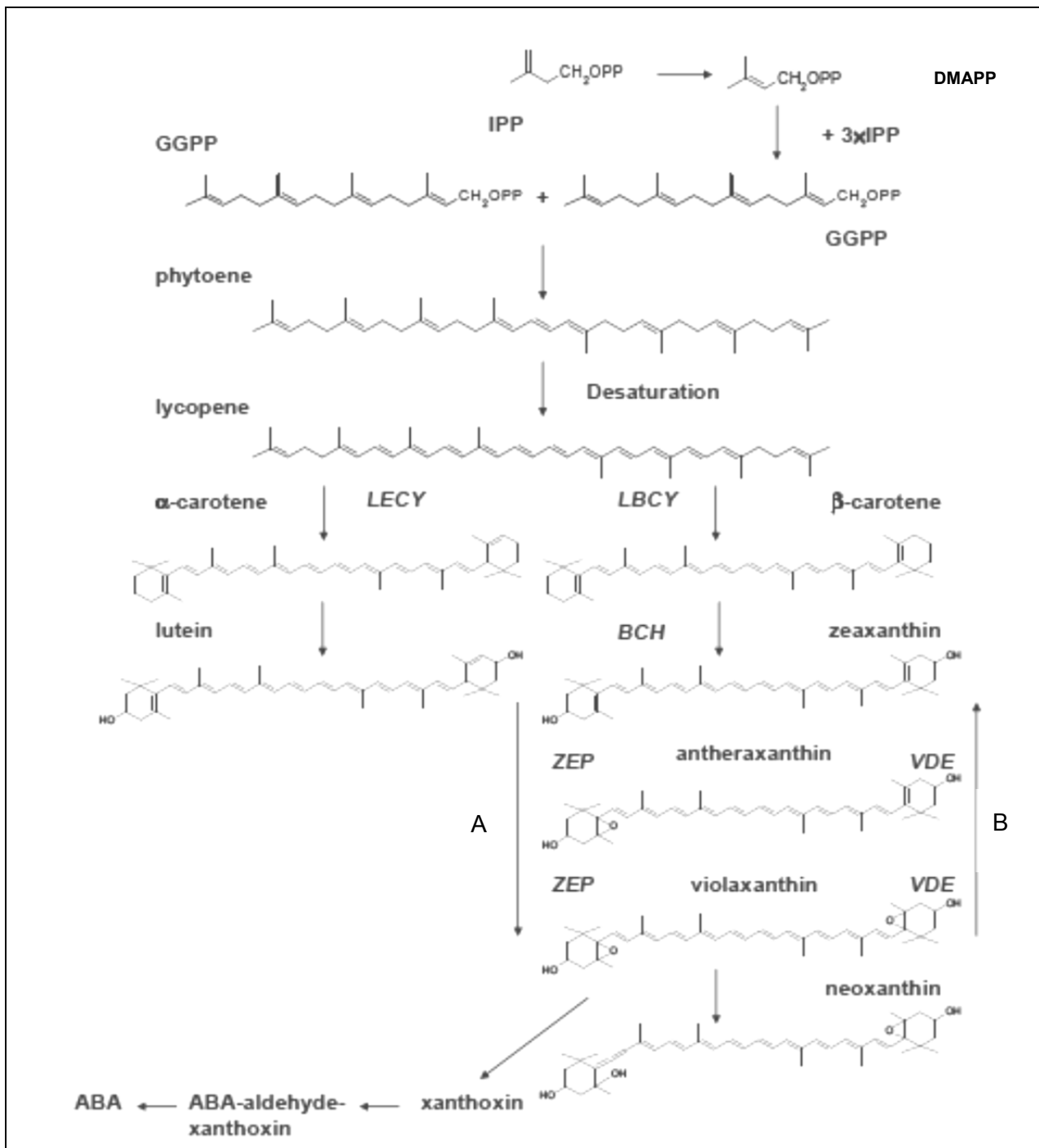


Figure 9 The carotenoid biosynthesis pathway in plants. IPP, isopentenyl diphosphate; GGPP, geranylgeranyl pyrophosphate; DMAPP, dimethylallyl diphosphate; LECY, lycopene ε-cyclase; LBCY, lycopene β-cyclase; BCH, β-carotene hydroxylase; ZEP, zeaxanthin epoxidase; VDE, violaxanthin de-epoxidase; ABA, abscisic acid. A: Epoxidation under limiting light (hours to days) B: De-epoxidation under excess light (within minutes) (Demmig-Adams, 1990; Demmig-Adams & Adams, 1996; Lichtenthaler *et al.*, 1997; Hirschberg, 2001).

2.4.8.2 Photoprotection

The protective function of carotenoids exists at two levels. Firstly, β-carotene acts to protect photosystems against photo-oxidative damage by quenching the excitation energy of triplet chlorophyll, which can form a toxic element, namely singlet oxygen (Demmig-Adams *et al.*, 1996).

Secondly, the xanthophyll cycle in thylakoid membranes involves the de-epoxidation of the light-harvesting carotenoid violaxanthin to zeaxanthin *via* antheraxanthin during stress conditions (Figure 9 and Figure 10). These enzymatic reactions are connected to the thermal dissipation of excess light energy within light harvesting antenna proteins, which can be measured as the non-photochemical quenching (NPQ) of chlorophyll fluorescence. Light energy reaching the chloroplasts is used to drive photosynthetic electron flow (Liakopoulos *et al.*, 2006) and when the photosynthetic compounds become light saturated, excess radiation may be dissipated by several biochemical mechanisms, among which the dissipation of excess energy as heat through the xanthophyll cycle is considered to be the most important photoprotective feature of leaves (Demmig-Adams & Adams, 1992). In *Vitis vinifera* L. leaves, thermal energy dissipation by the xanthophyll cycle accounts for almost all NPQ (Chaumont *et al.*, 1997), dissipating approximately 45 – 64% of the absorbed light energy under non-stressful environmental conditions, while under stress this may rise to 75 – 92%. Hendrickson *et al.* (2004b) showed that the de-epoxidation state of the xanthophyll cycle pigment pool (DEPS) can rise to relatively high levels (about 0.73) for grapevines illuminated under low temperatures. It is suggested that the xanthophyll cycle may become inadequate to dissipate absorbed energy when high irradiance is combined with other unfavourable factors, such as drought (Liakopoulos *et al.*, 2006). This may be one of the main factors involved in photodamage and leaf pigment degradation during the latter stages of grape ripening.

The levels of zeaxanthin in leaves were shown to be highly positively correlated to NPQ, and this relationship was species-independent (Demmig-Adams & Adams, 1996). It was also previously observed in field-grown, high light acclimated grapevines (Chaumont *et al.*, 1997; Flexas *et al.*, 2001). Chen & Cheng (2003) showed Fv/Fm (the maximum quantum efficiency of PSII primary photochemistry) to be negatively correlated with the zeaxanthin content of leaves. Efficient photoprotection of chlorophylls by carotenoids requires that these pigments are in close proximity and in a rigid environment, supplied by the pigment-protein complexes in PSI, PSII and the light harvesting complexes (Schoefs & Franck, 2003). The presence of the pigments in these structures also causes the spectral shifts observed between *in vivo* and extracted (*in vitro*) absorption spectra.

2.4.8.3 Structural roles of carotenoids

Carotenoids can have structural roles in the pigment-protein complexes, stabilising the photosynthetic components and lending these complexes its specific light absorption characteristics (Havaux, 1998). Without carotenoids these complexes cannot function properly.

2.4.8.4 Precursors of biochemical compounds

The carotenoids neoxanthin and violaxanthin are precursors of abscisic acid (ABA), a plant hormone participating in stomatal control and other physiological processes (Giuliano *et al.*, 2003; Peñuelas & Munné-Bosch, 2005). In *Arabidopsis*, ABA biosynthesis in response to stress occurred mainly *via* neoxanthin isomer precursors (North *et al.*, 2007). It is also known that carotenoids are precursors of aroma compounds (C₁₃-norisoprenoids) in grapes (Marais, 1992; Baumes *et al.*, 2002).

2.4.9 General physiological considerations (photo-protection)

The fraction of photosynthetically active radiation (PAR) absorbed by a plant canopy has previously been related to net primary productivity as a function of a light use efficiency (LUE) coefficient, which was defined as the carbon fixed per unit radiation intercepted (Blackburn, 2007). Such studies assume that each pigment has equal contribution to photosynthesis, but this may be flawed due to the underestimation of the contribution of accessory pigments such as chlorophyll b and carotenoids. Plants may therefore have varying photosynthetic potential, even if they are intercepting the same amounts of PAR, depending on accessory pigment contents unique to the species and environment in which it grows. As mentioned earlier, with interception of excess radiation, carotenoids in the xanthophyll cycle can dissipate excess energy and protect the reaction centres.

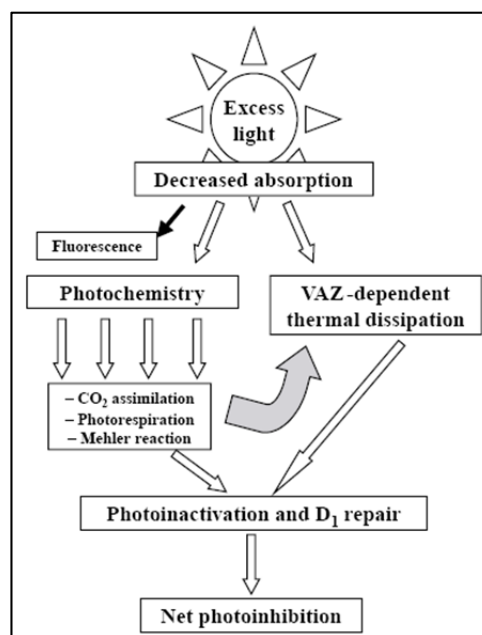


Figure 10 Energy dissipation mechanisms and photo-inactivation/photo-inhibition (Medrano *et al.* (2002).

Most photo-protective and photosynthetic responses to light follow a logarithmic pattern, with a higher response in the initial part of the curve (Sánchez-de-Miguel *et al.*, 2005). This implicates that in shade conditions small changes in irradiance may induce dramatic adjustments in the pools of photoprotective compounds (García-Plazaola *et al.*, 2008). This was confirmed in a study where functional PSII units were measured by flash-induced oxygen evolution, finding that the susceptibility of PSII to photo-inactivation was less in sun-exposed leaves than in shade leaves of *Vitis riparia* Michaux (an American rootstock variety) (Flexas *et al.*, 2001). It also corresponds to the general observation that plants that are acclimated to low light are more easily photo-inactivated. According to Flexas *et al.* (2001) photo-inactivation of a certain part of the PSII reaction centres during the day may be unavoidable, but may not affect light-saturation, of photosynthetic rates; it may rather contribute to photo-protection of remaining active photo-centres.

2.4.10 Chlorophyll *a:b* ratio and light interception

The chlorophyll *a:b* ratio is inversely proportional to the antenna size in the photosynthetic apparatus and an indicator of the PSII core complex relative to the light harvesting complex (LHC) ratio, considering that the latter has a lower chlorophyll *a:b* ratio (Lambers *et al.*, 1998; García-Plazaola *et al.*, 2008). It has been shown to increase with the onset of leaf fall, while chlorophyll content decrease, and also to respond greatly to changes in irradiance, suggesting a high adaptability in the structure of the photosynthetic apparatus of certain plants (García-Plazaola *et al.*, 2008). Besides the ratio decreasing during senescence, it also tends to decrease with decreasing light availability (Sanger, 1971; Castro & Sanchez-Azofeifa, 2008).

Photosystem I contains more chlorophyll *a* than chlorophyll *b* and therefore has a higher chlorophyll *a:b* ratio than PSII. The light harvesting complex II (LHCII) contains about half of the total chlorophyll and almost all the total chlorophyll *b* content of mature thylakoid membranes. The

chlorophyll *a:b* molar ratio in the LHCII for various higher plants is about 1.2, whereas in all other pigment-protein complexes the value of this ratio is much higher (Lambers *et al.*, 1998). A large change in the LHCII content must therefore be reflected in the chlorophyll *a:b* molar ratio and *vice versa*, and a substantial decrease in the chlorophyll *a:b* must be linked to accumulation in LHCII. This molar ratio therefore serves as an indicator of the LHCII content of photosynthetic membranes (Busheva *et al.*, 1991).

There appears to be a similarity in the response of chlorophyll *a:b* ratios to changing light spectral composition around the leaf, within a plant canopy and even within the leaf, suggesting a relationship between higher chlorophyll *b* (predominantly associated with PSII) in the shade leaf and increase in the absorption of red *versus* far-red light where a lower R:FR (675 - 680 nm :700 - 730 nm) prevails, as a mechanism of adaptation (Lei *et al.*, 1996).

2.5 Leaf pigment content and interrelations

2.5.1 Chlorophyll content and pigment ratios in grapevine leaves

Depending on the conditions in the study as well as the cultivar studied, and possibly also the method of pigment extraction, different ranges of total chlorophyll or chlorophyll *a:b* ratios have been reported in literature (Table 2).

Table 2 Typical chlorophyll ranges and ratios found in grapevine and some other species' leaves

Photosynthetic pigments	General ranges	References
Total chlorophyll	0.03-0.05 mg.cm ⁻² (young and mature leaves respectively)	Bertamini & Nedunchezian (2003)
	0.04-0.06 mg.cm ⁻² (600-800 ng.mg ⁻¹ FM) (converted using TSLM of 0.07 mg.cm ⁻²)	Hunter & Visser (1989)
	0.05-0.08 mg.cm ⁻²	Renzullo <i>et al.</i> (2006)
	Cabernet Sauvignon (field) – 0.08 mg.cm ⁻² (1160 ng.mg ⁻¹ FM) Shiraz (glasshouse) – 0.05 mg.cm ⁻² (700 ng.mg ⁻¹ FM) Pinot noir (field) – 0.17 mg.cm ⁻² (2400 ng.mg ⁻¹ FM)	Blanchfield <i>et al.</i> (2006)
Chlorophyll <i>a:b</i> ratio	2.3-3.5 (also other plant species)	Demmig-Adams (1998) Lichtenthaler & Burkart (1999) Bertamini & Nedunchezian (2003)
	Cabernet Sauvignon (field) – 2.0 - 2.5 Cabernet Sauvignon (field) – 2.0 Pinot noir (field) – 2.8	Hunter & Visser (1989) Blanchfield <i>et al.</i> (2006) Blanchfield <i>et al.</i> (2006)

2.5.2 Carotenoid and xanthophyll pigment relations in leaves

Similar to the ranges and ratios reported for chlorophylls, different ranges of total carotenoids, xanthophylls and ratios thereof have also been reported in literature (Table 3). According to Biswal (1995) the composition of carotenoids, particularly xanthophylls of different domains of the thylakoid membranes, may vary both qualitatively and quantitatively depending on light intensity, environmental factors and leaf physiology. A constant linear relationship of β -carotene to chlorophyll *a* found in a study by Eskins *et al.* (1982) showed that the P700 chlorophyll *a* protein

complex (CPI) comprised a steady percentage (approximately 13%) of the total chlorophyll during development while the P680 chlorophyll *a* protein complex (CPII) increased. The presence of lutein in the PSII reaction centre protein as well as in CPII and the PSI complex makes it difficult to predict its relationship to chlorophyll *a* during development (Eskins *et al.*, 1982).

In Griffith *et al.* (1944) the average ratio by weight of total chlorophyll to carotene of all varieties studied was 19.75, which is very close to what may be expected if nine molecules of chlorophyll *a* and three molecules of chlorophyll *b* were associated in the same protein group with one molecule of carotene.

Other studies that investigated the distribution of β -carotene and xanthophylls with respect to chlorophyll *a* and *b* in different fractions found a linear relationship of chlorophyll *b* with lutein and neoxanthin, which confirms the association of the xanthophylls with the light harvesting pigment complexes (Biswal, 1995). As in Eskins *et al.* (1982) a direct relation was shown between β -carotene and chlorophyll *a*, suggesting localisation of carotenes in the reaction centre of photosystems. Violaxanthin was shown to be uniformly distributed over the surface of thylakoids irrespective of variations in the chlorophyll *a:b* ratio.

With exception of the nonlinear relationship for violaxanthin, Eskins & Banks (1979) reported a significant linear correlation between individual accessory pigments and chlorophyll *a*, which was independent of genotype, light conditions and leaf age. Plotted against chlorophyll *a*, the extrapolated lines of β -carotene and lutein suggest that they exist prior to formation of chlorophylls *a* and *b*. The linear relation between chlorophyll *a* and neoxanthin was shown to be most consistent (Eskins *et al.*, 1982).

Table 3 Carotenoid content and ratios in plant leaves (as determined from HPLC measurements).

Formula	Significance	Common ranges	References
Total carotenoids		Cabernet Sauvignon (glasshouse) – 0.07 mg.cm ⁻² (995 ng.mg ⁻¹ FM) Shiraz (glasshouse) – 0.05 mg.cm ⁻² (660 ng.mg ⁻¹ FM)	Blanchfield <i>et al.</i> (2006)
XPS = (V+A+Z) or (V+A+Z)/total chlorophyll or (V+A+Z)/total carotenoids	Xanthophyll pool size. Indicates level of photoprotection and energy dissipation.	Different plant species and conditions – (78-151 mmol.mol ⁻¹)	Demmig-Adams & Adams (1992) Bertamini & Nedunchezian (2003) García-Plazaola <i>et al.</i> (2008)
		Cabernet Sauvignon (field) – 0.17 Pinot noir (field) – 0.07	Blanchfield <i>et al.</i> (2006) (VAZ/chl)
		134 mmol.mol ⁻¹ (average of field and glasshouse leaves)	Hendrickson <i>et al.</i> (2004b)
CPS = (XPS + β-carotene + lutein) in mmol.mol ⁻¹ chlorophyll	Carotenoid pool size / total chlorophyll	470-494 mmol.mol ⁻¹ total chlorophyll	Hendrickson <i>et al.</i> (2004b)
		481-601 mmol.mol ⁻¹ total chlorophyll	Bertamini & Nedunchezian (2003)
Carotenoid:chlorophyll ratio		Cabernet Sauvignon (field) – 0.45 Pinot noir (field) – 0.29	Blanchfield <i>et al.</i> (2006)
$DEPS = \frac{[A] + [Z]}{[V] + [A] + [Z]}$	Relative de-epoxidation state of the xanthophyll cycle pigment pool. (Note: some authors use 0.5 [A])	0.73 (high light)	Hendrickson <i>et al.</i> (2004b) Demmig-Adams & Adams (1992); Demmig-Adams & Adams (1996) Medrano <i>et al.</i> (2002)
Individual xanthophylls / CPS	Xanthophylls expressed relative to CPS	Neoxanthin 12% Lutein 38% β-Carotene 22% V+A+Z – 27.6%	Hendrickson <i>et al.</i> (2004b)

2.6 Viticultural and ecophysiological effects on leaf pigments

2.6.1 Grapevine leaf ageing and physiology

Leaf age can affect stomatal rhythm, leaf morphology, light absorbance as well as the biochemical composition of leaves (Sánchez-de-Miguel *et al.*, 2005). Leaf development in grapevines follow a well-defined sequence of emergence, unfolding, rapid lamina expansion, and eventually senescence and abscission (Kriedemann *et al.*, 1970). Grapevine leaves normally take from 30 to 40 days to reach full expansion (Kriedemann, 1968; Kriedemann *et al.*, 1970). An obvious “break” in chlorophyll content and other parameters was found for leaves transitioning from rapid expansion to the so-called “hardening phase” of development (between 50 and 100 cm² leaf area for Sultanina). Kriedemann (1968) also observed that older leaves take longer to reach maximum photosynthetic rate, compared to only a few minutes needed in young leaves. Poni *et al.* (1994b) showed a peak in assimilation rate (photosynthetic rate relative to the total chlorophyll per unit of leaf area) with a subsequent, gradual decline starting at 50-55 days leaf age. The assimilation rate was previously also related to the ratio of photosynthesis to absorbed light by Thayer & Bjorkman (1990). Photosynthetic activity decreased in aged leaves while chlorophyll concentrations continued to increase (Kriedemann, 1968) or decreased slightly (Kriedemann *et al.*, 1970) after full leaf expansion. Poni *et al.* (1994b) also showed that leaf chlorophyll content on a leaf area basis increased with photosynthesis during leaf expansion, but unlike the progressive photosynthesis decline thereafter, continued to increase beyond attainment of full leaf size. It was suggested that the chlorophyll-photosynthesis relationship is over-simplified and exist only for interior canopy, mature leaves under lower light conditions. It also has to be questioned whether it is optimal to express chlorophyll content on a leaf area basis, when leaf thickness increase substantially with ageing. Several factors other than chlorophyll concentration may have effects on photosynthesis, such as temperature, leaf morphological attributes and leaf age. Candolfi-Vasconcelos *et al.* (1994) reported an increase of photosynthesis with the onset of fruit maturation, which indicates that the source strength can also be sink-regulated.

2.6.1.1 Leaf age and pigment content/ratios

During the initial expansion phase, the chlorophyll content of grapevine leaves remained the same and photosynthesis increased sharply, which may be attributed to more intercellular air spaces as leaves age, offering less resistance to CO₂ assimilation (Kriedemann *et al.*, 1970). Poni *et al.* (1994b) showed chlorophyll content (leaf area basis) of leaves to be constant between bloom and véraison, reaching maximum values around harvest and dropping sharply after harvest. The chlorophyll content per leaf area in young apical leaves was significantly lower than basal and median leaves until véraison; thereafter, it increased sharply for mature apical leaves to reach the highest at the end of season as compared to median leaves. The plot of chlorophyll content against leaf age showed a peak at 70-80 days leaf age and a consistent decline after about 120 days leaf age. Other studies also confirmed chlorophyll a levels to be lower in older leaves (Hunter & Visser, 1989; Bertamini & Nedunchezian, 2002) (Table 4), with total carotenoids shown to be marginally less in older grapevine leaves (Steel & Keller, 2000).

Table 4 Properties of young, mature and senescing plant leaves.

Pigment/ratio	Young leaves	Mature leaves	Senescing leaves
Total chlorophyll	Lower on a leaf area basis (Bertamini & Nedunchezian, 2003) as well as on a leaf mass basis (Hunter & Visser, 1989)	Higher (Bertamini & Nedunchezian, 2003)	Lower on a mass basis (bunch leaves) at ripeness (Hunter & Visser, 1989)
Chlorophyll <i>a:b</i> ratio	No difference (Bertamini & Nedunchezian, 2003), higher (Lashbrooke <i>et al.</i> , 2010)	Lower chlorophyll <i>a</i> (Hunter & Visser, 1989)	Decreased (Hunter & Visser, 1989)
Carotenoid/chlorophyll	Higher (Bertamini & Nedunchezian, 2003)	Lower (Bertamini & Nedunchezian, 2003)	
XPS/chlorophyll	Higher (Bertamini & Nedunchezian, 2003)	Lower (Bertamini & Nedunchezian, 2003)	
DEPS	Higher (Lashbrooke <i>et al.</i> , 2010)	Lower (Lashbrooke <i>et al.</i> , 2010)	
Absorbance (visible radiation)	About 9% lower in young leaves (Bertamini & Nedunchezian, 2003)	Higher (Bertamini & Nedunchezian, 2003)	Lower (Demarez <i>et al.</i> , 1999)
Xanthophylls	Less lutein (Eskins & Banks, 1979)	Less violaxanthin, more lutein (Eskins & Banks, 1979)	

A higher susceptibility to photoinhibition was shown in younger leaves, apparently due to irradiance resulting in more excitation of chlorophylls due to their lower chlorophyll content per unit leaf area, therefore young leaves experience relatively more light stress (Bertamini & Nedunchezian, 2003). The author suggested different degrees of PSII inhibition in high light conditions dependent on leaf age. The chlorophyll *a:b* ratio was found to be similar between young and mature grapevine leaves, indicating that the photosynthetic apparatus was already fully developed in the young leaves. However, young leaves had a higher ratio of total carotenoids:chlorophyll as well as a higher xanthophyll pool size (XPS) relative to total chlorophyll (Bertamini & Nedunchezian, 2003).

More mature leaves of soybean and peanut showed less violaxanthin, with higher lutein levels (Eskins & Banks, 1979). A decrease in the chlorophyll *a:b* ratio corresponded to increases in chlorophyll *b* and neoxanthin and decreases in lutein, β -carotene and violaxanthin. The decrease in chlorophyll *a:b* ratio is associated with formation of grana from unstacked thylakoids (Eskins & Banks, 1979). We found in an earlier study that both the DEPS and chlorophyll *a:b* ratio showed an inverse correlation with leaf age, with older leaves also containing more lutein (Lashbrooke *et al.*, 2010). Higher chlorophyll *a:b* ratios correlate to increased photosynthetic activity in the younger, more exposed leaves (Lichtenthaler *et al.*, 1981). These leaves generally exhibit a higher DEPS value indicative of a shift in the xanthophyll cycle to zeaxanthin resulting in increased photoprotection.

2.6.1.2 Leaf senescence and pigment degradation

Senescence of leaves can be defined as a series of changes in the metabolism of mature plant organs, which include net protein breakdown, chlorophyll degradation, and death (Hill, 1980). Chlorophyll decrease cannot be seen as a reliable indicator of senescence, as it occurs only late in the process. Leaves senesce when demands of sinks for nutrients are expected to be high, therefore both nutrient starvation and hormonal changes have been suggested as causes of senescence (Hill, 1980). It has been proposed that fruit sink strength between véraison and harvest can delay or advance maturity of leaves (Sánchez-de-Miguel *et al.*, 2005). Environmental stimuli, such as low light, nutrient deficiencies and water stress can also attribute to senescence of leaves. Deficiency of mobile nutrients (N, P and K) generally advances senescence symptoms in older leaves, which can in turn lead to remobilisation of nutrients to the plant (Hill, 1980). During senescence and leaf yellowing, protein and nitrogen-containing compounds in chloroplasts are broken down, and ammonium ions are bound into glutamine and asparagine to prevent ammonium toxicity (Salisbury & Ross, 1978). Re-translocation of mineral nutrients from older leaves towards younger organs, as well as limitation of water use by older, senescing leaves are processes integrated with plant survival under difficult conditions (Munné-Bosch & Alegre, 2004). Poni *et al.* (1994b) reported that a possible remobilization of nitrogen occurred at a leaf age of about 50 - 55 days after unfolding, when the photosynthetic activity of these leaves was also suboptimal, and when chlorophyll has started to decline. This observation was based on the increase in nitrogen contents of younger leaves after véraison, in contrast with strongly decreasing levels in the older leaves, but it was not confirmed with translocation studies. .

Several oxidative cleavage reactions of carotenoids are known; this is important when for instance epoxy-carotenoids such as violaxanthin and neoxanthin breakdown initiate the synthesis of ABA (Giuliano *et al.*, 2003). In general, chlorophylls are susceptible to both chemical and enzymatic degradation. Weak acids, light, heat and oxygen can accelerate degradation, with a possible involvement of processes related to pheophytin formation, epimerization, and pyrolysis of chlorophyll. In terms of light damage, hydroxylation, oxidation or photo-oxidation, are the major chemical degradation routes. Chlorophylls *a* and *b* can readily be converted to pheophytin *a* or *b*, respectively, by adding a weak acid, which leads to replacement of the central magnesium atom by hydrogen (Lorenzen, 1967). Uncertainty exists about different enzymes involved and the order of the reactions and products formed in chlorophyll catabolism. According to Eckhardt *et al.* (2004) the first step of chlorophyll breakdown is the removal of the hydrophobic phytol chain catalysed by chlorophyllase, forming chlorophyllide, after which magnesium-dechelatase catalyses the release of the central magnesium atom to form pheophorbide (pheide). Hörtensteiner (2006) views chlorophyll degradation as a detoxification mechanism during senescence and outlines four steps of degradation: i) formation of a primary fluorescent tetrapyrrole intermediate, ii) species-specific modification of tetrapyrrole side chains iii) excretion of fluorescent catabolites into the vacuole, and iv) non-enzymatic tautomerization to the final non-fluorescent catabolites.

Some authors observed striking increases in chlorophyll *a:b* for five progressive stages of senescence of aspen leaves, a phenomenon not previously recorded among deciduous tree species, and possibly linked to earlier structural loss of grana lamellae compared to stroma lamellae (Castro & Sanchez-Azofeifa, 2008). A decline in the chlorophyll *a:b* ratio and the total chlorophyll:total carotenoid ratio (or increase in car:chl) suggests preferential loss of chlorophyll *a* containing proteins closely associated with the reaction centres over loss of light harvesting complex proteins (Lichtenthaler, 1987; Rosenthal & Camm, 1997). Bricker & Newman (1982) suggested the earlier structural loss of the chloroplast stroma lamellae (with PSI and most

chlorophyll *a*) compared to grana lamellae (PSII), which may explain a reduction in the chlorophyll *a:b* ratio observed during senescence.

Chlorophyll degradation would have been the process most likely to be affected by cytokinins (as it is known to inhibit senescence in leaves) but it was not the case in a study by Poni *et al.* (1994b). This result also confirms that exogenous cytokinins applied to intact organs kept under high light may not interact with leaf senescence. Studies under controlled environments have shown that light can entirely substitute cytokinins in preventing or retarding leaf senescence. The effect of cytokinins in reversing, or delaying, senescence in detached leaves and leaf pieces was however not observed in whole plants (Herold, 1980).

During the grape ripening period, the leaves close to the bunches are already undergoing senescence, and contribute little to canopy photosynthesis (Candolfi-Vasconcelos *et al.*, 1994). In Hunter *et al.* (1994) apical leaves on shoots were shown to contribute uniformly to photosynthesis throughout the season, with basal leaves showing a sharp decrease post-veraison and then retaining constant levels. This was also shown by Kriedemann *et al.* (1970). This retention is important to ensure sufficient carbohydrate contribution to the bunches during ripening and reserve accumulation in the vine post-harvest. Schultz (1993) observed a slower decline in photosynthetic activity after maximum assimilation was reached in his field study compared to glasshouse studies, with a decline starting only at about LPI 30. Leaf chlorophyll content started to decline after about 45 days after unfolding (which could be slightly earlier than the measurement of leaf age using the plastochron concept) (Kriedemann *et al.*, 1970) or only after 70 - 80 days leaf age (Poni *et al.*, 1994b). Some evidence exists that leaves could show retarded senescence and/or abscission in reaction to changed (lower) source:sink ratios or microclimate change (increased exposure) (Candolfi-Vasconcelos & Koblet, 1990; Poni & Giachino, 2000).

2.6.2 Microclimate effects on leaf structure/physiology

Some possible effects of leaf/canopy microclimate on leaf structure are shown in (Table 5). According to several authors (Kim *et al.*, 1993; Dietzel & Pfannschmidt, 2008; Ruban, 2009) shade plants grown under far-red enriched light may have a higher PSII/PSI ratio to compensate for the reduction in the amount of red light. Enrichment of far-red wavelengths observed in shaded conditions preferentially excites PSI, leading to a redox imbalance between the photosystems and oxidation of the PQ-pool. In this way a signal is generated, which leads to an adjustment of photosystem stoichiometry, thylakoid structure and metabolism. When pea and barley plants were irradiated with light believed to be preferentially absorbed by PSI (far-red light), the apparent light harvesting capacity of PSII increased, whilst that of PSI appeared to decrease (the PSII:PSI ratio increased) (Kim *et al.*, 1993).

2.6.3 Leaf/canopy microclimate effects on pigments

Grapevines have a strong capacity to compensate for a loss in leaf area in terms of photosynthetic efficiency (Hunter & Visser, 1988; Candolfi-Vasconcelos *et al.*, 1994). Grapevine leaves present in low light conditions are able to adapt and enhance its ability to utilise light in the canopy, which is also visible from the positive and significant correlation between the specific leaf mass (SLM) and photosynthesis (Cartechini & Palliotti, 1995). The SLM, and the leaf volume, density, and thickness are reduced with increased shading, leading to reduced light compensation points and dark respiration rates (Van den Heuvel *et al.*, 2004; Reynolds & Vanden Heuvel, 2009).

Leaves developing in or transferred to high light conditions develop larger pools of violaxanthin, antheraxanthin and zeaxanthin (all derived from β -carotene) relative to those developing in the

shade (Thayer & Bjorkman, 1990; Demmig-Adams & Adams, 1992). The xanthophyll pool size was also found to be significantly different between sun and shade leaves in a study by Demmig-Adams & Adams (1992) (Table 5).

Total carotenoid content of mature leaves was found to be less in grapevines grown under a UV screen (Steel & Keller, 2000). Levels of β -carotene were found to be lower in leaves growing in shaded conditions, and for sun-exposed leaves, the highest levels of lutein (derived from α -carotene) were found for leaves with the lowest photosynthetic rates, but this result may have been strongly affected by species differences in carotenoid composition (Demmig-Adams & Adams, 1992).

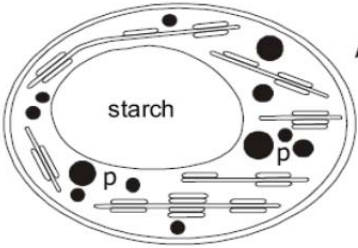
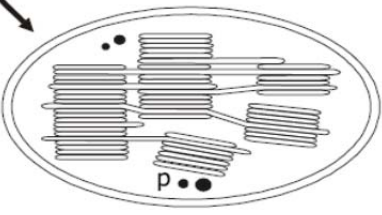
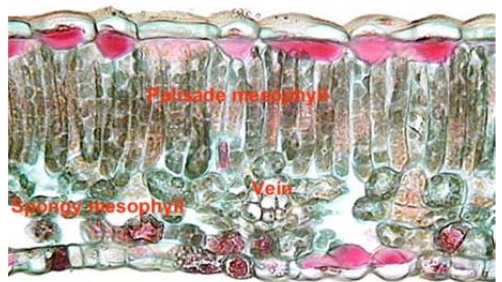
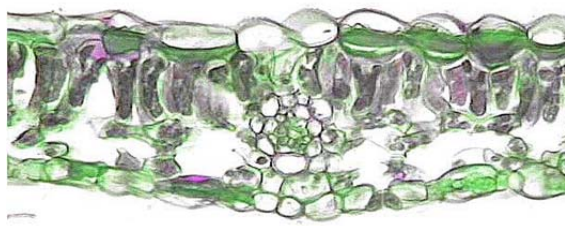
The discrepancies found in literature between total chlorophyll (or carotenoid) values are likely due to the effect of specific leaf mass. After extraction, pigments are derived from spectrophotometric equations on a mass per volume basis, which have to be converted to either pigment mass per area or pigment mass per dry or fresh leaf mass. In the case of pigment mass per area measurements, leaf specific mass and therefore thickness is not accounted for, and in the case of pigments expressed on a leaf DM or FM basis, the SLM has an important potential effect on the result. About half of the differences in pigment concentration of dark and burley tobaccos studied by Griffith *et al.* (1944) was attributed to differences in leaf thickness.

It seems that chlorophyll content, but not antenna size, acclimated to high light in grapevines, with a decrease in leaf chlorophyll not leading to significant leaf absorbance changes (Medrano *et al.*, 2002). Leaf absorbance was found in another study to only change significantly in very young or old leaves (Schultz, 1996).

Medrano *et al.* (2002) found no significant cultivar, time of season or drought stress effects on chlorophyll or total carotenoid content of leaves. The measurements were however performed only on a leaf area basis and effects of leaf thickness on the results can therefore not be excluded. They however reported a higher violaxanthin, antheraxanthin and zeaxanthin pool for Manto Negro, at the expense of β -carotene.

In the study by Castro & Sanchez-Azofeifa (2008) different species were not consistent regarding chlorophyll *a:b* ratios, as shade leaves of one of the species had consistently higher ratios, whereas for the others sun-exposed leaves showed higher values. Most studies have however shown a tendency for the chlorophyll *a:b* ratio to decrease in shade conditions.

Table 5 Comparison between sun and shade type chloroplasts and pigment composition [adapted from (Lambers *et al.*, 1998; Lichtenthaler & Burkart, 1999)]. Sun and shade leaf images from <http://lima.osu.edu/biology/images/>).

<p>Proplastid ↓ Etioplast</p> <div style="display: flex; justify-content: space-around;"> <div style="text-align: center;"> <p><i>sun, high light, blue light, kinetin</i></p>  </div> <div style="text-align: center;"> <p><i>shade, low light, red light, photosystem II-herbicides</i></p>  </div> </div>	
<p>Sun-type chloroplast</p> <ul style="list-style-type: none"> • Less thylakoids per chloroplast section <ul style="list-style-type: none"> • Narrow grana stacks • Few thylakoids per granum • Low stacking degree • More exposed chloroplast membranes • Higher proportion of Chl a-proteins CPI (P700 chlorophyll a protein complex) <ul style="list-style-type: none"> • Large starch grains • Many and large plastoglobuli • High rates of net CO₂ assimilation • Light saturation of photosynthesis at a high photon flux density 	<p>Shade type chloroplast</p> <ul style="list-style-type: none"> • High thylakoid frequency per chloroplast section <ul style="list-style-type: none"> • Broad grana stacks • Very high grana stacks • High stacking degree • More oppressed thylakoids • Higher amounts of light-harvesting chlorophyll a/b -proteins, predominantly chlorophyll b <ul style="list-style-type: none"> • No starch • Few small plastoglobuli • Low rates of net CO₂ assimilation • Early light saturation of photosynthesis
	
<p>Sun-acclimated leaves</p> <ul style="list-style-type: none"> • Higher SLM, thicker leaves, especially palisade parenchyma • High stomatal density (Lichtenthaler <i>et al.</i>, 2007)/ chloroplasts per leaf area. <ul style="list-style-type: none"> • Smaller leaf surface area • Greater leaf width (Gausman, 1984) • Thicker and/or multi-layered palisade mesophyll (Terashima <i>et al.</i>, 2006) • More dense mesophyll structure (Gamon & Surfus, 1999) • Higher light-saturated photosynthetic rates. • Smaller PSI and PSII antenna size (Ruban, 2009) and higher PSII per unit leaf area (Flexas <i>et al.</i>, 2001) 	<p>Shade acclimated leaves</p> <ul style="list-style-type: none"> • Lower SLM, thinner leaves <ul style="list-style-type: none"> • Lower stomatal density / chloroplasts per leaf area • Similar amounts of PSII to sun-acclimated leaves (due to higher chlorophyll and constant PSII/chl) (Flexas <i>et al.</i>, 2001) • Larger percent intercellular space (Castro & Sanchez-Azofeifa, 2008) • Relative higher amounts of spongy mesophyll (Lambers <i>et al.</i>, 1998) • Higher leaf light absorbance due to more internal light scattering (Vogelman <i>et al.</i>, 1996)

Pigment effects	
Total chlorophyll	
<ul style="list-style-type: none"> • Less on area basis (Demmig-Adams, 1998) (this result may also be influenced due to wide variety of species investigated). • More on an area basis (Flexas <i>et al.</i>, 2001; Lichtenthaler <i>et al.</i>, 2007), seem to be specific only for shade-tolerant plant species (Lambers <i>et al.</i>, 1998; Souza & Válio, 2003) • Lower chlorophyll concentration (on a mass basis or per chloroplast) (Gausman, 1984; Lichtenthaler & Burkart, 1999) 	<ul style="list-style-type: none"> • Increase in chlorophyll on a mass basis (an important adaptation in shade plants) (Lei <i>et al.</i>, 1996) • Less on an area basis (Flexas <i>et al.</i>, 2001) • During whole-vine shading experiments, Cartechini & Palliotti (1995) found leaf total chlorophyll <i>a</i> and <i>b</i> concentrations on a leaf area or leaf dry mass basis to be significantly higher the shaded treatments.
In different irradiance environments, chlorophyll concentration per unit leaf area were found to be similar, due to a greater chlorophyll concentration per unit FM in shade leaves compensating for a thinner leaf. The greater chlorophyll concentration per unit FM therefore does not overcompensate here, due to the smaller number and size of mesophyll cells (Lambers <i>et al.</i> , 1998).	
Chlorophyll <i>a</i> : <i>b</i>	
Higher (Demmig-Adams, 1998; Lichtenthaler & Burkart, 1999)	Chlorophyll <i>a</i> levels are lower in more shaded leaves (Bjorkman & Holmgren, 1963; Cartechini & Palliotti, 1995; Bertamini & Nedunchezian, 2004) therefore decreasing the ratio. This is ascribed to the increased association of chlorophyll with the LHC (with a lower chlorophyll <i>a</i> : <i>b</i> ratio) (Lambers <i>et al.</i> , 1998).
Carotenoid:chlorophyll ratio	
Higher (Demmig-Adams & Adams, 1992; Demmig-Adams & Adams, 1996; Demmig-Adams, 1998)	
XPS	
Higher amounts of photoprotective xanthophyll pigments (Gamon & Surfus, 1999) Much higher (Demmig-Adams, 1998) Higher xanthophylls per leaf area (Lambers <i>et al.</i> , 1998)	
β -Carotene:chlorophyll ratio	
Much higher (Demmig-Adams & Adams, 1992; Demmig-Adams, 1998).	
Lutein:chlorophyll ratio	
Only slightly higher (Demmig-Adams, 1998)	
XPS:carotenoid ratio	
	The VAZ:carotenoid and VAZ:chlorophyll ratios were found to increase in reaction to light increase, therefore were much lower in shade conditions (Montane <i>et al.</i> , 1998).
	Neoxanthin increases (also Lutein) was shown in shade leaves of beech and radish compared to high light exposed leaves(Lichtenthaler <i>et al.</i> , 2007) No differences between sun and shade leaves (Demmig-Adams, 1998; Hartel & Grimm, 1998; Krause <i>et al.</i> , 2003)

2.6.4 Plant water status/disease

2.6.4.1 Physiological effects

All stress/strain conditions that reduce the photosynthetic rate of a plant, such as water deficits, and nutrient or temperature stress, increase the degree to which incident radiation can become excessive, which would in turn lead to a higher need for energy dissipation *via* the xanthophyll cycle (Demmig-Adams & Adams, 1996). The authors stated that the kinetics of the xanthophyll

cycle are extremely dynamic, and also considerably decreased under stress conditions, which may lead to more long-term effects on xanthophyll ratios. Flexas *et al.* (2001) indicated that under water stress a relative increase of electron transport to alternate electron sinks, such as oxygen, may occur; this seems to be mediated by the Mehler reaction and photorespiration. The effect of plant water status on leaf pigment content and interrelations may also be indirect, as water deficits may also affect leaves structurally/morphologically through leaf size and/or density and/or thickness adaptations (Niinemets, 1999; Bertamini *et al.*, 2006; Palliotti *et al.*, 2009; Serrano *et al.*, 2010). Bertamini *et al.* (2006) reported marked leaf FM and DM reductions per leaf area, as well as a reduction in leaf size in water deficit plants and stated that the leaf DM reductions were mainly due to reduction in leaf thickness. Should leaf thickness for instance decrease, leaf transmittance of radiation may increase, potentially leading to increased risk of photodamage (Medrano *et al.*, 2002). Medrano *et al.* (2002) also stated that the XPS and CPS as well as the DEPS depend on the cultivar and its acclimation to light, which confirms the findings of Chaumont *et al.* (1997). Candolfi-Vasconcelos *et al.* (1994) reported that young leaves show increased transpiration, but also higher water use efficiency (WUE) than leaves opposite clusters, in accordance with work by Hunter & Visser (1988) and Schultz (1989).

2.6.4.2 Effect on pigments

In agreement with others, Bertamini *et al.* (2006) reported a marked reduction in chlorophyll in water deficit plants, but also that chlorophyll *a* was degraded more than chlorophyll *b* (lowering the chlorophyll *a:b* ratio). According to Medrano *et al.* (2002), the grapevine can be considered isohydric and similar LWP and RWC are reached at midday for both irrigated and water stressed plants. They found that high light with added water stress does not add further adjustment in chlorophyll content. Chaumont *et al.* (1997) also reported similar leaf chlorophyll content in irrigated and non-irrigated plants, but Maroco *et al.* (2002) found a significant reduction in field-grown drought-stressed plants. Medrano *et al.* (2002) also found a linear decrease in chlorophyll content with an increase in leaf water deficit during a 15 day drying cycle in glasshouse-grown Cabernet Sauvignon grapevines. A bigger pool size of precursors to the chlorophylls than to carotenoids or more sensitivity of the metabolic pathway of carotenoids to water deficit is suggested by Duysen & Freeman (1974). According to them, a progressive reduction of carotenoids in leaves of water stressed plants *versus* well watered leaves suggested that the precursors to carotenoid synthesis become increasingly limited in a stressed plant's leaves.

2.7 Destructive analysis of leaf pigments

The methods currently employed to determine leaf pigment content commonly include spectroscopic and chromatographic techniques. These techniques require an effective extraction protocol and analytical methods that prevent pigment degradation. In some HPLC protocols, the pigment contents are normalised to leaf fresh mass and chlorophyll *a* content (Hendrickson *et al.*, 2004a). Considering that chlorophyll *a* is one of the pigments most sensitive to degradation, it seems logical, but can lead to inconsistent results, considering that it is unlikely that different pigments will have identical degradation patterns. Further discussion on these considerations can be found in Chapter V.

2.8 Non-destructive analysis of leaf composition

2.8.1 General leaf spectral properties

2.8.1.1 Leaf interception of total radiation

A grapevine leaf is dorsiventral, and therefore consists of chlorophyll rich mesophyll tissue with two structurally different layers, namely the palisade and spongy parenchyma (Figure 11). The palisade chlorophyll absorbs most incoming visible radiation for use in photosynthesis, with increased absorption of red and blue light and therefore increased reflectance of green light, causing its green appearance (Figure 12 and Figure 13) (Short, 2010).

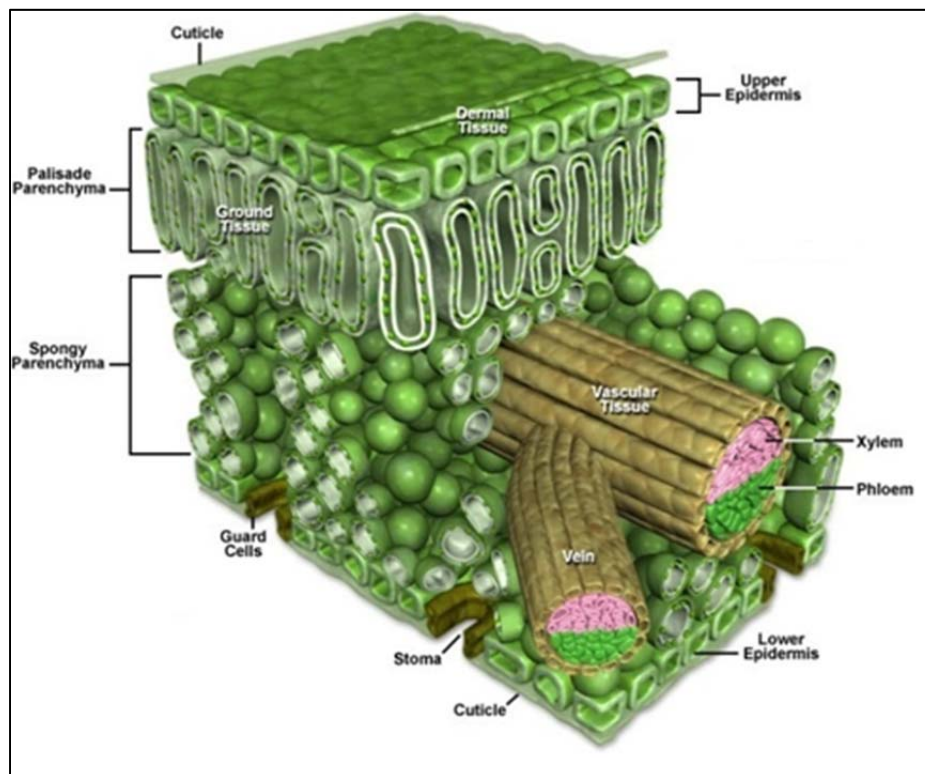


Figure 11 Cross-section through a dorsiventral leaf (Anonymous, 2011).

A model describing the possible actions of light reaching the surface of a leaf is shown in Figure 12. Although this may be affected by factors such as the cultivar, growing conditions and leaf age, a grapevine leaf generally reflects (R) about 10% of total incident radiation (I), while transmitting (T) only 9%. Of the 81% absorbed by the leaf, 20% is emitted, 60% is used in transpiration and convection and only about 1% is used in photosynthesis (Champagnol, 1984). For mature Shiraz leaves, only 9% of photosynthetically active radiation was transmitted, while 6% was reflected, and for Gewürztraminer in New Zealand 4% transmission, 6% reflection, and 90% absorption were indicated (Smart, 1985). While only about 10% of visible light is reflected by a leaf, infrared radiation is reflected to a much higher degree (40-50%) (Knipling, 1970; Woolley, 1971). According to Smart (1987) leaves absorb about 95% of red light, but only about 20% of infrared light, leading to the R:FR ratio in many dense canopies potentially being decreased to less than 10% of the ambient ratio.

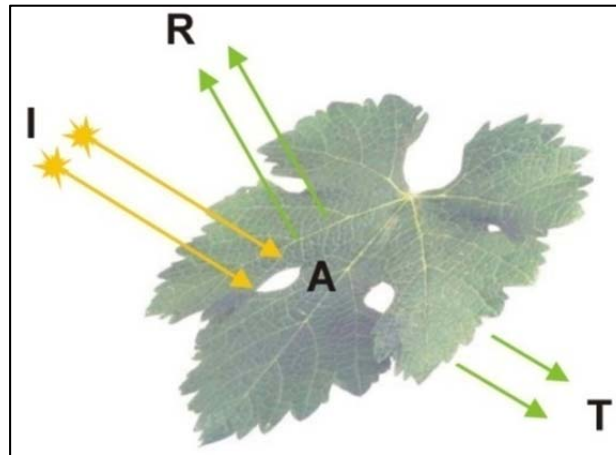


Figure 12 Absorption (A), reflection (R) and transmission (T) of incident radiation (I) for a grapevine leaf, adapted from Champagnol (1984).

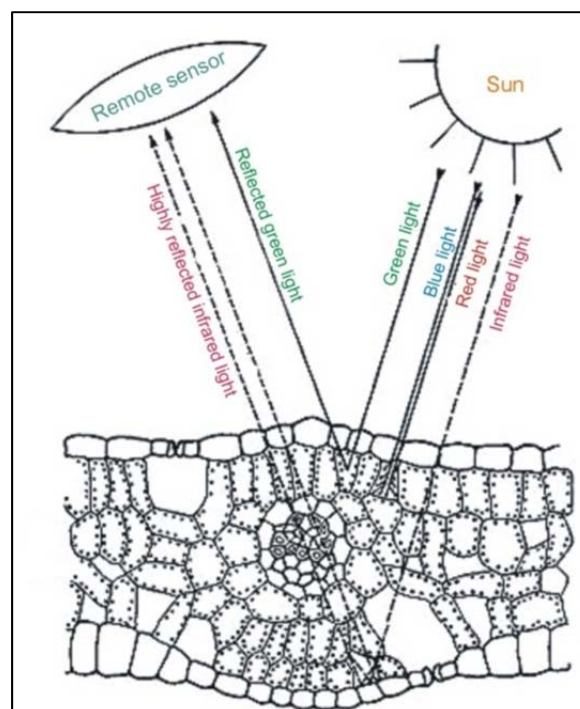


Figure 13 Plant leaf cell structure and interaction with radiation (Short, 2010).

Gausman (1977) found near-infrared light to be scattered by refractive index discontinuities, which can be found at the interface of hydrated cell walls with intercellular air spaces. Therefore a leaf with a relatively dense mesophyll should have a lower infrared reflectance and higher transmittance than a leaf with more air spaces. Leaf palisade cells are vertically aligned, propagating visible light deeper into the leaf, especially collimated (as opposed to diffuse) light (Vogelman *et al.*, 1996). Infrared light pass through the palisade cells without absorption by chlorophyll, but even though probably to a lesser extent than in the spongy mesophyll, small air spaces between palisade cells may still contribute to scattering (Knippling, 1970). Nevertheless, infrared energy that pass through the palisade cells meet an open cell structure in the spongy layer, which then enhances scattering and reflection back through the leaf, with the spongy parenchyma almost acting as “mirror-like structures” (Vogelman *et al.*, 1996; Slaton *et al.*, 2001). Grapevine leaves are heterobaric, containing different types of cells distributed randomly across a leaf section, which implies possible large variability in leaf pigments within single leaves (Flexas *et al.*, 2001).

Typical grapevine leaf and canopy reflectance spectra are shown in Figure 14. The peak in the canopy spectra (green) around 550 nm explains why plants appear green, while the trough around 690 nm can be ascribed primarily to chlorophyll absorption (Short, 2010). The canopy reflects less in the red region compared to the soil, but much more in the NIR, which can be ascribed to plant leaf structure. Incident radiation is absorbed strongly by chlorophyll *a* and chlorophyll *b* (60-75%) and carotenoids (25-35%) (Foody *et al.*, 2009). Absorption is centered at about 650 nm (red) by chlorophyll in chloroplasts of the palisade cells, and to a similar extent in the blue region. Light absorption by chlorophyll is a result of electronic transitions in the chlorophyll molecule. Carotenoids have strong absorption in the 350-500 nm (blue) region and are responsible for the colour of some flowers and fruits as well as leaves with less chlorophyll (Merzlyak & Gitelson, 1995).

Water in its liquid form, which comprises 65-90% of the FM of leaves, is transparent to the photosynthetically active radiation (PAR) wavelengths (350-700 nm) (Merzlyak *et al.*, 2003a). The NIR region has two main sub-divisions between 700 and 1100 nm, where reflectance is high, except for two minor water-related absorption bands (960 nm and 1100 nm), and between 1100 and 1300 nm, corresponding to the transition between the high near-infrared reflectance and the water-related absorption bands in the shortwave infrared region (SWIR, 1400-3000 nm). Since pigments do not absorb measurably in the NIR region, tissue reflectance in this region is determined by aspects such as leaf thickness, water content and light scattering (Merzlyak *et al.*, 2003a). Reflectance in the NIR area is dependent on the relative thickness of the mesophyll as well as the density of the leaf (as defined in combination by TSLM and SLM parameters). According to some researchers (Knipling, 1970; Slaton *et al.*, 2001; Castro-Esau *et al.*, 2006) the number or total area of the air-cell wall interfaces may be a more important parameter for determining reflectance than the volume of air space. Castro-Esau *et al.* (2006) also found significant correlations between leaf transmittance at 800 nm and both percent intercellular space and spongy mesophyll width for nine tropical plant species.

As mentioned, leaf pigments are transparent to NIR wavelengths and therefore leaf absorbance is very small in this region (10% maximum). Even this small absorbance was questioned by (Merzlyak *et al.*, 2002; Merzlyak *et al.*, 2003a), arguing that apparent absorption of light amounting to 10-15% in the range of 750 - 800 nm is likely to result from incomplete collection of transmitted light with integrating spheres. They demonstrated that a healthy leaf does not absorb significantly in the 780-900 nm region, and suggested that if the shapes of reflection and transmission spectra are examined and no structure whatsoever (apart from random fluctuations) is found, the measured transmittance should be corrected. Even with a particularly thick leaf, which contained enough water to give rise to a signal distinguishable from noise, the absorbance contributed by water was found to be much smaller than 1%. The importance of their findings is that when various damages to plants, causing browning or necrosis and a rise in absorbance in the 800 – 900 nm region, are analysed, such damages can be detected with more confidence when spectra have been properly corrected (Merzlyak *et al.*, 2002).

2.8.2 Factors that affect leaf interaction with radiation

2.8.2.1 Leaf microclimate

In terms of leaf microclimate, sun-exposed leaves are thicker due to longer palisade parenchyma cells or additional cell layers (Salisbury & Ross, 1978), It may be reasoned that they therefore may have a higher radiation absorption efficiency. Specific leaf mass (SLM) is an index that is sensitive to prevailing light conditions, increasing in sun-exposed leaves because of an increase in the

parenchyma layer thickness and/or density (Serrano, 2008). Shaded leaves of *V. vinifera* are able to adapt and enhance its ability to utilise diffuse light in the canopy; this is visible from the positive and significant correlation between SLM and photosynthesis (Cartechini & Palliotti, 1995), but SLM, leaf volume, density, and thickness are reduced with increased shading, leading to reduced light compensation points and dark respiration rates (Van den Heuvel *et al.*, 2004; Reynolds & Vanden Heuvel, 2009). Both visible and near-infrared transmittance of sun leaves were significantly less than that of shade leaves (Demarez *et al.*, 1999).

Table 6 Factors that affect leaf radiation interception and potential effects on reflectance (R), transmittance (T) and absorbance (A).

Factor	Status	Visible			Reference & Findings	Near-infrared			Reference & Findings
		R	T	A		R	T	A	
Microclimate	Sun-exposed		-		Less T (Demarez <i>et al.</i> , 1999)	+	-	-	More intercepting tissues in thicker leaves (R,T) (Knapp & Carter, 1998)
	Shaded		+			-	+	+	Counteraction in A where more air spaces occur in these leaves (Gausman, 1984; Gamon & Surfus, 1999)
Leaf age	Young	+	+	-		-	+		
	Old	-	-	+	Increase in A with ageing, decrease in R and T (Schultz, 1996)	+	-	+	Older, higher R, lower T. More scattering interfaces and cells split and cell contents shrink away from cell walls (Knipling, 1970; Gausman, 1985)
	Senescent	+	+	(-)	(Demarez <i>et al.</i> , 1999) (brown leaves)	-	-	(+)	R and T decrease with further mesophyll collapse (Knipling, 1970; Gausman, 1985).
Leaf water deficits	High	+	+	-	Will depend on pigment adaptation, some contradicting results (refer to section 2.6.4.2)	+(*)		-	Water loss in leaf, more air spaces and decreased A, also increase in multiple scattering of radiation (Jacquemoud <i>et al.</i> , 1996).
	Low	-	-	+	Transmittance may increase with high water content (Knipling, 1970)			+	

Note: It was accepted here, considering $R+T+A=1$, that if two of these factors decrease, one has to increase, and *vice versa*. The inferred response has been placed in brackets where applicable.

*Increase in R (Carter, 1993) in the range 1400-2500 nm only with severe leaf dehydration.

In the NIR (700-1300 nm) region, lower transmittance and increased reflectance of thicker sun-exposed leaves was attributed to their high quantity of intercepting leaf tissues, including cellular constituents and intercellular spaces (Knapp & Carter, 1998). Mature shade leaves may have a greater percentage of intercellular space than mature sun leaves (Gausman, 1984; Gamon & Surfus, 1999), where a higher proportion of loosely structured spongy mesophyll may serve to increase internal light scattering and absorbance under low light levels. This may lead to similar

optical properties in the NIR for sun and shade leaves (Knapp & Carter, 1998), as the NIR reflectance and transmittance may decrease in thicker leaves due to more intercepting tissues, and it may be increased in shade-adapted leaves due to more scattering of NIR because of a higher percentage of intercellular space. An earlier study by (Knapp & Carter, 1998) concluded that sun-adapted plants had similar optical properties than shade-adapted plants in the near-infrared region.

2.8.2.2 Leaf surface properties (such as cuticle thickness or leaf hair coverage)

Sims & Gamon (2002) proposed using reflectance at 445 nm to correct for leaf surface radiation scattering, and Serrano (2008) related leaf reflectance in this region to the absorption of carotenoids, which may react to the same conditions (high light) that leads to leaf mesophyll thickening.

2.8.2.3 General leaf age effects

As leaves age, a greater incidence of intercellular spaces as well as an overall increase in leaf thickness can be observed (Kriedemann *et al.*, 1970). Young leaves transmit 0.5 - 1 % more light than fully developed leaves. There are distinct anatomical changes in the expanding grapevine leaf: intercellular spaces and leaf thickness increase with age, which may contribute to lower mesophyll resistance to CO₂ influx (Kriedemann *et al.*, 1970). According to Medrano *et al.* (2002) a decrease in leaf chlorophyll does not necessarily lead to a significant change in absorbance. Schultz (1996) showed that leaf absorbance only changed significantly in very young or old leaves. In the case of damaged or senescing leaves, more visible light energy will be reflected owing to decreased chlorophyll levels and therefore decreased absorption of red and blue light energy. Healthy green leaves generally show a reflectance of 20% or less in the 500-700 nm range (green to red).

2.8.2.4 Leaf age and structural changes

As leaves age, a greater incidence of intercellular spaces, as well as an overall increase in leaf thickness can be observed (Kriedemann *et al.*, 1970). Poni *et al.* (1994b) showed that SLM of leaves increased steadily for all leaf ages from flowering until harvest, but also showed a SLM increase with leaf age according to the LPI index. The SLM trend shown by Poni *et al.* (1994b) supports the assumption that carbohydrate allocation in grapevine leaves takes place over a much longer period than the time needed for completing lamina expansion. Since exposure to light was optimal for each leaf along the shoot, this result was not affected by the variability of SLM, which can be found when large differences in light intensities during leaf expansion occur. Further, the fact that leaves of similar chronological age (80-90 days), but presumably differing in physiological age as they developed at different times during the season, had very similar SLM values, confirms a slight influence of the environment on this parameter.

2.8.2.5 Leaf age and visible radiation

In the visible range of the spectrum (400-680 nm), leaf transmittance decreases (absorbance increase) when the quantity of intercepting leaf tissues (number of palisade cells, intercellular spaces) and absorbing pigments (mainly chlorophyll and carotenoids) increases (Schultz, 1996). Leaf reflectance increases if the quantity of intercepting leaf tissue increases and/or if the quantity of absorbing leaf tissue decreases (Demarez *et al.*, 1999). Therefore leaf transmittance should decrease when SLM and leaf thickness/density increase. Leaf reflectance in the visible range should also decrease during the growing season, as there is generally an increase in SLM, which implies that the quantity of intercepting leaf tissue increases, and this could also be accompanied

by increases in the absorbing pigment content. After senescence, and chlorophyll degradation, both leaf reflectance and leaf transmittance increase, which cannot be explained by leaf thickness as it did not decrease significantly (Demarez *et al.*, 1999).

2.8.2.6 Leaf age and NIR radiation

With leaf ageing, NIR reflectance initially rises and transmittance decrease, as the number of scattering interfaces increases as cells split and cell contents pull away from cell walls; eventually reflectance and transmittance decrease in accordance with further mesophyll collapse during senescence (Knipling, 1970; Gausman, 1985).

2.8.2.7 Leaf water content

In contrast to the findings by Pisciotta *et al.* (2011), who found that leaf orientation can change in reaction to sunlight interception for different row directions, Medrano *et al.* (2002) suggested that leaf orientation changes during drought is simply due to leaf wilting, and not an acclimation response. Apart from leaf microclimatic conditions, plant water status may affect leaves structurally/morphologically through leaf size and/or density and/or thickness adaptations (Niinemets, 1999; Bertamini *et al.*, 2006; Palliotti *et al.*, 2009; Serrano *et al.*, 2010). Water deficits may therefore show directly in spectral measurements through changes in water absorption bands (Figure 14), or through the indirect adaptations. Furthermore, the leaf can adapt on a physiological level, potentially leading to pigment changes in the visible region of the spectra.

Laboratory measurements performed on leaves from five different plant species have shown a good relationship between the EWT and a "moisture stress index", calculated as the ratio between reflectance value measured at 1600 nm and reflectance value measured at 820 nm (Ceccato *et al.* (2001). Water, which comprises 65-90% of the FM of leaves, strongly absorbs radiation in portions of the NIR region. It is transparent to the PAR wavelengths between 350 and 700 nm, but may be a relevant factor in pigment analysis due to its potential secondary effect on transmittance of visible radiation, as shown by Knipling (1970). A bean leaf was infiltrated by water, leading to lower reflectance, as the elimination of air spaces increased transmittance of light through the leaf.

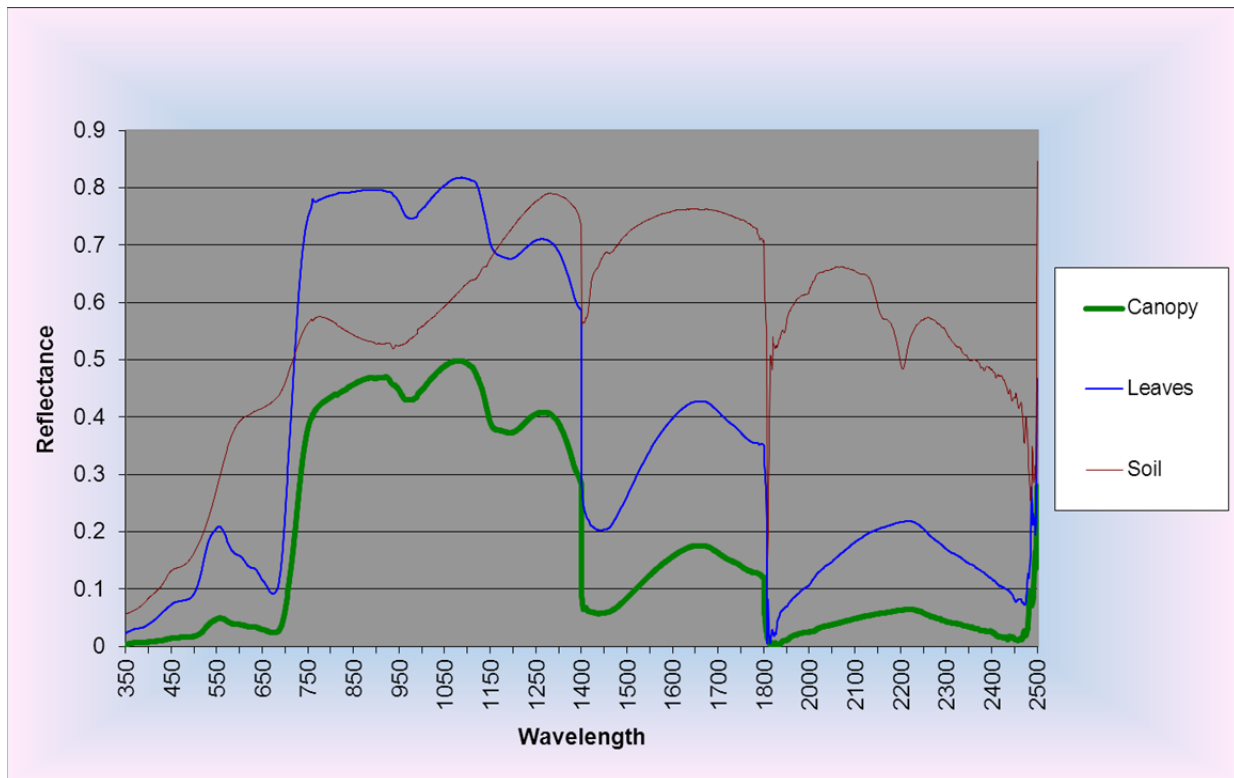


Figure 14 Typical reflectance spectra of individual grapevine leaves, whole canopy and soil (adapted from Strever (2003)).

Sims & Gamon (2002) reported that leaves with similar chlorophyll content, but more water, exhibited a change in a simple spectral ratio based on reflectance at 705 nm. Even small amounts of water in leaves tend to rapidly mask absorptions by minor features (such as protein, cellulose, lignin) in the leaf in the NIR region of the spectrum, but does not affect the visible area of pigment absorption (Jacquemoud *et al.*, 1996). It was also suggested that positive correlations found between leaf nitrogen and pigments are due to covariance of these compounds with pigment and water content in leaves (Jacquemoud *et al.*, 1996).

When a plant experiences water deficits, the water that is lost is replaced by air spaces in the leaf, as the desiccating cells contract. This causes two optical effects in the leaf, namely a decrease in the absorption in the NIR region, and an increase in multiple scattering of radiation (Jacquemoud *et al.*, 1996). Responses of the NIR and SWIR reflectance to water content are therefore caused by structural changes within the leaf and consequently changes in light absorption by water. As leaf water content decreases, leaf cells shrink and warp to accommodate the loss (Foley *et al.*, 2006); therefore air, water, and leaf cell interfaces will change in number and position. Air-water and air-cell wall interfaces have higher refractive indices than water-cell wall interfaces, therefore leading to an increase in light scattering when a leaf loses water (Carter, 1991; DeLucia *et al.*, 1996).

Most of the measured reflectance in the NIR is a result of the scattering properties of the leaf, with a moderate effect of water and other absorbers (Slaton *et al.*, 2001). The SWIR contains strong water absorption compared to other weaker absorbing agents, therefore it is easier to assess scattering/reflectance differences caused by structural variation in response to drying within leaves in the NIR region. In particular, the wavelengths at 1530 nm and 1720 nm seem to be most appropriate for assessing vegetation water content (Ceccato *et al.*, 2001).

A water index ($WI = R_{900}/R_{970}$) that closely followed leaf water content and stomatal conductance during water deficits has been defined (Penuelas & Filella, 1998; Cifre *et al.*, 2005). Its main disadvantage is that, because it involves structural changes like loss of cell wall elasticity, variations appear only when RWC drops below 85%, which precludes its use for mild water stress assessment or for assessment of plants, like many near-isohydric grapevine cultivars, capable of maintaining RWC within narrow ranges. Carter (1993) stated that NIR reflectance was, compared to visible reflectance, relatively unresponsive to stress, and only increased at 1400-2500 nm with severe leaf dehydration. An index or ratio that can predict water content successfully in a sample group with various internal structures must remove scattering effects of the leaves from the calculation (and therefore must include a wavelength region that accounts for internal leaf structure differences) (Foley *et al.*, 2006).

Ceccato *et al.* (2001) assessed five reflectance values per species at 1600 nm for a data set of 37 plant species having an EWT ranging from 0.0002 to 0.0524 g.cm⁻². These reflectance values were plotted as a function of EWT yielding a logarithmic relationship. This implies that when EWT is high, reflectance values are less sensitive to EWT variations but when the EWT decreases, reflectance values become more sensitive to EWT variations.

2.9 General indices for detecting vegetation condition

Different parameters reflecting changes in canopy reflectance at different wavelengths have been used for monitoring plant performance. Classical vegetation indices such as the normalised difference vegetation index (NDVI) represented by $(NIR-R)/(NIR+R)$ (Rouse *et al.*, 1974) and the simple ratio ($SR = NIR/R$) may serve as indicators of vegetation condition due to changes in canopy structure or pigment content. They may correlate with the amount of green biomass over an area and with the absorbed PAR (Cifre *et al.*, 2005). In forest environments, other simple ratios have been studied as indicators of plant condition (Carter, 1994). The results obtained suggested that reflectance in any waveband throughout the 760-800 nm range could be related to reflectance at 605, 695 or 710 nm to yield stress-sensitive ratios.

The red edge region can be found between the highly absorbing red region and the highly reflective NIR region at 680-750 nm. It is characterised by the combined effect of strong chlorophyll absorption and leaf internal scattering (Gitelson *et al.*, 1999). Plant nutrient/mineral stress is known to cause shifts in this region. A shift to shorter wavelengths is known as a "blue shift" and is associated with heavy metal-induced stress in several vegetation types (Peñuelas *et al.*, 1994). This blue shift has been attributed to reductions of chlorophyll *b* and a relative decrease of chlorophylls for vegetation under stress. Changes in the slope and position of the red edge with leaf chlorophyll concentrations have been discussed by Horler *et al.* (1983). The position and slope of the red edge may change as healthy leaves progress from active photosynthesis through various stages of senescence due to loss of chlorophyll and the addition of tannins (Knipling, 1970). Promising results were obtained by Vogelman *et al.* (1993) correlating red edge spectral parameters and chlorophyll content in sugar maple leaves affected by intensive insect damage. The indices used were the red edge inflection point (REIP), the ratio R_{740}/R_{720} , and the ratio of first derivative values at 705-715 nm (Table 7). The three indices demonstrated a high correlation with chlorophyll *a*, chlorophyll *b* and total chlorophyll content at a leaf level. Red edge position, amplitude of red edge peak and area of red edge peak were studied in the field at canopy level with hand-held radiometers and correlated with chlorophyll content, LAI and water content. The area of the red edge peak ($\sum dr$ 680-780 nm) was the best estimator of LAI, and the red edge position was highly correlated with chlorophyll content. When water stress was well developed, a

correlation with the amplitude of the derivative reflectance peak in the red edge was found (Filella & Penuelas, 1994).

Table 7 Reflectance indices or derivative reflectance related to the “red edge” region, used in the estimation of leaf chlorophyll content.

Index name	Formulation	Parameters estimated	References
Red edge inflection point (REIP)	R_{740}/R_{720}	Total chlorophyll (leaf level)	Vogelman <i>et al.</i> (1993)
Ratio of first derivative in red edge region	D_{715}/D_{705}		
Red edge (γ RE)	Wavelength of maximum slope in the increase of R from red to NIR	Total chlorophyll (canopy level)	Penuelas & Filella (1998)

2.10 Non-destructive analysis of leaf pigment content/profiles

The lists of studies that deal with remote sensing of vegetation properties are ever expanding, and the ranges of topics are just as diverse. Similarly, the amount of wide or narrow-waveband indices available to characterise vegetation at the leaf or canopy level are just as expansive. A number of reviews have been published that deal with this range of indices or derivations, including a collection of 79 indices discussed for water status in Rodríguez-Pérez *et al.* (2007). Similar reviews have been conducted for pigments (Le Maire *et al.*, 2004; Serrano, 2008).

It must, however, be noted that single or even complex ratios incorporating only few wavebands or wavelength regions would probably not be suitable for different targets (leaf, canopy or the entire vineyard) and for assessing different biochemical components in the diverse conditions found in vineyards. Static indices may therefore not be the desired approach when dealing with biochemically as well as physiologically diverse targets, which may show intra- or inter-leaf variability as well as temporal variability. It therefore seems relevant to design dynamic models capable of incorporating these variables.

Recent advances in chemometrics (defined for the purpose of this thesis as the application of multivariate statistical analysis to extract biochemical and physiological features from spectra) have changed the way large datasets incorporating narrow-band spectroscopy can be handled.

In general, the absorption spectra of pigments in extraction solvents do not correspond closely to spectra of intact leaves (Jacquemoud *et al.*, 1996). Reasons for this include the spectral influence of the solvent, pigment changes (for instance chlorophyll degradation) during extraction as well as the fact that in leaves, pigments are associated in pigment-protein complexes. Another issue in pigment spectral analysis is the chemical similarity between pigments in terms of their C-H, N-H, C-O and O-H bonds which can cause overlapping spectral features (Jacquemoud *et al.*, 1996).

According to Gitelson *et al.* (2002) the next step in the estimation of individual chlorophyll and carotenoid spectra would be to investigate how the carotenoid composition affects the accuracy of the total carotenoid estimation and how to quantify non-destructively different carotenoids (β -carotene, lutein, zeaxanthin, violaxanthin, neoxanthin and antheraxanthin).

2.10.1 Chlorophyll content

Earlier studies employing the 670-680 nm R minima for chlorophyll analysis, showed rapid saturation with an increase in the pigment content over 10-15 nmol.cm⁻², and it was stated by Merzlyak *et al.* (2003a) that the green (550-600 nm) and red (narrow band at 700-705 nm) areas of the spectrum are sensitive to chlorophyll levels from 0 to 50-60 nmol.cm⁻².

Chlorophyll meters are used for the *in vivo* measurement of the ratio of light transmittance through the leaf at two wavelengths, namely 650 nm (red) and 940 nm (near infrared) (Fanizza *et al.*, 1991). Data from one of these instruments were shown to be strongly related ($R^2 = 0.91$) to the laboratory measurement of chlorophyll concentration in grape leaves (Baldy *et al.*, 1996; Johnson *et al.*, 2001). Baldy *et al.* (1996) considered field chlorophyll measurements and the recording of the ratio vegetation index (NIR/R) with airborne sensors, to be the most practical way to quantify vine stress differences within vineyards. He particularly noted affordability, independence of readings to the meter operator (readings were comparable to those taken a year later, which is something not easily attainable with subjective vine scoring) and its non-invasive nature. The reader is referred to a comprehensive list of leaf chlorophyll indices used in non-destructive estimation that has been compiled by Le Maire *et al.* (2004), which included most of the indices published from 1973 to 2002.

2.10.2 Carotenoid content

The main obstacle in devising a non-destructive technique for carotenoid content estimation is the fact that the carotenoid content is much lower than the chlorophyll content in green plants and that carotenoids exhibit absorption wavebands overlapping with chlorophyll. To develop a technique for non-destructive estimation of leaf carotenoids, one needs to find spectral bands where reflectance is maximally sensitive to carotenoid content, where leaf structure and thickness affects it minimally. Alternatively, the contribution of chlorophyll to the reflectance in the selected spectral bands can be removed or a model can be devised that relates reflectance and carotenoid content for a variety of conditions (i.e. using multivariate techniques). Merzlyak *et al.* (2003a) firstly aimed at finding specific carotenoid features inherent in reflectance spectra. Secondly, after defining the 510 nm area as sensitive to the carotenoid content, a technique was developed to remove the effect of chlorophyll from reflectance in that range. The carotenoid reflectance index (CRI) is, however, not applicable to anthocyanin containing plant tissues, therefore whether it is applicable to grapevine cultivars with higher leaf anthocyanin content, is not known.

The photochemical reflectance index (PRI) is a physiological reflectance index that correlates with the epoxidation state of the xanthophyll cycle pigments and with the efficiency of photosynthesis in control and nitrogen stress canopies (Gamon *et al.*, 1992). Demmig-Adams (1990) already indicated that the different spectrum associated with the zeaxanthin-violaxanthin interconversions results in a signal near 531 nm in the reflectance spectra of intact leaves/canopies. The PRI was shown to be strongly correlated to the de-epoxidation state of the xanthophyll cycle (Peñuelas *et al.*, 1994; Penuelas & Filella, 1998), and it was shown to correlate with net photosynthesis (A_n) and stomatal conductance (G_s) and therefore capable to reflect drought at leaf level in many species (Penuelas & Filella, 1998), including grapevines (Evain *et al.*, 2004). The main disadvantages of the PRI measurements are that the precise PRI values as well as their relationship to A_n and G_s seem dependent on the species and/or the instrument used, and on occasions it failed to follow drought at the canopy scale, which was ascribed to leaf changes in orientation during wilting (Gamon & Pearcy, 1990; Peñuelas *et al.*, 1994) (also refer to section 2.8.2.7). The PRI (Table 8) reference wavelength minimizes complications associated with diurnal sun angle changes and the

corresponding effects on canopy reflectance. Filella *et al.* (1996) showed that PRI was significantly correlated with the epoxidation state and zeaxanthin and with photosynthetic radiation-use efficiency.

Chappelle *et al.* (1992) recommended using a ratio R_{760}/R_{500} as a quantitative measure of carotenoids. Blackburn (1998) suggested that the optimal individual waveband for carotenoid estimation is located at 470 nm and used the pigment-specific ratio R_{800}/R_{470} and a pigment-specific normalised difference $(R_{800}-R_{470})/(R_{800}+R_{470})$ for carotenoid content assessment. Analysing the coefficient of variation of reflectance spectra of yellow to dark-green leaves representing a wide-ranging process of senescence, Gitelson *et al.* (2002) found a prominent narrow peak in the range 500-520 nm. The magnitude of the peak decreased when yellow leaves with a high carotenoid:chlorophyll ratio were excluded from analysis. When only green to dark-green leaves were analysed, the peak disappeared. This suggested that the peak might be attributed solely to carotenoid absorption and that reflectance in the range 500-520 nm is maximally sensitive to the carotenoid content. In an attempt to find spectral bands that are maximally sensitive to carotenoid content in green leaves, Zur *et al.* (2000) suggested normalization of leaf absorbance spectra (A) to the red chlorophyll absorbance area at 678 nm. With this the contribution of chlorophyll was reduced and in the spectra of the standard deviation of A/A_{678} for leaves with a wide range of chlorophyll and carotenoid contents, a prominent peak was detected at 510-520 nm.

Table 8 Carotenoid content spectral indices from literature.

Index name	Formulation	Parameters estimated	References
Carotenoid reflectance index (CRI)	$R_{NIR}(1/R_{510}-1/R_{550})$ or $R_{NIR}(1/R_{510}-1/R_{700})$	Not applicable to anthocyanin containing leaves	Merzlyak <i>et al.</i> (2003a)
Photochemical reflectance index (PRI)	$(R_{REF}-R_{531})/(R_{REF}+R_{531})$ R_{REF} has been selected as R_{550} or R_{570} and R_{531} has been shifted to R_{530} or R_{539} to be an EPS-related region by Filella <i>et al.</i> (1996).	Epoxidation state of the xanthophyll cycle pigments and the efficiency of photosynthesis.	Gamon <i>et al.</i> (1992) Peñuelas <i>et al.</i> (1994) Filella <i>et al.</i> (1996)
Structure Intensive Pigment Index (SIPI)	$(R_{800} - R_1)/(R_{800} - R_2)$ Best results at a leaf level were obtained for the domains [400 nm < R_1 < 530 nm, 600 nm < R_2 < 700 nm] i.e. $(R_{800} - R_{445})/(R_{800} - R_{680})$	Carotenoid:chlorophyll ratio	Penuelas & Filella (1998)
Normalised difference pigment index (NDPI)	$(R_1 - R_2)/(R_1 + R_2)$		
Simple ratio	R_{760}/R_{500}	Carotenoid content	Chappelle <i>et al.</i> (1992)
Pigment-specific ratio	R_{800}/R_{470}	Carotenoid content	Blackburn (1998)
Pigment-specific normalised difference	$(R_{800}-R_{470})/(R_{800}+R_{470})$		
Merzlyak index	$(R_{680}-R_{500})/R_{750}$	Carotenoid:chlorophyll ratio – a quantitative measure of leaf senescence and fruit ripening.	Merzlyak <i>et al.</i> (2003b)

2.10.3 Carotenoid:chlorophyll ratio

To retrieve the carotenoid:chlorophyll ratio for a range of individual leaves and conditions, Penuelas & Filella (1998) proposed a structure-insensitive pigment index (SIPI) in the form $(R_{800}-R_{445})/(R_{800}-R_{680})$. Merzlyak *et al.* (1999) found that the difference $R_{680}-R_{500}$ depends on the pigment composition; the index $(R_{680}-R_{500})/R_{750}$ was found to be sensitive to the carotenoid:chlorophyll ratio and was used as a quantitative measure of leaf senescence and fruit ripening.

Penuelas *et al.* (1995a) indicated that the Simple Ratio Pigment Index (SRPI) (R_{430}/R_{680}) , based on the carotenoid/chlorophyll ratio, correlated well at leaf level with different levels of mite attacks in apple trees, where the ratio increased with an increasing level of attack. The SRPI demonstrated its sensitivity at a later phenological state, i.e. when chlorophyll concentration was lower.

2.10.4 Anthocyanin content and senescence detection

To estimate anthocyanin content non-destructively, Gitelson *et al.* (2009) found that the ARI and mARI can be used successfully in low or high anthocyanin containing leaf tissue. Another study also showed reduced reflectance in the 550 nm region, in reaction to more anthocyanins in leaves of anthocyanin rich cultivars such as Siriki (Liakopoulos *et al.*, 2006).

The normalised pheophytinisation index (NPQI), calculated as $(R_{415}-R_{435})/(R_{415}+R_{435})$, was considered responsive to chlorophyll degradation at leaf level (Penuelas *et al.*, 1995b). Yellowing of plant leaves under senescence or severe stress is the result of increased green as well as red reflectance, which in combination creates the yellow colour. During senescence the chloroplast plastoglobules, rather than the thylakoids, become the major sites of carotenoid localisation (Merzlyak *et al.*, 2003a). They proposed the plant senescence reflectance index (PSRI) = $(R_{678}-R_{500})/R_{NIR}$. Reflectance at 678 nm changed faster in the course of senescence than that of 500 nm, causing a positive PSRI. The stage when PSRI turns to zero was chosen as a criterion of the onset of senescence in plants that retained carotenoids during senescence, such as the grapevine.

Three spectral vegetation indices were computed over the time course of senescence, the modified simple ratio, $mSR_{705} = (R_{750}-R_{445})/(R_{705}-R_{445})$ (Sims & Gamon, 2002), the modified normalised difference index, $mND_{705} = (R_{750}-R_{705})/(R_{750}+R_{705}-2R_{445})$ (Sims & Gamon, 2002), and the plant senescence reflectance index $PSRI = (R_{678}-R_{500})/R_{750}$ (Merzlyak *et al.*, 1999).

2.10.5 Model approaches to determine pigments from spectra

The leaf radiation transfer model PROSPECT describes a leaf as a pile of elementary plates, composed of absorbing and diffusing constituents (Jacquemoud & Baret, 1990). The latest version of this model is a function of the chlorophyll *a* and *b* concentration ($C_a + b$), the EWT (C_w), the dry matter content (or SLM) (C_m), and an internal structure parameter (N) (Jacquemoud *et al.*, 2000). With the exception of N , all parameters can be measured. Several approaches have been proposed for quantifying the parameter N . Jacquemoud & Baret (1990) proposed a hyperbolic relationship between N and the specific leaf area (SLA), with a different relationship also used in a study by Ceccato *et al.* (2001). Jacquemoud *et al.* (1996) indicated that the N in glasshouse leaves of dicotyledons with differentiated mesophyll structure varied from 1.5 to 2.5. These approaches assumed that the vegetation chlorophyll content is proportional to vegetation water content, which is not true for all species (Ceccato *et al.*, 2001). Two other leaf parameters (internal structure and dry matter) are also responsible for leaf reflectance variations in the SWIR. A combination of information from both the NIR (only influenced by the internal structure and the dry matter) and SWIR wavelength ranges was clearly demonstrated to be necessary to provide a better estimation of vegetation water content, as measured by the EWT (Ceccato *et al.*, 2001).

2.11 Non-destructive estimation of leaf structural components

As discussed in section 2.10.5, the PROSPECT model can also be inverted to infer leaf EWT and SLM along with the leaf chlorophyll and carotenoid contents (Ceccato *et al.*, 2001).

Although indirectly most vegetation indices also incorporate wavelengths that account for leaf or canopy structural variability, there are very few studies (other than those based on leaf radiation transfer modelling), that deal directly with estimating leaf structure. The studies by Serrano (2008) and Slaton *et al.* (2001) are exceptions to this. Serrano (2008) studied the effects of leaf structural components, such as leaf thickness (LT), specific leaf mass (SLM) and leaf mass density (LMD) (which is similar to TD, but LT was measured with a micrometer and not derived from FM/LA) on

reflectance-based chlorophyll indices using regression and correlation analyses for seven Mediterranean plant species. The chlorophyll indices used were corrected for differences in internal scattering and surface scattering or based on reflectance first derivatives. Within species, chlorophyll indices showed similar correlation with chlorophyll content ($R^2 > 0.80$), while across species, indices corrected for surface scattering and first reflectance derivative indices were more closely related to chlorophyll content ($R^2 = 0.78$ and $R^2 = 0.75$, respectively) than simple reflectance ratio indices ($R^2 = 0.70$). Plant species with thicker leaves showed lower index values at similar chlorophyll content than species with thinner leaves. In species with thicker leaves, the increases in chlorophyll content were associated with increases in TD rather than to changes in LT and were accompanied by significant reductions in NIR radiation scattering at 800 nm. Both Serrano (2008) and Slaton *et al.* (2001) proposed that light scattering within the leaf is more related to leaf internal structure rather than thickness *per se*.

2.12 Conclusions

The importance of leaf age, leaf structure, pigment and water content cannot be over-emphasised with respect to grapevine physiological studies. During the growing season, different environmental or internal plant factors may affect these parameters, and with ageing, each leaf within the canopy accumulates a “physiological history” of these different events.

The environmental factors may include, amongst others, ambient temperature, humidity, plant and soil water status as well as nutrient content, while different scion and rootstock combinations may adapt differently to all or some of these factors, while altered growing conditions add to this complexity. These complex relationships need to be taken into account when conducting studies to derive leaf or canopy properties non-destructively.

A multitude of vegetation indices have been published in order to estimate the named parameters non-destructively. Considering, however, the complex interaction of the grapevine canopy with radiation, and similarly complex interaction with radiation on leaf level, in-situ calibration of models such as the PROSPECT model or multivariate calibration models may be a more desired approach.

2.13 Literature cited

- Anonymous, 2011. Cross-section through a dorsiventral leaf. URL: www.photobucket.com, album cc105, user "dob1234".
- Archer, E., 1981. Klassifikasie, anatomie en morfologie. In *Wingerdbou in Suid-Afrika*. Burger and Deist (eds.), pp. 1-32. ARC-Infruitec-Nietvoorbij, Stellenbosch.
- Baldy, R., Baldy, M., DeBenedictis, J., Granett, J., Osborn, B., Bledsoe, A., Bosch, D., Hlavka, C., Johnson, L. & Weber, E., 1996. Assessment of leaf area, vine vigour, and grape yield and quality of phylloxera-infested and non-infested grapevines in Napa County and their relationship to leaf reflectance, chlorophyll, and mineral content. Final report: NASA/Ames Research Centre Joint Research Interchange, NCC2-5062.
- Baumes, R., Wirth, J., Bureau, S., Gunata, Y. & Razungles, A., 2002. Biogenesis of C13-norisoprenoid compounds: experiments supportive for an apo-carotenoid pathway in grapevines. *Anal. Chim. Acta.* 458.
- Bertamini, M. & Nedunchezian, N., 2002. Leaf age effects on chlorophyll, Rubisco, photosynthetic electron transport activities and thylakoid membrane protein in field grown grapevine leaves. *Journal of Plant Physiology* 159., 799-803.
- Bertamini, M. & Nedunchezian, N., 2003. Photoinhibition of photosynthesis in mature and young leaves of grapevine (*Vitis vinifera* L.). *Plant Science* 164, 635-644.
- Bertamini, M. & Nedunchezian, N., 2004. Photosynthetic responses for *Vitis vinifera* plants grown at different photon flux densities under field conditions. *Biologia Plantarum* 48, 149-152.
- Bertamini, M., Zulini, L., Muthuchelian, K. & Nedunchezian, N., 2006. Effect of water deficit on photosynthetic and other physiological responses in grapevine (*Vitis vinifera* L. cv. Riesling) plants. *Photosynthetica* 44, 151-154.
- Biswal, B., 1995. Carotenoid catabolism during leaf senescence and its control by light. *Journal of Photochemistry and Photobiology B: Biology* 30, 3-13.
- Bjorkman, O. & Holmgren, P., 1963. Adaptability of the photosynthetic apparatus to light intensity in ecotypes from exposed and shaded habitats. *Physiologia Plantarum* 16, 889-914. .
- Blackburn, G.A., 1998. Quantifying Chlorophylls and Carotenoids at Leaf and Canopy Scales: An Evaluation of Some Hyperspectral Approaches. *Remote Sensing of Environment* 66, 273-285.
- Blackburn, G.A., 2007. Wavelet decomposition of hyperspectral reflectance data for quantifying photosynthetic pigment concentrations in vegetation. *International Journal of Remote Sensing* 28, 2831-2855.
- Blanchfield, A.L., Robinson, S.A., Renzullo, L.J. & Powell, K.S., 2006. Phylloxera-infested grapevines have reduced chlorophyll and increased photoprotective pigment content—can leaf pigment composition aid pest detection? *Functional plant biology* 33, 507-514.
- Bricker, T. & Newman, D., 1982. Changes in the chlorophyll proteins and electron transport activities of soybean (*Glycine Max* L. CV. Wayne) cotyledon chloroplasts during senescence. *Photosynthetica* 16, 239-244.
- Britton, G., 1979. Carotenoid biosynthesis - a target for herbicide activity. . *Z. Naturforsch* 34, 979-985.
- Britton, G., 1982. Carotenoid biosynthesis in higher plants. *Physiol. Veg.* 20, 735-755.
- Busheva, M., Garab, G., Liker, E., Toth, Z., Szell, M. & Nagy, F., 1991. Diurnal Fluctuations in the Content and Functional Properties of the Light Harvesting Chlorophyll a/b Complex in Thylakoid Membranes. *Plant Physiol.* 95, 997-1003.
- Candolfi-Vasconcelos, M.C. & Koblet, W., 1990. Yield, fruit quality, bud fertility and starch reserves of the wood as a function of leaf removal in *Vitis vinifera*. Evidence of compensation and stress recovering. *Vitis* 29, 199-221.
- Candolfi-Vasconcelos, M.C., Koblet, W., Howell, G.S. & Zweifel, W., 1994. Influence of Defoliation, Rootstock, Training System, and Leaf Position on Gas Exchange of Pinot noir Grapevines. *American Journal of Enology and Viticulture* 45, 173-180.

- Cartechini, A. & Palliotti, A., 1995. Effect of Shading on Vine Morphology and Productivity and Leaf Gas Exchange Characteristics in Grapevines in the Field. *American Journal of Enology and Viticulture* 46, 227-234.
- Carter, G.A., 1991. Primary and Secondary Effects of Water Content on the Spectral Reflectance of Leaves. *American Journal of Botany* 78, 916-924.
- Carter, G.A., 1993. Responses of leaf spectral reflectance to plant stress. *American Journal of Botany* 80, 239-243.
- Carter, G.A., 1994. Ratios of leaf reflectances in narrow wavebands as indicators of plant stress. *International Journal of Remote Sensing* 15, 697-703.
- Castro-Esau, K.L., Sanchez-Azofeifa, G.A., Rivard, B., Wright, S.J. & Quesada, M., 2006. Variability in leaf optical properties of Mesoamerican trees and the potential for species classification. *Am. J. Bot.* 93, 517-530.
- Castro, K.L. & Sanchez-Azofeifa, G.A., 2008. Changes in Spectral Properties, Chlorophyll Content and Internal Mesophyll Structure of Senescing *Populus balsamifera* and *Populus tremuloides* Leaves. *Sensors* 8, 51-69.
- Ceccato, P., Flasseb, S., Tarantolac, S., Jacquemoud, S. & Gregoirea, J.-M., 2001. Detecting vegetation leaf water content using reflectance in the optical domain. *Rem. Sens. Environ.* 77, 22-33.
- Champagnol, F., 1984. *Elements de physiologie de la vigne et de viticulture générale*. Déhan, Montpellier.
- Chappelle, E.W., Kim, M.S. & McMurtrey Iii, J.E., 1992. Ratio analysis of reflectance spectra (RARS): An algorithm for the remote estimation of the concentrations of chlorophyll A, chlorophyll B, and carotenoids in soybean leaves. *Remote Sensing of Environment* 39, 239-247.
- Chaumont, M., Osorio, M., Chaves, M., Vanacker, H., Morot-Gaudry, J.-F. & Foyer, C., 1997. The absence of photoinhibition during the midmorning depression of photosynthesis in *Vitis vinifera* grown in semi-arid and temperate climates. *Journal of Plant Physiology* 150, 743-751.
- Chen, L. & Cheng, L., 2003. Both xanthophyll cycle-dependent thermal dissipation and the antioxidant system are up-regulated in grape (*Vitis labrusca* L. cv. Concord) leaves in response to N limitation. *Journal of Experimental Botany* 54, 2165-2175.
- Cifre, J., Bota, J., Escalona, J.M., Medrano, H. & Flexas, J., 2005. Physiological tools for irrigation scheduling in grapevine (*Vitis vinifera* L.) An open gate to improve water-use efficiency? *Agriculture, Ecosystems and Environment* 106, 159-170.
- Croce, R., Remelli, R., Varotto, C., Breton, J. & Bassi, R., 1999. The neoxanthin binding site of the major light harvesting complex (LHCII) from higher plants. *FEBS letters* 456, 1-6.
- Danson, F.M., Steven, M.D., Malthus, T.J. & Clark, J.A., 1992. High-spectral resolution data for determining leaf water content. *International Journal of Remote Sensing* 13, 461-470.
- DeLucia, E.H., Nelson, K., Vogelmann, T.C. & Smith, W.K., 1996. Contribution of intercellular reflectance to photosynthesis in shade leaves. *Plant, Cell & Environment* 19, 159-170.
- Demarez, V., Gastellu-Etchegorry, J.P., Mouglin, E., Marty, G., Proisy, C., Dufrene, E. & Le Dantec, V., 1999. Seasonal variation of leaf chlorophyll content of a temperate forest. Inversion of the PROSPECT model. *International Journal of Remote Sensing* 20, 879-894.
- Demmig-Adams, B., 1990. Carotenoids and photoprotection in plants. A role for the xanthophyll zeaxanthin. *Biochim. Biophys. Acta* 1020, 1-24.
- Demmig-Adams, B., 1998. Survey of thermal energy dissipation and pigment composition in sun and shade leaves. *Plant Cell Physiol.* 39, 474-482.
- Demmig-Adams, B. & Adams, W., 1996. Xanthophyll cycle and light stress in nature: Uniform response to excess direct sunlight among higher plant species. *Planta* 198, 460-470.
- Demmig-Adams, B. & Adams, W.W., 1992. Photoprotection and other responses of plants to high light stress. *Annual Review of Plant Physiology and Plant Molecular Biology* 43, 599-626.
- Demmig-Adams, B., Gilmore, A.M. & Adams, W.W., 1996. In vivo functions of carotenoids in higher plants. *FASEB J.* 10, 403-412.

- Dietzel, L. & Pfannschmidt, T., 2008. Photosynthetic acclimation to light gradients in plant stands comes out of shade. *Plant Signaling and Behavior* 3, 1116-1118.
- Duysen, M. & Freeman, T., 1974. Effects of Moderate Water Deficit (Stress) on Wheat Seedling Growth and Plastid Pigment Development. *Physiol. Plant.* 31, 262-266.
- Eckhardt, U., Grimm, B. & Hörtensteiner, S., 2004. Recent advances in chlorophyll biosynthesis and breakdown in higher plants. *Plant Mol. Biol.* 56, 1-14.
- Eskins, K. & Banks, D.J., 1979. The relationship of accessory pigments to chlorophyll a content in chlorophyll-deficient peanut and soybean varieties. *Photochem Photobiol* 30, 585-588.
- Eskins, K., Kwolek, W.F. & Harris, L., 1982. The accumulation of accessory pigments as a function of chlorophyll a. A comparison of development and genetic control. *Physiol. Plant.* 54, 409-413.
- Evain, S., Flexas, J. & Moya, I., 2004. A new instrument for passive remote sensing: 2. Measurement of leaf and canopy reflectance changes at 531 nm and their relationship with photosynthesis and chlorophyll fluorescence. *Remote Sensing of Environment* 91, 175-185.
- Fanizza, G., Della Gatta, C. & Bagnulo, C., 1991. A non-destructive determination of leaf chlorophyll in *Vitis vinifera*. *Annals of Applied Biology* 119, 203-205.
- Filella, I., Amaro, T., Araus, J.L. & Pefuelas, J., 1996. Relationship between photosynthetic radiation-use efficiency of barley canopies and the photochemical reflectance index (PRI). *Physiologia Plantarum* 96, 211-216.
- Filella, I. & Penuelas, J., 1994. The red edge position and shape as indicators of plant chlorophyll content, biomass and hydric status. *International Journal of Remote Sensing* 15, 1459-1470.
- Fleming, I., 1967. Absolute Configuration and the Structure of Chlorophyll. *Nature* 216, 151-152.
- Flexas, J., Hendrickson, L. & Chow, W.S., 2001. Photoinactivation of photosystem II in high light-acclimated grapevines. *Aust. J. Plant Physiol.* 28, 755-764.
- Foley, S., Rivard, B., Sanchez-Azofeifa, G.A. & Calvo, J., 2006. Foliar spectral properties following leaf clipping and implications for handling techniques. *Rem. Sens. Environ.* 103, 265-275.
- Foody, G.M., Warner, T.A. & Nellis, M.D., 2009. *The SAGE handbook of remote sensing*. SAGE.
- Gamon, J.A. & Pearcy, R.W., 1990. Photoinhibition in *Vitis californica*: interactive effects of sunlight, temperature and water status. *Plant, Cell & Environment* 13, 267-275.
- Gamon, J.A., Penuelas, J. & Field, C.B., 1992. A Narrow-Waveband Spectral Index That Tracks Diurnal Changes in Photosynthetic Efficiency. *Rem. Sens. Environ.* 41, 35-44.
- Gamon, J.A. & Surfus, J.S., 1999. Assessing leaf pigments content and activity with a reflectometer. *New Phytol.* 143, 105-117.
- García-Plazaola, J.I., Esteban, R., Hormaetxe, K. & María Becerril, J., 2008. Seasonal reversibility of acclimation to irradiance in leaves of common box (*Buxus sempervirens* L.) in a deciduous forest. *Flora - Morphology, Distribution, Functional Ecology of Plants* 203, 254-260.
- Garnier, E., Shipley, B., Roumet, C. & Laurent, G., 2001. A Standardized Protocol for the Determination of Specific Leaf Area and Leaf Dry Matter Content. *Functional Ecology* 15, 688-695.
- Gausman, H.W., 1977. Reflectance of leaf components. *Remote Sensing of Environment* 6, 1-9.
- Gausman, H.W., 1984. Evaluation of factors causing reflectance differences between sun and shade leaves. *Rem. Sens. Environ.* 15, 177-181.
- Gausman, H.W., 1985. *Plant leaf optical properties in visible and near-infrared light*. . Texas Tech Press, Lubbock, Texas.
- Gholami, M., Coombe, B.G., Robinson, S.P. & Williams, P.J., 1996. Amounts of glycosides in grapevine organs during berry development. *Australian Journal of Grape and Wine Research* 2, 59-63.
- Gitelson, A.A., Buschmann, C. & Lichtenthaler, H., 1999. The Chlorophyll Fluorescence Ratio F735/F700 as an Accurate Measure of the Chlorophyll Content in Plants. *Rem. Sens. Environ.* 69, 296-302.

- Gitelson, A.A., Chivkunova, O.B. & Merzlyak, M.N., 2009. Nondestructive estimation of anthocyanins and chlorophylls in anthocyanic leaves. *American Journal of Botany* 96, 1861-1868.
- Gitelson, A.A., Zur, Y., Chivkunova, O.B. & Merzlyak, M.N., 2002. Assessing carotenoid content in plant leaves with reflectance spectroscopy. *Photochem Photobiol* 75, 272-81.
- Giuliano, G., Al-Babili, S. & von Lintig, J., 2003. Carotenoid oxygenases: cleave it or leave it. *Trends in Plant Science* 8, 145-149.
- Goodwin, T.W. & Lester, P., 1993. Biosynthesis of carotenoids: An overview. *In Methods in Enzymology*. pp. 330-340. Academic Press.
- Goussard, P.G. & Orffer, C.J., 2011. Grapevine anatomy and morphology - Viticulture 424 class notes. Department of Viticulture and Oenology, Stellenbosch.
- Gradinaru, C.C., van Stokkum, I.H.M., Pascal, A.A., van Grondelle, R. & van Amerongen, H., 2000. Identifying the pathways of energy transfer between carotenoids and chlorophylls in LHCII and CP29. A multicolor, femtosecond pump-probe study. *The Journal of Physical Chemistry B* 104, 9330-9342.
- Griffith, R.B., Valleau, W.D. & Jeffrey, R.N., 1944. Chlorophyll and carotene content of eighteen tobacco varieties. *Plant Physiol.* 19, 689-693.
- Hartel, H. & Grimm, B., 1998. Consequences of chlorophyll deficiency for leaf carotenoid composition in tobacco synthesizing glutamate 1-semialdehyde aminotransferase antisense RNA: dependency on developmental age and growth light. *Journal of Experimental Botany* 49, 535-546.
- Havaux, M., 1998. Carotenoids as membrane stabilizers in chloroplasts. *Trends in Plant Science* 3, 147-151.
- Havaux, M., Tardy, F. & Lemoine, Y., 1998. Photosynthetic light-harvesting function of carotenoids in higher-plant leaves exposed to high light irradiances. *Planta* 205, 242-250.
- Hendrickson, L., Ball, M.C., Wood, J.T., Chow, W.S. & Furbank, R.T., 2004a. Low temperature effects on photosynthesis and growth of grapevine. *Plant, Cell & Environment* 27, 795-809.
- Hendrickson, L., Forster, B., Furbank, R.T. & Chow, W.S., 2004b. Processes contributing to photoprotection of grapevine leaves illuminated at low temperature. *Physiologia Plantarum* 121, 272-281.
- Herold, A., 1980. Regulation of photosynthesis by sink activity - the missing link. *New Phytol.* 86, 131-144.
- Hill, J., 1980. The remobilization of nutrients from leaves. *Journal of Plant Nutrition* 2, 407-444.
- Hirschberg, J., 2001. Carotenoid biosynthesis in flowering plants. *Current Opinion in Plant Biology* 4, 210-218.
- Horler, D.N.H., Dockray, M. & Barber, J., 1983. The red edge of plant leaf reflectance. *International Journal of Remote Sensing* 4, 273-288.
- Hörtensteiner, S., 2006. Chlorophyll degradation during senescence. *Annu. Rev. Plant. Biol.* 57, 55-77.
- Huglin, P. & Schneider, C., 1998. *Biologie et écologie de la vigne*. Lavoisier, Paris.
- Hunter, J.J., Skrivan, R. & Ruffner, H.P., 1994. Diurnal and seasonal physiological changes in leaves of *Vitis vinifera* L.: CO₂ assimilation rates, sugar levels and sucrolytic enzyme activity. *Vitis* 33, 189-195.
- Hunter, J.J. & Visser, J.H., 1988. The effect of partial defoliation, leaf position and developmental stage of the vine on photosynthetic activity of *Vitis vinifera* L. cv Cabernet Sauvignon. *S. Afr. J. Enol. Vitic.* 9, 9-15.
- Hunter, J.J. & Visser, J.H., 1989. The effect of partial defoliation, leaf position and developmental stage of the vine on leaf chlorophyll concentration in relation to the photosynthetic activity and light intensity in the canopy of *Vitis vinifera* L. cv. Cabernet Sauvignon. *S. Afr. J. Enol. Vitic.* 10, 67-73.
- Jacquemoud, S., Bacour, C., Poilve, H. & Frangi, J.P., 2000. Comparison of Four Radiative Transfer Models to Simulate Plant Canopies Reflectance:: Direct and Inverse Mode. *Remote Sensing of Environment* 74, 471-481.
- Jacquemoud, S. & Baret, F., 1990. PROSPECT: A model of leaf optical properties spectra. *Remote Sensing of Environment* 34, 75-91.

- Jacquemoud, S., Ustin, S.L., Verdebout, J., Schmuck, G., Andreoli, G. & Hosgood, B., 1996. Estimating leaf biochemistry using the PROSPECT leaf optical properties model. *Remote Sensing of Environment* 56, 194-202.
- Johnson, L.F., Bosch, D.F., Williams, D.C. & Lobitz, B.M., 2001. Remote sensing of vineyard management zones: implications for wine quality. *Appl. Eng. Agric.* 17, 557-560.
- Keller, M., 2010. *The science of grapevines: anatomy and physiology*.
- Kim, J.H., Click, R.E. & Melis, A., 1993. Dynamics of Photosystem Stoichiometry Adjustment by Light Quality in Chloroplasts. *Plant Physiol.* 102, 181-190.
- Knapp, A.K. & Carter, G.A., 1998. Variability in leaf optical properties among 26 species from a broad range of habitats. *Am. J. Bot.* 85, 940-946.
- Knipling, E.B., 1970. Physical and physiological basis for the reflectance of visible and near-infrared radiation from vegetation. *Rem. Sens. Environ.* 1, 155-159.
- Krause, G.H., Gallé, A., Gademann, R. & Winter, K., 2003. Capacity of protection against ultraviolet radiation in sun and shade leaves of tropical forest plants. *Functional Plant Biology* 30, 533-542.
- Kriedemann, P.E., 1968. Photosynthesis in vine leaves as a function of light intensity, temperature, and leaf age. *Vitis* 7, 213-220.
- Kriedemann, P.E., Kliewer, W.M. & Harris, J.M., 1970. Leaf age and photosynthesis in *Vitis vinifera* L. *Vitis* 9, 97-104.
- Lambers, H., Chapin, F.S. & Pons, T.L., 1998. *Plant physiological ecology*. Springer, New York, USA.
- Lashbrooke, J.G., Young, P.R., Strever, A.E., Stander, C. & Vivier, M.A., 2010. The development of a method for the extraction of carotenoids and chlorophylls from grapevine leaves and berries for HPLC profiling. *Australian Journal of Grape and Wine Research* 16, 349-360.
- Le Maire, G., François, C. & Dufrêne, E., 2004. Towards universal broad leaf chlorophyll indices using PROSPECT simulated database and hyperspectral reflectance measurements. *Rem. Sens. Environ.* 89, 1-28.
- Lei, T.T., Tabuchi, R., Kitao, M. & Koike, T., 1996. Functional relationship between chlorophyll content and leaf reflectance, and light-capturing efficiency of Japanese forest species. *Physiol. Plant.* 96, 411-418.
- Liakopoulos, G., Nikolopoulos, D., Klouvatou, A., Vekkos, K., Manetas, Y. & Karabourniotis, G., 2006. The Photoprotective Role of Epidermal Anthocyanins and Surface Pubescence in Young Leaves of Grapevine (*Vitis vinifera*). *Annals of Botany* 98, 257-265.
- Lichtenthaler, H., Babani, F. & Langsdorf, G., 2007. Chlorophyll fluorescence imaging of photosynthetic activity in sun and shade leaves of trees. *Photosynthesis Research* 93, 235-244.
- Lichtenthaler, H., Buschmann, C., Döll, M., Fietz, H.J., Bach, T., Kozel, U., Meier, D. & Rahmsdorf, U., 1981. Photosynthetic activity, chloroplast ultrastructure, and leaf characteristics of high-light and low-light plants and of sun and shade leaves. *Photosynthesis Research* 2, 115-141.
- Lichtenthaler, H.K., 1987. Chlorophylls and carotenoids: Pigments of photosynthetic biomembranes. *In* *Methods in Enzymology*. pp. 350-382. Academic Press.
- Lichtenthaler, H.K., 1999. The 1-deoxy-D-xylulose-5-phosphate pathway of isoprenoid biosynthesis in plants. *Annual Review of Plant Biology* 50, 47-65.
- Lichtenthaler, H.K. & Burkart, S., 1999. Photosynthesis and high light stress. *Bulg. J. Plant Physiol.* 25, 3-16.
- Lichtenthaler, H.K., Schwender, J., Disch, A. & Rohmer, M., 1997. Biosynthesis of isoprenoids in higher plant chloroplasts proceeds via a mevalonate independent pathway. *FEBS letters* 400, 271-274
- Lorenzen, C.J., 1967. Determination of Chlorophyll and Pheo-Pigments: Spectrophotometric Equations. *Limnology and Oceanography* 12, 343-346.
- Marais, J., 1992. 1,1,6-Trimethyl-1,2-dihydronaphthalene (TDN): a possible degradation product of lutein and beta-carotene. *S. Afr. J. Enol. Vitic.* 13, 52-55.

- Maroco, J.P., Rodrigues, M.L., Lopes, C. & Chaves, M.M., 2002. Limitations to leaf photosynthesis in field-grown grapevine under drought—metabolic and modelling approaches. *Functional Plant Biology* 29, 451-459.
- Medrano, H., Bota, J., Abadia, A., Sampol, B., Escalona, J. & Flexas, J., 2002. Effects of drought on light-energy dissipation mechanisms in high-light acclimated, field-grown grapevines *Functional Plant Biology* 29, 1197-1207.
- Merzlyak, M.N., Chivkunova, O.B., Melø, T.B. & Naqvi, K.R., 2002. Does a leaf absorb radiation in the near infrared (780–900 nm) region? A new approach to quantifying optical reflection, absorption and transmission of leaves. *Photosynth. Res.* 72, 263–270.
- Merzlyak, M.N. & Gitelson, A., 1995. Why and what for the leaves are yellow in autumn? On the interpretation of optical spectra of senescing leaves (*Acer platanoides* L.). *Journal of Plant Physiology* 145, 315-315.
- Merzlyak, M.N., Gitelson, A.A., Chivkunova, O.B., Solovchenko, A.E. & Pogosyan, S.I., 2003a. Application of reflectance spectroscopy for analysis of higher plant pigments. *Plant Physiol.* 50, 704-710.
- Merzlyak, M.N., Gitelson, A.A., Chivkunovaa, O.B. & Rakitinc, V.Y., 1999. Non-destructive optical detection of pigment changes during leaf senescence and fruit ripening. *Physiologia Plantarum* 106, 135–141.
- Merzlyak, M.N., Solovchenko, A.E. & Gitelson, A.A., 2003b. Reflectance spectral features and non-destructive estimation of chlorophyll, carotenoid and anthocyanin content in apple fruit. *Postharvest Biology and Technology* 27, 197-211.
- Montane, M.-H., Tardy, F., Kloppstech, K. & Havaux, M., 1998. Differential Control of Xanthophylls and Light-Induced Stress Proteins, as Opposed to Light-Harvesting Chlorophyll a/b Proteins, during Photosynthetic Acclimation of Barley Leaves to Light Irradiance. *PLANT PHYSIOLOGY* 118, 227-235.
- Munné-Bosch, S. & Alegre, L., 2004. Die and let live: leaf senescence contributes to plant survival under drought stress. *Functional Plant Biology* 31, 203-216.
- Niinemets, U., 1999. Research Review: Components of Leaf Dry Mass Per Area-Thickness and Density-Alter Leaf Photosynthetic Capacity in Reverse Directions in Woody Plants. *New Phytologist* 144, 35-47.
- North, H.M., Almeida, A.D., Boutin, J.-P., Frey, A., To, A., Botran, L., Sotta, B. & Marion-Poll, A., 2007. The *Arabidopsis* ABA-deficient mutant *aba4* demonstrates that the major route for stress-induced ABA accumulation is via neoxanthin isomers. *The Plant Journal* 50, 810–824.
- Palliotti, A., Cartechini, A. & Ferranti, F., 2000. Morpho-anatomical and Physiological Characteristics of Primary and Lateral Shoot Leaves of Cabernet Franc and Trebbiano Toscano Grapevines Under Two Irradiance Regimes. *American Journal of Enology and Viticulture* 51, 122-130.
- Palliotti, A., Silvestroni, O. & Petoumenou, D., 2009. Photosynthetic and Photoinhibition Behavior of Two Field-Grown Grapevine Cultivars under Multiple Summer Stresses. *American Journal of Enology and Viticulture* 60, 189-198.
- Peñuelas, J. & Filella, I., 1998. Visible and near-infrared reflectance techniques for diagnosing plant physiological status. *Trends in Plant Science* 3, 151-156.
- Peñuelas, J., Filella, I. & Gamon, J.A., 1995a. Assessment of photosynthetic radiation-use efficiency with spectral reflectance. *New Phytologist* 131, 291-296.
- Peñuelas, J., Filella, I., Lloret, P., Munoz, F. & Vilajeliu, M., 1995b. Reflectance assessment of mite effects on apple trees. *International Journal of Remote Sensing* 16, 2727-2733.
- Peñuelas, J., Gamon, J.A., Fredeen, A.L., Merino, J. & Field, C.B., 1994. Reflectance indices associated with physiological changes in nitrogen- and water-limited sunflower leaves. *Remote Sensing of Environment* 48, 135-146.
- Peñuelas, J. & Munné-Bosch, S., 2005. Isoprenoids: an evolutionary pool for photoprotection. *Trends in Plant Science* 10, 166-169.

- Pisciotta, A., Di Lorenzo, R., Volschenk, C.G. & Hunter, J.J., 2011. Relation between row and leaf orientation of Syrah/101-14 MGT. In: Proc. Seventeenth International GiESCO Symposium, 29 August - 2 September, Asti - Alba (CN), Italy. pp. 555-558.
- Pogson, B., McDonald, K.A., Truong, M., Britton, G. & DellaPenna, D., 1996. Arabidopsis Camtenoid Mutants Demonstrate That Lutein is Not Essential for Photosynthesis in Higher Plants. *The Plant Cell* 8, 1627-1639.
- Poni, S. & Giachino, E., 2000. Growth, photosynthesis and cropping of potted grapevines (*Vitis vinifera* L. cv. Cabernet Sauvignon) in relation to shoot trimming. *Australian Journal of Grape and Wine Research* 6, 216-226.
- Poni, S., Intrieri, C. & Silvestroni, O., 1994. Interactions of LeafAge, Fruiting, and Exogenous Cytokinins in Sangiovese Grapevines Under Non-Irrigated Conditions. II. Chlorophyll and Nitrogen Content. *Am. J. Enol. Vitic.* 45, 278-284.
- Pratt, C., 1974. Vegetative Anatomy of Cultivated Grapes--A Review. *American Journal of Enology and Viticulture* 25, 131-150.
- Renzullo, L.J., Blanchfield, A.L., Guillermin, R., Powell, K.S. & Held, A.A., 2006. Comparison of PROSPECT and HPLC estimates of leaf chlorophyll contents in a grapevine stress study. *International Journal of Remote Sensing* 27, 817-823.
- Reynolds, A.G. & Vanden Heuvel, J.E., 2009. Influence of Grapevine Training Systems on Vine Growth and Fruit Composition: A Review. *American Journal of Enology and Viticulture* 60, 251-268.
- Rodríguez-Pérez, J.R., Riaño, D., Carlisle, E., Ustin, S. & Smart, D.R., 2007. Evaluation of Hyperspectral Reflectance Indexes to Detect Grapevine Water Status in Vineyards. *Am. J. Enol. Vitic.* 58, 302-317.
- Rosenthal, S.I. & Camm, E.L., 1997. Photosynthetic decline and pigment loss during autumn foliar senescence in western larch (*Larix occidentalis*). *Tree Physiology* 17, 767-775.
- Rouse, J.W., Haas, R.H., Schell, J.A., Deering, D.W. & Harlan, J.C., 1974. Monitoring the vernal advancement and retrogradation (greenwave effect) of natural vegetation. *In* NASA/GSFC Type III Final Report. Greenbelt, Md., 371p.
- Ruban, A.V., 2009. Plants in light. *Commun Integr Biol.* 2, 50-55.
- Sajilata, M.G., Singhal, R.S. & Kamat, M.Y., 2008. The Carotenoid Pigment Zeaxanthin—A Review. *Comprehensive Reviews in Food Science and Food Safety* 7, 29-49.
- Salisbury, F.B. & Ross, C.W., 1978. *Plant Physiology*. Wadsworth Publishing, Belmont, California.
- Sánchez-de-Miguel, P., Centeno, A., Baeza, P. & Lissarrague, J.R., 2005. Photosynthetic response to light of 'Tempranillo' leaves in the field: effects of leaf age, position and water potential. *Acta Hort. (ISHS)* 689, 357-364.
- Sanger, J.E., 1971. Quantitative investigations of leaf pigments from their inception in buds through autumn coloration to decomposition in falling leaves. *Ecology* 52, 1075-1089.
- Schoefs, B. & Franck, F., 2003. Protochlorophyllide reduction: Mechanisms and Evolution. *Photochem Photobiol* 78, 543-557.
- Schultz, H.R., 1989. CO₂-Gaswechsel und Wassertransport von Stark- und Schwachlichttrieben bei *Vitis vinifera* L. (cv. Riesling) in Abhängigkeit von Klima- und Pflanzenfaktoren - Ansatz eines empirischen Assimilationsmodells. *Geisenheimer Berichte, Veröffentlichungender FA Geisenheim* Band 5, 221 pp.
- Schultz, H.R., 1993. Photosynthesis of sun and shade leaves of field-grown grapevine (*Vitis vinifera* L.) in relation to leaf age. Suitability of the plastochron concept for the expression of physiological age. *Vitis* 32, 197-205.
- Schultz, H.R., 1996. Leaf absorptance of visible radiation in *Vitis vinifera* L.: estimates of age and shade effects with a simple field method. *Scientia Horticulturae* 66, 93-102.
- Serrano, L., 2008. Effects of leaf structure on reflectance estimates of chlorophyll content. *International Journal of Remote Sensing* 29, 5265-5274.

- Serrano, L., González-Flor, C. & Gorchs, G., 2010. Assessing vineyard water status using the reflectance based Water Index. *Agriculture, Ecosystems & Environment* 139, 490-499.
- Short, N., 2010. Remote sensing tutorial. VEGETATION APPLICATIONS: AGRICULTURE, FORESTRY, AND ECOLOGY General Principles For Recognizing Vegetation. URL: Available: <http://rst.gsfc.nasa.gov/Front/tofc.html>.
- Sims, D.A. & Gamon, J.A., 2002. Relationships between leaf pigment content and spectral reflectance across a wide range of species, leaf structures and developmental stages. *Rem. Sens. Environ.* 81, 337-354.
- Slaton, M.R., Hunt, E.R. & Smith, W.K., 2001. Estimating near-infrared leaf reflectance from leaf structural characteristics. *Am. J. Bot.* 88, 278-284.
- Smart, R., 1987. Influence of light on composition and quality of grapes. *Acta Hort.* 206, 37-47.
- Smart, R.E., 1985. Principles of Grapevine Canopy Microclimate Manipulation with Implications for Yield and Quality. A Review. *American Journal of Enology and Viticulture* 36, 230-239.
- Souza, R.P. & Válio, I.F.M., 2003. Leaf optical properties as affected by shade in saplings of six tropical tree species differing in successional status. *Braz. J. Plant Physiol.* 15, 49-54.
- Steel, C.C. & Keller, M., 2000. Influence of UV-B irradiation on the carotenoid content of *Vitis vinifera* tissues. *Biochemical Society Transactions* 28, 883-885.
- Strever, A., 2003. A study of within-vineyard variability with conventional and remote sensing technology. MSc(Agric)Viticulture Thesis thesis, Stellenbosch University.
- Szabó, I., Bergantino, E. & Giacometti, G.M., 2005. Light and oxygenic photosynthesis: energy dissipation as a protection mechanism against photo-oxidation. *EMBO reports* 6, 629-634.
- Taiz, L. & Zeiger, E., 1998. *Plant physiology*. Sinauer Associates, Inc., Sunderland, Massachusetts.
- Terashima, I., Hanba, Y.T., Tazoe, Y., Vyas, P. & Yano, S., 2006. Irradiance and phenotype: comparative eco-development of sun and shade leaves in relation to photosynthetic CO₂ diffusion. *Journal of Experimental Botany* 57, 343-354.
- Thayer, S.S. & Bjorkman, O., 1990. Leaf xanthophyll content and composition in sun and shade determined by HPLC. *Photosynth. Res.* 23, 331-343.
- Tsukaya, H., 2006. Mechanism of leaf-shape determination. *Annu. Rev. Plant Biol.* 57, 477-496.
- Van den Heuvel, J.E., Proctor, J.T.A., Fisher, K.H. & Sullivan, J.A., 2004. Shading Affects Morphology, Dry-matter Partitioning, and Photosynthetic Response of Greenhouse-grown 'Chardonnay' Grapevines. *HortScience* 39, 65-70.
- Van Volkenburgh, E., 1999. Leaf expansion – an integrating plant behaviour. *Plant, Cell & Environment* 22, 1463-1473.
- Vogelman, J.E., Rock, B.N. & Moss, D.M., 1993. Red edge spectral measurements from sugar maple leaves. *international Journal of Remote Sensing* 14, 1563-1575.
- Vogelman, T.C., Nishio, J.N. & Smith, W.K., 1996. Leaves and light capture: Light propagation and gradients of carbon fixation within leaves. *Trends in Plant Science* 1, 65-70.
- Williams, L.E., 1987. Growth of Thompson Seedless grapevines: I. Leaf area development and dry weight distribution. *J. Am. Soc. Hortic. Sci.* 112, 325-330.
- Witkowski, E.T.F. & Byron, B.L., 1991. Leaf Specific Mass Confounds Leaf Density and Thickness. *Oecologia* 88, 486-493.
- Woolley, J.T., 1971. Reflectance and transmittance of light by leaves. *PLANT PHYSIOLOGY* 47, 656.
- Zur, Y., Gitelson, A.A., Chivkunova, O.B. & Merzlyak, M.N., 2000. The spectral contribution of carotenoids to light absorption and reflectance in green leaves. In: *Proc. Second International Conference on Geospatial Information in Agriculture and Forestry, Lake Buena Vista, FL.* pp. 17-23.

Chapter III

Research Results

Interactive effects of growth manipulation
and water deficit in grapevine (*Vitis vinifera*
L.) cv. Shiraz

Chapter III: Interactive effects of growth manipulation and water deficit in grapevine (*Vitis vinifera* L.) cv. Shiraz

3.1 Introduction

Grapevine canopy manipulation/management is considered an integral and important practice in grapevine seasonal management with potential large impacts on the physiology of the grapevine and consequently grape and wine composition (Hunter & Le Roux, 2000; Hunter & Archer, 2002). The timing and methods of application of canopy management are of critical importance (Hunter, 1999, 2000). Along with this, the timing and intensity of irrigation practices, which may lead to plant water deficits, may also inhibit shoot and leaf growth due to stomatal closure and consequently lower photosynthetic activity in leaves (Archer & Strauss, 1989; Fanizza & Ricciardi, 1990; Schultz, 1995b; Myburgh *et al.*, 1996; Myburgh, 2005b). It may also impact on phenological development (Coombe, 1992), leading to a shorter growing season and possibly earlier leaf senescence and abscission, whereas berry growth, which may potentially reduce berry size (Ojeda *et al.*, 2002; Ellis, 2008) and consequently yield, may be affected. Positive effects observed with respect to grape ripening and composition when mild water deficits exist in grapevines (Van Zyl & Weber, 1977) are often ascribed to a reduction in vegetative growth (Smart & Coombe, 1983) and consequently increased leaf and fruit exposure. The latter can also cause reduced berry mass and yield due to increased berry water loss (Smart & Coombe, 1983). However, other studies found no differences in sugar concentration at harvest in reaction to different levels of water constraints (Myburgh, 2005a; Myburgh, 2006), also on a total soluble solids relative to berry mass basis (Ojeda *et al.*, 2002). Shiraz grapevines in the Stellenbosch area, South Africa, that were exposed to strong water deficits during the pre-véraison period, those receiving an irrigation one month after véraison, as well as those receiving frequent irrigation showed reduced grape phenolics compared to non-irrigated grapevines and those only receiving an irrigation at véraison (Ellis, 2008). Water deficits may decrease leaf area, leaf number per shoot, leaf size and leaf thickness (Schultz & Matthews, 1988; Gómez-del-Campo *et al.*, 2002; Bertamini *et al.*, 2006) as well as potentially exposed leaf area (Carbonneau, 1995). Hardie & Martin (2000) suggested that the growth rate of de-fruited shoots is even more sensitive to soil moisture deficit. It was also suggested that once the fruiting constraint on shoot growth is removed, shoot growth rate becomes a sensitive indicator of vine water status when leaf water potential is more negative than -700 kPa during active shoot growth. Shoot growth generally ceases below this threshold (Van Zyl & Kennedy, 1983).

Shoot growth is strongly influenced by temperature, soil moisture, grapevine nutrient and reserve status, pruning level, plant age or genetic characteristics of the rootstock or scion (Keller, 2010). The growth of shoots accelerates with temperature increases up to 25 to 30°C, and slows with further temperature increase above 35°C, but respiratory losses may also increase with night-time temperatures above 20°C, which could limit growth (Buttrose, 1969). Initial shoot growth may be affected to different degrees by apical dominance and correlative inhibition (dependent mostly on the cultivar and pruning system), and seems to be under strong control of growth hormones (Ferguson & Beveridge, 2009). Secondary shoots may start developing, even under conditions of apical dominance, presumably due to increased cytokinin formation in and translocation from the roots (Keller, 2010). Conversely, conditions leading to stimulated cytokinin delivery to the axillary buds, such as warm temperatures, high transpiration levels, high nitrogen levels (Keller & Koblet, 1995) and rapid shoot growth, may stimulate secondary shoot growth. Also, higher abscisic acid to

cytokinin ratios, caused by water deficit conditions, may inhibit secondary shoot growth due to an increased apical dominance effect (Stoll *et al.*, 2000; Lebon *et al.*, 2006).

In the northern hemisphere, a decrease in day length and lower temperatures before ripening may trigger the cessation of cell division in the apical meristem and cambium of the shoot marking the initiation of dormancy, brought about by a decrease in auxin and an increase in the root-derived abscisic acid in the plant sap (Mwange *et al.*, 2005; Rohde & Bhalerao, 2007). In warmer winegrowing countries/regions, ambient temperatures during ripening are still very high, and shoot growth reduction is more likely in response to increased water deficit conditions. The onset of senescence is probably day length regulated, but enhanced by temperature effects, with both cooler- and heat stress conditions accelerating it (Thomas & Stoddart, 1980; Fracheboud *et al.*, 2009). It can be debated as to when senescence actually sets in for a grapevine during the growth season, but it seems that the physiological symptoms of senescence set in well in advance of visual symptoms (leaf yellowing and abscission). This of course depends on the definition of senescence, which in some cases are associated with initial reductions in leaf chlorophyll content and decreased photosynthetic activity in leaves (Poni *et al.*, 1994b).

Although several studies monitored shoot growth, particularly its cessation, specific guidelines or thresholds for monitoring are not always provided. Coipel *et al.* (2006) evaluated shoot growth cessation from observations of the shoot apex. Apexes were sampled on several dates and a value of “2” was attributed to an actively growing apex, “1” to an apex of which the growth was starting to slow down (defined as an apex that is hidden when the last two established leaves are folded together), and “0” to a dried apex showing no growth activity. This is also an approach that is used by trained viticulturists in the field to monitor plant water status along with the reaction of the second tendril (usually dropping under stressful conditions) relative to the growth tip of a shoot (Archer, E., personal communication). Van Leeuwen *et al.* (2004) considered shoot growth to have ceased when the mean growth within a plot was less than 5 mm/day, with the total shoot length at growth cessation used as an indicator of vine vigour.

The period from budburst to flowering is important for the initiation and differentiation of inflorescence primordia (Swanepoel & Archer, 1988), with the light environment of the canopy playing an important role to improve bud fruitfulness (Smart *et al.*, 1982; Hunter & Visser, 1990b; May, 2000). During this period, suckering (removal of infertile shoots that are not allocated during pruning) is therefore often performed when shoots are shorter than 30 cm. The excision of shoots also potentially removes major sources of auxins and gibberelin and is likely to increase the availability of nutrients and root-produced metabolites such as cytokinins to the remaining parts because of the increased root:canopy ratio (Herold, 1980). Shoot removal (or more severe pruning) could cause increased vigour, as the plant aims to re-establish its root:shoot ratio (Clingeffer, 1984). Grapevines with higher shoot numbers also tend to show earlier cessation of shoot growth, along with reduced lateral bud break (Keller, 2010).

Leaf thinning can lead to compensatory increases in photosynthesis in remaining leaves as well as a delay in their senescence (Hunter & Visser, 1988; Hunter & Visser, 1989; Candolfi-Vasconcelos & Koblet, 1991; Hunter *et al.*, 1995; Iacono *et al.*, 1995), but if excessive, the compensation may not be sufficient, with resulting negative effects on fruit composition and ripening (Petrie *et al.*, 2000). Grapevines have a strong capacity to compensate for a loss in leaf area through changes in photosynthetic activity, export of carbohydrates and re-translocation of carbohydrate reserves (Johnson *et al.*, 1982; Hunter & Visser, 1988; Candolfi-Vasconcelos & Koblet, 1990; Candolfi-Vasconcelos *et al.*, 1994).

Partial or total crop reduction in grapevines may lead to premature leaf senescence, which may be triggered by surplus sugar accumulation in leaves (Rolland *et al.*, 2002; Lim *et al.*, 2007; Keller, 2010). Early fruit removal or loss may be compensated for by stimulated growth of remaining fruit, leading to berry size increases (Keller *et al.*, 2008).

Poni & Giachino (2000) pointed out the limited value of total leaf area:fruit ratio as an indicator of grape quality (untripped shoots had a significantly higher ratio than trimmed vines, but similar vine performance), thereby justifying the need to assess also the 'quality' of the source, i.e. the 'effective' leaf area:fruit ratio.

The goal of this study was to assess the interactive effects of canopy manipulation and water deficit on pruning mass, shoot characteristics, grape ripening and harvest parameters in Shiraz, laying the foundation for determining the interactions between age, structure and pigment content of leaves in reaction to the modified conditions.

3.2 Materials and methods

3.2.1 Vineyard

Experiments were conducted in a *Vitis vinifera* L. cv. Shiraz (clone SH9C) vineyard grafted on 101-14 Mgt (*Vitis riparia* x *Vitis rupestris*) rootstock. The vineyard was established in 2000 with a north-south row direction on a flat terrain at the Welgevallen experiment farm of the Department of Viticulture and Oenology, Stellenbosch University, South Africa (33°56'S, 18°52'E, 157 m mean height above sea level). The Stellenbosch winegrowing region is characterised by a Mediterranean climate. Vines are spaced 2.7 x 1.5 m and trellising consisted of a 7-wire hedge trellis system (vertically shoot positioned) with three sets of moveable canopy wires. Irrigation was applied using a pressure compensated drip system spaced 40 cm, at a rate of 2.3 L/h. Spur pruning was applied. In this chapter, "season one" refers to the 2008/09 growing season, "season two" to the 2009/10 growing season, and "season three" to the 2010/11 growing season.

3.2.2 Experiment layout and treatments

The experiment was designed according to a split-plot design incorporating six main plots with an irrigation treatment assigned to each, namely non-stressed (NS) and stressed (S), with two sub-plots of 12 grapevines each subjected to a different canopy manipulation treatment, namely full canopy (F) or reduced canopy (R) (refer to Figure 69 and Figure 70 in Addendum A). In season three the trial layout was modified to represent the same main plots, but sub-plots were modified to 18 sub-plots of three grapevines each for the canopy manipulation treatments. The irrigation trial was set up according to measurements of predawn leaf water potential (Ψ_{PD}), with targets for NS and S grapevines of less negative than -400 KPa and less negative than -1700 KPa, respectively. For the canopy reduction treatment, shoot removal was performed at 19 DAB in season one and 55-60 DAB in seasons two and three by removing the apical shoot on a two-bud spur, followed by suckering to a single shoot per bearer (Figure 15). In season three, secondary shoots were continuously removed in the lower 25-30 cm of the reduced canopy treatment (bunch zone), to study the effects on fruit composition when the compensatory secondary shoot growth is not present.

3.2.3 Climate measurements

Temperature data was obtained from a weather station approx. 1500 m from the vineyard (Heritage Garden, Infruitec, Stellenbosch, Lat -33.92714; Long 18.87226, Alt 112 m, courtesy of the Agro-Climatology Division of the Institute of Soil Climate and Water of the Agricultural

Research Council: Agro-Climatology, ARC – ISCW, Pretoria, ZA). Thermal time (TT) or heat units expressed in degree days ($^{\circ}\text{C}\cdot\text{day}^{-1}$) (Winkler & Williams, 1939; Gallagher, 1979; Schultz, 1992) was calculated daily from budburst from Equation 1, with the base temperature representing a theoretical lower limit for growth of the grapevine (accepted to be 10°C) (Schultz, 1989). The accumulation of TT was started at phenological Stage EL5 according to the Eichhorn-Lorenz system, as adapted by Coombe (1995). This stage, hereafter referred to as budburst, corresponded to a stage when 50% of the shoots were 2 cm long, their first leaves have unfolded and the leaves have reached a length of approximately 20 mm. After this stage leaf and shoot measurements could be conducted easily.

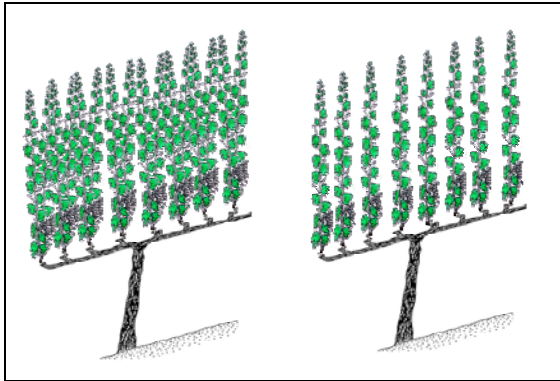


Figure 15 Illustration of the canopy reduction treatment imposed (secondary shoots not shown). Left: full canopy, right: reduced canopy suckered to a single shoot per spur position.

Equation 1 Thermal time calculation

$$TT = \sum_{i=1}^n \frac{(T_{\max,i} + T_{\min,i})}{2} - T_b$$

TT – thermal time

T_{\max} , T_{\min} - maximum and minimum temperatures

T_b - base temperature

3.2.4 Soil and plant water status

Soil water status was determined using a 503 DR Hydroprobe Neutron Depth Moisture Gauge (Campbell Pacific Nuclear International Inc., CA, USA) at three depths (0-30 cm; 30-60 cm and 60-90 cm) throughout the growing season. For all the treatments, pre-dawn leaf water potential (Ψ_{PD}) was determined using a pressure chamber on fully expanded leaves on primary shoots, according to Scholander *et al.* (1965). Classification of values were done by combining suggested categories from (Carbonneau, 1998) and (Deloire *et al.*, 2004) in Table 9. The latter reference also specifies vegetative and reproductive growth and physiological implications of some of these levels.

Table 9 Classification of Ψ_{PD} values adapted according to existing literature.

Class	Ψ_{PD} range (-kPa)	Classification of plant water status
1	0-200	Water stress absent
2	200-400	Mild to moderate water stress
3	400-600	Moderate to severe water stress
4	600 to 900	Severe water stress
5	900+	Critical water stress

3.2.5 Light measurements

The ratio of red:far red (660:730 nm) radiation was measured in the bunch zone for the full and reduced canopy treatments about a month after the treatments were carried out using a R:FR sensor (Skye instruments, Powys, UK). An AccuPAR LP-80 Ceptometer, Decagon Devices, Inc., Pullman, WA was also used to perform canopy light measurements on 178 DAB in season two. The measurements were performed at solar noon in the bunch zone for the NSR and NSF treatments, and are expressed as a ratio of ambient radiation measured in units of $\mu\text{E}\cdot\text{m}^{-2}\cdot\text{s}^{-1}$.

3.2.6 Vegetative measurements

3.2.6.1 Pruning measurements

All grapevines in the experiment were pruned during full dormancy to two-bud spurs and dormant canes were weighed and counted for each vine. Detailed cane measurements were performed on a sub-set of the pruned shoots, and it included primary cane length, number of secondary shoots and total length of secondary shoots per primary cane as well as the node number on primary canes. The apical sections of each primary cane were also inspected, and it was noted if it had been topped or not.

3.2.6.2 Shoot growth, leaf length and leaf plastochron index (LPI) measurements

Shoot length was monitored on shoots tagged from the beginning of the growth season on different grapevines throughout the season. Due to wind damage in both seasons as well as shoot topping performed in the first season, shoots had to be changed during the season and only a limited number of shoots could be monitored throughout the season. Non-linear least-square regression analysis of shoot growth can be performed on a chronological or thermal time basis (Lebon *et al.*, 2004; Tarara *et al.*, 2009). Due to the nature of shoot growth in the grapevine, logistical growth curves are the most appropriate to use in shoot growth analysis. An example of a logistical growth curve is shown in Figure 16, with the accompanying formula used to calculate indicated parameters shown in Equation 2.

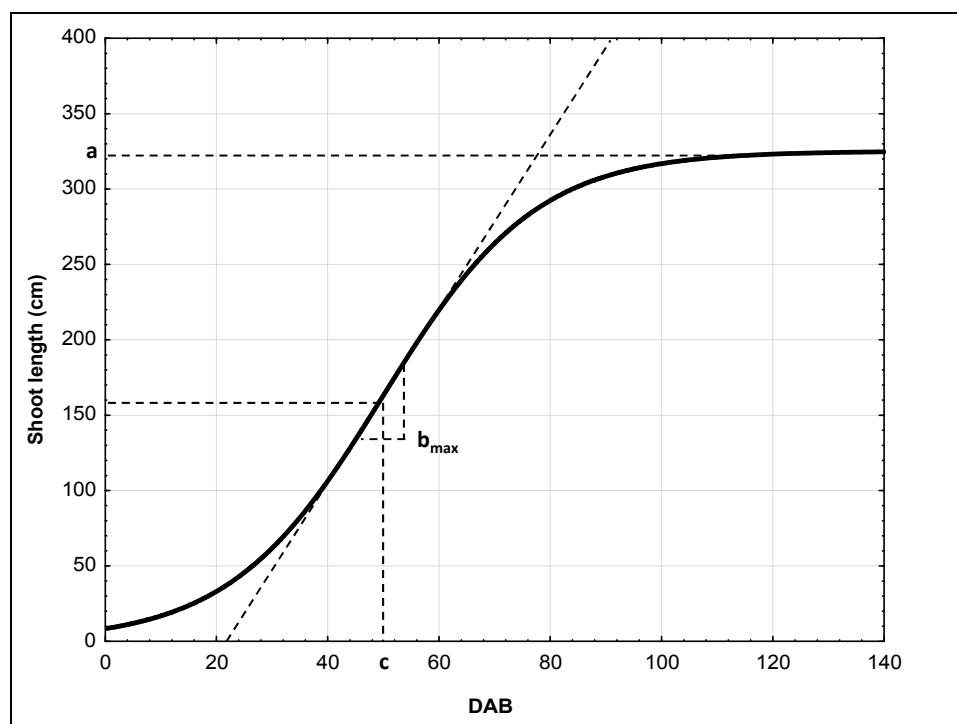


Figure 16 Example of logistic shoot growth curve and parameters measured.

The parameter x can be expressed relative to chronological or thermal time. Shoot growth rate can be calculated from the first-order derivative of the curve shown in Figure 16, using Equation 3. This equation has the same parameter definition as Equation 2, only differing in parameter b , representing the response coefficient of the curve.

For a selection of shoots (refer to Chapter IV), leaf main vein (L1) lengths as well as the shoot plastochron index (PI) and leaf plastochron index (LPI) of each leaf were also measured.

Equation 2 Equation of logistical growth curves used to determine growth curve fit parameters.

$\text{Shoot length } (y) = \frac{a}{1 + \exp[b_{max}(x - c)]}$	
a	theoretical maximum shoot length attained
c	x-value at the inflexion point midway respective to the shoot growth duration (number of days required to reach 50% of a)
b_{max}	maximum slope around the inflexion point
x	chronological or thermal time (days after budburst)

Equation 3 Equation used to determine the derivative of the growth fit curve.

$\frac{dy}{dx} = -b \cdot y \left(1 - \frac{y}{a}\right)$	
b	– response coefficient of the growth curve (Refer to Equation 2 for a description of the other parameters)

3.2.6.3 Leaf area

For each of the measurement dates shown in Table 10, three to eight shoots were collected from different grapevines per treatment.

Table 10 Leaf area measurement dates for the different seasons.

Season	DAB	Measurement details
1	61	Eight shoots each for F/R (all from NS), all secondary shoots quantified
2	213	3 primary shoots per treatment.
3	142	Six primary shoots each for F/R all main plots, NS only, all secondary shoots quantified

Leaf area was measured destructively for each leaf on primary and secondary shoots separately, using an electronic leaf surface area meter (Delta-T devices Ltd, Cambridge, UK), and leaf L1 length was also determined for a sub-set of shoots. The leaf area meter was calibrated using a white paper with a calibration line prior to measurements. Regressions were created between the square of the leaf L1 length and individual leaf area (Poni *et al.*, 1994b). Each primary shoot length was recorded along with the total length of all secondary shoots as well as the number of secondary shoots. Only secondary shoots that exceeded 5 cm in length were recorded.

3.2.7 Reproductive measurements

3.2.7.1 Berry sampling and analyses

Berry development was monitored on 50-berry samples collected randomly from véraison onwards in the different sub-plots within the trial. Total soluble solid concentration (TSS) was determined using a digital pocket refractometer (Atago PAL-1, Tokyo, Japan). Titratable acidity (TA) was measured with an automatic titration device (Metrohm 785 DMP Titrino, Herisau, Switzerland) and pH using a bench pH meter (Crison Basic 20 with Crison 5531 PT1000 electrode, Barcelona, Spain). Berry fresh mass (g) and volume (mL) were determined by weighing or water displacement, respectively.

3.2.8 Statistical analysis

Statistical analysis was conducted using Statistica 10 ® software (Statsoft, Tulsa, UK) and Unscrambler® 9.2 (CAMO PROCESS AS, Oslo, Norway). For analysis of pruning and yield data, a mixed model repeated measures ANOVA was used. The statistical package R (Version 2.14.0, the R Foundation for Statistical Computing) was used in conjunction with Statistica 10 (programming for integration with courtesy of prof M Kidd, Director of the Centre of Statistical Consultation, Stellenbosch University) for performing logistic growth curve fitting and analysis according to the procedures described by Ritz & Streibig (2005), using the ‘drc’ package in R developed by the same authors to analyse dose response curves.

3.3 Results and discussion

3.3.1 Climatic data

Marked differences in climatic data were found between the three seasons. The date of budburst for this vineyard differed from season to season, the latest budburst being recorded in season one. A total of 163 mm of rainfall was recorded a month before budburst in season one compared to 91 mm in season two and only 23 mm in season three (see Addendum B). This most likely caused lower soil temperature, which may have delayed budburst as well as initial shoot growth. Cool and rainy conditions prevailed until quite late during season two. This is evident from the daily and accumulated thermal time results in Figure 17 and Figure 18. In general, temperatures were lower during most of the growing season in season two, whereas for season three, lower temperatures were recorded earlier (before 80 DAB) in the season, with the latter part showing the highest mean temperature of all seasons.

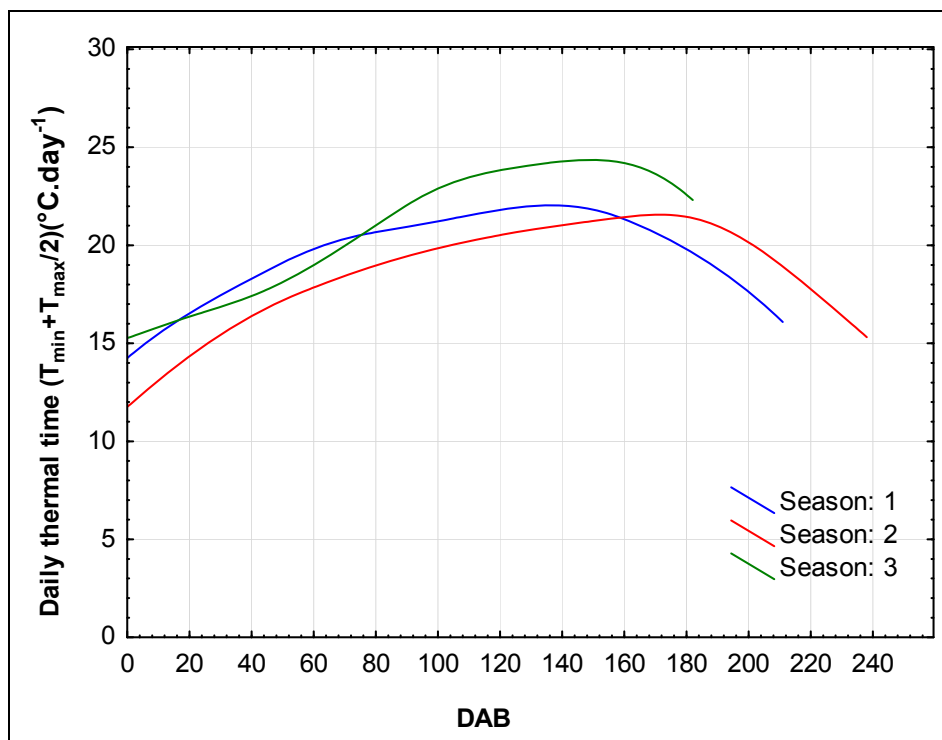


Figure 17 Daily thermal time ($^{\circ}\text{C}\cdot\text{day}^{-1}$) relative to date after budburst (DAB) calculated for the different seasons and shown using a distance-weighted least squares fit.

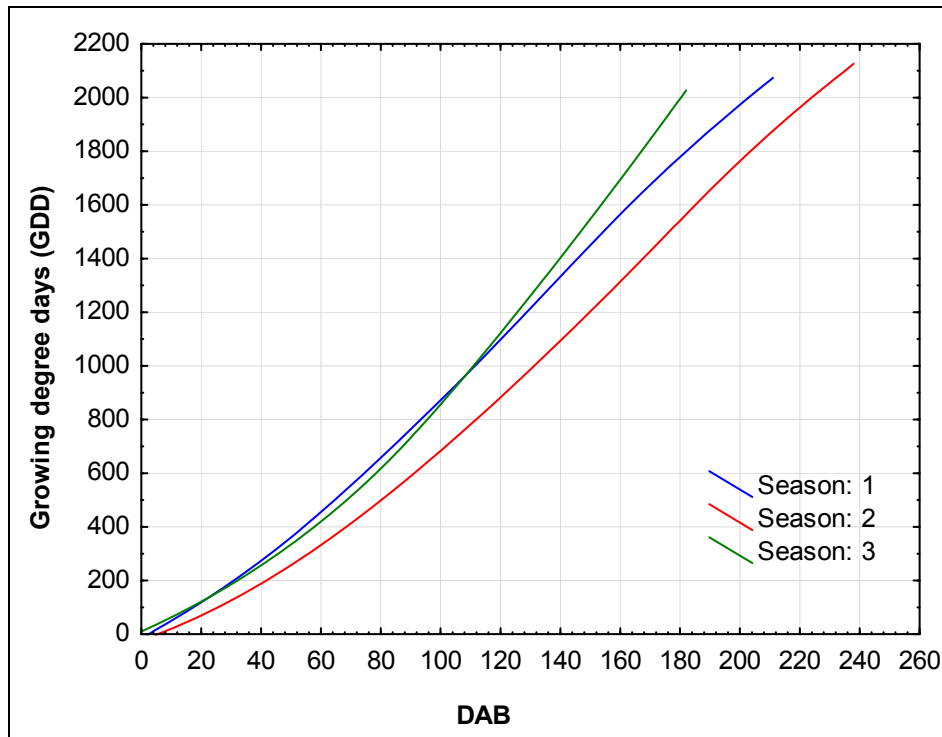


Figure 18 Growing degree days (GDD) relative to date after budburst (DAB) calculated for the different seasons and shown using a distance-weighted least squares fit.

3.3.2 Soil water status

It was expected that the canopy reduction treatment would increase the gap fraction in the vineyard, but compared to the full canopy treatment, it could possibly lead to increased air flow as well as transpiration and consequently water use. However, this seems to be negated by the reduction in leaf area brought about by the treatment, possibly leading to lower transpiration per unit leaf area (higher photosynthetic efficiency). In addition to this, the reduced canopies, with relatively increased secondary shoot leaf areas in seasons one and two (refer to Section 3.3.5.2), possibly had higher water use efficiency in the canopy in the remaining, as well as newly developed leaves. This is in accordance with Palliotti *et al.* (2011) and Flore & Lakso (1989) hypothesising that a severe source reduction may lead to newly developed leaves benefitting from increased root supply of nutrients, water and hormones, conversely leading to more efficient leaf tissue in the mature stages. The canopy manipulation treatment seemed to be more important in determining soil water depletion, compared to the irrigation treatment (Figure 19 and Figure 20), with the full canopies generally showing lower soil water content as measured by neutron count ratios compared to the reduced canopies. The reduced canopy, cultivated under essentially rain-fed conditions, seemed to have resulted in a wetter 90 cm soil layer (data not shown). This may be the result of less depletion of water from the 0-60 cm layers, where the highest root concentration is expected, leading to more drainage towards the 90 cm layer as a consequence of a smaller leaf transpiration surface area. In season three, the full canopy seemed to react different from the other two seasons, with the intensively irrigated treatments showing lower soil water contents than the non-irrigated treatments. A possible explanation for this could be that the cooler conditions during the initial part of this season led to more growth, with the full canopy possibly having a larger transpiration surface when conditions changed later in the season. When water was applied, the vines did not seem to regulate well under these conditions, leading to fast transpiration and increased extraction of soil water. *Vitis vinifera* cv. Shiraz generally seem to display anisohydric (“optimistic”) behaviour (Schultz, 2003a). The reduced canopies in seasons one and two used less

water, and soil was wetter due to more rain during these seasons. This was not the case in season three, leaving soils much drier than during the other two seasons, especially for the SR and NSF treatments, the former not receiving water, and the latter seemingly transpiring most of the water received.

Heilman *et al.* (1996) found that grapevine water use was increased for a sprawling-type canopy compared to a restricted hedge trellis, due to higher canopy latent heat flux per unit leaf area in the open canopy. In studies that attempt to model grapevine evapotranspiration, the decrease in porosity or gap fraction of the canopy is an important parameter that needs to be estimated along with the increase in canopy dimensions during the season (Lebon *et al.*, 2003). Canopy gap fraction can be estimated from digital image analysis (Trambouze & Voltz, 2001; Williams & Ayars, 2005) and generally a decrease in gap fraction would mean increased transpiration as linked to the transpiration models (in terms of the inference of a larger canopy when gap fraction decrease). Trambouze & Voltz (2001), however, found that differences in gap fraction from 5 to 16% would only decrease transpiration by 1.6%.

It seems very important not to underestimate the importance of canopy size and the transpiration of available soil water when irrigating grapevines, especially considering the physiological behaviour of Shiraz. From the results of all seasons, the full canopy treatments (especially NSF) consistently tended to extract more water from the soil. As a consequence of soil available water as well as canopy size, soil water extraction curves of the full- and restricted canopy vines are closer together under stressed conditions. The amounts of irrigation water applied to the treatments are shown in Addendum B.

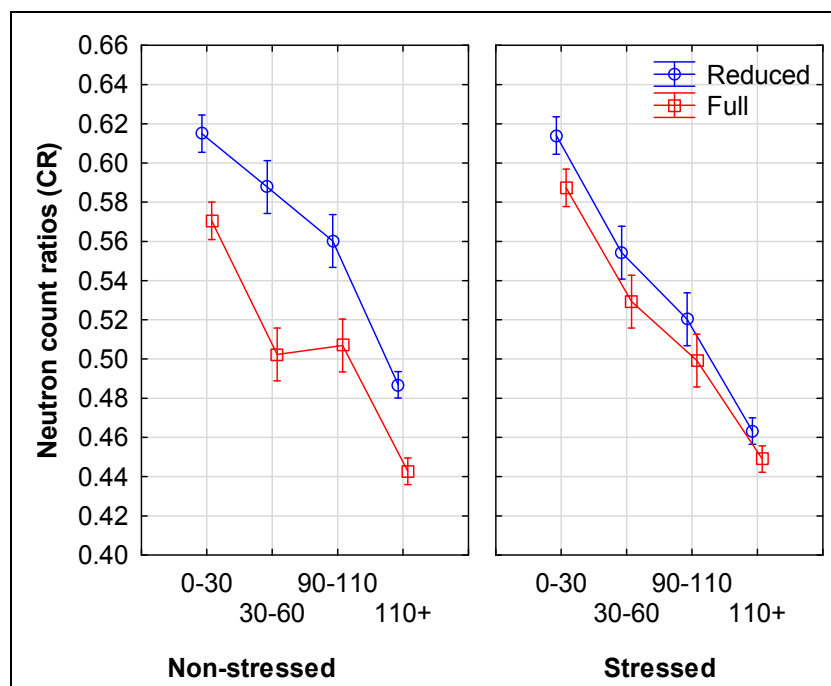


Figure 19 Neutron count ratios (CR) relative to date after budburst (DAB) categories (30-day intervals) shown for the different irrigation and canopy manipulation treatments for the second season (means calculated over 0-90 cm depth levels). Vertical bars denote 95% confidence intervals.

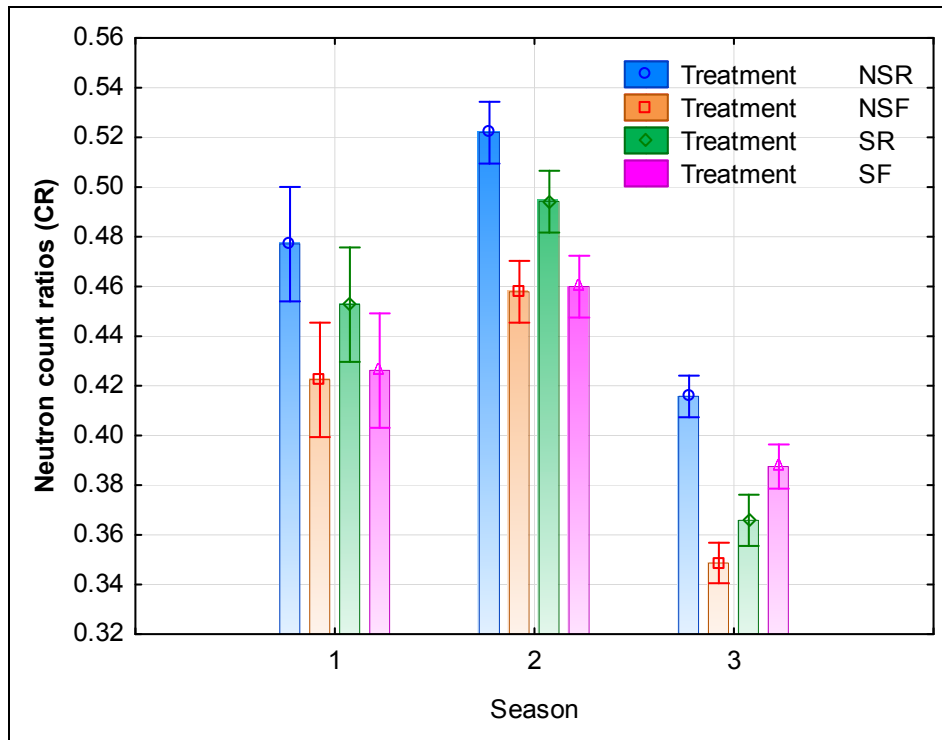


Figure 20 Neutron count ratios (CR) shown for the different irrigation and canopy manipulation treatments as well as seasons, with only dates after 110 DAB shown and the 90 cm depth level excluded. Vertical bars denote 95% confidence intervals.

3.3.3 Plant water status

The mean predawn leaf water potential (Ψ_{PD}) values for the three seasons, and all treatments combined, over time (Figure 21) generally transcended the threshold from class 1 (no stress) to class 2 after about 80 DAB, with values increasing to classes 3 and higher (moderate to severe) after about 100 DAB.

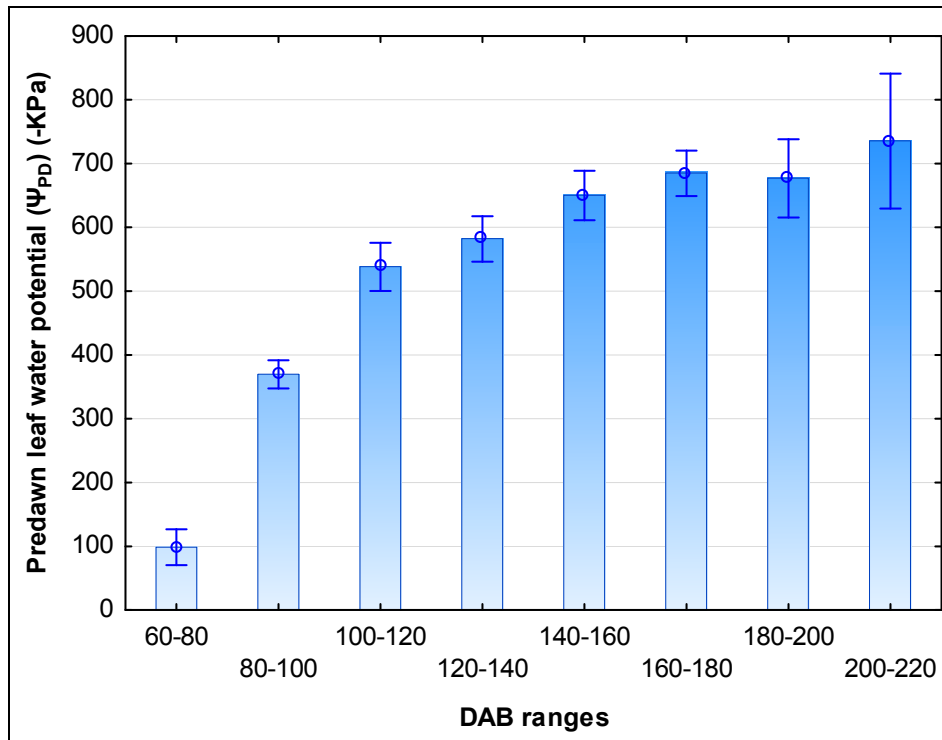


Figure 21 Predawn leaf water potential (Ψ_{PD}) relative to date categories (20 day intervals) shown for the mean values calculated over all three seasons and all the treatments. Vertical bars denote 95% confidence intervals.

In order to evaluate the results from leaf pigment measurements conducted in season one (refer to Chapter V for the analysis), it was assumed that water stress, as quantified using predawn leaf water potential measurements, was absent between 0 and 80 DAB (concurrent with the classes described in Table 9) (Figure 22). During this period, the canopy treatment effect is therefore considered as a dominant microclimate effect, considering possible interactions between plant water status and the canopy manipulation treatments later in the different seasons (discussion later in this section). Figure 23 to Figure 27 indicate results from Ψ_{PD} measurements throughout the different seasons. The first irrigation was applied at 107 DAB in season one and Ψ_{PD} measurements only commenced in the S treatments after this. With respect to measuring dates C and D it was considered that the NSR treatments have lower Ψ_{PD} values than the NSF treatments, and that the Ψ_{PD} values on measurement date D was higher (more negative) than that of measurement date C. These assumptions are confirmed by consistent seasonal trends in the treatments (lower values seemed to persist for NSR treatments) as well as lower soil water contents observed in the NSF *versus* NSR treatments. Furthermore, the boundaries of values for which these assumptions are made, transcend the classification of water status previously reported in literature (refer to Table 9).

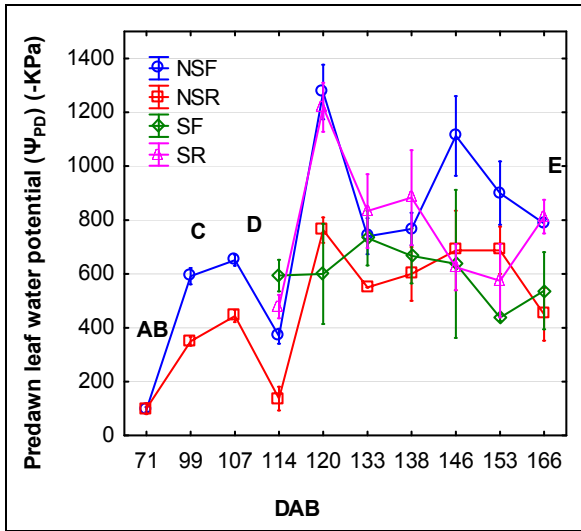


Figure 22 Predawn leaf water potentials (Ψ_{PD}) relative to date after budburst (DAB) for the treatments in season one (including specified measurement dates for pigment sampling indicated as letters from A to E) (means with +/- standard errors shown).

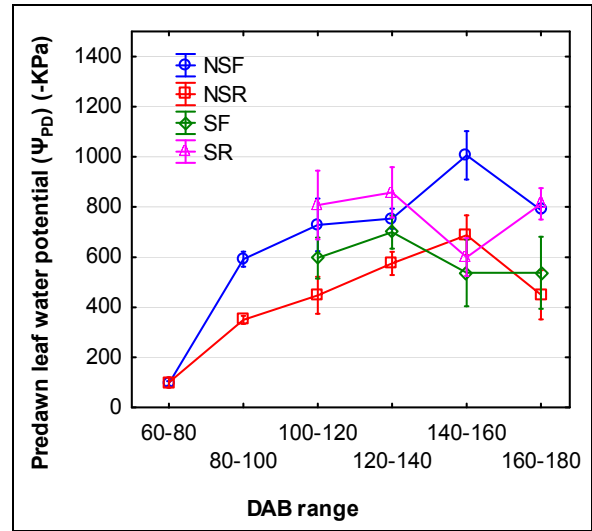


Figure 23 Predawn leaf water potentials (Ψ_{PD}) relative to date categories (20-day intervals) for the different treatments in season one (means with +/- standard errors shown).

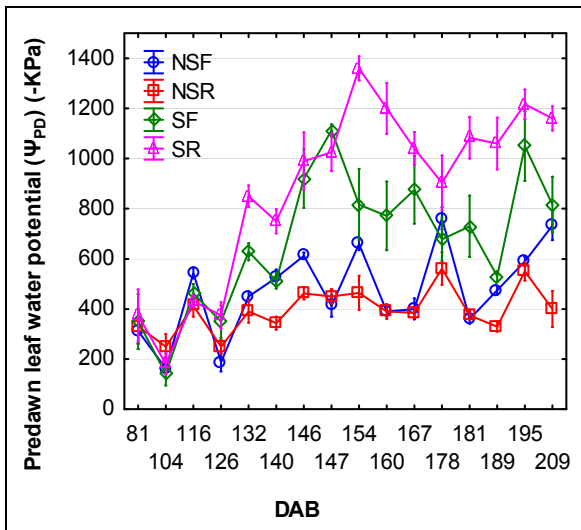


Figure 24 Predawn leaf water potentials (Ψ_{PD}) relative to date after budburst (DAB) for the different treatments in season two (means with +/- standard errors shown).

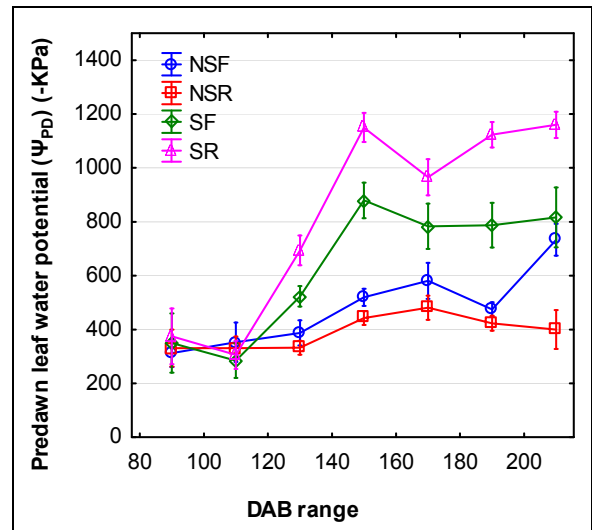


Figure 25 Predawn leaf water potentials (Ψ_{PD}) relative to date categories (20-day intervals) for the different treatments in season two (means with +/- standard errors shown).

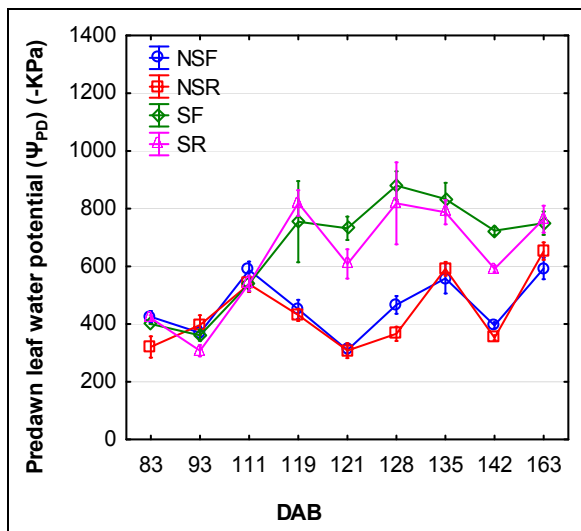


Figure 26 Predawn leaf water potentials (Ψ_{PD}) relative to date after budburst (DAB) for the different treatments in season three (means with \pm standard errors shown).

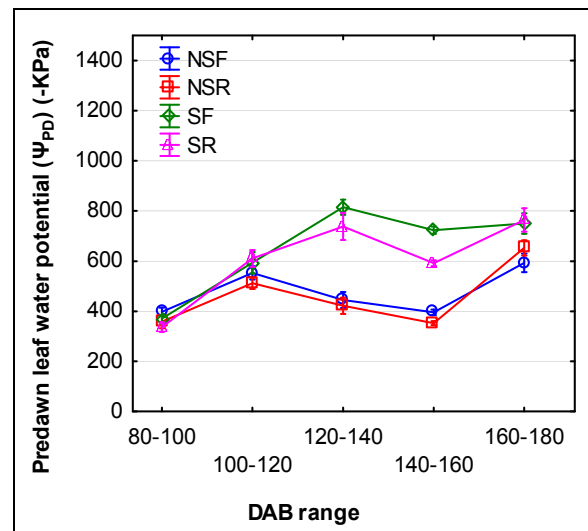


Figure 27 Season three predawn leaf water potentials (Ψ_{PD}) relative to date categories (20-day intervals) for the different treatments in season three (means with \pm standard errors shown).

Relatively high negative mean Ψ_{PD} values were measured for the NSF treatment during season one (Figure 28). It is possible that during this relatively warm season, the larger transpiration surface in the full canopies led to more negative Ψ_{PD} values than for the NSR canopies. This is in accordance with studies finding that larger leaf areas deplete soil water faster and lead to earlier stomatal closure (Schultz, 2003a). The relative slow response of Shiraz with respect to stomatal closure, however, also have to be considered (Schultz, 2003a); this may lead to continuous transpiration even in water stress conditions. In seasons two and three, the amounts of irrigation water, as well as the intervals of irrigation applied to the NS treatments were increased, in an attempt to lower the Ψ_{PD} values for the NS treatments. For the “stressed” treatments, the reduced canopies tended to show more negative Ψ_{PD} values than the full canopies, except in season three. This may be due to much less and shorter secondary shoots per primary shoot present in season three (see Section 3.3.5.3), probably in reaction to the lower soil water contents in this season, but also aggravated by the removal of secondary shoots in the bunch zone. The higher water deficits in seasons one and two for the SR treatments may have been due to a significant increase in the secondary:primary shoot leaf area (refer to Table 15 in Section 3.3.5.3), and the previously observed higher transpiration rates of younger leaves in the canopy (Hunter & Visser, 1988; Schultz, 1989). It may be expected for more isohydric cultivars that a higher root:shoot ratio, which may be the case when shoots are removed as in this study, may lead to improved stomatal control. Here, the root:shoot ratio may not have increased that much, as the canopy was allowed to compensate for the reduction in leaf area during the first two seasons of the study. The same general trend was observed for season two (Figure 29), but it is interesting that the highest Ψ_{PD} values were registered in this season for the S treatment, even though it was the cooler and wetter of the three seasons. Crop load in terms of the yield:pruning mass ratio (refer to Section 3.3.5) appeared to be higher in season two, compared to the other seasons; this may have played a role. The larger differences between irrigation treatments observed in Figure 29 and Figure 30, compared to Figure 28, may be attributed to higher irrigation volumes applied to the NS treatments in seasons two and three, in an attempt to keep Ψ_{PD} values under the accepted threshold values. This also seemed to decrease the differences induced by canopy manipulation as observed for the NS treatments in season one.

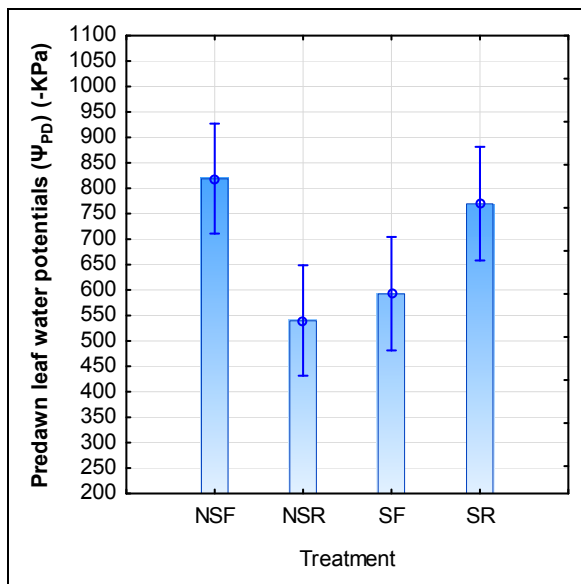


Figure 28 Predawn leaf water potentials (Ψ_{PD}) for the different treatments in the first season. Vertical bars denote 95% confidence intervals.

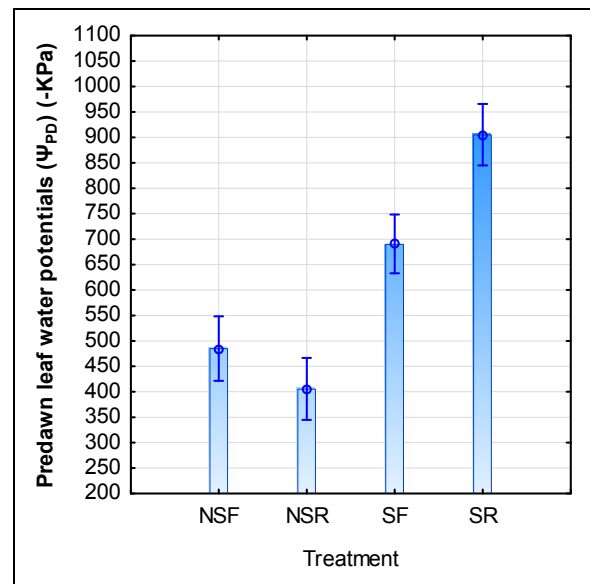


Figure 29 Predawn leaf water potentials (Ψ_{PD}) for the different treatments in the second season. Vertical bars denote 95% confidence intervals.

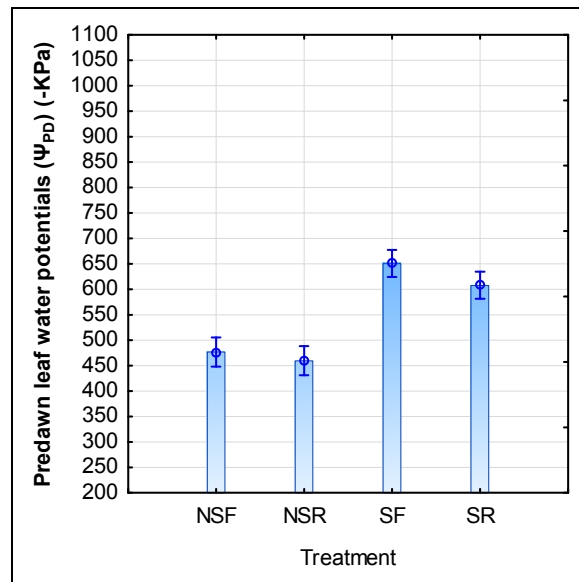


Figure 30 Predawn leaf water potentials (Ψ_{PD}) for the different treatments in the third season. Vertical bars denote 95% confidence intervals.

3.3.4 Light measurements

The reduced canopies in season one had significantly higher levels of red *versus* far-red radiation (R:FR) compared to the full canopies (Table 11). The measurements were conducted one month after the canopy manipulation treatment was applied (just prior to measurement date A in Season one). Dokoozlian & Kliewer (1995) reported that R:FR ratios in the fruit zone at berry set ranged from 0.58 to 0.40 in low density canopies and 0.2 or less in high density canopies, for which similar values were also previously found by Smart *et al.* (1988). They also reported R:FR ratios to decrease between fruit set and véraison, with values ranging from 0.52 to 0.35 for low density canopies to less than 0.1 for high density canopies. A relationship between the R:FR ratio and photosynthetic photon flux density ($r = 0.98$) was shown for a range of vineyard sites. In this study, even the reduced canopies seemed to correspond more to high-density canopy values found in literature, highlighting the vigour experienced at this site, especially where no canopy manipulation was done.

Table 11 Red:far red ratios measured in the bunch zone for the different canopy manipulation treatments on 52 DAB in season one (means with different letters are significantly different at the $p \leq 0.01$ level according to a Mann-Whitney t -test).

Treatment	R:FR means	N	SD
Full canopy	0.14 a	17	0.05
Reduced canopy	0.26 b	19	0.12
All measurements	0.20	36	

At the end of season two, measurements of photosynthetically active radiation (PAR) in the bunch zone indicated significantly lower values for the full canopies (140% lower). Light penetration values relative to ambient PAR radiation were reduced to below 2% for these canopies. Considering that these values are even lower than those reported for vertical canopies with 15% canopy gaps and 15% bunch exposure as well as 4.5 leaf layers (Volschenk & Hunter, 2001), these canopies can be considered excessively dense. Higher levels of variability were also observed in the measurements conducted in the reduced canopies, compared to those of the full canopies, indicating a more heterogeneous canopy distribution (Table 12).

Table 12 Photosynthetically active radiation (PAR) measurements performed 178 DAB in season two. Means with different letters are significantly different at the $p \leq 0.05$ level (Mann-Whitney t -test).

Treatment	Mean PAR ($\mu\text{E}\cdot\text{m}^{-2}\cdot\text{s}^{-1}$)	N	SD	Min PAR ($\mu\text{E}\cdot\text{m}^{-2}\cdot\text{s}^{-1}$)	Max PAR ($\mu\text{E}\cdot\text{m}^{-2}\cdot\text{s}^{-1}$)
Reduced canopy	70.7 [3.4]* a	15	75.7 [0.7]	13 [0.6]	252 [12.1]
Full canopy	29.5 [1.4] b	15	16.9 [0.7]	7 [0.3]	73 [3.5]
All treatments	50.1	30	57.8	7	252

* Values in square brackets represent calculations from % of ambient readings

3.3.5 Vegetative measurements

3.3.5.1 Shoot growth

Shoot growth was slow during the initial growth stages in season two, which could be ascribed to the lower TT/day values during the first 30 DAB. Even though budburst occurred almost a month earlier in season two compared to season one, shoots were much shorter at the same DAB due to more moderate temperatures in the early stages of shoot growth after budburst. This highlights the value of later pruning, where in similar seasons, later budburst would have been more beneficial. Differences in initial shoot growth and slower shoot growth, as observed in season two of this study, were also observed between seasons by Schultz (1992). Although the shoot growth curve was not affected, the initial lag in shoot growth in season two was sustained and shoots remained shorter than in the other two seasons (Figure 31).

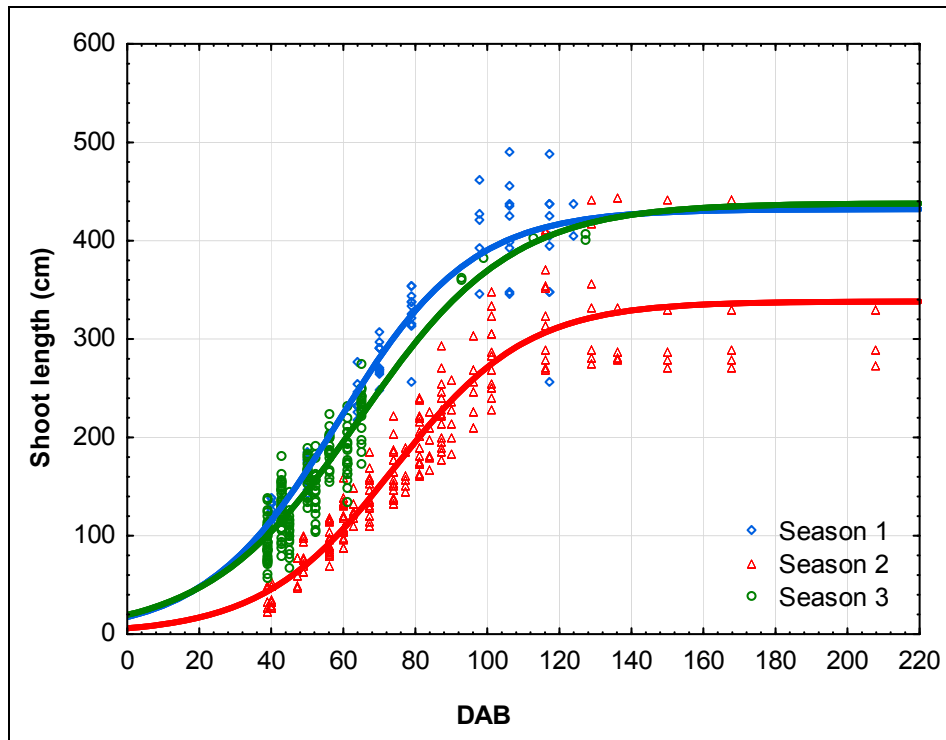


Figure 31 Fitted logistic growth curves of shoot length (cm) relative to date after budburst (DAB) for the different seasons (season one $R^2 = 0.95$; season two $R^2 = 0.94$; season three $R^2 = 0.95$).

Shoot growth rate ($\text{cm}\cdot\text{day}^{-1}$) for the different seasons is shown in Figure 32. Shoot growth less than $5 \text{ mm}\cdot\text{day}^{-1}$ was considered shoot growth cessation (Van Leeuwen *et al.*, 2004), which in this case also represented values of approximately one tenth of the maximum shoot growth rate. Before about 80 DAB, shoot growth was faster in the first and third seasons compared to the second season, which can be explained from the different thermal time/day values measured between these seasons. The reduced shoot growth rate in the third season compared to the first, despite similar thermal time values, may be explained by much lower soil water contents before budburst and also in general during this season. It would seem that ambient temperatures and soil/plant water status are major factors in shoot growth. It is also peculiar that season three, which in general showed the least negative Ψ_{PD} values, showed lower shoot growth rates than season one. Theoretical shoot growth cessation was reached for season one at ± 130 DAB and for seasons two and three at ± 140 DAB. Season one was characterised by the most negative Ψ_{PD} values in the period from 80 to 140 DAB, which probably led to about ten days earlier shoot growth cessation compared to the other two seasons. No re-growth of shoots was also observed after these dates in any of the seasons; this was also the case for secondary shoots. This is in contrast to findings by Lategan (2011), where re-growth was observed in all seasons of the study for grapevines that were exposed to high or severe water deficits before véraison, followed by more frequent irrigation during ripening.

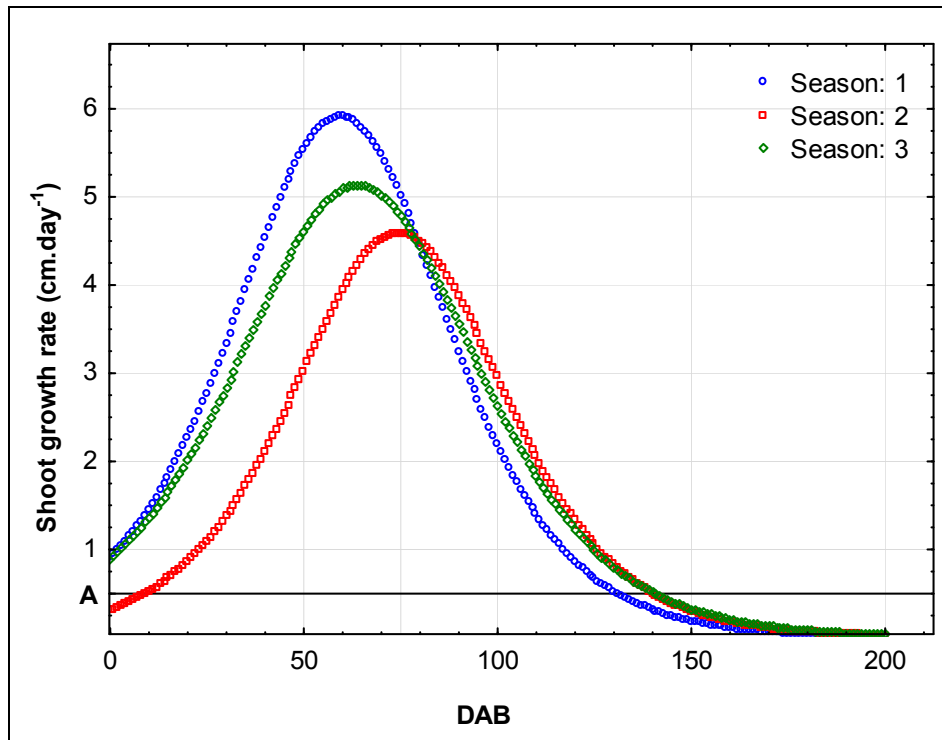


Figure 32 Shoot growth rate ($\text{cm}\cdot\text{day}^{-1}$) relative to date after budburst (DAB) for the three seasons. The reference line at A represents theoretical shoot growth cessation ($5 \text{ mm}\cdot\text{day}^{-1}$).

The maximum slope (b_{max}) calculated around the inflexion point (c) (Table 13) represents the maximum shoot growth rate for the specific fit (also visible in Figure 32). Other parameters were part of the fit estimation and therefore it was possible to perform a t -test on the data of the different shoots. Maximum shoot growth rate was reached significantly earlier in season one (Table 13), more than two weeks earlier than in season two. The lower sustained growth rate of the latter (until maximum shoot growth rate was reached), also led to a significantly lower maximum potential shoot length (upper asymptote, a) than in seasons one and three. The b -parameters indicate that the shape of the estimated fits of the curves was not significantly different.

Table 13 Estimated growth curve fit parameters related to shoot length (cm) measurements for the different seasons. Means with the same letters are not significantly different at the $p \leq 0.05$ level according to paired t -tests performed on the growth curve fit parameters.

Season	b	a	c	b_{max}
1	-0.054 a	432.09 a	58.58 c	5.90
2	-0.054 a	338.28 b	74.18 a	4.58
3	-0.047 a	438.11 a	64.49 b	5.13

Shoot length (cm) was also evaluated relative to growing degree days (GDD) and some changes could be observed in the growth fit calculations. Here, the c -parameters showed no significant differences, indicating that the differences in time required for shoots to reach maximum growth rate was now eliminated (i.e. shoots need similar thermal time units to reach the maximum shoot growth rate). The a -parameter was not affected by expressing shoot length relative to thermal time, but now a significant response coefficient (b) difference between seasons one and two was found, which was not previously detected. Season two had a significantly more negative response coefficient than season one (-0.0066 versus -0.0054). This was expected, as setting a constant c -parameter in Equation 3 would result in the response coefficient being only dependent on the asymptote a and the b_{max} value, which both differed in season two.

Growth fit curve parameters were also calculated for the different treatments in the respective seasons (Figure 33 to Figure 35).

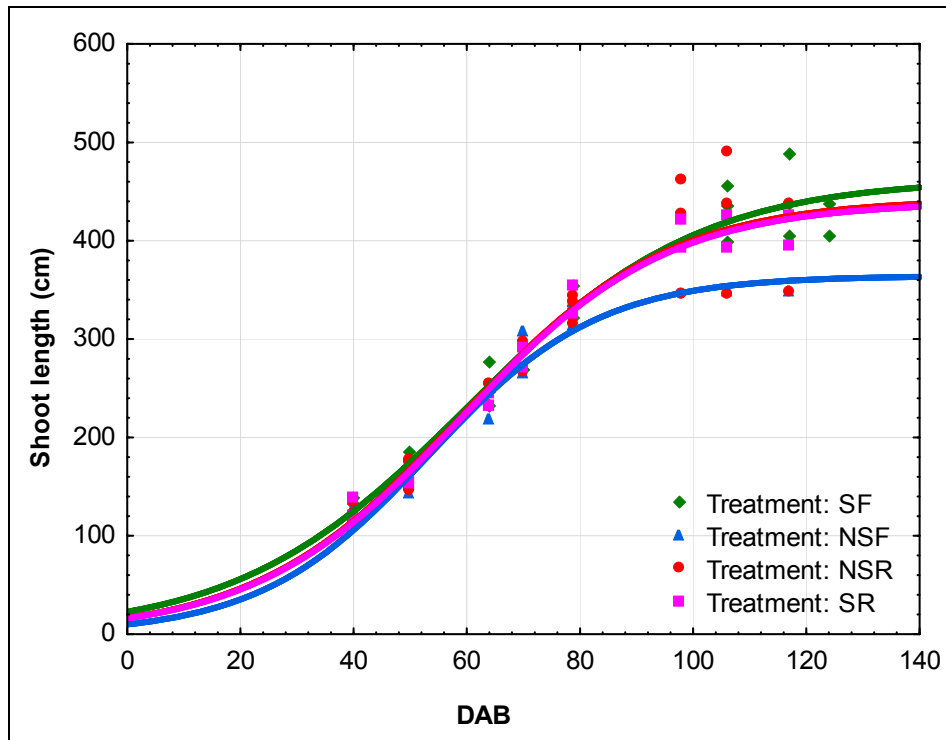


Figure 33 Fitted logistic growth curves of shoot length (cm) relative to date after budburst (DAB) for the different treatments in the first season (SF $R^2 = 0.98$; NSF $R^2 = 0.98$; NSR $R^2 = 0.95$; SR $R^2 = 0.99$).

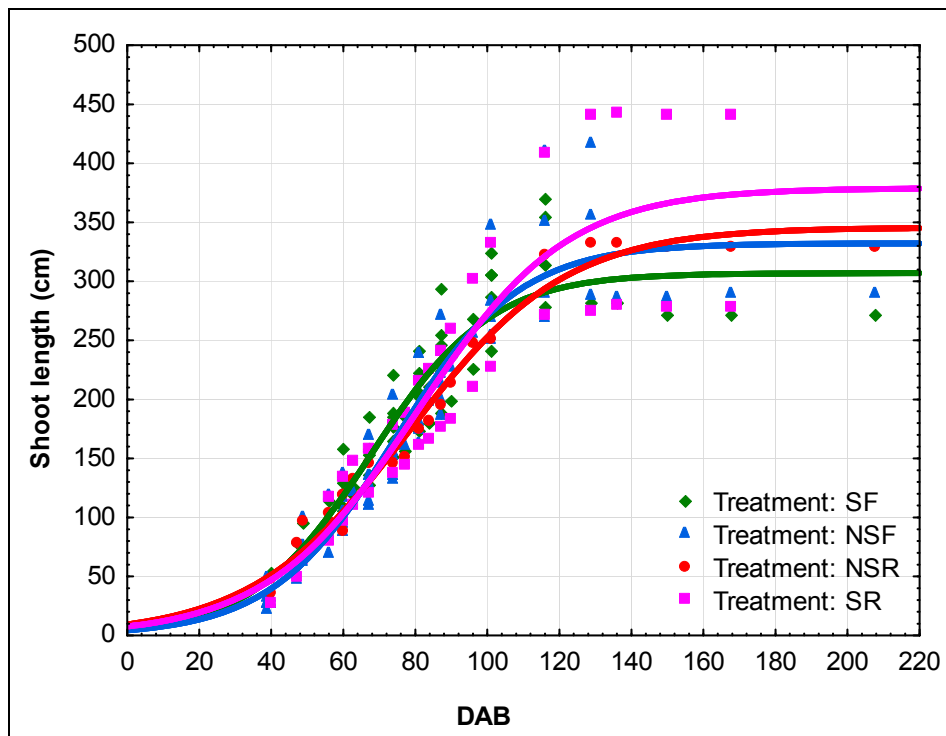


Figure 34 Fitted logistic growth curve of shoot length (cm) relative to date after budburst (DAB) for the different treatments in the second season (SF $R^2 = 0.93$; NSF $R^2 = 0.96$; NSR $R^2 = 0.99$; SR $R^2 = 0.90$).

In season three, logistical issues prevented sufficient measurements to be performed after 70 DAB for all treatments, therefore growth fit analysis was performed assuming similar shoot asymptotes (Figure 35). This was done by setting the a -parameter to a constant value, in this case the mean of

the shoot length values measured during leaf area analysis at 142 DAB when shoot growth has stopped. The transformed analysis showed that the maximum shoot growth rate was reached about five days earlier for the NS treatments (Table 14). The b -parameter of the SF treatment was significantly less negative than that of the NSR treatment, which is also shown by much lower maximum shoot growth rates measured for this treatment.

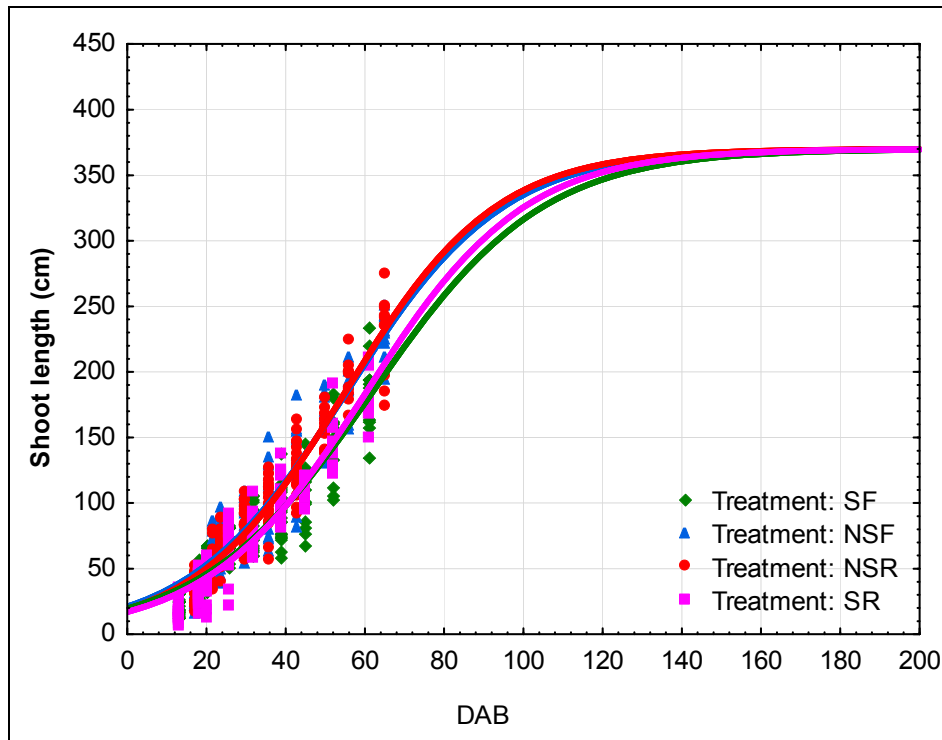


Figure 35 Fitted logistic growth curve of shoot length (cm) relative to date after budburst (DAB) for the different treatments in the third season, with the upper asymptote set to the mean maximum shoot length observed after cessation of growth (142 DAB) (NSF $R^2 = 0.94$; NSR $R^2 = 0.96$; SF $R^2 = 0.92$; SR $R^2 = 0.94$).

No significant differences could be detected in the b -parameters for treatments in seasons one and two, but the a -parameter for the NSF treatment was significantly lower in the first season (Table 14). This could have resulted from more negative Ψ_{PD} values leading up to shoot growth cessation in this treatment. In season two the NSF treatment also had significantly lower a -parameter values than the SR treatment, but care has to be taken interpreting the result from the SR treatment due to a single shoot that grew to almost 450 cm, against the expectation for the most stressed treatment in this season (see Figure 34). Shoot parameters were often found to be quite variable, for instance in season one the upper asymptote displayed a range in 95% confidence intervals of up to 80 cm for some treatments. This highlights the fact that care has to be taken when estimating parameters such as shoot growth cessation by only sampling a few shoots from a vineyard without considering the variability between shoots. Furthermore, it stands to reason that this variability also needs to be taken into account when leaf age estimations are done from shoot parameters (refer to Chapter IV). The only other significant difference observed in season two was for the SF treatment that reached maximum shoot growth rate earlier than the other treatments. It is not clear why this happened, as plant water deficits did not seem to differ a lot between treatments prior to this date (but it seems from all seasons as well as the comparison between seasons that shoots reaching this point earlier also seem to cease growth earlier). Leaf size was also found to be larger in this treatment (refer to section 3.3.5.2). The b_{max} values seemed similar between treatments in season one, but lower for the NSR treatment in season two. This parameter was, however, not part of the statistical analysis of individual shoots in the method used for growth curve comparison, therefore

(according to the formulae used) it could only be interpreted as significant, should all other parameters involved in its estimation also be significant. This was the case in season three, which means the NSR treatment had a significantly higher maximum shoot growth rate than the SF treatment. On the first date of Ψ_{PD} measurements (83 DAB) in season three, the NSR treatment seemed to have less negative values than the other treatments (Figure 26), but we did not perform measurements before this date to confirm this as the reason for increased shoot growth rates. It is interesting that the NS treatments showed significantly earlier *c*-parameter values (about 5 days) in season three, despite the fact that no irrigation was applied before 90 DAB. Considering that our main plots of the split plot design (the irrigation treatments) were still the same in season three compared to the previous two seasons, this could be a carry-over effect from the previous season. It is possible that the stressed treatments had fewer reserves available for initial shoot growth, therefore lagging slightly and reaching maximum shoot growth rate later in season three. In season two, budburst was severely delayed due to environmental conditions and the impact of reserves on initial shoot growth may have been lower under the more favourable growth conditions.

Table 14 Results from growth curve fit parameters related to shoot length (cm) measurements for the different seasons and treatments. Means with the same letters are not significantly different at the $p \leq 0.05$ level according to paired *t*-tests performed on the growth curve fit parameters.

Season	Treatment	<i>b</i>	<i>a</i>	<i>c</i>	<i>b_{max}</i>
1	SF	-0.049 a	462.97 a	60.22 a	5.70
	NSF	-0.067 a	364.40 b	53.33 a	6.10
	NSR	-0.055 a	442.54 a	58.99 a	6.08
	SR	-0.055 a	439.39 a	58.98 a	6.07
2	SF	-0.060 a	306.97 bc	67.73 b	4.61
	NSF	-0.058 a	332.23 b	74.36 a	4.82
	NSR	-0.046 a	345.67 ab	78.14 a	3.96
	SR	-0.048 a	379.04 a	80.45 a	4.57
3*	SF	-0.047 b	370*	61.98 b	4.32
	NSF	-0.051 ab	370*	55.42 a	4.46
	NSR	-0.053 a	370*	55.09 a	5.25
	SR	-0.050 ab	370*	60.39 b	3.85

* Season three upper asymptote was set to 370 cm prior to growth curve fit estimation.

Shoot growth ceased (according to the theoretical threshold) on different dates for the treatments in season one (Figure 36). This dataset was chosen for the shoot growth rate analysis as well as evaluating shoot growth cessation, as it had the highest number of shoots measured throughout for the different treatments until cessation. The NSF treatment ceased growth at 111 DAB, followed by the NSR and SR at 129 DAB, and the SF treatment at approximately 137 DAB. The latter treatment also showed the lowest maximum shoot growth rate. The earlier shoot growth cessation in the NSF treatment was probably due to increased soil/plant water deficits leading up to the date of cessation. A shoot growth restriction actually seemed to start from as early as 53 DAB (Figure 32 and Figure 36). It is possible that the environmental and internal factors that play a role in growth cessation do not exert their impact abruptly, but that an accumulative, probably synergistic effect, may lead to an almost linear decrease in the rate of shoot growth until cessation is reached. It may therefore be problematic to calculate leaf physiological age up to shoot growth cessation and then update it chronologically, for the simple reason that this date could be quite variable between shoots, possibly also due to differences in crop load on different grapevines and possibly

also shoots. Hardie & Martin (2000) addressed this issue by dropping the crop from selected grapevines, which were then used as “indicator vines” for irrigation scheduling.

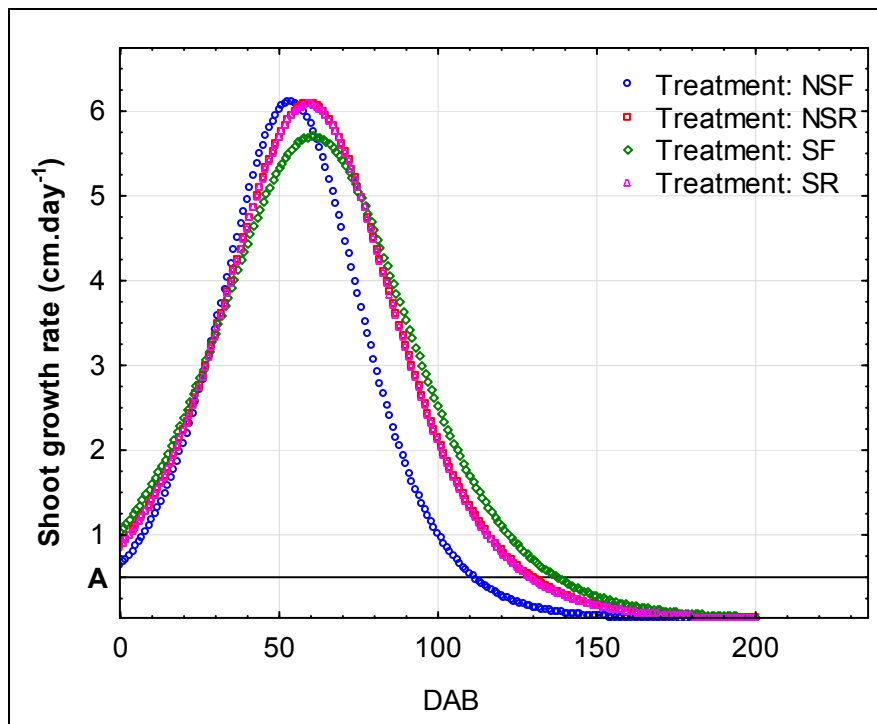


Figure 36 Shoot growth rate ($\text{cm}\cdot\text{day}^{-1}$) relative to date after budburst (DAB) in season one for the different treatments. The reference line at A represents a theoretical shoot growth cessation threshold of 5 mm/day.

3.3.5.2 Leaf area

Results from destructive leaf area analysis performed in season one are shown in Table 15. Canopy reduction led to increased primary and secondary shoot lengths as well as mean area per leaf on primary as well as secondary shoots. The total leaf area per primary and secondary shoot was increased in accordance with the lengths of these shoots. The mean leaf area per vine [considering mean shoot number per vine (refer to section 3.3.5.3) and the total leaf areas per primary and secondary shoot] of the different treatments showed values of $45\,132\text{ cm}^2$ and $55\,480\text{ cm}^2$ for the full and reduced canopies, respectively (determined for the NS treatments only). Canopy reduction also led to an increase in the total secondary leaf area:total primary shoot leaf area ratio.

Table 15 Shoot and leaf area data from destructive analysis performed on 61 DAB in season one (N=8 per treatment, significance is indicated according to a Student's *t*-test. Shoots were only collected from NS grapevines).

Treatment	Full (means)	Reduced (means)	% change	All treatments (means)	Significance ^a
Mean primary shoot length (cm)	183.80	267.50	46%	225.6	*
Mean secondary shoot length (cm)	19.40	56.00	188%	37.7	***
Primary shoot leaf size (cm^2)	133.00	167.60	26%	150.3	*
Leaf size on secondary shoots (cm^2)	44.90	70.50	57%	57.7	**
Total leaf area per primary shoot (cm^2)	1793.00	2570.20	43%	2181.6	*
Total leaf area of secondary shoots per primary shoot (cm^2)	1421.50	4122.20	190%	2771.8	***
Ratio secondary:primary leaf area	0.79	1.60			

^a (*, ** and *** indicate significance at $p \leq 0.05$, 0.01, 0.001 respectively)

The relationship between the area per leaf (cm^2) and leaf main (L1) vein length (cm) for primary and secondary shoot leaves corresponded to Schultz (1992) as well as Louarn *et al.* (2007), yielding an exponential relationship (Figure 37). It was previously noted that the ratio of leaf width to leaf length changes as leaves age, probably due to differential expansion of the leaf blade (Elsner & Jubb, 1988), which explains why an exponential relationship is observed. Alternatively, a linear regression can be calculated between the square of the leaf main vein length and the area of the leaf (Figure 38), which is shown as a combined graph for all the leaf area calibration datasets in Figure 39. The calibration equation created in the first season was used to predict leaf area in the second season, followed by a comparison of the predicted values to those measured in the second season. This yielded an excellent ($R^2 = 0.97$) correlation and a root-mean square error of prediction (RMSEP) of 14.4 cm^2 (Figure 40). Predicted leaf area per shoot [calculated from leaf lengths measured on a shoot and the regression equation: $\text{area per leaf (cm}^2\text{)} = -3.36 + 1.135 (\text{leaf } L1^2)$ ($R^2 = 0.97$)] yielded an excellent correlation ($R^2 = 0.93$) with primary and secondary shoot length (Figure 41). The same equation was used to estimate leaf area for both shoot types in further work, as separate correlations did not improve the correlation coefficients or modify the regression equation significantly (data not shown).

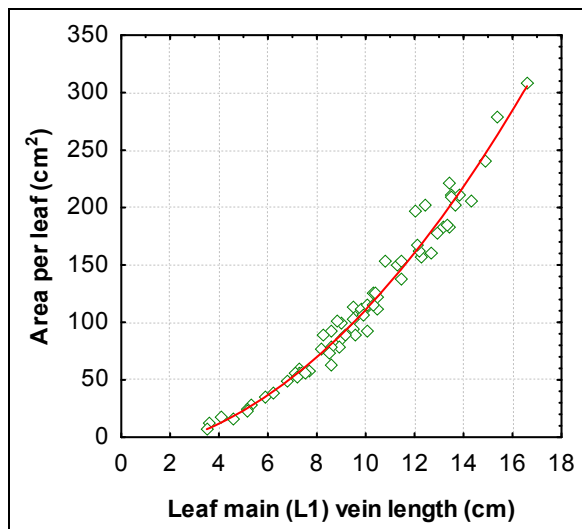


Figure 37 Relationship between the area per leaf (cm^2) and the leaf main vein (L1) length (cm) measured in the second season for primary and secondary shoot leaves ($y = -13.04 + 2.11x + 1.03x^2$; $r = 0.97$).

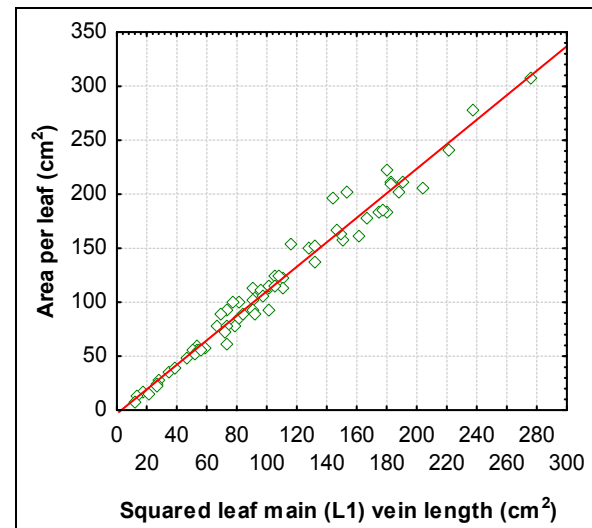


Figure 38 Relationship between the area per leaf (cm^2) and the squared leaf main vein (L1) length (cm^2) measured in the second season for primary and secondary shoot leaves ($y = -3.36 + 1.135x$; $R^2 = 0.97$).

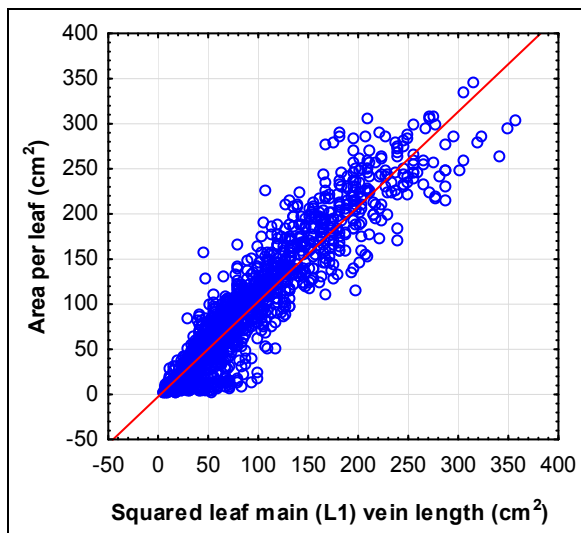


Figure 39 Relationship between the area per leaf (cm^2) and the squared leaf main (L1) vein length (cm^2) for all three seasons, including primary and secondary shoot leaves ($y = -2.29 + 1.05x$; $R^2 = 0.87$).

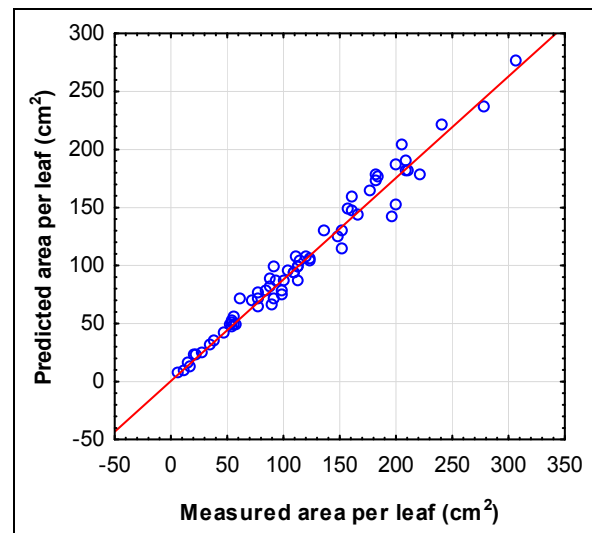


Figure 40 Relationship between predicted area per leaf (cm^2) versus measured area per leaf (cm^2) in the second season, using a leaf area regression equation created in the first season ($y = 0.59 + 0.87x$; $R^2 = 0.97$).

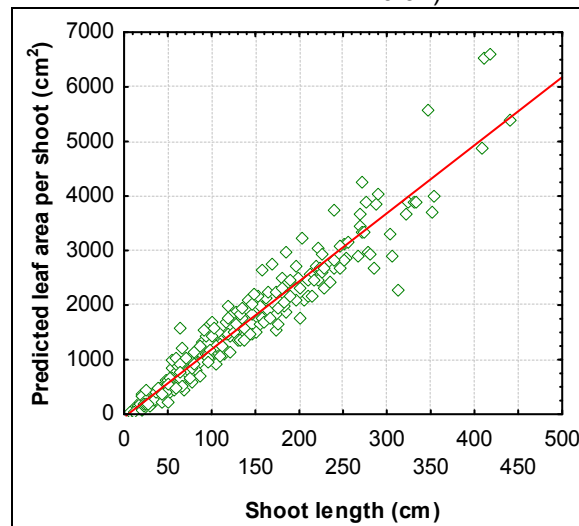


Figure 41 Relationship between the predicted leaf area per shoot (cm^2) and the shoot length (cm) measured in the second season ($y = 57.10 + 12.47x$); ($R^2 = 0.93$).

The relationship between the area per leaf (cm^2), which also represents leaf size, relative to the leaf plastochron index (LPI) values is shown for a shoot selected in season one (Figure 42) (also refer to Chapter IV). Possible seasonal and treatment-related effects on leaf area have to be evaluated by also considering the observed variability in leaf size/area of single leaves found on a shoot. One approach would be to remove the data of the smaller leaves on the first few nodes on the shoot (LPI 21 and 22 shown on Figure 42) and to fit growth curves to the remaining data. The parameters that can be estimated from these curves would then represent the maximum leaf size on a shoot (a), while the c -parameter represents the LPI value (or node position) where leaves reached half of its fully expanded states. The b_{max} parameter is not relevant in this type of analysis and is excluded.

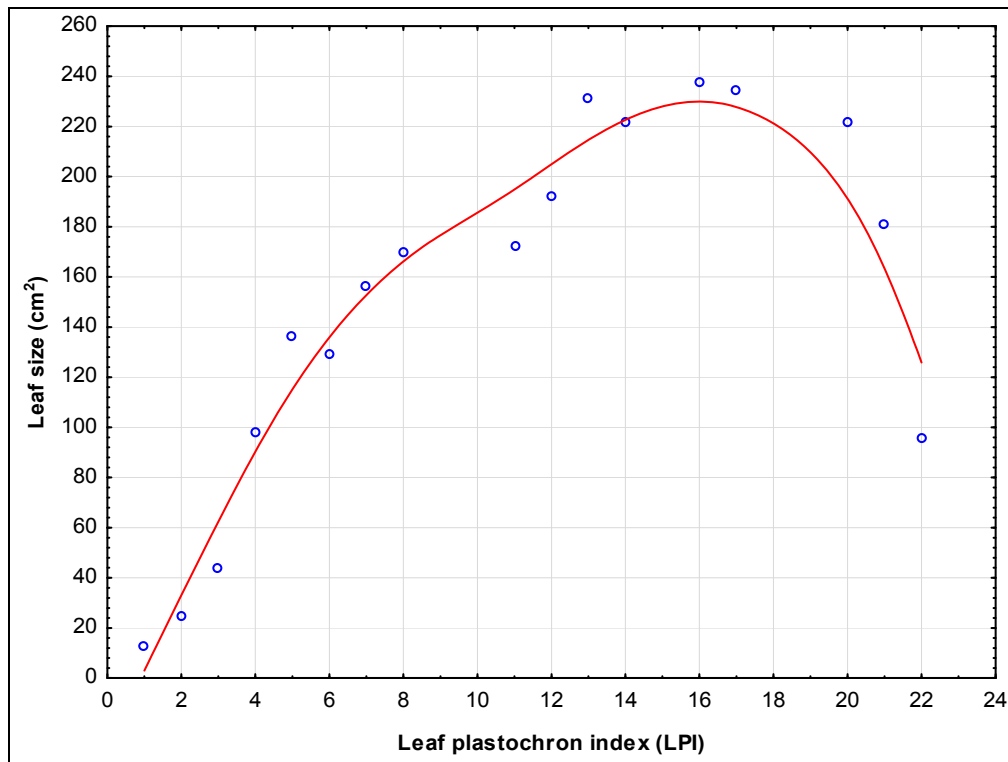


Figure 42 Example of the relationship between leaf size (cm²) and the leaf plastochron index (LPI) for a single primary shoot in season one, shown with a distance-weighted least-square fit.

The maximum leaf size (cm²) (*a*-parameter) was significantly less in the second season, as evaluated from the calculated fit parameters (Table 16). This was expected, considering the mild growth conditions during this season, as mentioned previously. With similar *a*-parameters, a shift in the *c*-parameter of shoots towards higher values, will lead to a reduced slope of the leaf size:LPI relation for the low LPI values, signifying larger portions of the apical parts of a shoot, with smaller leaf areas. Conversely, a shift to lower *c*-parameter values may mean that more leaves on the shoot have reached the fully expanded state before shoot growth cessation. This may imply restricted leaf growth during the active growth phase of the leaf (exponential or linear relative to chronological time) or more consistent young leaf production on a shoot, which may be linked to a longer active shoot growth period. Another explanation for smaller leaves in the apical region may be increased leaf exposure, which may lead to decreased leaf size (Cartechini & Palliotti, 1995). In season two, the first mentioned scenario seemed to apply, with the growing conditions leading to smaller maximum leaf sizes, as well as smaller apical leaves. In season one, the NSF treatment had significantly lower maximum leaf size on a shoot, and this was combined with lower *c*-parameter value, in accordance with the early growth cessation on these shoots. The largest leaves found in the SR treatment, in accordance with its significantly lower crop load (refer to yield:pruning mass ratios discussed in Section 3.3.6.2). The *c*-parameters were significantly higher in the reduced canopies, which could have been caused by increased exposure of the apical parts of shoots. In season two, the lowest maximum leaf sizes were found on the shoots of the reduced (especially NSF) treatments, which also had lower *c*-parameters. There seemed to be significantly more and longer secondary shoots per primary shoot in season two (refer to Section 3.3.5.3), especially in the reduced canopies, which could explain smaller primary shoot leaves as a result of increased carbohydrate allocation to secondary growth. The reasons for the lower *c*-parameter in the NSF treatment is not entirely clear, but it also had a much lower *b*_{max} value than the other treatments, which was probably the result of very strong secondary growth at the expense of shoot

elongation. This may have also led to less young leaves being formed on these shoots and conversely lower c-parameter values.

Table 16 Results from growth curve fit parameters related to primary shoot leaf size (cm^2) versus leaf plastochron index (LPI) for the different seasons and treatments. Means with the same letters are not significantly different at the $p \leq 0.05$ level according to paired t -tests performed on the growth curve fit parameters.

Season	Treatment	b	a	c	Regression R^2 -values
1	All	-0.499 a	198.95 a	3.93 a	0.79
2		-0.518 a	184.91 b	4.66 b	0.79
1	NSF	-0.658 a	177.47 a	3.50 a	0.75
	NSR	-0.535 ab	203.32 b	4.13 b	0.83
	SF	-0.468 ab	200.34 b	3.33 a	0.75
	SR	-0.401 b	215.31 c	4.72 b	0.84
2	NSF	-0.494 a	188.25 a	4.80 a	0.79
	NSR	-0.830 b	164.05 b	3.61c	0.85
	SF	-0.437 a	201.16 c	5.23 b	0.79
	SR	-0.437 a	179.15 d	4.69 ab	0.80

The percentage of leaf loss on shoots was estimated for season two as the amount of leaves that were utilised for main (L1) vein length measurements on a shoot versus the total nodes counted on that same shoot. This could be done, as normally all leaves on a shoot were measured, but not severely damaged or lost leaves. Leaf loss increased as the season progressed, especially after 140 DAB (Figure 43). Leaf loss before harvest seemed to be less in the NSF treatment. Initial (before 80 DAB) leaf loss also seemed to be more in the SF and SR treatments. The lost leaves were mainly observed in the basal shoot sections (data not shown).

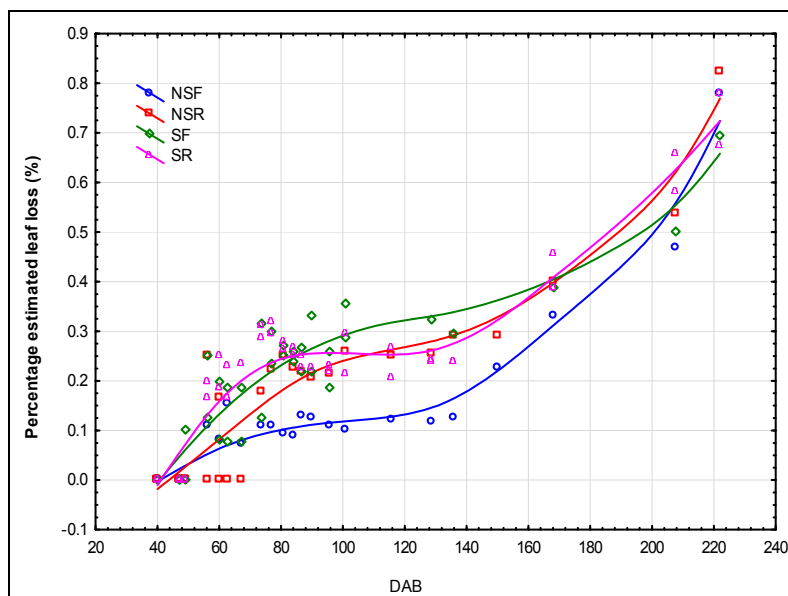


Figure 43 Estimated percentage leaf loss (%) relative to date after budburst (DAB) for the different treatments in the second season, shown using a distance-weighted least-square fit for each treatment.

3.3.5.3 Pruning measurements

Results from analyses performed during winter pruning are presented in Table 21 to Table 26 in Addendum C. The reduction in shoots achieved by this treatment (as measured from number of

primary canes left on a vine) were 41%, 30% and 50% respectively for seasons one, two and three. A higher number of primary canes were measured in season three (as seen in the NSF treatment), probably due to an improved budburst percentage. The 4% higher number of primary canes per vine in the stressed treatments of season three is probably attributable to an experimental error.

The mass per primary cane (including secondary canes) was increased by 53% for the reduced canopies in season one; the number of secondary canes per primary cane was increased by 59% in reaction to the canopy reduction. This is the only season in which the number of secondary shoots was affected by the treatments, which could have been due to the early application of the treatment in comparison to the other two seasons. In season two the primary and secondary canes were kept separate and the mean mass per cane increased by 35% and 23%, respectively. The total secondary shoot length also responded to canopy manipulation, but only when the topping status of the shoots was considered (see discussion later). The total mass of the secondary canes on a primary cane was, however, increased (without consideration of the topping status) by 59% in reaction to canopy manipulation. In season three the mass per cane was decreased by 11% in the water stressed treatments and increased by 61% in the reduced canopy treatments. Even though the number of secondary shoots did not change, they were on average 24% longer. The decrease in the mass per primary cane of the stressed treatments was more pronounced in season two (29%).

In seasons two and three the “topping status” of a shoot was also included in the statistical analysis as a separate factor and the results are shown in Table 23 and Table 24. This is not a treatment *per se*, but a classification of shoots that was necessary during pruning measurements, as it was not only non-topped shoots that were collected during pruning measurements. In season two there was a significant interaction between the topping status and the canopy manipulation treatment, with the reduced canopies showing a 76% increase in the total secondary shoot length per primary cane (cm), compared to the full canopies. The total secondary shoot length per primary cane was also longer (31%) for non-topped shoots, indicating a canopy manipulation-induced response, being increased by topping. In seasons two and three, topped shoots also showed 36% and 23% reductions in the mass per primary cane and it seems that the topping was more severe in season two, as the mean primary cane length was reduced by 63% compared to the 13% reduction in season three. This severe topping in shoots observed in season two also significantly increased the mean length of a secondary shoot by about 31%.

The length of primary canes measured during pruning was not significantly affected by any treatments in season one, but it has to be noted that here the topping status of shoots was not known. There seemed to be less secondary shoot growth in season three, which could have been a result of the drier conditions that prevailed in this season. The mean secondary shoot length was increased by 31% in reaction to canopy reduction, but it was still much less than the other two seasons.

The number and mass of non-bearing canes were also determined and included in the results, but contributions to the total cane numbers or mass per vine are small and therefore not discussed further.

The total cane mass (or “pruning mass”) per vine (kg) was only affected significantly in season three by the canopy reduction treatment, showing an 18% reduction. This could be explained by the removal of secondary shoots that were performed in the lower 25 cm of the canopy during this

season, therefore possibly reducing the secondary shoot growth compensation effect observed in the other seasons.

3.3.6 Reproductive measurements

3.3.6.1 Yield per vine and bunch mass results

The total number of bunches per vine seemed to be less in season one, and it was significantly reduced by 37%, 40% and 48%, respectively, in seasons one, two and three by the canopy manipulation treatment (Table 25).

Yield per vine (kg) was the highest (5.59 kg.vine⁻¹) for the NSF grapevines in season three, compared to all seasons (Table 22), and it was decreased in the reduced canopy treatments by 43% and 33%, respectively, in seasons one and two (Table 25). In season three there was a significant second-order interaction between canopy manipulation and irrigation strategy with respect to the yield per vine, showing a similar yield reduction with canopy manipulation, specifically 41% in the NSR and 42% for the SR grapevines. The yield decrease due to water deficits amounted to 31%. The combined effect (NSF versus SR) was a yield reduction of about 60%. This is also the only season where there were significant main effects with respect to the change in the mass per bunch (kg). Bunches from “stressed” grapevines were on average 33% lighter, and canopy reduction increased bunch mass by 11%. The higher-order interaction was, however, non-significant. It is interesting that yield was not reduced by water deficits in season two, even though it seemed to be the season with the most negative Ψ_{PD} values. This may point to a dominant effect of soil and plant water status on yield in the first part of the season, i.e. during the berry set phase of grape development (Williams & Matthews, 1990).

3.3.6.2 Yield:pruning mass ratios

The yield:pruning mass ratio was affected significantly by both the irrigation and canopy manipulation treatments in season one (Table 22). There was a significant reduction in the ratio for the SF compared to the NSF treatments, but not for the SR compared to the NSR treatments. The ratio was, however, reduced in both NS and S treatments by canopy reduction and by almost half of the original ratio in the case of the NS treatments. In season two the yield:pruning mass ratio was reduced from a ratio of 3.75 to 2.57 and in season three both the reduced canopies and stressed treatments showed significantly lower ratios, even though the higher-order interaction was non-significant. Although it seems logical that these reductions in the yield:pruning mass ratios are expected to have positive effects on fruit ripening and possibly reserve accumulation in the vines, the ratio of leaf area relative to the yield also has to be considered. The leaf area:fruit mass ratio (cm².g⁻¹) in season one was calculated from the mean total leaf area per vine and the yield per vine values determined during harvest, yielding 5.51 cm².g⁻¹ in the NSF grapevines and 10.24 cm².g⁻¹ in the NSR grapevines. Furthermore the “quality” of the source is also of relevance, and it is expected that improved exposure, a higher leaf area:fruit mass ratio and a lower yield:pruning mass ratio would accelerate ripening in the fruit. The extent to which the grapevine would compensate for all these modifications by way of source:sink regulation (lower photosynthetic activity due to lower crop load) would need to be evaluated based on the reaction of berry growth and ripening to the treatments.

The first season of this study corresponded to earlier studies showing that fully expanded leaf size is inversely related to crop size (Pandey & Farmahan, 1977; Edson *et al.*, 1995b), if the results from maximum leaf size relative to the yield:pruning mass ratios are compared. This was, however, not the case in season two.

3.3.6.3 Berry growth

Even though the budburst of season one was delayed (refer to section 3.3.1), it seems that berry development took place even earlier and faster than in the other two seasons (Figure 44). Véraison was recorded 20 days later in season two. When berry development was plotted against thermal time units (Figure 45), differences between seasons one and two seemed to be largely eliminated, while season three showed delayed development. Season three was much drier than the other two seasons, and berry development seemed delayed. Plant water deficits seemed much more pronounced in general for season two compared to season three, but the levels of water deficit were not that much different in the pre-véraison period (refer to Section 3.3.3). It would therefore seem that berry size is not only determined by plant water status, but also dependent on soil water status in this period, and probably linked to the dynamic turgor changes in the berry during a diurnal cycle (Thomas *et al.*, 2006). In the early berry growth stages, berries grow mostly at night, with a loss in berry mass, due to transpiration, happening mostly during the day (Greenspan *et al.*, 1994; Greenspan *et al.*, 1996). It seems that even though plant water status partially recovered at night time, leading to higher predawn leaf water potential values, reduced soil water availability did not allow for sufficient berry turgor recovery allowing growth to continue unhindered in this period.

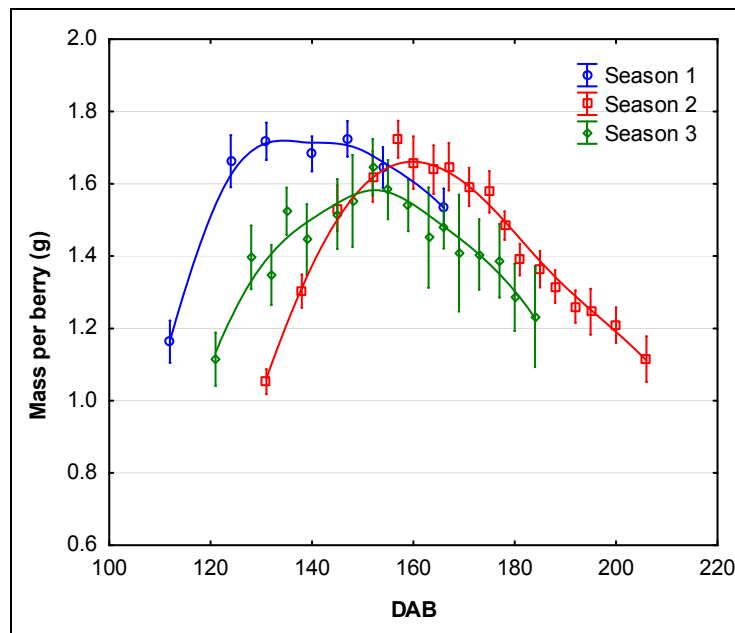


Figure 44 Mass per berry (g) relative to date after budburst (DAB) for the different seasons. For each season a distance-weighted least-square fit is shown, with the vertical bars around the means indicating 95% confidence intervals.

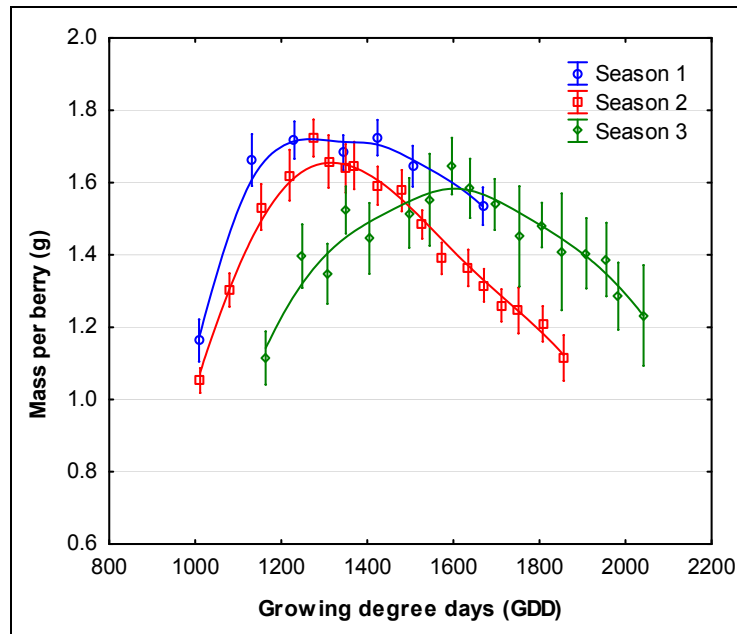


Figure 45 Mass per berry (g) relative to growing degree days (GDD) for the different seasons. For each season a distance-weighted least-square fit is shown, with the vertical bars around the means indicating 95% confidence intervals.

Growth curve analysis could be used to compare treatments within the respective seasons, but only prior to reduction in the mass per berry. No significant treatment differences were found in season one, but this could also have been affected by the limited amount of measurements available before maximum mass per berry was reached. There was however a tendency for the NSR treatment to have larger berries and the NSF to have smaller berries, especially in the 120-130 DAB period (data not shown). In general, the NS treatments displayed higher maximum mass per berry in both seasons, with the *c*-parameter only differing significantly between the NSR and SF treatments in season three (Table 17). The SF berry mass increase was delayed, reaching lower maximum values.

Table 17 Results from growth curve fit parameters related to mass per berry (g) measurements relative to date after budburst (DAB) for the different seasons and treatments. Means with the same letters are not significantly different at the $p \leq 0.05$ level according to paired *t*-tests performed on the growth curve fit parameters. All *b*-parameters were non-significant and are not shown.

Season	Treatment	<i>a</i>	<i>c</i>
2	NSF	1.74a	140.12 a
	NSR	1.76a	137.61 a
	SF	1.60b	140.12 a
	SR	1.68ab	138.77 a
3	NSF	1.66a	125.49 ab
	NSR	1.70a	124.28 a
	SF	1.49ab	132.32 b
	SR	1.51b	126.98 ab

3.3.6.4 Berry total soluble solids accumulation

Total soluble solid accumulation in the berries showed a delay in season two relative to the other seasons, consistent with cool and wet ripening conditions, but a constant rate was maintained until late season, where the other two seasons showed a decline (Figure 46). Differences between

seasons (especially season two, relative to the others) seemed to be reduced if expressed relative to thermal time units (Figure 47), season three apparently showing lower total soluble solid values. The latter may be ascribed to the drier conditions that prevailed during this season. The role of secondary shoots could also have played a major part here, especially late season, considering that, even though water deficits seemed a lot higher post-veraison in season two, there was a much higher ratio of secondary to primary leaf area in this season.

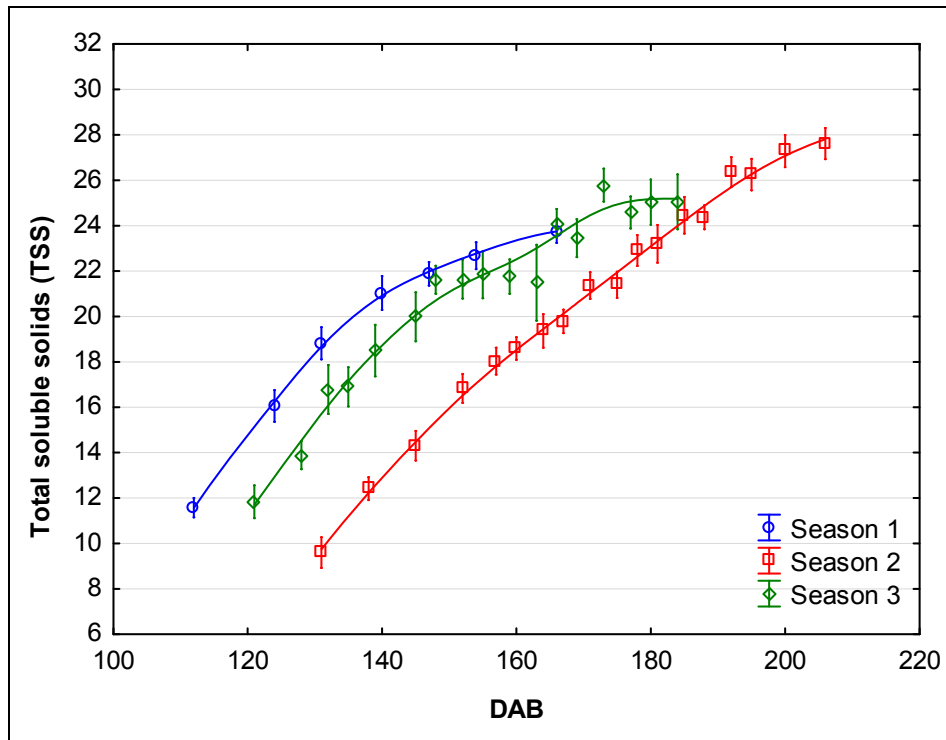


Figure 46 Berry total soluble solids (TSS, °B) accumulation relative to days after budburst (DAB) for the different seasons as measured from véraison onwards. A distance-weighted least-squares fit is shown for clarity. Vertical bars denote +/- standard errors.

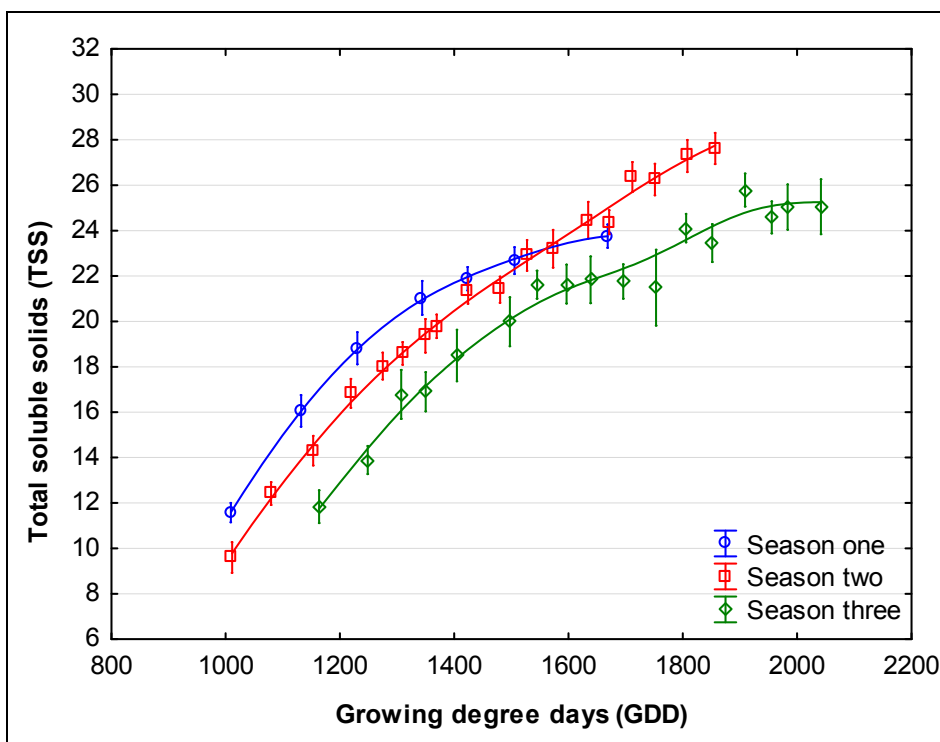


Figure 47 Berry total soluble solids (TSS, °B) accumulation relative to growing degree days (GDD) for the different seasons as measured from véraison onwards. A distance-weighted least-squares fit is shown for clarity. Vertical bars denote +/- standard errors.

Sugar loading is defined as the evolution of a quantity of sugar per berry ($\text{mg}\cdot\text{berry}^{-1}$) from véraison onwards (Wang *et al.*, 2003). Monitoring the evolution in sugar content of the berry during ripening can indirectly aid in quantifying changes in the physiological functioning of the plant, as affected by factors such as grapevine water status and microclimate (Carbonneau & Deloire, 2001; Wang *et al.*, 2003; Hunter & Deloire, 2005; Deloire, 2011). In this study, sugar loading was calculated on the basis of berry volume using the procedure outlined in Deloire (2011) and the data displayed on the basis of growth response curves, as previously indicated. With measurements commencing at véraison, the lower boundaries of the growth curves were not set to zero, but to the mean values measured at véraison for the ripeness parameter evaluated. When sugar loading was evaluated relative to date after budburst, a trend similar to that obtained for total soluble solids was found, with the warmest season showing the earliest maximum rate of sugar loading and season two showing delayed sugar accumulation (Figure 48), leading to significant differences in the maximum potential sugar loaded into the berry (a -parameters) (Table 19).

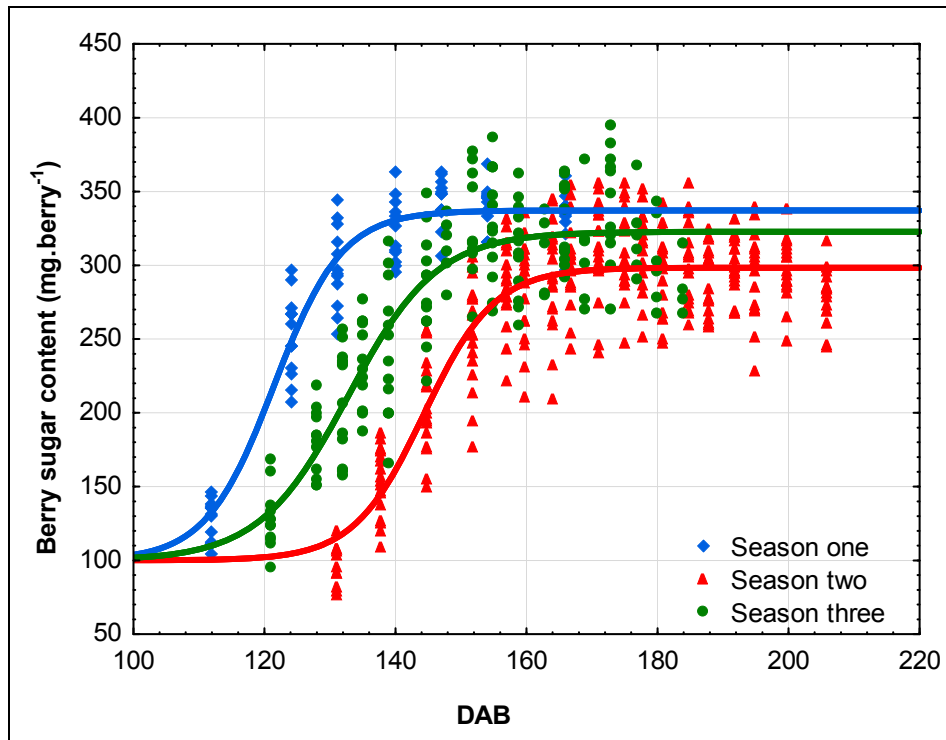


Figure 48 Fitted logistic growth curves of berry sugar content (mg.berry^{-1}) relative to date after budburst (DAB) for the different seasons, with the lower asymptote set to $100 \text{ mg.berry}^{-1}$ (season one $R^2 = 0.96$; season two $R^2 = 0.87$; season three $R^2 = 0.88$).

Table 18 Results from growth curve fit parameters of berry sugar content (mg.berry^{-1}) relative to days after budburst (DAB) for the different seasons, with the lower asymptote set to $100 \text{ mg.berry}^{-1}$. Means with the same letters are not significantly different at the $p \leq 0.05$ level according to paired t -tests performed on the growth curve fit parameters.

Season	b	a	c
1	-0.192a	337.15a	121.49a
2	-0.186a	298.38b	144.37b
3	-0.147a	322.74c	132.79c

When this apparent thermal time effect was accounted for by expressing sugar loading relative to growing degree day (GDD) units (Figure 49), seasons one and two showed similar fitted curves, still differing in the a -parameters as previously shown relative to date after budburst (Table 19). Season three, however, showed a significantly delayed c -parameter (about $200 \text{ }^\circ\text{C.day}^{-1}$), emphasising a delay in berry sugar loading, probably owing mostly to the drier conditions prevailing in season three and despite plant water status not indicating the most stress in this season. The calculated b_{max} value for both seasons one and two was $1.42 \text{ mg.berry}^{-1} \cdot (\text{ }^\circ\text{C.day}^{-1})^{-1}$, whereas it was only $0.82 \text{ mg.berry}^{-1} \cdot (\text{ }^\circ\text{C.day}^{-1})^{-1}$ in season three.

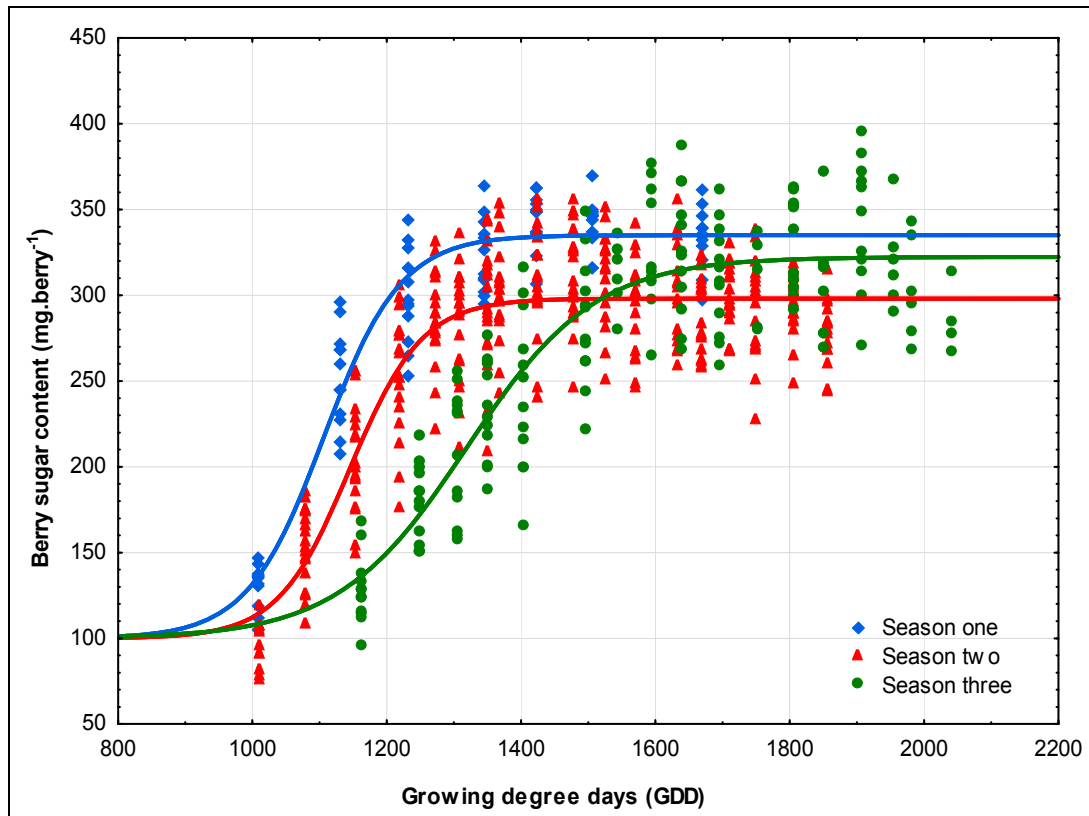


Figure 49 Fitted logistic growth curves of berry sugar content (mg.berry^{-1}) relative to growing degree days (GDD) for the different seasons, with the lower asymptote set to $100 \text{ mg.berry}^{-1}$ (season one $R^2 = 0.96$; season two $R^2 = 0.87$; season three $R^2 = 0.88$).

Table 19 Results from growth curve fit parameters of berry sugar content (mg.berry^{-1}) relative to growing degree days (GDD) for the different seasons, with the lower asymptote set to $100 \text{ mg.berry}^{-1}$. Means with the same letters are not significantly different at the $p \leq 0.05$ level according to paired t -tests performed on the growth curve fit parameters.

Season	b	a	c
1	-0.017 a	335.08 a	1106.71 a
2	-0.019 a	298.11 b	1145.40 b
3	-0.010 b	322.33 c	1319.17 c

If the value of $3 \text{ mg.berry}^{-1} \cdot \text{day}^{-1}$, as suggested by Deloire (2011) as indicative of the cessation of sugar loading (in order to determine the harvesting window relative to sugar loading), is considered, this threshold was reached almost 20 days later in season two compared to season one (Figure 50). Relative to thermal time units, the threshold was reached at levels of about $250 \text{ }^\circ\text{C} \cdot \text{day}^{-1}$ higher in season three compared to the other seasons (Figure 51).

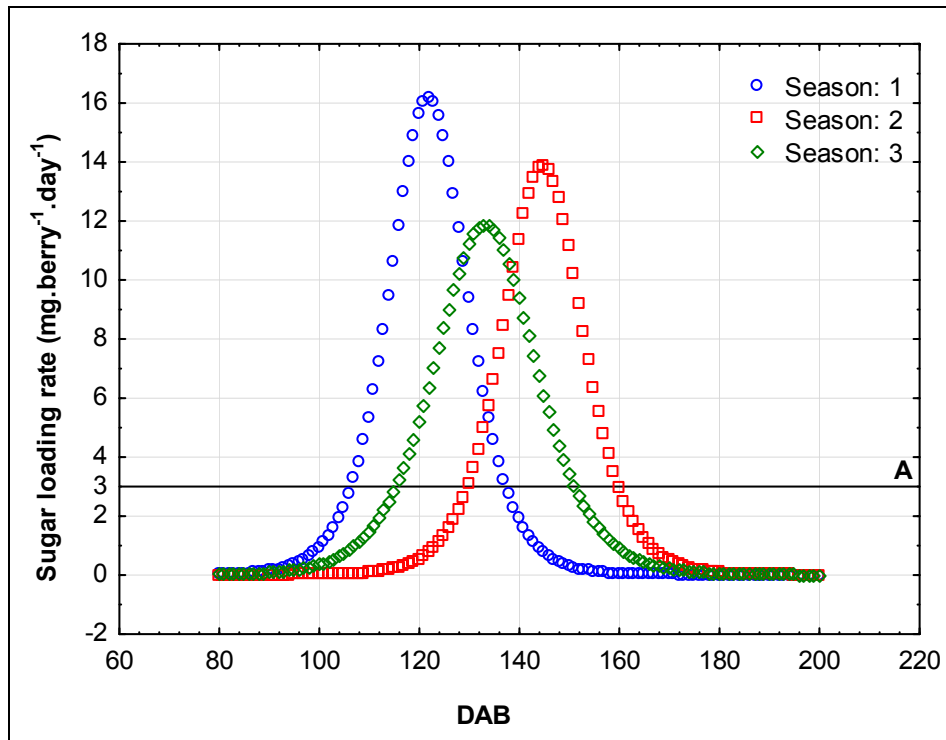


Figure 50 Sugar loading rate (mg.berry⁻¹.day⁻¹) relative to days after budburst (DAB) for the three seasons. The reference line at A represents theoretical cessation of sugar loading.

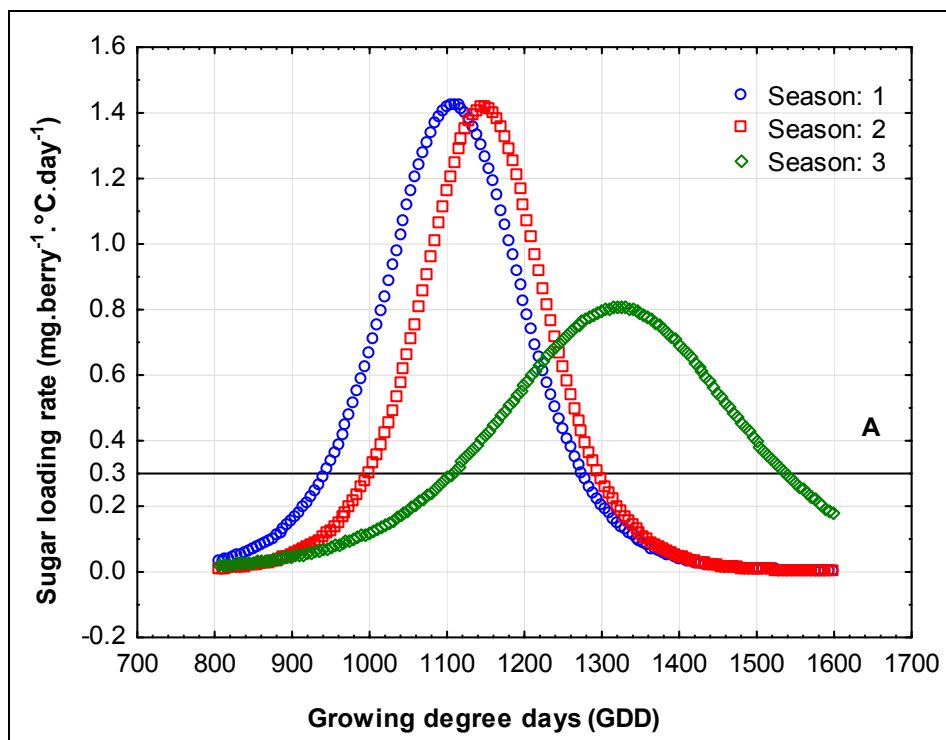


Figure 51 Sugar loading rate (mg.berry⁻¹.°C.day⁻¹) relative to growing degree days (GDD) for the three seasons. The reference line at A represents theoretical cessation of sugar loading.

Canopy manipulation effects seemed to dominate the differences in treatments with respect to sugar loading (Figure 52), considering differences observed (some not significant at the $p \leq 0.05$ confidence level) in the c -parameters (Table 20). This also concurs with leaf area development in the full canopies (Table 15) and thus with canopies having less young leaves; this may have led to reduced sucrose transport to bunches (lower photosynthetic activity in older leaves during the

ripening period). It is possible that this could have been aggravated by shaded canopy conditions, as may have been the case if the PAR radiation levels are considered (section 3.3.4). The same effects were observed for the maximum sugar loaded (a -parameter) in season one, but in season two and three effects of the irrigation treatments were also visible, where the S treatments also led to significantly lower values.

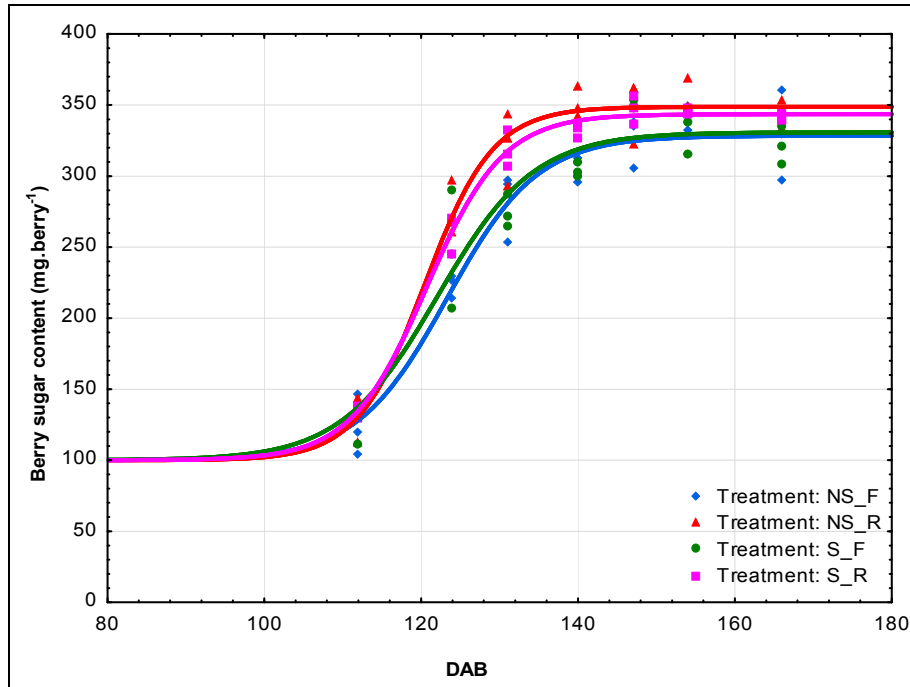


Figure 52 Fitted logistic growth curves of berry sugar content (mg.berry^{-1}) relative to dates after budburst (DAB) for the different treatments in season one, with the lower asymptote set to $100 \text{ mg.berry}^{-1}$ (NSF $R^2 = 0.97$; NSR $R^2 = 0.98$; SF $R^2 = 0.96$; SF $R^2 = 0.99$).

Table 20 Results from growth curve fit parameters of berry sugar content (mg.berry^{-1}) related to dates after budburst (DAB) for the different season and treatments. Means with the same letters are not significantly different at the $p \leq 0.05$ level according to paired t -tests performed on the growth curve fit parameters.

Season	Treatment	b	a	c
1	NSF	-0.173 a	328.41 a	123.33a
	NSR	-0.230a	348.76 b	120.50b
	SF	-0.163a	330.85 a	122.09ab
	SR	-0.205a	343.58 ab	120.71b
2	NSF	-0.195a	301.01a	145.50b
	NSR	-0.212a	321.49c	141.09a
	SF	-0.177a	279.48b	146.27b
	SR	-0.202a	308.34 a	142.82a
3	NSF	-0.133a	329.67b	133.34a
	NSR	-0.122a	369.83a	131.68a
	SF	-0.140a	290.49c	136.46b
	SR	-0.135a	338.95b	133.77ab

It was also clear that the highest maximum rate of sugar loading (Figure 53) was reached in the reduced canopy treatments in season one, with the full canopy treatments reaching the theoretical point of sugar loading cessation about 5 days later than the other treatments, indicating delayed ripening. No differences were apparent with respect to the irrigation treatments.

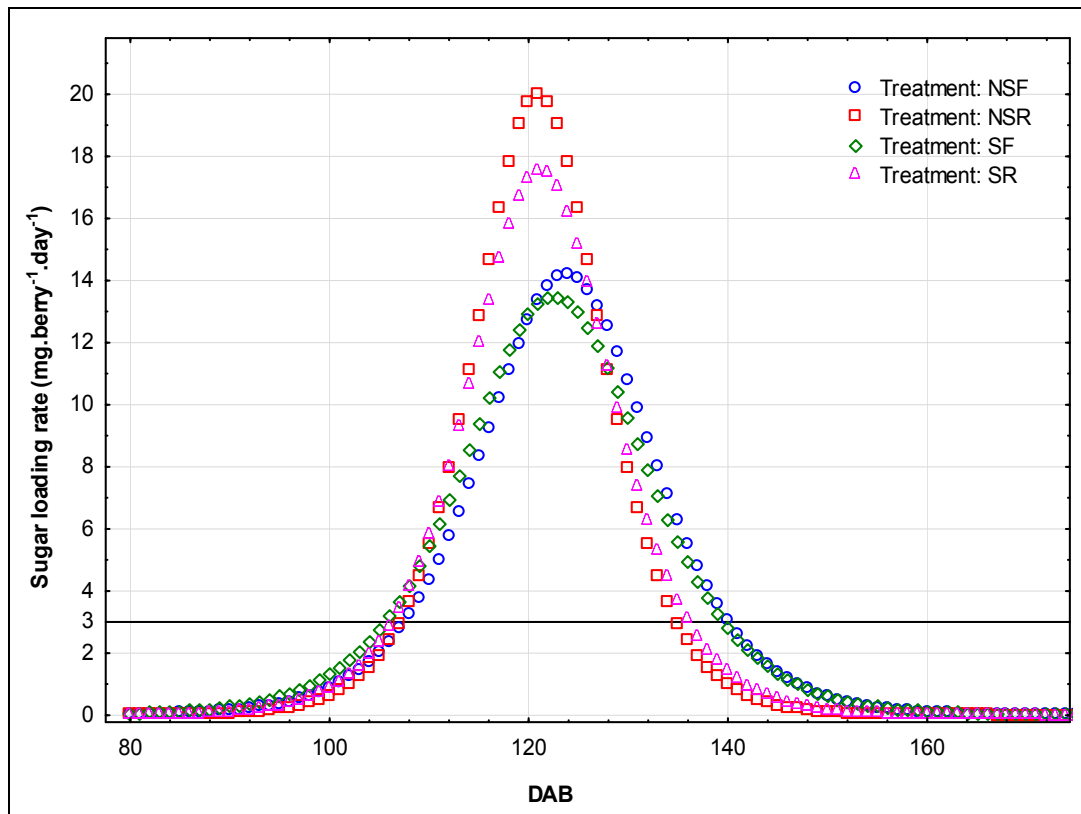


Figure 53 Sugar loading rate ($\text{mg.berry}^{-1}.\text{day}^{-1}$) relative to date after budburst (DAB) for the different treatments in season one. The reference line at A represents theoretical cessation of sugar loading ($3 \text{ mg.berry}^{-1}.\text{day}^{-1}$).

3.3.6.5 Titratable acidity and pH

The cooler growing season clearly showed higher titratable acidity values at equivalent days after budburst, compared to the other seasons (Figure 54). When TA was expressed relative to growing degree days, however, season one seemed to show earlier reduction, while in season three the TA seemed resilient early in the season, but decreased quickly during the final ripening stages (Figure 55).

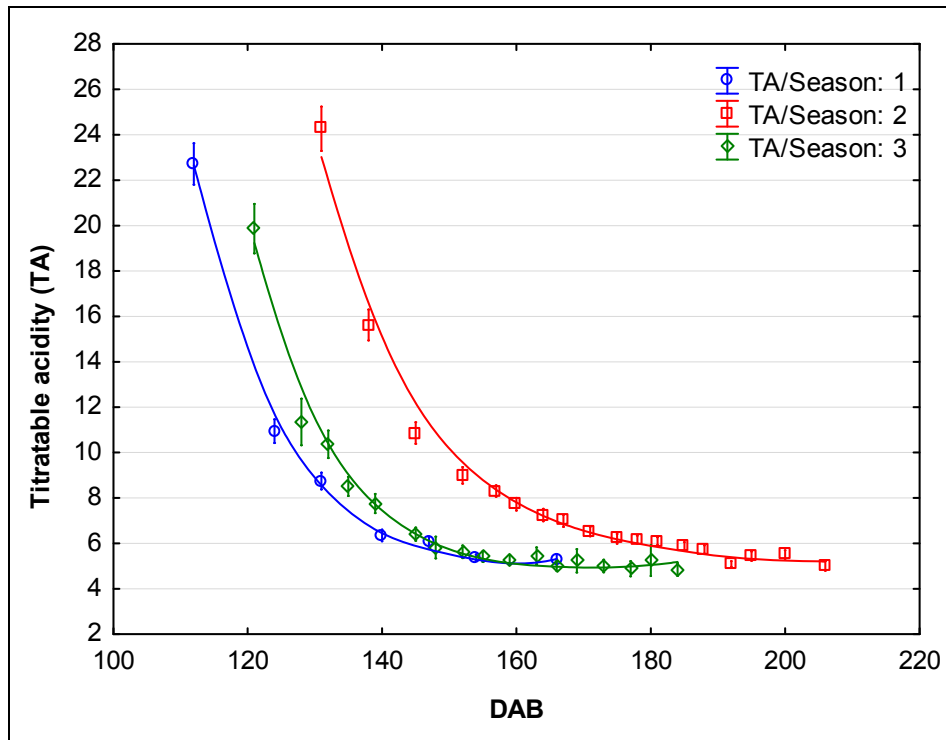


Figure 54 Titratable acidity (TA) relative to date after budburst (DAB) measured from véraison in the different seasons. Distance-weighted least-square fits are shown and vertical bars denote means with standard errors.

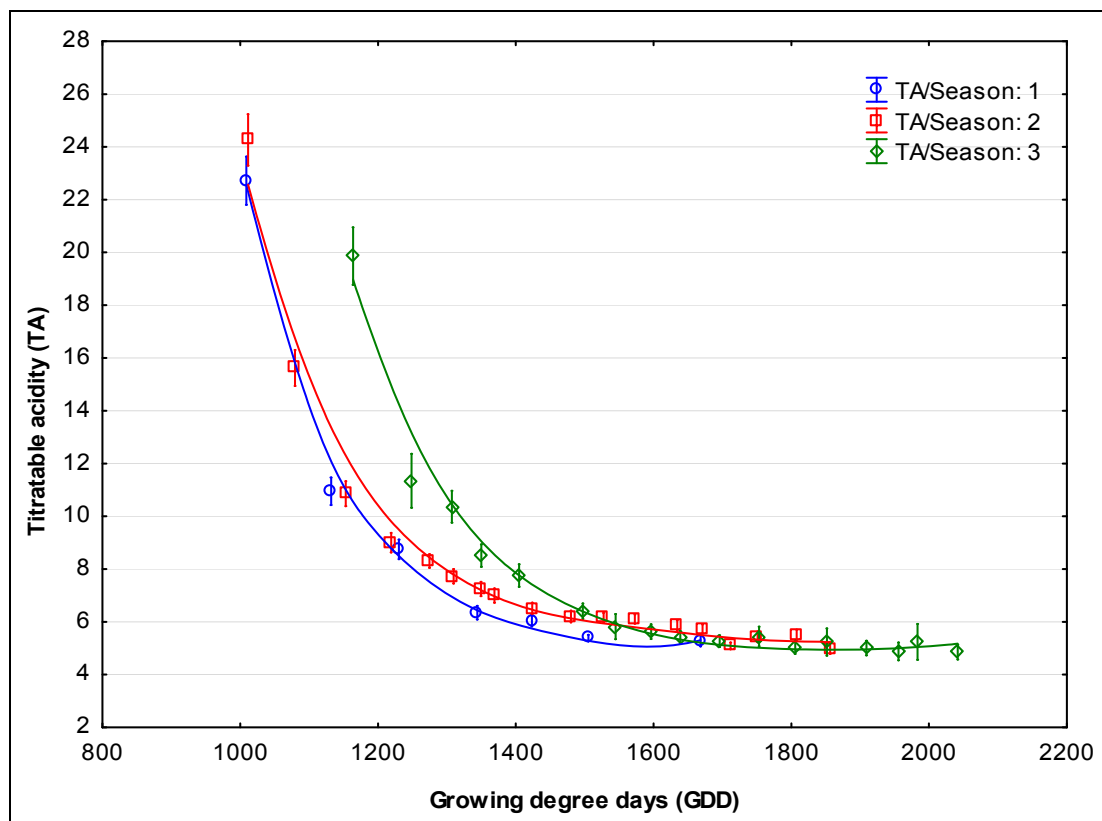


Figure 55 Titratable acidity (TA) relative to growing degree days (GDD) measured from véraison in the different seasons. Distance-weighted least-square fits are shown and vertical bars denote means with standard errors.

In general, for seasons two and three, the NS treatments seemed to have lower TA values (Figure 57 and Figure 58), which may be linked to increased maximum berry sizes in these treatments

(Table 17), resulting in lower organic acid concentrations (Mullins *et al.*, 1992; Yuste *et al.*, 2004; Lategan, 2011). However, the reduction in berry size was not quantified, as the growth fit curves were only calculated until berry mass started to decline. Yet, the most prominent effect of lower acidity in the NS treatments was observed in season three, in which the most significant and largest magnitude of maximum berry mass difference between the NS and S treatments occurred. In season three, the SF treatment seemed to retain the most titratable acidity. This treatment was also shown to be the least ripe according to sugar loading curve fitting (Table 20).

During season one, a faster decrease in TA for the NSF treatment (Figure 56), despite apparent smaller berry sizes, could have been a result of higher plant water deficits. Especially on 120 DAB large differences existed between the NSF and SF treatments (Figure 22). The pH in this treatment seemed unaffected, so the decrease in acidity could have been due to malic acid decrease, rather than tartaric acid. It was expected that the reduced canopies would have lower TA values, as more bunch exposure could contribute to accelerated malic acid degradation (Kliewer & Lider, 1968; Bergqvist *et al.*, 2001). It could be that during ripening berry exposure could have been enhanced by leaf loss due to water deficits in the NSF treatment, reducing malic acid, but this was unfortunately not quantified for this season.

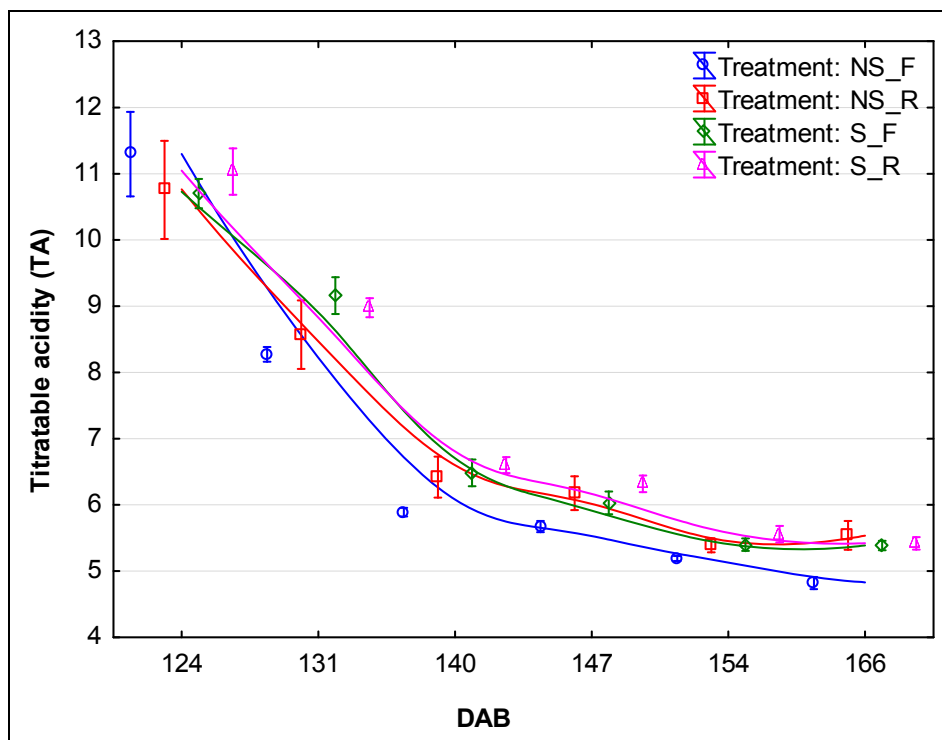


Figure 56 Titratable acidity (TA) relative to days after budburst (DAB) for the different treatments measured in the harvesting period (three different harvest dates) in season one. (Distance-weighted least-square fits are shown and vertical bars denote means with standard errors. Treatments are offset for clarity, but fits are drawn through non-offset mean values).

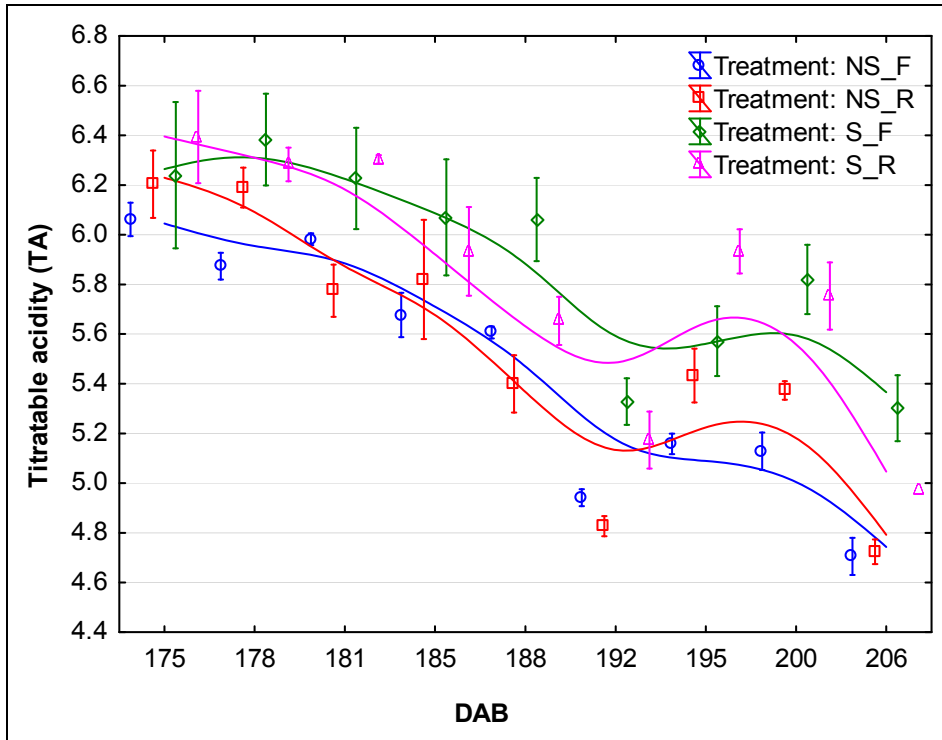


Figure 57 Titratable acidity (TA) relative to days after budburst (DAB) for the different treatments measured in the harvesting period of season two (Distance-weighted least-square fits are shown and vertical bars denote means with standard errors. Treatments are offset for clarity, but fits are drawn through non-offset mean values).

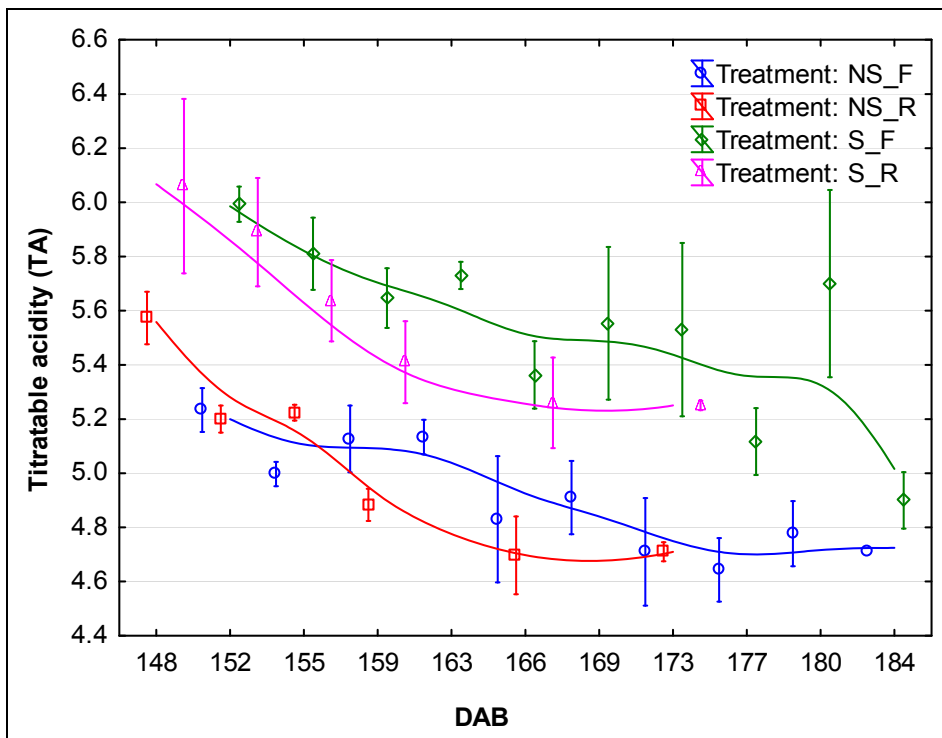


Figure 58 Titratable acidity (TA) relative to days after budburst (DAB) for the different treatments measured in the harvesting period of season three (Distance-weighted least-square fits are shown and vertical bars denote means with standard errors. Treatments are offset for clarity, but fits are drawn through non-offset mean values. The reduced treatments were not available for sampling after 173 DAB, as they were already harvested).

Season two resulted in the lowest pH values during ripening (Figure 59). This was expected due to the higher titratable acidity in this season. If the pH was expressed relative to degree days (Figure 60), season three showed lower values for corresponding thermal time ($^{\circ}\text{C}\cdot\text{day}^{-1}$) values. This was expected, considering delayed ripening relative to thermal time in this season mentioned earlier.

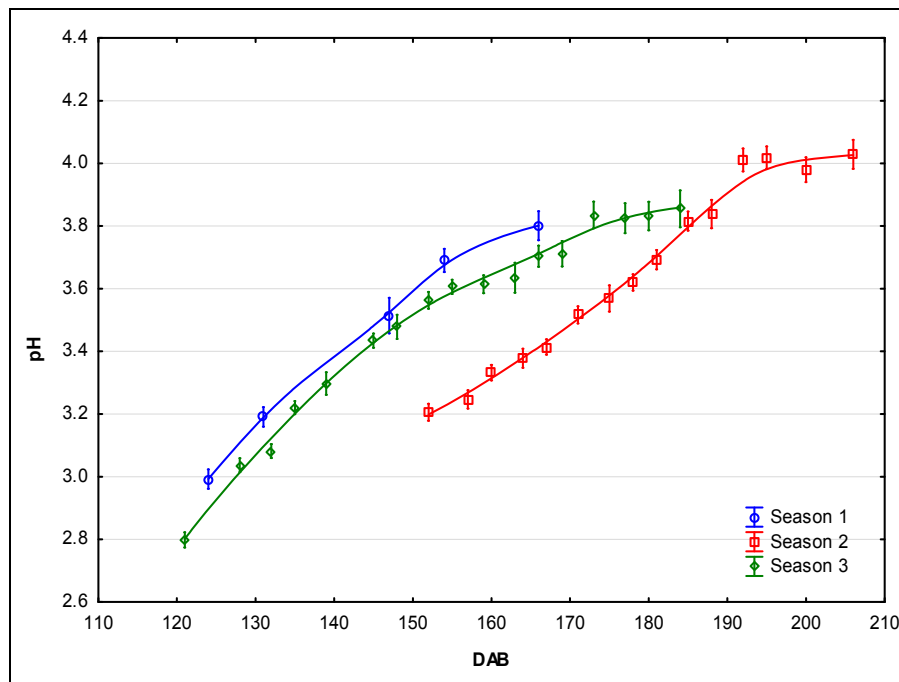


Figure 59 Measured pH values relative to date after budburst (DAB) from véraison onwards in the different seasons. Distance-weighted least-square fits are shown and vertical bars denote means with standard errors.

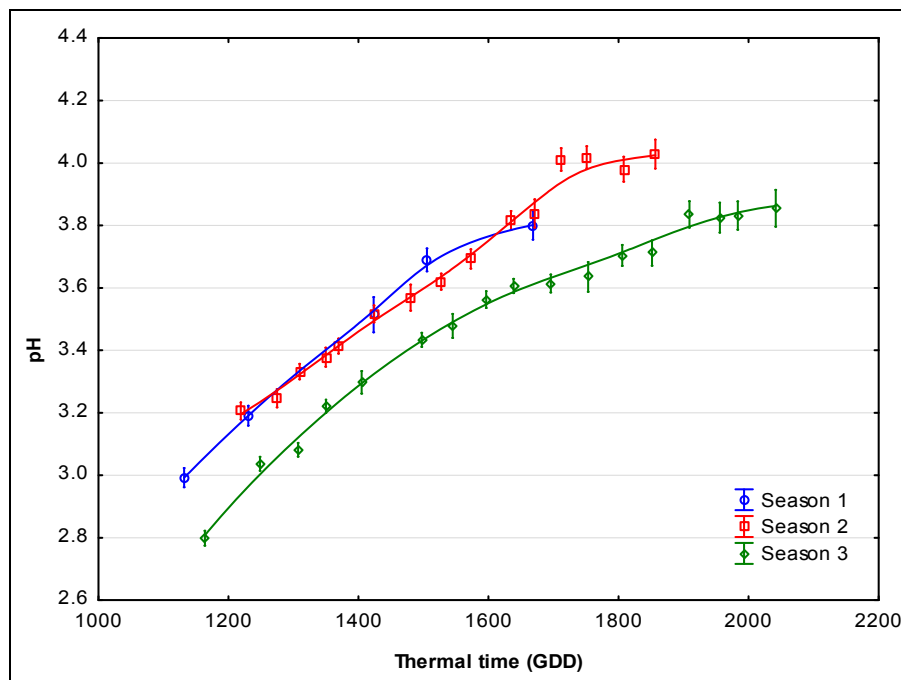


Figure 60 Measured pH values relative to growing degree days (GDD) from véraison onwards in the different seasons. Distance-weighted least-square fits are shown and vertical bars denote means with standard errors.

No treatment effects were evident from pH values measured during ripening in season one (Figure 61). In season two the reduced canopies seemed to have higher pH values during ripening (Figure 62). This was in contrast to what we expected, considering that well-exposed canopies normally

exhibit lower pH values (Haselgrove *et al.*, 2000). However, this may have been the result of advanced ripening in the reduced canopies, leading to higher pH, in concurrence with the trend of pH to increase sharply as ripening progresses (see also Ellis (2008). This was also observed in season three (Figure 63), the pH value differentiation coinciding with the trends seen from the sugar loading growth fit parameters, i.e. the NSR treatment having the highest maximum sugar loading values, the NSF and SR treatments could not be differentiated, and the SF treatment showing lower maximum values and slow sugar loading. Elevated pH is expected in luxuriously irrigated, or luxuriously growing grapevines, due to increased availability of potassium and possible decreased acidity due to tartaric acid salt formation (bi- and di-potassium tartrate) in the must (Smart & Coombe, 1983; Jackson & Lombard, 1993).

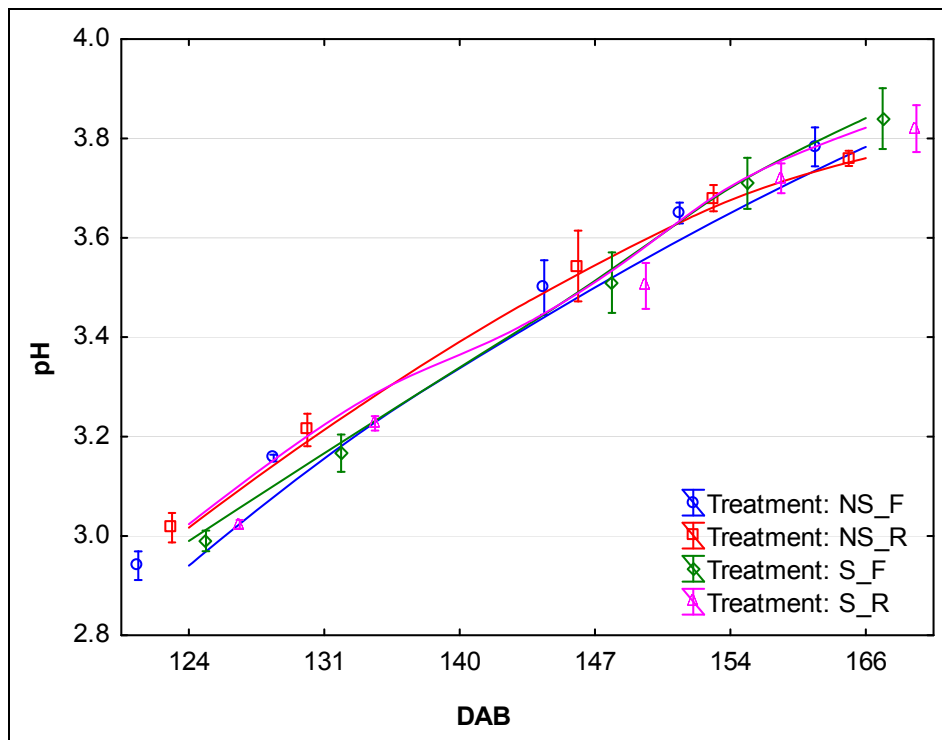


Figure 61 Measured pH values relative to days after budburst (DAB) for the different treatments in the harvesting period of season one (Distance-weighted least-square fits are shown and vertical bars denote means with standard errors. Treatments are offset for clarity, but fits are drawn through non-offset mean values).

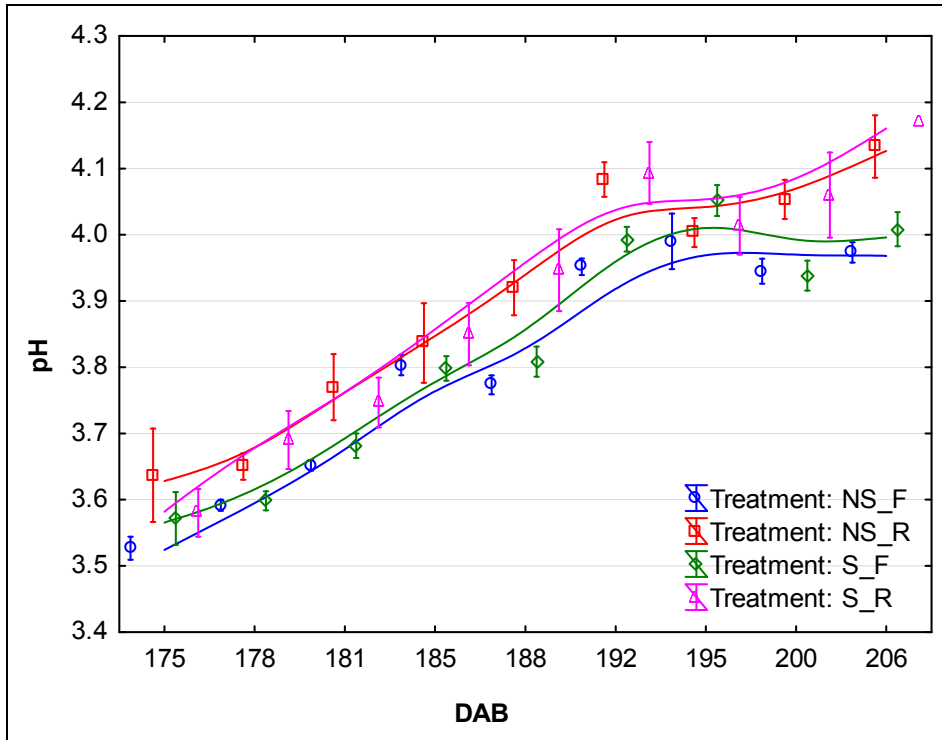


Figure 62 Measured pH values relative to days after budburst (DAB) for the different treatments in the harvesting period of season two (Distance-weighted least-square fits are shown and vertical bars denote means with standard errors. Treatments are offset for clarity, but fits are drawn through non-offset mean values).

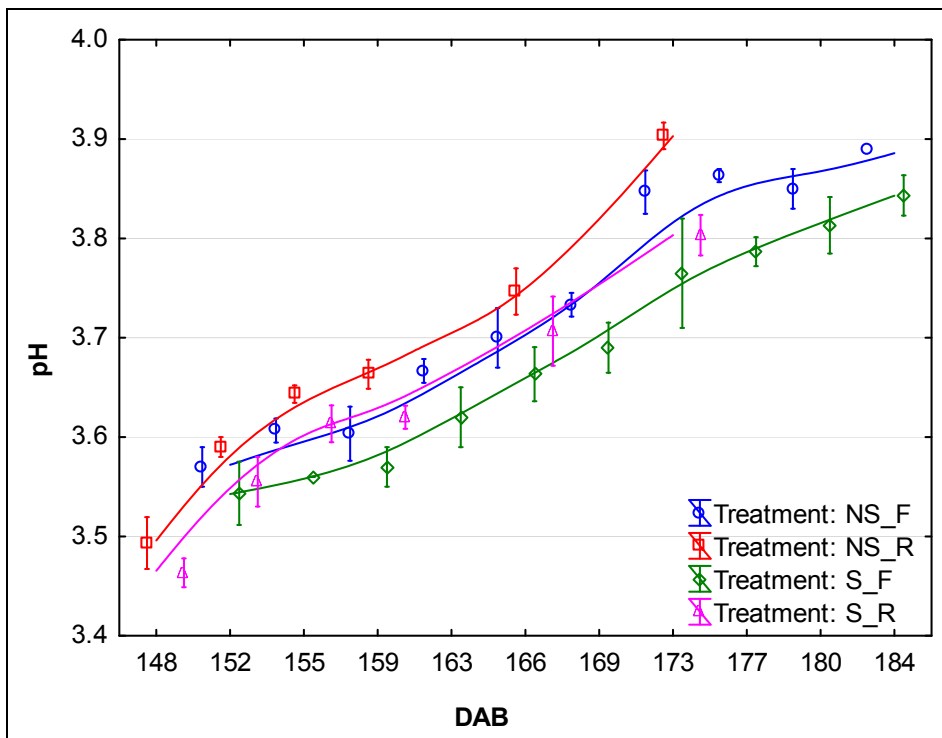


Figure 63 Measured pH values relative to days after budburst (DAB) for the different treatments in the harvesting period of season three (Distance-weighted least-square fits are shown and vertical bars denote means with standard errors. Treatments are offset for clarity, but fits are drawn through non-offset mean values).

3.3.6.6 Ratio of total soluble solids to titratable acidity

The total soluble solids:titratable acidity ratio ($^{\circ}\text{B}:\text{TA}$) progressed much slower as expected in season two and displayed a linear increase with days after budburst (Figure 64) as well as with growing degree days (Figure 65); for the latter the difference between seasons was reduced.

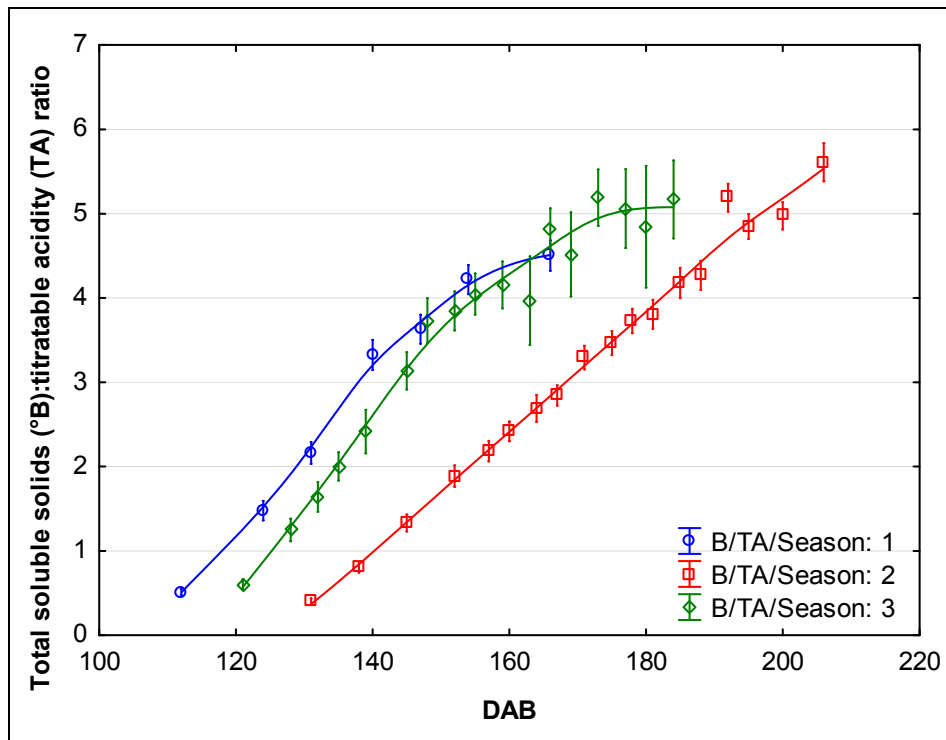


Figure 64 Total soluble solids ($^{\circ}\text{B}$):titratable acidity (TA) ratios relative to date after budburst (DAB) from véraison onwards in the different seasons. Distance-weighted least-square fits are shown and vertical bars denote means with standard errors.

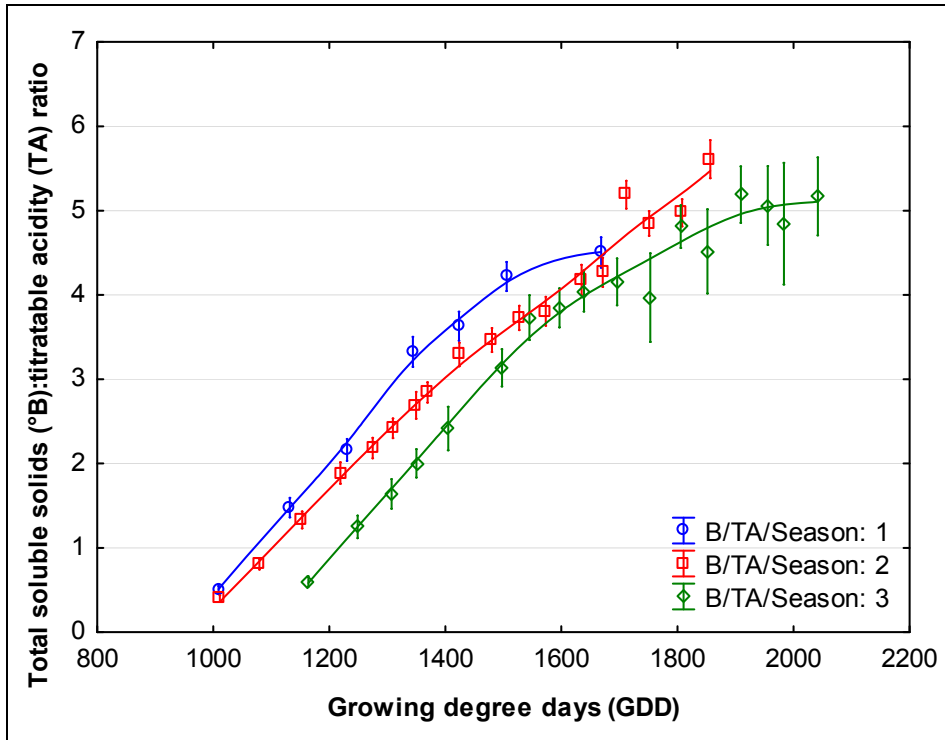


Figure 65 Total soluble solids (°B):titratable acidity (TA) ratios relative to growing degree days (GDD) from véraison onwards in the different seasons. Distance-weighted least-square fits are shown and vertical bars denote means with standard errors.

With respect to treatment differences, results from the °B:TA ratio were similar to those shown for pH (Figure 66 to Figure 68). However, the differences between treatments seemed more pronounced, especially for season three.

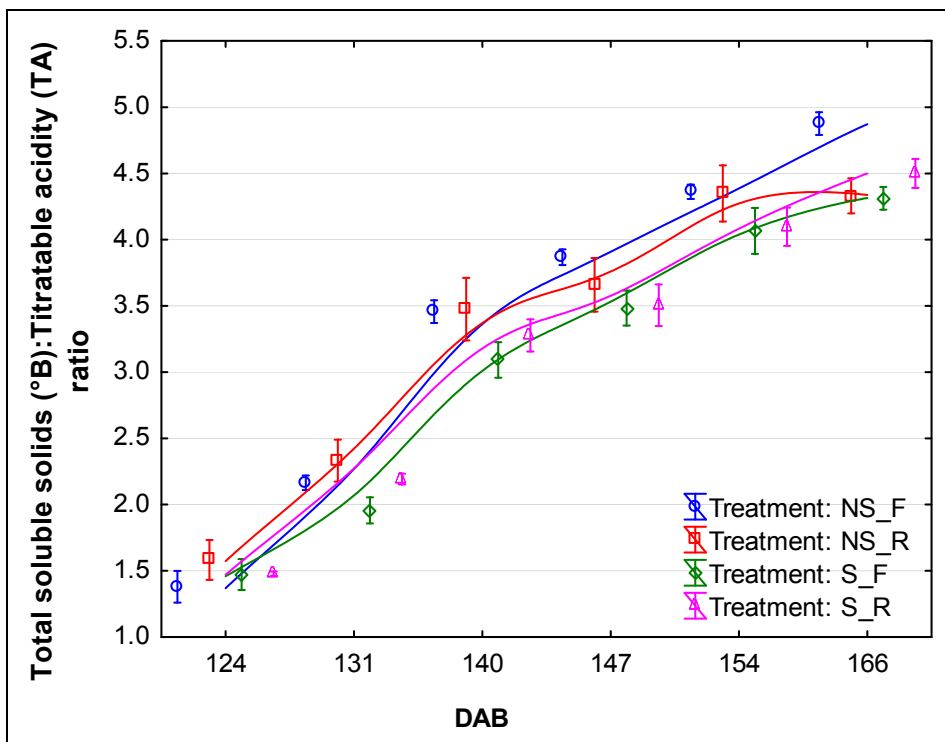


Figure 66 Total soluble solids (°B):Titratable acidity (TA) ratios relative to days after budburst (DAB) for the different treatments in the harvesting period of season one (Distance-weighted least-square fits are shown and vertical bars denote means with standard errors. Treatments are offset for clarity, but fits are drawn through non-offset mean values).

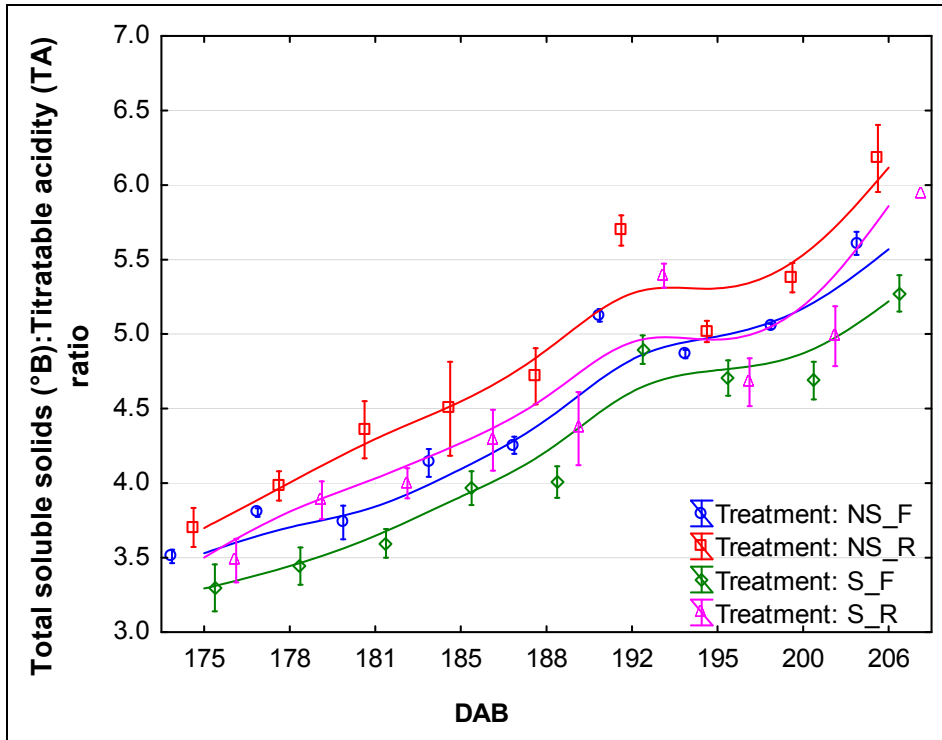


Figure 67 Total soluble solids (°B):Titratable acidity (TA) ratios relative to days after budburst (DAB) for the different treatments in the harvesting period of season two (Distance-weighted least-square fits are shown and vertical bars denote means with standard errors. Treatments are offset for clarity, but fits are drawn through non-offset mean values).

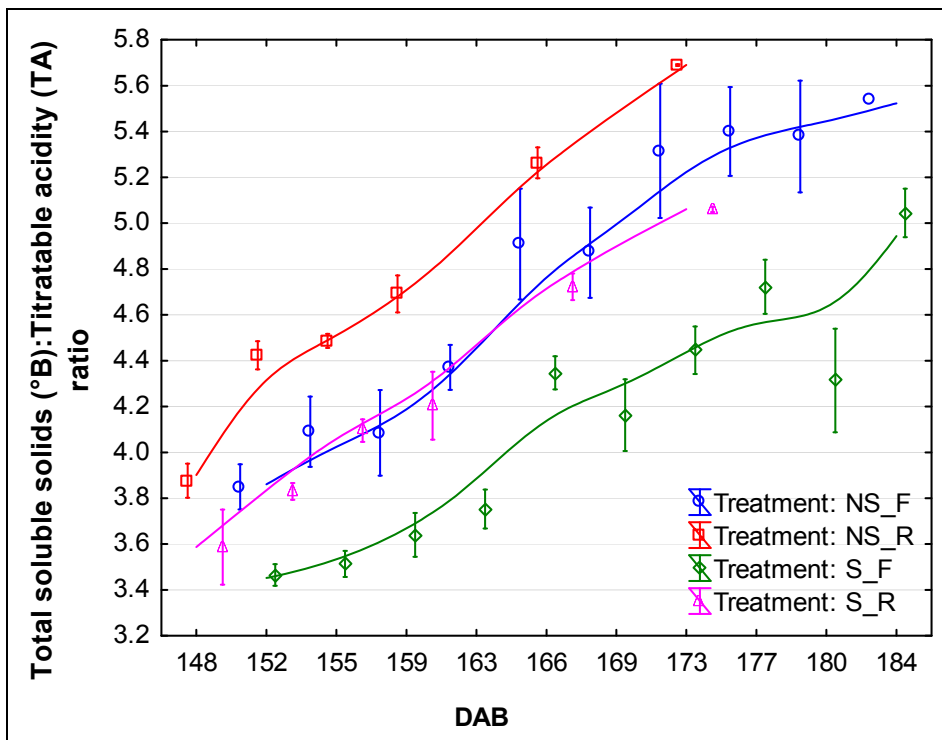


Figure 68 Total soluble solids (°B):Titratable acidity (TA) ratios relative to days after budburst (DAB) for the different treatments in the harvesting period of season three (Distance-weighted least-square fits are shown and vertical bars denote means with standard errors. Treatments are offset for clarity, but fits are drawn through non-offset mean values).

3.4 Conclusions

The three seasons studied differed considerably in terms of temperature and rainfall as well as the apparent available soil moisture.

It was expected that by removing almost half of the shoots (including the grapes) a drastic modification in microclimate, but not necessarily in the above-ground source:sink ratio, would be obtained. This is different from early leaf removal practices. Early defoliation applied before flowering is mostly aimed at limiting yield per vine, bunch or berry mass, bunch compactness and rot incidence. With these practices, the leaf area:fruit mass ratio drops dramatically, but recovers fully as secondary shoot growth compensates for the removed leaf area. Similarly, in this study secondary shoot growth compensated fully for the removed leaf area, leaving the vines with a ratio of increased leaf area (albeit younger) to fruit mass in the reduced canopies, with a much lower yield:pruning mass ratio.

Inadequate irrigation scheduling in the first season and high temperatures led to the targets of Ψ_{PD} not being reached for the NS grapevines. The transpiration losses of the full canopy vines seemed much higher than those of the reduced canopy vines, apparently decreasing the available soil water much faster. Higher water use efficiency may have occurred in the reduced canopies due to the increased secondary:primary shoot leaf area ratios. Despite the apparently wettest soil water conditions in season two, the S treatments reached the lowest Ψ_{PD} values, indicating high plant water deficits. In contrast, season three with the lowest rainfall and apparently also soil water content, did not lead to the lowest Ψ_{PD} values in the S treatments. It would seem that Shiraz does in fact display some isohydric characteristics, but it seems to be limited to dry soil conditions.

Light quality and quantity were increased for the reduced canopies, but unfortunately one limitation in this study was that it was not measured at a regular basis throughout all the seasons.

Logistic growth curve fitting was effective in analysing seasonal and treatment differences in shoot growth, with the theoretical shoot growth cessation point ($5 \text{ mm}\cdot\text{day}^{-1}$) providing an adequate cut-off point to compare seasons and treatments. Expressing shoot growth relative to thermal time units seemed to effectively eliminate time differences between seasons in terms of shoot growth rate, confirming the dependence of shoot growth on ambient temperature. The variability in growth between shoots also seemed to amplify after the shoots reached 50% of its final length, confirming that the decrease and cessation of growth between shoots are not very uniform. Despite the variability, however, logistic growth curve fitting made it possible to analyse differences between shoots for the seasons and treatments, incorporating statistical analysis into the results.

The interaction of crop load (as measured by the yield:pruning mass ratio) and shoot growth was not consistent. It was expected that the reduced canopies, with reduced ratio would show increased shoot growth rates and longest shoot lengths. This may have been counteracted by the compensatory growth of secondary shoots.

Maximum leaf size could be effectively modelled using growth curve fitting on the relationship between leaf size and node position or leaf plastochron index values.

The only season when increased bunch mass was measured for the reduced canopy treatment was season three, which could have resulted from secondary shoot removal in this season leading to the compensation reaction directed more towards bunch/berry development.

It seemed that plant water status played a dominant role in yield determination early season, which was also evident from season two showing no yield decrease despite the lowest Ψ_{PD} values

late-season compared to the other seasons. The date of harvesting would play a dominant role in yield reduction, as considerable berry mass decline occurred in all three seasons from 140 to 160 DAB.

The importance of noting the "topping status" of canes during pruning measured was confirmed from the results differing drastically between topped and non-topped shoots, especially with regards to secondary shoot length as well as primary cane mass and length.

When sugar loading was expressed relative to thermal time, the dry and warm conditions during ripening in season three appeared as less sugar loaded per thermal time unit. The maximum sugar loaded was higher in seasons two and three where crop load was reduced, with the secondary shoot compensation also possibly playing a positive role during ripening. It was surprising that sugar loading in this study seemed more difficult to predict from thermal time values than from chronological time values.

3.5 Literature cited

- Archer, E. & Strauss, H.C., 1989. The effect of plant spacing on the water status of soil and grapevines. *S. Afr. J. Enol. Vitic* 10, 49-58.
- Bergqvist, J., Dokoozlian, N. & Ebisuda, N., 2001. Sunlight exposure and temperature effects on berry growth and composition of Cabernet Sauvignon and Grenache in the Central San Joaquin Valley of California. *American Journal of Enology and Viticulture* 52, 1-7.
- Bertamini, M., Zulini, L., Muthuchelian, K. & Nedunchezian, N., 2006. Effect of water deficit on photosynthetic and other physiological responses in grapevine (*Vitis vinifera* L. cv. Riesling) plants. *Photosynthetica* 44, 151-154.
- Buttrose, M.S., 1969. Vegetative growth of grapevine varieties under controlled temperature and light intensity. *Vitis* 8, 280-285.
- Candolfi-Vasconcelos, M.C. & Koblet, W., 1990. Yield, fruit quality, bud fertility and starch reserves of the wood as a function of leaf removal in *Vitis vinifera*. Evidence of compensation and stress recovering. *Vitis* 29, 199-221.
- Candolfi-Vasconcelos, M.C. & Koblet, W., 1991. Influence of partial defoliation on gas exchange parameters and chlorophyll content of field-grown grapevines: mechanisms and limitations of the compensation capacity. *Vitis* 30, 129-141.
- Candolfi-Vasconcelos, M.C., Koblet, W., Howell, G.S. & Zweifel, W., 1994. Influence of Defoliation, Rootstock, Training System, and Leaf Position on Gas Exchange of Pinot noir Grapevines. *American Journal of Enology and Viticulture* 45, 173-180.
- Carbonneau, A., 1995. General relationship within the whole-plant: examples of the influence of vigour status, crop load and canopy exposure on the sink "berry maturation" for the grapevine. *Strategies to Optimize Wine Grape Quality* 427, 99-118.
- Carbonneau, A., 1998. Irrigation, vignoble et produits de la vigne. *Traité d'Irrigation*. J.-R. Tiercelin, coord.. Paris, Lavoisier Tec & Doc. Chapitre IV: Aspects Qualitatifs, 257-298.
- Carbonneau, A. & Deloire, A., 2001. Plant organization based on source-sink relationships: New findings on developmental, biochemical and molecular responses to environment. *In Molecular Biology and Biotechnology of the Grapevine*. Roubelakis-Angelakis, K.A. (ed.), pp. 263-268. Kluwer Academic Publishers.
- Cartechini, A. & Palliotti, A., 1995. Effect of Shading on Vine Morphology and Productivity and Leaf Gas Exchange Characteristics in Grapevines in the Field. *American Journal of Enology and Viticulture* 46, 227-234.
- Clingeffer, P.R., 1984. Production and growth of minimal pruned Sultana vines. *Vitis* 23, 42-54.

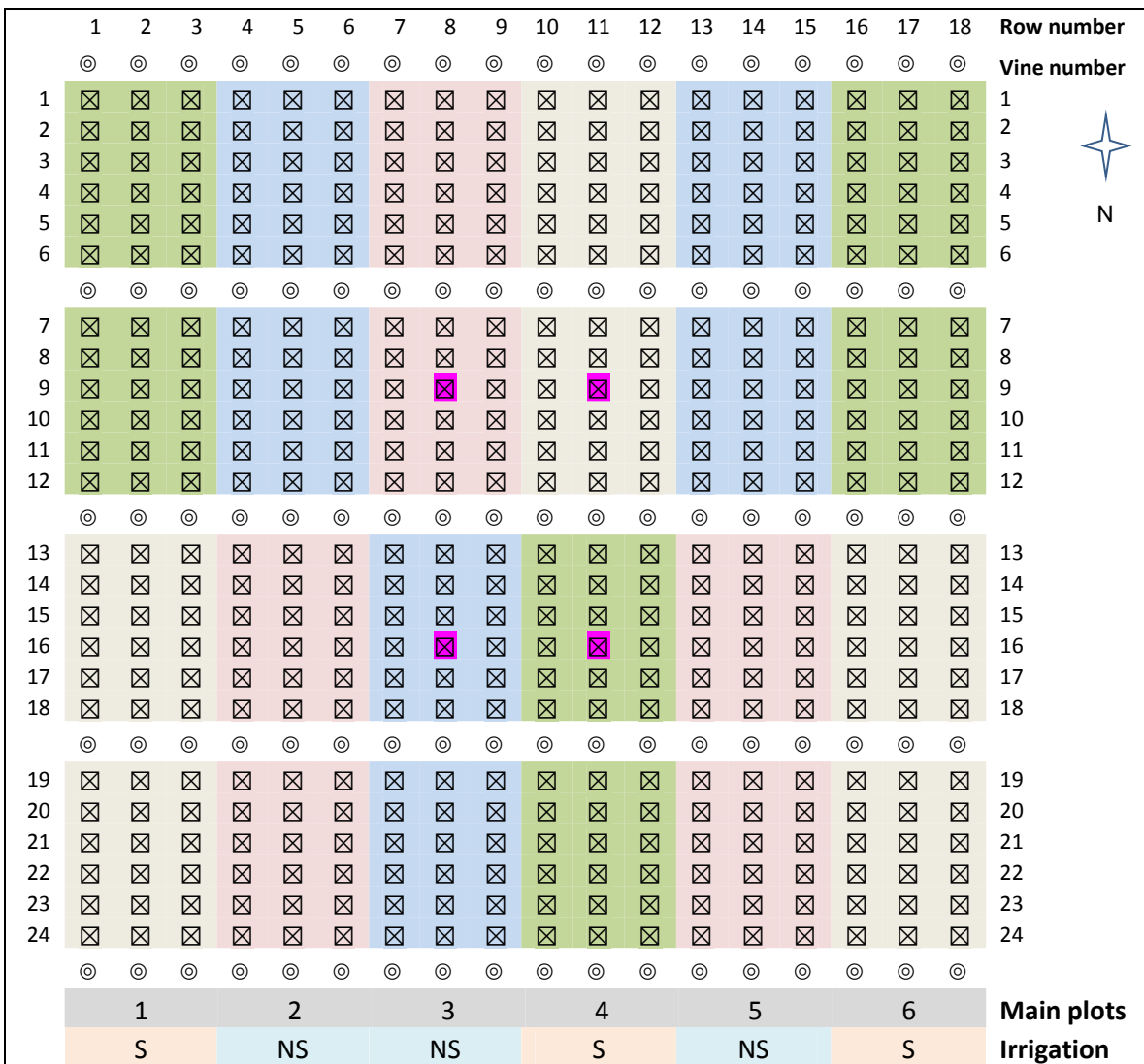
- Coipel, J., Rodriguez Lovelle, B., Sipp, C. & Van Leeuwen, C., 2006. "Terroir" effect as a result of environmental stress, depends more on soil depth than on soil type (*Vitis vinifera* L. cv. Grenache noir, Cotes du Rhone, France, 2000). *J. Int. Sci. Vigne Vin.* 40, 177-185.
- Coombe, B.G., 1992. Research on Development and Ripening of the Grape Berry. *American Journal of Enology and Viticulture* 43, 101-110.
- Coombe, B.G., 1995. Growth Stages of the Grapevine: Adoption of a system for identifying grapevine growth stages. *Australian Journal of Grape and Wine Research* 1, 104-110.
- Deloire, A., 2011. The concept of berry sugar loading. *In Wineland*, January 2011, pp. 93-95.
- Deloire, A., Carbonneau, A., Wang, Z. & Ojeda, H., 2004. Vine and water: a short review. *Journal International des Sciences de la Vigne et du Vin*, 1-14.
- Dokoozlian, N.K. & Kliewer, W.M., 1995. The Light Environment Within Grapevine Canopies. I. Description and Seasonal Changes During Fruit Development. *American Journal of Enology and Viticulture* 46, 209-218.
- Edson, C.E., Howell, G.S. & Flore, J.A., 1995. Influence of Crop Load on Photosynthesis and Dry Matter Partitioning of Seyval Grapevines. III. Seasonal Changes in Dry Matter Partitioning, Vine Morphology, Yield, and Fruit Composition. *American Journal of Enology and Viticulture* 46, 478-485.
- Ellis, W., 2008. Grapevine (Shiraz/Richter 99) water relations during berry ripening. MSc(Agric) Viticulture thesis, Stellenbosch University.
- Elsner, E.A. & Jubb, G.L.J.R., 1988. Leaf Area Estimation of Concord Grape Leaves from Simple Linear Measurements. *American Journal of Enology and Viticulture* 39, 95-97.
- Fanizza, G. & Ricciardi, L., 1990. Influence of drought stress on shoot, leaf growth, leaf water potential, stomatal resistance in wine grape genotypes (*Vitis vinifera* L.). *Vitis* (Special edition), 371-381.
- Ferguson, B.J. & Beveridge, C.A., 2009. Roles for auxin, cytokinin, and strigolactone in regulating shoot branching. *PLANT PHYSIOLOGY* 149, 1929-1944.
- Flore, J.A. & Lakso, A.N., 1989. Environmental and physiological regulation of photosynthesis in fruit crops. *Horticultural reviews*, 111-157.
- Fracheboud, Y., Luquez, V., Björkén, L., Sjödin, A., Tuominen, H. & Jansson, S., 2009. The Control of Autumn Senescence in European Aspen. *PLANT PHYSIOLOGY* 149, 1982-1991.
- Gallagher, J.N., 1979. Field studies of cereal leaf growth. I. Initiation and expansion in relation to temperature and ontogeny. *J. Exp. Bot.* 30, 625-636.
- Gómez-del-Campo, M., Ruiz, C. & Lissarrague, J.R., 2002. Effect of water stress on leaf area development, photosynthesis, and productivity in Chardonnay and Airén grapevines. *American Journal of Enology and Viticulture* 53, 138-143.
- Greenspan, M.D., Schultz, H.R. & Matthews, M.A., 1996. Field evaluation of water transport in grape berries during water deficits. *Physiologia Plantarum* 97, 55-62.
- Greenspan, M.D., Shackel, K.A. & Matthews, M.A., 1994. Developmental changes in the diurnal water budget of the grape berry exposed to water deficits. *Plant, Cell & Environment* 17, 811-820.
- Hardie, W.J. & Martin, S.R., 2000. Shoot growth on de-fruited grapevines: a physiological indicator for irrigation scheduling. *Australian Journal of Grape and Wine Research* 6, 52-58.
- Haselgrove, L., Botting, D., van Heeswijck, R., HØJ, P.B., Dry, P.R., Ford, C. & Land, P.G.I., 2000. Canopy microclimate and berry composition: The effect of bunch exposure on the phenolic composition of *Vitis vinifera* L cv. Shiraz grape berries. *Australian Journal of Grape and Wine Research* 6, 141-149.
- Heilman, J.L., McInnes, K.J., Gesch, R.W., Lascano, R.J. & Savage, M.J., 1996. Effects of trellising on the energy balance of a vineyard. *Agricultural and Forest Meteorology* 81, 79-93.
- Herold, A., 1980. Regulation of photosynthesis by sink activity - the missing link. *New Phytol.* 86, 131-144.
- Hunter, J. & Visser, J., 1990. The effect of partial defoliation on growth characteristics of *Vitis vinifera* L. cv. Cabernet Sauvignon II. Reproductive growth. *South African Journal of Enology and Viticulture* 11, 26-32.

- Hunter, J.J., 1999. Present status and prospects of winegrape viticulture in South Africa – focus on canopy related aspects/practices and relationships with grape and wine quality. In: Proc. 11th Meeting of the Study Group for Vine Training Systems (GESCO), 6-12 June 1999, Sicily, Italy. pp. 70-85.
- Hunter, J.J., 2000. Implications of seasonal canopy management and growth compensation in grapevine. South african journal for enology and viticulture 21, 81-91.
- Hunter, J.J. & Archer, E., 2002. Status of grapevine canopy management and future prospects (Papel actual y perspectivas futuras de la gestión del follaje). In ACE Revista de Enología, May 2002, pp.
- Hunter, J.J. & Deloire, A., 2005. Relationship between sugar loading and berry size of ripening Syrah/R99 grapes as affected by grapevine water status. In: Proc. Gesco XIVeme journees du groupe europeen d'etude des systems de conduit de la vigne, 23-27Août, Geisenheim, Allemagne. pp. 127-133.
- Hunter, J.J. & Le Roux, D.J., 2000. Canopy management effects on yield, labour input, and growth compensation-new canopy composition perspectives. Acta Hort. (ISHS) 526, 81-90.
- Hunter, J.J., Ruffner, H.P., Volschenk, C.G. & Le Roux, D.J., 1995. Partial Defoliation of *Vitis vinifera* L. cv. Cabernet Sauvignon/99 Richter: Effect on Root Growth, Canopy Efficiency; Grape Composition, and Wine Quality. American Journal of Enology and Viticulture 46, 306-314.
- Hunter, J.J. & Visser, J.H., 1988. The effect of partial defoliation, leaf position and developmental stage of the vine on photosynthetic activity of *Vitis vinifera* L. cv Cabernet Sauvignon. S. Afr. J. Enol. Vitic. 9, 9-15.
- Hunter, J.J. & Visser, J.H., 1989. The effect of partial defoliation, leaf position and developmental stage of the vine on leaf chlorophyll concentration in relation to the photosynthetic activity and light intensity in the canopy of *Vitis vinifera* L. cv. Cabernet Sauvignon. S. Afr. J. Enol. Vitic. 10, 67-73.
- Iacono, F., Bertamini, M., Scienza, A. & Coombe, B.G., 1995. Differential effects of canopy manipulation and shading of *Vitis vinifera* L. cv. Cabernet Sauvignon. Leaf gas exchange, photosynthetic electron transport rate and sugar accumulation in berries. Vitis 34, 201-206.
- Jackson, D.I. & Lombard, P.B., 1993. Environmental and management practices affecting grape composition and wine quality-a review. American Journal of Enology and Viticulture 44, 409-430.
- Johnson, J.O., Weaver, R.J. & Paige, D.F., 1982. Differences in the mobilization of assimilates of *Vitis vinifera* L. grapevines as influenced by an increased source strength. American Journal of Enology and Viticulture 33, 207-213.
- Keller, M., 2010. The science of grapevines: anatomy and physiology.
- Keller, M. & Koblet, W., 1995. Dry matter and leaf area partitioning, bud fertility and second season growth of *Vitis vinifera* L.: Responses to nitrogen supply and limiting irradiance. Vitis 34, 77-83.
- Keller, M., Smithyman, R.P. & Mills, L.J., 2008. Interactive Effects of Deficit Irrigation and Crop Load on Cabernet Sauvignon in an Arid Climate. American Journal of Enology and Viticulture 59, 221-234.
- Kliwer, W.M. & Lider, L.A., 1968. Influence of cluster exposure to the sun on the composition of Thompson Seedless fruit. American Journal of Enology and Viticulture 19, 175-184.
- Lategan, E.L., 2011. Determining of optimum irrigation schedules for drip irrigated Shiraz vineyards in the Breede River Valley. MSc(Agric) Soil Science thesis, Stellenbosch University, Stellenbosch.
- Lebon, E., Dumas, V., Pieri, P. & Schultz, H.R., 2003. Modelling the seasonal dynamics of the soil water balance of vineyards. Functional Plant Biology 30, 699-710.
- Lebon, E., Pellegrino, A., Louarn, G. & Lecoeur, J., 2006. Branch Development Controls Leaf Area Dynamics in Grapevine (*Vitis vinifera*) Growing in Drying Soil. Annals of Botany 98, 175-185.
- Lebon, E., Pellegrino, A., Tardieu, F. & Lecoeur, J., 2004. Shoot Development in Grapevine (*Vitis vinifera*) is Affected by the Modular Branching Pattern of the Stem and Intra- and Inter-shoot Trophic Competition. Annals of Botany 93, 263-274.
- Lim, P.O., Kim, H.J. & Gil Nam, H., 2007. Leaf Senescence. Annual Review of Plant Biology 58, 115-136.
- Louarn, G., Guedon, Y., Lecoeur, J. & Lebon, E., 2007. Quantitative Analysis of the Phenotypic Variability of Shoot Architecture in Two Grapevine (*Vitis vinifera*) Cultivars. Annals of Botany 99, 425-437.

- May, P., 2000. From bud to berry, with special reference to inflorescence and bunch morphology in *Vitis vinifera* L. Australian Journal of Grape and Wine Research 6, 82-98.
- Mullins, M.G., Bouquet, A. & Williams, L.E., 1992. Biology of the grapevine. Cambridge University Press, Cambridge.
- Mwange, K., Hou, H., Wang, Y., He, X. & Cui, K., 2005. Opposite patterns in the annual distribution and time-course of endogenous abscisic acid and indole-3-acetic acid in relation to the periodicity of cambial activity in *Eucommia ulmoides* Oliv. Journal of Experimental Botany 56, 1017-1028.
- Myburgh, P.A., 2005a. Effect of altitude and distance from the Atlantic Ocean on mean February temperatures in the Western Cape Coastal Region. In Wynboer technical yearbook, pp. 49-52.
- Myburgh, P.A., 2005b. Water status, vegetative growth and yield responses of *Vitis vinifera* L. cvs. Sauvignon blanc and Chenin blanc to timing of irrigation during berry ripening in the coastal region of South Africa. South african journal for enology and viticulture 26, 59.
- Myburgh, P.A., 2006. Juice and wine quality responses of *Vitis vinifera* L. cvs. Sauvignon blanc and Chenin blanc to timing of irrigation during berry ripening in the coastal region of South Africa. South african journal for enology and viticulture 27, 1.
- Myburgh, P.A., Van Zyl, J.L. & Conradie, W.J., 1996. Effect of soil depth on growth and water consumption of young *Vitis vinifera* L. cv. Pinot noir. South african journal for enology and viticulture 17.
- Ojeda, H., Andary, C., Kraeva, E., Carbonneau, A. & Deloire, A., 2002. Influence of Pre- and Postveraison Water Deficit on Synthesis and Concentration of Skin Phenolic Compounds during Berry Growth of *Vitis vinifera* cv. Shiraz. American Journal of Enology and Viticulture 53, 261-267.
- Palliotti, A., Gatti, M. & Poni, S., 2011. Early Leaf Removal to Improve Vineyard Efficiency: Gas Exchange, Source-to-Sink Balance, and Reserve Storage Responses. American Journal of Enology and Viticulture.
- Pandey, R.M. & Farmahan, H.C., 1977. Changes in the rate of photosynthesis and respiration in leaves and berries of *Vitis vinifera* grapevines at various stages of berry development. Vitis 16, 106-111.
- Petrie, P.R., Trought, M.C.T. & Howell, G.S., 2000. Fruit composition and ripening of Pinot Noir (*Vitis vinifera* L.) in relation to leaf area. Australian Journal of Grape and Wine Research 6, 46-51.
- Poni, S. & Giachino, E., 2000. Growth, photosynthesis and cropping of potted grapevines (*Vitis vinifera* L. cv. Cabernet Sauvignon) in relation to shoot trimming. Australian Journal of Grape and Wine Research 6, 216-226.
- Poni, S., Intrieri, C. & Silvestroni, O., 1994. Interactions of Leaf Age, Fruiting, and Exogenous Cytokinins in Sangiovese Grapevines Under Non-Irrigated Conditions. II. Chlorophyll and Nitrogen Content. Am. J. Enol. Vitic. 45, 278-284.
- Ritz, C. & Streibig, J.C., 2005. Bioassay analysis using R. Journal of Statistical Software 12, 1-22.
- Rohde, A. & Bhalerao, R.P., 2007. Plant dormancy in the perennial context. Trends in Plant Science 12, 217-223.
- Rolland, F., Moore, B. & Sheen, J., 2002. Sugar Sensing and Signaling in Plants. The Plant Cell Online 14, S185-S205.
- Scholander, P.F., Hammel, H.T., Bradstreet, E.D. & Hemmingsen, E.A., 1965. Sap pressure in vascular plants. Science 148, 339-346.
- Schultz, H.R., 1989. CO₂-Gaswechsel und Wassertransport von Stark- und Schwachlichttrieben bei *Vitis vinifera* L. (cv. Riesling) in Abhängigkeit von Klima- und Pflanzenfaktoren - Ansatz eines empirischen Assimilationsmodells. Geisenheimer Berichte, Veröffentlichungender FA Geisenheim Band 5, 221 pp.
- Schultz, H.R., 1992. An empirical model for the simulation of leaf appearance and leaf area development of primary shoots of several grapevine (*Vitis vinifera* L.) canopy-systems. Scientia Horticulturae 52, 179-200.
- Schultz, H.R., 1995. Water relations and photosynthetic responses of two grapevine cultivars of different geographical origin during water stress. Strategies to Optimize Wine Grape Quality 427, 251-266.

- Schultz, H.R., 2003. Differences in hydraulic architecture account for near-isohydric and anisohydric behaviour of two field-grown *Vitis vinifera* L. cultivars during drought. *Plant, Cell & Environment* 26, 1393-1405.
- Schultz, H.R. & Matthews, M.A., 1988. Vegetative Growth Distribution during Water Deficits in *Vitis vinifera* L. *Aust. J. Plant Physiol.* 15, 641-656.
- Smart, R.E. & Coombe, B.G., 1983. Water relations of grapevines. *In Water Deficits and Plant Growth*, Vol. VII, Additional Woody Crop Plants. Kozlowski, T.T. (ed.), pp. 137-196. Academic Press, New York.
- Smart, R.E., Shaulis, N.J. & Lemon, E.R., 1982. The effect of Concord vineyard microclimate on yield. II. The interrelations between microclimate and yield expression. *American Journal of Enology and Viticulture* 33, 109-116.
- Smart, R.E., Smith, S.M. & Winchester, R.V., 1988. Light Quality and Quantity Effects on Fruit Ripening for Cabernet Sauvignon. *American Journal of Enology and Viticulture* 39, 250-258.
- Stoll, M., Loveys, B. & Dry, P., 2000. Hormonal changes induced by partial rootzone drying of irrigated grapevine. *Journal of Experimental Botany* 51, 1627.
- Swanepoel, J.J. & Archer, E., 1988. The ontogeny and development of *Vitis vinifera* L. cv. Chenin blanc inflorescence in relation to phenological stages. *Vitis* 27.
- Tarara, J.M., Blom, P.E., Shafii, B., Price, W.J. & Olmstead, M.A., 2009. Modeling Seasonal Dynamics of Canopy and Fruit Growth in Grapevine for Application in Trellis Tension Monitoring.
- Thomas, H. & Stoddart, J.L., 1980. Leaf Senescence. *Annual Review of Plant Physiology* 31, 83-111.
- Thomas, T.R., Matthews, M.A. & Shackel, K.A., 2006. Direct in situ measurement of cell turgor in grape (*Vitis vinifera* L.) berries during development and in response to plant water deficits. *Plant, Cell & Environment* 29, 993-1001.
- Trambouze, W. & Voltz, M., 2001. Measurement and modelling of the transpiration of a Mediterranean vineyard. *Agricultural and Forest Meteorology* 107, 153-166.
- Van Leeuwen, C., Friant, P., Chone, X., Tregoat, O., Koundouras, S. & Dubourdieu, D., 2004. Influence of climate, soil and cultivar on terroir. *American Journal of Enology and Viticulture* 55, 207-217.
- Van Zyl, J. & Kennedy, C., 1983. Vine response to water stress induced by polyethylene glycol. *S. Afr. J. Enol. Vitic* 4, 15.
- Van Zyl, J.L. & Weber, H.W., 1977. Irrigation of Chenin blanc in the Stellenbosch area within the framework of the climate-soil-water-plant continuum. . *In: Proc. International Symposium on the Quality of the Vintage*, 14-21 February 1977, Cape Town, South Africa. pp. 331-349.
- Volschenk, C.G. & Hunter, J., 2001. Effect of trellis conversion on the performance of Chenin blanc/99 Richter grapevines. *South African Journal of Enology and Viticulture* 22, 31-35.
- Wang, Z.P., Deloire, A., Carbonneau, A., Federspiel, B. & Lopez, F., 2003. An in vivo experimental system to study sugar phloem unloading in ripening grape berries during water deficiency stress. *Annals of Botany* 92, 523-528.
- Williams, L.E. & Ayars, J.E., 2005. Grapevine water use and the crop coefficient are linear functions of the shaded area measured beneath the canopy. *Agricultural and Forest Meteorology* 132, 201-211.
- Williams, L.E. & Matthews, M.A., 1990. Grapevine. *In Agronomy: Irrigation of Agricultural Crops*. Stewart, B.A. and Nielson, N.R. (eds.), pp. 1019-1055. ASA-CSSA-SSSA, Madison, WI, USA.
- Winkler, A.J. & Williams, W.O., 1939. The heat required to bring Tokay grapes to maturity. *Proc. Am. Soc. Hortic. Sci.* 37, 650-652.
- Yuste, J., Asenjo, J.L., Martín, H. & Yuste, R., 2004. Influence of irrigation on water status, productivity, yield and must composition in Tempranillo grapevine under Duero Valley zone conditions. *In: Proc. Joint International Conference on Viticultural Zoning*, 15-19 November 2004, Cape Town, South Africa. pp. 416-421.

3.6 Addendum A - Experiment layout



Irrigation	Canopy treatment
Non stressed	Full canopy
Non stressed	Reduced canopy
Stressed	Full canopy
Stressed	Reduced canopy
⊠ Neutron probe positions	

Figure 69 Experiment layout according to a split-plot design in seasons 1 and 2. Main plots are shown and sub-plots are represented by the different canopy manipulation treatments shown within a main plot.

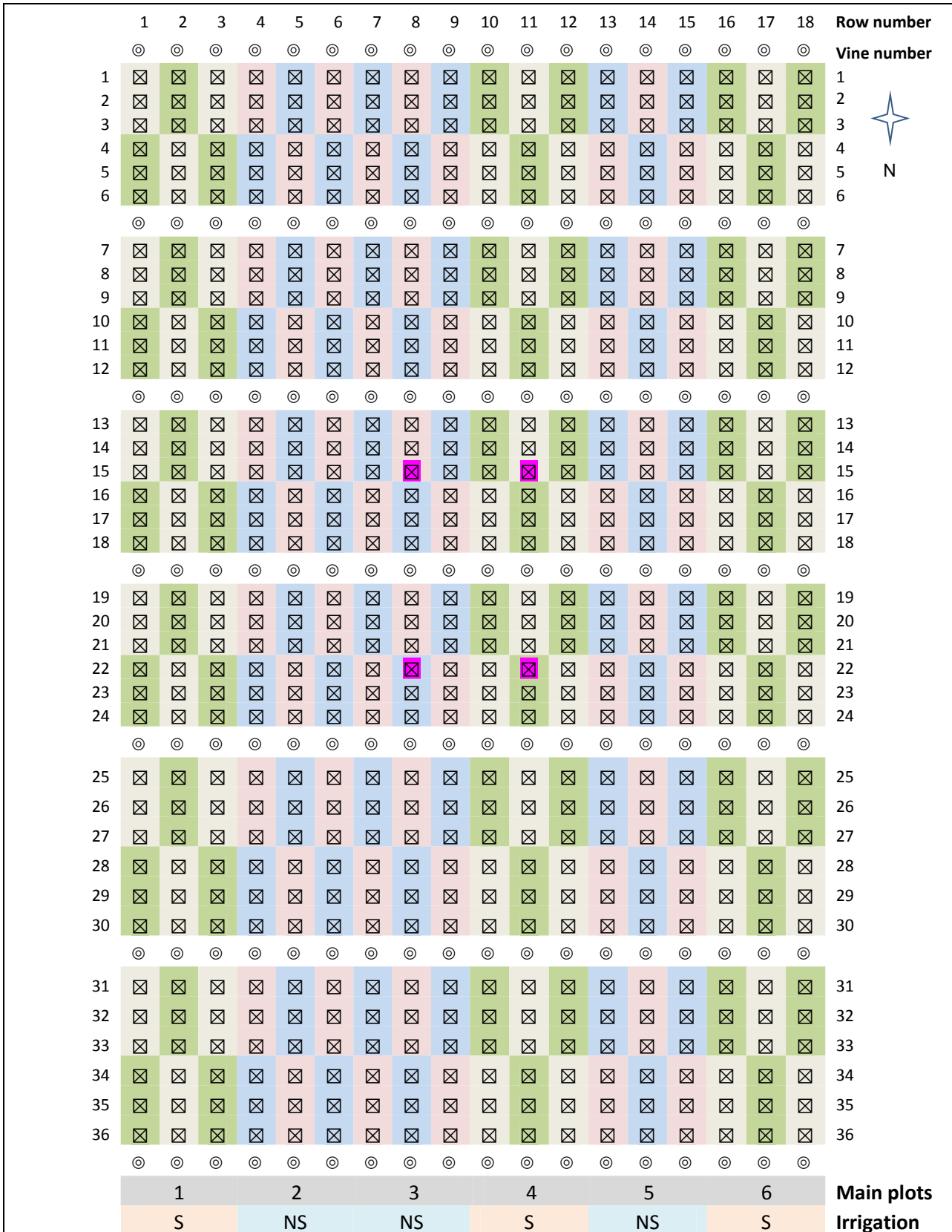


Figure 70 Experiment layout according to a split-plot design in season 3. Main plots are shown and sub-plots are represented by the different individual plots of canopy manipulation treatments shown within a main plot.

3.7 Addendum A - Phenology

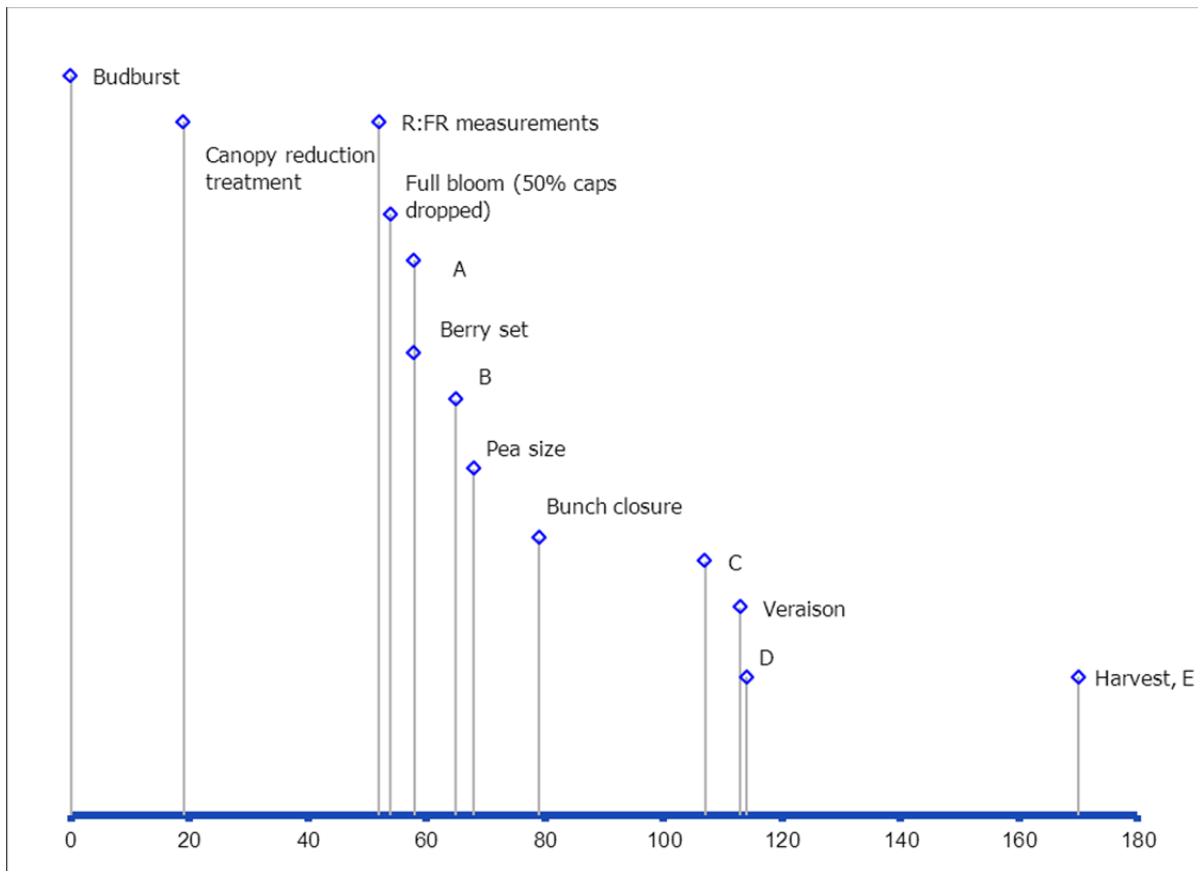


Figure 71 Main phenological stages according to days after budburst (DAB) for the trial vineyard during season one, also indicating main pigment measurement dates (A to E) (Budburst was recorded on 1 Oct 2008).

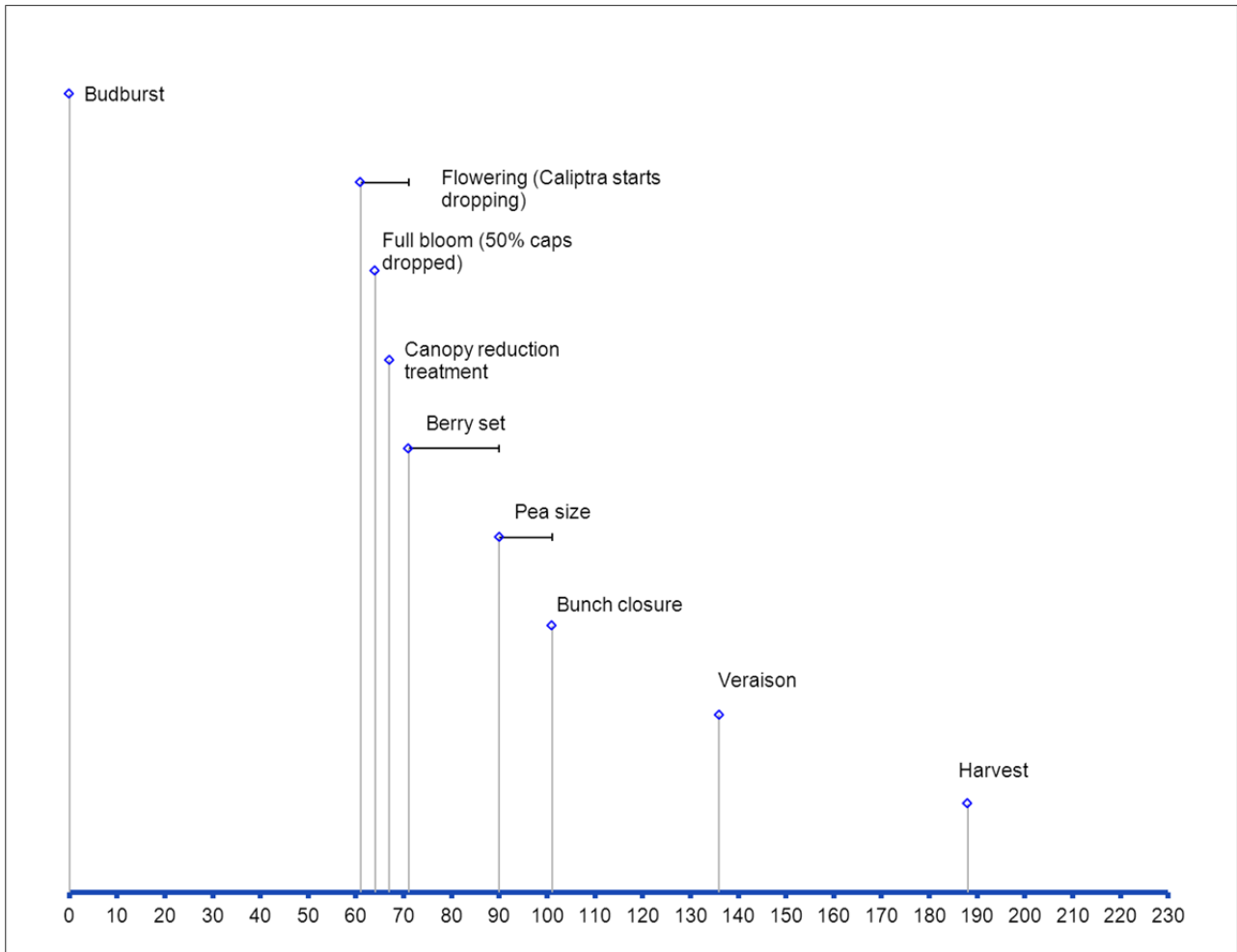


Figure 72 Main phenological stages according to days after budburst (DAB) for the trial vineyard during season two (Budburst was recorded on 4 Sept 2009).

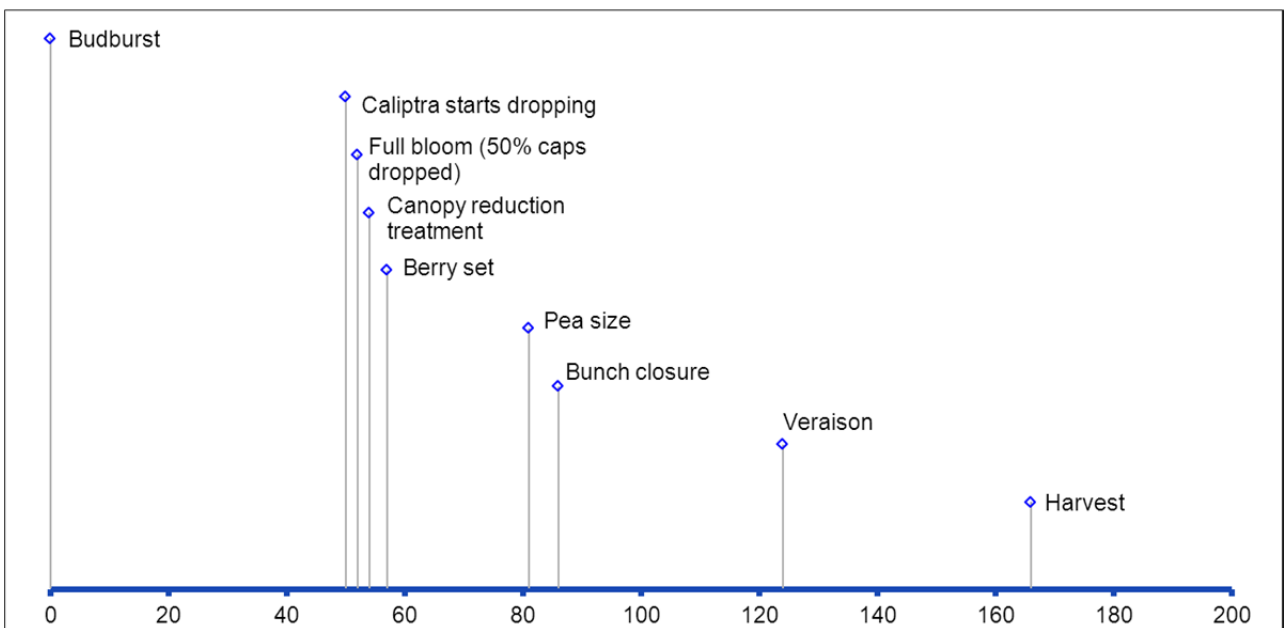


Figure 73 Main phenological stages according to days after budburst (DAB) for the trial vineyard during season three (Budburst was recorded on 15 Sept 2010).

3.8 Addendum B - Rainfall / ET

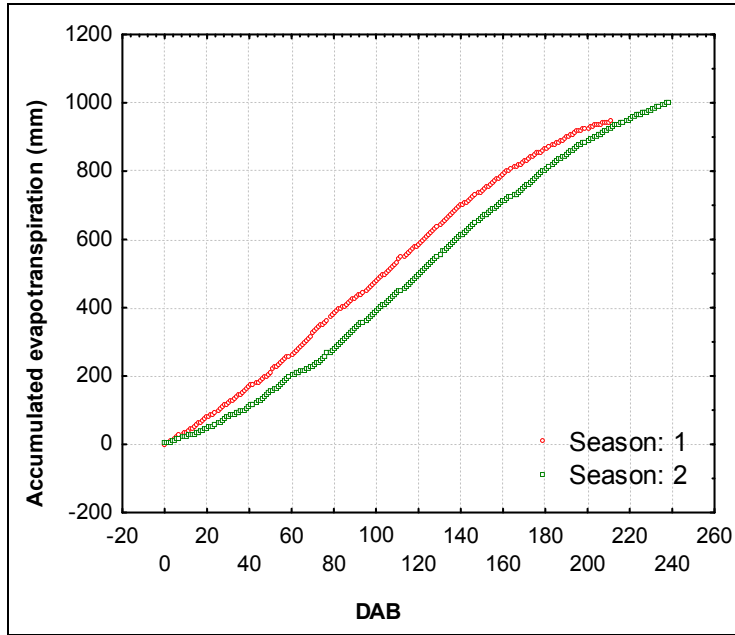


Figure 74 Accumulated evapotranspiration (mm) shown for the first two seasons of the study.

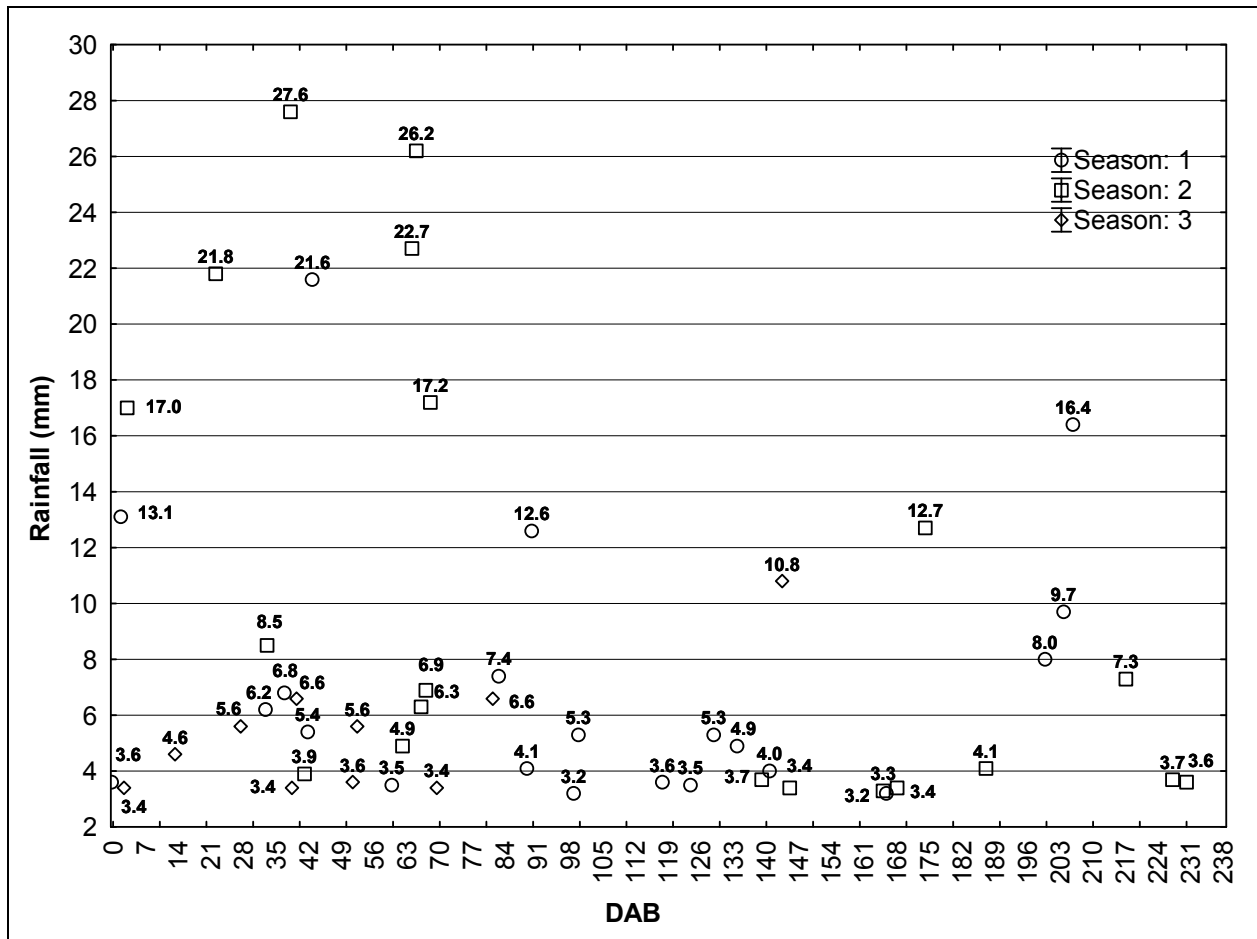


Figure 75 Rainfall (mm) recorded during the growing seasons.

3.9 Addendum B - Irrigation

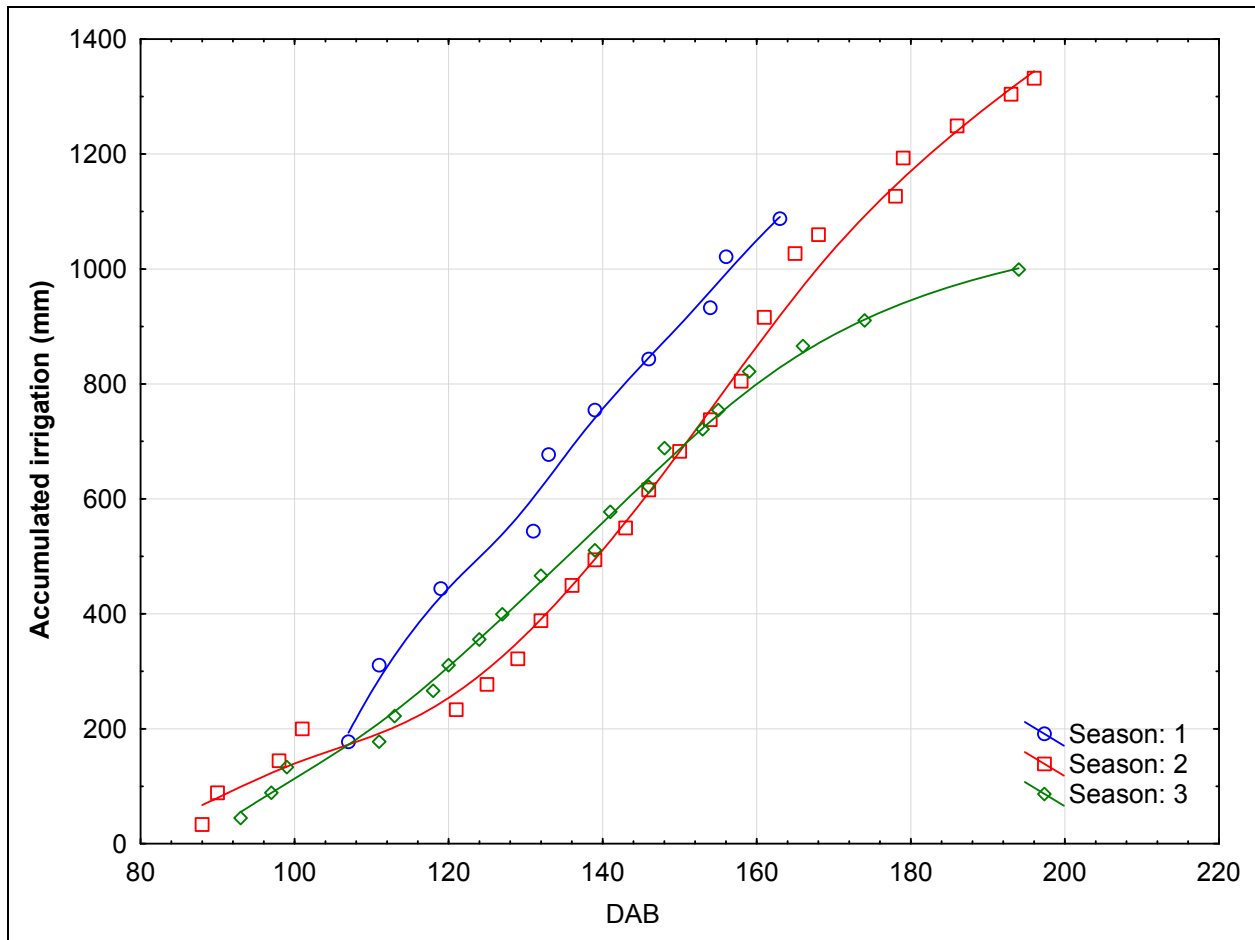


Figure 76 Accumulated irrigation (mm) applied to the NS treatments. A distance-weighted least-square fit is shown for clarity.

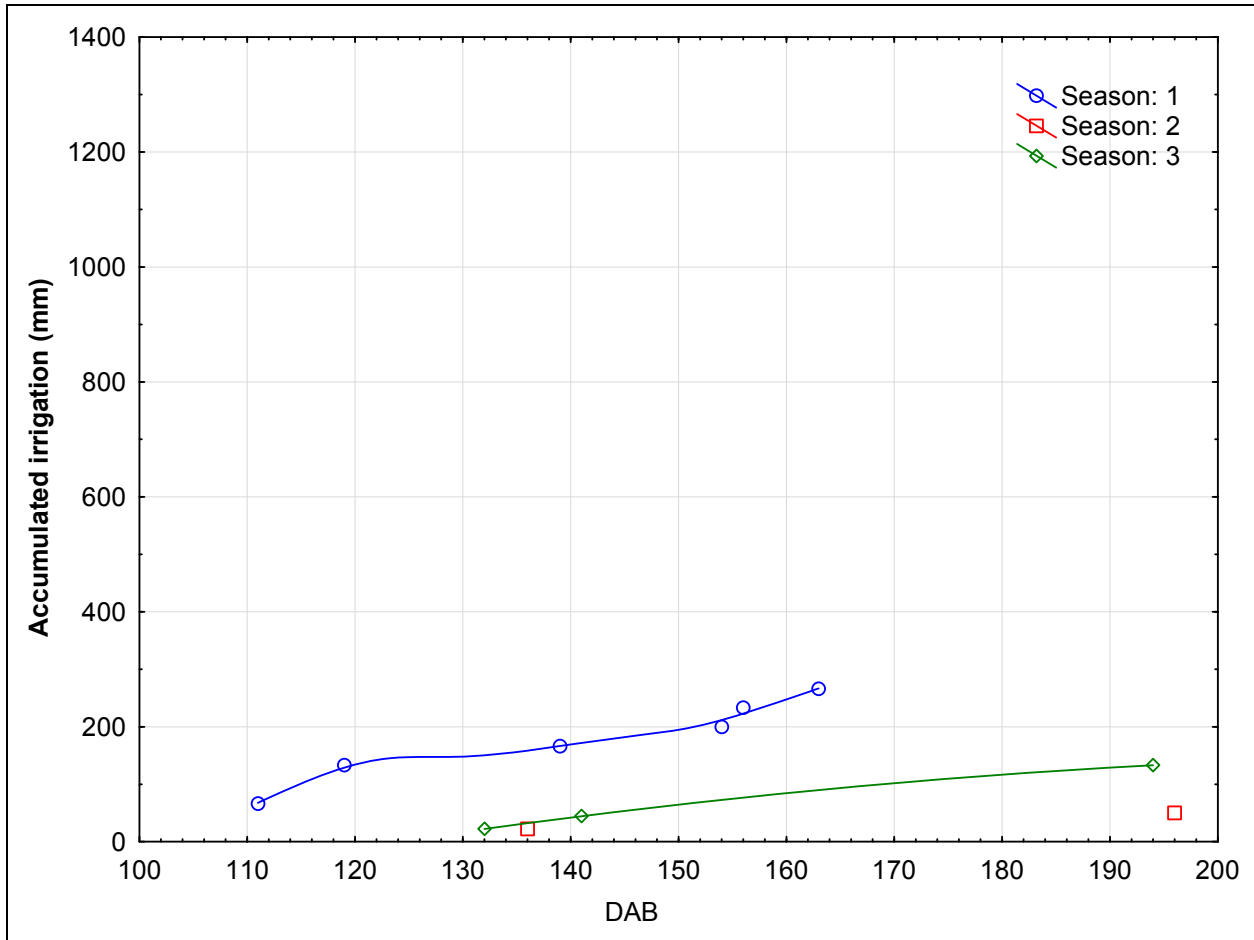


Figure 77 Accumulated irrigation (mm) applied to the S treatments. A distance-weighted least-square fit is shown for clarity.

3.10 Addendum C - Pruning and yield data results

Table 21 Results from measurements conducted during winter pruning in the different seasons (all parameters shown have non-significant ($p \leq 0.05$) main effects, second- and third-order interactions).

		Season 1	Season 2	Season 3
Mass/bunch (g)	N	19	24	
	Mean	206.59	182.23	
	SD	35.05	26.87	
Total cane mass/vine (kg)	N	20	24	
	Mean	1.45	1.38	
	SD	0.29	0.21	
Primary cane length (cm)	N	12	20	
	Mean	257.78	215.67	
	SD	26.80	67.28	
Node number per cane	N	12		
	Mean	24.28		
	SD	1.85		
Number of secondary shoots per primary cane	N		20	126
	Mean		4.40	2.69
	SD		1.64	1.88
Total secondary shoot length per primary cane (cm)	N	12		126
	Mean	174.45		47.55
	SD	54.37		46.67
Mean secondary shoot length (cm)	N	12		
	Mean	54.38		
	SD	14.19		
Total secondary cane mass per primary cane (g)	N			126
	Mean			24.94
	SD			34.02

Table 22 Second-order interactions between irrigation and canopy manipulation treatments for measurements conducted during winter pruning in the different seasons (only parameters that show significant second-order interactions at $p \leq 0.05$ are indicated, the third table indicates % differences between the significant interactions where applicable).

Season 1		Irrigation*Canopy			
		Non-stressed		Stressed	
		Full	Reduced	Full	Reduced
Yield:PM ratio	N	3	6	4	6
	Mean	4.00 c	2.04 ab	2.72 a	1.83 b
	SD	0.47	0.28	0.92	0.37

Season 3		Irrigation*Canopy			
		Non-stressed		Stressed	
		Full	Reduced	Full	Reduced
Yield/vine (kg)	N	54	55	54	53
	Mean	5.59 b	3.28 a	3.88 a	2.26 c
	SD	1.23	0.68	1.77	1.07
Non-bearing canes/vine	N	54	55	48	47
	Mean	0.86 b	0.08 a	1.40 c	0.13 a
	SD	0.76	0.18	1.28	0.25

Season 3		NSF	NSR	SF	SR
Yield/vine (kg)	NSF		-41%	-31%	-60%
	NSR	-41%			-31%
	SF	-31%			-42%
	SR	-60%	-31%	-42%	
Non-bearing canes/vine	NSF		-90%	62%	
	NSR	-90%			NS
	SF	62%			-91%
	SR		NS	-91%	

Table 23 Second-order interactions between cane topping status and canopy manipulation treatments for measurements conducted during winter pruning in season two (only parameters that show significant second-order interactions at $p \leq 0.05$ are shown, the second table indicates % differences between the significant interactions where applicable).

Season 2		Canopy*Topping			
		Topped		Non-topped	
		Full	Reduced	Full	Reduced
Total secondary shoot length per primary cane (cm)	N	5	5	5	5
	Mean	219.71 bc	387.77 a	173.65 c	229.18 ab
	SD	100.84	90.85	100.68	76.51

		TF	TR	NTF	NTR
Total secondary shoot length per primary cane (cm)	TF		76%	-21%	
	TR	76%			-41%
	NTF	-21%			31%
	NTR		-41%	31%	

Table 24 Main effects of shoot topping status for measurements conducted during winter pruning in the different seasons (only parameters that show significant first-order interactions at $p \leq 0.05$ are shown).

		Season 2			Season 3		
		Topping status			Topping status		
		Topped	Non-topped	% diff.	Topped	Non-topped	% diff.
Mass per primary cane (g)	N	10	10	36%	79	112	23%
	Mean	114.6994	156.3475		130.38	159.87	
	SD	29.38237	36.96236		55.92	64.98	
Primary cane length (cm)	N	10	10	63%	79	112	13%
	Mean	164.1623	267.1867		124.21	140.23	
	SD	29.6732	52.7237		63.16	66.13	
Mean secondary shoot length (cm)	N	10	10	-31%			
	Mean	66.22	45.74				
	SD	19.92	10.94				

Table 25 Main effects of canopy manipulation treatments for measurements conducted during winter pruning in the different seasons (only parameters that show significant first-order interactions at $p \leq 0.05$ are shown).

		Season 1			Season 2			Season 3		
		Canopy manipulation			Canopy manipulation			Canopy manipulation		
		Full	Reduced	% diff.	Full	Reduced	% diff.	Full	Reduced	% diff.
Total number of bunches per vine	N	7	12	-37%	12	12	-40%	108	108	-48%
	Mean	20.79	13.00		28.74	17.29		28.98	15.09	
	SD	4.02	2.08		1.41	1.37		4.49	2.14	
Yield/vine (kg)	N	7	12	-43%	12	12	-33%			
	Mean	4.57	2.60		4.97	3.32				
	SD	1.09	0.73		0.68	0.60				
Mass/bunch (g)	N							108	108	11%
	Mean							164.97	183.76	
	SD							57.13	62.46	
Total primary canes/vine	N	8	12	-41%	12	12	-30%	108	108	-50%
	Mean	14.04	8.29		14.45	10.16		15.85	8.00	
	SD	2.43	0.42		0.72	0.96		1.48	0.60	
Bearing canes/vine	N				12	12	-40%	108	108	-47%
	Mean				13.09	7.79		14.80	7.90	
	SD				0.57	0.22		1.11	0.51	
Bearing cane mass (kg)	N				12	12	-19%	108	108	-17%
	Mean				0.98	0.80		1.60	1.33	
	SD				0.14	0.13		0.37	0.34	
Non-bearing canes/vine	N				12	12	50%	102	102	-91%
	Mean				2.16	3.23		1.12	0.10	
	SD				0.74	0.85		1.07	0.21	
Total cane mass/vine (kg)	N							108	108	-18%
	Mean							1.63	1.34	
	SD							0.37	0.35	

		Season 1			Season 2			Season 3		
		Canopy manipulation			Canopy manipulation			Canopy manipulation		
		Full	Reduced	% diff.	Full	Reduced	% diff.	Full	Reduced	% diff.
Mean secondary cane mass (g)	N				12	12	23%			
	Mean				21.09	26.00				
	SD				4.31	3.75				
Mass per primary cane (g)	N	8	12	53%	12	12	35%	108	108	61%
	Mean	111.44	170.71		76.23	102.89		104.66	168.73	
	SD	25.28	34.98		10.49	15.31		25.90	42.52	
Yield:PM ratio	N	7	12	-41%	12	12	-31%	108	108	-28%
	Mean	3.27	1.93		3.75	2.57		3.22	2.30	
	SD	0.98	0.33		0.34	0.36		1.20	0.93	
Number of secondary shoots per primary cane	N	6	6	59%						
	Mean	2.50	3.98							
	SD	0.58	0.86							
Total secondary cane mass per primary cane (g)	N				10	10	59%			
	Mean				51.85	82.55				
	SD				28.72	34.86				
Mean secondary shoot length (cm)	N							65	61	31%
	Mean							13.75	18.03	
	SD							6.74	9.18	

Table 26 Main effects of irrigation treatments for measurements conducted during winter pruning in the different seasons (only parameters that show significant first-order interactions at $p \leq 0.05$ are shown).

		Season 2			Season 3		
		Non-stressed	Stressed	% diff.	Non-stressed	Stressed	% diff.
Mass/bunch (kg)	N				109	107	-33%
	Mean				207.94	140.17	
	SD				38.76	59.52	
Total primary canes/vine	N				109	107	4%
	Mean				11.68	12.17	
	SD				3.94	4.25	
Bearing cane mass (kg)	N				109	107	-9%
	Mean				1.54	1.40	
	SD				0.35	0.40	
Non-bearing canes/vine	N				109	95	64%
	Mean				0.47	0.77	
	SD				0.67	1.12	
Non-bearing cane mass (kg)	N	12	12	-44%			
	Mean	0.13	0.07				
	SD	0.03	0.04				
Mass per primary cane (g)	N	8	12	-29%	109	107	-11%
	Mean	164.33	116.32		144.47	128.77	
	SD	29.70	32.33		45.29	48.76	
Yield:PM ratio	N				109	107	-18%
	Mean				3.04	2.48	
	SD				0.84	1.36	

Chapter IV

Research Results

Response of *Vitis vinifera* L. cv. Shiraz leaves to canopy manipulation and water deficit, with specific reference to leaf age

Chapter IV: Response of *Vitis vinifera* L. cv. Shiraz leaves to canopy manipulation and water deficit, with specific reference to leaf age

4.1 Introduction

In many studies of plant reaction to its environment, leaf age effects are avoided by implicitly sampling from a variety of leaves from different plant canopy positions. Other studies, however, specify leaf age by incorporating date after emergence or unfolding (Kriedemann *et al.*, 1970; Liakopoulos *et al.*, 2006) or by grouping leaves in different categories according to position on the shoot (Hunter & Visser, 1988; Hunter & Visser, 1989; Bertamini & Nedunchezian, 2002; Bertamini & Nedunchezian, 2003).

The “plastochron” term has been proposed more than a century ago by Askenasy (1880) to define the interval of time between formation of two successive internode cells in *Nitella flexilis*, but it was adapted by Erickson & Michelini (1957) to include leaf length as a measurement of leaf development and to extend the definition to the time interval between corresponding stages of leaf development. It was also recognized that when successive plastochrons are of equal duration the plastochron may be used to quantify shoot development as well.

The leaf plastochron index (LPI) needs to be determined on shoots measured during its active shoot growth period (Erickson & Michelini, 1957) and incorporates a specified leaf reference lamina length. This reference length has to be in the range of exponential leaf growth, showing linearity between the logarithm of lamina length vs. time, for the period of measurement. A length of 30 mm for grapevine leaves was shown to be relatively easy to measure accurately without damaging leaves (Freeman & Kliewer, 1984).

According to Erickson & Michelini (1957), and Lamoreaux *et al.* (1978), the criteria that must be met by plant organs that are measured, include: i) early growth of the organ must be exponentially; ii) early growth of successors on a single plant must occur at the same relative rate; and iii) successive plastochrons must be of the same duration for a particular plant. One criticism against the use of the LPI to define leaf morphological age, is that the specified conditions are rarely met in conditions outside of controlled (glasshouse/pot studies) environments and that in field studies the duration of a plastochron can be prone to high variance between plants (Chen *et al.*, 2009).

The mean shoot PI can be related to chronological time, calculating the reciprocal of the linear regression coefficient ($1/b$), which represents the number of days elapsing between the appearances of two consecutive leaves on the main shoot, termed the plastochron duration (PD). Leaf age can then be calculated as $(LPI \times 1/b)$ days (Poni & Giachino, 2000). Schultz (1992) calculated plastochron development rate (PDR) by following the same procedure, only using thermal time and not chronological time in the calculation. The PDR is expressed in units of plastochrons per degree day from the formula: $PDR = dPI/dTT$. Its reciprocal is termed the “phyllochron”, with units of $^{\circ}\text{C}\cdot\text{day}^{-1}\cdot\text{PI}^{-1}$, denoting the heat unit requirement for the development of a single plastochron. A possible complication with the approach of incorporating thermal time into leaf age monitoring is that the accepted base temperature (10°C) for the calculation could be invalid, but this may be addressed using the technique specified by Moncur *et al.* (1989).

Schultz (1992) indicated that the number of leaves and rate of appearance (PDR) are independent of leaf irradiance, but found the PI not to be applicable to secondary shoots due to its irregular growth. This is in contrast to Poni & Giachino (2000), who stated that the technique can also be

used to determine the age of leaves on secondary shoots forming along the main shoot during the phase of linear growth, after which the age of all leaves can be updated chronologically.

It was also indicated by Schultz (1992) that the requirements for using the plastochron index (PI) are not strictly met by grapevines (if the whole growing season is considered), as rates of leaf appearance commonly decrease during the season, so that the linearity of log PI against chronological time are not sustained. However, Schultz (1993) showed that the plastochron is an adequate indicator of time as experienced by the plant and was superior to chronological and thermal time when it comes to assessing photosynthesis for leaves differing in age. In a study investigating the relation between leaf potassium content and leaf age throughout the growing season, similar potassium concentrations were found in leaf blades of leaves with similar LPI values (Freeman & Kliewer, 1984).

The goals of this part of the study were to evaluate the use of logistic shoot growth modelling to aid in leaf age determination of Shiraz, assess the relationships between shoot growth parameters (shoot length, node number and the plastochron index) and finally to assess the reaction of Shiraz leaf age to canopy manipulation and irrigation treatments. The main aim was therefore to establish a basis for leaf age determination and classification for further work on leaf structure, and leaf water and pigment content in the same vineyard.

4.2 Materials and methods

The experiment layout, vineyard conditions, climatic conditions, and the shoot growth and plant water status measurements are identical to those mentioned in Chapter III, therefore only the relevant differences are given.

4.2.1 Plastochron measurements

Non-destructive shoot and leaf measurements were conducted throughout the growing seasons on shoots tagged from the beginning of the season on different grapevines. Due to wind damage in all seasons as well as shoot topping performed in the first season, shoots had to be changed during the season where possible and only a limited number of shoots could be monitored for the whole period. Shoot length was measured for each marked shoot and main (L1) vein lengths were recorded from the leaf petiole attachment to the tip of the leaf for leaves with a vein length longer than 20 mm. Node numbers of the measured leaves were also noted (first node counted at the base of the shoot). The plastochron index (PI) was calculated from Equation 4 with n being the number of leaves equal to or longer than the reference length (30 mm), L_n the length of leaf n and L_{n+1} is the length of the leaf smaller than leaf n . Leaf plastochron index (LPI) can then be defined as the developmental age of each leaf on a measured shoot, expressed on a common scale of plastochrons calculated according to Equation 5 where i is the serial number (node number) of the leaf in question. In the study by Pilar *et al.* (2007) only n was measured, reasoning that the second summand as shown in Equation 4 only affects decimals. It was however reasoned in this study that the decimals may cause some error in leaf age estimation, thus it was retained.

Equation 4 Shoot plastochron index calculation.

$$PI = n + \frac{\log_e L_n - \log_e 30}{\log_e L_n - \log_e L_{n+1}}$$

Equation 5 Leaf plastochron index calculation.

$$LPI_i = PI - i$$

4.2.2 Statistical analysis

Statistical analysis was conducted using Statistica 10 ® software (Statsoft, Tulsa, USA) and Unscrambler® 9.2 (CAMO PROCESS AS, Oslo, Norway). Refer to Chapter III for the statistical procedure used to perform logistical growth curve analysis.

4.3 Results and discussion

4.3.1 Plastochron development on shoots for the measurement seasons

The growth rate of individual shoots will determine node number accumulated over time, therefore rate of leaf formation on that shoot. Also at the budburst stage as defined previously (refer to Chapter III), shoots are not at exactly the same node numbers, which was evident from plastochron results of individual shoots (data not shown). Although there were some differences detected for individual shoots, most adhered to a logistic growth curve, as was also visible in Schultz (1992) for shoots sampled from different trellis systems. These logistic curves were also used here, considering the strength of the shoot length:plastochron index relationship (see Section 4.3.2), to relate shoot plastochron development to time for the different seasons (Figure 78). The results from growth fit parameter calculations are shown in Table 27. The maximum PI was significantly less in season two, and the duration until maximum plastochron development (c -parameter) was significantly longer along with a lower b_{max} parameter, confirming the sluggish shoot growth discussed in Chapter III for this season.

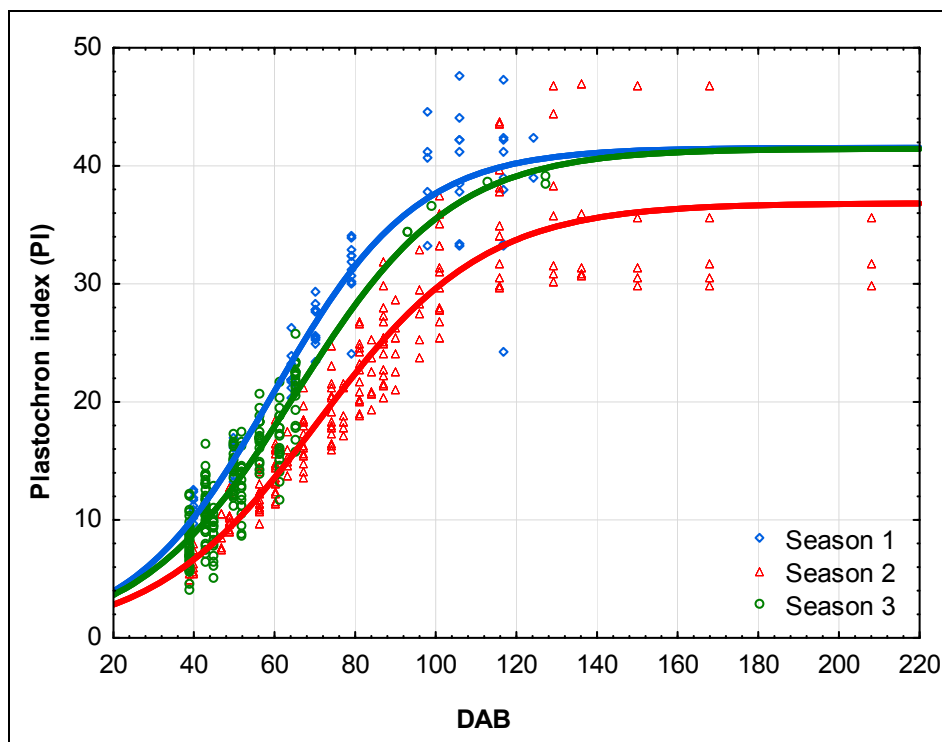


Figure 78 Fitted logistic growth curves of plastochron index (PI) derived from shoot length relative to date after budburst (DAB) for the different seasons (season one $R^2 = 0.95$; season two $R^2 = 0.94$; season three $R^2 = 0.95$).

Table 27 Results from logistic growth curve fit parameters for plastochron index (PI) measurements relative to date after budburst (DAB) over the different seasons. Means with the same letters are not significantly different at the $p \leq 0.05$ level according to paired t -tests performed on the growth curve fit parameters.

Season	b	a	c	b_{max}
1	-0.057 a	41.54 a	59.77 a	0.59
2	-0.049 a	36.84 b	71.03 b	0.45
3	-0.052 a	41.46 a	65.32 c	0.55

When expressing the plastochron index relative to thermal time units (Table 28), the response coefficients (b) were still not significantly different, the a -parameter showed similar results, and differences in the c -parameter were reduced, with only seasons one and two showing significant differences ($p \leq 0.05$). This reduction in differences observed relative to DAB in the c -parameter was also observed in shoot growth measurements (refer to Chapter III).

Table 28 Results from logistic growth curve fit parameters for plastochron index (PI) measurements relative to thermal time units (GDD) over the different seasons. Means with the same letters are not significantly different at the $p \leq 0.05$ level according to paired t -tests performed on the growth curve fit parameters.

Season	b	a	c	b_{max}
1	-0.0054 a	42.3 a	456.7 a	0.057
2	-0.0060 a	36.2 b	415.6 b	0.054
3	-0.0074 b	39.0 a	434.6 ab	0.072

The plastochron development rate (PDR, $\text{PI} \cdot \text{day}^{-1}$) was much slower in season two, especially during the first part of the season, and the decline in this rate also seemed to shift slightly later relative to the other two seasons (Figure 79). When it was expressed relative to thermal time however, season three showed the highest PDR, which would also mean the lowest phyllochron ($^{\circ}\text{C} \cdot \text{day}^{-1} \cdot \text{PI}^{-1}$). This means that in this season the lowest heat unit requirement existed for shoots to reach maximum PDR, which is interesting, considering that the major difference between seasons one and three, was drier soil conditions in season three, limiting secondary shoot growth. This may suggest that PDR was faster due to reduced lateral development in the canopy.

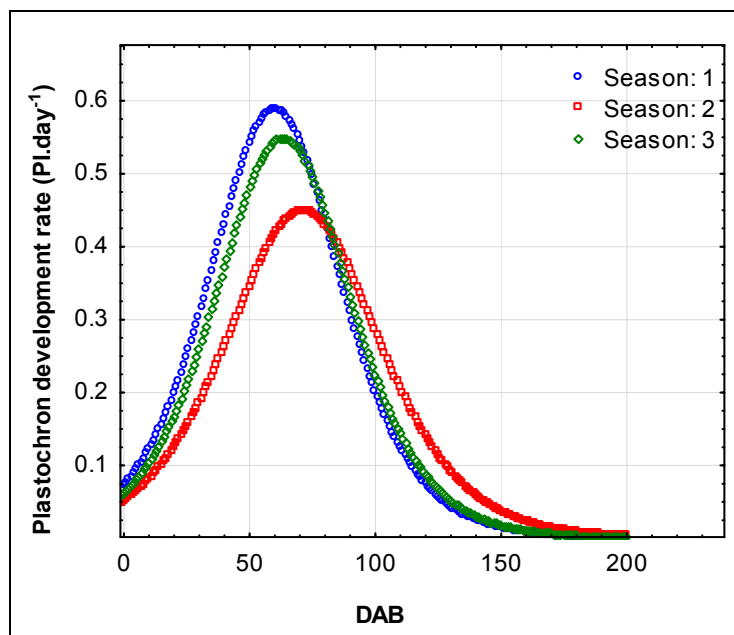


Figure 79 Plastochron development rate ($\text{PI} \cdot \text{day}^{-1}$) on main shoots relative to days after budburst (DAB) for the different seasons.

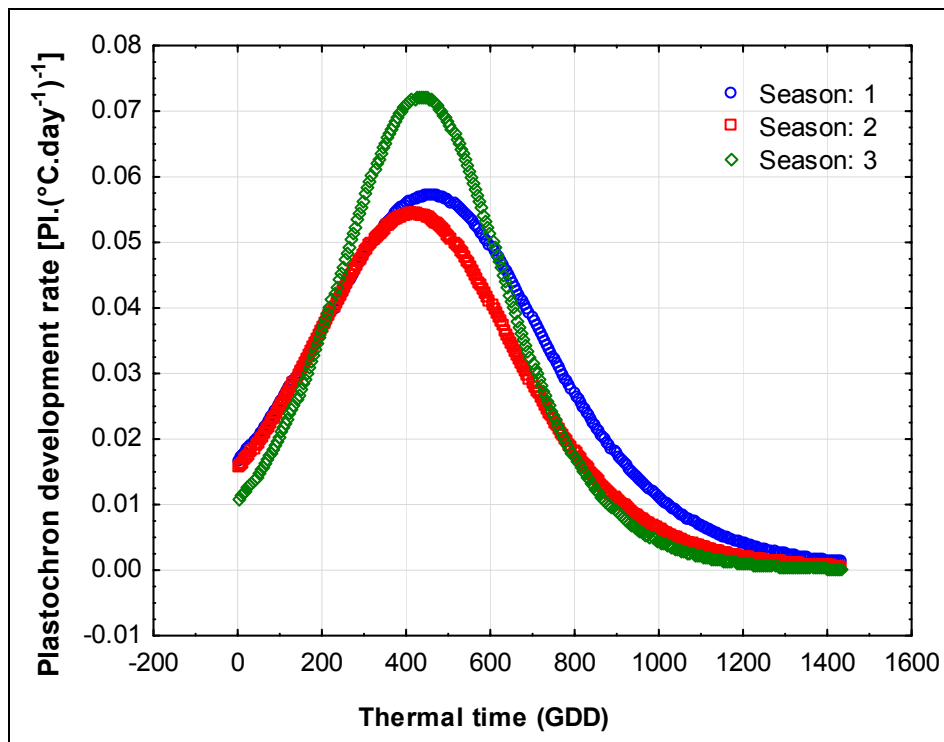


Figure 80 Plastochron development rate [$\text{PI} \cdot (\text{°C} \cdot \text{day}^{-1})^{-1}$] on main shoots relative to thermal time (GDD) for the different seasons.

It is important to consider the variability in shoot PI values, which can lead to large errors in leaf chronological age estimation, should means of shoot measurements be used to calculate LPI and leaf chronological age throughout the vineyard. The goal of creating PI:DAB relations using means of measured shoots, is to establish a mean PD value from the regression slope, but it is important to use individual shoot PI values to estimate leaf age on a shoot to account for differences between shoots. When most of the leaves are measured within the active growth period, as specified in several studies (Freeman & Kliewer, 1984; Schultz, 1992, 1996; Poni & Giachino, 2000), it would not be necessary to fit logistic growth curves when PI needs to be estimated from shoot lengths, which can be seen from the linearity of the shoot length as well as PI values relative to dates after budburst (Figure 82 and Figure 81). It is, however, not always specified in these studies how “active shoot growth” was determined and how the initial lag phases or differences in shoot growth decline were accounted for. Possible errors in the slope estimation from the linear PI:DAB relationship can also impact leaf age estimation. Another advantage therefore of shoot growth curve fitting is that it is relatively easy to determine lower and upper asymptote as well as slope differences statistically between shoots prior to leaf age estimation.

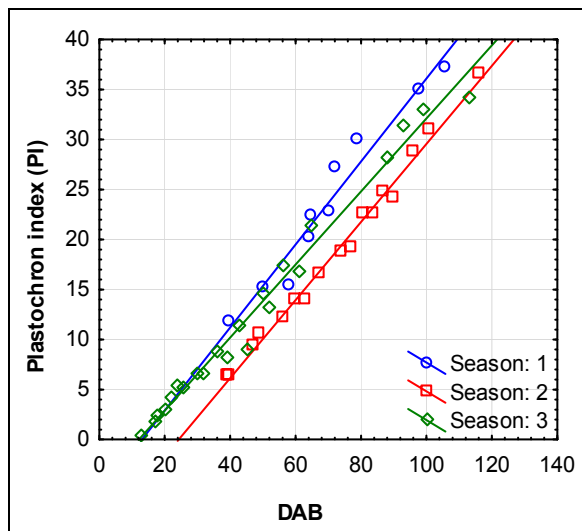


Figure 81 Mean plastochron index (PI) development on shoots until shoot growth cessation for the three seasons (season one $y = -5.37 + 0.41x$; $R^2 = 0.93$; season two $y = -9.46 + 0.39x$; $R^2 = 0.99$; season three $y = -4.39 + 0.37x$; $R^2 = 0.99$; all seasons $p \leq 0.001$).

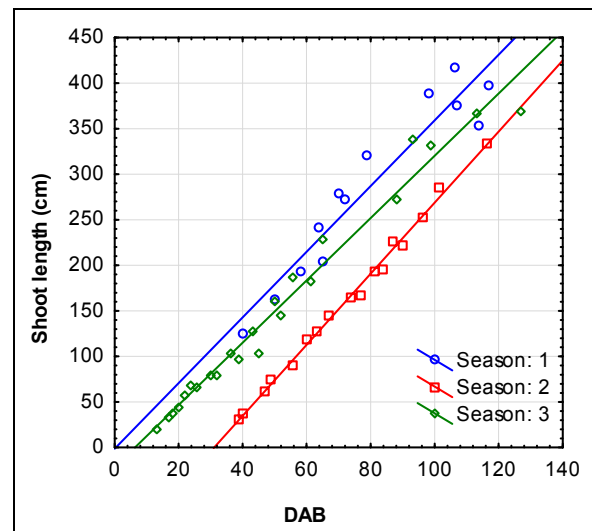


Figure 82 Mean shoot length (cm) until shoot growth cessation for the three seasons (season one $y = -1.27 + 3.60x$; $R^2 = 0.91$; season two $y = 121.39 + 3.90x$; $R^2 = 0.75$; season three $y = -21.75 + 3.42x$; $R^2 = 0.98$; all seasons $p \leq 0.001$).

4.3.2 Relationships between shoot growth parameters

Very strong relationships were found between the plastochron index (PI), shoot length (cm) and node numbers of shoots in seasons one and two (

Figure 83 to Figure 85), making it possible to derive the PI of these shoots from either its shoot length or node number. Measurements in season three were only performed after 88 DAB (closer to shoot growth cessation), which could explain the slope difference observed in the PI:shoot length regression as well as in the PI:node number regression. If the PI is to be estimated from shoot length measurements, the same equation could be used for all seasons, depending on the goal of the measurements and accuracy required. The seemingly higher PI:shoot length values observed for season two need some explanation (

Figure 83). Plastochron duration values were longer in this season, as previously noted, and it could be expected that due to the longer time it takes for a leaf to form on the shoot, there should be lower PI values per shoot length. However, with lower shoot growth rates, internode lengths may be reduced in the active growth region of the shoot (Schultz & Matthews, 1988), explaining more nodes formed for a shorter shoot length in season two (Figure 85). This was also observed in Chapter III (section 3.3.5.2), showing slower growing shoots in season two with larger portions of smaller leaves on shoots, which could be due to the relation found in limiting growth conditions between leaf and internode growth (Schultz & Matthews, 1988). It seems that reduced internode lengths may compensate fully for higher PD values, but this remains to be evaluated in other scenarios as well. It also explains why seasons one and two could have a similar PI:node number relationship, as the longer PD (less nodes formed in the same time) in season two were seemingly fully counteracted by shorter internodes.

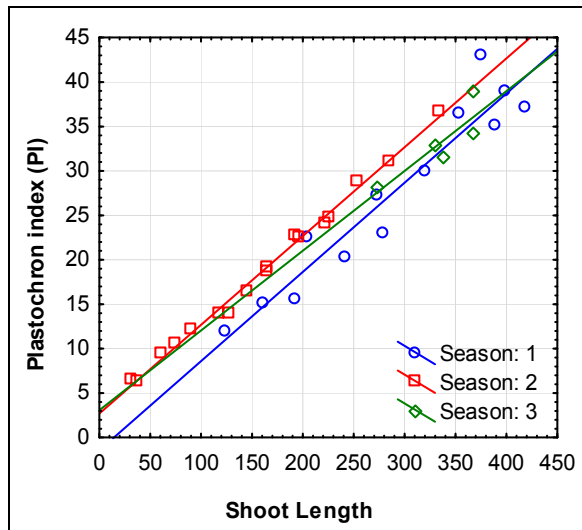


Figure 83 Relationship between the mean main shoot plastochron index (PI) and the mean main shoot length for the different seasons (season one: $y = -1.43 + 0.10x$; $R^2 = 0.91$; season two: $y = 2.70 + 0.10x$; $R^2 = 0.99$; season three: $y = 3.10 + 0.09x$ $R^2 = 0.76$; all seasons $p \leq 0.05$).

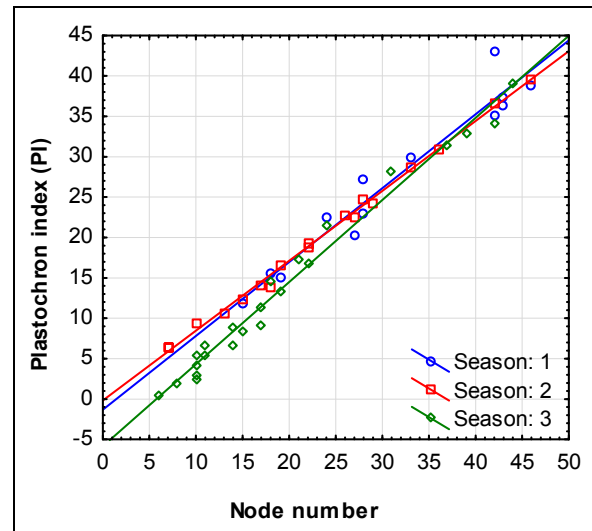


Figure 84 Relationship between the mean shoot plastochron index (PI) and node number on a shoot for the seasons (season one: $y = -1.31 + 0.91x$; $R^2 = 0.94$; season two: $y = -0.16 + 0.86x$; $R^2 = 1.00$; season three: $y = -5.84 + 1.02x$; $R^2 = 0.98$; all seasons $p \leq 0.001$).

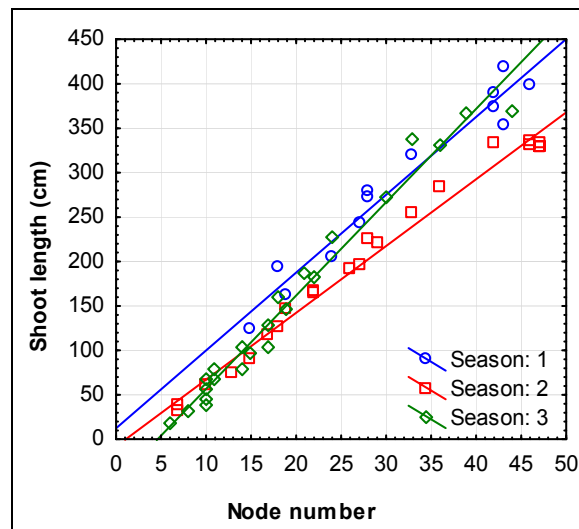


Figure 85 Relationship between mean shoot length (cm) and node number for the different seasons (season one $y = 12.36 + 8.75x$; $R^2 = 0.95$; season two: $y = -8.04 + 7.51x$; $R^2 = 0.98$; season three: $y = -48.4 + 10.50x$; $R^2 = 0.98$; all seasons $p \leq 0.001$).

Separate regressions analysed for the PI and shoot length relationships of main and secondary shoots indicated that the same regression would be valid for both shoot types (data not shown). This was determined in season two by subjecting some shoots to topping on 63 DAB (post anthesis) and then measuring PI on the stimulated secondary shoot growth. Schultz (1992) used a “remaining leaf number” strategy to account for topped shoots, which was not applicable in this study as we only measured plastochron index for non-topped shoots.

4.3.3 Plastochron development on shoots from different treatments

In general, the PI measurements in season one followed closely the trend of shoot growth, with a tendency for the PI development on the NSF shoots to decline earlier in the season than the other treatments (Figure 86 and Figure 87). The a -parameter and c -parameter were significantly lower for the NSF treatments (Table 29). This corresponded to results from logistic shoot growth curve fitting (Chapter III); the c -parameter for the NSF treatment in season one was, however, not

significantly lower. The plastochron development rates ($\text{PI}\cdot\text{day}^{-1}$) (Figure 87) were similar between treatments during the period preceding time point c (maximum plastochron development rate), which was also observed from shoot growth rate analysis in Chapter III. The similarity in the results confirmed that, during the phase of linear (or close to linear) shoot growth, there are negligible effects on shoot growth rate, even when drastic canopy manipulation took place (the irrigation treatment effect was not expected to be significant before soil and plant water status indicated growth-limiting conditions). It would also seem as if the plastochron index is not superior to shoot growth monitoring in reducing differences between shoots with different growth rates. The PI does, however, seem to have the property (as mentioned in section 4.3.2) to incorporate a counteraction between shoot features, as shown in Table 30.

The more rapid decline after 50 DAB in the NSF treatment with respect to the plastochron development rate corresponded to the shoot growth decline discussed in Chapter III. Results from growth fit parameters for the PI values of the treatments during seasons two and three largely corresponded to what was analysed during shoot growth analysis [note that the upper asymptote was also set to a constant value (as in Chapter III) to analyse plastochron development parameters in season three].

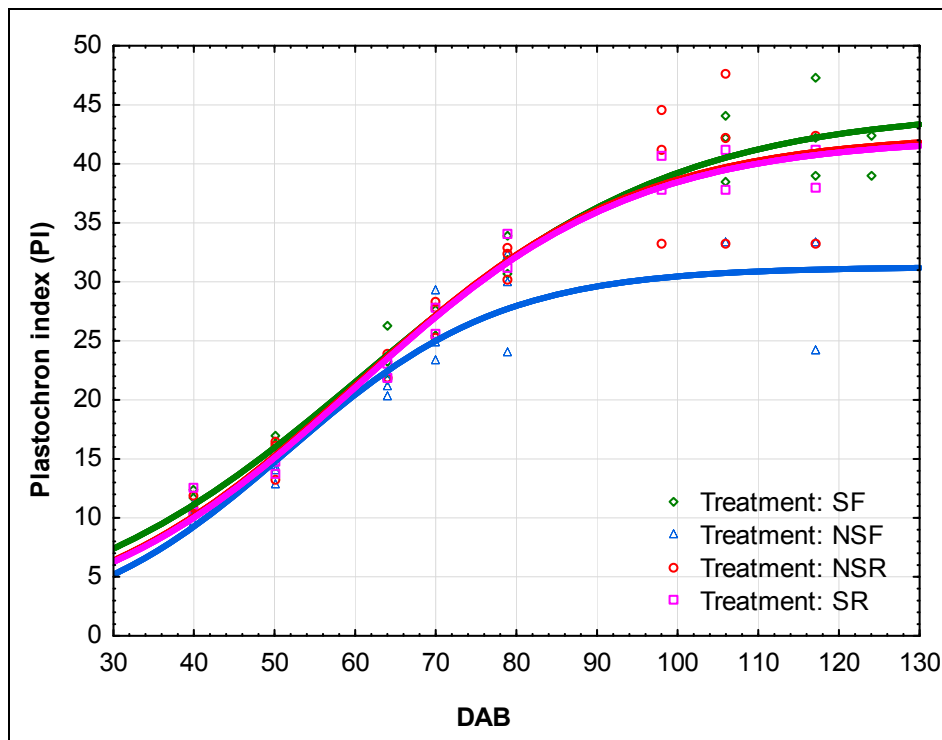


Figure 86 Fitted logistic growth curves of plastochron index (PI) relative to days after budburst (DAB) for the different treatments in season one (SF $R^2 = 0.95$; NSF $R^2 = 0.94$; NSR $R^2 = 0.95$; SR $R^2 = 0.99$).

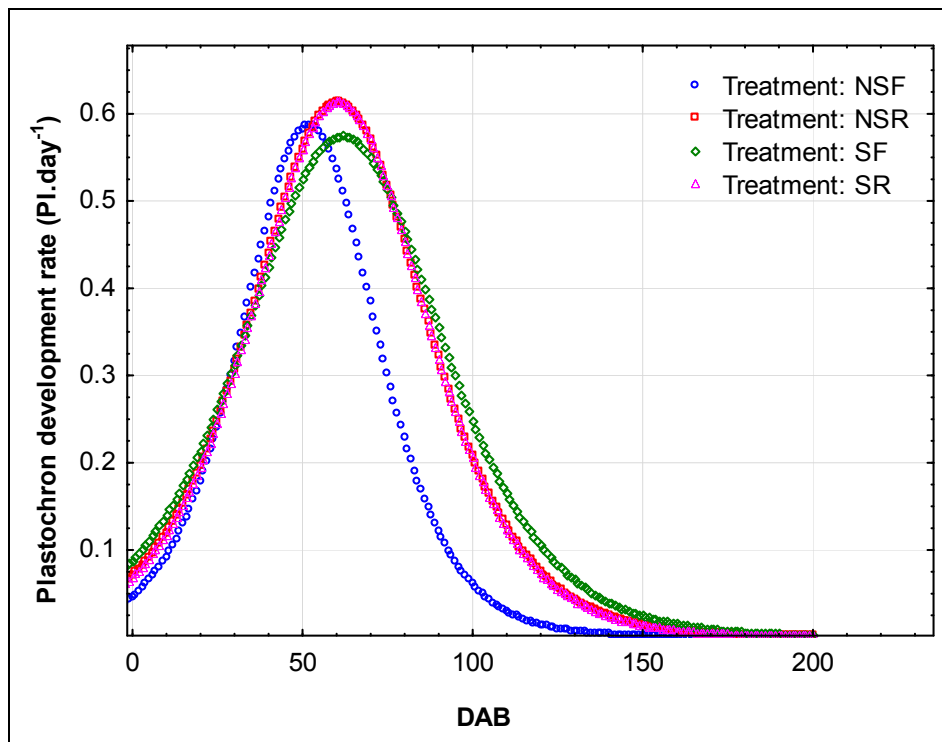


Figure 87 Plastochron development rate ($\text{PI}\cdot\text{day}^{-1}$) relative to days after budburst (DAB) for the different treatments during season one.

Table 29 Results from growth curve fit parameters related to plastochron index (PI) measurements relative to days after budburst (DAB) for the different seasons and treatments. Means with the same letters are not significantly different at the $p \leq 0.05$ level according to paired t -tests performed on the growth curve fit parameters. The PD_{max} parameter is the maximum plastochron durations as calculated from the inverse of the b_{max} values.

Season	Treatment	b	a	c	b_{max}	PD_{max}
1	SF	-0.051 a	44.61 a	61.38 a	0.57	1.75
	NSF	-0.075 b	31.27 b	51.53 b	0.59	1.69
	NSR	-0.058 ab	42.55 a	60.11 a	0.61	1.64
	SR	-0.058 ab	42.23 a	60.11 a	0.61	1.64
2	SF	-0.055 a	33.59 a	64.59 a	0.46	2.17
	NSF	-0.051 a	36.31 ab	71.29 b	0.46	2.17
	NSR	-0.041 a	37.61 bc	74.52 b	0.38	2.63
	SR	-0.044 a	41.05 c	77.55 b	0.45	2.22
3	NSF	-0.055 a	37*	58.75 a	0.51	1.96
	NSR	-0.058 a	37	58.30 a	0.53	1.89
	SF	-0.054 a	37	64.39 b	0.50	2.00
	SR	-0.057 a	37	62.99 b	0.53	1.89

*Season three upper asymptote was set to PI 37 prior to growth curve fit estimation

Table 30 Shoot growth features that could lead to similar PI values under differing growth conditions.

Slow growth	Fast growth
Longer PD (less nodes formed per day)	Shorter PD (more nodes formed per day)
Shorter shoots at similar DAB	Longer shoots at similar DAB
More internodes per shoot length	Less internodes per shoot length

4.3.4 Chronological leaf age estimation

As mentioned previously, the chronological leaf age is a function of the leaf plastochron index (LPI) and the plastochron duration (PD). The dynamics of the PD values for different shoots or changes in PD as growth progresses and environmental or internal plant conditions change, seem to be determining in separating chronological and plastochron leaf age on shoots. In order to assess the possibility of using a constant PD in leaf age estimation, the LPI of leaves \times mean PD for the active growth period was calculated for the first node from the base of the shoot (node 1). The result showed that for some shoots and stages in the season, the error in leaf age estimation can be as large as 40 days (data not shown) due to differences between shoots, especially in terms of growth cessation.

An alternative to using a mean PD for the active growth period is to compute leaf chronological age from Equation 6. Theoretically, the LPI of a leaf being fully unfolded can be simplified as LPI=0 (equivalent to the selected reference length), which will also mean that the PI of the shoot and the node number of the leaf would be equal (considering Equation 5). This also implies that either the PI or node number could be substituted into Equation 7 to determine the DAB of leaf unfolding from the PI:DAB logistic curve regression equation. In this way, the uncertainty of shoot growth cessation estimation (needed when leaf age is chronologically updated after leaf age cessation in some studies) is eliminated. Also, the possible lagging growth of shoots early in the season will be incorporated here (provided it was measured and included in the growth curve fit calculation), which means that there is no need to take into account offsets from linear shoot growth relationships that can occur in PI:shoot length regression and then has to be taken into account for every leaf during leaf age estimation.

Equation 6 Calculation of leaf chronological age (days) from the time of leaf emergence

$Leaf\ chronological\ age\ (days) = DAB - DAB_{LE}$
DAB – date after budburst at time of leaf age determination
DAB_{LE} – date after budburst when leaf emerged (calculated from Equation 7)

Equation 7 Estimation of date after budburst (DAB) from plastochron index (PI) and growth curve parameters calculated from the PI:DAB logistic relationship

$Date\ after\ budburst\ of\ leaf\ emergence\ (DAB_{LE}) = \frac{\ln\left(\frac{a}{PI_{LE}} - 1\right)}{b_{max}} + c$	
a	theoretical maximum PI
c	x-value at the inflexion point midway respective to the PI formation period (number of days required to reach 50% of a)
b_{max}	maximum slope around the inflexion point
PI_{LE}	Plastochron index value of the shoot when the leaf in question was formed
DAB	Refers to the date after budburst of the unfolding for the leaf in question

The estimation of leaf age on secondary shoots is problematic. The different secondary shoots can have different emergence dates, as well as plastochron duration values on the shoots, which complicates leaf age estimation.

An estimation of final canopy leaf age can therefore be made from the *a*-parameter as well as the mean plastochron duration until shoot growth cessation, of which the value needs to be specified. The development of the mean canopy age can also be determined from the mean PI, shoot length or node number values at a defined time point and the mean of the plastochron duration up to that point.

4.3.5 Leaf age classification according to LPI

Classification of leaf age according to LPI was done in relation to published results on the relationship between leaf age and photosynthesis. Schultz (1996) classified the upper three leaves on a shoot as young leaves and in a successive study (Schultz, 2003b) the upper three to five leaves on secondary shoots were also classified as young leaves. Poni *et al.* (1994b) noted that four month old leaves still retained 70% of maximum photosynthesis reached at 40 days, and that a strong limitation of photosynthesis could be observed for young apical leaves. The consistent decline in photosynthesis after 45 to 50 days of leaf age raised some questions as to which mechanism of leaf senescence is triggered. Taking into account observations and previous classifications from literature (Table 31), leaves in this study were also classified to represent leaf physiological age transitions in order to simplify statistical analysis and data interpretation (Table 32 and Table 33). This was done only for main shoot leaves, considering that chronological age derivation of leaves on secondary shoots is impossible without knowing their date of emergence as well as individual plastochron durations and potential effect of the phytomer sequence and characteristics, i.e. if the secondary shoot emerged from a node position where tendrils or bunches originate, or a position with only a leaf (Lebon *et al.*, 2004).

Table 31 Existing leaf age classifications according to literature (Poni *et al.*, 1994b; Schultz, 1995a).

Category	LPI range	Leaf age (Kriedemann <i>et al.</i> , 1970)	SLM
Young	0 to 5	0-20d	4-5 mg/cm ²
Max	5-25 [10-25 in Schultz (1995a)]	20-70d	5-7 mg/cm ²
Old	> 25	> 70d	>7 mg/cm ²

Table 32 Adapted chronological leaf age classification.

Class	Category	Leaf age (main)
1	Young	<20
2	Approaching max	20-50d
3	Max	50-90d
4	Declining	90-120
5	Old	> 120d

Table 33 Adapted physiological leaf age classification.

Class	LPI range
1	<5
2	5-10
3	10-15
4	15-20
5	>20

4.3.6 Canopy age

In literature, determination of canopy age is simplified as an estimation from mean age values of individual leaves in the canopy (Poni & Giachino, 2000). This is, however, considered as an oversimplification in relation to field studies, where the factors affecting canopy ageing can be complex, including potential leaf loss due to canopy manipulation (thinning, topping), damage or abscission; shoot growth variability (lengths, node numbers); plastochron variability (plastochron duration and the LPI value distribution in the canopy), as well as leaf physiological condition (pigment content or leaf structural differences). The presence, emergence dates and physiology of secondary shoots add to this complexity.

In this study, canopy age is simplified to a representation of mean leaf chronological age on primary shoots in response to canopy manipulation and plant water status (treatments as discussed in Chapter III). Between seasons, differences in leaf age on shoot positions, as defined by LPI values, seem minute (Figure 88), possibly due to the counteracting features in shoots described in Table 30.

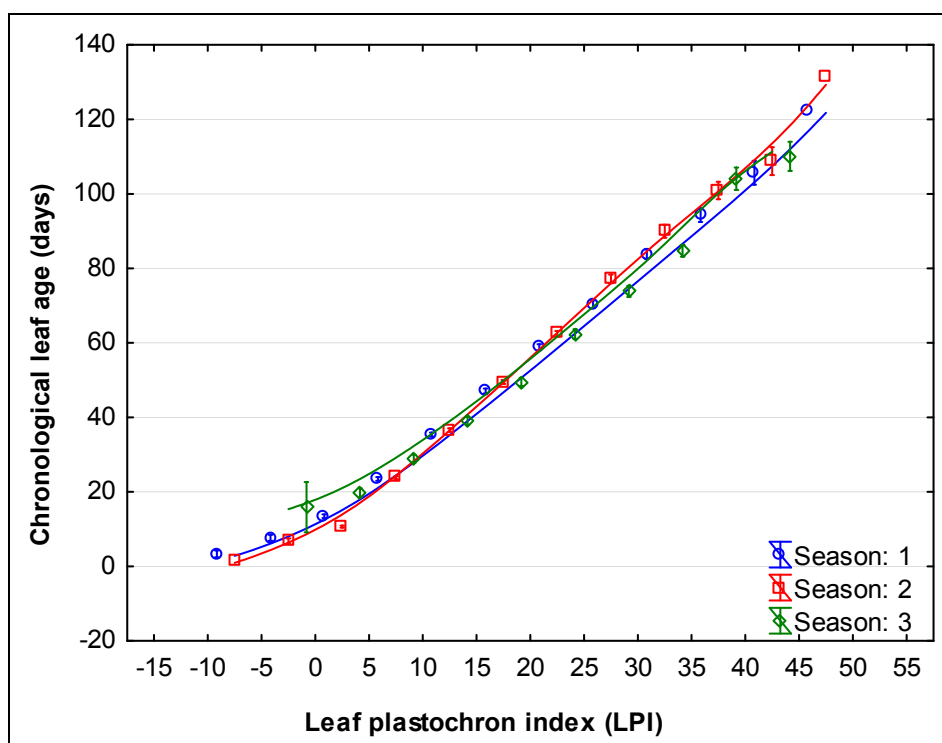


Figure 88 Chronological leaf age (days) relative to leaf plastochron index (LPI) showed in five-LPI intervals for main shoots of the different seasons. Vertical bars denote standard errors. The DAB range was set to 0-140 DAB prior to measurement to represent the same period between seasons. Seasons are offset for clarity, but the distance-weighted least-square fits shown are drawn through the means of the respective seasons.

In season one, the NSF treatment showed reduced shoot growth rates from about 50 DAB as well as lower final shoot lengths, and reduced leaf size (refer to Chapter III). The shoots of this treatment showed lower LPI values, as expected, but the older leaves still had high leaf ages, therefore potentially increasing the mean age of the canopies for this treatment (Figure 10). In season two, the NSR treatment seemed to show the highest leaf age values (Figure 90), which corresponded to earlier observations of lower b_{max} values (maximum shoot growth rate), as well as smaller maximum leaf size along with a lower c -parameter, signifying a smaller portion of the apical part of the shoot with low LPI values (refer to Chapter III). Some care should, however, also be taken to interpret the low (< 5 LPI) and high (> 30 LPI) ranges on these graphs, considering the asymptotic nature of the growth curves that were used to obtain the date of leaf formation, which

implies that as the PD increase, the possible error in estimation may also increase. In season three, sufficient measurements were not performed throughout the season to allow the same comparison than the other seasons.

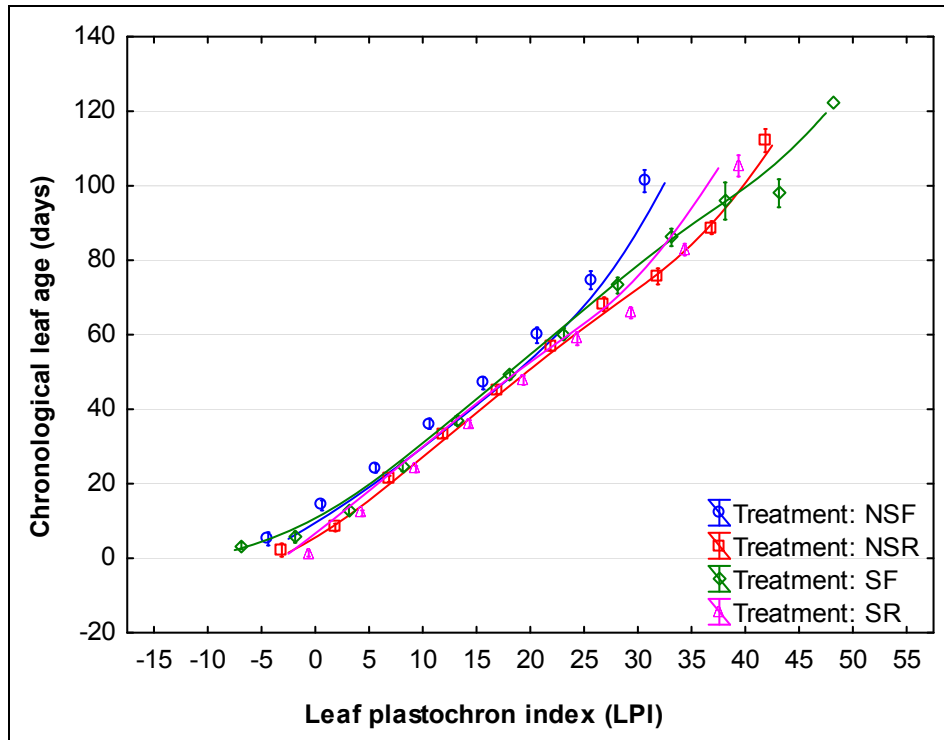


Figure 89 Leaf chronological age (days) relative to leaf plastochron index (LPI) showed in five-LPI intervals for main shoots of the different treatments in season one. Vertical bars denote standard errors. Treatments are offset for clarity, but the distance-weighted least-square fits shown are drawn through the means of the respective treatments.

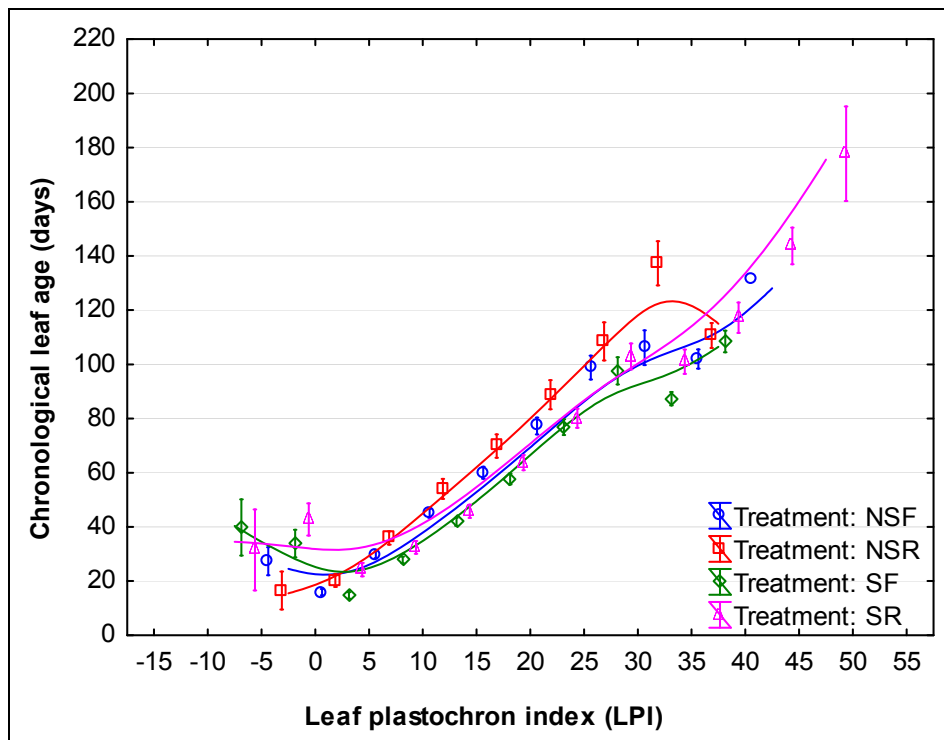


Figure 90 Leaf chronological age (days) relative to leaf plastochron index (LPI) showed in five-LPI intervals for main shoots of the different treatments in season two. Vertical bars denote standard errors. Treatments are offset for clarity, but the distance-weighted least-square fits shown are drawn through the means of the respective treatments.

4.4 Conclusions

One of the requirements for measuring the plastochron index (PI) is that shoots should be actively growing. When environmental and internal factors cause shoot growth in the grapevine to slow significantly or cease, shoot length, node formation and hence PI would either show limited change or no change at all over time. As a consequence, PD would increase. From the results of the shoot growth rate and plastochron formation rate presented here, there were similarities between the two parameters. An increased PD in season two until 75 DAB corresponded with a decreased shoot growth rate for the same period. This was expected considering the good correlation between shoot length and PI.

Even though it is possible to use a constant PD (implying linear shoot growth) over time to derive leaf age for the active shoot growth period, and then switch over to chronological time when shoot growth ceases, it would be necessary with this approach to consider offsets in the PI:DAB linear regression (used to calculate PD). These offsets are likely, as differences in the length of the lag phase of shoot growth between seasons do occur. In addition to this, variability in shoot PI values needs to be considered, preferably by calculating leaf age on a shoot from the PI of that specific shoot, rather than from a mean PI for the treatment of even the vineyard. Even though in this study the logistic growth curve fitting was determined from individual shoots and the mean fit equation used to estimate leaf age, it would theoretically be possible to determine fit equation in an automated procedure for each shoot in order to ensure incorporation of shoot variability into the model when estimating leaf age on a shoot.

The benefit of the plastochron index may be questioned if leaf age can be determined on a chronological time scale from budburst. However, in practice it is difficult to tag leaves to monitor chronological time. The value of the PI in viticulture may be the relation that it has with shoot growth through the PD parameter. The PI stabilises in growth limiting conditions, which should correspond to a decrease in physiological activity in the grapevine. Conversely, this may be the major limitation of expressing leaf age only relative to LPI units, as after shoot growth cessation, a leaf in a certain position will have a stable LPI value, but its physiological age will change. This study provides a method of incorporating leaf ageing after shoot growth cessation into the canopy ageing concept. Our data also suggest that the shoot PI can simply be derived from node number, and it may be argued whether it is at all useful or of any practical value to measure leaf vein lengths in order to add decimal accuracy to the LPI values. Considering that it is difficult to monitor leaf ageing during the season by tagging and monitoring individual leaves, the PI change during active shoot growth can be used to infer leaf ageing during the season.

The approach followed here deviated from the general approach of monitoring leaf plastochron index only in the period of linear shoot growth by incorporating changes in shoot plastochron duration during the growing season. These changes were monitored from logistic shoot growth fitting of the PI:DAB relationship and subsequent calculation of leaf chronological age by inferring the date of leaf formation from the fit equation. The approach is therefore an attempt to incorporate inevitable changes in shoot growth rate and hence plastochron duration throughout the season into leaf age determination.

For grapevines it is therefore proposed that phytomer formation, shoot growth and node number increase are strongly linked to leaf age determination in canopies of grapevine, and considering the correlation between parameters, it could be sufficient to choose the easiest one to measure, which may possibly be to count the number of nodes on a shoot and measure the shoot length. The strength of the plastochron index (which already deviates significantly from its original inception) may therefore lie in its insensitivity to internode length differences between shoots, as it

essentially records organogenesis rather than increase in mass or length. It, however, remains to be shown for a variety of cultivars and growing conditions if the relations between PI and other shoot parameters remain valid.

4.5 Literature cited

- Askenasy, E., 1880. Über eine neue Methode um die Verteilung der Wachstumsintensität in wachsenden Teilen zu bestimmen. *Verh. Naturh. Medic. Ver. Heidelberg* 2, 70-153.
- Bertamini, M. & Nedunchezian, N., 2002. Leaf age effects on chlorophyll, Rubisco, photosynthetic electron transport activities and thylakoid membrane protein in field grown grapevine leaves. *Journal of Plant Physiology* 159., 799-803.
- Bertamini, M. & Nedunchezian, N., 2003. Photoinhibition of photosynthesis in mature and young leaves of grapevine (*Vitis vinifera* L.). *Plant Science* 164, 635-644.
- Chen, C.C., Chen, H. & Chen, Y., 2009. A new method to measure leaf age: Leaf measuring-interval index. *American Journal of Botany* 96, 1313-1318.
- Erickson, R.O. & Michelini, F.J., 1957. The Plastochron Index. *American Journal of Botany* 44, 297-305.
- Freeman, B.M. & Kliewer, W.M., 1984. Grapevine leaf development in relationship to potassium concentration and leaf dry weight density. *Am. J. Bot.* 3, 294-300.
- Hunter, J.J. & Visser, J.H., 1988. The effect of partial defoliation, leaf position and developmental stage of the vine on photosynthetic activity of *Vitis vinifera* L. cv Cabernet Sauvignon. *S. Afr. J. Enol. Vitic.* 9, 9-15.
- Hunter, J.J. & Visser, J.H., 1989. The effect of partial defoliation, leaf position and developmental stage of the vine on leaf chlorophyll concentration in relation to the photosynthetic activity and light intensity in the canopy of *Vitis vinifera* L. cv. Cabernet Sauvignon. *S. Afr. J. Enol. Vitic.* 10, 67-73.
- Kriedemann, P.E., Kliewer, W.M. & Harris, J.M., 1970. Leaf age and photosynthesis in *Vitis vinifera* L. *Vitis* 9, 97-104.
- Lamoreaux, R.J., Chaney, W.R. & Brown, K.M., 1978. The plastochron index: A review after two decades of use. *American Journal of Botany* 65, 586-593.
- Lebon, E., Pellegrino, A., Tardieu, F. & Lecoeur, J., 2004. Shoot Development in Grapevine (*Vitis vinifera*) is Affected by the Modular Branching Pattern of the Stem and Intra- and Inter-shoot Trophic Competition. *Annals of Botany* 93, 263-274.
- Liakopoulos, G., Nikolopoulos, D., Klouvatou, A., Vekkos, K., Manetas, Y. & Karabourniotis, G., 2006. The Photoprotective Role of Epidermal Anthocyanins and Surface Pubescence in Young Leaves of Grapevine (*Vitis vinifera*). *Annals of Botany* 98, 257-265.
- Moncur, M.W., Rattigan, K., Mackenzie, D.H. & McIntyre, G.N., 1989. Base Temperatures for Budbreak and Leaf Appearance of Grapevines. *American Journal of Enology and Viticulture* 40, 21-26.
- Pilar, B., Sanchez-de-Miguel, P., Centeno, A., Junquera, P., Linares, R. & Lissarrague, J.R., 2007. Water relations between leaf water potential, photosynthesis and agronomic vine response as a tool for establishing thresholds in irrigation scheduling. *Scientia Horticulturae* 114, 151-158.
- Poni, S. & Giachino, E., 2000. Growth, photosynthesis and cropping of potted grapevines (*Vitis vinifera* L. cv. Cabernet Sauvignon) in relation to shoot trimming. *Australian Journal of Grape and Wine Research* 6, 216-226.
- Poni, S., Intrieri, C. & Silvestroni, O., 1994. Interactions of Leaf Age, Fruiting, and Exogenous Cytokinins in Sangiovese Grapevines Under Non-Irrigated Conditions. II. Chlorophyll and Nitrogen Content. *Am. J. Enol. Vitic.* 45, 278-284.
- Schultz, H.R., 1992. An empirical model for the simulation of leaf appearance and leaf area development of primary shoots of several grapevine (*Vitis vinifera* L.) canopy-systems. *Scientia Horticulturae* 52, 179-200.
- Schultz, H.R., 1993. Photosynthesis of sun and shade leaves of field-grown grapevine (*Vitis vinifera* L.) in relation to leaf age. Suitability of the plastochron concept for the expression of physiological age. *Vitis* 32, 197-205.

- Schultz, H.R., 1995. Grape canopy structure, light microclimate and photosynthesis. I: A two-dimensional model of the spatial distribution of surface area densities and leaf ages in two canopy systems. *Vitis* 34, 211-215.
- Schultz, H.R., 1996. Leaf absorptance of visible radiation in *Vitis vinifera* L.: estimates of age and shade effects with a simple field method. *Scientia Horticulturae* 66, 93-102.
- Schultz, H.R., 2003. Extension of a Farquhar model for limitations of leaf photosynthesis induced by light environment, phenology and leaf age in grapevines (*Vitis vinifera* L. cvv. white riesling and zinfandel). *Functional plant biology* 30, 673-687.
- Schultz, H.R. & Matthews, M.A., 1988. Vegetative Growth Distribution during Water Deficits in *Vitis vinifera* L. *Aust. J. Plant Physiol.* 15, 641-656.

Chapter V

Research Results

Leaf chlorophyll and carotenoid profiles during growth of *Vitis vinifera* L. cv. Shiraz

Chapter V: Leaf chlorophyll and carotenoid profiles during growth of *Vitis vinifera* L. cv. Shiraz

5.1 Introduction

Leaf pigment content is dynamic and responsive to abiotic and biotic conditions and therefore important as indicators of plant health and performance. Both the loss and formation of pigments can be important to assess, as pigment loss may be the result of microclimatic conditions (Flexas *et al.*, 2001; Bertamini & Nedunchezian, 2004), water deficits (Medrano *et al.*, 2002), virus infection (Sampol *et al.*, 2003), phylloxera infestation (Blanchfield *et al.*, 2006) as well as senescence, while pigment synthesis may also result from some of these conditions in reaction to triggered photoprotective mechanisms in leaves.

Spectrophotometric techniques are often used for pigment analysis. However, it is difficult to determine degradation components, especially when analysing individual pigments. In many cases it is also difficult to compare results from pigment analyses between studies. Porra (2002) outlined the inaccuracies of the spectrophotometric equations of Arnon (1949), which were derived from the specific extinction coefficients of Mackinney (1941). The inaccuracies, confirmed by atomic absorption spectrometry (Porra *et al.* (1989), were largely due to the use of dried solid chlorophyll *a* and *b* samples that were not purified prior to analysis to remove degradation products. This has also been shown to affect chlorophyll *a:b* ratios quite severely, but can be corrected post-analysis using a quadratic equation published by Porra (2002).

Considering that similar extraction procedures are used for high-performance liquid chromatography (HPLC) analysis and that with some methods degradation components can go undetected, the same diligence applies when using this technique. Recently, methods were developed to optimise extraction and minimise degradation in grapevine leaf extracts, while facilitating measurement of chlorophyll and carotenoids, including the major xanthophylls (Lashbrooke *et al.*, 2010). Photosynthetic pigments pose several challenges when accurate assessment is required, for instance the characteristic conjugated double bonds of carotenoids render them particularly instable and susceptible to degradation by light, heat, oxygen and acidic conditions (Oliver & Palou, 2000).

The goals of this study were to evaluate the interaction between leaf pigment content, as measured by means of HPLC, leaf age and changing water deficit conditions during the growing season, in reaction to canopy manipulation.

5.1 Materials and methods

The vineyard, climatic conditions, leaf area and plant water relations were identical to those described in Chapter III. The analyses presented here were performed exclusively during season one. Leaf plastochron index and leaf age measurements are described in Chapter IV.

5.1.1 Experiment layout

The experiment layout shown in Figure 91 is part of a larger trial of which details are discussed in Chapter III. Treatment application was identical to what was described there.

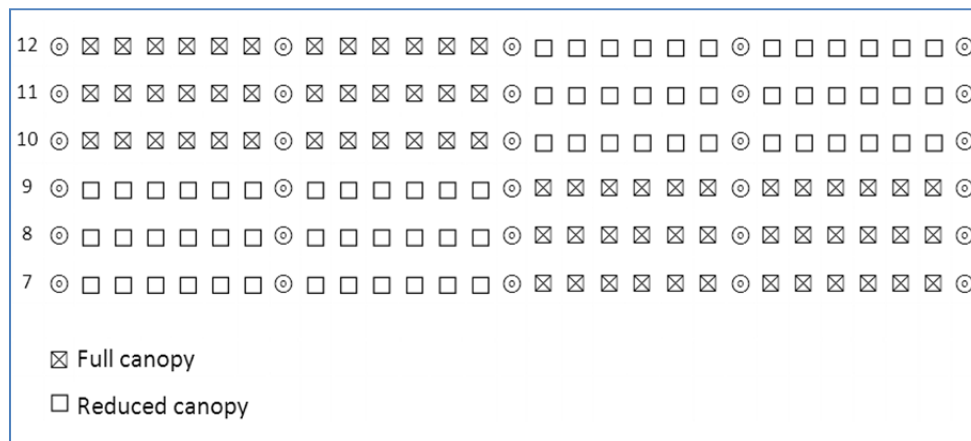


Figure 91 Experiment layout as part of a field experiment on the interaction of water deficits and canopy manipulation in Shiraz. Round markers indicate vineyard poles.

5.1.2 Destructive pigment determination (HPLC)

To study pigment content on a mass per leaf area basis has value when comparing pigments or assessing pigment ratios, but when assessing treatment effects and effects on pigments during leaf development, expression against specific leaf mass or total specific leaf mass (see Chapter VI) may be more useful, as it aids in defining leaf structural changes such as thickening or change in mesophyll structure. It is clear from especially remote sensing articles, but also generally in plant sciences that expression of pigments on a leaf area basis remains popular. However, in numerous recent articles, especially in those dealing with HPLC measurements, leaf mass-based expression is favoured, without reference to leaf area. From a leaf microclimate and physiology perspective, however, neither of these approaches should be favoured, as it is only by measuring both, or assessing TSLM (and preferably also SLM, see Chapter VI) separately, that it would be possible to elucidate *why* pigments are changing. This is illustrated by hypothetical leaf measurements (A to D) indicated in Figure 92 and Table 35. The expansion of leaf area is only relevant in leaf pigment analysis if pigments will be expressed on a per-leaf basis, which is not commonly found in plant physiology studies. It is also relevant in a remote sensing context, where total plant pigment content per soil surface area becomes important. In field studies leaf area and microclimate interact within a defined canopy configuration, with consequences for pigment formation and function (JJ Hunter, personal communication).

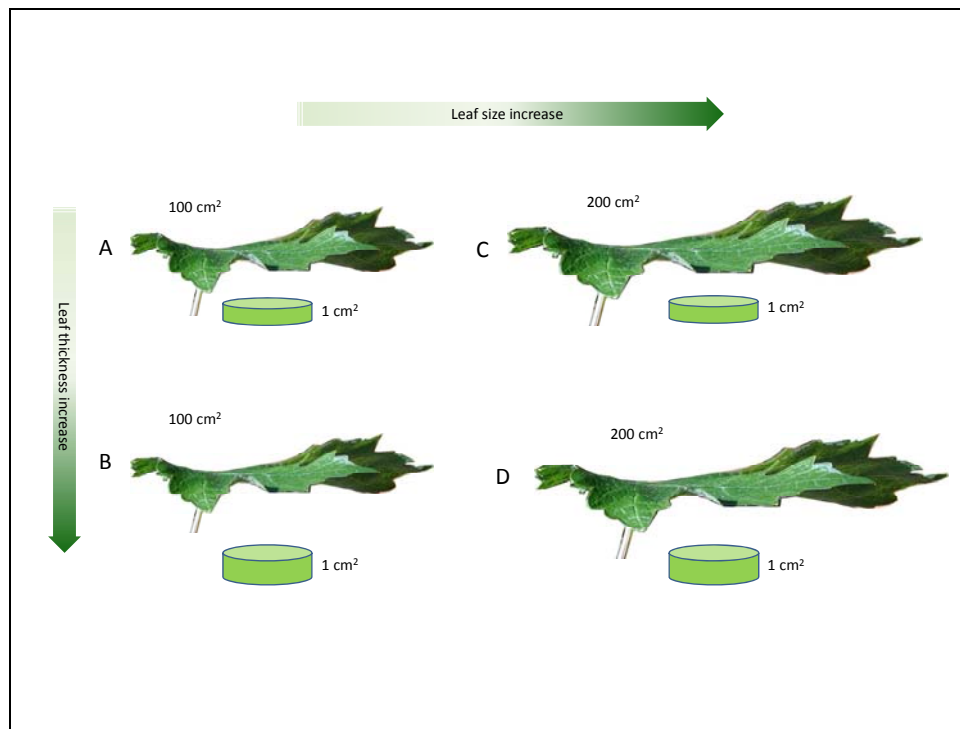


Figure 92 Leaf size and thickness increase (shown as leaf discs) during growth to demonstrate effects on pigment expression methods.

Table 34 Pigment content change on a leaf area and leaf mass basis on account of leaf growth illustrated in Figure 92.

Scenario	Pigment content in leaf disc (ng)	Leaf disc mass (mg)	Leaf area (cm ²)	SLM (mg.cm ⁻²)	Pigment concentration (ng.mg ⁻¹)	Pigment content (area basis) (mg.cm ²)	Pigment content per leaf (mg)
A	10000	5.0	100	5.0	2000	0.01	1.0
B	20000	10.0	100	10.0	2000	0.02	2.0
C	10000	5.0	200	5.0	2000	0.01	2.0
D	20000	10.0	200	10.0	2000	0.02	4.0

In Freeman & Kliewer (1984) leaf lamina potassium concentration (mg.g⁻¹ DM) decreased when expressed relative to increasing LPI values, mainly due to the commonly observed increase in SLM (mg.cm⁻²) in older (higher LPI value) leaves. The values were relatively constant when expressed on a leaf area (g.m⁻²) basis. Similarly, during leaf development pigment content is expected to increase on an area basis, but its increase on a mass basis will depend if it increases *more* than the increase in TSLM and SLM commonly observed during leaf development. Some characteristics and differences between the two methods of pigment or nutrient expression are shown in Table 35.

Table 35 Methods of pigment expression and some observed characteristics.

Method of pigment expression	Units (example)	Characteristics
Area-basis	mg.cm ⁻²	Insensitive to changes in SLM, only dependent on pigment change per leaf area
Mass-basis	mg.g ⁻¹ FM or DM	May increase if pigments increase more than specific leaf mass or if pigment content remains constant, but specific leaf mass decreases (specific leaf mass can decrease or increase due to leaf density or thickness decrease or increase). May remain similar if pigment content and specific leaf mass increase. May decrease if specific leaf mass increase without pigment content increase Dependent on both pigment change and leaf mass per area (TSLM or SLM) change.

In season one, destructive pigment analysis was performed on four leaf disks punched out with a cork borer (2.26 cm² area) from inter-vein areas of single, detached, fully unfolded leaves from main and secondary shoots, respectively. All sampling was conducted during early morning (07:00 to 10:00). Leaves used in measurements were from representative, non-topped shoots, collected on five measuring dates (A-E) during the season (see Results & Discussion). Leaf main (L1) vein length was also recorded for every leaf on which photosynthetic pigments were determined. Leaf discs were placed in an eppendorf tube, frozen in the field using liquid nitrogen, kept in the dark and stored at -80°C until further processing. Prior to extraction, tissue was ground with a mortar and pestle in liquid nitrogen to a visually homogenous powder. Approximately 20 mg of tissue were weighed off into pre-weighed tubes, and the mass was again determined for each tube. The full method and validation for the HPLC measurement method are supplied in Lashbrooke *et al.* (2010), which is an adaptation of methods found in literature where grapevine pigments were analysed. These methods were found during initial experimentation to yield abnormal amounts of chlorophyll and carotenoid degradation products, caused by conditions during extraction, storage and analysis. These obstacles, and solutions are presented in Lashbrooke *et al.* (2010).

All solvents used during the sample extraction, preparation and analyses were of HPLC grade. *tert*-butyl methyl ether (TBME), methanol, acetone, ethyl acetate and chloroform were purchased from Sigma–Aldrich (Steinheim, Germany). Butylated hydroxytoluene (BHT), N-ethyl-di-isopropylamine (NED) and analytical grade sodium chloride (NaCl) were purchased from Fluka Chemie (Buchs, Switzerland). Tri-ethylamine (TEA) and ammonium acetate were purchased from Merck (Hohenbrunn, Germany); Tris base was purchased from Roche Diagnostics (Mannheim).

The authentic standards *trans*- β -carotene (β -carotene), chlorophyll *b* and the internal standard (IS), β -apo-caroten-8-al were all purchased from Fluka Chemie. CaroteNature GmbH (Lupsingen, Switzerland) supplied zeaxanthin, neoxanthin, violaxanthin and antheraxanthin. Lutein and chlorophyll *a* were obtained from Sigma-Aldrich. Standard curves constructed for the authentic standards showed linearity over the concentration range injected. All R^2 -values were above 0.99 with recoveries from leaf extracts (relative to the recovery of the internal standard) evaluated to be above 95% for all pigments, except violaxanthin with a recovery of about 80% (Lashbrooke *et al.*, 2010).

Frozen tissue from leaves (± 20 mg) was extracted in 2.0 mL micro-centrifuge tubes in a cold laboratory (8°C), taking care to minimise exposure to air and light. The leaf samples were suspended in 1.8 mL acetone and the internal standard, β -apocaroten-8-al (2 μ g), added to all extracts. The tubes were vortexed for 30 minutes, followed by pelleting of the tissue residue *via* centrifugation (10,000 rpm, 3 minutes). A 300 μ L aliquot of the acetone supernatant (now

containing pigment) was removed, 1 mL of extraction buffer added and the solution mixed by vortexing for 5 minutes. Ethyl acetate (200 μ L) was added and the mixture vortexed briefly, followed by centrifugation (10,000 rpm, 5 minutes) for partitioning. A 50 μ L aliquot of the 150-200 μ L top ethyl acetate phase (containing pigment) was removed, added to 200 μ L methanol containing 0.125% (mass/volume) BHT, and 200 μ L transferred to amber HPLC vials (containing 200 μ L vial inserts, filled to the brim) and sealed.

All pigments were separated by reverse-phase high-performance liquid chromatography (RP-HPLC) on an Agilent 1100 series HPLC system (Agilent Technologies, Palo Alto, CA, USA), equipped with a diode array detector (DAD) system. A YMC30 column (250 mm \times 2.1 mm) and YMC30 guard cartridge (10 mm \times 2.1 mm, particle size 3 μ m) from YMC Europe (Schermbek, Germany) were used. Chemstation software for LC3D (Rev.A.10.01 [1635]; Hewlett-Packard, Waldbronn, Germany) was used for data processing. The chromatographic conditions were optimised to facilitate baseline separation of the major pigments extracted from grapevine tissue. A binary mobile phase of 3% (v/v) ddH₂O in methanol containing 0.2% (w/v) ammonium acetate and 0.05% (v/v) tri-ethylamine (solvent A) and TBME containing 0.05% (v/v) tri-ethylamine (solvent B) was employed. The flow rate was 1 mL.min⁻¹ and temperature was maintained at 25°C. The elution program was isocratic at 20% solvent B for 12 minutes followed by a linear increase from 20% to 50% solvent B in 6 minutes, isocratic at 50% solvent B for 4 minutes, a linear increase to 68% solvent B in 2 minutes, isocratic at 68% for 4 minutes followed by a linear decrease to 20% solvent B in 2 minutes. The column was equilibrated for 15 minutes before each injection, and regularly flushed to maintain column condition. Pigments were identified by comparison of their retention times and spectral properties with the authentic standards and published data. For more details see Lashbrooke *et al.* (2010).

To facilitate comparison to molar concentration values found in some literature sources, molecular masses of pigments shown in Table 36 were used.

Table 36 Molar masses of different pigments analysed used to convert values to mmol.mol⁻¹ units.

Pigment	Molar mass (g.mol ⁻¹)
Chlorophyll <i>a</i> (Blanchfield <i>et al.</i> , 2006)	892.9
Chlorophyll <i>a</i> (Blanchfield <i>et al.</i> , 2006)	906.9
Lutein	568.85
B-carotene	536.85
Violaxanthin	600.85
Neoxanthin	600.85
Antheraxanthin	584.871
Zeaxanthin	568.88

Pigments determined relative to the standard curves created for each pigment were expressed in ng.mg⁻¹ FM (fresh mass), and the effect of TSLM was incorporated by multiplying this amount by the total specific leaf mass (mg.cm⁻² FM), yielding the amount of pigment on an area basis (ng.cm⁻²). Where applicable, values were transformed to molar ratios using Equation 8.

Equation 8 Conversion of pigments to molar mass units.

$$\text{Pigment A} \left(\frac{\text{ng}}{\text{mg}} \right) \times \text{molar mass of A} \left(\frac{\text{nmol}}{\text{ng}} \right) = \text{Pigment A} \left(\frac{\text{nmol}}{\text{mg}} \right)$$

The de-epoxidation state of the xanthophyll cycle (DEPS) (Demmig-Adams & Adams, 1992; Demmig-Adams & Adams, 1996) was calculated from:

$$DEPS = \frac{A+Z}{V+A+Z}$$

where A represents antheraxanthin, Z represents zeaxanthin and V represents violaxanthin.

5.1.3 Leaf age classification

The methods used for leaf age classification is discussed in Chapter IV.

5.1.4 Statistic and chemometric analysis

The results from pigment analysis were based on measurements of leaf discs collected from leaves on selected shoots for five different measurement dates (A to E). Data were grouped into chronological leaf age categories as defined in Chapter IV. Statistical analysis was conducted using Statistica 10 ® software (Statsoft, Tulsa, USA). Three-way analysis of variance was performed of sampling dates, canopy manipulation treatments and leaf chronological age classes for different pigments or pigment ratios determined from HPLC analysis. The ANOVA consisted of an initial *F*-test followed by a Fisher's LSD test. Only primary shoot leaves were included in the analysis, except where specified otherwise. The analyses shown are only the interactions that were significant at the $p \leq 0.05$ level. All ANOVA results represent Type I decompositions, and on graphs non-weighted means are presented.

5.2 Results and discussion

According to Chapter III, shoot growth rate reached maximum values on measurement date A, when shoot lengths were approximately 200 cm, and then slowed down to the theoretical threshold of 5 mm.day⁻¹ after measurement date D (depending on the treatment, see Chapter III). The reduced canopy treatment was performed very early in the season (19 DAB), and was characterised in this season by significant secondary shoot growth compensation in reaction to the treatment.

5.2.1 Light measurements

The reduced canopies in season one had significantly higher levels of red *versus* far-red radiation (R:FR) compared to the full canopies (Table 11). The measurements were conducted one month after the canopy manipulation treatment was applied (just prior to measurement date A). Dokoozlian & Kliewer (1995) reported that R:FR ratios in the fruit zone at berry set ranged from 0.58 to 0.40 in low density canopies and 0.2 or less in high density canopies, for which similar values were also previously found by Smart *et al.* (1988). They also reported R:FR ratios to decrease between fruit set and véraison, with values ranging from 0.52 to 0.35 for low density canopies to less than 0.1 for high density canopies. A relationship between the R:FR ratio and photosynthetic photon flux density ($r = 0.98$) was shown for a range of vineyard sites. In this study, even the reduced canopies seemed to correspond more to high-density canopy values found in literature, highlighting the vigour experienced at this site, especially where no canopy manipulation was done.

Table 37 Red:far red ratios measured in the bunch zone for the different canopy manipulation treatments on 52 DAB in season one (means with different letters are significantly different at the $p \leq 0.01$ level according to a Mann-Whitney *t*-test).

Treatment	R:FR means	N	SD
Full canopy	0.14 a	17	0.05
Reduced canopy	0.26 b	19	0.12
All measurements	0.20	36	

5.2.2 Leaf water potential (pre-dawn)

For season one it was assumed that water stress, as quantified using predawn leaf water potential (Ψ_{PD}) measurements, was absent between 0 and 80 DAB (concurrent with the classes described in Chapter III) (Figure 22). During this period, the canopy reduction treatment may therefore be

considered a dominant microclimate effect, with possible interactions between plant water status and the canopy manipulation treatments occurring later in the season. The first irrigation was applied at 107 DAB and Ψ_{PD} measurements only commenced in the S treatments after this. With respect to measuring dates C and D it was considered that the NSR treatments have lower Ψ_{PD} values than the NSF treatments, and that the Ψ_{PD} values on measurement date D was lower (more negative) than that of measurement date C. These assumptions are confirmed by consistent seasonal trends in the treatments (higher values seemed to persist for NSR treatments) as well as lower soil water contents observed in the NSF *versus* NSR treatments (refer to Chapter III). Relatively low (more negative) mean Ψ_{PD} values were measured for the NSF treatment during season one (refer to Chapter III). It is possible that during this relatively warm season, the larger transpiration surface in the full canopies led to more negative Ψ_{PD} values than for the NSR canopies.

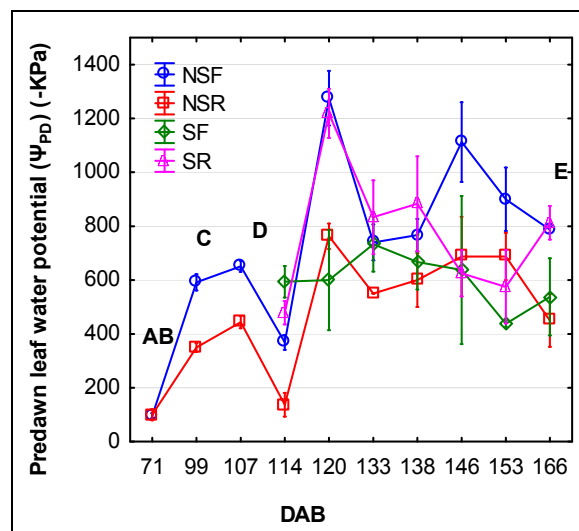


Figure 93 Predawn leaf water potentials (Ψ_{PD}) relative to date after budburst (DAB) for the treatments in season one (including specified measurement dates for pigment sampling indicated as letters from A to E) (means with +/- standard errors shown).

5.2.3 Leaf age on the measuring dates

The chronological leaf age (days) for the different sampling dates and canopy manipulation treatments are shown in Figure 94. Although the interaction shown was non-significant, the age increase shown in measurement dates D and E for the full canopy treatment and for E in the reduced canopy treatment, as well as the difference between the means of the full and reduced canopies was significant at the $p \leq 0.05$ level. From this interaction it was found that the leaves were significantly younger for the reduced canopy on measurement date D, which may be ascribed to shoot growth. In Chapter III a strong shoot growth decline was described for the NSF treatment after 50 DAB, relative to the other treatments, as well as theoretical growth cessation at date C. This could have caused a consistent increase in leaf age (considering that no new leaves are formed on primary shoots) compared to the NSR treatments, which only ceased growing between dates D and E. (shown in Chapter III), which could have contributed to the observed sharp increase in leaf age for the NSR canopies from date D to date E.

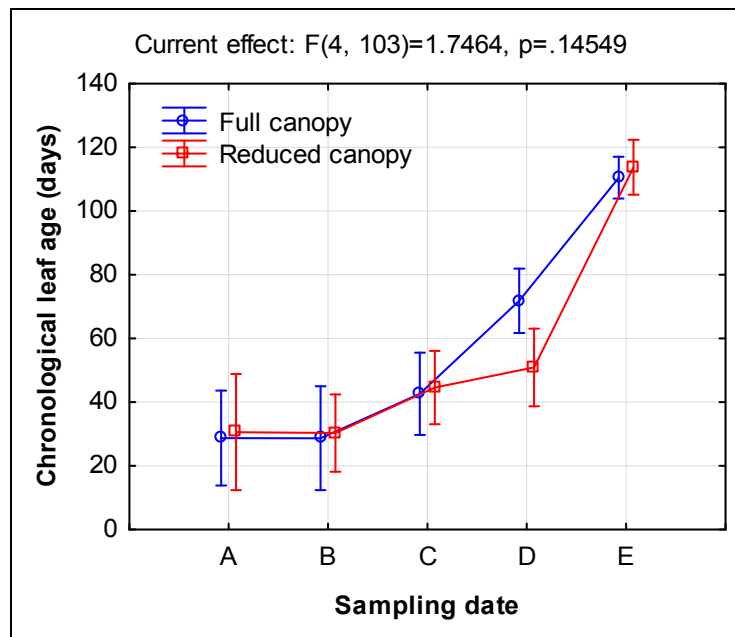


Figure 94 Chronological leaf age (days) for the different measurement dates and canopy manipulation treatments. Vertical bars denote 95% confidence intervals ($p \geq 0.05$).

5.2.4 Range of measured pigments

In general, the results of mean leaf pigment content, as measured using HPLC from primary and secondary shoots of all treatments, indicate high chlorophyll a contents relative to the other pigments, with lutein being the most abundant carotenoid (Figure 95). The ranges of pigments and pigment ratios measured using HPLC for primary shoot leaves are shown in Table 39, Addendum A, and pigments as well as pigment ratios correlations are shown in Table 40, Addendum A.

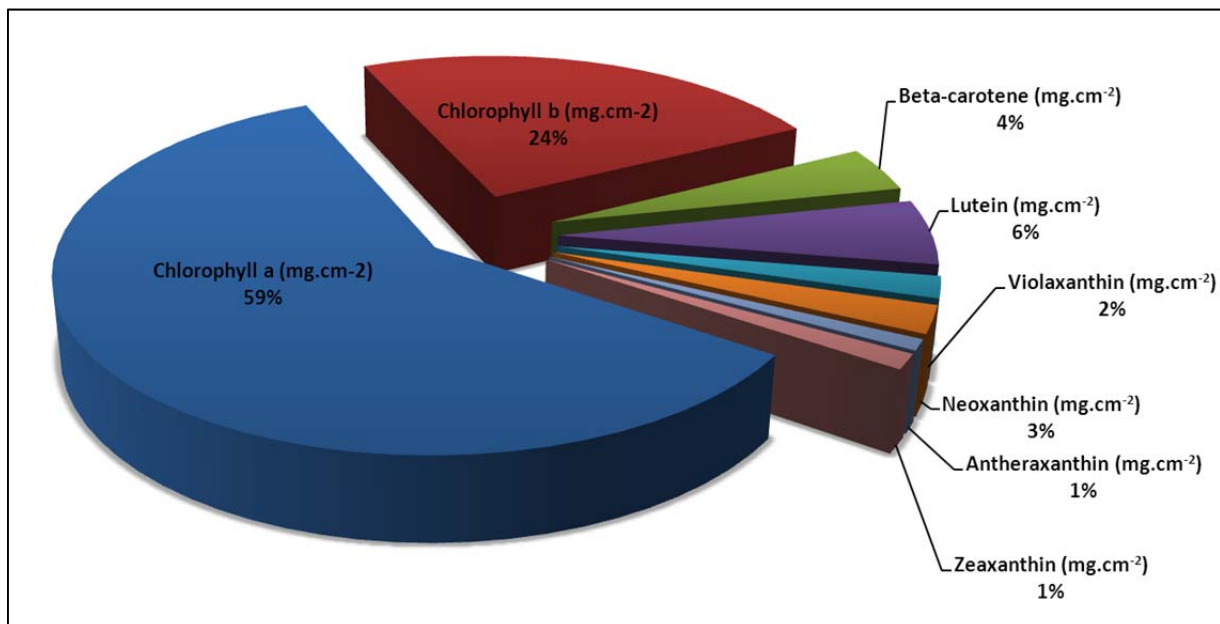


Figure 95 Mean values of pigments extracted from grapevine leaves collected from primary and secondary shoots from all treatments and measurement dates.

5.2.5 Results from destructive pigment measurements

5.2.5.1 Leaf total chlorophyll content

Mean total chlorophyll (mg.cm⁻²) values in this study generally corresponded to values reported in Blanchfield *et al.* (2006) (Cabernet Sauvignon grown in the field: 0.020 mg.cm⁻², Shiraz grown in

the glasshouse: 0.013 mg.cm^{-2} and Pinot noir in the field: 0.042 mg.cm^{-2}) as well as Hunter & Visser (1989) (Cabernet Sauvignon in a field study: from a maximum of 0.026 mg.cm^{-2} for leaves opposite and below the bunches at berry set to a minimum of about 0.009 mg.cm^{-2} at ripeness) (Table 39).

The highest total chlorophyll levels were measured in leaves from chronological age class 3 on measurement date A (Figure 96). For this age class, leaf total chlorophyll levels declined sharply between dates A and B and then again from date D to E (total decrease of 60%). The results in this study differs from earlier studies (Hunter & Visser, 1989), as younger leaves reached maximum total chlorophyll levels relatively early in the season and declined from as early as measurement date B, more than a month prior to véraison on measurement date C. In Poni *et al.* (1994b) apical leaves reached maximum total chlorophyll levels (area basis) about a month after véraison (midway between our dates D and E) after a sharp increase from véraison. A simple explanation for these observed differences could be the difference in our definition of young/apical leaves. In Poni *et al.* (1994b), the mean age of apical leaves changed from 8-20 days before September, to 58 days and older past 7 September. Therefore in both studies shoot growth cessation brought about a change in the age level of apical leaves, leading to the observation of a sharp increase in chlorophyll levels. In this study, leaf age classification performed from chronological leaf age calculation will lead to these leaves ending up in an older age class after shoot growth cessation. Other studies have also considered leaf age rather than shoot zone classification to investigate pigment content and photosynthesis. For example, maximum chlorophyll levels were reached in Kriedemann *et al.* (1970) at a leaf age of about 45 days after unfolding, corresponding to the point of maximum net photosynthesis. In the study by Poni *et al.* (1994b) maximum chlorophyll levels were reported for leaves 60-80 days old, but with maximum photosynthesis at about 30-40 days (corresponding to 100% leaf expansion) or an LPI of about 17-18, similar to the results found in this study.

Another factor that needs to be taken into account in comparison with other studies in which pigments are expressed on a mass-basis, is potential differences in specific leaf mass (SLM) that could exist between leaves differing in age or canopy position. For example, in Hunter & Visser (1989) a recalculation of the mass-based results using the SLM results for each leaf could lead to some changes in the results. This can also be seen in the study by Cloete *et al.* (2008), where significantly different results of leaf chlorophyll concentration ($\mu\text{g.g}^{-1}$) between normal and underdeveloped shoots in Shiraz, were non-significant when expressed on a leaf area basis, caused by the significant lower SLM in the underdeveloped shoots.

Leaf chlorophyll content seemed to be a more reliable indicator of photosynthetic capacity only for basal or apical shoot zones in the studies by Hunter & Visser (1989) as well as Poni *et al.* (1994b), with middle leaves showing weak correlations between the two parameters. The reason suggested for these observations is that these leaves (in this study leaves of class three, between 50-90 days of age) are stable with regards to SLM development and also reached maximum chlorophyll levels, which means there are too small variability in chlorophyll content and photosynthesis to drive correlations. However, it seems that when outside canopy leaves are selected exclusively from this class, as in the study by Cartechini & Palliotti (1995), the relationship between photosynthesis and SLM holds strong, but possibly only if chlorophyll content does not become limiting. This is evident from the total chlorophyll (mg.cm^{-2}) of 100% irradiated mid-canopy leaves being considerably higher than that found in other studies at the end of the season.

For the youngest leaves, leaf total chlorophyll content was found to initially increase and then decrease from sampling date B, coinciding with the onset of more severe water deficits (predawn leaf water potential values more negative than -500 KPa, refer to Chapter III) (Figure 96).

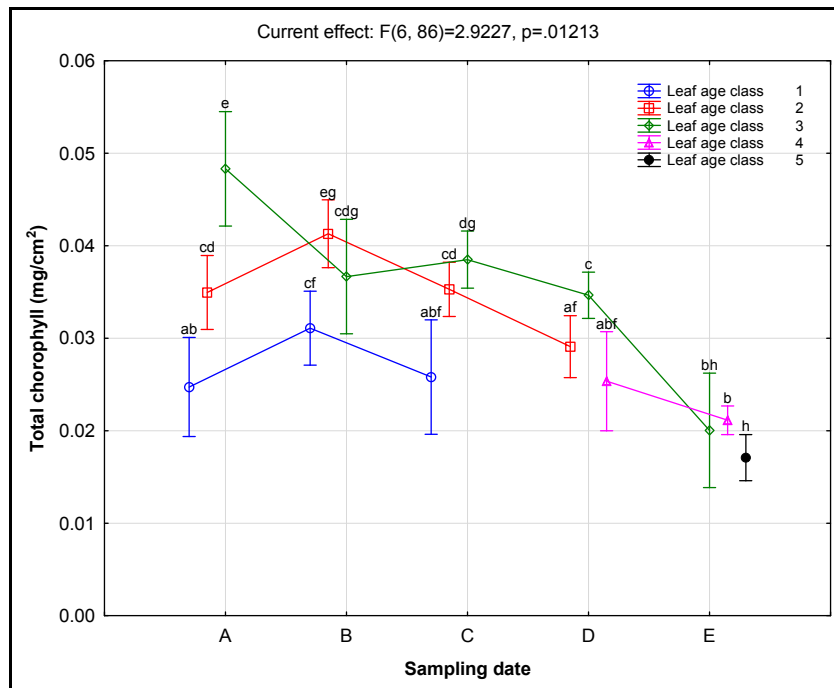


Figure 96 Primary shoot leaf total chlorophyll content ($\text{mg}\cdot\text{cm}^{-2}$) for the different measuring dates and chronological age classes (vertical bars denote 95% confidence intervals).

From the mean total chlorophyll values recorded for primary and secondary shoots on the different measurement dates, the secondary shoots seem to make an important contribution on measurement dates C and D, where maximum chlorophyll levels were reached, but the decline in the last part of the season (date D to E) was similar to that of the main shoots. Considering the abundant presence of secondary shoots in the reduced canopy treatments this may strengthen the observed importance of these leaves in the ripening period (Schultz, 1989; Candolfi-Vasconcelos & Koblet, 1990; Candolfi-Vasconcelos & Koblet, 1991), and removal of secondary shoots are therefore not recommended, apart from it not being economically viable (Hunter, 2000).

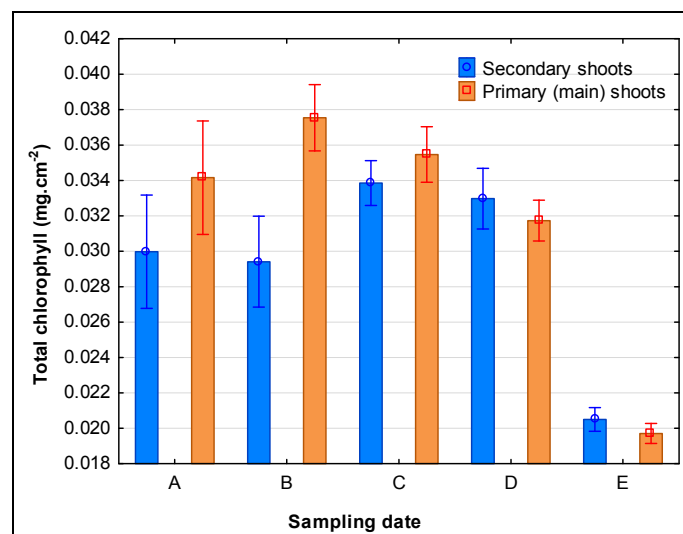


Figure 97 Mean leaf total chlorophyll content ($\text{mg}\cdot\text{cm}^{-2}$) for the different measuring dates and shoot types measured (primary and secondary) (vertical bars denote 95% confidence intervals).

The total chlorophyll content of the primary leaves in the reduced canopy treatment showed an earlier decline (from dates B to C) compared to the full canopy treatment, leading to significantly lower values measured on date C (Figure 98). This result is not likely to have been caused by leaf age differences, even though leaf age differences may have led to the reduced canopy showing higher chlorophyll content on date D. Unfortunately canopy light measurements were not available at date C to confirm this, but it was deemed possible that continued growth of the NSR canopies at date C (in contrast to the NSF canopies), combined with the strong secondary shoot compensation reaction measured at 61 DAB (see Chapter III), may have caused a more dense canopy than expected in this treatment at this point in time. The lower chlorophyll values measured on date C were accompanied by significantly lower total carotenoids (Figure 100). On closer inspection, it seemed to be mostly the younger (class one and two) leaves that had decreased total chlorophyll levels on date C, which makes the shading theory an unlikely one. It is also possible that the abundance of secondary shoots, and actively growing shoot tips, may have led to distribution of carbohydrates to the actively growing sinks, counteracting possible positive effects that could have been the result of improved microclimate in the reduced canopies (Koblet, 1969; Hunter & Visser, 1988; Hunter *et al.*, 1995). In the study by Candolfi-Vasconcelos & Koblet (1991) secondary shoot removal caused significantly higher chlorophyll levels, a compensatory mechanism that was also shown by Hofäcker (1978) as well as Hunter & Visser (1989) in reaction to partial defoliation. It can therefore be expected that significant compensatory secondary shoot growth in reaction to the reduced canopy treatment, may have had the opposite effect, lowering leaf pigment levels.

After measurement date C, the total chlorophyll levels in the reduced canopy treatment were stable and it declined less until the last measurement date, finally having significantly higher values than the full canopies. Lower reduction from date D to E may be due to inhibition in senescence of more exposed leaves, as suggested in partial defoliation studies (Hunter & Visser, 1989; Candolfi-Vasconcelos & Koblet, 1990; Candolfi-Vasconcelos & Koblet, 1991). It was also peculiar that the NSF treatment's total chlorophyll or total carotenoid contents did not decrease in reaction to increased water deficits between measurement dates B and C. It could be that water deficits did not increase significantly enough for the effect to become apparent in chlorophyll or carotenoid breakdown, however the de-epoxidation state of the xanthophylls (DEPS) did increase in NSF young leaves for date C (see Section 5.2.5.5).

It was interesting that, even with possible considerable differences in canopy microclimate between the reduced and full canopy treatments, no differences could be seen between them for the first two measurement dates with reference to leaf total chlorophyll values, also not when analysed on a mass basis (ng.mg^{-1}) (data not shown).

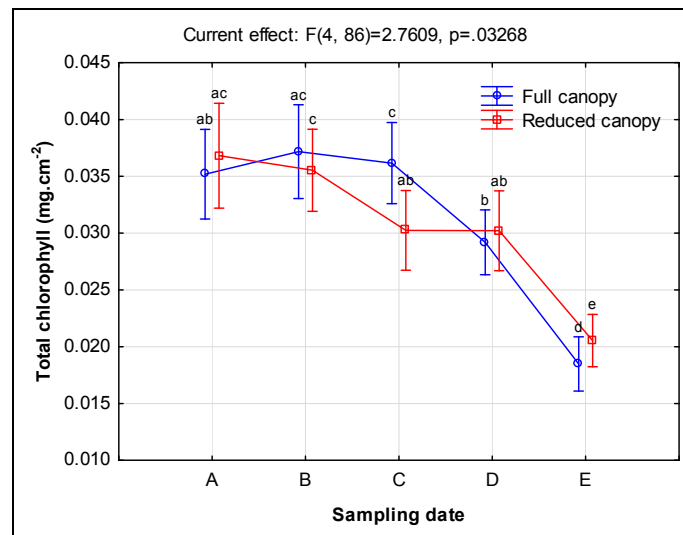


Figure 98 Primary shoot leaf mean total chlorophyll content ($\text{mg}\cdot\text{cm}^{-2}$) for the different measuring dates in reaction to canopy manipulation (vertical bars denote 95% confidence intervals).

5.2.5.2 Total carotenoids

In accordance with the total chlorophyll content, total carotenoid content (calculated as the sum of β -carotene, lutein and all the xanthophylls) in primary shoot leaves was the highest in leaf age classes two and three, significantly lower for the youngest leaf age class, and second lowest and lowest for classes four and five, respectively. The oldest leaves had 50% lower values than the two leaf classes with the highest values (Figure 99).

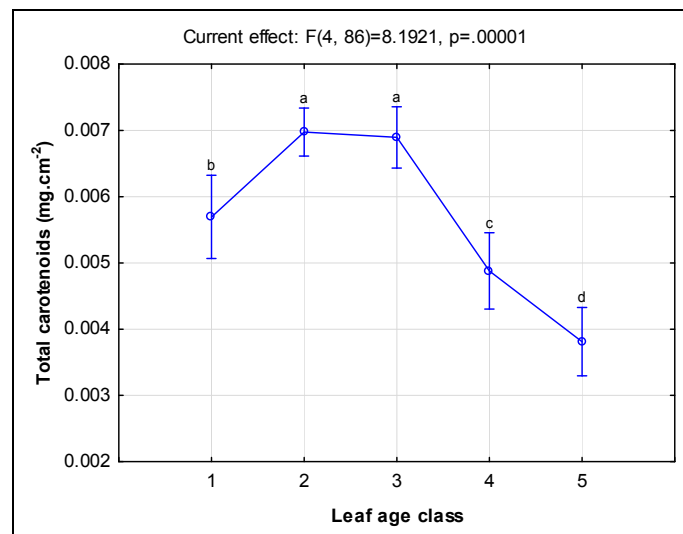


Figure 99 Primary shoot leaf total carotenoid content ($\text{mg}\cdot\text{cm}^{-2}$) for the different chronological leaf age categories (vertical bars denote 95% confidence intervals).

The reduced canopy had approximately 20% higher total carotenoid content at the first measuring date, which was the closest date to the canopy manipulation treatment (Figure 100). This reaction could have been the result of higher leaf exposure levels increasing the carotenoid:chlorophyll ratio, especially for leaf age class two (Figure 101), which is in accordance with the findings of Bertamini & Nedunchezian (2003) related to photoprotection of young grapevine leaves. The compensation reactions following up to date C in this treatment, however, seemed to counteract these higher values, reducing it to levels even below that of the full canopies. Possible reasons for this were discussed in the previous section.

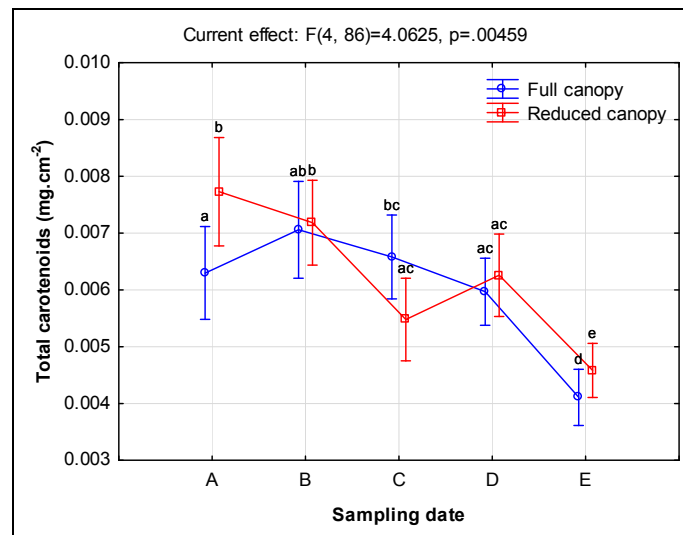


Figure 100 Primary shoot leaf total carotenoid content ($\text{mg}\cdot\text{cm}^{-2}$) for the different measurement dates in reaction to the canopy manipulation treatment (vertical bars denote 95% confidence intervals).

5.2.5.3 Carotenoid:chlorophyll ratios

Higher total carotenoid:total chlorophyll ratios were recorded in the younger leaves of the reduced canopy treatment, in accordance with Bertamini & Nedunchezian (2003), reporting similar results for young leaves, and some studies reporting higher ratios in exposed *versus* shaded leaves (Demmig-Adams & Adams, 1992; Demmig-Adams & Adams, 1996; Demmig-Adams, 1998) (Figure 101). This ratio seemed to increase consistently for leaf age class three and generally in all leaves after véraison, corresponding to ambient temperature increase, which is normal for this time of the growing season. There was a tendency for the class two leaves to show higher increase in this ratio after date C in the NSF treatment, where increased water deficits (according to predawn leaf water potential measurements) were observed on date D, compared to the near-absent water stress in the NSR treatment. No significant differences for any treatments or leaf age classes could be observed on measurement date C.

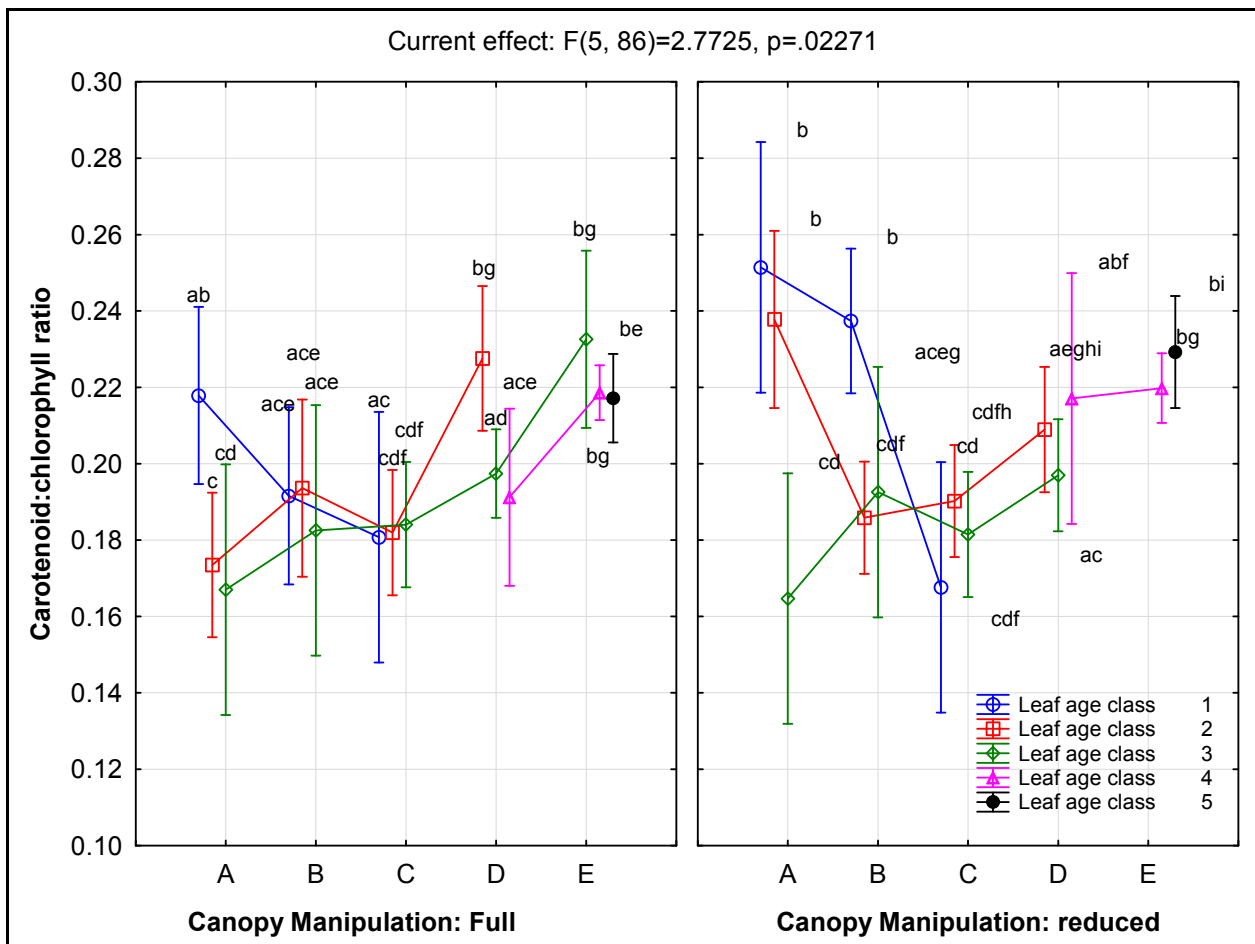


Figure 101 Primary shoot leaf carotenoid:chlorophyll ratios for the different measurement dates as well as chronological leaf age categories in reaction to the canopy manipulation treatment (vertical bars denote 95% confidence intervals).

5.2.5.4 Chlorophyll *a:b* ratios

Chlorophyll *a:b* ratios were generally higher in young leaves during the first part of the season, but even for the youngest leaf age class the values declined considerably up to measurement date C, and stayed low where leaf age was increased (Figure 102) in accordance with Hunter & Visser (1989) as well as Bertamini & Nedunchezian (2002), where a decrease in the chlorophyll *a* levels of basal leaves were noted. It also corresponds to leaves differing in age in the study by Kriedemann *et al.* (1970). Considering the decrease that was also observed in the youngest leaf age class up to measurement date C, the possible role of water deficits increasing during the season cannot be excluded. In Bertamini *et al.* (2006) water deficits were shown to degrade chlorophyll *a* more than chlorophyll *b*, therefore lowering the ratio. It was also confirmed here that chlorophyll *a* values declined between measurement dates B and C, with chlorophyll *b* remaining fairly constant (data not shown). The increase in the values for age class two from date C to D seemed to be primarily due to an increase in the chlorophyll *a:b* ratio of the reduced canopy leaves (Figure 103). This could have resulted from more young leaves observed in the reduced canopies for measurement date D, but it is peculiar that it was limited only to leaf age class two. A decrease in the chlorophyll *a:b* ratio can also occur in conditions of low irradiance (Bjorkman & Holmgren, 1963; Bertamini & Nedunchezian, 2004). In general, the reduced canopies showed significantly higher chlorophyll *a:b* ratios (Table 38), even though the measurement date interaction was non-significant (Figure 103).

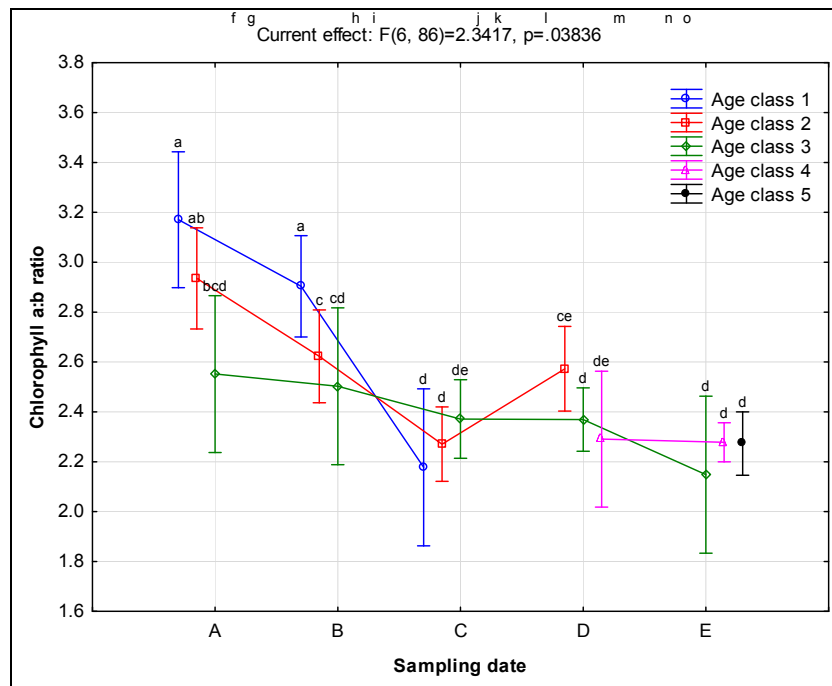


Figure 102 Primary shoot leaf chlorophyll *a:b* ratios for the different measurement dates and chronological leaf age classes (vertical bars denote 95% confidence intervals).

Table 38 Canopy manipulation treatment effect on chlorophyll *a:b* ratios for main shoot leaves ($F = 4.45$, $p \leq 0.05$).

Treatment	N	Chlorophyll <i>a:b</i> mean	Chlorophyll <i>a:b</i> SD
Full canopy	64	2.37 a	0.30
Reduced canopy	51	2.46 b	0.34

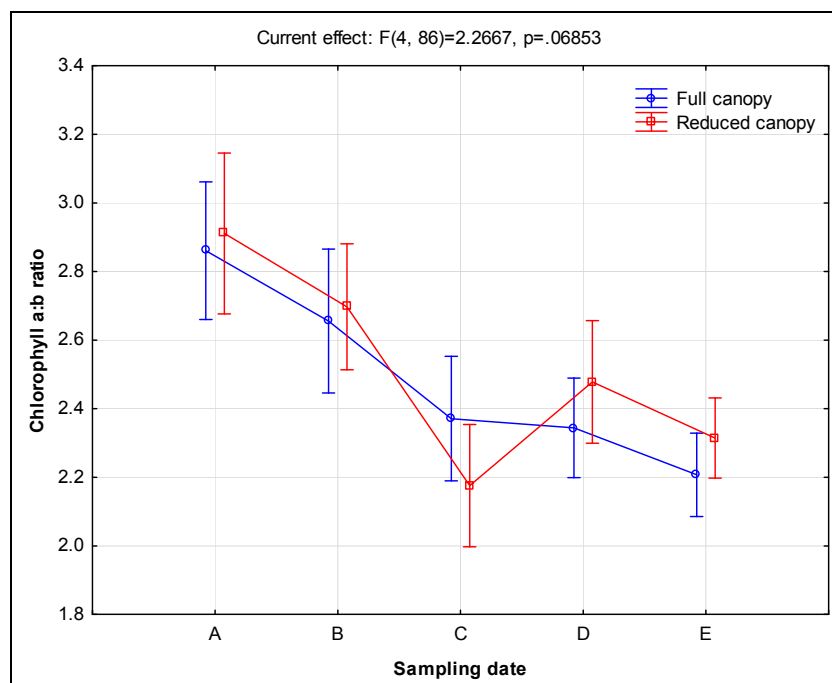


Figure 103 Chlorophyll *a:b* ratios for the different measurement dates in reaction to canopy manipulation (vertical bars denote 95% confidence intervals).

5.2.5.5 De-epoxidation state of the xanthophylls

It has been shown that the DEPS ratio may increase in reaction to high light conditions (Demmig-Adams, 1998), but also to light quality differences, with increases in the DEPS ratio reported with

increased red or UV light (Woitsch & Römer, 2003; Sobrino *et al.*, 2005). In contrast to the reduced canopy treatment, the full canopy DEPS in the primary shoot leaves increased after date B towards date D, as water deficits developed (Figure 104). The reduced canopies initially showed higher levels in the young leaf age classes, decreasing to general low levels, also in the younger leaves. Medrano *et al.* (2002) found drought-stressed grapevines to show significantly higher DEPS values in a diurnal cycle, with the largest differences found when irradiance reached maximum levels. In this study higher DEPS values were found in the youngest leaves of more exposed canopies, even when apparently no water deficits were present. It therefore seems that canopy microclimate in addition to water deficits may impact the DEPS levels, and this is more pronounced in young leaves, as there is probably an increased need for photoprotection when photosynthetic rates are high in these leaves. The DEPS levels seemed unresponsive when leaf senescence was more advanced (date E). The DEPS levels were also assessed in secondary shoots, without consideration of leaf age on these shoots (data not shown) and it was found that the NSF secondary shoot leaves had higher levels than the NSR leaves on dates B, C and D, with no difference on date E.

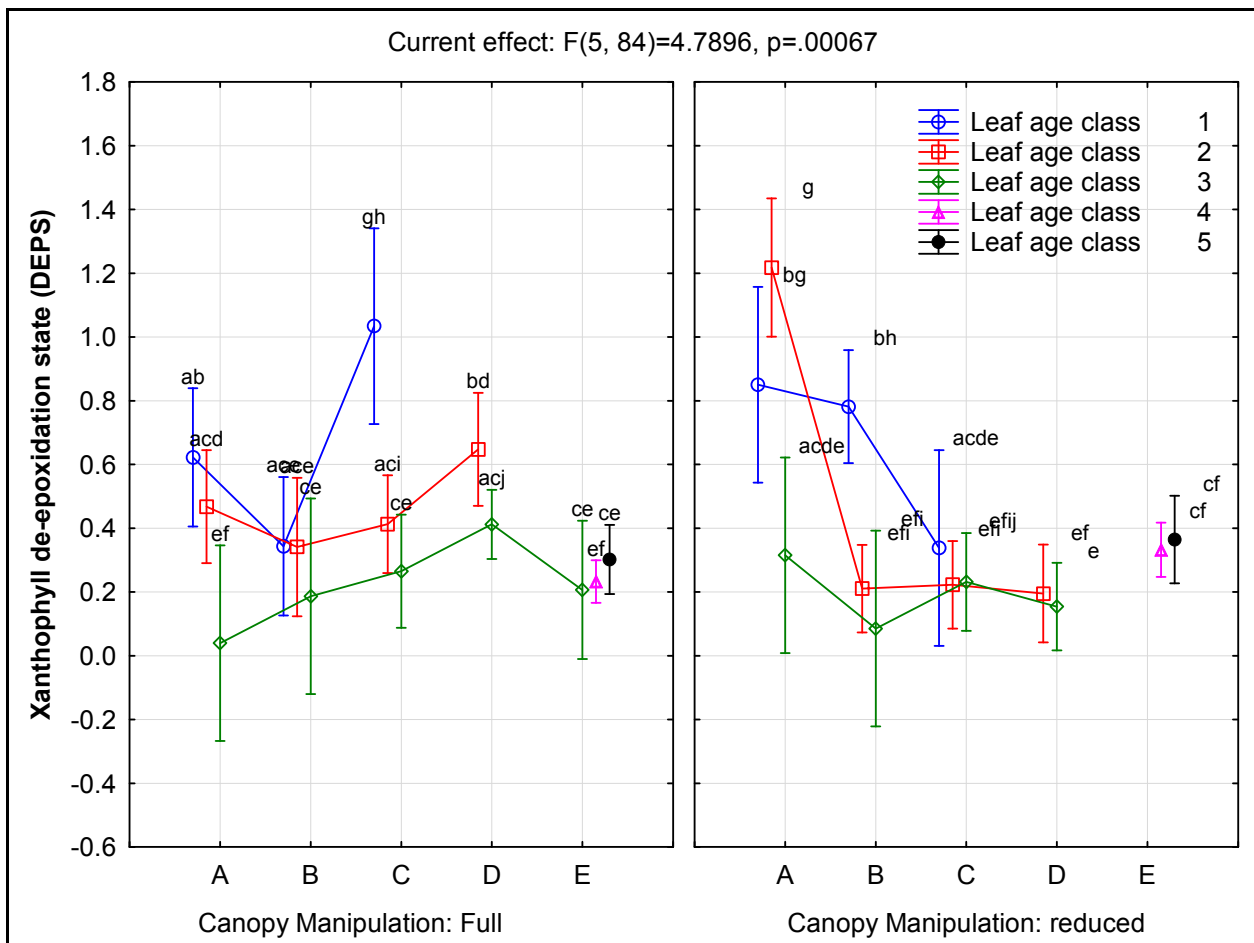


Figure 104 Primary shoot leaf xanthophyll de-epoxidation state (DEPS) for the different measurement dates and chronological leaf age classes in reaction to canopy manipulation (vertical bars denote 95% confidence intervals).

Regression analysis of the DEPS ratio with leaf chronological age was performed (Figure 105 to Figure 107) and even though the variability was quite high [possibly also considering the strong diurnal variability of DEPS shown in Medrano *et al.* (2002) and slight differences in the time of early morning when leaves were destructed], the trends of higher values in the younger leaves of the reduced canopies were visible for dates A and B combined (Figure 105). When leaves were classified according to their leaf water potential values (measured close to the date of pigment

analysis - refer to Chapter III) on date C, a clear differentiation was visible between leaf water potential classes three and four, marking the transition from moderate-severe (-400 to -600 KPa) to severe (-600 to -900 KPa) plant water deficits (Figure 106), and on date D the differentiation was between absent to moderate and moderate to severe classes (Figure 107). No correlations could be detected on measurement date E, possibly due to leaf senescence and lower photosynthesis tempos, reducing the need for photoprotection in the leaves.

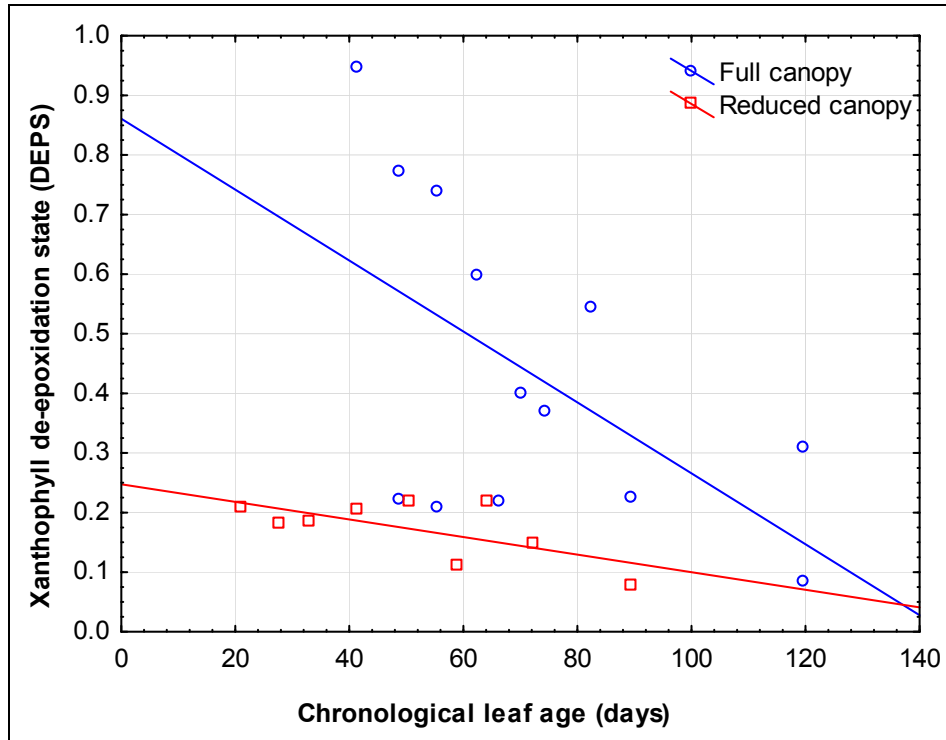


Figure 105 Relationship between the xanthophyll de-epoxidation state (DEPS) and leaf age for primary shoot leaves on measurement dates A and B for the different canopy manipulation treatments (full canopy: $R^2 = 0.32$; reduced canopy: $R^2 = 0.44$; all regressions significant at the $p \leq 0.01$ level).

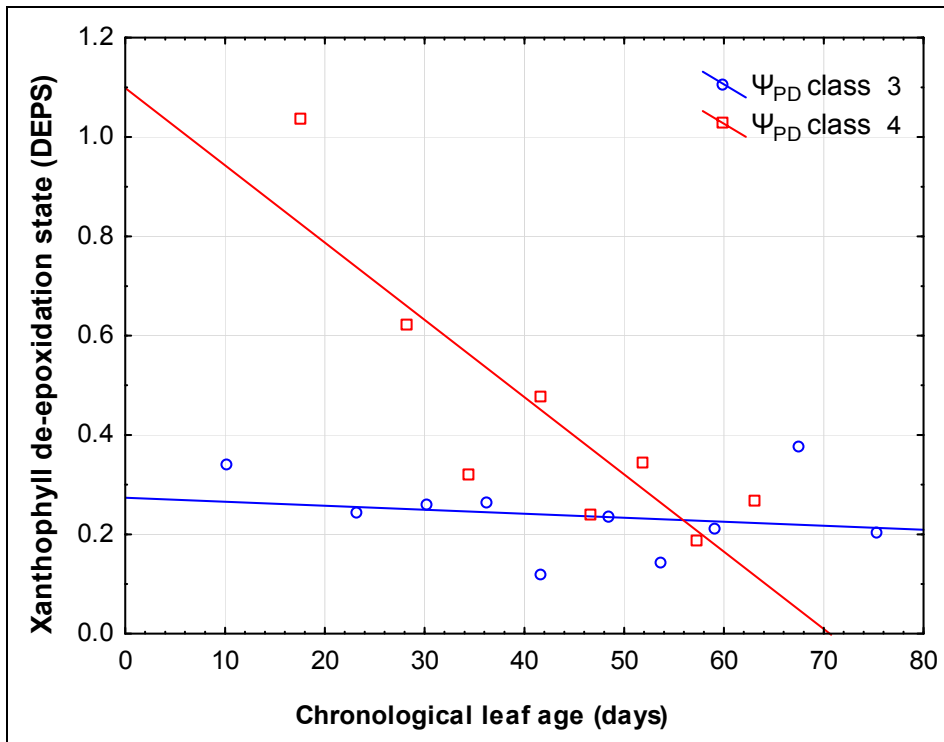


Figure 106 Relationship between the xanthophyll de-epoxidation state (DEPS) and leaf age for primary shoot leaves on measurement date C for different predawn leaf water potential classes (Ψ_{PD}) (class 3: $r^2 = 0.04$, non-significant; class 4: $R^2 = 0.73$; significant at the $p \leq 0.01$ level).

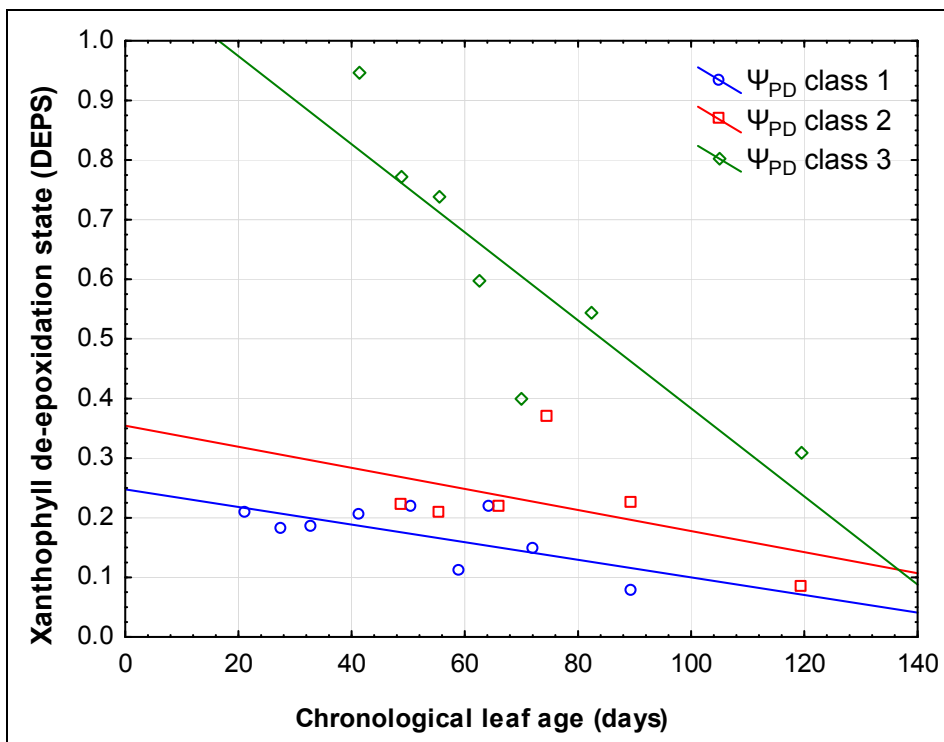


Figure 107 Relationship between the xanthophyll de-epoxidation state (DEPS) and leaf age for primary shoot leaves on measurement date D for different predawn leaf water potential classes (Class 1: $R^2 = 0.44$, $p = 0.052$; class 2: $R^2 = 0.25$, non-significant; class 3: $R^2 = 0.76$, $p = 0.01$).

5.2.5.6 Xanthophyll pool size:chlorophyll ratio

The reaction in the xanthophyll pool size:total chlorophyll ratio (XPS:chl) was similar to that of the DEPS ratio, but the same increase was not seen for the youngest leaf age class on date C, and

only leaf age class three seemed to increase slightly from date B to C. It seems therefore as if the DEPS ratio is more sensitive to water deficits, while the xanthophyll pool size is still sensitive to exposure levels in young leaves, similar to the DEPS ratio, and with even more pronounced differences between the leaf age classes on measurement date A (Figure 108). In the study by Blanchfield *et al.* (2006) this ratio also increased in phylloxera-infested grapevines, indicating that photoprotective mechanisms were activated, probably as a consequence reduced water uptake by infested roots.

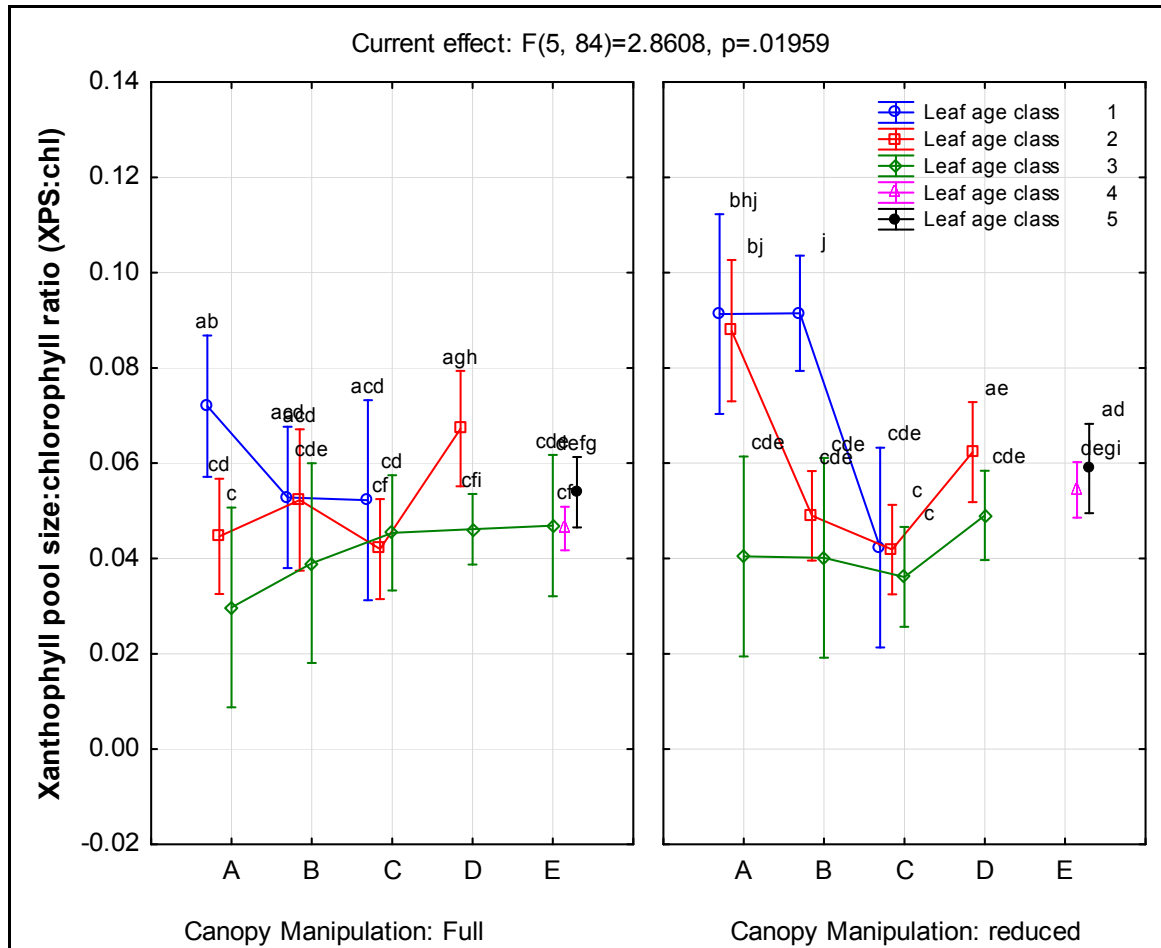


Figure 108 Xanthophyll pool size:chlorophyll ratio (XPS:chl) for the different measurement dates and chronological leaf age classes in reaction to canopy manipulation (vertical bars denote 95% confidence intervals).

5.2.5.7 Lutein:chlorophyll ratio

The lutein:chlorophyll ratio was initially highest in the youngest leaf class, but showed consistent increases as the growing season progressed past measurement date B in all other leaf classes (Figure 109). The increases seemed to be more in the NSF canopies past date C, ending with significantly higher levels on date E (Figure 110).

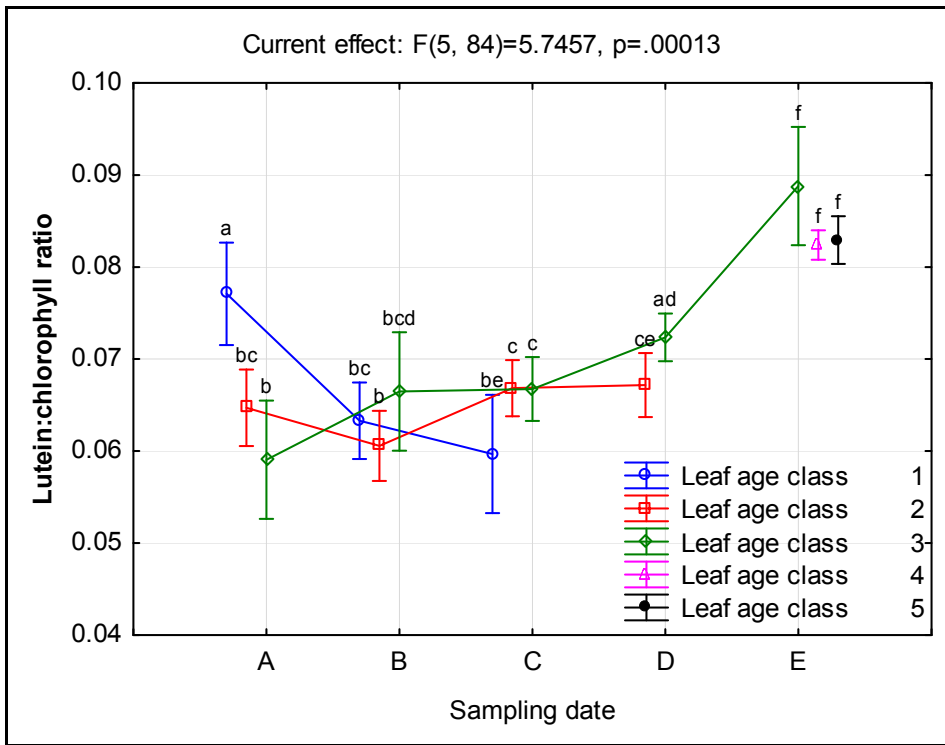


Figure 109 Lutein content relative to total chlorophyll for the different measurement dates and chronological leaf age classes (vertical bars denote 95% confidence intervals).

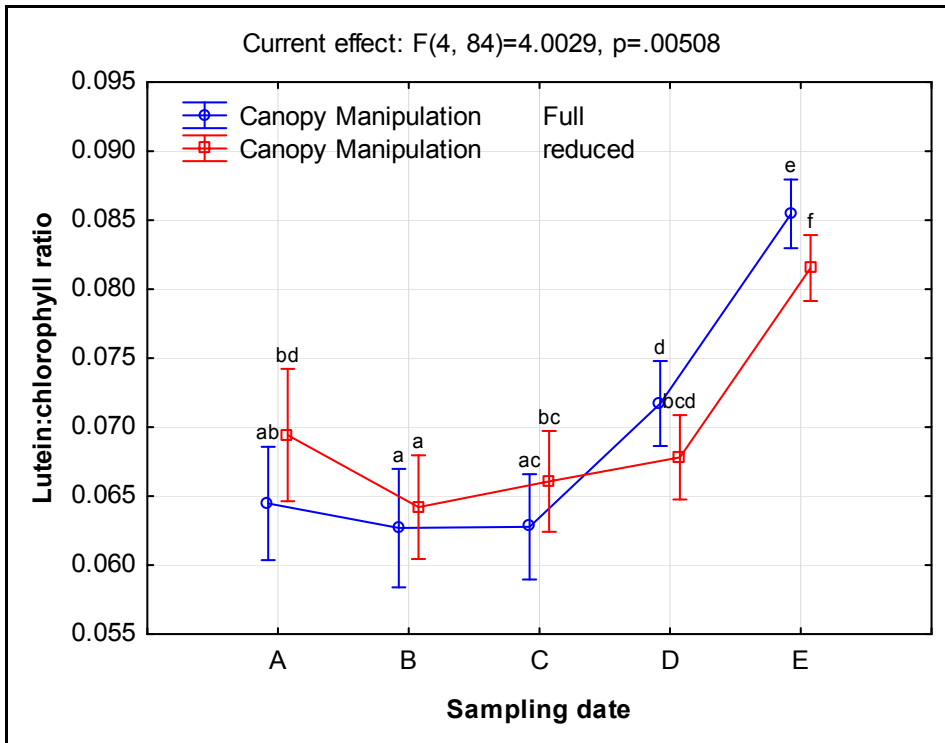


Figure 110 Lutein content relative to total chlorophyll for the different measurement dates and canopy manipulation treatments (vertical bars denote 95% confidence intervals).

5.3 Conclusions

As the canopy age from just before pea size (measurement date B), a decline in total chlorophyll and total carotenoids seemed to be consistent for all leaf ages on primary shoots, with the secondary shoots still showing increases of total chlorophyll content up to date C, just before véraison. The carotenoid:chlorophyll ratios and chlorophyll *a:b* ratios seemed to decrease up to measurement date C, the former also increased thereafter, while the latter was quite stable, except

for an apparent increase in the younger leaves of the reduced canopy. The DEPS ratio, carotenoid:chlorophyll ratio as well as the XPS:chlorophyll ratio reacted to higher exposure levels measured for the reduced canopies initially, when water deficits was not really apparent (before berry set). After this, the DEPS ratio in particular seemed reactive to water deficits increasing, especially for young leaves and especially in the NSF treatments where these deficits were more pronounced particularly at measurement date D. Although it is problematic, even in a non-topped canopy to obtain sufficiently young leaves to assess DEPS as a water status indicator closer to véraison and thereafter, it seems that secondary shoots may offer a solution in this regard. It seems from the regression results that DEPS values could be monitored in leaves younger than about 70 days of age, from the onset of water deficits ($\Psi_{PD} < -400$ KPa) with a threshold value of about 0.50 and higher, indicating increased water deficit stress levels.

5.4 Literature cited

- Arnon, D.I., 1949. Copper enzymes in isolated chloroplasts. Polyphenoloxidase in *Beta vulgaris*. *PLANT PHYSIOLOGY* 24, 1.
- Bertamini, M. & Nedunchezian, N., 2002. Leaf age effects on chlorophyll, Rubisco, photosynthetic electron transport activities and thylakoid membrane protein in field grown grapevine leaves. *Journal of Plant Physiology* 159., 799-803.
- Bertamini, M. & Nedunchezian, N., 2003. Photoinhibition of photosynthesis in mature and young leaves of grapevine (*Vitis vinifera* L.). *Plant Science* 164, 635-644.
- Bertamini, M. & Nedunchezian, N., 2004. Photosynthetic responses for *Vitis vinifera* plants grown at different photon flux densities under field conditions. *Biologia Plantarum* 48, 149-152.
- Bertamini, M., Zulini, L., Muthuchelian, K. & Nedunchezian, N., 2006. Effect of water deficit on photosynthetic and other physiological responses in grapevine (*Vitis vinifera* L. cv. Riesling) plants. *Photosynthetica* 44, 151-154.
- Bjorkman, O. & Holmgren, P., 1963. Adaptability of the photosynthetic apparatus to light intensity in ecotypes from exposed and shaded habitats. *Physiologia Plantarum* 16, 889-914. .
- Blanchfield, A.L., Robinson, S.A., Renzullo, L.J. & Powell, K.S., 2006. Phylloxera-infested grapevines have reduced chlorophyll and increased photoprotective pigment content—can leaf pigment composition aid pest detection? *Functional plant biology* 33, 507-514.
- Candolfi-Vasconcelos, M.C. & Koblet, W., 1990. Yield, fruit quality, bud fertility and starch reserves of the wood as a function of leaf removal in *Vitis vinifera*. Evidence of compensation and stress recovering. *Vitis* 29, 199-221.
- Candolfi-Vasconcelos, M.C. & Koblet, W., 1991. Influence of partial defoliation on gas exchange parameters and chlorophyll content of field-grown grapevines: mechanisms and limitations of the compensation capacity. *Vitis* 30, 129-141.
- Cartechini, A. & Palliotti, A., 1995. Effect of Shading on Vine Morphology and Productivity and Leaf Gas Exchange Characteristics in Grapevines in the Field. *American Journal of Enology and Viticulture* 46, 227-234.
- Cloete, H., Archer, E., Novello, V. & Hunter, J.J., 2008. Shoot heterogeneity effects on Shiraz/Richter 99 grapevines. III, Leaf chlorophyll content.
- Demmig-Adams, B., 1998. Survey of thermal energy dissipation and pigment composition in sun and shade leaves. *Plant Cell Physiol.* 39, 474–482.
- Demmig-Adams, B. & Adams, W., 1996. Xanthophyll cycle and light stress in nature: Uniform response to excess direct sunlight among higher plant species. *Planta* 198, 460-470.
- Demmig-Adams, B. & Adams, W.W., 1992. Photoprotection and other responses of plants to high light stress. *Annual Review of Plant Physiology and Plant Molecular Biology* 43, 599–626.
- Dokoozlian, N.K. & Kliewer, W.M., 1995. The Light Environment Within Grapevine Canopies. I. Description and Seasonal Changes During Fruit Development. *American Journal of Enology and Viticulture* 46, 209-218.
- Flexas, J., Hendrickson, L. & Chow, W.S., 2001. Photoinactivation of photosystem II in high light-acclimated grapevines. *Aust. J. Plant Physiol.* 28, 755-764.

- Freeman, B.M. & Kliewer, W.M., 1984. Grapevine leaf development in relationship to potassium concentration and leaf dry weight density. *Am. J. Bot.* 3, 294-300.
- Hofäcker, W., 1978. Untersuchungen zur photosynthese der rebe. Einfluß der entblätterung, der dekapitierung, der ringelung und der entfernung der traube. *Vitis* 17, 10-22.
- Hunter, J.J., 2000. Implications of seasonal canopy management and growth compensation in grapevine. *South african journal for enology and viticulture* 21, 81-91.
- Hunter, J.J., Ruffner, H.P., Volschenk, C.G. & Le Roux, D.J., 1995. Partial Defoliation of *Vitis vinifera* L. cv. Cabernet Sauvignon/99 Richter: Effect on Root Growth, Canopy Efficiency; Grape Composition, and Wine Quality. *American Journal of Enology and Viticulture* 46, 306-314.
- Hunter, J.J. & Visser, J.H., 1988. The effect of partial defoliation, leaf position and developmental stage of the vine on photosynthetic activity of *Vitis vinifera* L. cv Cabernet Sauvignon. *S. Afr. J. Enol. Vitic.* 9, 9-15.
- Hunter, J.J. & Visser, J.H., 1989. The effect of partial defoliation, leaf position and developmental stage of the vine on leaf chlorophyll concentration in relation to the photosynthetic activity and light intensity in the canopy of *Vitis vinifera* L. cv. Cabernet Sauvignon. *S. Afr. J. Enol. Vitic.* 10, 67-73.
- Koblet, W., 1969. Translocation of photosynthate in vine shoots and influence of leaf area on quantity and quality of the grapes. *Wein-Wiss* 24, 277-319.
- Kriedemann, P.E., Kliewer, W.M. & Harris, J.M., 1970. Leaf age and photosynthesis in *Vitis vinifera* L. *Vitis* 9, 97-104.
- Lashbrooke, J.G., Young, P.R., Strever, A.E., Stander, C. & Vivier, M.A., 2010. The development of a method for the extraction of carotenoids and chlorophylls from grapevine leaves and berries for HPLC profiling. *Australian Journal of Grape and Wine Research* 16, 349-360.
- Mackinney, G., 1941. Absorption of light by chlorophyll solutions. *Journal of Biological Chemistry* 140, 315-322.
- Medrano, H., Bota, J., Abadia, A., Sampol, B., Escalona, J. & Flexas, J., 2002. Effects of drought on light-energy dissipation mechanisms in high-light acclimated, field-grown grapevines *Functional Plant Biology* 29, 1197-1207.
- Oliver, J. & Palou, A., 2000. Chromatographic determination of carotenoids in foods. *Journal of chromatography A* 881, 543-555.
- Poni, S., Intrieri, C. & Silvestroni, O., 1994. Interactions of LeafAge, Fruiting, and Exogenous Cytokinins in Sangiovese Grapevines Under Non-Irrigated Conditions. II. Chlorophyll and Nitrogen Content. *Am. J. Enol. Vitic.* 45, 278-284.
- Porra, R.J., 2002. The chequered history of the development and use of simultaneous equations for the accurate determination of chlorophylls a and b. *Photosynth. Res.* 73, 149-156.
- Porra, R.J., Thompson, W.A. & Kriedemann, P.E., 1989. Determination of accurate extinction coefficients and simultaneous equations for assaying chlorophylls a and b extracted with four different solvents: verification of the concentration of chlorophyll standards by atomic absorption spectroscopy. *Biochimica et Biophysica Acta (BBA)-Bioenergetics* 975, 384-394.
- Sampol, B., Bota, J., Riera, D., Medrano, H. & Flexas, J., 2003. Analysis of the virus-induced inhibition of photosynthesis in malmsey grapevines. *New Phytologist* 160, 403-412.
- Schultz, H.R., 1989. CO₂-Gaswechsel und Wassertransport von Stark- und Schwachlichttrieben bei *Vitis vinifera* L. (cv. Riesling) in Abhängigkeit von Klima- und Pflanzenfaktoren - Ansatz eines empirischen Assimilationsmodells. *Geisenheimer Berichte, Veröffentlichungender FA Geisenheim Band 5*, 221 pp.
- Smart, R.E., Smith, S.M. & Winchester, R.V., 1988. Light Quality and Quantity Effects on Fruit Ripening for Cabernet Sauvignon. *American Journal of Enology and Viticulture* 39, 250-258.
- Sobrino, C., Neale, P.J., Montero, O. & Lubián, L.M., 2005. Biological weighting function for xanthophyll de-epoxidation induced by ultraviolet radiation. *Physiologia Plantarum* 125, 41-51.
- Woitsch, S. & Römer, S., 2003. Expression of xanthophyll biosynthetic genes during light-dependent chloroplast differentiation. *Plant Physiology* 132, 1508.

5.5 Addendum A

Table 39 Ranges of pigments and pigment ratios measured for primary shoot leaves (all treatments and measurement dates) in Shiraz. Mean values, minimum and maximum values, as well as the standard deviations (SD) and coefficients of variation (CV) are shown.

Pigment/ratio	N	Mean	Min	Max	SD	CV
Violaxanthin (ng.mg ⁻¹)	115	36.68	11.06	115.35	19.18	52.3
Neoxanthin (ng.mg ⁻¹)	115	47.97	14.29	94.55	16.22	33.8
Antheraxanthin (ng.mg ⁻¹)	115	17.70	4.60	53.10	10.32	58.3
Chlorophyll <i>b</i> (ng.mg ⁻¹)	115	461.71	139.39	879.81	154.69	33.5
Lutein (ng.mg ⁻¹)	115	112.51	40.41	192.92	30.16	26.8
Zeaxanthin (ng.mg ⁻¹)	115	25.40	0.00	126.28	22.07	86.9
Chlorophyll <i>a</i> (ng.mg ⁻¹)	115	1115.14	338.79	2005.48	401.06	36.0
β-carotene (ng.mg ⁻¹)	115	77.79	24.21	135.44	23.76	30.5
Total chlorophyll (ng.mg ⁻¹)	115	1576.85	478.17	2857.76	547.62	34.7
Total carotenoids (ng.mg ⁻¹)	115	318.06	117.60	523.66	93.98	29.6
Chlorophyll <i>a:b</i> ratio	115	2.4	1.7	3.2	0.3	13.2
DEPS ratio	115	0.35	0.04	1.45	0.24	70.6
XPS (ng.mg ⁻¹)	115	79.79	31.41	178.43	33.92	42.5
XPS:chlorophyll ratio	115	0.051	0.028	0.11	0.015	29.0
XPS:carotenoid ratio	115	0.246	0.16	0.432	0.0516	20.9
Carotenoid:chlorophyll ratio (car:chl)	115	0.207	0.161	0.263	0.0238	11.5
Lutein:chlorophyll ratio	115	0.074	0.055	0.092	0.01	13.6
β-carotene:chlorophyll ratio	115	0.051	0.035	0.066	0.0071	14.1
Neoxanthin:chlorophyll ratio	115	0.031	0.024	0.037	0.0029	9.6
Violaxanthin:chlorophyll ratio	115	0.024	0.006	0.049	0.0089	37.2
Antheraxanthin:chlorophyll ratio	115	0.011	0.004	0.036	0.0057	49.6
Zeaxanthin:chlorophyll ratio	115	0.016	0.000	0.067	0.0123	75.8
Neoxanthin:carotenoid ratio	115	0.15	0.097	0.198	0.0198	13.2
Violaxanthin:carotenoid ratio	115	0.115	0.031	0.22	0.0401	34.8
Antheraxanthin:carotenoid ratio	115	0.055	0.017	0.14	0.0231	42.2
Zeaxanthin:carotenoid ratio	115	0.077	0.000	0.275	0.0524	68.5
Lutein:carotenoid ratio	115	0.359	0.263	0.434	0.0368	10.3
β-Carotene:carotenoid ratio	115	0.244	0.195	0.298	0.0207	8.5

... **Table 40** (continued)

Pigment/ratio	N	Mean	Min	Max	SD	CV
Violaxanthin (mg.cm ⁻²)	115	0.0007	0.0002	0.0020	0.0003	52.8
Neoxanthin (mg.cm ⁻²)	115	0.0009	0.0003	0.0015	0.0003	32.2
Antheraxanthin (mg.cm ⁻²)	115	0.0003	0.0001	0.0010	0.0002	59.4
Chlorophyll <i>b</i> (mg.cm ⁻²)	115	0.0082	0.0026	0.0138	0.0026	31.6
Lutein (mg.cm ⁻²)	115	0.0020	0.0008	0.0031	0.0005	24.7
Zeaxanthin (mg.cm ⁻²)	115	0.0004	0.0000	0.0021	0.0004	85.5
Chlorophyll <i>a</i> (mg.cm ⁻²)	115	0.0199	0.0064	0.0361	0.0070	35.2
β-carotene (mg.cm ⁻²)	115	0.0014	0.0005	0.0025	0.0004	31.1
Total chlorophyll (mg.cm ⁻²)	115	0.028	0.009	0.050	0.0095	33.7
Total carotenoids (mg.cm ⁻²)	115	0.006	0.002	0.009	0.0016	28.7
XPS (mg.cm ⁻²)	115	0.001	0.001	0.003	0.0006	42.4
Violaxanthin (nmol.mg ⁻¹)	115	0.061	0.018	0.192	0.0319	52.3
Neoxanthin (nmol.mg ⁻¹)	115	0.08	0.024	0.157	0.027	33.8
Antheraxanthin (nmol.mg ⁻¹)	115	0.03	0.008	0.091	0.0176	58.3
Chlorophyll <i>b</i> (nmol.mg ⁻¹)	115	0.509	0.154	0.970	0.1706	33.5
Lutein (nmol.mg ⁻¹)	115	0.198	0.071	0.339	0.053	26.8
Zeaxanthin (nmol.mg ⁻¹)	115	0.045	0.000	0.222	0.0388	86.9
Chlorophyll <i>a</i> (nmol.mg ⁻¹)	115	1.249	0.379	2.246	0.4492	36.0
Beta-carotene (nmol.mg ⁻¹)	115	0.145	0.045	0.252	0.0443	30.5
Total chlorophyll (nmol.mg ⁻¹)	115	1.758	0.533	3.185	0.6107	34.7
Total carotenoids (nmol.mg ⁻¹)	115	0.558	0.206	0.915	0.1648	29.5
Carotenoid:chlorophyll (mmol.mol ⁻¹)	115	325.388	254.019	414.427	37.4899	11.5
Zeaxanthin:chlorophyll (nmol.mol ⁻¹)	115	25.459	0.000	106.214	19.3161	75.9
XPS:chlorophyll ratio (nmol.mol ⁻¹)	115	78.620	41.895	170.236	23.2354	29.6
XPS:carotenoid ratio (nmol.mol ⁻¹)	115	239.065	153.491	425.795	51.2661	21.4
Chlorophyll <i>a</i> : <i>b</i> ratio (nmol.mol ⁻¹)	115	2448.599	1763.808	3269.959	322.3675	13.2

Table 40 Correlation matrix for pigments and pigment ratios measured for primary shoot leaves in season one (*r*-values are shown in the matrix, increasing shades of red indicate stronger negative correlations while increasing shades of blue indicate stronger positive correlations).

		1	2	3	4	5	6	7	8	9	10	11	12	13	14	15	16
1	DEPS	1.00	0.26	0.31	-0.11	-0.02	-0.27	-0.49	-0.11	0.46	-0.09	-0.06	0.92	0.00	-0.01	-0.03	0.12
2	Chlorophyll a:b	0.26	1.00	0.10	-0.47	0.07	-0.64	0.38	0.19	0.74	0.09	0.23	0.41	0.45	0.45	0.36	0.49
3	Carotenoid/Chlorophyll	0.31	0.10	1.00	0.67	0.79	0.23	-0.18	-0.55	0.17	-0.65	-0.43	0.21	-0.54	-0.25	-0.58	-0.26
4	Lutein/chl	-0.11	-0.47	0.67	1.00	0.53	0.58	-0.43	-0.65	-0.49	-0.69	-0.53	-0.29	-0.79	-0.62	-0.78	-0.65
5	Beta-carotene/chl	-0.02	0.07	0.79	0.53	1.00	0.15	0.05	-0.39	0.05	-0.46	-0.27	-0.04	-0.37	0.04	-0.40	-0.13
6	Neoxanthin/chl	-0.27	-0.64	0.23	0.58	0.15	1.00	-0.12	-0.01	-0.51	-0.13	-0.10	-0.32	-0.35	-0.28	-0.29	-0.26
7	Violaxanthin (mg/cm ²)	-0.49	0.38	-0.18	-0.43	0.05	-0.12	1.00	0.61	0.29	0.52	0.59	-0.25	0.63	0.69	0.61	0.66
8	Neoxanthin (mg/cm ²)	-0.11	0.19	-0.55	-0.65	-0.39	-0.01	0.61	1.00	0.34	0.96	0.95	0.17	0.93	0.84	0.96	0.89
9	Antheraxanthin (mg/cm ²)	0.46	0.74	0.17	-0.49	0.05	-0.51	0.29	0.34	1.00	0.29	0.38	0.66	0.53	0.57	0.47	0.65
10	Chlorophyll b (mg/cm ²)	-0.09	0.09	-0.65	-0.69	-0.46	-0.13	0.52	0.96	0.29	1.00	0.93	0.17	0.93	0.81	0.96	0.85
11	Lutein (mg/cm ²)	-0.06	0.23	-0.43	-0.53	-0.27	-0.10	0.59	0.95	0.38	0.93	1.00	0.24	0.92	0.88	0.94	0.92
12	Zeaxanthin (mg/cm ²)	0.92	0.41	0.21	-0.29	-0.04	-0.32	-0.25	0.17	0.66	0.17	0.24	1.00	0.29	0.29	0.26	0.43
13	Chlorophyll a (mg/cm ²)	0.00	0.45	-0.54	-0.79	-0.37	-0.35	0.63	0.93	0.53	0.93	0.92	0.29	1.00	0.90	0.99	0.94
14	Beta-carotene (mg/cm ²)	-0.01	0.45	-0.25	-0.62	0.04	-0.28	0.69	0.84	0.57	0.81	0.88	0.29	0.90	1.00	0.89	0.96
15	Total chlorophyll (mg/cm ²)	-0.03	0.36	-0.58	-0.78	-0.40	-0.29	0.61	0.96	0.47	0.96	0.94	0.26	0.99	0.89	1.00	0.93
16	Total carotenoids (mg/cm ²)	0.12	0.49	-0.26	-0.65	-0.13	-0.26	0.66	0.89	0.65	0.85	0.92	0.43	0.94	0.96	0.93	1.00

Chapter VI

Research Results

Leaf structural components and water content during growth of *Vitis vinifera* L. cv. Shiraz

Chapter VI: Leaf structural components and water content during growth of *Vitis vinifera* L. cv. Shiraz

6.1 Introduction

Specific leaf mass (SLM) has been shown to correlate with photosynthesis in grapevines (Gaudillere & Carbonneau, 1986; Poni *et al.*, 1994a; Cartechini & Palliotti, 1995) and in many other plants (Sims & Pearcy, 1992; Niinemets *et al.*, 1998; Niinemets, 1999). It also forms part of an important triangle in plant growth, between leaf thickness, leaf density and SLM (Niinemets, 2001).

Leaf thickness and density are relatively easy to determine, and in addition to SLM it can aid in providing a better understanding of the relationship between physiological processes, leaf structure and environmental conditions (Witkowski & Byron, 1991). The equivalent water thickness (EWT) corresponds to a hypothetical thickness of a single layer of water averaged over the whole leaf area (Danson *et al.*, 1992). Results from Ceccato *et al.* (2001) showed that a unique leaf water content relative to fresh mass (LWC_f) value may correspond to different EWT values. Conversely, a unique EWT value may correspond to different LWC_f values. These examples showed that EWT and LWC_f are two different ways to define vegetation water content and that they are not directly related. The EWT parameter is often used in remote sensing studies, as it has been shown to vary less in relation to canopy position or leaf age (Rodríguez-Pérez *et al.*, 2007). This parameter however did not yield very strong correlations with vegetation spectral indices at the canopy level, even though it is generally very well-correlated at the leaf level (Ceccato *et al.*, 2001).

It was found by Cartechini & Palliotti (1995) that whole-vine shading using shade netting, significantly reduced the SLM during the entire growing season, and a positive and significant relationship was also confirmed between the SLM and photosynthesis. Decreased leaf SLM in shade leaves is an adaptation to increase leaf radiation absorbance, which is often associated with increased mass based chlorophyll levels in the leaf (Lei *et al.*, 1996; Lambers *et al.*, 1998) to compensate for the thinner leaf. It is therefore always relevant in plant physiological studies to consider the interaction between leaf age and microclimate that could lead to adaptations in the SLM parameter, and conversely change the way pigment, nutrient or leaf water content may be interpreted in reaction to the environment.

Leaf water content can be considered an important parameter in leaves, but its physiological relation to leaf water potential is not simple, and requires using psychrometric techniques to monitor the interaction between leaf osmotic potential, turgor pressure and leaf relative water content (Patakas *et al.*, 1997). In the study of Ellis (2008), it was noted that lower leaf water potentials did indicate lower leaf water contents, measured relative to leaf fresh mass (%).

The goals of this study were to determine leaf structural components and leaf water content in order to study its possible interaction with leaf age, canopy light conditions as well as selected canopy management and irrigation treatments during two growing seasons. The datasets generated were also used to calibrate non-destructive field spectroscopy models (refer to Chapter VII).

6.2 Materials and methods

6.2.1 Vineyard

The vineyard used in this study is described in Chapter III.

6.2.2 Experiment layout

Refer to Chapter V for the experiment layout. In this chapter, “season two” refers to the 2009/10 growing season and “season three” to the 2010/11 growing season during which experiments were conducted. The canopy reduction treatment and the irrigation treatments were performed as specified in Chapter III. A description of the data sets discussed in this chapter is provided in Table 41.

6.2.3 Leaf sampling

Visually representative shoots were chosen from healthy vines and leaves were collected randomly according to the specified experiment layout. Leaves were mostly collected from main shoots, except for the young leaves selected from secondary shoots, where the first unfolded, suitably sized apical leaf on a secondary shoot were selected. Four leaf disks were punched from the inter-vein areas of the leaf (same position as spectral measurements defined in Chapter VII) using a cork borer with an area of 2.075 cm². The disks were immediately put into previously weighed micro-centrifuge tubes to avoid any moisture loss. The tubes were then weighed again to determine leaf fresh mass (FM). The leaf material was oven-dried at 65⁰C until constant dry mass (DM). Leaf thickness measurements were conducted with a Sundoo digital thickness gauge (Model LP-D1030, Wenzhou Sundoo Instruments, Wenzhou, China) on inter-vein areas of intact leaves on the same positions where spectral non-destructive measurements were made (refer to Chapter VII for details on field spectrophotometer measurements). Mean leaf thickness was calculated from the four positions measured per leaf.

Where leaves from secondary shoots were collected, it was done from shoots of similar length and canopy position, and only recently unfolded leaves were chosen.

Table 41 Leaf structural component and water content measurement dataset description.

Dataset	Season (DAB)	Measurements conducted	Goal/experiment procedure
2011A	3 (93-127)	Leaf age Mean leaf thickness SLM and TSLM LWCf and LWCd EWT LMD	Measurements were only conducted in the NS treatments, with leaves collected from randomly selected shoots, but with the leaf age of each leaf defined from plastochron measurements (see Chapter IV).
2011B	3 (147)	Mean leaf thickness SLM and TSLM LWCf and LWCd EWT LMD	Leaf age (young leaves less than five nodes from primary shoot growth tip, old leaves from nodes 2-4 on primary shoot) and shading level (fully exposed leaves from canopy perimeter, shaded leaves at least two leaf layers from canopy perimeter) were studied for leaves collected in NSF treatment (predawn leaf water potential on this date < -400 KPa).
2010A	2 (137)	SLM and TSLM LWCf and LWCd EWT	Basal (node 3-4), middle (node 8-14) and youngest leaves on secondary shoots sampled from SF and SR treatments.
2010B	2 (161)	SLM and TSLM LWCf and LWCd EWT	Basal, middle, apical and young leaves from secondary shoots sampled for all treatments.

6.2.4 Statistical analysis

Statistica 10 ® software (Statsoft, Tulsa, UK) was used for statistical analysis. Multi-way analyses of variance (ANOVA) was performed, as determined by the dataset in question. The ANOVA analyses consisted of an initial *F*-test followed by a Fisher's LSD test.

6.2.5 Leaf age determination/classification

Refer to Chapter V.

6.2.6 Leaf water potential measurements

Refer to Chapter III.

6.3 Results and discussion

6.3.1 Results from Dataset 2011A

Predawn leaf water potential values for the two treatments and three measurement dates indicated moderate water deficits, but although the full canopy treatment tended to have lower values, there seemed to be little difference between treatments (Figure 111).

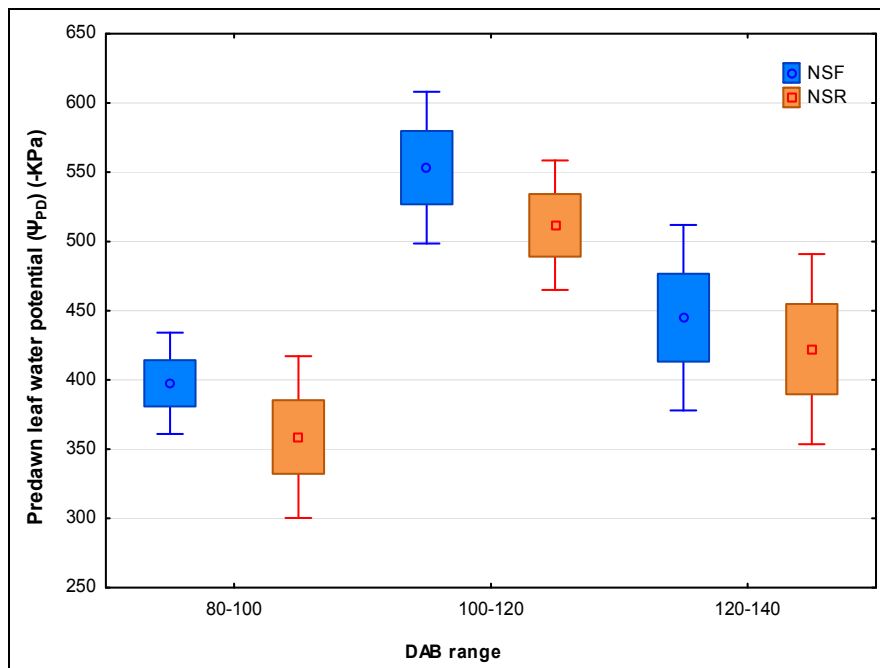


Figure 111 Predawn leaf water potential (Ψ_{PD}) (-KPa) for the date after budburst ranges relevant in analysis of dataset 2011A, with differences between the NSF and NSR treatments indicated (means with standard errors as boxes and 95% confidence intervals as vertical bars are shown).

6.3.1.1 Total specific leaf mass (TSLM) and specific leaf mass (SLM)

In contrast to what was found in a study performed in pots, where the specific leaf mass (SLM) and leaf plastochron index relationship was studied (Freeman & Kliewer, 1984), significant variability existed for this parameter between different shoots in the canopy (Figure 112). In the study by Poni *et al.* (1994a), relationships were much stronger, due to the calculation of means of leaves over different shoot zones, in combination with severe shoot thinning at the beginning of the study. The variability observed in the SLM values are likely due to differences in the exposure levels and growth responses on the same shoot within the canopy, as this is also expected to be reduced considerably in single-shoot or severely shoot-thinned conditions where natural plant response is restricted by manipulative interference. The strengths of the logarithmic fits also diminish as the season progresses, with all leaves ending up with higher values on the last measuring date.

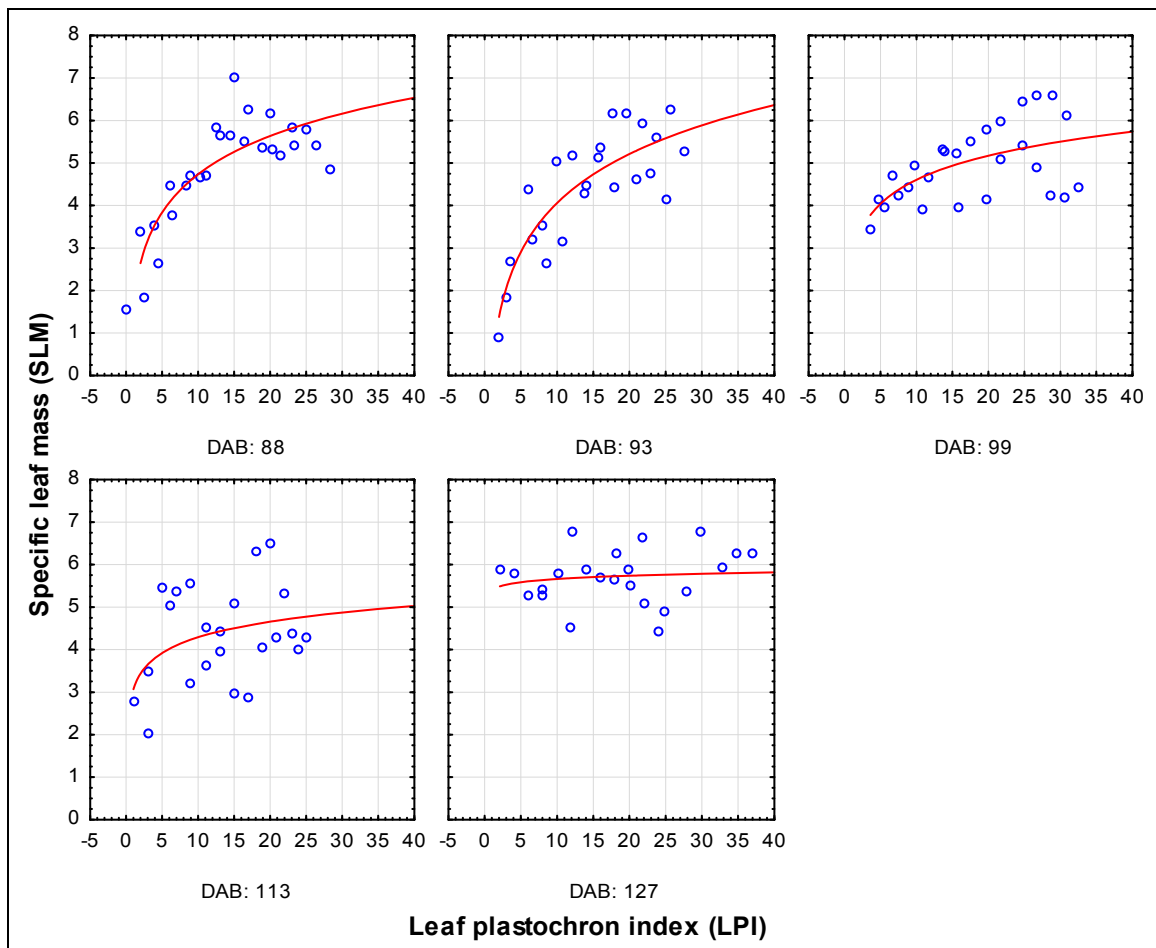


Figure 112 Relationship between main shoot specific leaf mass (SLM) and leaf plastochron index (LPI) for the different measurement dates in season three (dataset 2011A) [88 DAB: $SLM = 2.20 + 2.62 \cdot \log_{10}(LPI)$, $R^2 = 0.59$; 93 DAB: $SLM = 0.78 + 3.40 \cdot \log_{10}(LPI)$, $R^2 = 0.52$; 99 DAB: $SLM = 2.73 + (1.88) \cdot \log_{10}(LPI)$, $R^2 = 0.33$; 113 DAB: $R^2 = 0.07$; 127 DAB: $R^2 = 0.02$].

If values of SLM are compared to studies on other plant species, such as those by Serrano (2008), the highest SLM values for Shiraz corresponded to some of the lowest values measured in those studies. In general, lower TSLM values were also measured in this study (even with late-season measurements, as discussed for dataset 2010B), compared to those measured in other studies on Shiraz (approximately $22 \text{ mg} \cdot \text{cm}^{-2}$ in normally developed shoots) (Cloete *et al.*, 2006; Ellis, 2008). This highlights the high vigour that occurred in this specific vineyard, accompanied by low light conditions in the canopy. Secondary shoots were also removed in the bunch zone in season three, as specified in Chapter III to investigate effects on fruit composition when compensatory growth is removed, therefore chronological age classes three and four were likely more exposed compared to the other seasons in the NSR treatments. Significantly higher TSLM and SLM values were found in leaf age classes three and four compared to the first two classes, with values also increasing towards the last measurement date, especially for SLM (Figure 113 to Figure 116).

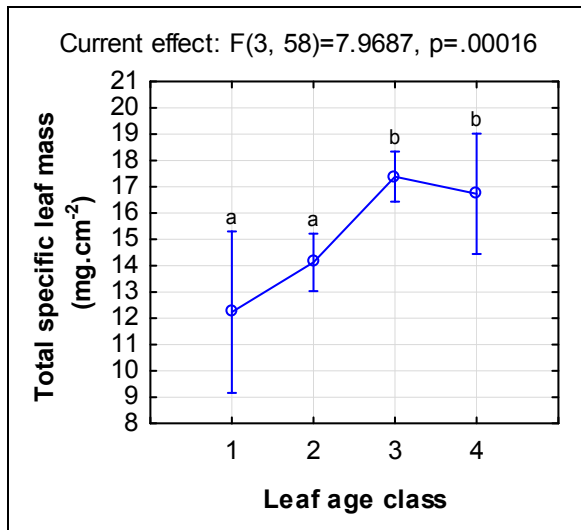


Figure 113 Total specific leaf mass (mg.cm⁻²) for the different leaf age classes in season three (dataset 2011A) ($p \leq 0.001$) (vertical bars denote 95% confidence intervals and means with the same letters are not significantly different at the $p \leq 0.05$ level).

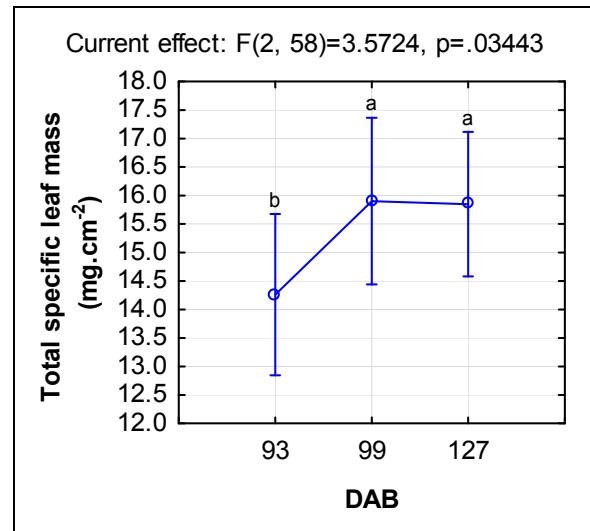


Figure 114 Total specific leaf mass (mg.cm⁻²) for the different measurement dates in season three (dataset 2011A) ($p \leq 0.05$) (vertical bars denote 95% confidence intervals and means with the same letters are not significantly different at the $p \leq 0.05$ level).

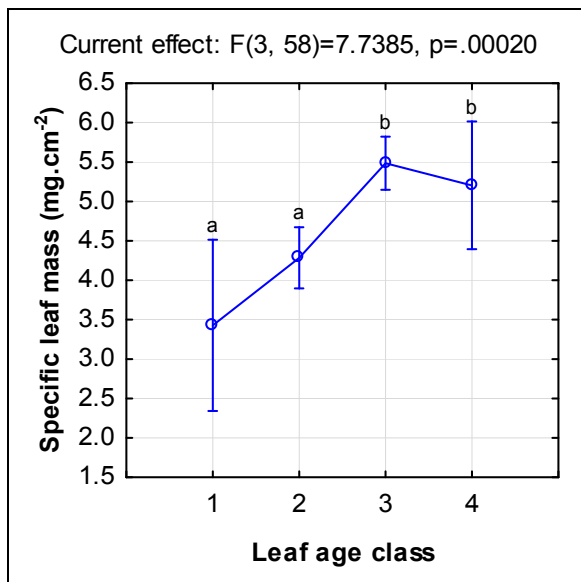


Figure 115 Specific leaf mass (mg.cm⁻²) for the different leaf age classes in season three (dataset 2011A) ($p \leq 0.001$) (vertical bars denote 95% confidence intervals and means with the same letters are not significantly different at the $p \leq 0.05$ level).

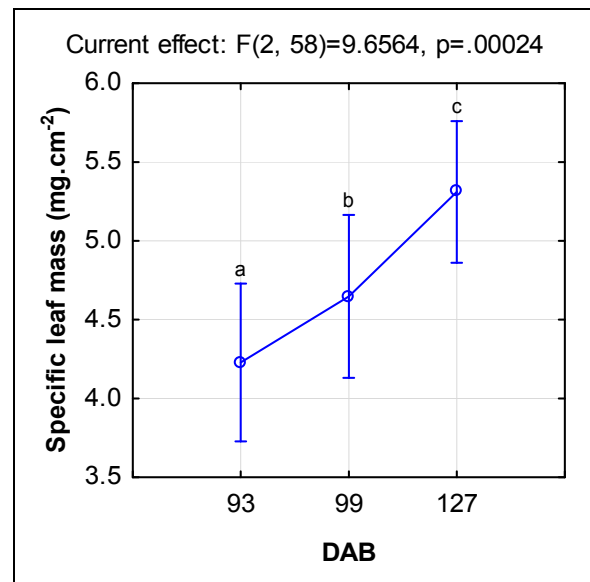


Figure 116 Specific leaf mass (mg.cm⁻²) for the different measurement dates in season three (dataset 2011A) ($p \leq 0.001$) (vertical bars denote 95% confidence intervals and means with the same letters are not significantly different at the $p \leq 0.05$ level).

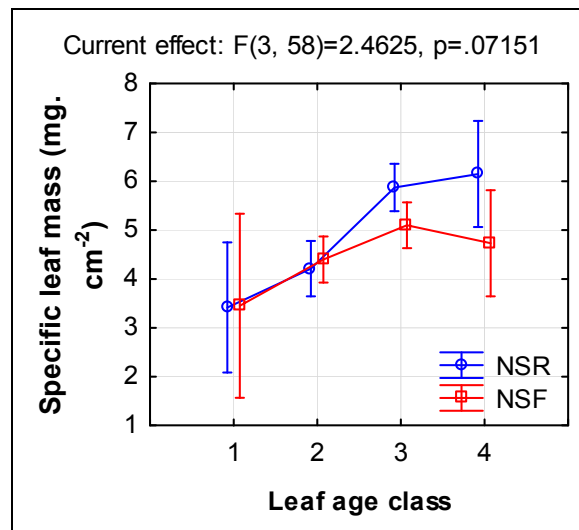


Figure 117 Specific leaf mass ($\text{mg}\cdot\text{cm}^{-2}$) for the different leaf age classes and canopy manipulation treatments in season three (dataset 2011A) ($p \leq 0.10$) (vertical bars denote 95% confidence intervals).

6.3.1.2 Mean leaf thickness measurements

The relationship between mean leaf thickness and the total specific leaf mass (Figure 118) indicates that values below a TSLM of $12 \text{ mg}\cdot\text{cm}^{-2}$ are not well-defined by the leaf calliper. This was also found for SLM values below $3 \text{ mg}\cdot\text{cm}^{-2}$ and EWT values below $8 \text{ mg}\cdot\text{cm}^{-2}$. These low values were not recorded in any other dataset presented in this chapter, and therefore are removed for further analysis of leaf thickness. In terms of measured thickness, leaves were mostly found to be in the range of 0.20 to 0.50 mm. This differs significantly from our own unpublished data from microscope studies, and those of other workers, suggesting leaf thickness values of between 0.08 and 0.20 mm (Boso *et al.*, 2010). The observed insensitivity of the electronic caliper may be due to leaf indentations and trichomes on the abaxial surface that may have a significant effect, especially for measurements below 0.30 mm.

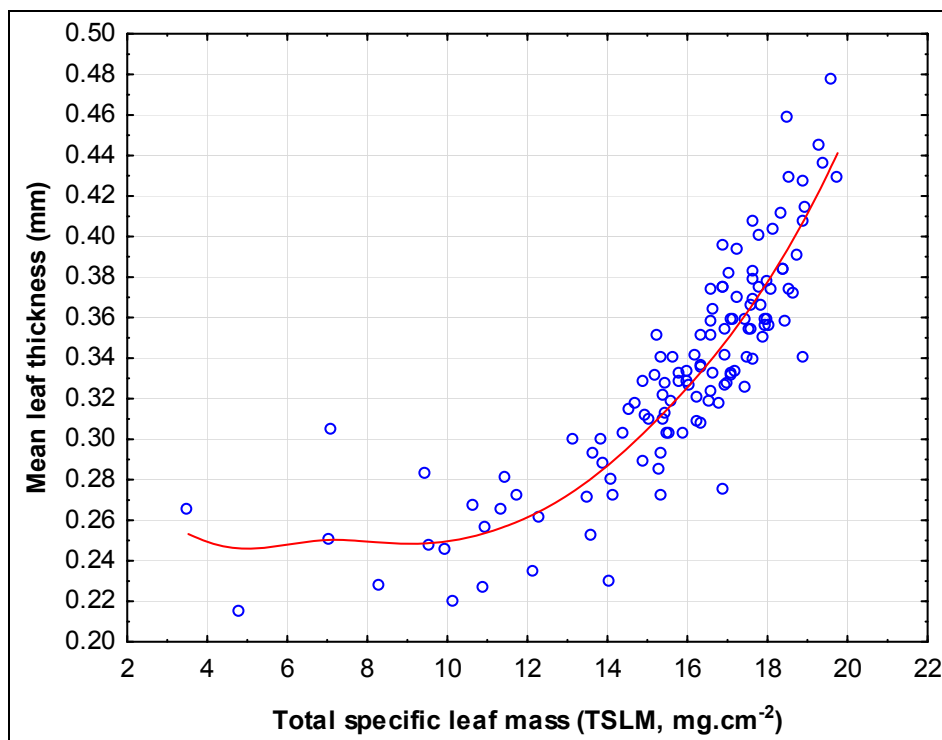


Figure 118 Relationship between mean leaf thickness and total specific leaf mass (TSLM) for the 2011A dataset (a distance-weighted least-square fit is shown).

Mean leaf thickness (mm) was significantly lower in leaf age class one and in class four, compared to class three (Figure 119). Thinner young leaves were expected, but it seems that leaves in leaf chronological age class four also showed reduced thickness. Leaf thickness was also lower in the last two measurement dates, compared to the first (Figure 120). It is not clear whether leaves were actually thinner or just slightly more compressed during calliper measurements in the older leaf stages (due to increased air spaces), which may have affected the calliper measurements. This was, however, unlikely, as the spring-loaded calliper exerts very little pressure on the leaf surface during measurement, and also because leaves were not in such an advanced stage of senescence (only up to leaf age class four measured). Another possible explanation for thinner leaves as the canopy ages, is progressively increased shading in the lower parts of the canopy, which may restrict the increase in leaf thickness (Van den Heuvel *et al.*, 2004; Cloete *et al.*, 2006). Leaf thickness in the full canopies was also significantly less than in the reduced canopies, which can probably be attributed to the reduction in leaf thickness brought about by shading in the canopy (Table 42). Buisson & Lee (1993) showed that the R:FR ratio and phytochrome ratio, apart from low irradiance can have additional effects on leaves and stems of papaya, including reduced chlorophyll a:b ratios, longer internodes and further reduced SLM as well as leaf thickness.

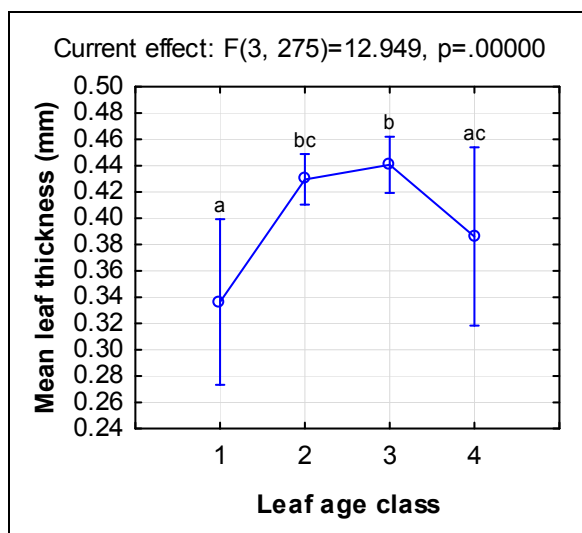


Figure 119 Mean leaf thickness (mm) for the different leaf age classes in season three (dataset 2011A). Vertical bars denote 95% confidence intervals and means with the same letters are not significantly different at the $p \leq 0.05$ level).

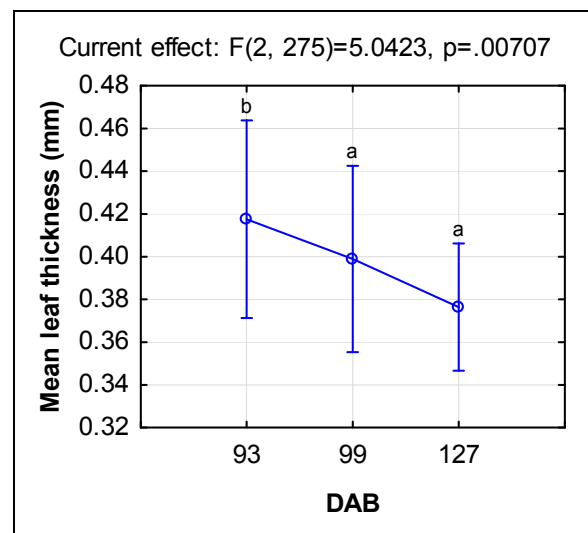


Figure 120 Mean leaf thickness (mm) for the different dates of measurement in season three (dataset 2011A) ($p \leq 0.01$). Vertical bars denote 95% confidence intervals and means with the same letters are not significantly different at the $p \leq 0.05$ level).

Table 42 Mean leaf thickness (mm) for the different treatments in season three (dataset 2011A). Means with different letters are significantly different at the $p \leq 0.001$ level ($F = 18.633$).

Treatment	N	Mean leaf thickness (mm)	SD	% difference
NSR	201	0.46 a	0.11	12%
NSF	89	0.41 b	0.11	

6.3.1.3 Leaf mass density (LMD)

It is important to consider that leaf density and thickness can vary independently within the specific leaf mass (SLM) parameter (Equation 9). Witkowski & Byron (1991) found that in sun-exposed leaves SLM was correlated to leaf density, but not in shaded leaves. In this study, the correlation was found to be more related to leaf age (strongest correlation in youngest leaf age class) (Figure 121). However, the probable higher exposure levels of these young leaves cannot be excluded.

Equation 9 Components of specific leaf mass

$$SLM = \frac{DM}{LA} = \frac{DM}{LA \times LT} \times \frac{LT}{1} = \frac{DM}{Volume} \times \frac{LT}{1} = LD \times LT$$

Refer to Chapter II for parameter definitions

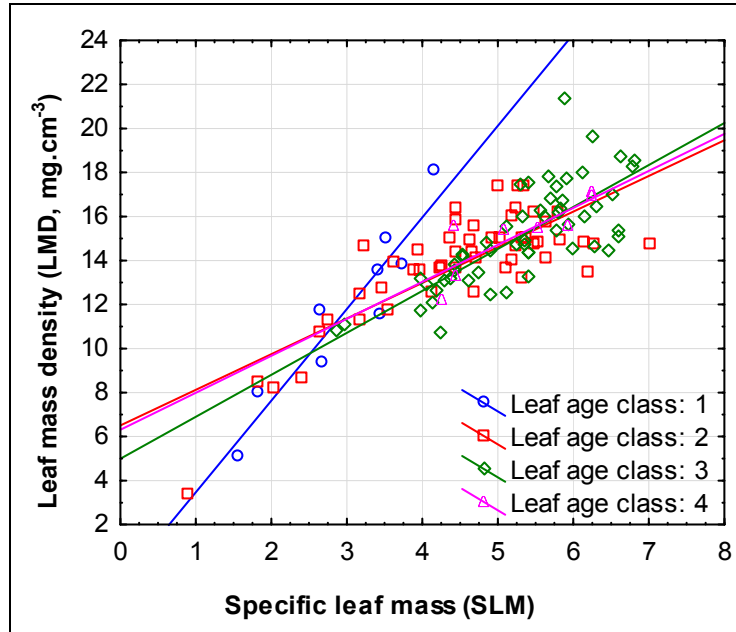


Figure 121 Relationship between leaf mass density (LMD) and specific leaf mass (SLM) for the different leaf age classes in the 2011A dataset (age class 1: $r^2 = 0.89$; age class 2: $r^2 = 0.63$; age class 3: $r^2 = 0.62$; age class 4: $r^2 = 0.69$).

Leaf mass density increased with measurement date (Figure 122), and also tended to be higher in the reduced canopies (Figure 123). Water deficits may reduce cell turgor pressure and – expansion, resulting in similar dry mass being contained in a smaller leaf area, potentially leading to higher leaf density (Hsiao, 1973; Witkowski & Byron, 1991). Higher light intensity may also increase leaf density (Chabot & Chabot, 1977; Witkowski & Byron, 1991).

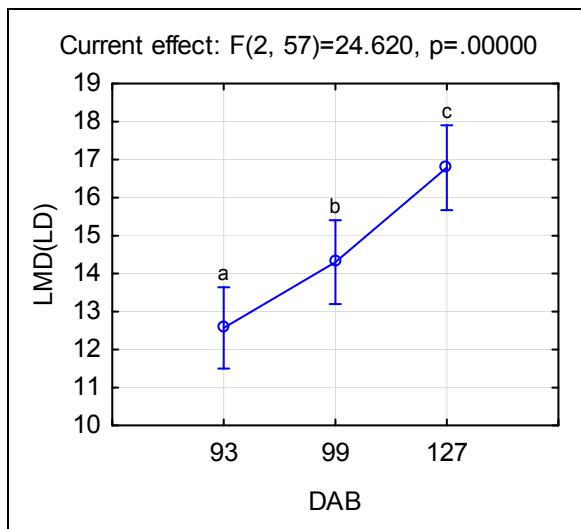


Figure 122 Leaf mass density (LMD, mg.cm^{-3}) for the different leaf age classes and measurement dates in season three (dataset 2011A) ($p \leq 0.001$) (vertical bars denote 95% confidence intervals and means with the same letters are not significantly different at the $p \leq 0.05$ level).

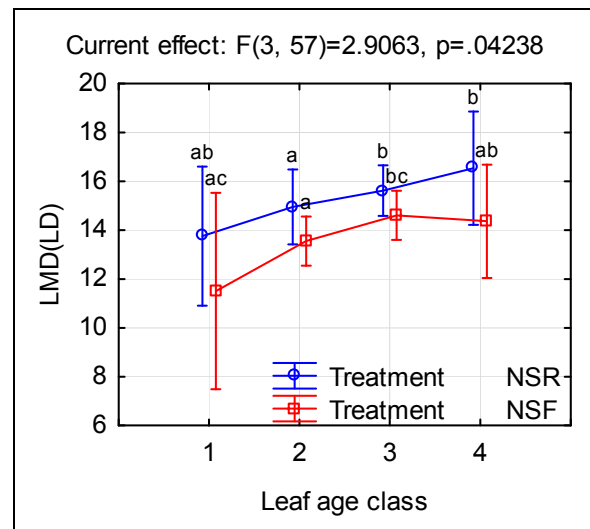


Figure 123 Leaf mass density (LMD, mg.cm^{-3}) for the different leaf age classes and measurement dates in season three (dataset 2011A) ($p \leq 0.001$) (vertical bars denote 95% confidence intervals and means with the same letters are not significantly different at the $p \leq 0.05$ level).

6.3.1.4 Leaf water content on a mass (LWC_d and LWC_f) and area basis (equivalent water thickness, EWT)

Leaf water content measurements are expected to be affected by the specific leaf mass (lower leaf water contents are expected when SLM increase), which can also be derived from the regression between the different measures of leaf water content (LWC) and SLM in Figure 124. Lower LWC_d and LWC_f in leaf age classes three and four for the reduced canopy treatments can therefore possibly be explained by the trend for these leaves to have higher SLM values (Figure 125 and Figure 127). This result is in accordance with the work of Hunter & Visser (1990a), where partial defoliation in Cabernet Sauvignon grapevines led to decreased leaf water contents, especially in the bunch and basal leaves in the canopy. Lower leaf water contents were also measured for the last measurement date, in accordance with higher SLM values, and significantly older leaves (Figure 126 and Figure 128).

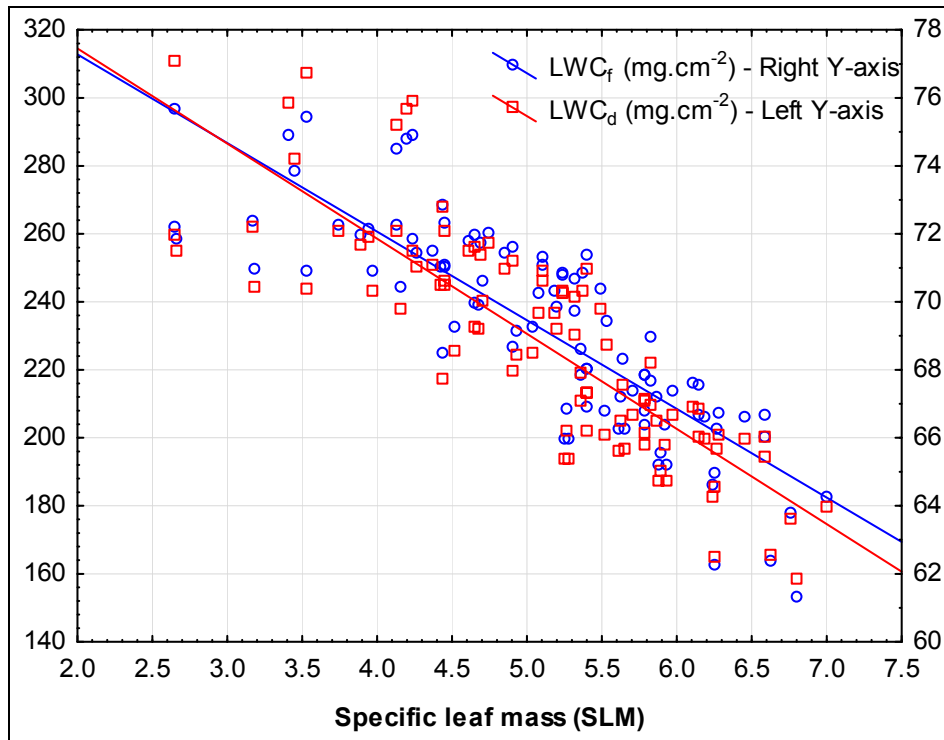


Figure 124 Relationship between leaf water content (LWC_d and LWC_f) and specific leaf mass (SLM) (SLM: LWC_f $r = 0.84$, $R^2 = 0.71$ and SLM: LWC_d $r = 0.84$, $R^2 = 0.71$, all $p \leq 0.001$).

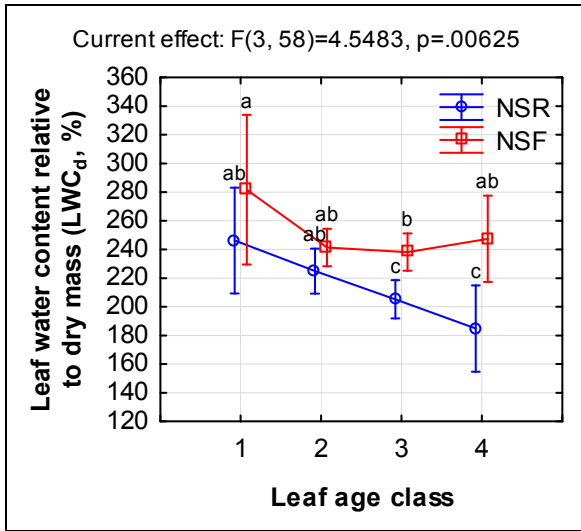


Figure 125 Mean leaf water content relative to leaf dry mass (%) for the different leaf age classes and canopy manipulation treatments in season three (dataset 2011A; $p \leq 0.01$; vertical bars denote 95% confidence intervals and means with the same letters are not significantly different at the $p \leq 0.05$ level).

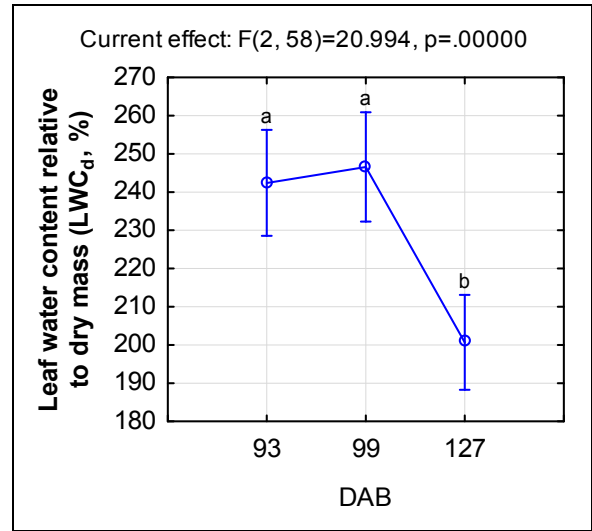


Figure 126 Mean leaf water content relative to leaf dry mass (%) for the different measurement dates in season three (dataset 2011A; $p \leq 0.001$; vertical bars denote 95% confidence intervals and means with the same letters are not significantly different at the $p \leq 0.05$ level).

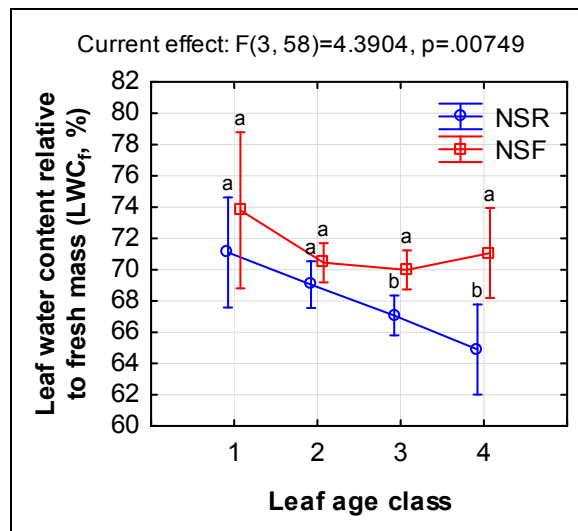


Figure 127 Mean leaf water content relative to leaf fresh mass (%) for the different leaf age classes and canopy manipulation treatments in season three (dataset 2011A; $p \leq 0.01$; vertical bars denote 95% confidence intervals and means with the same letters are not significantly different at the $p \leq 0.05$ level).

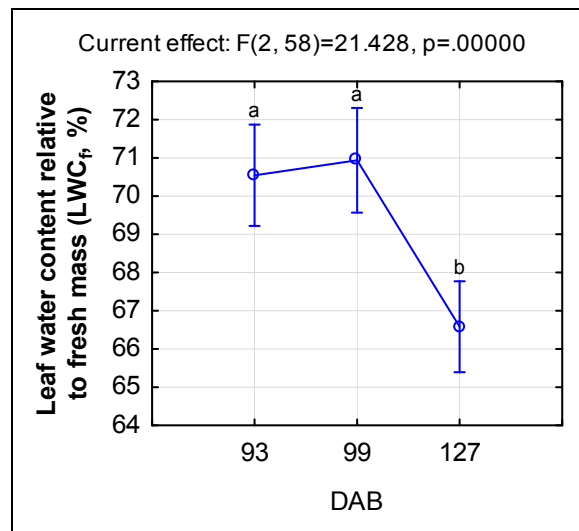


Figure 128 Mean leaf water content relative to leaf fresh mass (%) for the different measurement dates in season three (dataset 2011A; $p \leq 0.001$; vertical bars denote 95% confidence intervals and means with the same letters are not significantly different at the $p \leq 0.05$ level).

Equivalent water thickness (EWT, $\text{mg}\cdot\text{cm}^{-2}$) was lower in the younger leaf classes (Figure 129), and increased between the first and second sampling dates (Figure 130). This parameter is, similar to leaf pigment content measured on a leaf area basis, not directly affected by changes in SLM in the leaf. It is, however, sensitive to the relationship between the TSLM and SLM, which relates to its formula derivation.

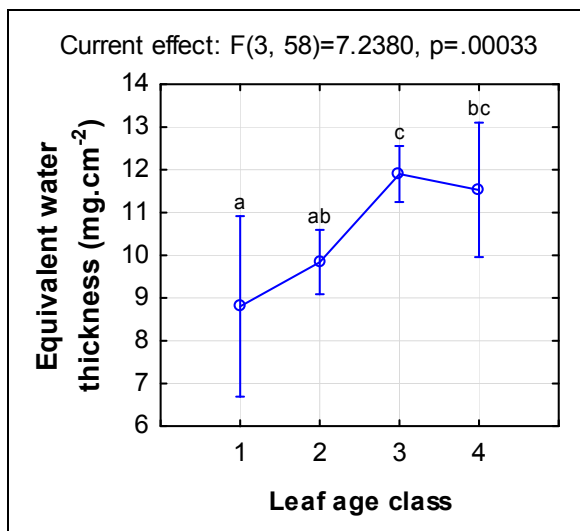


Figure 129 Equivalent water thickness ($\text{mg}\cdot\text{cm}^{-2}$) for the different leaf age classes in season three (dataset 2011A) ($p \leq 0.001$) (vertical bars denote 95% confidence intervals and means with the same letters are not significantly different at the $p \leq 0.05$ level).

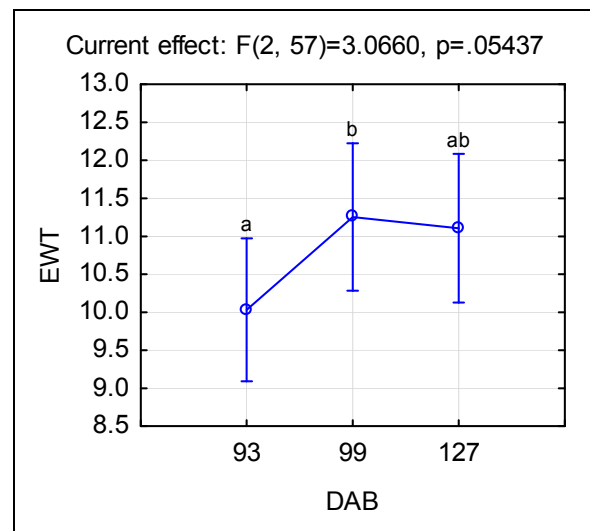


Figure 130 Equivalent water thickness ($\text{mg}\cdot\text{cm}^{-2}$) for the different leaf age classes in season three (dataset 2011A) ($p \leq 0.001$) (vertical bars denote 95% confidence intervals and means with the same letters are not significantly different at the $p \leq 0.05$ level).

6.3.2 Results from dataset 2011B

Shading did not affect leaf thickness significantly for young leaves (Figure 131), which were significantly thinner than older leaves, both for shaded and exposed positions. Old exposed leaves were 73% thicker than the old shaded leaves. Older leaves were also significantly less dense than younger leaves, with exposed young leaves having considerable higher density than the older leaves as well as the young shaded leaves (Figure 132). These results are in contrast to the dataset collected earlier and suggest that the older leaves collected here are already in a more

advanced stage of senescence, which can also be seen from its lower TSLM and EWT values compared to the oldest leaves measured in the previous dataset. Shaded leaves had higher leaf water contents (fresh and dry mass basis) than exposed leaves, consistent with their lower SLM values (Table 43). The EWT was not significantly different for leaves with different exposure, but older leaves showed significantly higher values, consistent with their higher TSLM values. The TSLM values were also higher for exposed leaves. The TSLM parameter can be calculated from the SLM and EWT, explaining why its significance follows that of the two parameters. The interaction between leaf age and shading was, however, not found to be significant for the TSLM. Exposed leaves showed higher SLM values, but no significant difference could be found between young and old leaves. This dataset confirms the important role of leaf exposure in determining the SLM parameter in leaves. It also shows the relative insensitivity of leaf water content relative to leaf area (EWT) to exposure, yet its dependency on leaf age.

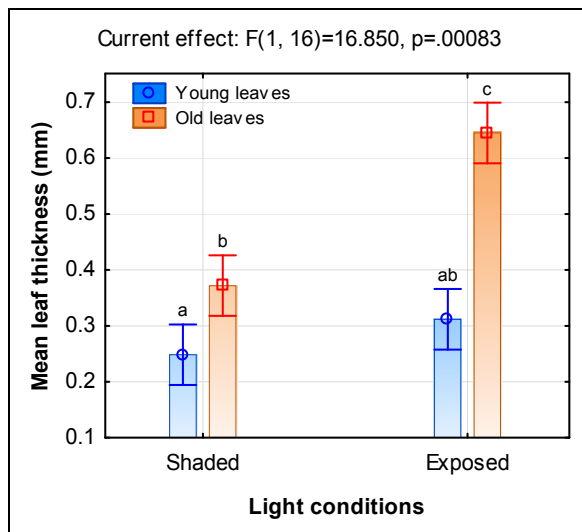


Figure 131 Mean leaf thickness (mm) for different leaf age and canopy light conditions (means with the same letters are not significantly different at the $p \leq 0.05$ level, vertical bars denote 95% confidence intervals).

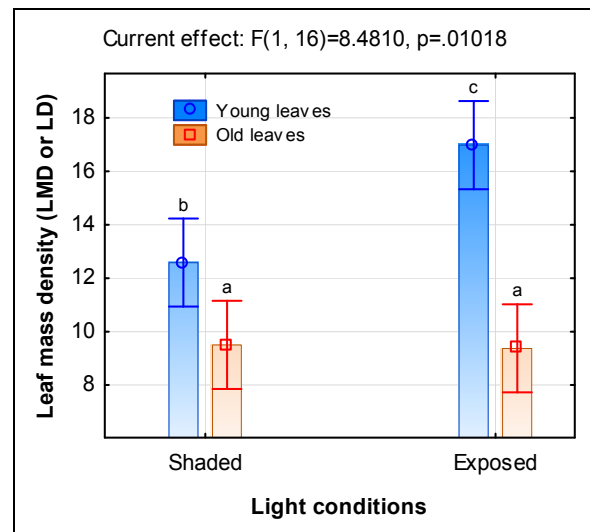


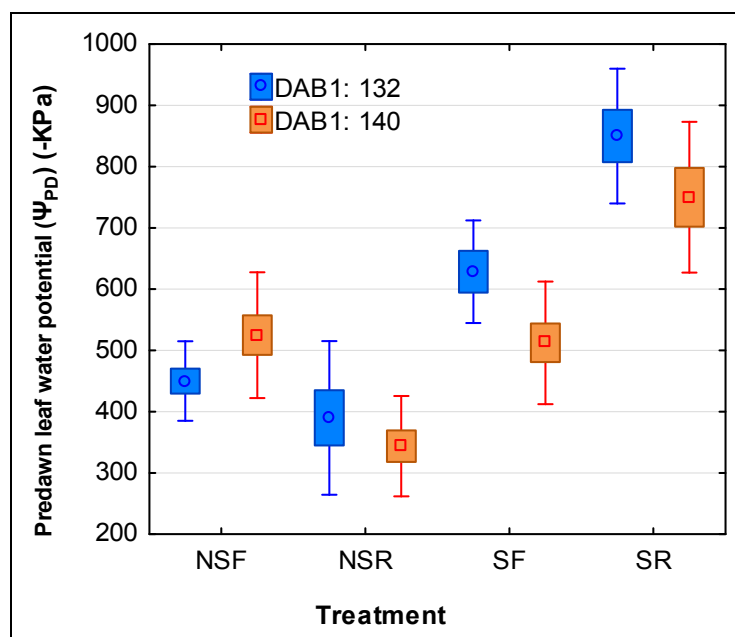
Figure 132 Leaf mass density (LMD or LD) for different leaf age and canopy light conditions (means with the same letters are not significantly different at the $p \leq 0.05$ level, vertical bars denote 95% confidence intervals).

Table 43 Leaf structural component results for Dataset 2011B (Only significant interactions shown - according to a Fischer LSD test).

Measurement	Light conditions	Leaf Age	% diff.	N	Means	SD	Significance	
LWC _d	Shaded		64.8	10	274.28	49.58	$p \leq 0.01$	
	Exposed			10	166.40	20.63		
LWC _f	Shaded		17.1	10	72.87	3.46	$p \leq 0.001$	
	Exposed			10	62.25	2.97		
TSLM	Shaded		21.9	10	12.31	2.53	$p \leq 0.05$	
	Exposed			10	15.00	2.15		
			Young	19.6	10	12.44	2.26	$p \leq 0.05$
			Old		10	14.88	2.59	
SLM	Shaded	67.3	10	3.38	0.92	$p \leq 0.001$		
	Exposed		10	5.65	0.83			
EWT		Young	23.1	10	8.20	1.11	$p \leq 0.01$	
		Old		10	10.09	1.46		

6.3.3 Results from Dataset 2010A

The predawn leaf water potential values around 137 days after budburst in season two showed considerably higher water deficits in especially the SR treatments (Figure 133).

**Figure 133** Predawn leaf water potential (Ψ_{PD}) (-KPa) for dates adjacent to the measurement date for Dataset 2010 A with different treatments indicated (boxes show standard errors and vertical bars denote 95% confidence intervals).

The full canopy treatment had significantly lower SLM values (Figure 134), especially for the young leaves sampled from secondary shoots. This could be due to shaded conditions in the canopies causing lower SLM values. The TSLM differences (Figure 135) were non-significant in the basal and middle leaves, presumably due to the parameter including leaf water, but it was significantly lower for the full canopy treatment in the young secondary shoot leaves. In this dataset, the only differences observed with regards to canopy position were between the main and secondary shoot leaves, but only in the full canopy treatment.

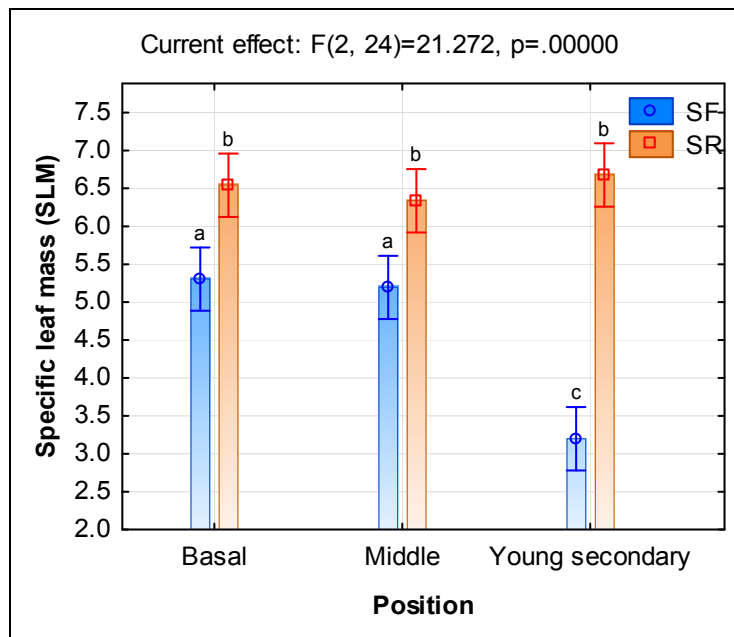


Figure 134 Specific leaf mass (SLM) for different leaf positions and treatments for dataset 2010A (means with the same letters are not significantly different at the $p \leq 0.05$ level; vertical bars denote 95% confidence intervals).

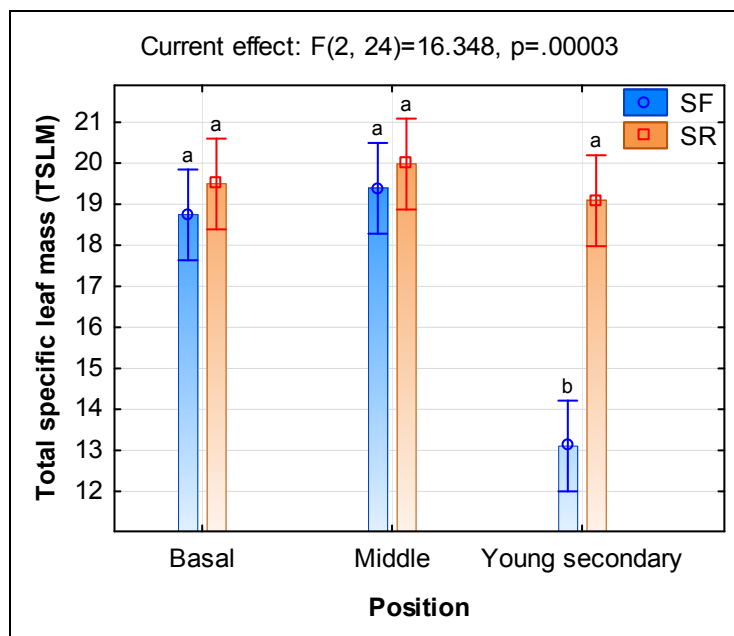


Figure 135 Total specific leaf mass (TSLM) for different leaf positions and treatments in dataset 2010A (means with the same letters are not significantly different at the $p \leq 0.05$ level; vertical bars denote 95% confidence intervals).

The LWC_d and LWC_f trends were similar to those described for dataset 2011A (Figure 125), with higher values in younger leaves; this was, however, only the case in the full canopy treatment (Figure 136 and Figure 137). Leaves of the SR treatment seemed to be considerably more stressed than those of the other treatments, from which it may be expected that leaf water contents could be less, especially in the secondary shoot leaves. This result is, however, more likely due to the higher SLM values for the SR treatment. In agreement with this, the EWT parameter (Figure 138) suggested similar water contents relative to leaf area between the treatments in the basal and middle leaves, with lower values measured in the SF treatment for the young leaves on secondary shoots. These results are peculiar and contrary to what were expected in the SR treatments, in relation to its predawn leaf water potential values.

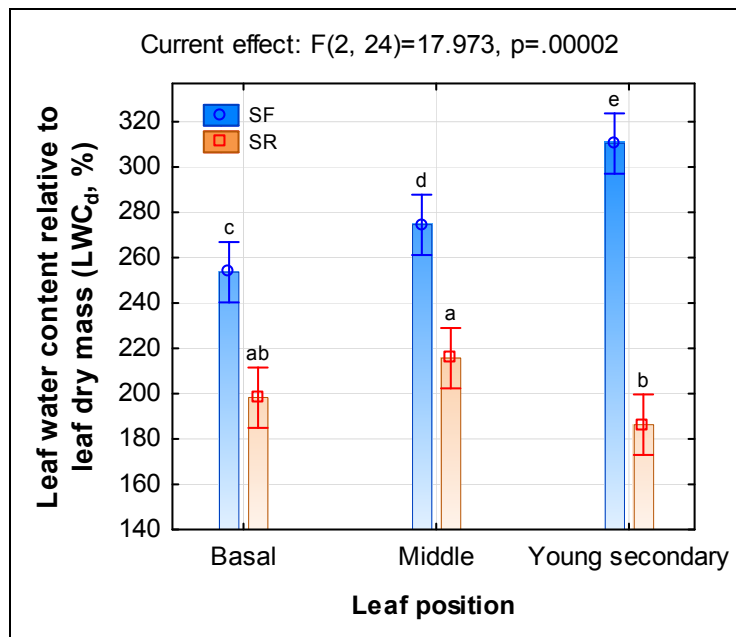


Figure 136 Leaf water content relative to leaf dry mass (LWC_d) for different leaf positions and treatments in dataset 2010A (means with the same letters are not significantly different at the $p \leq 0.05$ level; vertical bars denote 95% confidence intervals).

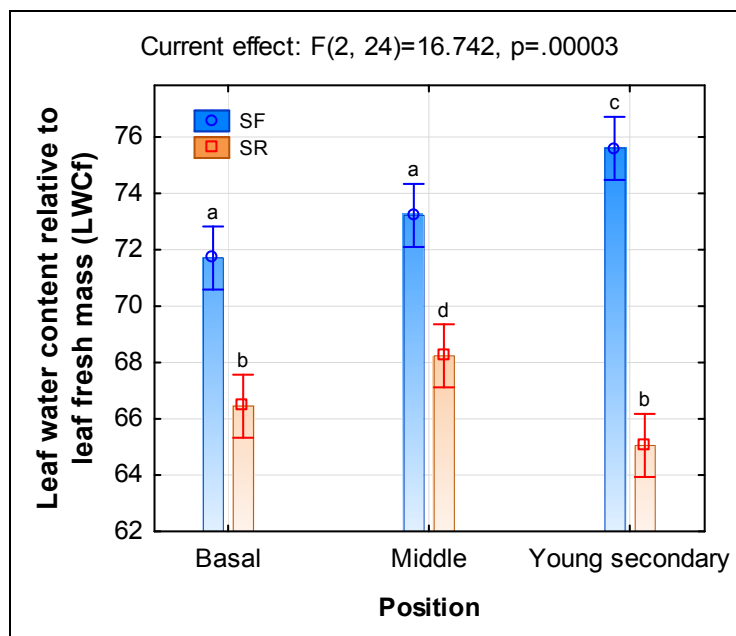


Figure 137 Leaf water content relative to leaf fresh mass (LWC_f) for different leaf positions and treatments in dataset 2010A (means with the same letters are not significantly different at the $p \leq 0.05$ level; vertical bars denote 95% confidence intervals).

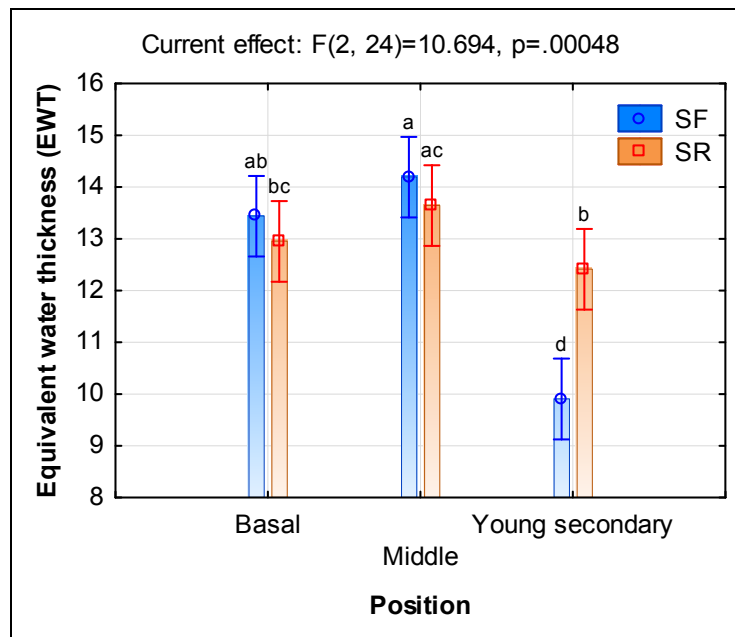


Figure 138 Equivalent water thickness (EWT) for different leaf positions and treatments in dataset 2010A (means with the same letters are not significantly different at the $p \leq 0.05$ level; vertical bars denote 95% confidence intervals).

6.3.4 Results from Dataset 2010B

The predawn leaf water potential values seemed to be much higher in the SF and SR treatments for this dataset, also in comparison to the previous dataset discussed for this season (Figure 139).

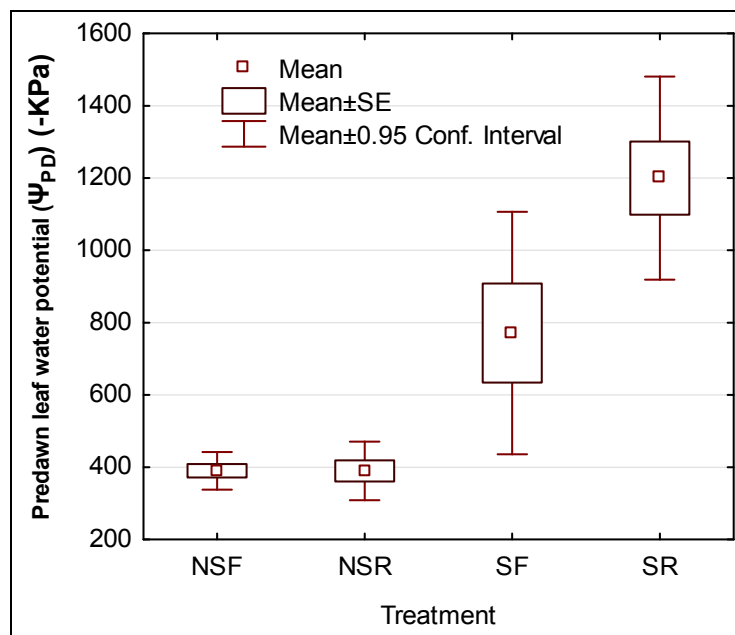


Figure 139 Predawn leaf water potential (Ψ_{PD}) (-KPa) a day before the measurement date (160 DAB) for dataset 2010B, with different treatments indicated (means are indicated with standard errors as boxes and with vertical bars indicating 95% confidence intervals).

Significantly lower TSLM and SLM values were found in the middle leaves of the full canopy treatments (Figure 140 and Figure 141), presumably due to shaded conditions in this part of the canopy. There was a tendency for the TSLM values to be higher in the apical leaves for the SR and SF treatments (which was also seen in the EWT interaction – data not shown). The leaf water content (LWC_d) (Figure 142) and LWC_f (Figure 143) values inversely followed the TSLM and SLM trends for the middle canopy leaves. The results from this dataset are more in accordance with the

work of Ellis (2008), as the LWC_f tended to be higher in the basal leaves compared to the apical and secondary shoot leaves. Hunter & Visser (1990a) however also found that bunch and basal leaves apparently had higher water contents than apical leaves at ripeness, but that this relationship was reversed for early season (berry set and pea size) measurements. It also has to be taken into account that canopy zones are applicable, while in dataset 2011A, leaf age classification was used, which mean that leaves could have been situated in different segments of the canopy. Considering that shoot growth decreased considerably after about 100 DAB (refer to Chapter III), less leaves emerged and therefore more resources may be allocated to the existing newly formed young leaves compared to early season, when continuing primary and newly emerging secondary shoot growth competed for nutrients and water. This may be another reason for the late-season higher values of TSLM found in the younger leaf zones.

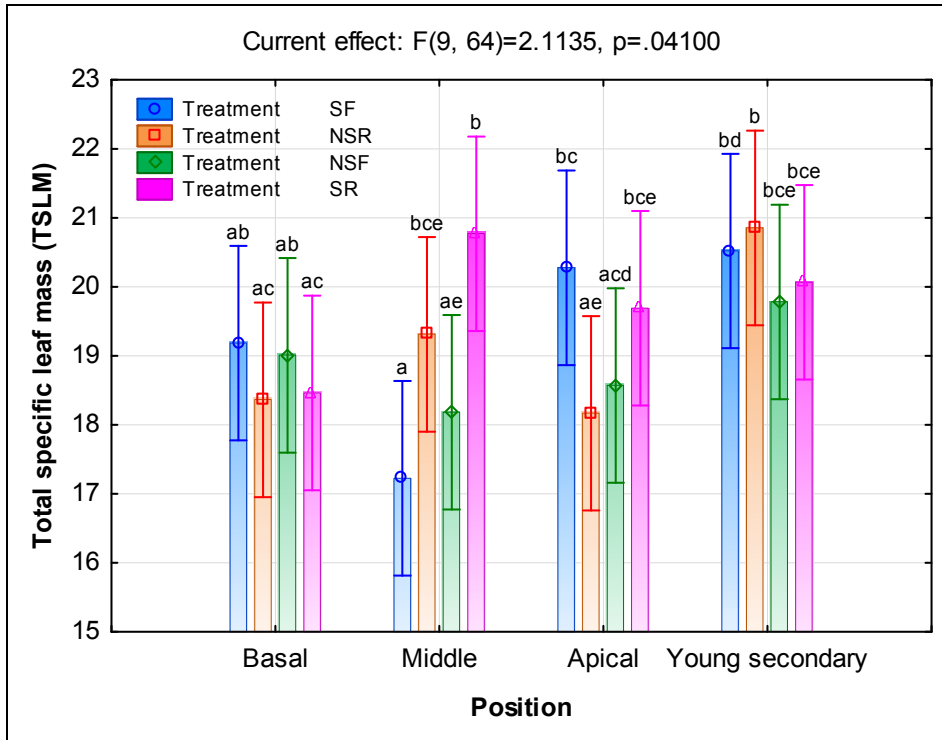


Figure 140 Total specific leaf mass (TSLM) for different leaf positions and treatments in dataset 2010B (means with the same letters are not significantly different at the $p \leq 0.05$ level; vertical bars denote 95% confidence intervals).

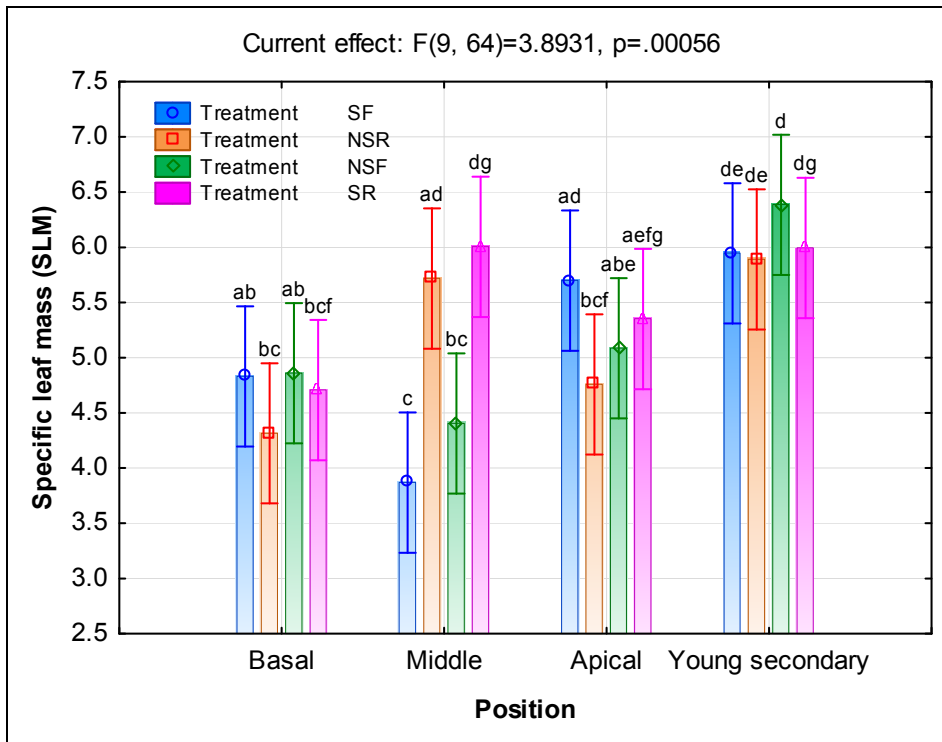


Figure 141 Specific leaf mass (SLM) for different leaf positions and treatments in dataset 2010B (means with the same letters are not significantly different at the $p \leq 0.05$ level; vertical bars denote 95% confidence intervals).

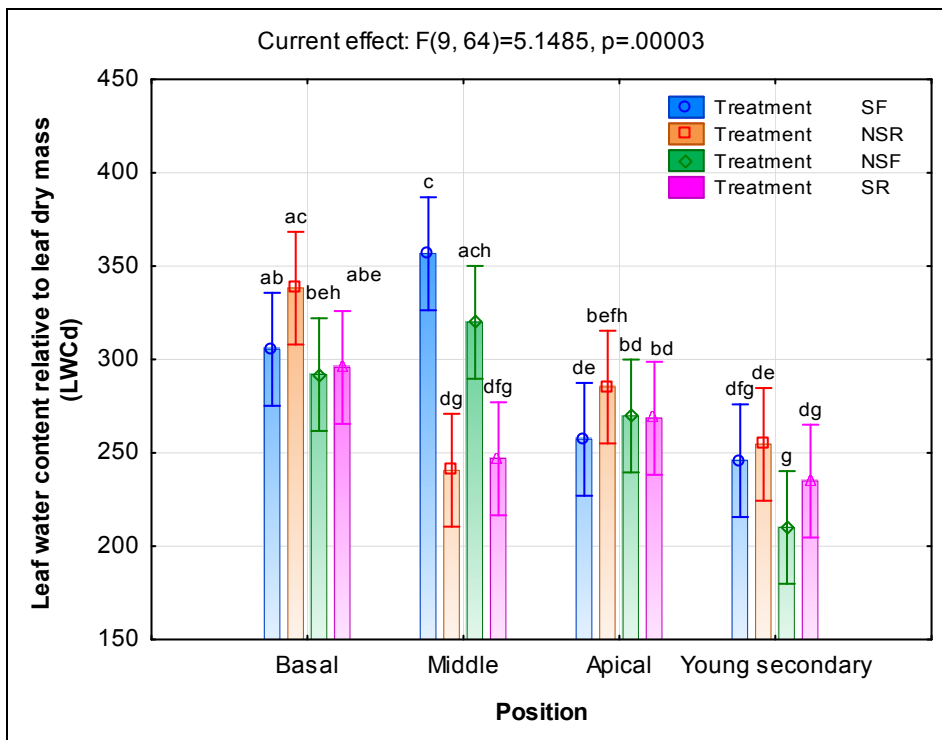


Figure 142 Leaf water content relative to leaf dry mass (LWCd) for different leaf positions and treatments in dataset 2010B (means with the same letters are not significantly different at the $p \leq 0.05$ level; vertical bars denote 95% confidence intervals).

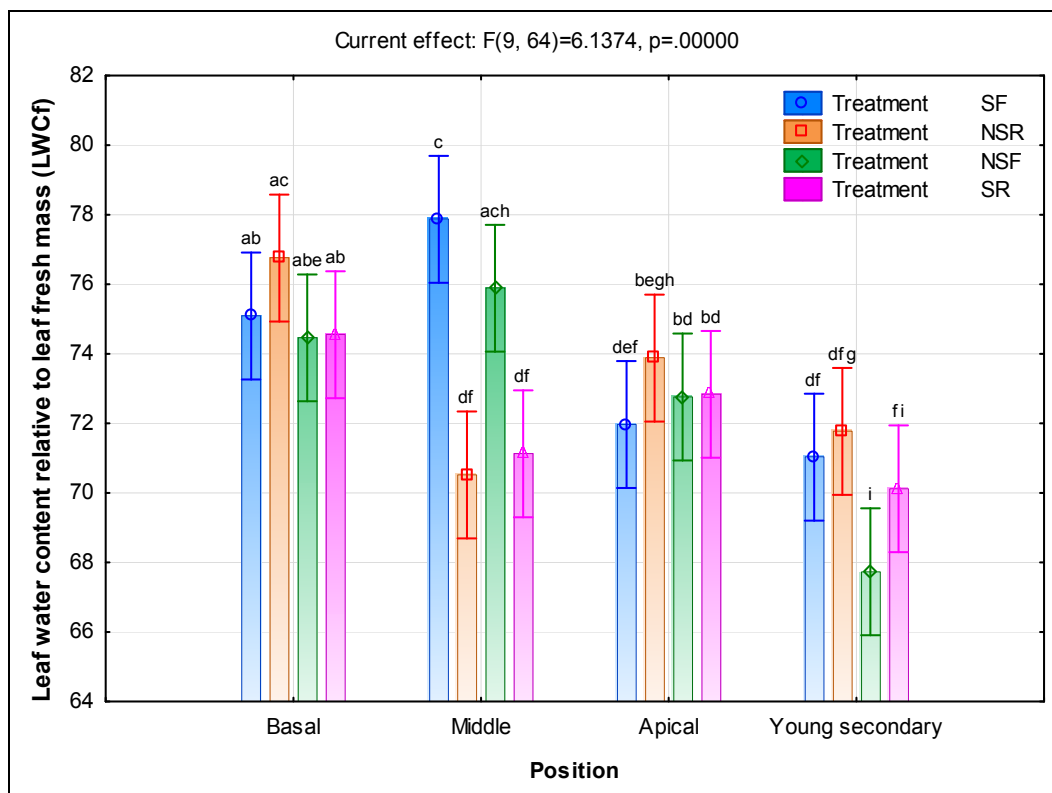


Figure 143 Leaf water content relative to leaf fresh mass (LWCf) for different leaf positions and treatments in dataset 2010B (means with the same letters are not significantly different at the $p \leq 0.05$ level; vertical bars denote 95% confidence intervals).

6.4 Conclusions

Leaf thickness, structure and water content are clearly related to leaf age and exposure levels, but there seems to be little, if any, effect on these parameters due to plant water status differences. The dynamics of leaf structure and water content in the canopy throughout the season, apparently with véraison as a pivotal point is evident. Specific leaf mass generally increase through the season, but the region in the canopy of high specific leaf mass shift from the lower parts to the apical parts (including secondary shoots) of the canopy as the season progresses. This relates to the change in functional dynamics of the canopy, with the secondary shoot leaves gaining higher importance as photosynthate contributing units as the season progresses. These interactions and characteristics of the canopy need to be taken into account in remote sensing studies, during leaf-level measurements, but especially where *scaling-up* methods are to be used to estimate canopy biomass/water content or pigment content.

The difficulty with relating leaf water potential to leaf or canopy water content may be illustrated by severe stress conditions. This may decrease growth and reduce shading in the canopy, potentially leading to increases in SLM, while the actual stress conditions that decrease growth may also inhibit leaf expansion and growth. This may be counteracted by a reduction in SLM.

6.5 Literature cited

- Boso, S., Alonso-Villaverde, V., Santiago, J.L., Gago, P., Dürrenberger, M., Düggelin, M., Kassenmeyer, H.H. & Martinez, M.C., 2010. Macro- and microscopic leaf characteristics of six grapevine genotypes (*Vitis* spp.) with different susceptibilities to grapevine downy mildew. *Vitis* 49, 43-50.
- Buisson, D. & Lee, D.W., 1993. The Developmental Responses of Papaya Leaves to Simulated Canopy Shade. *American Journal of Botany* 80, 947-952.

- Cartechini, A. & Palliotti, A., 1995. Effect of Shading on Vine Morphology and Productivity and Leaf Gas Exchange Characteristics in Grapevines in the Field. *American Journal of Enology and Viticulture* 46, 227-234.
- Ceccato, P., Flasseb, S., Tarantolac, S., Jacquemoud, S. & Gregoirea, J.-M., 2001. Detecting vegetation leaf water content using reflectance in the optical domain. *Rem. Sens. Environ.* 77, 22-33.
- Chabot, B.F. & Chabot, J.F., 1977. Effects of light and temperature on leaf anatomy and photosynthesis in *Fragaria vesca*. *Oecologia* 26, 363-377.
- Cloete, H., Archer, E. & Hunter, J.J., 2006. Shoot heterogeneity effects on Shiraz/Richter 99 grapevines. I. Vegetative growth. *South african journal for enology and viticulture* 27, 68.
- Danson, F.M., Steven, M.D., Malthus, T.J. & Clark, J.A., 1992. High-spectral resolution data for determining leaf water content. *International Journal of Remote Sensing* 13, 461-470.
- Ellis, W., 2008. Grapevine (Shiraz/Richter 99) water relations during berry ripening. MSc(Agric) Viticulture thesis, Stellenbosch University.
- Freeman, B.M. & Kliewer, W.M., 1984. Grapevine leaf development in relationship to potassium concentration and leaf dry weight density. *Am. J. Bot.* 3, 294-300.
- Gaudillere, J.P. & Carbonneau, A., 1986. Training system and photosynthetic activity of the vine. In: Dejong, T.M. (ed). *Proc. International Workshop on Regulation of Photosynthesis in Fruit Crops*, University of California, Davis. pp. 61-71
- Hsiao, T.C., 1973. Plant responses to water stress. *Annual Review of Plant Physiology* 24, 519-570.
- Hunter, J. & Visser, J., 1990. The effect of partial defoliation on growth characteristics of *Vitis vinifera* L. cv. Cabernet Sauvignon I. Vegetative growth. *South African Journal of Enology and Viticulture* 11, 18-25.
- Lambers, H., Chapin, F.S. & Pons, T.L., 1998. *Plant physiological ecology*. Springer, New York, USA.
- Lei, T.T., Tabuchi, R., Kitao, M. & Koike, T., 1996. Functional relationship between chlorophyll content and leaf reflectance, and light-capturing efficiency of Japanese forest species. *Physiol. Plant.* 96, 411-418.
- Niinemets, Ä., 2001. Global-scale climatic controls of leaf dry mass per area, density, and thickness in trees and shrubs. *Ecology* 82, 453-469.
- Niinemets, U., 1999. Research Review: Components of Leaf Dry Mass Per Area-Thickness and Density-Alter Leaf Photosynthetic Capacity in Reverse Directions in Woody Plants. *New Phytologist* 144, 35-47.
- Niinemets, Ü., Kull, O. & Tenhunen, J.D., 1998. An analysis of light effects on foliar morphology, physiology, and light interception in temperate deciduous woody species of contrasting shade tolerance. *Tree Physiology* 18, 681-696.
- Patakas, A., Noitsakis, B. & Stavrakas, D., 1997. Water relation parameters in *Vitis vinifera* L in drought period. *Effects of leaf age. Agronomie* 17, 129-138.
- Poni, S., Intrieri, C. & Silvestroni, O., 1994. Interactions of Leaf Age, Fruiting, and Exogenous Cytokinins in Sangiovese Grapevines Under Non-Irrigated Conditions. I. Gas Exchange. *American Journal of Enology and Viticulture* 45, 71-78.
- Rodríguez-Pérez, J.R., Riaño, D., Carlisle, E., Ustin, S. & Smart, D.R., 2007. Evaluation of Hyperspectral Reflectance Indexes to Detect Grapevine Water Status in Vineyards. *Am. J. Enol. Vitic.* 58, 302-317.
- Serrano, L., 2008. Effects of leaf structure on reflectance estimates of chlorophyll content. *International Journal of Remote Sensing* 29, 5265-5274.
- Sims, D.A. & Pearcy, R.W., 1992. Response of leaf anatomy and photosynthetic capacity in *Alocasia macrorrhiza* (Araceae) to a transfer from low to high light. *American Journal of Botany*, 449-455.
- Van den Heuvel, J.E., Proctor, J.T.A., Fisher, K.H. & Sullivan, J.A., 2004. Shading Affects Morphology, Dry-matter Partitioning, and Photosynthetic Response of Greenhouse-grown 'Chardonnay' Grapevines. *HortScience* 39, 65-70.

Witkowski, E.T.F. & Byron, B.L., 1991. Leaf Specific Mass Confounds Leaf Density and Thickness. *Oecologia* 88, 486-493.

Chapter VII

Research Results

Non-destructive assessment of leaf pigment content, specific leaf mass and water content during growth of *Vitis vinifera* L. cv. Shiraz

Chapter VII: Non-destructive assessment of leaf pigment content, specific leaf mass and water content during growth of *Vitis vinifera* L. cv. Shiraz

7.1 Introduction

Several remote sensing techniques aim at detecting grapevine vigour differences, which may integrate complex factors, such as canopy size, density, leaf age, pigment content, nutrient and water status differences. The need exists to investigate the contribution of different elements of the canopy to the signal on a spatial and temporal basis, while also assessing the leaf compositional aspects (in terms of morphology and pigment composition) that underlie the signal. A better understanding of the spectral properties of grapevine leaves could also shed more light on the dynamics of canopy efficiency, and eventually aid in scaling up these measurements to the canopy and vineyard level, where hyperspectral airborne (Zarco-Tejada *et al.*, 2005; Meggio *et al.*, 2010) or, eventually, satellite sensors may be used to monitor canopy changes. Non-destructive measurements such as leaf temperature (Grant *et al.*, 2007) and pigment fluorescence (Flexas *et al.*, 2002; Hendrickson *et al.*, 2004c) already show potential to complement conventional measurements in determining grapevine water status, with remote sensing indices also holding promise in this regard (Cifre *et al.*, 2005; De Bei *et al.*, 2011).

The grapevine leaf age and environment can affect its structural components (area, mass, thickness and density) as well as pigment composition and therefore its interaction with radiation (Kriedemann, 1968; Kriedemann *et al.*, 1970; Hunter & Visser, 1989; Poni *et al.*, 1994b; Schultz, 1996). Non-destructive techniques have the potential of allowing measurements to be conducted on the same leaves in the canopy during growth of the plant, thus enabling detection of change without drastic intervention. Leaf thickness and density may change during ageing (refer to chapter II for discussion), also potentially affecting its interaction with radiation. This is not only relevant in leaf-level pigment measurements, but also in remote sensing, as the amount, orientation (Pisciotta *et al.*, 2011) and structure of leaves all contribute to the signal interpreted from an aerial or space-borne platform. Considering that specific leaf mass, which is determined by leaf density and thickness, also relates positively to leaf photosynthetic capacity per unit leaf area (Gaudillere & Carbonneau, 1986; Cartechini & Palliotti, 1995; Niinemets, 1999), it can be considered a very important parameter to assess non-destructively. The interaction of this parameter with row and leaf orientation have also previously been shown for Shiraz (Pisciotta *et al.*, 2011).

Several approaches can be followed to assess the relationships between spectral data and biochemical constituents. Apart from vegetation indices and radiation transfer modelling (that were briefly dealt with in chapter II), uni- and multivariate regression techniques, such as multiple linear regression (MLR), principal component analysis and -regression (PCA and PCR) as well as partial least-squares regression (PLS) can also be used in spectral data interpretation. These techniques enable the analyst to visualise and interpret large spectral datasets (especially with powerful computing platforms now being readily available) and to study relations with the parameters of interest. Another advantage of partial least squares (PLS) regression is that it can deal with strongly correlated data, commonly found in spectroscopy (Esbensen *et al.*, 2002), which is made possible by performing calibration over latent variables that are defined as linear combinations (or “projections”) of the original variables with factors extracted in such a way that they have the maximum covariance with the property of interest (Pedro & Ferreira, 2007; Li *et al.*, 2008).

The objectives of this study were, firstly, to assess the use of field spectroscopy to estimate specific leaf mass, leaf water and leaf pigment content using a calibration-validation approach and,

secondly, to investigate if relationships exist between the predicted values and these parameters, with consideration of the existing plant water status (as assessed by predawn leaf water potential measurements). The third objective was to investigate the possibility of using leaf spectral features to assess plant water status, which could be of use when designing field instruments that may be useful in irrigation scheduling.

7.2 Materials and methods

7.2.1 Vineyard, experiment layout and leaf sampling

Refer to chapter III for details on the vineyard where the experiments were conducted, and to chapter VI for details on the experiment layout. Refer to chapters V and VI for details on leaf sampling procedures.

7.2.2 Non-destructive measurements

Leaf sampling was accompanied with adaxial leaf spectral measurements, which were conducted using an ASD[®] FieldSpec Pro spectroradiometer (Analytical Spectral Devices Inc., Boulder, CO, USA) detecting reflectance in the 350-2500 nm spectral region. The spectroradiometer is characterised by a spectral resolution of 3 nm (full-width-at-half-maximum, FWHM) and a 1.4 nm sampling interval across the 350-1050 nm spectral range. The FWHM and the sampling interval for the 1051-2500 nm spectral range are 30 nm and 2 nm, respectively. It was deployed using an ASD[®] high intensity plant probe with a leaf clip assembly and a halogen light source (Figure 144). The instrument was set to a spectral averaging in the field of 20 scans and instrument dark current correction as well as white reference (Spectralon, Labsphere Inc., Ltd., USA) collection was performed regularly (after every four to five leaf measurements). This set-up combined reflectance and transmittance properties into a single measurement, which should theoretically be less variable with respect to leaf internal structural variability (Lillesaeter, 1982; Stuckens *et al.*, 2009; Dzikiti *et al.*, 2010). The low intensity of the halogen lamp in the UV region caused some excessive noise in the lower wavelength regions, which were avoided during analysis of the spectra (analysis was confined to wavelengths longer than 400 nm).

Spectral measurements were conducted on four leaf positions as indicated on Figure 145, which corresponded to positions where discs were collected for destructive leaf pigment or leaf structure and water content measurements.

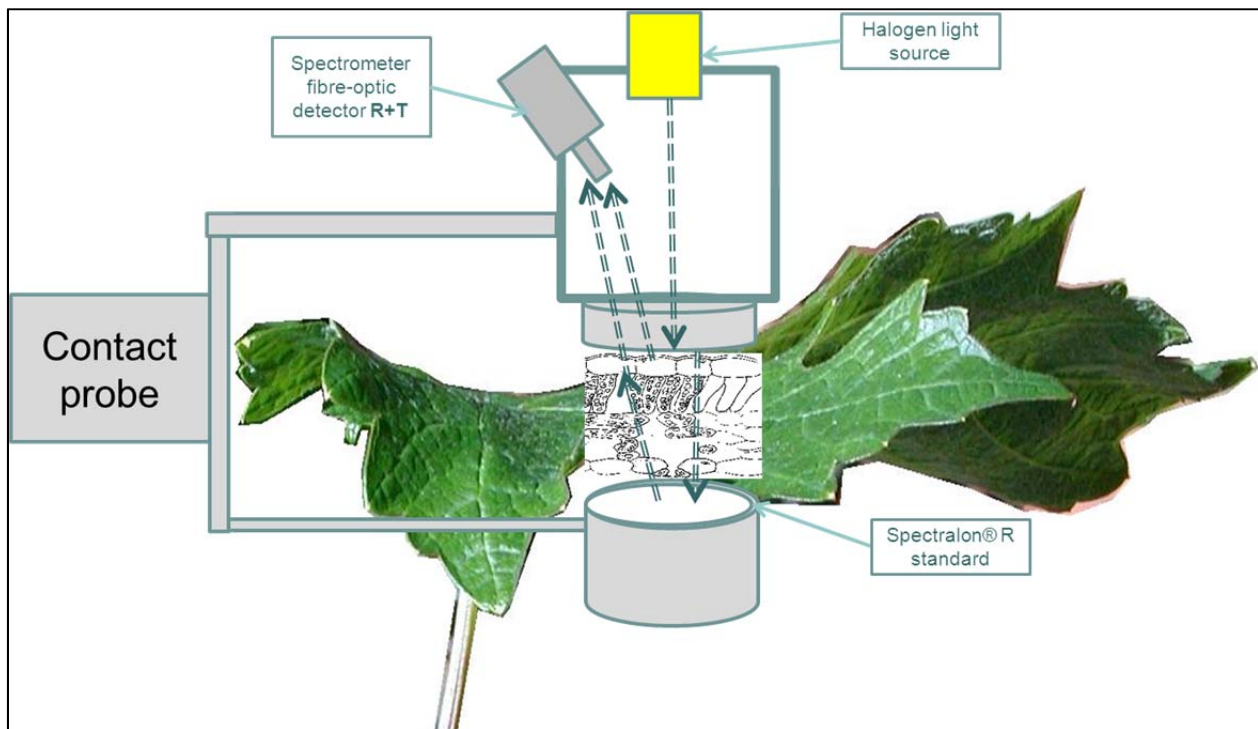


Figure 144 Leaf spectrometer and contact probe set-up during leaf spectral measurements



Figure 145 Image showing sampling positions on the leaf as well as instruments used during sampling.

7.2.3 Statistical analysis

Statistica 10 ® software (Statsoft, Tulsa, USA) was used for general statistical analysis. Multivariate analysis of spectra was done using Unscrambler® 9.2 (CAMO PROCESS AS, Oslo, Norway). A calibration-validation approach was used to create partial least squares (PLS 1 and PLS 2) models for leaf structural and pigment data as well as in attempting leaf age prediction (Pedro & Ferreira, 2007). The PLS 1 approach involves calibrating properties one by one, but they can also be calibrated at once using PLS 2. In PLS 1, a single set of factors is needed for each calibration model, while with PLS 2 modelling a single set of factors is extracted from multiple factors. The convenience of PLS 2 is therefore that results are obtained in a single execution of the calculation routine, but in many cases, PLS 1 models may be more precise. The PLS 2 regressions will give models with similar predictive abilities to PLS1, if the dependent variables (chemical constituents) are strongly correlated. The advantage of PLS 2 is seen when dependent variables that can be determined quite precisely are put together with properties that are more difficult to

measure using its reference methods (Pedro & Ferreira, 2007). This property will be explored with regards to specific leaf mass, that is often found to be difficult to predict in spectroscopic studies (Jacquemoud *et al.*, 1996; Feret *et al.*, 2008; Stuckens *et al.*, 2009).

Spectral data transformations are indicated where applicable, but in general, all data were mean-centred, but not scaled, as scaling is generally not recommended in spectral datasets. Models were also evaluated with scaling of spectra, but no improvement in the models was detectable. Full cross-validation was performed on all datasets. In order to avoid over-fitting of the models, the optimum number of principal components (PC's) were selected by evaluating the number closest to the minimum root-mean square error of cross-validation (RMSECV) (Esbensen *et al.*, 2002). The datasets used for calibration purposes included all leaf structure and water content datasets discussed in Chapter VI, as well as pigment data from leaves of primary shoots in season one discussed in Chapter V. Leaf age calibration was conducted from all shoot measurement data from all three seasons in the study.

7.2.4 Leaf radiation transfer modelling

An inversion of the PROSPECT (version 5) model (Jacquemoud & Baret, 1990) was used to estimate leaf total chlorophyll ($\text{mg}\cdot\text{cm}^{-2}$), total carotenoid content ($\text{mg}\cdot\text{cm}^{-2}$), equivalent water thickness (EWT, $\text{mg}\cdot\text{cm}^{-2}$), a leaf structure parameter (N) as well as leaf dry matter content or specific leaf mass (SLM) ($\text{mg}\cdot\text{cm}^{-2}$). The inversion script was configured to use leaf reflectance data measured against a white Spectralon® background and the inversion algorithm was chosen according to the work of Stuckens *et al.* (2009) who found the constrained Nelder–Mead minimization (Nelder & Mead, 1965) to be optimal under similar measurement conditions than what were used in this study. Based on the ranges found, the initial values were constrained in the range 2-3 for N, 0.009-0.050 $\text{mg}\cdot\text{cm}^{-2}$ for chlorophyll content, 0.002-0.009 $\text{mg}\cdot\text{cm}^{-2}$ for carotenoid content, 0.002-0.016 $\text{mg}\cdot\text{cm}^{-2}$ for EWT and 0.0009-0.0073 $\text{mg}\cdot\text{cm}^{-2}$ for SLM. Leaf spectra measured against a white Spectralon® background gave the best inversion results compared to the black background, consistent with the observations of Stuckens *et al.* (2009). Inversion of the PROSPECT model is generally considered reliable and well-validated to retrieve leaf water content and probably more so than using simple spectral ratio indices (Ceccato *et al.*, 2001; Colombo *et al.*, 2008; Dziki *et al.*, 2010).

7.2.5 Leaf age determination/classification

For every measured leaf as well as an additional seasonal dataset comprising of several non-destructive spectral measurements, leaf plastochron analysis was performed in order to determine leaf age along with each measurement. For details of the procedure, refer to chapter V.

7.2.6 Leaf water potential measurements

Refer to chapter III.

7.3 Results and discussion

7.3.1 General spectral properties of leaves

Reflectance and transmittance ($R+T$) spectra [equivalent to $(1 - \text{absorbance})$] in the visible region (400-700 nm) seemed to increase with leaf ageing in a leaf selected from a basal position on a primary shoot, with the infrared $R+T$ (700-1400 nm) initially increasing, and then decreasing towards the last sampled date (Figure 146). The leaves were first measured when fully unfolded and when they were suitably sized to fit into the spectrometer leaf clip assembly. In a young apical leaf, the visible $R+T$ was high initially, then decreased as leaf absorbance increased on the second

date, with an increase again shown when the leaf became senescent (Figure 147). In this leaf, the infrared $R+T$ decreased consistently from the first measurement.

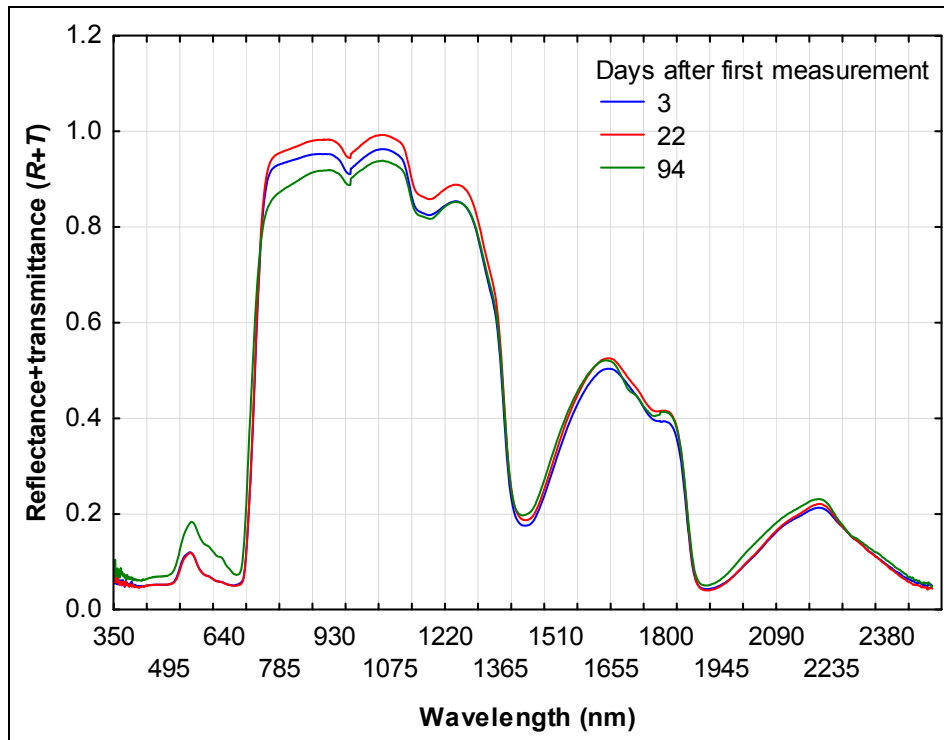


Figure 146 Reflectance + transmittance ($R+T$) spectra of an intact basal (node five) leaf measured on three different dates (3, 22 and 94 DAB). The last date corresponded to about 120 days leaf age.

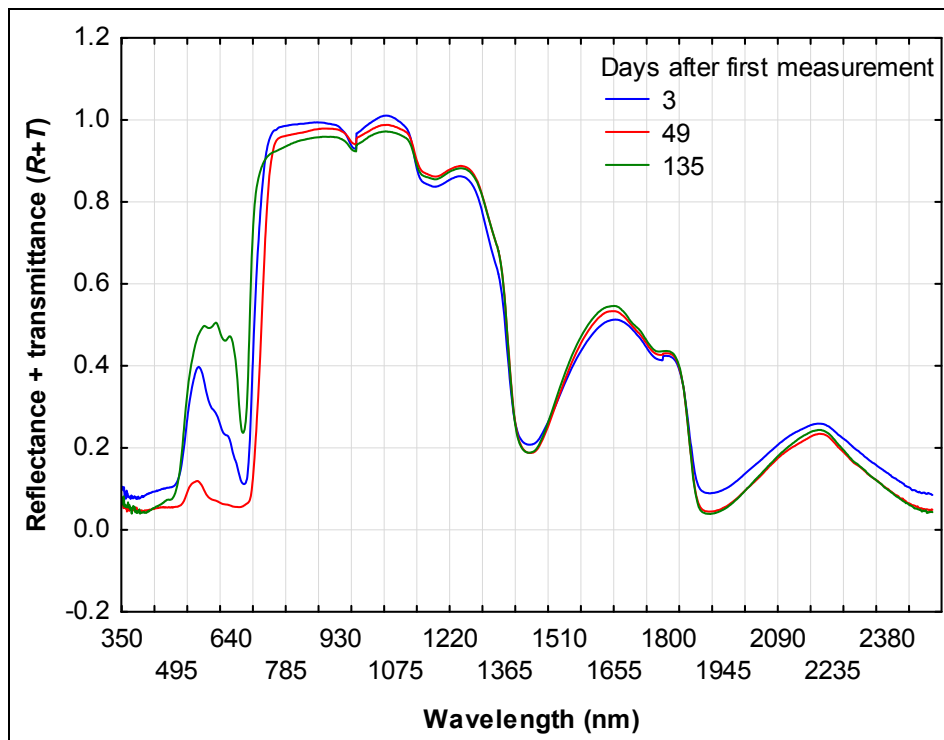


Figure 147 Reflectance + transmittance ($R+T$) spectra of an intact apical (node 23) leaf measured on three different dates (3, 49 and 135 DAB). The last date corresponded to a leaf age of more than 132 days.

7.3.1.1 Leaf absorption of visible (400-700 nm) radiation

An increase in leaf absorption of visible radiation [A (VIS)] from date A to dates B and C in season one (Figure 148) was expected with leaf ageing, associated with an increase in intercepting tissue and pigments, which should coincide with decrease in visible R and T (Schultz, 1996). The final

decrease in A (VIS), as seen here for dates D and especially E, could be linked to pigment loss and leaf senescence (Demarez *et al.*, 1999). Note that in this study changes observed in A could be due to changes in R and/or T . If the trends in pigment content change for the measuring dates observed in chapter V are considered, chlorophyll and carotenoid content peaked on measurement date B, while leaf absorbance in the visible region only seemed to peak on date C (Figure 149), with the highest absorption of visible radiation observed for leaf age classes two and three (Figure 150).

Similar A (VIS) trends were observed in Schultz (1996), but the range of values in this study was markedly higher than the average of about 85% for mature, non-senescent grapevine leaves found by Schultz, and also previously reported by Smart (1987).

The A (VIS) values seemed to be lower in the NSF treatment for leaves aged more than 50 days (Figure 151). It may be possible that these leaves were situated in positions where increased shading prevailed in the full canopies, where the TSLM of the leaves could also be lower (see discussion later in this chapter). This could negate the effects of possible higher area-based chlorophyll values in shaded conditions, as found by Cartechini & Palliotti (1995). Flexas *et al.* (2001) found lower total leaf chlorophyll ($\mu\text{mol}\cdot\text{m}^{-2}$) in shade leaves of *Vitis riparia* Michaux, which also confirms that even though leaf total chlorophyll content in shade leaves may be more on a mass basis, the content on an area basis would in some cases be significantly affected by the TSLM of the leaves.

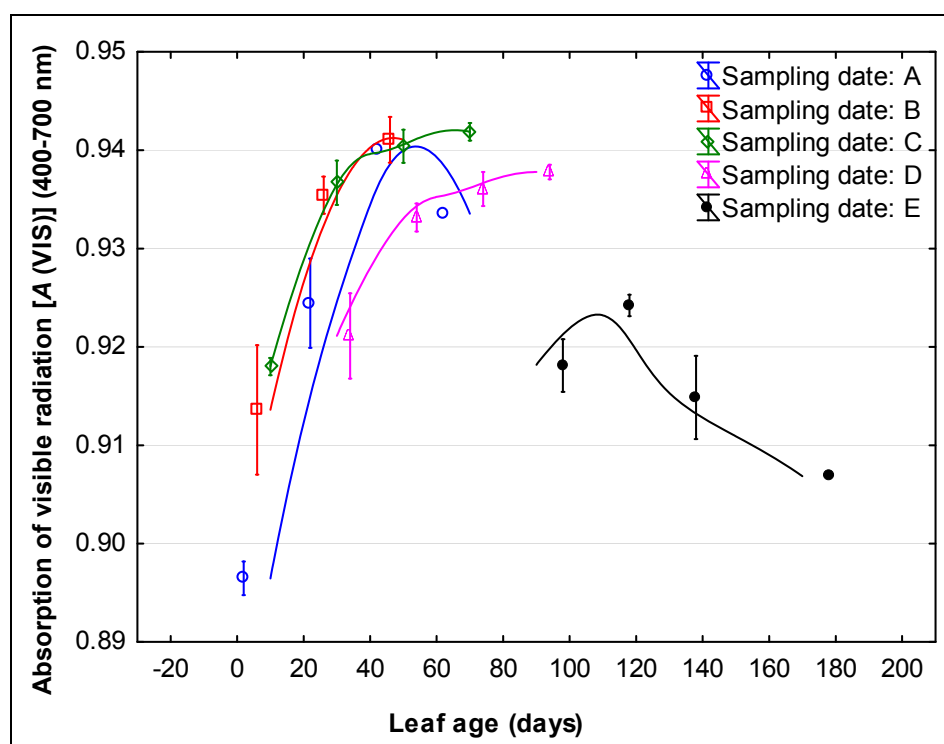


Figure 148 Relationship between the absorption of visible radiation [A (VIS)] (400-700 nm) and leaf chronological age for the different measurement dates in season one (distance-weighted least-squares fits are shown for each measurement date fitted to mean values, while standard errors, shown as vertical bars, and means are offset for clarity).

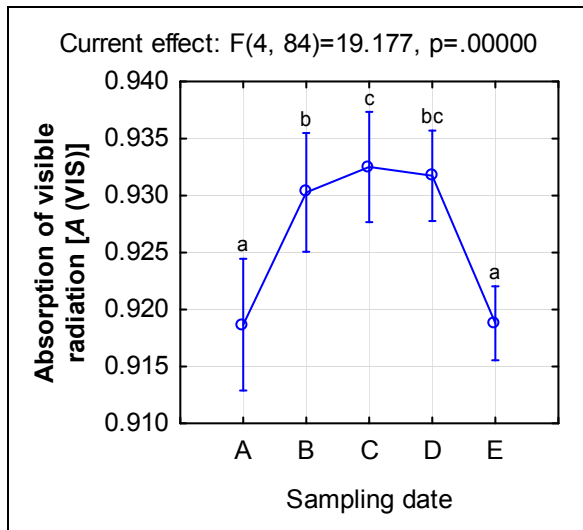


Figure 149 Primary shoot leaf absorption of visible radiation [A (VIS)] (400-700 nm) for the different measuring dates in season one (vertical bars denote 95% confidence intervals).

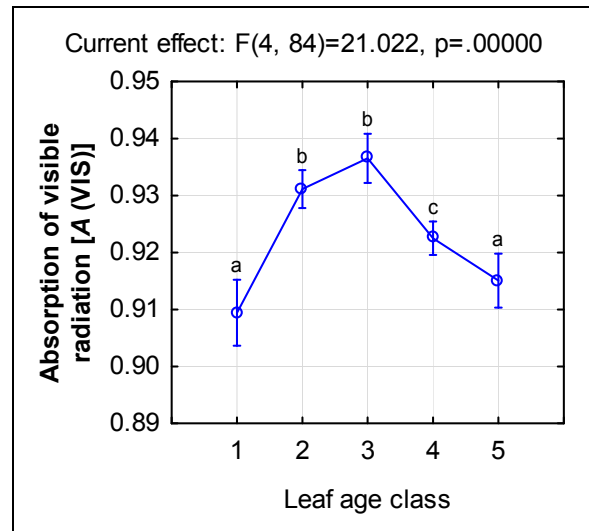


Figure 150 Primary shoot leaf absorption of visible radiation [A (VIS)] (400-700 nm) for the different leaf age classes in season one (vertical bars denote 95% confidence intervals).

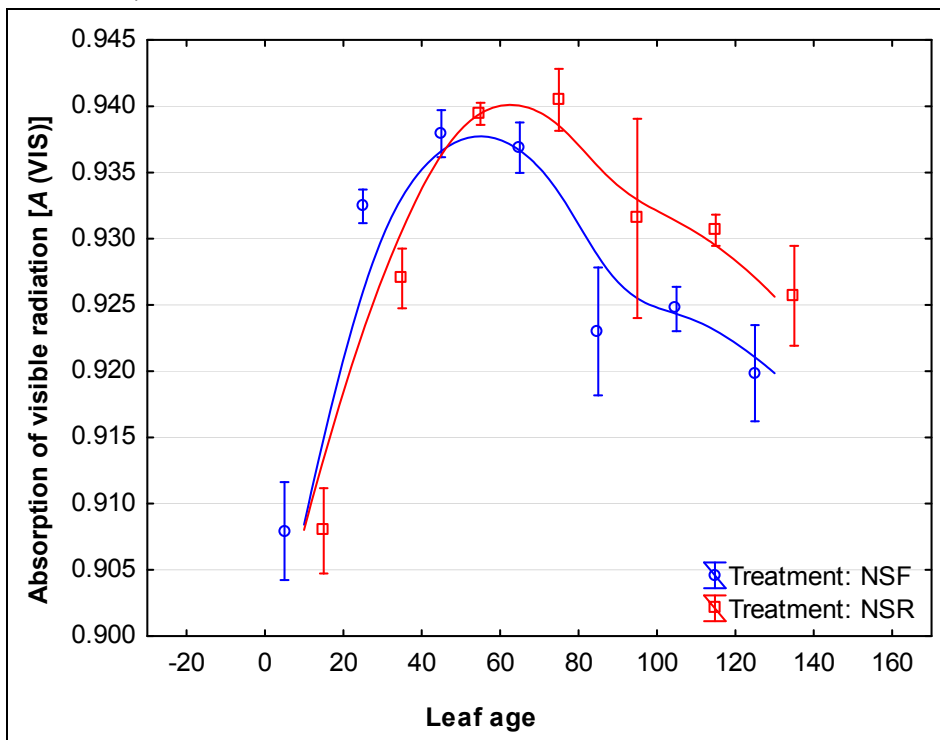


Figure 151 Relationship between the absorption of visible radiation [A (VIS)] (400-700 nm) and leaf chronological age for the different canopy manipulation treatments in season one (distance-weighted least-squares fits are shown for each measurement date fitted to mean values, while standard errors, shown as vertical bars, and means are offset for clarity).

Absorption of visible radiation [A (VIS)] seemed to be higher initially in the SF treatments in season two, which was peculiar considering the canopy manipulation treatment was only performed on 67 DAB (Figure 152). A reason for this can be the faster initial shoot growth in the SF treatments (the shoots reached 50% of maximum shoot length earlier than the other treatments, refer to chapter III), as well as formation of the largest leaves (also refer to chapter III), which may indicate higher carbon allocation towards shoot and leaf growth, with the potential of increasing the SLM (see predicted SLM values later in this chapter). The increased SLM could then also be associated with increased chlorophyll content on a leaf area basis. The A (VIS) seemed to increase for the SF and SR treatments up to 67 DAB when the canopy manipulation treatment was performed and when

shoot growth in the SF treatments reached maximum values, decreasing thereafter and increasing again up to 168 DAB. The final decrease after this date (probably linked to general leaf senescence) seemed to be much less in the SR treatment. Leaf age class one only reached A (VIS) of about 0.90 after 100 DAB (Figure 153) compared to season one, when this age class already reached this level at 58 DAB. The youngest leaf classification obviously experienced less of the previous events in the canopy, and apart from having lower A (VIS), it also seemed more responsive in terms of changing levels throughout the season. The decrease after 67 DAB is associated with simultaneous increase in EWT of the same leaf class (data not shown), with strong decrease in EWT for this class after 81 DAB. It is therefore possible that for this young leaf class, spectral measurements in the visible domain are dominated by leaf water content changes during the season (see discussion on the work of Knipling (1970) later in this section). The other leaf age classes show consistent decrease in A (VIS) from 67 DAB.

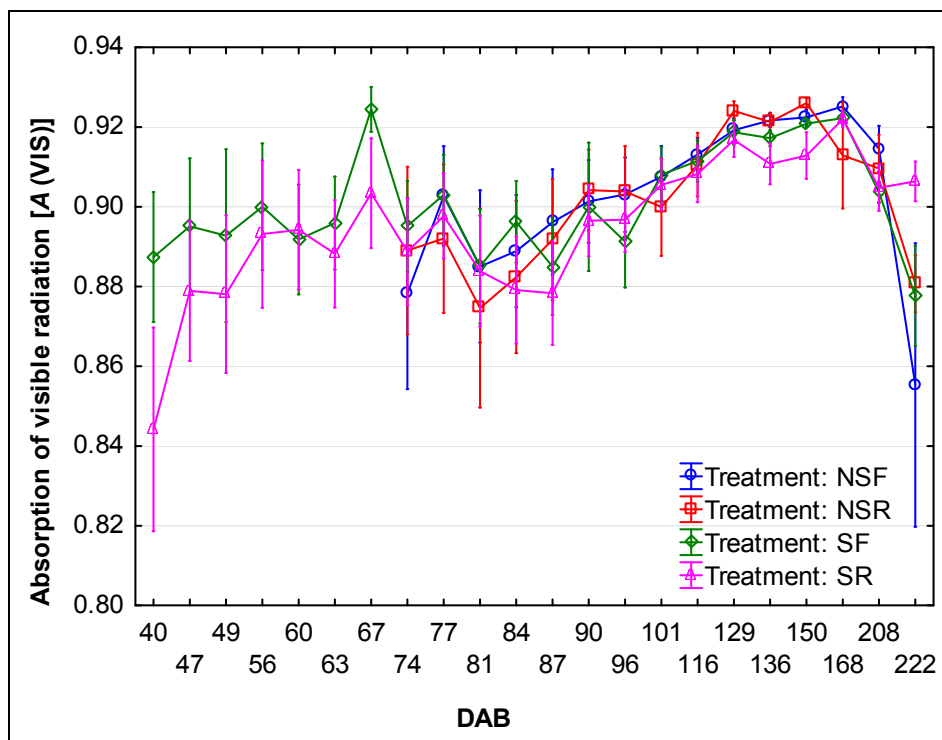


Figure 152 Relationship between the absorption of visible radiation [A (VIS)] (400-700 nm) and date after budburst (DAB) for the different canopy manipulation treatments in season two (vertical bars denote standard errors).

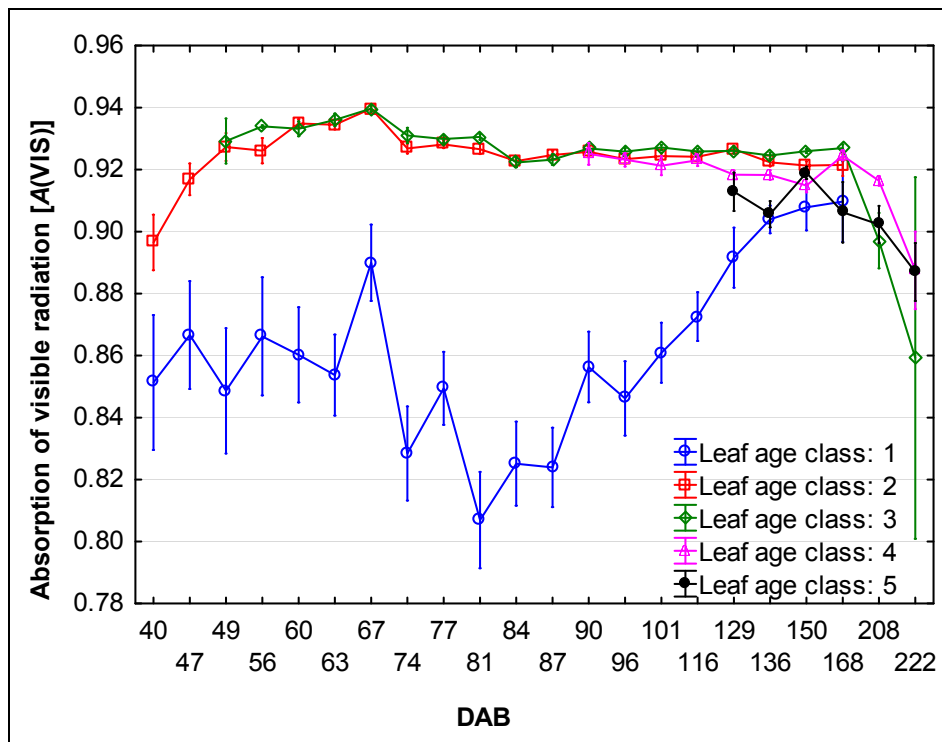


Figure 153 Relationship between the absorption of visible radiation [A (VIS)] (400-700 nm) and date after budburst (DAB) for the different leaf age classes in season two (vertical bars denote standard errors).

When the relationship in Figure 152 was plotted against leaf age rather than DAB, the NS treatments seemed to show more decrease in A (VIS) for leaves older than 130 days compared to the S treatments (data not shown). This could possibly be explained by the effect of leaf water content on visible absorption. Knipling (1970) indicated that transmittance can increase in leaves with higher water content, decreasing absorbance of visible radiation. This is possible here, as the EWT was also shown to be higher in leaf age class four for the NSR treatments (refer to Section 7.3.9). In season three the A (VIS) was much lower for leaf class one compared to the other classes, but also in general the A (VIS) seemed to be lower compared to the other two seasons (Figure 154 and Figure 155). This could be due to the observation that the TSLM levels in leaves were much lower for this season (refer to section 7.3.2). Besides the trend for young (class one) leaf A (VIS) to decrease from 99 to 127 DAB, it was not the case if leaves were analysed together for 93, 99 and 127 DAB (Figure 156).

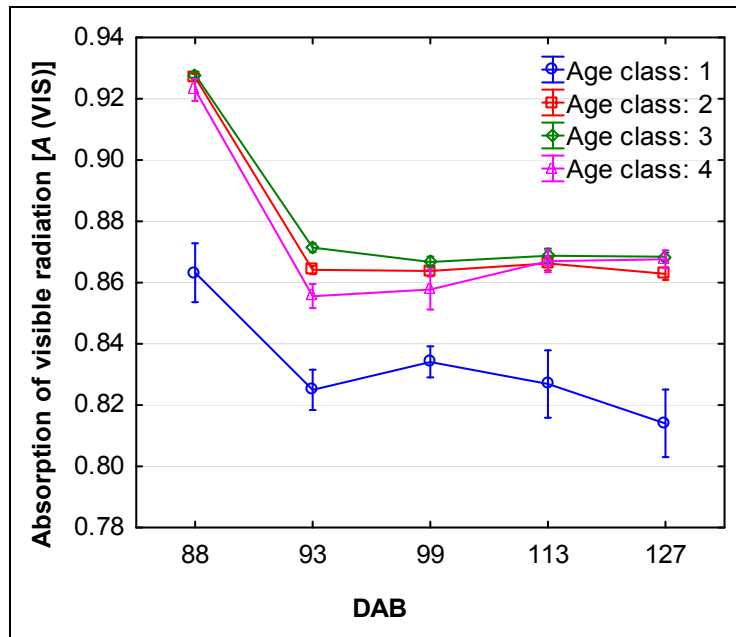


Figure 154 Relationship between the absorption of visible radiation [A (VIS)] (400-700 nm) and leaf chronological age for the different measurement dates in season three (vertical bars denote standard errors).

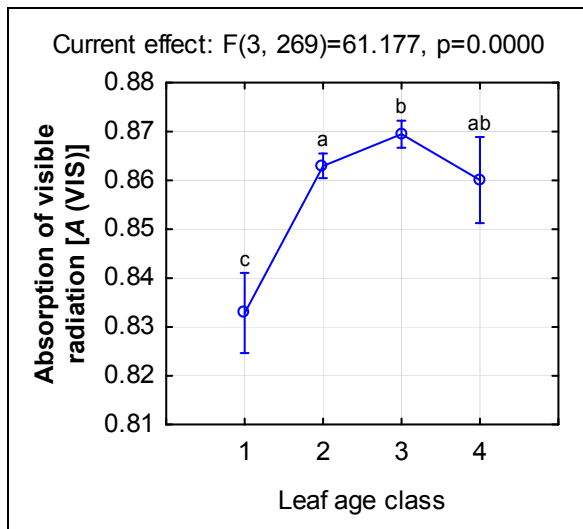


Figure 155 Primary shoot leaf absorption of visible radiation [A (VIS)] (400-700 nm) for the different leaf age classes in season three (means with the same letters are not significantly different at the $p \leq 0.05$ level, vertical bars denote 95% confidence intervals).

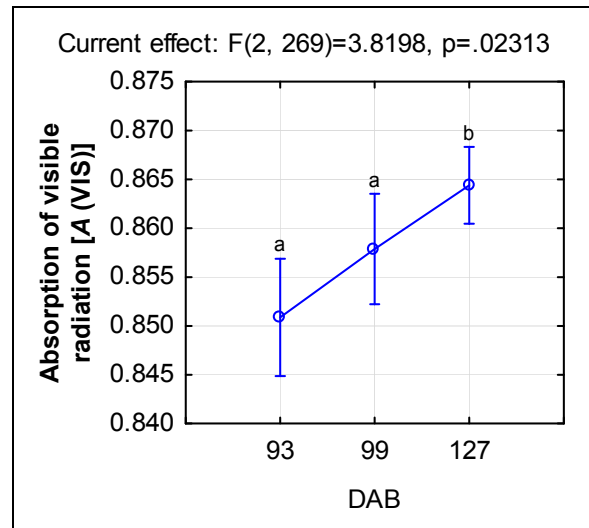


Figure 156 Primary shoot leaf absorption of visible radiation [A (VIS)] for different measurement dates in season three (means with the same letters are not significantly different at the $p \leq 0.05$ level, vertical bars denote 95% confidence intervals).

7.3.1.2 Leaf absorption of infrared (700-1400 nm) radiation

The initial increase in A (NIR), may be due to a strong decrease in T, commonly seen in young leaves as they thicken (Figure 157 and Figure 158). The increase in A (NIR) in old/senescent leaves, especially leaf age class five (Figure 159) could be due to mesophyll collapse (Knipling, 1970; Gausman, 1985). The strong decline in A (NIR) from date B to C may be due to water loss in the leaf and increase in the number of air spaces, which may increase multiple scattering of radiation (Jacquemoud *et al.*, 1996), but can also be associated with increased shading in all canopies as canopy filling completes up to véraison and before shoot growth cessation. Significant interactions were not seen with the canopy manipulation treatments. If canopy shading had prevailed, A (NIR) might have increased due to increased air spaces found in shaded leaves (Gausman, 1984; Gamon & Surfus, 1999). The increase in A (NIR) for leaf ages older than 90 days

in the NSR canopies was expected with senescing leaves, and it could be that water deficits interacted to curb this increase in the NSF treatments [water deficits may lead to increased air spaces in the leaf and decreased A (NIR), the latter which can also be caused by the increase in multiple scattering of radiation (Jacquemoud *et al.*, 1996)].

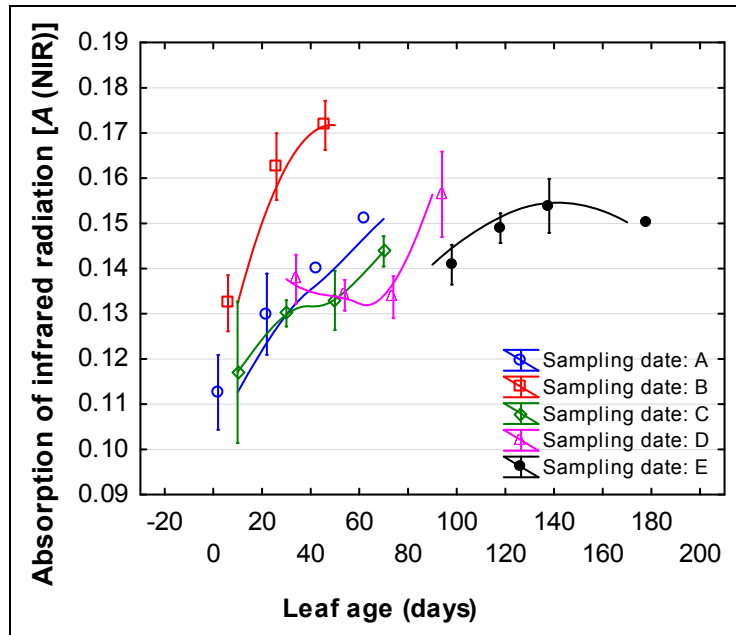


Figure 157 Relationship between the absorption of infrared radiation [A (NIR)] (700-1400 nm) and leaf chronological age for the different measurement dates in season one (distance-weighted least-squares fits are shown for each measurement date fitted to mean values, while standard errors, shown as vertical bars, and means are offset for clarity).

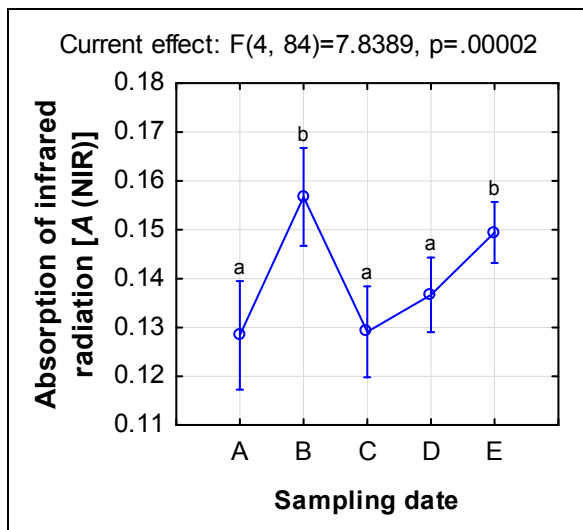


Figure 158 Primary shoot leaf absorption of infrared radiation [A (NIR)] (700-1400 nm) for the different measurement dates in season one (means with the same letters are not significantly different at the $p \leq 0.05$ level, vertical bars denote 95% confidence intervals).

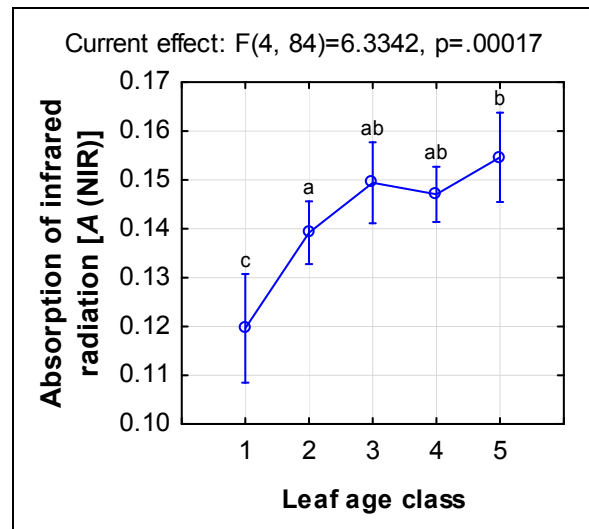


Figure 159 Primary shoot leaf absorption of infrared radiation [A (NIR)] (700-1400 nm) for the different leaf age classes in season one (means with the same letters are not significantly different at the $p \leq 0.05$ level, vertical bars denote 95% confidence intervals).

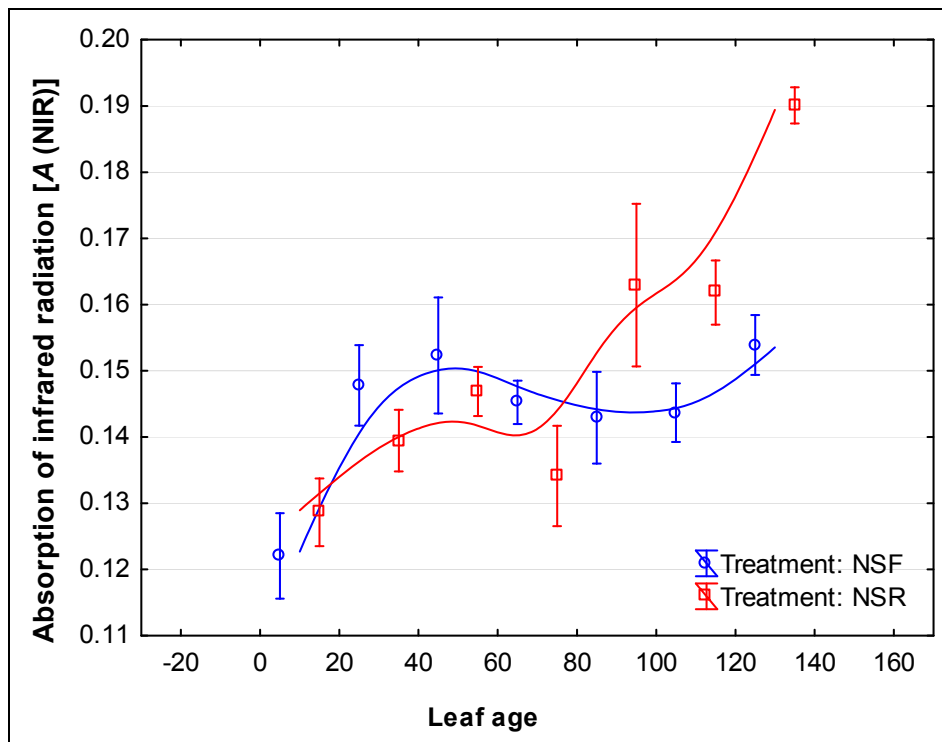


Figure 160 Relationship between the absorption of infrared radiation [A (NIR)] (700-1400 nm) and leaf chronological age for the different canopy manipulation treatments in season one (distance-weighted least-squares fits are shown for each measurement date fitted to mean values, while standard errors, shown as vertical bars, and means are offset for clarity).

The initial increase in A (NIR) at 60 DAB (Figure 161) was also observed between 58 and 65 DAB in season one. It did not seem logical at first that leaf structure could change so much over the course of three to four days (and further studies should determine whether this was not an instrument problem on the day). However, the initial stages of leaf formation in a canopy have been shown to incorporate a critical transition phase for the leaves, also referred to as a “hardening phase” (Kriedemann *et al.*, 1970). The short time-span of this apparent change in the canopy as a whole, however, needs to be given more attention in future studies. Young (class one) leaves seemed to have consistently lower A (NIR), followed by class two leaves, and with the highest values mid-season measured in the class three leaves. Treatment differences were not very pronounced for A (NIR) values in season two, with the exception of the SF treatment that seemed to show higher values initially, and the NSR treatment between 84 and 101 DAB (Figure 162). The A (NIR) trends for season three were similar to those of season two, but with less difference between leaf age classes two, three and four (Figure 163).

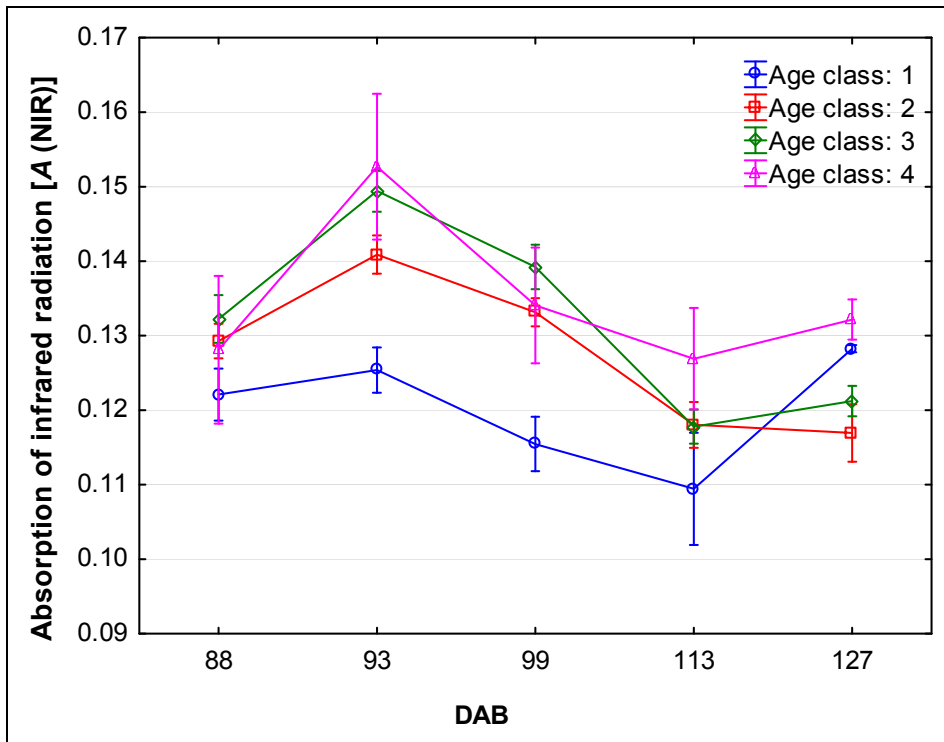


Figure 161 Relationship between the absorption of infrared radiation [A (NIR)] (700-1400 nm) and date after budburst for the different leaf chronological age classes in season two (vertical bars denote standard errors).

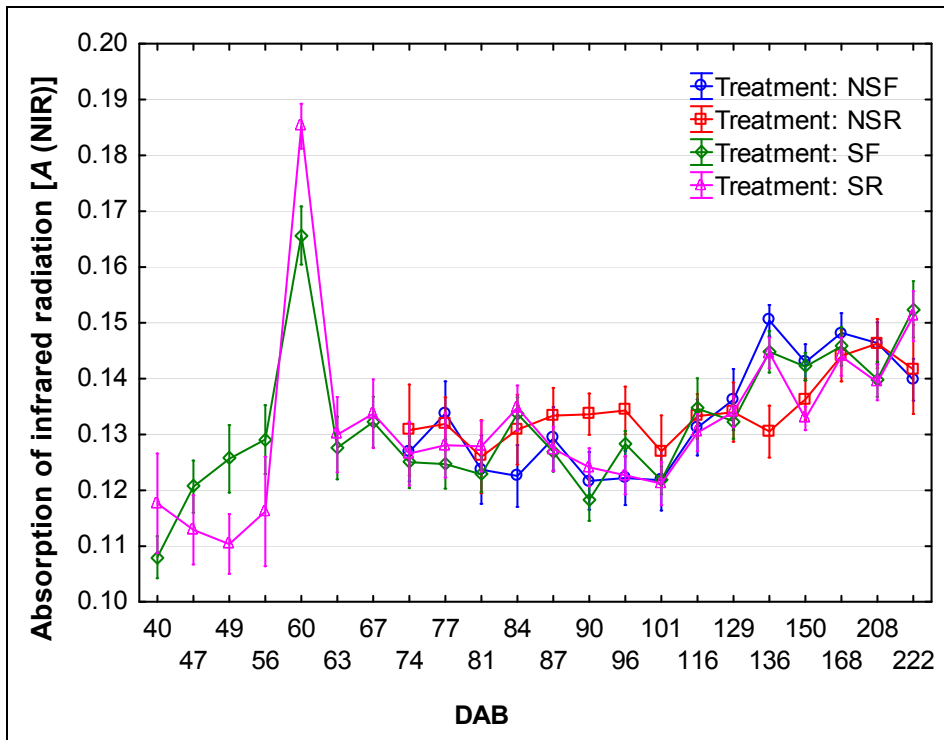


Figure 162 Relationship between the absorption of infrared radiation [A (NIR)] (700-1400 nm) and leaf chronological age for the treatments in season two (vertical bars denote standard errors).

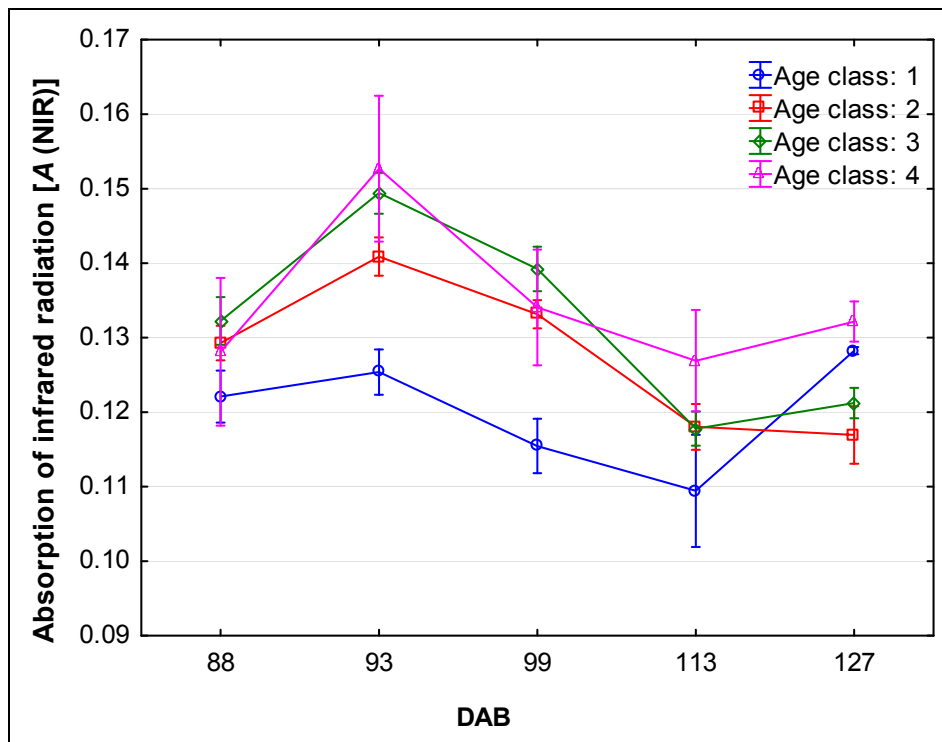


Figure 163 Relationship between the absorption of infrared radiation [A (NIR)] (700-1400 nm) and date after budburst for the different leaf chronological age classes in season three (vertical bars denote standard errors).

7.3.2 Multivariate calibration and prediction of leaf structure and water content

Principal component analysis (PCA) was used to screen leaf spectra collected from the four datasets (Table 44) described in chapter VII for outliers as well as structure in the spectral dataset related to seasonal or treatment differences.

Table 44 Calibration dataset used in partial least squares analysis of spectral data

Dataset	Parameter	Valid N	Mean	Minimum	Maximum	Std.Dev.
All groups	TSLM (mg.cm ⁻²)	253	16.95	3.53	22.66	3.26
	SLM (mg.cm ⁻²)	253	5.01	0.90	7.30	1.20
	EWT (mg.cm ⁻²)	253	11.93	2.63	16.13	2.34
	Mean leaf thickness (mm)	574	0.44	0.20	0.93	0.12
	Leaf density (mg.cm ⁻³)	143	14.04	3.38	21.40	2.89
2010A	TSLM (mg.cm ⁻²)	30	18.30	11.94	21.74	2.63
	SLM (mg.cm ⁻²)	30	5.54	2.81	7.30	1.28
	EWT (mg.cm ⁻²)	30	12.76	9.03	15.14	1.61
	Mean leaf thickness (mm)	Not determined				
2010B	TSLM (mg.cm ⁻²)	80	19.28	13.11	22.66	1.76
	SLM (mg.cm ⁻²)	80	5.24	2.46	6.84	0.96
	EWT (mg.cm ⁻²)	80	14.04	10.65	16.13	1.01
	Mean leaf thickness (mm)	Not determined				
2011A	TSLM (mg.cm ⁻²)	123	15.64	3.53	19.76	3.10
	SLM (mg.cm ⁻²)	123	4.82	0.90	7.01	1.22
	EWT (mg.cm ⁻²)	123	10.82	2.63	13.48	2.02
	Mean leaf thickness (mm)	554	0.44	0.22	0.93	0.12
	Leaf density (mg.cm ⁻³)	123	14.36	3.38	21.40	2.65
2011B	TSLM (mg.cm ⁻²)	20	13.66	8.44	17.94	2.67
	SLM (mg.cm ⁻²)	20	4.51	1.90	6.81	1.45
	EWT (mg.cm ⁻²)	20	9.14	6.10	11.88	1.59
	Mean leaf thickness (mm)	20	0.39	0.20	0.75	0.16
	Leaf density (mg.cm ⁻³)	20	12.11	7.46	19.80	3.55

Large differences seemed to exist between the EWT values of the four datasets (Figure 164), with the datasets collected in season two (2010) apparently having higher EWT values than those collected in 2011. The same trend was observed for the SLM values, but differences seemed much less between the years (Figure 165). These differences therefore seemed to be mainly due to leaf tissue water content differences, which could have been caused by the cooler, wetter conditions in season two. The same trend and magnitude of differences were observed for the TSLM values, which compared well to the EWT results (data not shown).

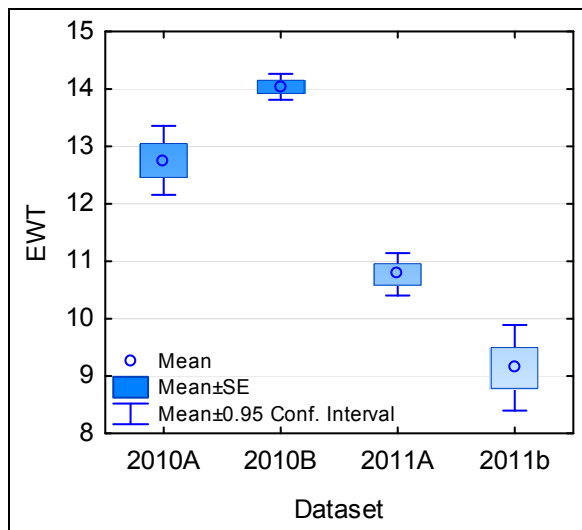


Figure 164 Equivalent water thickness (EWT, $\text{mg}\cdot\text{cm}^{-2}$) for the different spectral datasets collected for leaf structure and water content calibration (means, standard errors and 95% confidence intervals as indicated on graph).

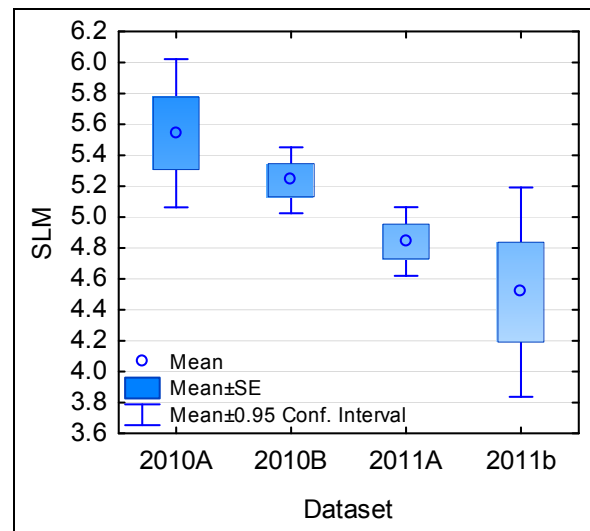


Figure 165 Specific leaf mass (SLM, $\text{mg}\cdot\text{cm}^{-2}$) for the different spectral datasets collected for leaf structure and water content calibration (means, standard errors and 95% confidence intervals as indicated on graph).

Linear regression analysis of the relationship between TSLM and the leaf absorption of NIR radiation (Figure 166) revealed some outlying values. These represented the youngest leaves, with TSLM values below $8 \text{ mg}\cdot\text{cm}^{-2}$. Considering that these leaves accounted for less than 2.5% of the total dataset, they were removed, thereby improving the relationship to $R^2 = 0.70$ ($p \leq 0.001$).

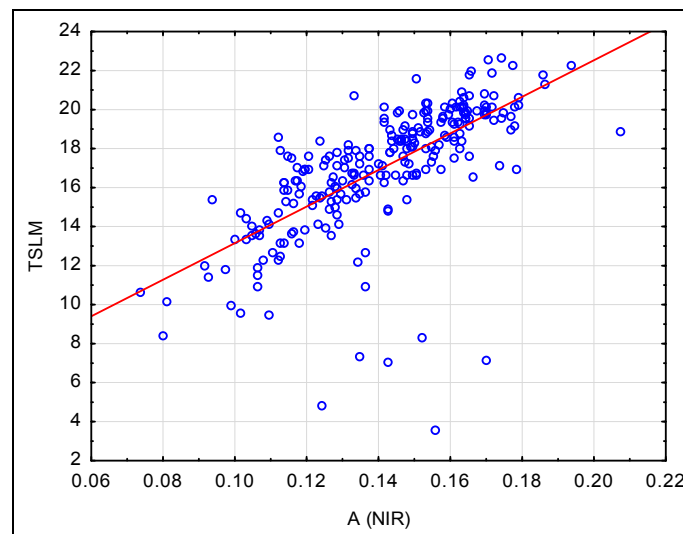


Figure 166 Relationship between total specific leaf mass (TSLM) and the absorption of near-infrared radiation [A (NIR), 700-1400 nm] for the spectral datasets used to predict leaf structure and water content parameters, $R^2 = 0.46$ ($p \leq 0.001$).

Results from PLS 1 prediction of specific leaf mass (SLM) were not very promising, with a minimum of six principal components (PC's) required to minimise the y -residual validation variance, and relatively higher root-mean square error of cross-validation (RMSECV) (Table 45). Even though the RMSECV may be acceptable, considering the variable conditions found in these canopies, it is always risky to include more PC's due to the danger of over-fitting and noise amplification in the data (Esbensen *et al.*, 2002). It was therefore decided to use PLS 2 regression to model total specific leaf mass (TSLM) along with the EWT, with both showing better PLS 1 results. The PLS 2 model performed better, which means that it was possible to compute the SLM from these two modelled parameters (TSLM - EWT = SLM) in a single prediction. Both parameters

were effectively modelled in three principal components, leading to a model with a root mean square error of prediction (RMSEP) for EWT and TSLM of less than 1.00 mg.cm⁻². Basic statistics from the predicted values are shown in Table 46. The TSLM and EWT linear relationship was also very strong ($R^2 = 0.90$; $p \leq 0.001$), creating another option for calculating SLM by using the linear regression equation along with a PLS 1 regression from either one of the parameters (TSLM or EWT).

Table 45 Prediction diagnostics for leaf structural and water content parameters using partial least squares (PLS) regression.

Parameter (mg.cm ⁻²)	N	Min PC's	RMSECV (mg.cm ⁻²)	RMSECV (%)	Slope	Offset	R ²
TSLM	253	2	1.22	7.2	0.83	2.92	0.83
EWT	253	3	0.78	6.5	0.86	1.71	0.85
SLM	253	6	0.50	10.0	0.79	1.06	0.78
TSLM and	253	3 (PLS2)	0.97	5.7	0.88	2.11	0.88
EWT	253		0.77	6.5	0.87	1.63	0.86

Min PC's - Minimum principal components required to minimise the RMSECV
RMSECV (%) is expressed relative to the means of the respective parameters.

Table 46 Results from leaf structure and water content parameters predicted using PLS 2 regression calibration of TSLM and EWT, with manual calculation of the SLM values.

Dataset	Parameter	Valid N	Mean	Minimum	Maximum	Std.Dev.
All groups	TSLM (mg.cm ⁻²)	253	17.18	7.29	22.49	2.69
	SLM (mg.cm ⁻²)	253	5.08	1.42	6.51	0.88
	EWT (mg.cm ⁻²)	253	12.10	5.87	16.31	1.93
2010A	TSLM (mg.cm ⁻²)	30	18.32	11.87	22.00	2.49
	SLM (mg.cm ⁻²)	30	5.11	2.41	6.51	1.03
	EWT (mg.cm ⁻²)	30	13.20	9.47	15.49	1.46
2010B	TSLM (mg.cm ⁻²)	80	19.28	14.38	22.00	1.41
	SLM (mg.cm ⁻²)	80	5.39	3.43	6.46	0.57
	EWT (mg.cm ⁻²)	80	13.89	10.94	15.68	0.85
2011A	TSLM (mg.cm ⁻²)	123	15.95	9.00	22.49	2.19
	SLM (mg.cm ⁻²)	123	4.95	2.13	6.26	0.85
	EWT (mg.cm ⁻²)	123	11.00	6.87	16.31	1.37
2011B	TSLM (mg.cm ⁻²)	20	14.70	7.29	19.28	3.26
	SLM (mg.cm ⁻²)	20	4.57	1.42	6.43	1.36
	EWT (mg.cm ⁻²)	20	10.13	5.87	12.85	1.91

When only spectra above 700 nm was considered (Figure 167), the grouping between the datasets from different years became evident, which was not the case when visible spectra were included. There were also very slight improvements in the model performance.

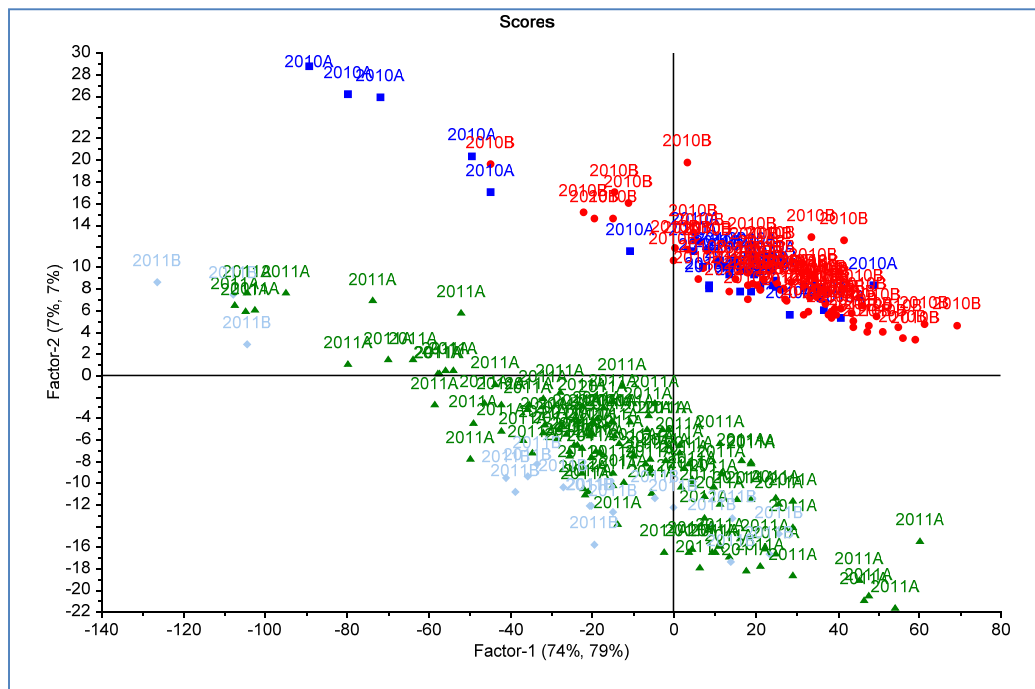


Figure 167 Score plot of partial least squares (PLS 2) regression of TSLM and EWT using spectral data in the 700-2500 nm range for the leaf structure and water content calibration dataset.

Univariate regression analysis of the TSLM and EWT parameters against spectral data (Figure 168) revealed strong correlations in certain wavelengths above 1300 nm for both parameters. A selection of two wavelengths was made to evaluate to what extent the x-matrix (spectral data) in the PLS 2 can be minimised. A region with strong correlations for both parameters were selected, and the single wavelengths, 1836 nm and 1837 nm, were isolated (PLS 2 analysis requires at least two wavelengths). The analysis yielded a PLS 2 model needing a single PC to reach minimum validation variance, with a RMSEP of 1.08, slope of 0.85, offset of 2.53 and correlation (R^2) of 0.85, which suggests the whole model is still valid, and even more so due to less noise, for only two wavelengths. It therefore seems possible to create linear regressions for both TSLM and EWT, using any one of the strong correlating wavelengths, use the equations to predict these two parameters, and then calculate the SLM (Figure 169). Similar approaches than these can be followed to create or evaluate simple spectral ratio indices from the results of uni- or multivariate analyses. What has to be considered, however, is that the spectral source from which prediction is performed may have specific complicating factors in the selected wavelengths (noise, baseline shifts, etc.), which may make the use of single-wavelengths (or narrow-band selections) more risky than modelling full or partial spectra.

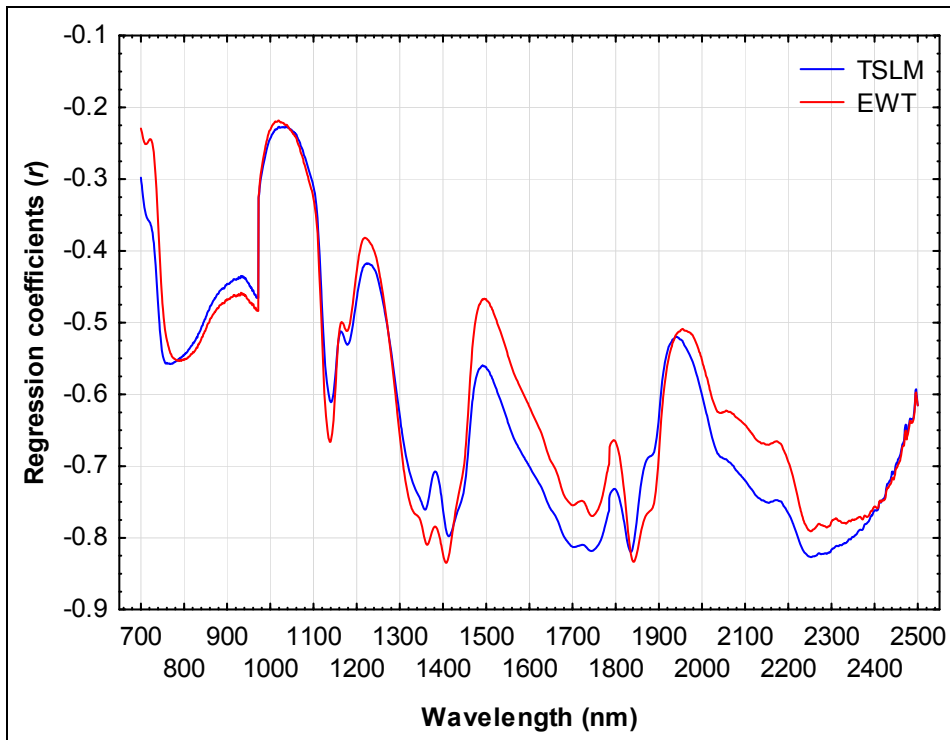


Figure 168 Correlogram of regression coefficients retrieved from assessing the linear relationship between spectral data and TSLM as well as EWT.

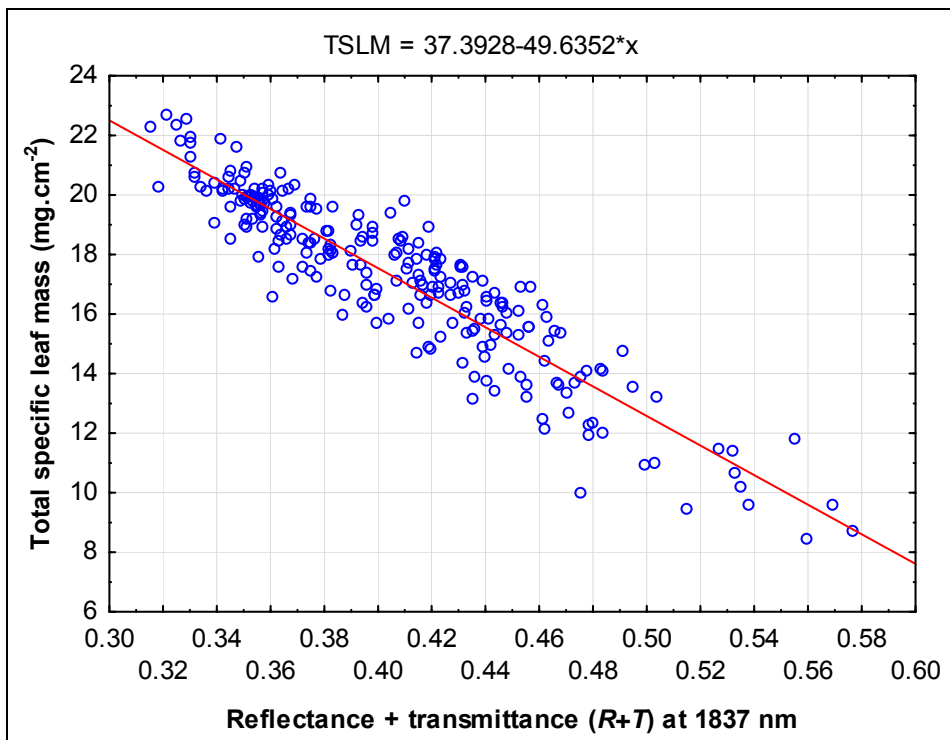


Figure 169 Relationship between total specific leaf mass (TSLM) and a single wavelength (1837 nm) measured for the leaf dataset used for spectral calibration of leaf structure and water content, $R^2 = 0.85$ ($p \leq 0.001$).

7.3.3 Univariate regressions of leaf pigments

Univariate regressions were performed for several grapevine leaf pigments or related ratios and leaf reflectance + transmittance data (Figure 170).

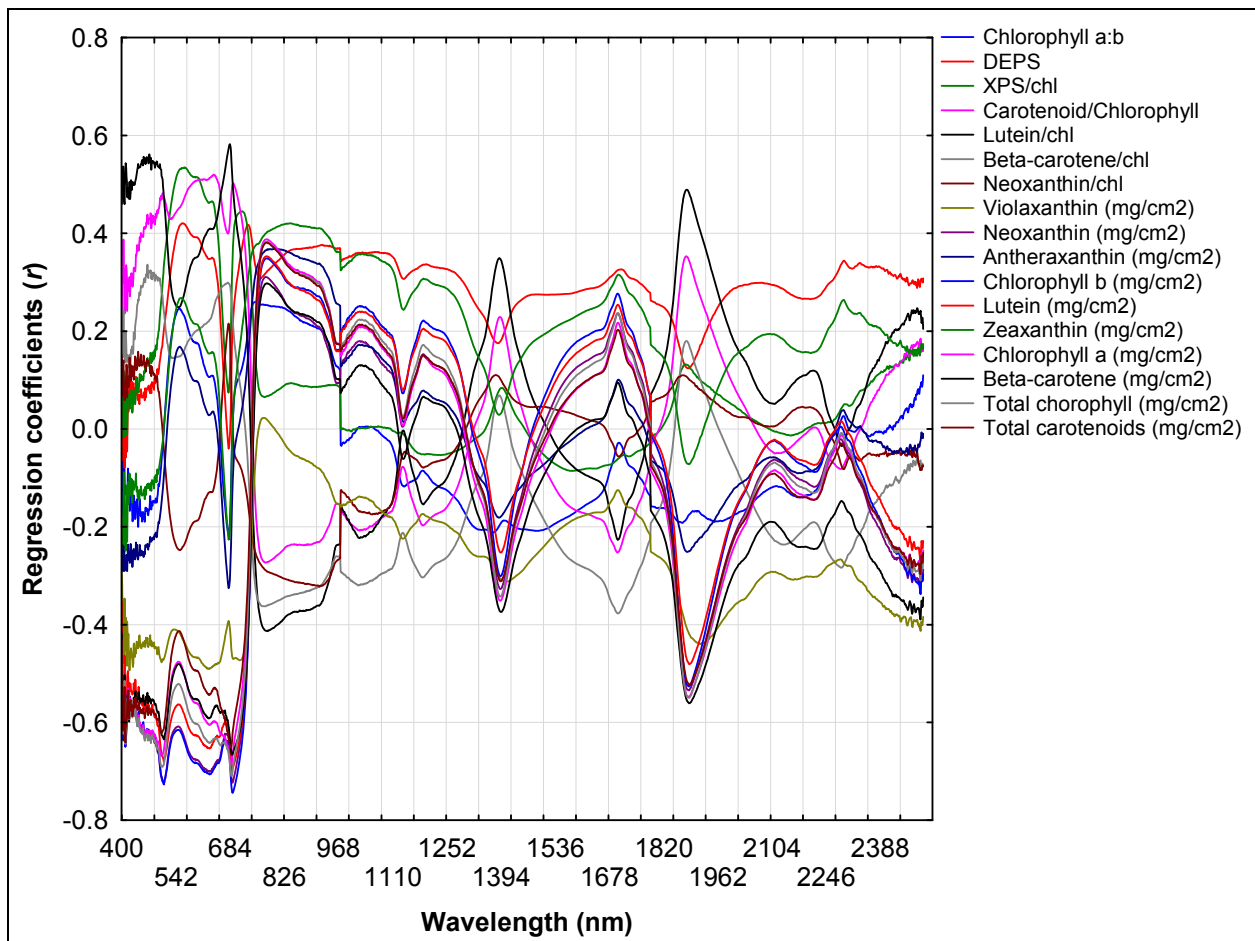


Figure 170 Univariate regressions for several grapevine leaf pigments or related ratios created from relationships with leaf reflectance + transmittance data.

Two of the strongest negative and positive regression coefficient wavelengths (778 and 687 nm) were selected for total chlorophyll, and a modified simple spectral ratio (Rodríguez-Pérez *et al.*, 2007) was computed for each leaf. The relationship with measured total chlorophyll values was strong (Figure 171), but still inferior to the result from PLS 1 regression (Figure 172).

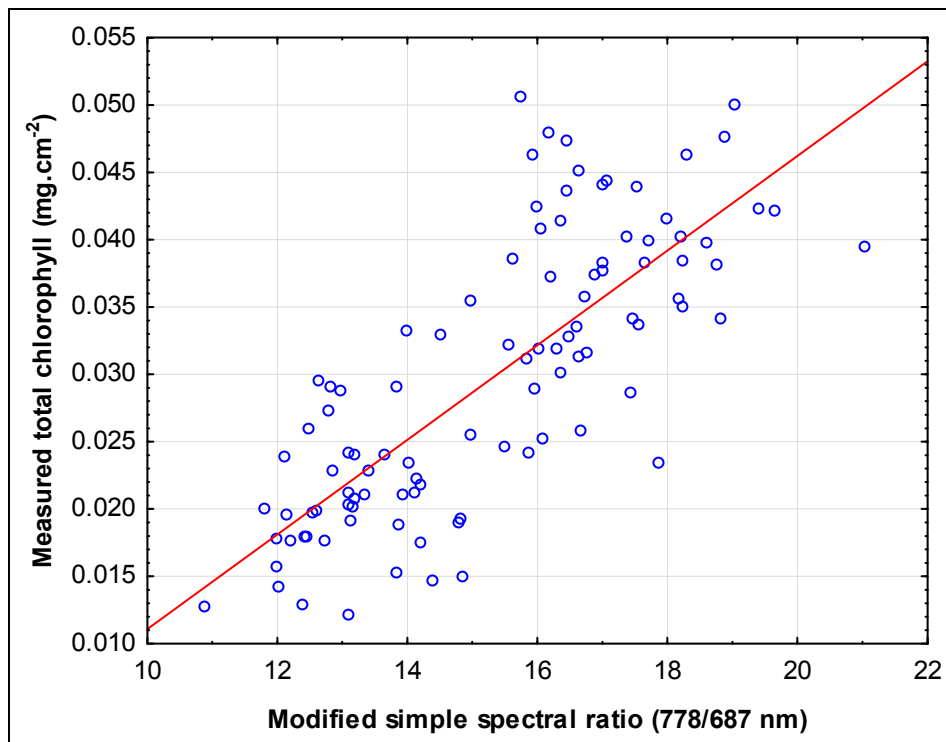


Figure 171 Measured total chlorophyll values for primary shoot leaves *versus* a simple ratio (778/787 nm) calculated from reflectance+transmittance spectra, $R^2 = 0.60$ ($p \leq 0.001$)

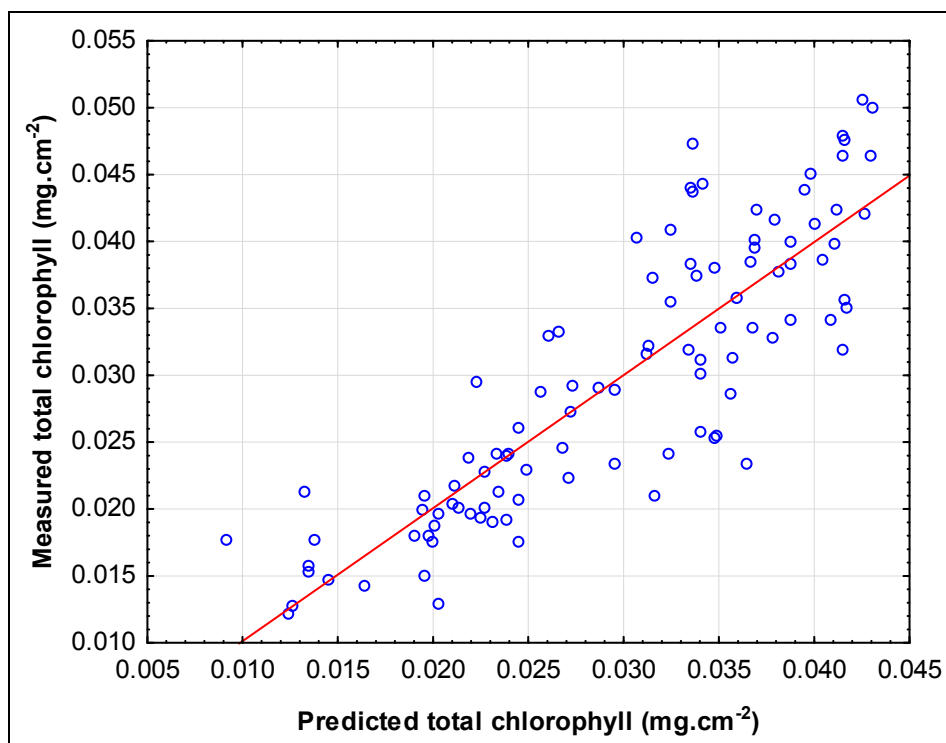


Figure 172 Measured total chlorophyll values for primary shoot leaves *versus* total chlorophyll, predicted using PLS regression, $R^2 = 0.74$ ($p \leq 0.001$).

7.3.4 Multivariate calibration and prediction of leaf pigment content

Chlorophyll *b* and lutein turned out to be the easiest pigments to model using the PLS approach in Shiraz primary shoot leaves (Table 47). The modelling of the DEPS ratio and the xanthophylls, except for neoxanthin, was problematic. A closer inspection of the score and loading plots in the PLS model of the DEPS ratio revealed differential effects of leaf age and water status, which would be difficult to separate prior to modelling. Non-linear behaviour was also detected in the predicted

versus measured value plots, especially for violaxanthin and antheraxanthin, but possibly also for chlorophyll *a*. Another advantage of PLS modelling is that it tolerates slight non-linearity in the data, with the effect being a model with more PC's (Esbensen *et al.*, 2002). This non-linearity was for instance very strong in violaxanthin, which rendered the model virtually useless. For chlorophyll *a* the observed non-linearity may be related to the saturation effect in certain spectral wavelengths caused by high chlorophyll values, which was also mentioned by Merzlyak *et al.* (2003a). In general, the PLS models seemed to account for this well enough, even though the RMSECV was relatively high. Here, the RMSECV was, however, conservatively expressed relative to mean pigment values. If the RMSECV is calculated according to the range of measured total chlorophyll values, it would be reduced to 13.2%. Basic statistics of the prediction of season one's pigment data are shown in Table 48, which can be compared to the basic statistics for the same dataset shown in Chapter V.

Table 47 Prediction diagnostics for leaf pigment content parameters using partial least squares (PLS) regression analysis of reflectance + transmittance (*R+T*) spectra (raw spectra, no smoothing or derivation).

Parameter	N	Min PC's	RMSECV (mg.cm ⁻²)	RMSECV (%)	Slope	Offset	R ²
Total chlorophyll (mg.cm ⁻²)	102	7	0.0054	19.3	0.74	0.0070	0.72
Total carotenoids (mg.cm ⁻²)	102	7	0.0010	16.7	0.71	0.0017	0.66
Chlorophyll <i>a:b</i> ratio	102	8	0.24	10.0	0.54	1.120	0.46
DEPS ratio	102	10	0.171	48.9	0.63	0.134	0.52
Carotenoid:chloro-phyll ratio	102	6	0.018	8.7	0.51	0.101	0.45
Lutein (mg.cm ⁻²)	102	4	0.00030	15.0	0.66	0.0007	0.64
β-carotene (mg.cm ⁻²)	102	6	0.00028	20.0	0.67	0.0005	0.62
Neoxanthin (mg.cm ⁻²)	102	9	0.00014	15.6	0.82	0.00016	0.78
Antheraxanthin (mg.cm ⁻²)	102	8	0.00015	50.0	0.52	0.00016	0.45
Chlorophyll <i>b</i> (mg.cm ⁻²)	102	4	0.0014	17.1	0.77	0.0019	0.76
Zeaxanthin (mg.cm ⁻²)	102	8	0.00030	75.0	0.57	0.00021	0.47
Chlorophyll <i>a</i> (mg.cm ⁻²)	102	7	0.0040	20.1	0.76	0.0050	0.72
Violaxanthin (mg.cm ⁻²)	102	4	0.00032	45.7	0.30	0.00048	0.25

Min PC's - Minimum principal components required to minimise the RMSECV
 RMSECV (%) is expressed relative to the means of the respective parameters.

Table 48 Basics statistics of prediction results from partial least squares (PLS) regression analysis of reflectance + transmittance (*R+T*) spectra collected in season one.

Parameter	N	Mean	Min	Max	SD
Total chlorophyll (mg.cm ⁻²)	102	0.0295	0.0022	0.0470	0.0096
Total carotenoids (mg.cm ⁻²)	102	0.0060	0.0018	0.0087	0.0015
Chlorophyll <i>a:b</i> ratio	102	2.4275	1.9174	3.1906	0.2546
DEPS ratio	102	0.3536	-0.0435	1.1658	0.2110
Carotenoid:chlorophyll ratio	102	0.2064	0.1731	0.2451	0.0180
Lutein (mg.cm ⁻²)	102	0.0021	0.0010	0.0028	0.0004
β-carotene (mg.cm ⁻²)	102	0.0015	0.0004	0.0023	0.0004
Violaxanthin (mg.cm ⁻²)	102	0.0007	0.0000	0.0012	0.0002
Neoxanthin (mg.cm ⁻²)	102	0.0009	0.0003	0.0014	0.0003
Antheraxanthin (mg.cm ⁻²)	102	0.0003	0.0001	0.0008	0.0002
Chlorophyll <i>b</i> (mg.cm ⁻²)	102	0.0086	0.0027	0.0126	0.0025
Zeaxanthin (mg.cm ⁻²)	102	0.0005	-0.0001	0.0017	0.0003
Chlorophyll <i>a</i> (mg.cm ⁻²)	102	0.0210	0.0028	0.0343	0.0067

Principal component analysis (PCA) was also performed on the *R+T* spectra collected for primary shoot leaves on measurement dates A to E. Groupings in the score plots were well-defined for measurement dates D and E and the merged dataset was used in further investigations. The first principal component, which explained 73% of the spectral variance in the dataset according to the x-loadings plot (Figure 173), mostly incorporated differences in the TSLM (levels indicated on Figure 174). This was also probably linked to the higher loadings in the spectra above 800 nm. The second principal component was explained mostly by the differences between measurement dates (D and E), and was probably linked to pigment and water content differences that could have caused the high loadings in the pigment absorption area (400-700 nm) and the water absorption areas (1400 and 1900 nm) (Figure 175 and Figure 176). Together, these two principal components described 86% of spectral variance. The strength of the 800 nm region for pigment ratios or water content (Slaton *et al.*, 2001) was confirmed by the reaction in PC2. The third PC was similar to the second, with lower influence in the longer wavelengths and with no clear grouping observed in the score plots (Figure 177). Large differences in chlorophyll and carotenoid contents have already been shown between measurement dates D and E (chapter V). The dynamics between pigment content and water content in tissue need further attention.

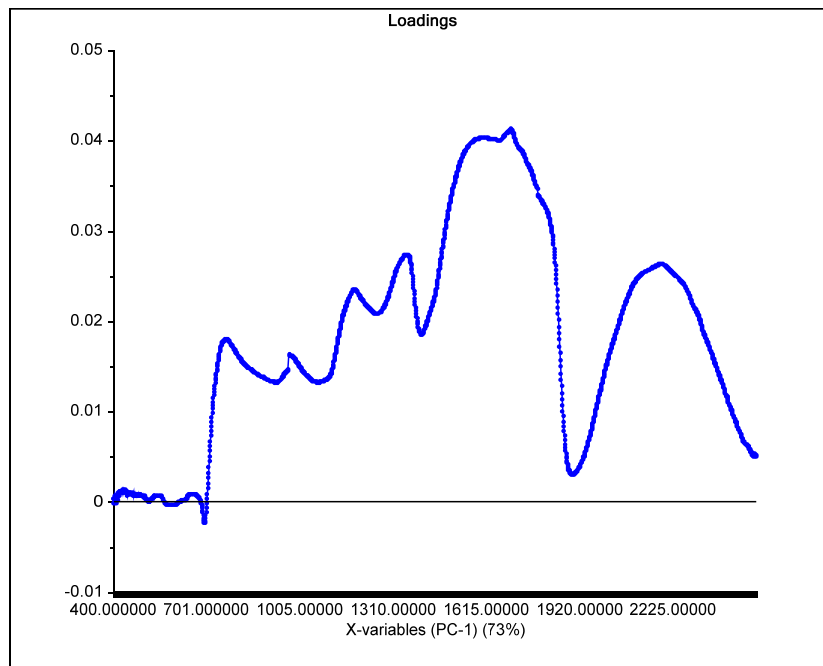


Figure 173 Spectral loadings in the first principal component calculated during principal component analysis of primary shoot leaf spectra in season one.

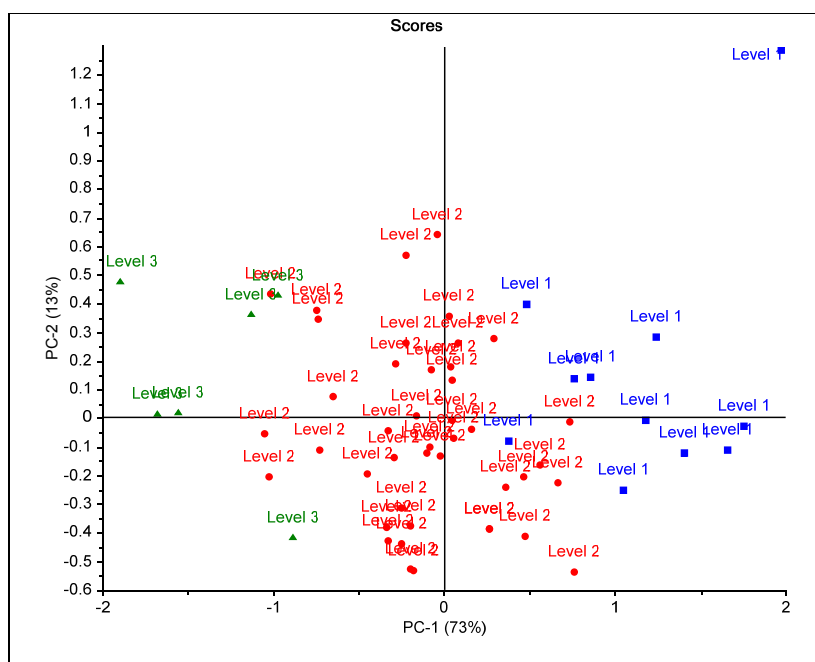


Figure 174 Score plot for the first (horizontal) and second (vertical) principal component calculated during principal component analysis of primary shoot leaf spectra in season one (level one represents TSLM values between 14.7 and 17.1 $\text{mg}\cdot\text{cm}^{-2}$, level two between 17.1 and 19.5 $\text{mg}\cdot\text{cm}^{-2}$ and level three between 19.5 and 21.9 $\text{mg}\cdot\text{cm}^{-2}$).

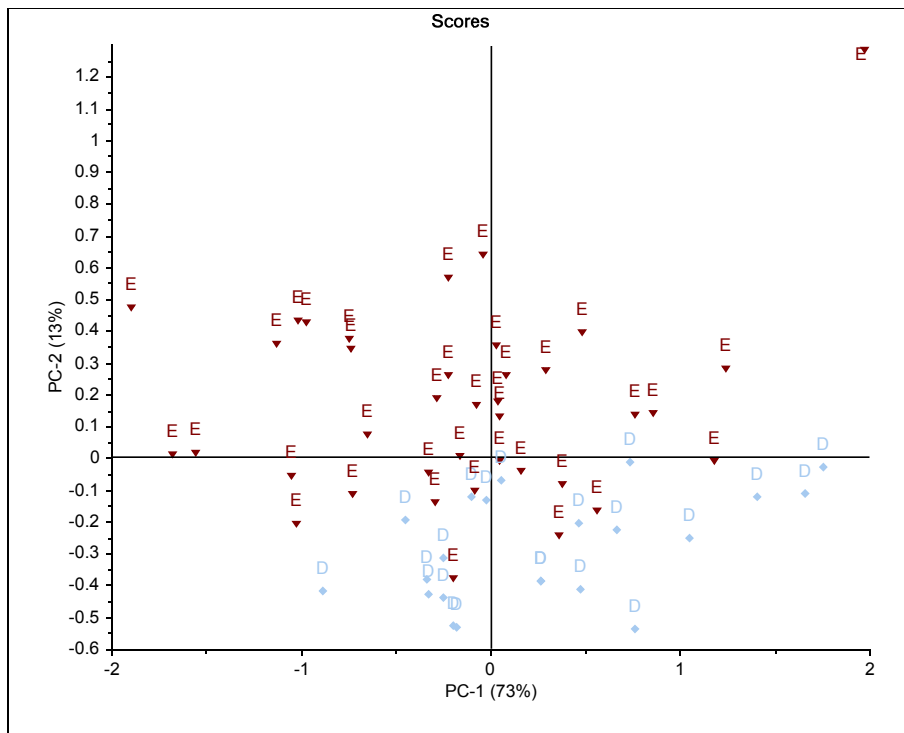


Figure 175 Score plot for the first (horizontal) and second (vertical) principal component calculated during principal component analysis of primary shoot leaf spectra in season one (The letter D represents measurement date D and E represents measurement date E).

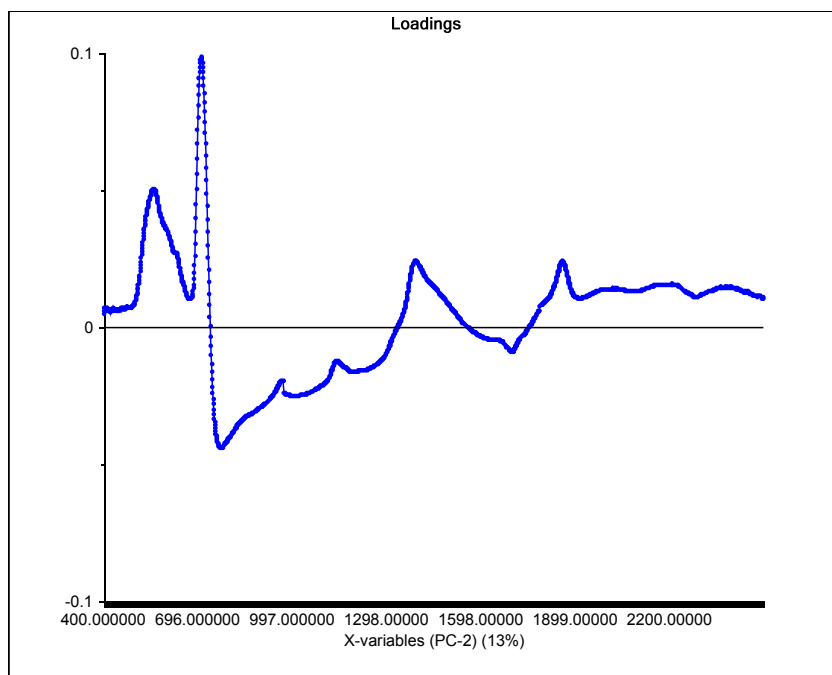


Figure 176 Spectral loadings in the second principal component calculated during principal component analysis of primary shoot leaf spectra in season one.

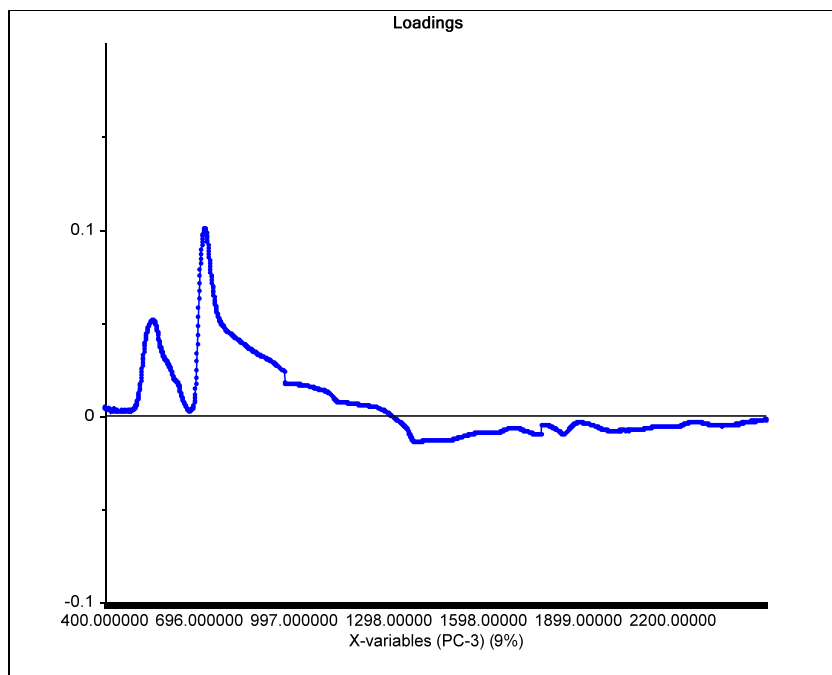


Figure 177 Spectral loadings in the third principal component calculated during principal component analysis of primary shoot leaf spectra in season one.

Additional validation was performed to evaluate the prediction models for a different dataset (test set) which was compiled from only secondary shoot leaves for which pigments were also measured. Leaf total chlorophyll content prediction was acceptable for the secondary shoot leaves, even though these leaves generally had lower chlorophyll contents (refer to Chapter V) (Figure 178). The other parameters were not always reliably predicted for the secondary shoot leaves (Table 49), and it is interesting that the results suggest that it is better to calculate the chlorophyll *a:b* ratio after prediction on a new dataset than to use the chlorophyll *a:b* predicted values. This was also the case for primary shoot leaves in the original model. Contrary to this, it seems advisable to calculate total carotenoids from the carotenoid:chlorophyll ratio, as this was more reliably predicted. This illustrates the importance of reviewing prediction diagnostics before performing prediction on a new dataset, as the chlorophyll *a:b* ratio showed a low coefficient of determination ($R^2 = 0.46$) along with a high number of PC's required for modelling (eight), compared to the lower number of PC's required in the carotenoid:chlorophyll model (six), but a similar coefficient of determination ($R^2 = 0.45$). The low predicted *versus* measured coefficients of determination for lutein and β -carotene was surprising, considering acceptable modelling from full cross-validation on the primary shoot leaves. This may be due to a different carotenoid pigment composition in the generally younger leaves of the secondary shoots.

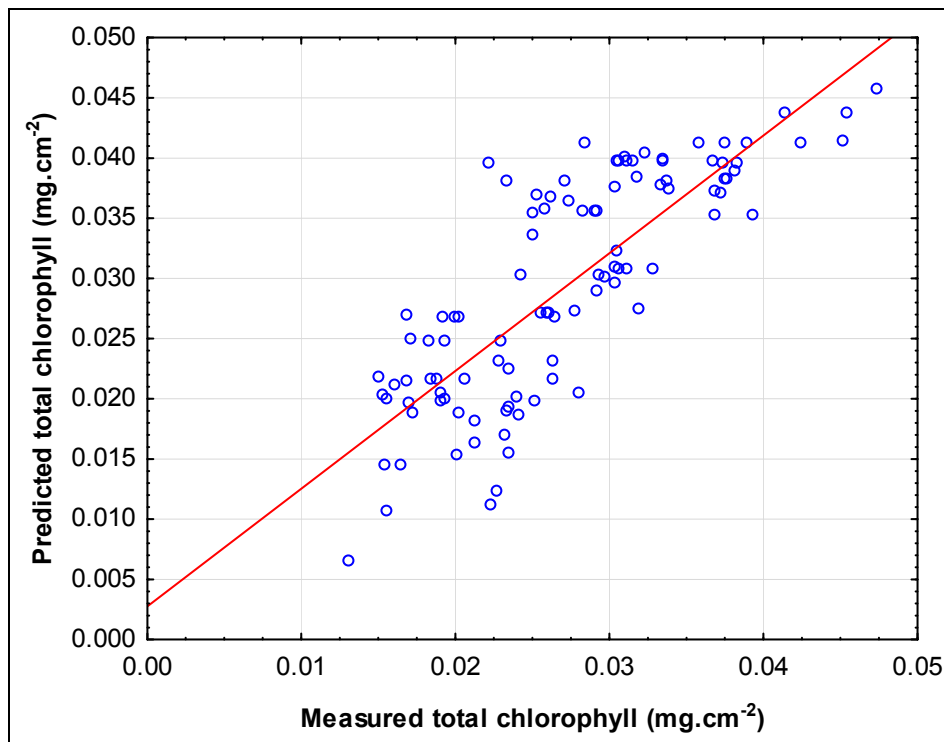


Figure 178 Predicted versus measured total chlorophyll content ($\text{mg}\cdot\text{cm}^{-2}$) of secondary shoot leaves from a partial least-squares (PLS) model created from primary shoot leaves, $r = 0.81$, $R^2 = 0.65$ ($p \leq 0.001$).

Table 49 Results from regression analysis between the predicted and measured values of secondary shoot leaves, based on a partial least-squares (PLS) model created from primary shoot leaves.

Parameter	Regression results
Total chlorophyll ($\text{mg}\cdot\text{cm}^{-2}$)	$r = 0.81$; $p \leq 0.001$; $R^2 = 0.65$
Total carotenoids ($\text{mg}\cdot\text{cm}^{-2}$)	$r = 0.62$; $p \leq 0.001$; $R^2 = 0.38$
Chlorophyll a:b ratio	$r = 0.64$; $p \leq 0.001$; $R^2 = 0.41$
DEPS ratio	$r = 0.77$; $p \leq 0.001$; $R^2 = 0.59$
Carotenoid:chlorophyll ratio	$r = 0.79$; $p \leq 0.001$; $R^2 = 0.63$
Lutein ($\text{mg}\cdot\text{cm}^{-2}$)	$r = 0.55$; $p \leq 0.001$; $R^2 = 0.30$
B-carotene ($\text{mg}\cdot\text{cm}^{-2}$)	$r = 0.59$; $p \leq 0.001$; $R^2 = 0.35$
Neoxanthin ($\text{mg}\cdot\text{cm}^{-2}$)	$r = 0.79$; $p \leq 0.001$; $R^2 = 0.62$
Chlorophyll b ($\text{mg}\cdot\text{cm}^{-2}$)	$r = 0.77$; $p \leq 0.001$; $R^2 = 0.60$
Chlorophyll a ($\text{mg}\cdot\text{cm}^{-2}$)	$r = 0.80$; $p \leq 0.001$; $R^2 = 0.64$

7.3.5 “Photochemical reflectance index” performance

The photochemical reflectance index (PRI) (Gamon *et al.*, 1997) was developed to assess changes in the photoprotective xanthophyll pigments, but was also shown to respond to carotenoid:chlorophyll ratios (Sims & Gamon, 2002). In accordance with the results from this study (Figure 179), Blanchfield *et al.* (2006) also found relatively weak ($R^2 < 0.45$) correlations between the PRI index and carotenoid:chlorophyll ratios, and it seemed to be driven more by the differences between cultivars than between leaves/treatments in that study.

Results were also split into different sampling dates and leaf age classes (Table 50 and Table 51), which revealed that the correlation was the strongest for the first two sampling dates and youngest leaf age class, indicating that it is more sensitive to leaf age differences than water status/stress differences in leaves *per se*.

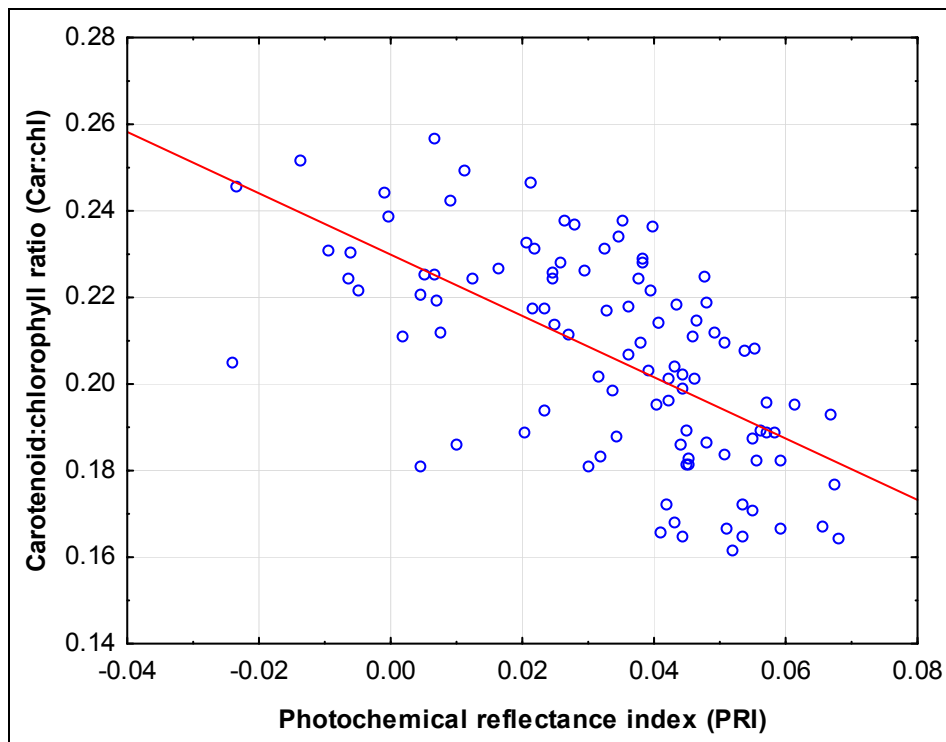


Figure 179 Relationship between the carotenoid:chlorophyll ratios of primary shoot leaves and the photochemical reflectance index (PRI), $r = -0.62$, $R^2 = 0.39$ ($p \leq 0.001$).

Table 50 Results from regression analysis between the carotenoid:chlorophyll ratio and PRI index ($531 \text{ nm} - 570 \text{ nm}) / (531 \text{ nm} + 570 \text{ nm})$ calculated from reflectance+transmittance spectral of primary shoot leaves in Shiraz for the different sampling dates.

Sampling date	Regression results
A	$r = -0.96$, $p = 0.00001$; $R^2 = 0.93$
B	$r = -0.81$, $p = 0.0004$; $R^2 = 0.66$
C	$r = -0.18$, $p = 0.4687$; $R^2 = 0.03$
D	$r = -0.43$, $p = 0.0477$; $R^2 = 0.18$
E	$r = -0.31$, $p = 0.0577$; $R^2 = 0.10$

Table 51 Results from regression analysis between the carotenoid:chlorophyll ratio and PRI index ($531 \text{ nm} - 570 \text{ nm}) / (531 \text{ nm} + 570 \text{ nm})$ calculated from reflectance+transmittance spectral of primary shoot leaves in Shiraz for the different chronological leaf age classes.

Leaf age class	Regression results
1	$r = -0.74$, $p = 0.0137$; $R^2 = 0.55$
2	$r = -0.64$, $p = 0.0003$; $R^2 = 0.41$
3	$r = -0.47$, $p = 0.0151$; $R^2 = 0.22$
4	$r = -0.58$, $p = 0.0018$; $R^2 = 0.34$
5	$r = -0.29$, $p = 0.3654$; $R^2 = 0.08$

7.3.6 PROSPECT inversion

Good results were obtained with PROSPECT ($R^2 = 0.68$) for the EWT inversion, but results for SLM ($R^2 = 0.11$) as well as for total chlorophyll ($R^2 = 0.26$) and total carotenoids ($R^2 = 0.10$) were disappointing. According to Stuckens *et al.* (2009), dry matter content has a much smaller impact on reflectance than hydrated cells, making it more difficult to model. This was also reported by others (Jacquemoud *et al.*, 1996; Feret *et al.*, 2008). Preliminary work using the “dorsiventral leaf model” (DLM) of Stuckens *et al.* (2009) also did not lead to improved models, but further work is required to optimise the minimisation algorithm as well as the plate model parameters for grapevine leaves. It was not yet possible to accurately predict chlorophyll and carotenoid values for

individual leaves using either PROSPECT inversion of the spectra or multivariate modelling. It seems that the interaction between leaf structure, pigment composition and radiation are complex, especially when small changes in pigments have to be detected.

7.3.7 Results from spectral predictions of TSLM, SLM and EWT

Changes in modelled TSLM, SLM and EWT values were almost exactly similar in trend over the measurement dates, showing an increase up to date B, a sharp decrease and then retaining constant levels for the last three measurement dates (Figure 180, Figure 182 and Figure 184). This was peculiar, as SLM is mostly reported to increase gradually with time as well as with higher leaf plastochron index values (Williams, 1987; Poni *et al.*, 1994b). Possible explanations for these trends are provided in section 7.3.1.2. These parameters also increased with leaf age up to class three, showing decreased levels in class four, and increasing again in the oldest leaf age class (Figure 181, Figure 183 and Figure 185). The decrease observed in leaf age class four could be due to shading in the part of the canopy where these leaves would mostly occur (lower half of the canopy for the largest part of the season). This age class was also only observed from measurement date D, when water deficits were already more developed. The increased values in class five indicate more advanced senescence in these leaves. The canopy manipulation treatments also had small (but statistically significant) effects on these parameters (Table 42, Table 53 and Table 54).

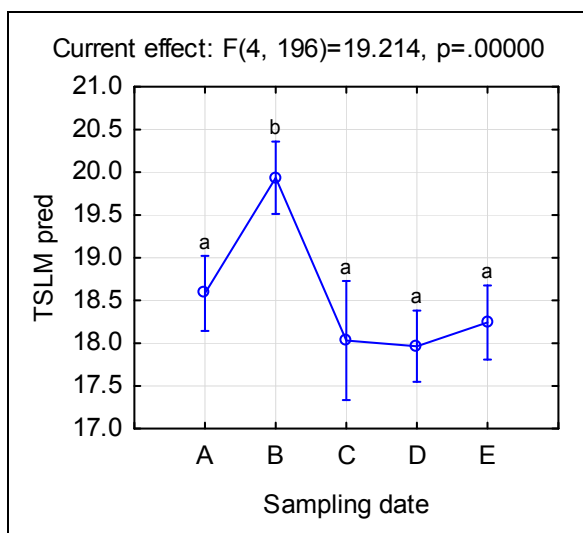


Figure 180 Primary shoot leaf predicted TSLM for the different sampling dates in season one (means with the same letters are not significantly different at the $p \leq 0.05$ level, vertical bars denote 95% confidence intervals).



Figure 181 Primary shoot leaf predicted TSLM for the different leaf age classes in season one (means with the same letters are not significantly different at the $p \leq 0.05$ level, vertical bars denote 95% confidence intervals).

Table 52 Predicted TSLM for the different treatments in season one. Means with different letters are significant at the $p \leq 0.05$ level ($F = 5.88$).

Treatment	N	TSLM	SD	% difference
NSF	113	18.37 a	1.47	2%
NSR	112	18.77 b	1.52	

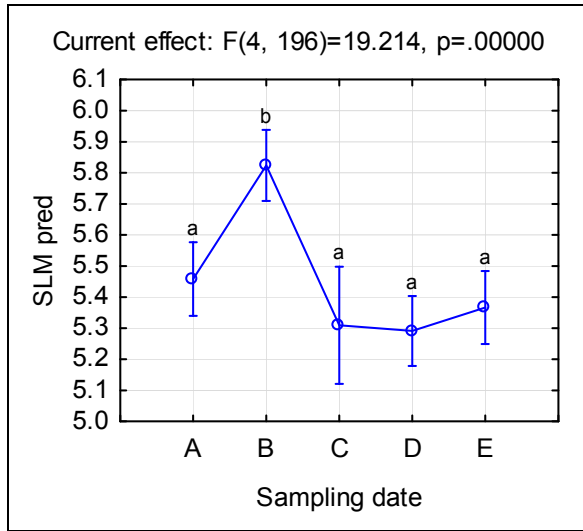


Figure 182 Primary shoot leaf predicted SLM for the different measurement dates in season one (means with the same letters are not significantly different at the $p \leq 0.05$ level, vertical bars denote 95% confidence intervals).

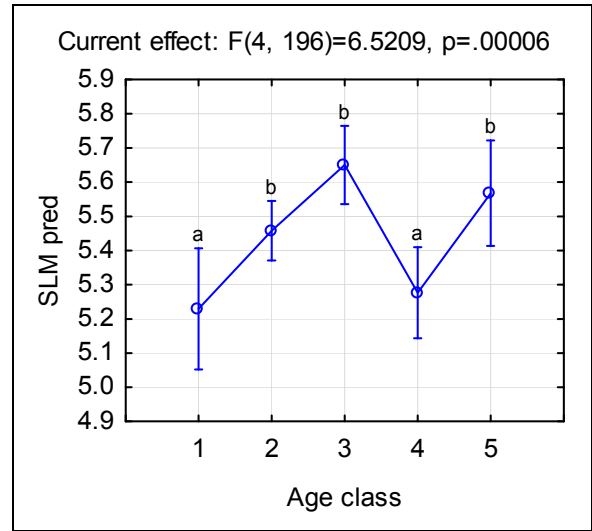


Figure 183 Primary shoot leaf predicted SLM for the different leaf age classes in season one (means with the same letters are not significantly different at the $p \leq 0.05$ level, vertical bars denote 95% confidence intervals).

Table 53 Primary shoot leaf predicted SLM for the different treatments in season one (means with different letters are significant at the $p \leq 0.05$ level, $F = 5.88$).

Treatment	N	SLM	SD	% difference
NSF	113	5.40	0.40	2%
NSR	112	5.51	0.41	

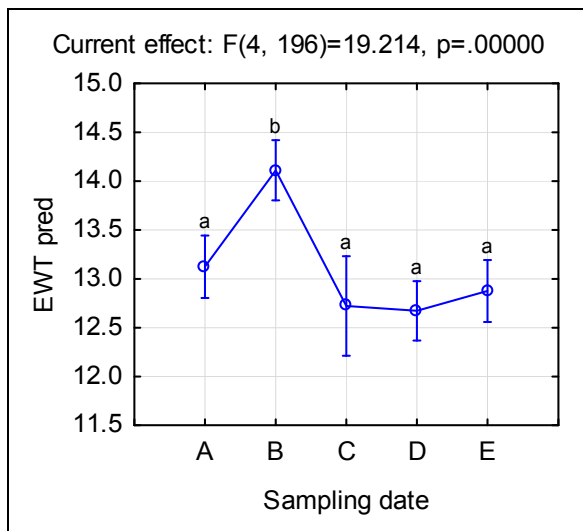


Figure 184 Primary shoot leaf predicted EWT for the different measurement dates in season one (means with the same letters are not significantly different at the $p \leq 0.05$ level, vertical bars denote 95% confidence intervals).



Figure 185 Primary shoot leaf predicted EWT for the different leaf age classes in season one (means with the same letters are not significantly different at the $p \leq 0.05$ level, vertical bars denote 95% confidence intervals).

Table 54 Primary shoot leaf predicted EWT for the different treatments in season one (means with different letters are significant at the $p \leq 0.05$ level, $F = 5.88$).

Treatment	N	EWT	SD	% difference
NSF	113	12.97	1.07	2%
NSR	112	13.26	1.11	

The predicted SLM values in season two showed almost consistent increase as the season progressed (Figure 186) and only seemed to marginally decrease for some treatments after 208 DAB. Possible reasons for the higher SLM values initially in the SF treatment were discussed in section 7.3.1.2. It is not clear what could have caused the fluctuations in the predicted SLM values between 56 and 74 DAB. The decrease seen at 56 DAB could be due to canopy filling at that stage in the full canopy treatment due to fast shoot growth, enhancing shaded conditions, which did not happen in the SR canopies.

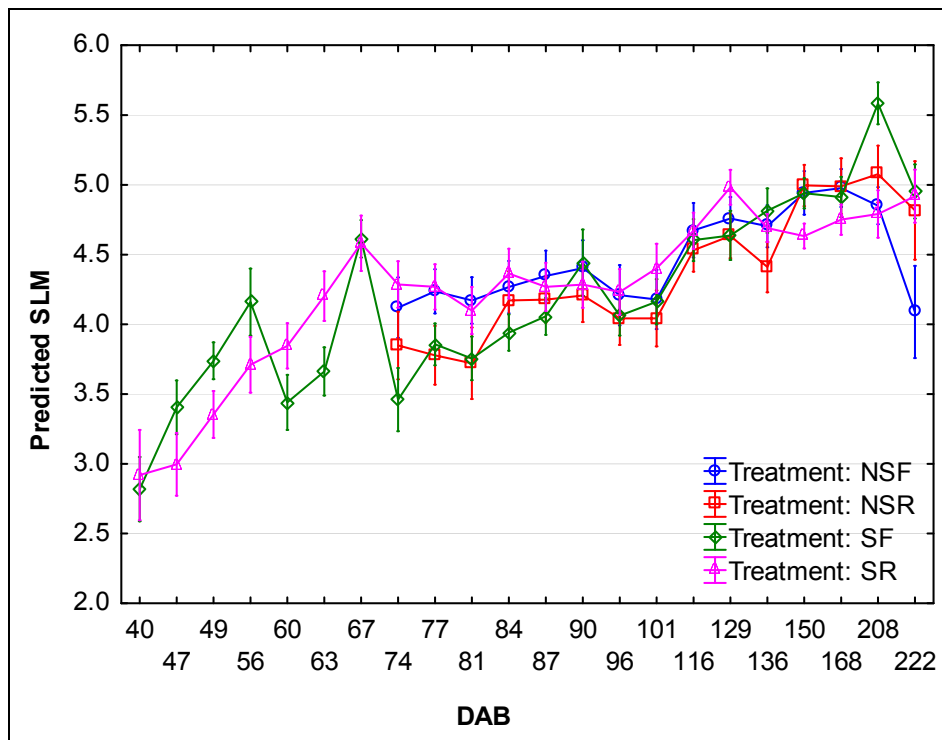


Figure 186 Predicted SLM values for the different dates after budburst and treatments in season two.

7.3.8 Leaf age prediction from spectra

A total of 2866 leaves, with defined chronological ages and spectra measured non-destructively on the same leaves throughout seasons two and three, were analysed using PLS analysis of mean-centered data. Model performance was weak with raw spectra, but modelling from first-derivative transformation of the spectra [Savitzky-Golay smoothing (Savitzky & Golay, 1964), with seven smoothing points yielded improved results] (Table 55).

Table 55 Leaf chronological age (days) prediction diagnostics

Parameter	Min PC's	RMSECV (days)	RMSECV (%)	Slope	Offset	R^2
Leaf chronological age (days) ¹	10	15.9	9.8	0.76	10.8	0.76
Leaf chronological age (days) ²	7	13.2 days	8.1	0.84	7.37	0.83

Min PC's - Minimum principal components required to minimise the RMSECV

RMSECV (%) is expressed relative to the maximum leaf age measured for these datasets, namely 163 days.

¹ computed using only mean-centered spectral data

² computed from Savitzky-Golay smoothing with seven smoothing points

7.3.9 Non-destructive prediction evaluation

Direct prediction of Ψ_{PD} from season two primary shoot leaf spectral data was not very successful, with the PLS models needing 11-15 PC's, therefore indicating very complex models, which may not be optimal when predicting Ψ_{PD} in new datasets (Table 56). The youngest leaf age class's prediction was much better, but still needed 11 PC's to reach minimum RMSECV.

Table 56 Prediction diagnostics and general statistics for predawn leaf water potential (Ψ_{PD}) (-KPa) using partial least squares (PLS) regression analysis of reflectance + transmittance (R+T) spectra collected during season two (raw spectra, no smoothing or derivation).

Parameter (mg.cm ⁻²)	N	Min PC's	RMSECV (- KPa)	RMSECV (%)	Slope	Offset	R ²
All leaf age classes	468	15	251.1	20	0.65	232.1	0.57
Age class 2	132	15	178.4	14	0.82	106.4	0.70
Age class 1	79	11	156.0	12	0.79	95.7	0.77

Min PC's - Minimum principal components required to minimise the RMSECV

RMSECV (%) is expressed relative to the range of the Ψ_{PD} values for this dataset.

	N	Mean	Minimum	Maximum	Range	Std.Dev.
Ψ_{PD} (- KPa)	468	659.2	256.0	1508.6	1252.6	384.8

A selection was made of leaf spectral data collected on primary shoots during season two in order to investigate possible interactions between leaf structure and water content, pigment content and predawn leaf water potential. The dataset represented a critical stage in the season with respect to plant water status, with two selected treatments, namely NSR and SR, showing different behaviour in terms of predawn leaf water potential (Figure 187). The portion where the SR treatment showed linear increase in Ψ_{PD} values was selected for further analysis (100 to 160 DAB) and the linear regression equations for these two treatments were used to estimate Ψ_{PD} for the dates on which spectral measurements were conducted (Figure 188).

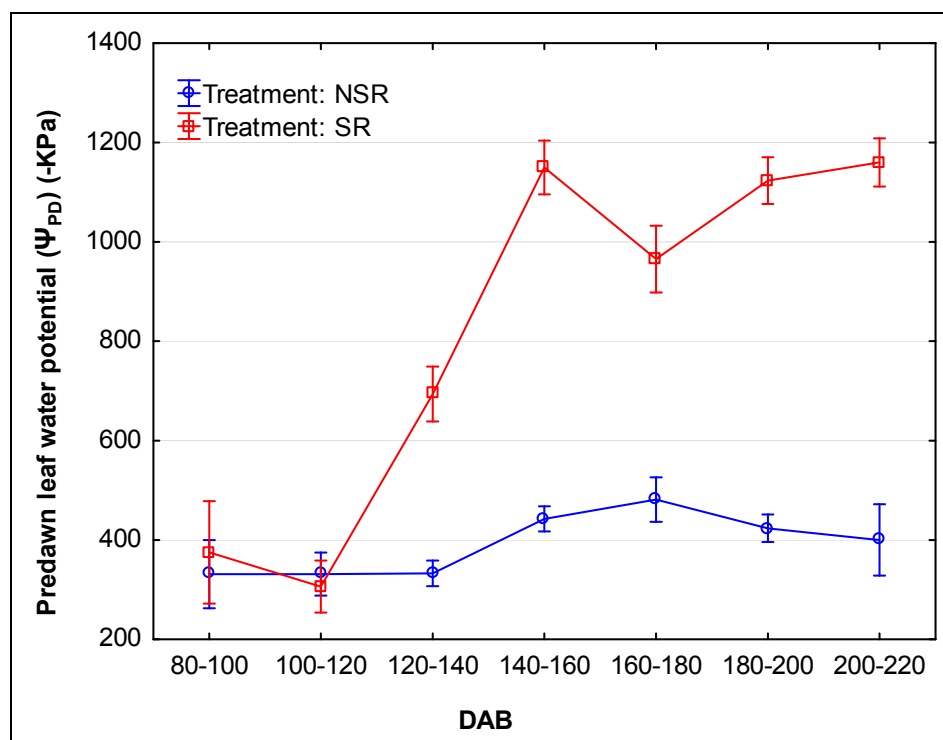


Figure 187 Predawn leaf water potential (Ψ_{PD}) (-KPa) for the NSR and SR treatments in season two for 20-day intervals of date after budburst (DAB) (vertical bars represent standard errors).

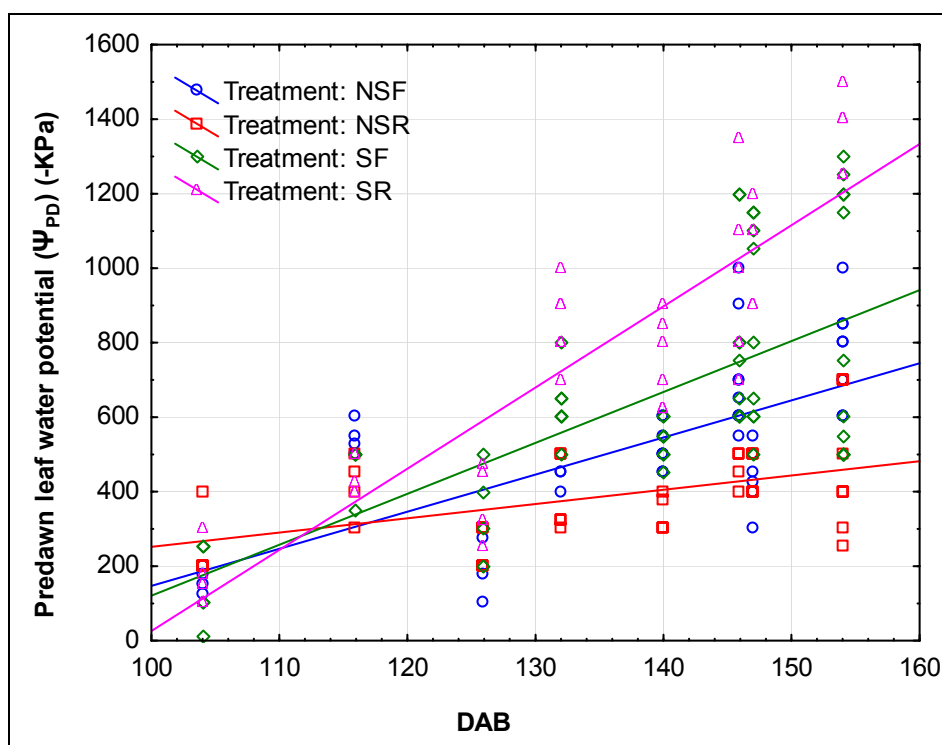


Figure 188 Relationship between predawn leaf water potential (Ψ_{PD}) (-KPa) and date after budburst (DAB) for the different treatments in season two (NSR: $\Psi_{PD} = -129.6 + 3.82$ (DAB); $R^2 = 0.24$; SR - $\Psi_{PD} = -2153.2 + 21.8$ (DAB); $R^2 = 0.78$; all $p \leq 0.001$).

The predicted TSLM and SLM values (Figure 189 and Figure 190) seemed to be higher in the SR treatments for the first measurement dates. This seemed to be limited to the youngest and oldest leaf age classes. For leaf age class four, this could have been due to possible increased early (pre 80 DAB) leaf loss (refer to % leaf loss results in Chapter III) in the SR and SF treatments compared to the NS treatments, which could have increased canopy exposure further in the lower canopy sections. The SR treatment also tended to have lower main cane mass per vine compared to the NSR treatment, but this was not accompanied by smaller leaves or shorter shoot lengths. Only the results of leaf chronological age classes two to four are presented, as the other classes were not well enough represented in all of the measurement dates for comparison purposes. The absence of any measurable class five leaves in the SR treatments up to 208 DAB, in contrast to the NSR treatment, confirms the early main shoot leaf loss/damage observed earlier.

The EWT decreased, especially in older leaves, when the lowest Ψ_{PD} values were reached in the SR treatment. However, regressions that were created for the different leaf age classes as well as treatments between EWT and Ψ_{PD} all yielded coefficients of determination of less than $R^2 = 0.11$. The decrease in EWT therefore seemed not to be progressive, but only occurred after prolonged critical water deficit levels. Even then, the levels were in general (for all leaf classes) not below that of the NSR canopy. In this part of the season, the lowest EWT was found in the younger leaf classes, which is in contrast to the findings of Rodríguez-Pérez *et al.* (2007) for Pinot noir canopies.

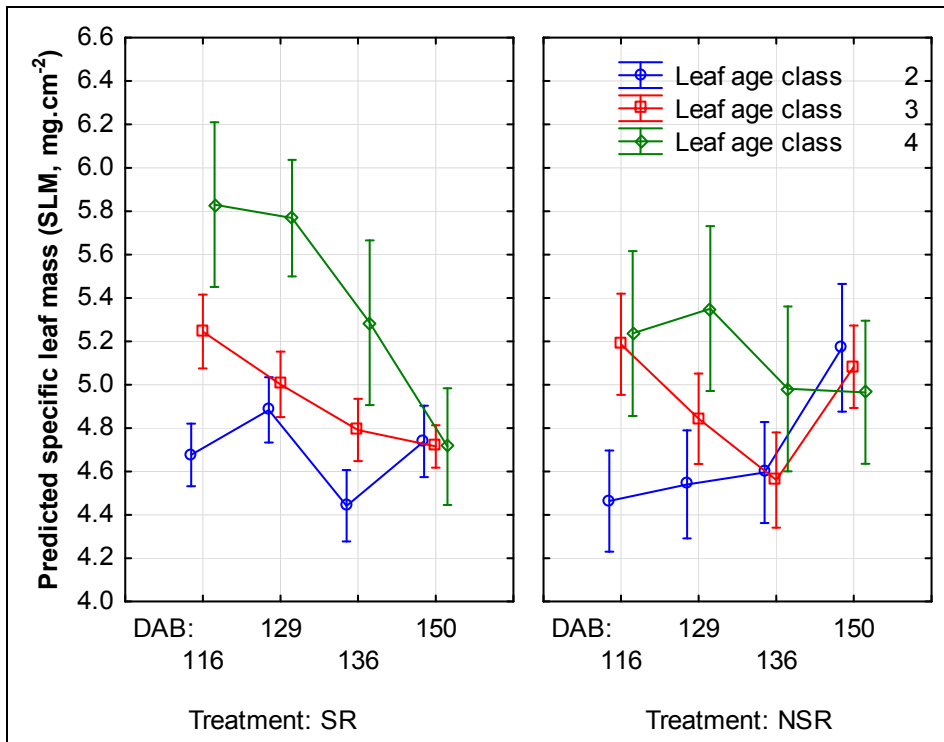


Figure 189 Predicted specific leaf mass (mg.cm^{-2}) values for selected measurement dates, leaf chronological age classes and treatments in season two (vertical bars denote standard errors).

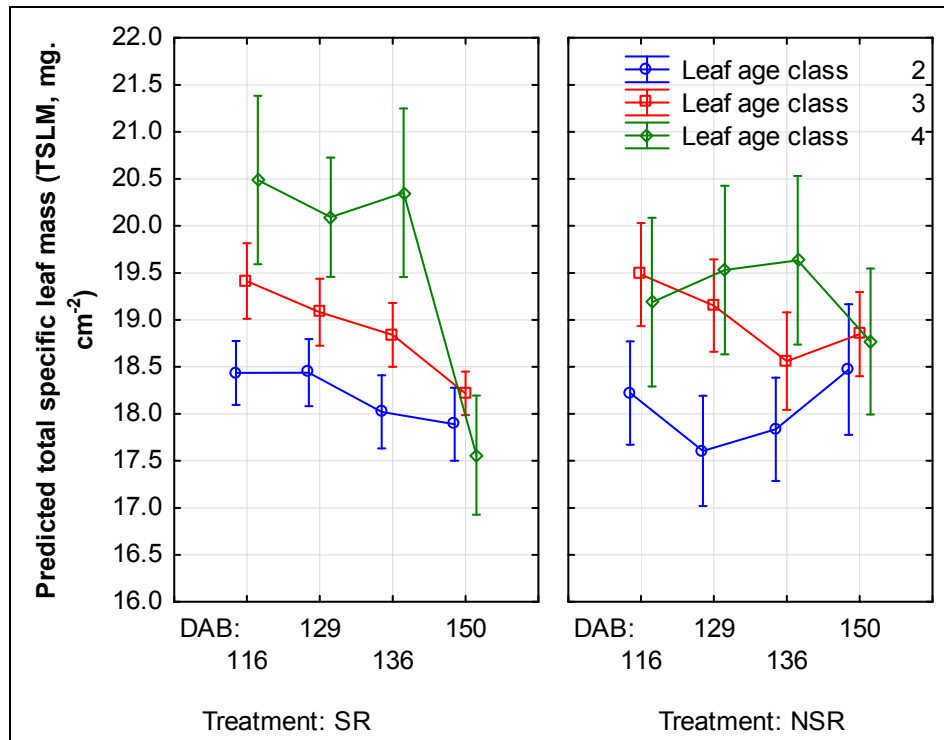


Figure 190 Predicted total specific leaf mass (mg.cm^{-2}) values for selected measurement dates, leaf chronological age classes and treatments in season two (vertical bars denote standard errors).

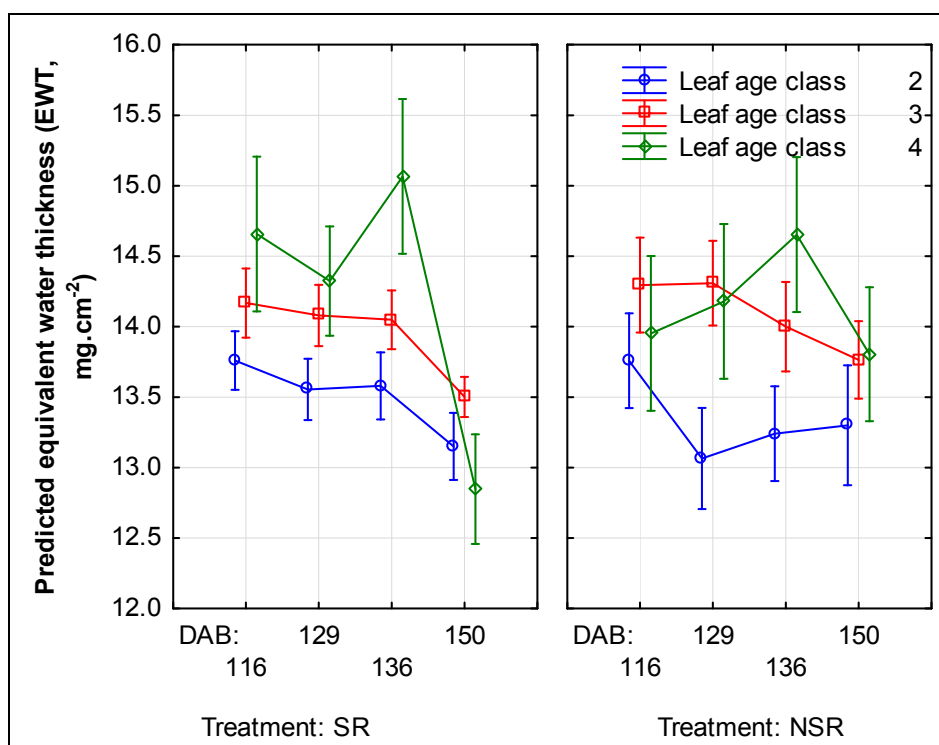


Figure 191 Predicted equivalent water thickness ($\text{mg}\cdot\text{cm}^{-2}$) values for selected measurement dates, leaf chronological age classes and treatments in season two (vertical bars denote standard errors).

The predicted leaf total chlorophyll content seemed to decrease more in the older leaves (class four) of the SR treatment (Figure 192). The increase in chlorophyll for leaf age class three after 129 DAB in this treatment is peculiar, and was also seen on a mass-basis (Figure 193). On a mass- as well as area basis this seemed to be especially due to chlorophyll *a* increasing (Figure 194 and Figure 195). There seemed to be no other water deficit effects related to the predicted total chlorophyll values which seemed stable in the youngest leaf class despite critical water deficits. The levels in the class three leaves also seemed to be lower for the first two measurement dates in the SR treatment (also on a mass-basis). These leaves seemed to have lower carotenoid:chlorophyll ratios (refer to Figure 201), but similar chlorophyll *a*:*b* ratios (Figure 198). Shading is therefore unlikely to have played an important role here, as similar SLM values were also found in the two treatments for these leaves. The differences here may be attributable to either pigment synthesis or degradation differences between the two treatments, caused by the irrigation treatments, but not detectable as major differences in the Ψ_{PD} values. Carotenoids seemed to be affected more than chlorophyll, judging by the apparently lower carotenoid:chlorophyll ratios. When critical water deficit levels were reached in the SR treatment, the predicted chlorophyll *b* values seemed to decrease more than chlorophyll *a* in the class four leaves (Figure 196 and Figure 197), leading to a large increase in the chlorophyll *a*:*b* ratio (Figure 198). Decreases were also recorded in the predicted chlorophyll *b* levels for this period in the class two leaves, but this was similar to what was observed for the NSR treatment. It would seem that in this season water deficit effects could not be detected, in terms of chlorophyll *a*:*b* ratio or carotenoid:chlorophyll ratio differences in the class two leaves. In the class four leaves the carotenoid:chlorophyll ratio seemed to be increased in the SR treatment for all of the measurement dates, especially the last. The trend in the SR chlorophyll *a*:*b* ratio to decrease towards véraison and then increase, was also seen in season one (refer to Chapter V). Only the NSR class four leaves showed no final increase in the chlorophyll *a*:*b* ratio. The reason for this is not clear.

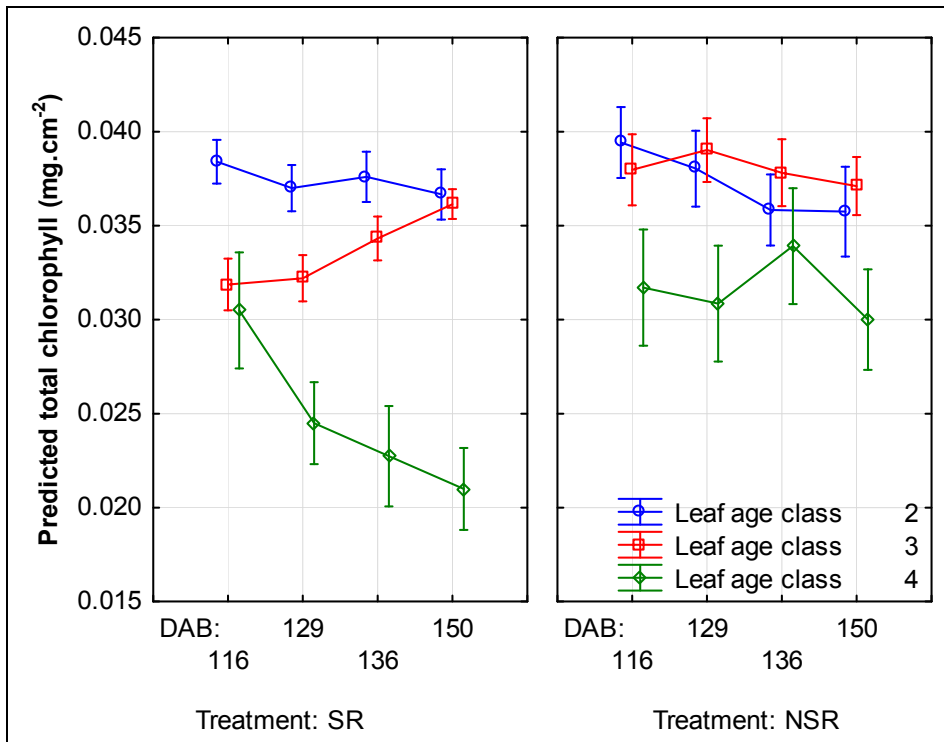


Figure 192 Predicted total chlorophyll (mg.cm⁻²) values for selected measurement dates, leaf chronological age classes and treatments in season two (vertical bars denote standard errors).

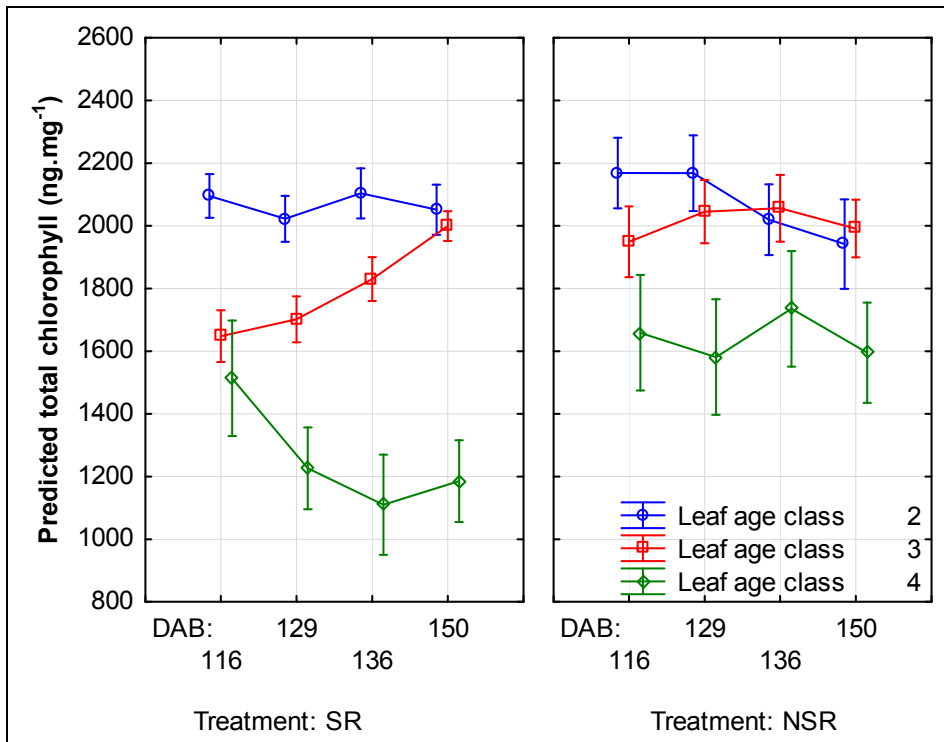


Figure 193 Predicted total chlorophyll (ng.mg⁻¹) values for selected measurement dates, leaf chronological age classes and treatments in season two (vertical bars denote standard errors).

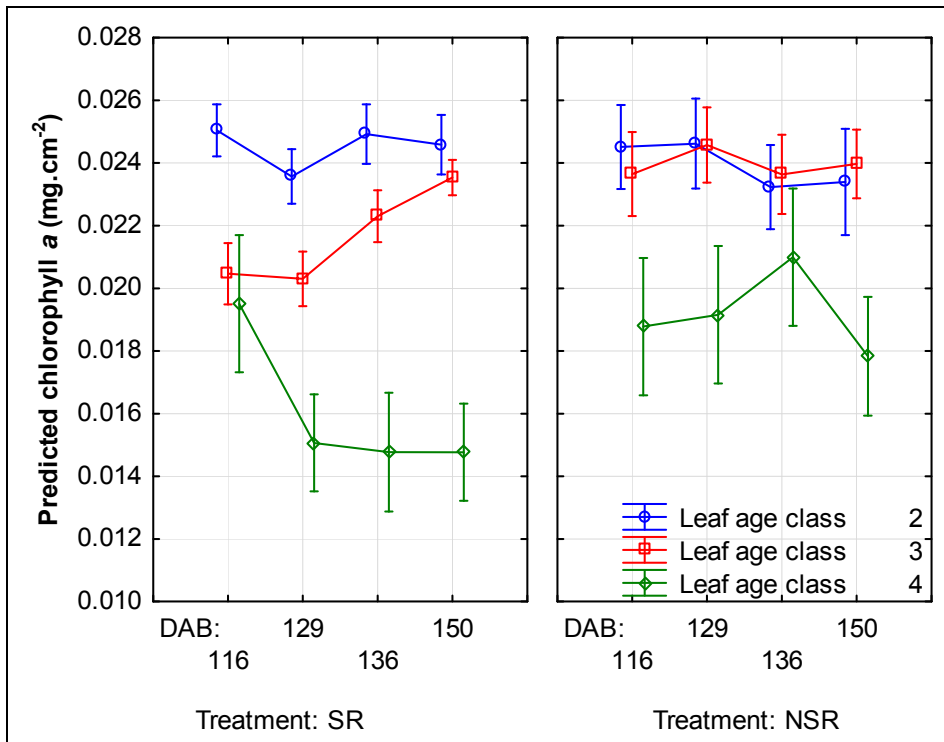


Figure 194 Predicted chlorophyll a (mg.cm⁻²) values for selected measurement dates, leaf chronological age classes and treatments in season two (vertical bars denote standard errors).

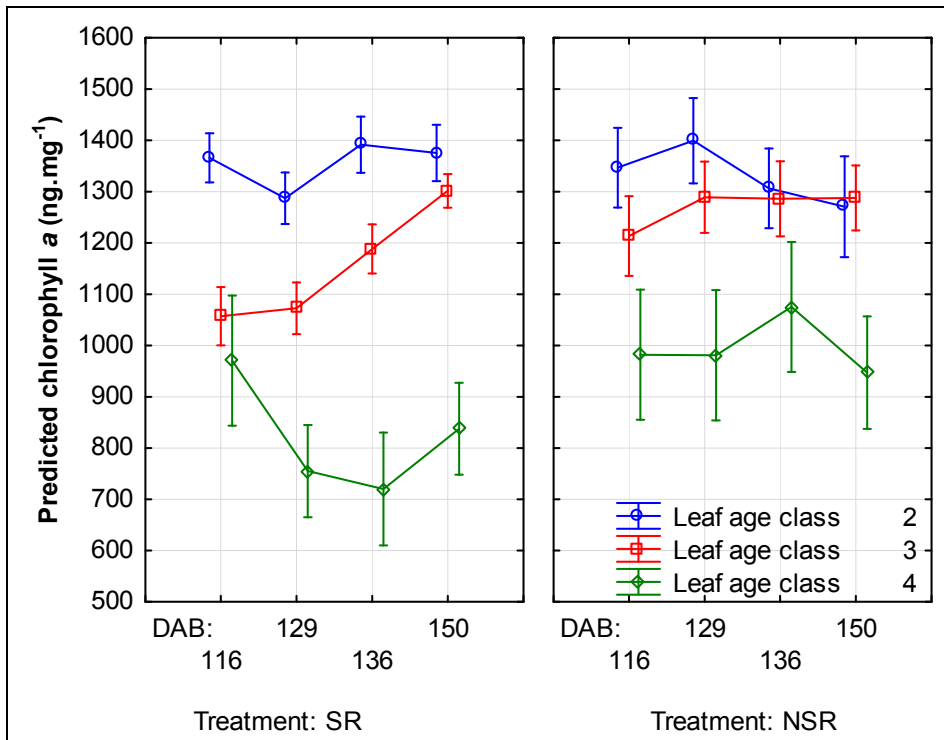


Figure 195 Predicted chlorophyll a (ng.mg⁻¹) values for selected measurement dates, leaf chronological age classes and treatments in season two (vertical bars denote standard errors).

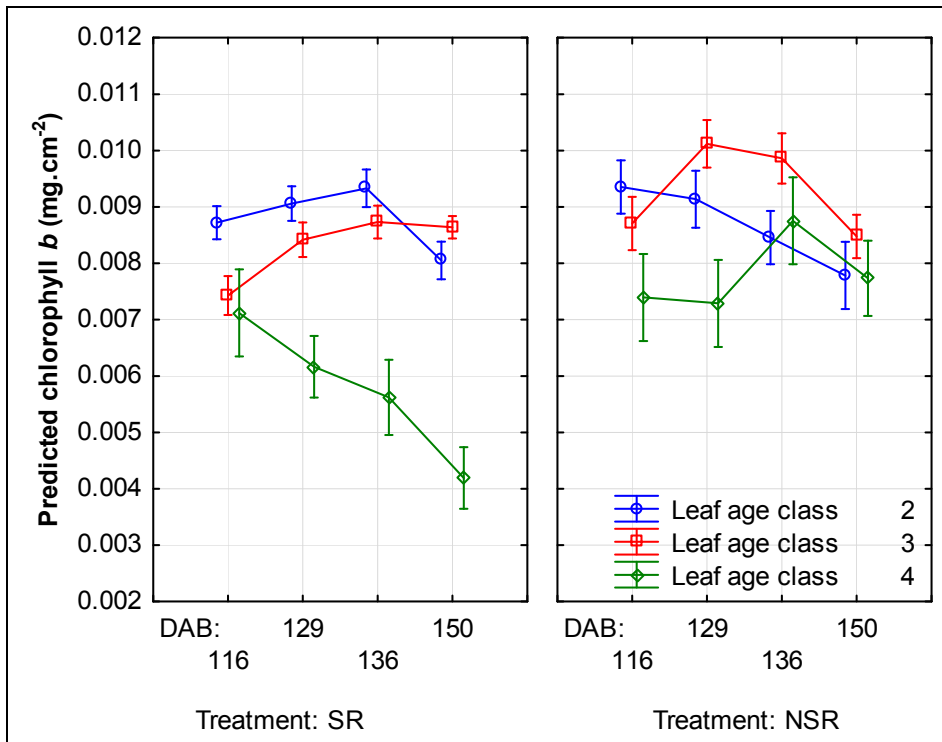


Figure 196 Predicted chlorophyll *b* (mg.cm⁻²) values for selected measurement dates, leaf chronological age classes and treatments in season two (vertical bars denote standard errors).

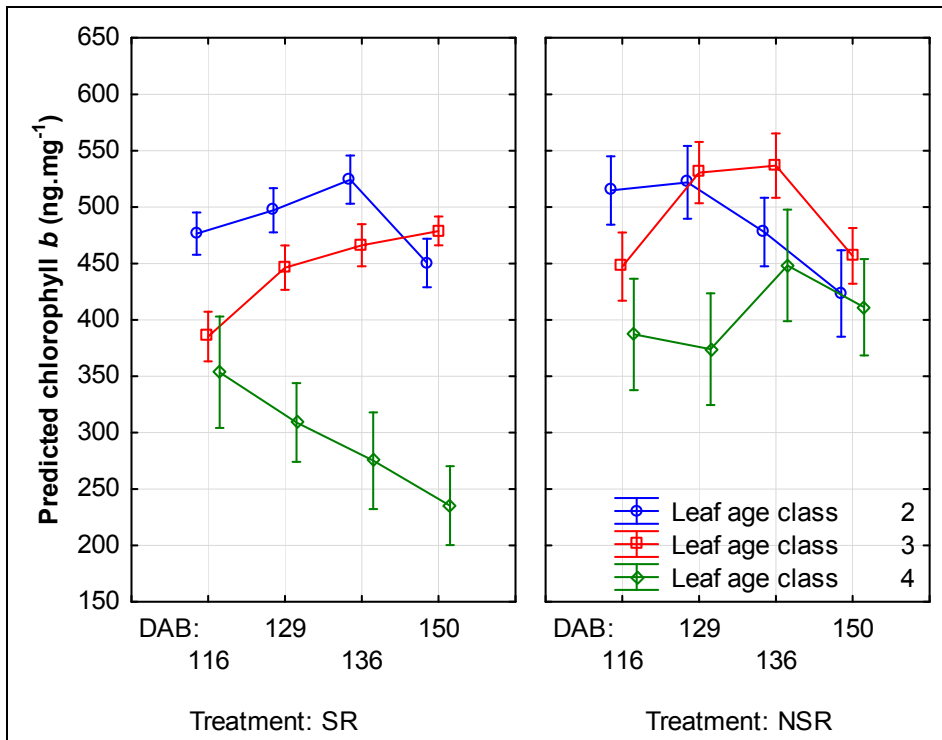


Figure 197 Predicted chlorophyll *b* (ng.mg⁻¹) values for selected measurement dates, leaf chronological age classes and treatments in season two (vertical bars denote standard errors).

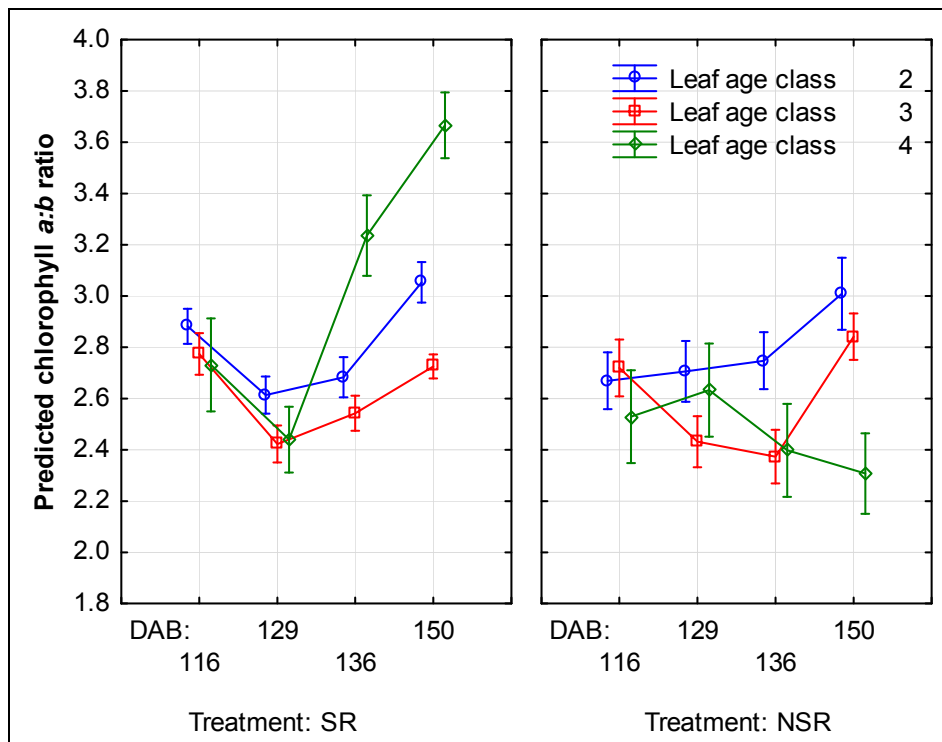


Figure 198 Predicted chlorophyll *a:b* ratios for selected measurement dates, leaf chronological age classes and treatments in season two (vertical bars denote standard errors).

The predicted leaf total carotenoid levels seemed to increase in leaf age classes two and three from the second measurement date for the SR treatments (Figure 199 and Figure 200). The initial carotenoid:chlorophyll ratio values in the class four leaves of the SR treatment were also higher and was different to the chlorophyll *a:b* result (Figure 201). The suggested leaf loss in the lower canopy sections could have caused this, but higher chlorophyll *a:b* ratios were also expected, had this only been an exposure effect. It is suggested that the chlorophyll *a:b* ratio may be less dynamic (i.e. established before leaf loss and then being less adaptive) than the carotenoid:chlorophyll ratio with regards to leaf exposure. In Chapter V, a similar result was obtained, as chlorophyll *a:b* ratios were not increased on measurement date A after canopy manipulation was established. Results from the DEPS ratio were not very consistent, probably due to limited prediction reliability and possible non-linearity in its defining elements (Figure 202). The initial values did, however, seem higher in the SR treatment for class four leaves, which could also have been linked to increased exposure. No response to water stress was, however, evident, which was not consistent with the results of season one.

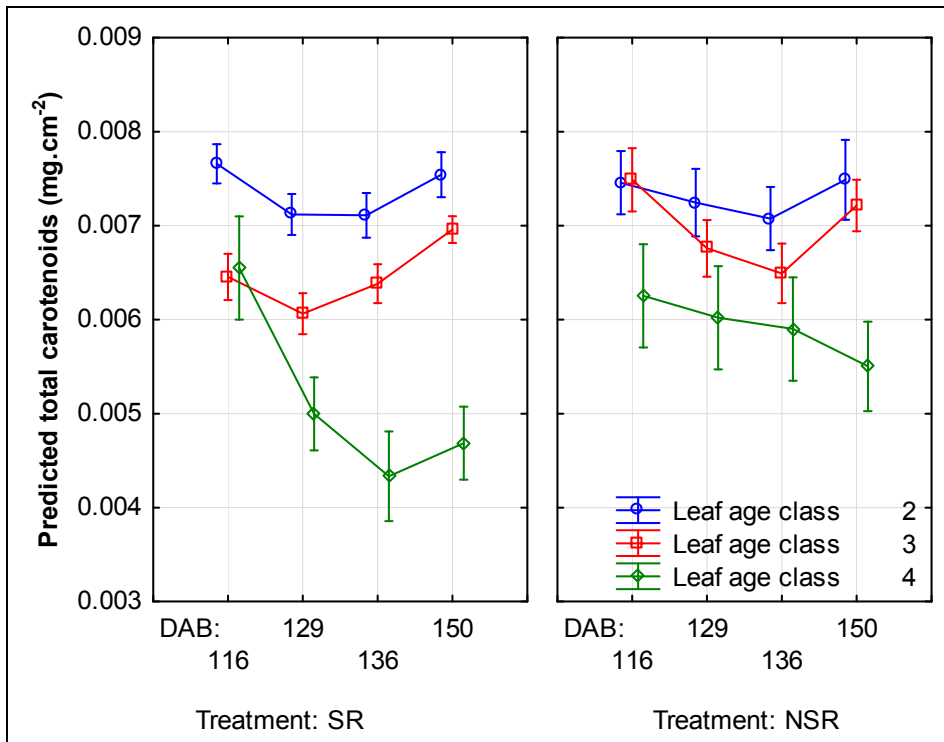


Figure 199 Predicted total carotenoid (mg.cm⁻²) values for selected measurement dates, leaf chronological age classes and treatments in season two (vertical bars denote standard errors).

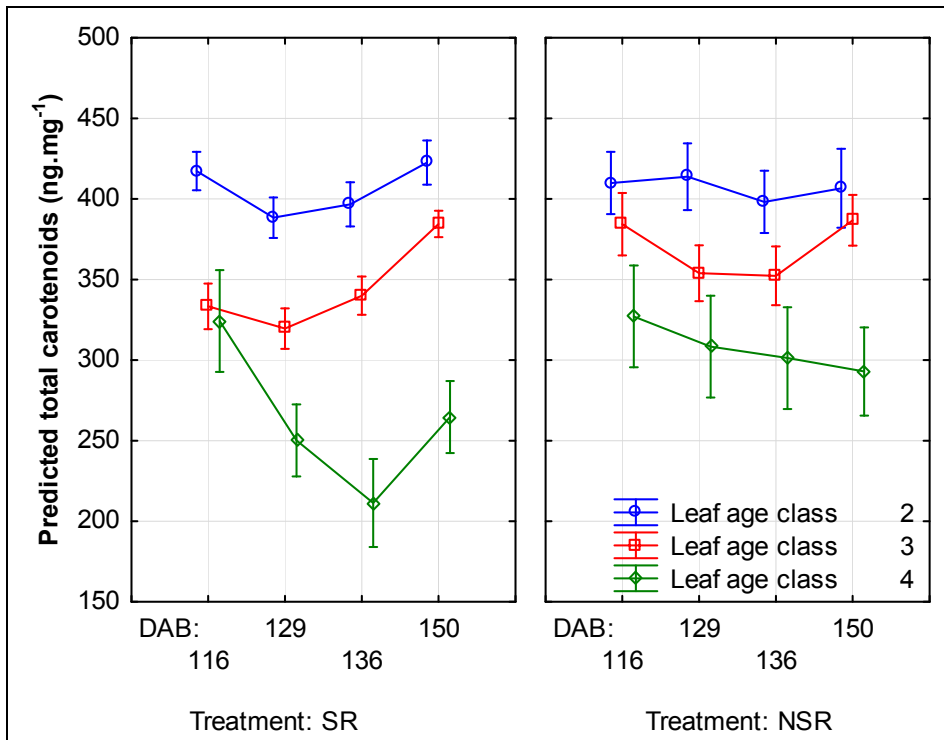


Figure 200 Predicted total carotenoid (ng.mg⁻¹) values for selected measurement dates, leaf chronological age classes and treatments in season two (vertical bars denote standard errors).

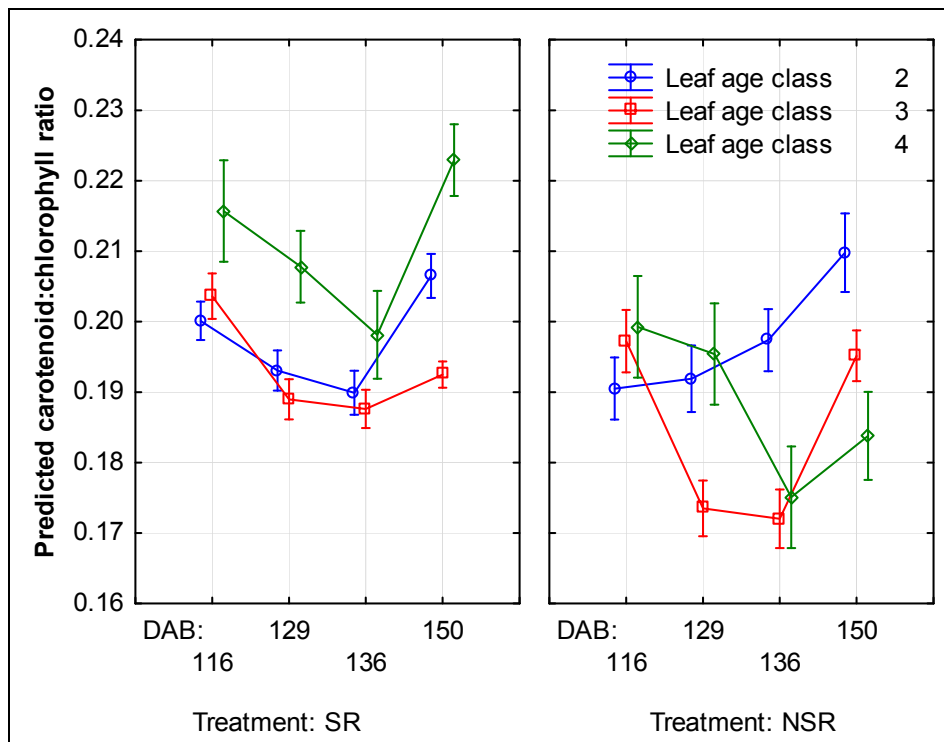


Figure 201 Predicted carotenoid:chlorophyll ratios for selected measurement dates, leaf chronological age classes and treatments in season two (vertical bars denote standard errors).

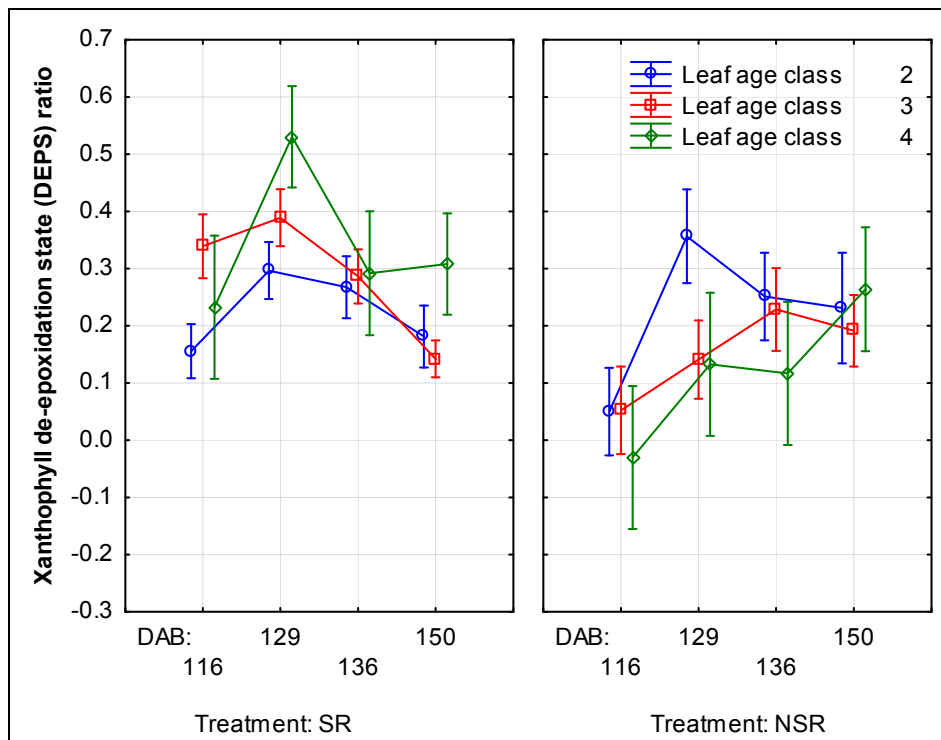


Figure 202 Predicted xanthophyll de-epoxidation state (DEPS) ratios for selected measurement dates, leaf chronological age classes and treatments in season two (vertical bars denote standard errors).

The predicted neoxanthin levels seemed lower in class three and four leaves for the SR treatments, in response to increased water deficit stress (Figure 203 and Figure 204). Interestingly, for the class two leaves higher values seemed to be found as water deficit stress increased. Neoxanthin and chlorophyll *b* values were strongly correlated, which explains the similarity in the trends between the two parameters.

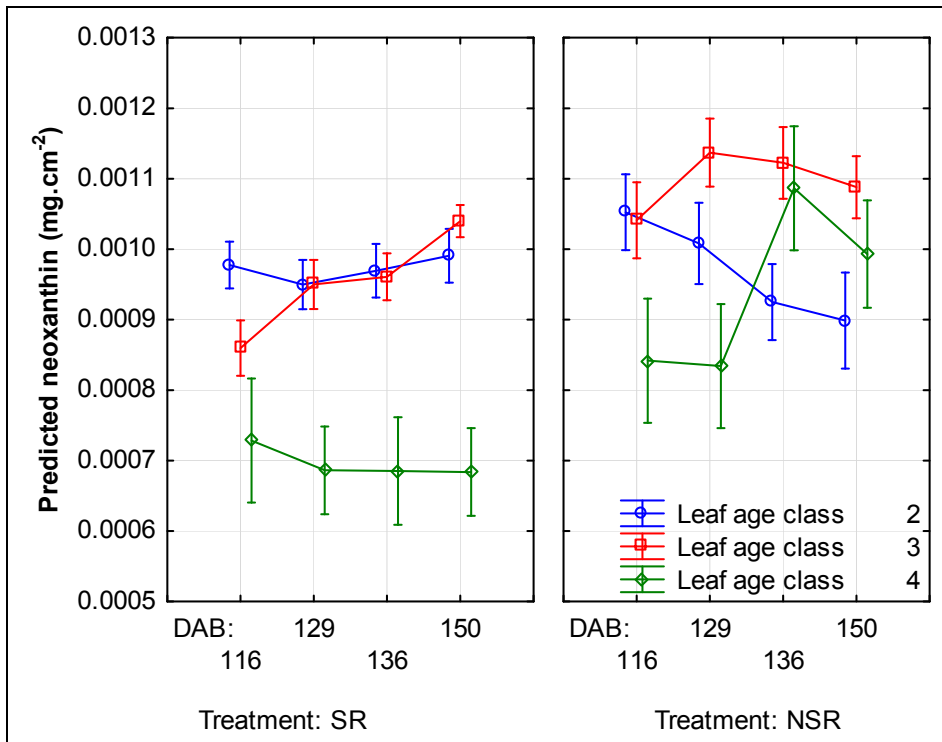


Figure 203 Predicted neoxanthin (mg.cm⁻²) values for selected measurement dates, leaf chronological age classes and treatments in season two (vertical bars denote standard errors).

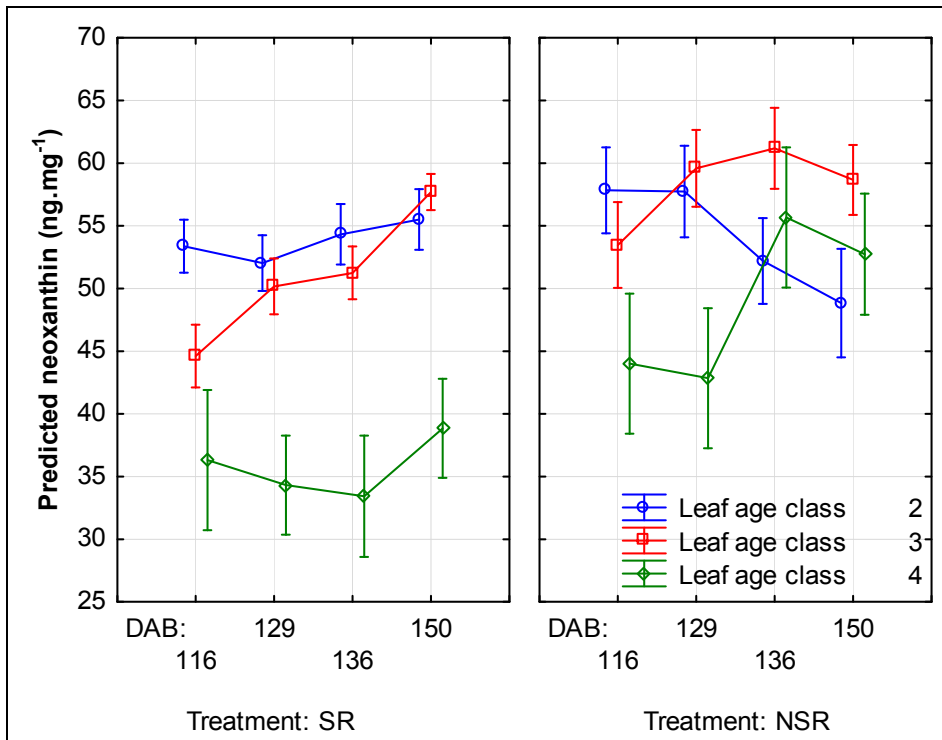


Figure 204 Predicted neoxanthin (ng.mg⁻¹) values for selected measurement dates, leaf chronological age classes and treatments in season two (vertical bars denote standard errors).

7.3.10 Prediction application

From a practical viewpoint, the transition from Ψ_{PD} values higher than -400 KPa (absent to moderate stress) to lower than -600 KPa (moderate to severe stress) from 116 to 129 DAB can be considered of some importance in irrigation scheduling prior to véraison in the context of season two. This section aims to propose the parameters from the previous section that would be most appropriate to use in non-destructive identification of this transition, which may then be of use in

irrigation scheduling. The requirements for such a parameter would then be that it should increase or decrease between the two dates for the SR treatment, but not in the NSR treatment. Secondly it should also preferably be distinguishable also with further stress progression.

There seemed to be differences initially for the SLM and EWT parameters, but this was not stable during development of water deficits, making it less reliable as predictor further in the season (Table 57). A range of other parameters show suitability to monitor water deficit change, and some (such as the carotenoid:chlorophyll ratio and the chlorophyll *a:b* ratio) can be used with slight adaptation for monitoring after véraison as well.

Table 57 Predicted leaf parameters responding to water deficit changes in the SR treatment between 116 and 129 DAB in season two.

Parameter	Leaf age class	Response	Stability
SLM ($\text{mg}\cdot\text{cm}^{-2}$)	2	Increase	Not stable
EWT($\text{mg}\cdot\text{cm}^{-2}$)	2	Stable	Not stable
Total chlorophyll ($\text{mg}\cdot\text{cm}^{-2}$)	4	Decrease	Stable
Chlorophyll <i>a</i> ($\text{mg}\cdot\text{cm}^{-2}$)	2/4	Decrease	More stable in older class
Chlorophyll <i>b</i> ($\text{mg}\cdot\text{cm}^{-2}$)	2/4	Decrease	
Chlorophyll <i>a:b</i> ratio	2/4	Decrease /increase	Increase after véraison in class four, can be combined for prediction
Total carotenoids ($\text{mg}\cdot\text{cm}^{-2}$)	2/4	Decrease	More stable in older class
Carotenoid:chlorophyll ratio	2/4	Decrease	Young leaves better initially, older leaves better after véraison
DEPS ratio	4	Increase	Not stable later, but good indicator before véraison

7.4 Conclusions

The general spectral properties of leaves in the visible and near-infrared spectral regions agreed with what was expected during leaf ageing and structural as well as leaf water content changes. Visible absorption of radiation seemed to correspond to pigment change in the leaves, with a consistent chlorophyll decrease in leaf age classes two to five in season two. The absorption of infrared radiation mostly consistently increased with leaf maturation, water loss and further maturation and senescence. This was consistent between the seasons.

Leaf structure, water content and age prediction from PCA, PLS and PLS 2 techniques proved effective and also provides methods to develop customised simple ratios, as was illustrated for leaf TSLM. Pigment predictions were also within acceptable error margins for the major pigments in grapevine leaves, but further work is required to improve the modelling of xanthophylls, which probably would also require non-linear techniques such as neural networks or data transformation. The pigment and pigment ratio prediction models were also validated on secondary shoot leaves, with models generally proving to be stable.

PROSPECT inversion was not very effective, but it could be that the measurement set-up needs specific pre-processing steps to be effective. Previous studies also used adapted spectral response curves for different pigments in the PROSPECT model, but in this study it was decided to rather focus further on the multivariate techniques.

Up-scaling of measurements to the canopy level would require integration of models incorporating leaf age and leaf- and canopy structure as well as pigment composition within the canopy in order to be used effectively in hyperspectral aerial or satellite applications.

Non-destructive prediction in conjunction with increased water deficits in season two yielded some surprising results with no clear relation between EWT and increasing Ψ_{PD} values with the exception of leaf age class four on 150 DAB. For the pigments, the increase in total chlorophyll with

increasing water deficits in the SR treatment of leaf age class three was interesting, but in general the older leaves (leaf age class four) responded as expected with earlier pigment decrease. The carotenoid:chlorophyll ratios that seemed higher in leaf age class three for the SR treatments also seemed to be a reliable indicator of the increasing water deficits. Together with the chlorophyll a:b ratio, it can be monitored on selected leaves from leaf age classes two and four to monitor water deficits. Although it does not seem possible to monitor small changes in water deficits, as confirmed by difficult direct prediction of predawn leaf water potentials, it seems that the specified leaves can be used to monitor important transitions of water deficits in grapevine. This has to be confirmed in further studies for other developmental stages and water deficit thresholds.

7.5 Literature cited

- Blanchfield, A.L., Robinson, S.A., Renzullo, L.J. & Powell, K.S., 2006. Phylloxera-infested grapevines have reduced chlorophyll and increased photoprotective pigment content—can leaf pigment composition aid pest detection? *Functional plant biology* 33, 507-514.
- Cartechini, A. & Palliotti, A., 1995. Effect of Shading on Vine Morphology and Productivity and Leaf Gas Exchange Characteristics in Grapevines in the Field. *American Journal of Enology and Viticulture* 46, 227-234.
- Ceccato, P., Flasseb, S., Tarantolac, S., Jacquemoud, S. & Gregoirea, J.-M., 2001. Detecting vegetation leaf water content using reflectance in the optical domain. *Rem. Sens. Environ.* 77, 22-33.
- Cifre, J., Bota, J., Escalona, J.M., Medrano, H. & Flexas, J., 2005. Physiological tools for irrigation scheduling in grapevine (*Vitis vinifera* L.) An open gate to improve water-use efficiency? *Agriculture, Ecosystems and Environment* 106, 159–170.
- Colombo, R., Meroni, M., Marchesi, A., Busetto, L., Rossini, M., Giardino, C. & Panigada, C., 2008. Estimation of leaf and canopy water content in polar plantations by means of spectral indices and inverse modeling. *Rem. Sens. Environ.* 112, 1820-1834.
- De Bei, R., Cozzolino, D., Sullivan, W., Cynkar, W., Fuentes, S., Dambergs, R., Pech, J. & Tyerman, S., 2011. Non-destructive measurement of grapevine water potential using near infrared spectroscopy. *Australian Journal of Grape and Wine Research* 17, 62-71.
- Demarez, V., Gastellu-Etchegorry, J.P., Mougine, E., Marty, G., Proisy, C., Dufrene, E. & Le Dantec, V., 1999. Seasonal variation of leaf chlorophyll content of a temperate forest. Inversion of the PROSPECT model. *International Journal of Remote Sensing* 20, 879-894.
- Dzikiti, S., Verreyne, J.S., Stuckens, J., Strever, A., Verstraeten, W.W., Swennen, R. & Coppin, P., 2010. Determining the water status of Satsuma mandarin trees [*Citrus Unshiu* Marcovitch] using spectral indices and by combining hyperspectral and physiological data. *Agricultural and Forest Meteorology* 150, 369-379.
- Esbensen, K.H., Guyot, D., Westad, F. & Houmøller, L.P., 2002. *Multivariate data analysis: in practice: an introduction to multivariate data analysis and experimental design*. Multivariate Data Analysis.
- Feret, J.-B., François, C., Asner, G.P., Gitelson, A.A., Martin, R.E., Bidet, L.P.R., Ustin, S.L., le Maire, G. & Jacquemoud, S., 2008. PROSPECT-4 and 5: Advances in the leaf optical properties model separating photosynthetic pigments. *Remote Sensing of Environment* 112, 3030-3043.
- Flexas, J., Escalona, J.M., Evain, S., Gulías, J., Moya, I., Osmond, C.B. & Medrano, H., 2002. Steady-state chlorophyll fluorescence (Fs) measurements as a tool to follow variations of net CO₂ assimilation and stomatal conductance during water-stress in C₃ plants. *Physiologia Plantarum* 114, 231-240.
- Flexas, J., Hendrickson, L. & Chow, W.S., 2001. Photoinactivation of photosystem II in high light-acclimated grapevines. *Aust. J. Plant Physiol.* 28, 755-764.
- Gamon, J.A., Serrano, L. & Surfus, J.S., 1997. The Photochemical Reflectance Index: An Optical Indicator of Photosynthetic Radiation Use Efficiency across Species, Functional Types, and Nutrient Levels. *Oecologia* 112, 492-501.

- Gamon, J.A. & Surfus, J.S., 1999. Assessing leaf pigments content and activity with a reflectometer. *New Phytol.* 143, 105-117.
- Gaudillere, J.P. & Carbonneau, A., 1986. Training system and photosynthetic activity of the vine. In: Dejong, T.M. (ed). *Proc. International Workshop on Regulation of Photosynthesis in Fruit Crops*, University of California, Davis. pp. 61-71
- Gausman, H.W., 1984. Evaluation of factors causing reflectance differences between sun and shade leaves. *Rem. Sens. Environ.* 15, 177-181.
- Gausman, H.W., 1985. *Plant leaf optical properties in visible and near-infrared light*. . Texas Tech Press, Lubbock, Texas.
- Grant, O.M., Tronina, A.u., Jones, H.G. & Chaves, M.M., 2007. Exploring thermal imaging variables for the detection of stress responses in grapevine under different irrigation regimes. *Journal of Experimental Botany* 58, 815-825.
- Hendrickson, L., Furbank, R.T. & Chow, W.S., 2004. A simple alternative approach to assessing the fate of absorbed light energy using chlorophyll fluorescence. *Photosynthesis Research* 82, 73-81.
- Hunter, J.J. & Visser, J.H., 1989. The effect of partial defoliation, leaf position and developmental stage of the vine on leaf chlorophyll concentration in relation to the photosynthetic activity and light intensity in the canopy of *Vitis vinifera* L. cv. Cabernet Sauvignon. *S. Afr. J. Enol. Vitic.* 10, 67-73.
- Jacquemoud, S. & Baret, F., 1990. PROSPECT: A model of leaf optical properties spectra. *Remote Sensing of Environment* 34, 75-91.
- Jacquemoud, S., Ustin, S.L., Verdebout, J., Schmuck, G., Andreoli, G. & Hosgood, B., 1996. Estimating leaf biochemistry using the PROSPECT leaf optical properties model. *Remote Sensing of Environment* 56, 194-202.
- Knipling, E.B., 1970. Physical and physiological basis for the reflectance of visible and near-infrared radiation from vegetation. *Rem. Sens. Environ.* 1, 155-159.
- Kriedemann, P.E., 1968. Photosynthesis in vine leaves as a function of light intensity, temperature, and leaf age. *Vitis* 7, 213-220.
- Kriedemann, P.E., Kliewer, W.M. & Harris, J.M., 1970. Leaf age and photosynthesis in *Vitis vinifera* L. *Vitis* 9, 97-104.
- Li, L., Cheng, Y.B., Ustin, S., Hu, X.T. & Riaño, D., 2008. Retrieval of vegetation equivalent water thickness from reflectance using genetic algorithm (GA)-partial least squares (PLS) regression. *Advances in Space Research* 41, 1755-1763.
- Lillesaeter, O., 1982. Spectral reflectance of partly transmitting leaves: laboratory measurements and mathematical modeling. *Rem. Sens. Environ.* 12, 247-254.
- Meggio, F., Zarco-Tejada, P.J., Núñez, L.C., Sepulcre-Cantó, G., González, M.R. & Martín, P., 2010. Grape quality assessment in vineyards affected by iron deficiency chlorosis using narrow-band physiological remote sensing indices. *Remote Sensing of Environment* 114, 1968-1986.
- Merzlyak, M.N., Gitelson, A.A., Chivkunova, O.B., Solovchenko, A.E. & Pogosyan, S.I., 2003. Application of reflectance spectroscopy for analysis of higher plant pigments. *Plant Physiol.* 50, 704-710.
- Nelder, J.A. & Mead, R., 1965. A simplex method for function minimization. *Comput. J.* 7, 308-313.
- Niinemets, U., 1999. Research Review: Components of Leaf Dry Mass Per Area-Thickness and Density- Alter Leaf Photosynthetic Capacity in Reverse Directions in Woody Plants. *New Phytologist* 144, 35-47.
- Pedro, A.M.K. & Ferreira, M.M.C., 2007. Simultaneously calibrating solids, sugars and acidity of tomato products using PLS2 and NIR spectroscopy. *Anal. Chim. Acta.* 595, 221-227.
- Pisciotta, A., Di Lorenzo, R., Volschenk, C.G. & Hunter, J.J., 2011. Relation between row and leaf orientation of Syrah/101-14 MGT. In: *Proc. Seventeenth International GiESCO Symposium*, 29 August - 2 September, Asti - Alba (CN), Italy. pp. 555-558.

- Poni, S., Intrieri, C. & Silvestroni, O., 1994. Interactions of LeafAge, Fruiting, and Exogenous Cytokinins in Sangiovese Grapevines Under Non-Irrigated Conditions. II. Chlorophyll and Nitrogen Content. *Am. J. Enol. Vitic.* 45, 278-284.
- Rodríguez-Pérez, J.R., Riaño, D., Carlisle, E., Ustin, S. & Smart, D.R., 2007. Evaluation of Hyperspectral Reflectance Indexes to Detect Grapevine Water Status in Vineyards. *Am. J. Enol. Vitic.* 58, 302-317.
- Savitzky, A. & Golay, M.J.E., 1964. Curve smoothing by local polynomial fits. *Anal. Chem* 36, 1627-1639.
- Schultz, H.R., 1996. Leaf absorptance of visible radiation in *Vitis vinifera* L.: estimates of age and shade effects with a simple field method. *Scientia Horticulturae* 66, 93-102.
- Sims, D.A. & Gamon, J.A., 2002. Relationships between leaf pigment content and spectral reflectance across a wide range of species, leaf structures and developmental stages. *Rem. Sens. Environ.* 81, 337-354.
- Slaton, M.R., Hunt, E.R. & Smith, W.K., 2001. Estimating near-infrared leaf reflectance from leaf structural characteristics. *Am. J. Bot.* 88, 278-284.
- Smart, R., 1987. Influence of light on composition and quality of grapes. *Acta Hort.* 206, 37-47.
- Stuckens, J., Verstraeten, W.W., Delalieux, S. & Coppin, P., 2009. A dorsiventral leaf radiative transfer model: development, validation and improved model inversion techniques. *Rem. Sens. Environ.* 113, 2560-2573.
- Williams, L.E., 1987. Growth of Thompson Seedless grapevines: I. Leaf area development and dry weight distribution. *J. Am. Soc. Hortic. Sci.* 112, 325-330.
- Zarco-Tejada, P.J., Berjón, A., López-Lozano, R., Miller, J.R., Martín, P., Cachorro, V., González, M.R. & De Frutos, A., 2005. Assessing vineyard condition with hyperspectral indices: Leaf and canopy reflectance simulation in a row-structured discontinuous canopy. *Remote Sensing of Environment* 99, 271-287.

Chapter VIII

General Discussion and Conclusions

Chapter VIII: General discussion and conclusions

8.1 Brief overview

In this study, large amounts of growth and leaf spectral absorbance data were collected in a *Vitis vinifera* cv. Shiraz vineyard showing considerable variability in vigour. Irrigation and canopy manipulation treatments were also imposed. Spectral measurements were conducted over three growing seasons at different developmental stages and for leaves with known canopy positions and ages. The study aimed to provide new insights into assessing the grapevine leaf and possibly also the canopy growth and ageing dynamics as well as pigment content as a basis of validating a non-destructive measurement approach. The application of multivariate techniques in leaf spectroscopy was investigated with the goal of simplifying non-destructive leaf pigment, structure and water content estimation in future studies. The main objective of this study was therefore to use field spectroscopy to study leaf composition and some factors (including canopy growth manipulation and water status changes) that may impact on it. The approach was not to avoid variability, but to describe and analyse it with as many parameters as possible.

8.2 General discussion of findings according to original objectives

8.2.1 Objective I: Interactive effects of growth manipulation and water deficits

Even though relatively large climatic differences existed between the seasons during which this study was conducted, the importance of canopy size in determining grapevine water relations could be seen from the interactions between treatments. It was also visible between seasons, as the Ψ_{PD} was lowest in the non-irrigated treatments for season two, despite cooler and wetter conditions, which was possibly due to larger canopies in this, relative to the other seasons.

The results for shoot removal in this study are in agreement with those found by Hunter & Visser (1990a) with leaf thinning, where drastic compensation effects in terms of secondary shoot growth could be observed. In this study, a full recovery in leaf area per vine was found in season one, with the final leaf area in the reduced canopies seemingly even exceeding that of the full canopy. However, it has to be considered that the composition of the leaf area also changed dramatically. This was not so prevalent in season three, where drier conditions, along with cooler conditions in the first part of the season, probably led to significantly less secondary shoot growth. The reduced canopies also had an increased leaf area:fruit mass ratio along with much lower yield:pruning mass ratios.

Although no measurements were done, it may be that the reduced canopies also had higher water use efficiency, if expressed relative to carbon gains, due to increased secondary:primary shoot leaf area ratios. It is not certain, however, if water use efficiency would also be higher relative to yield, which should be confirmed in follow-up studies.

Light quality and quantity were improved/increased for the reduced canopies, and even though there may have been significant compensatory secondary growth, it has to be considered that the younger leaves would also have higher reflectance and transmittance of visible radiation in particular (especially initially) and higher transmittance of infrared radiation. They can therefore be expected to have less of an effect in reducing the R:FR ratio in the canopies, compared to primary shoot leaves.

Logistic growth curve fitting revealed larger between-season differences in the time that maximum shoot growth was reached, with smaller differences in the time of shoot growth reduction/cessation between seasons. However, shoot growth seemed to respond more to treatments, especially where water deficits were severe from early in the season (NSF treatment). It was expected that

the reduced canopies, with reduced yield:pruning mass ratio would show increased shoot growth rates and maximum shoot length, but this seemed to be counteracted by compensatory growth.

In general, the reduced canopy treatments offered the possibility of attaining technological ripeness at an earlier stage, and at comparatively lower potential alcohol levels (refer to sugar loading results). It is notable that the reduced canopy treatments in season one reached the plateau of sugar loading at about 135 DAB, which was just three weeks after véraison.

Results from the SF treatment in season two suggest that it had larger maximum leaf sizes and it was also noticed that it had lower SLM values. This suggested shaded conditions in the canopy, which were not quantified by light measurements. Less and shorter secondary shoots and a lower mass per primary cane were found; the maximum growth rate was reached earlier in season two. It also showed the lowest maximum sugar loading compared to all treatments and seasons. This example highlights the difficulty in separating water deficit stress and shading effects, as all of the characteristics that were mentioned (with exception of maximum leaf size) could potentially also have been caused by increased water deficit stress conditions. It also confirms why the measurement of water deficits (from some of the mentioned parameters, but also in spectral determination) would be favoured on fully exposed leaves in the canopy.

According to Silvestroni *et al.* (2005) grapevine compensation behaviour in response to several stress conditions were affected by cultivar and the age and position of leaves in the canopy. Changes in leaf inclination, lower leaf visible light absorbance (linked to lower chlorophyll content) and higher transmittance due to lower SLM values apparently allowed Sangiovese to evade excessive light absorption and use less water. Basal leaves (90-120 days old), however, experienced irreversible photo-inhibition and necrosis when exposed to direct light and high temperatures. Younger leaves showed no photo-inhibition.

8.2.2 Objective II: Logistic growth models to determine leaf age and its response to canopy manipulation and water deficit

Shoot plastochron measurements in this study confirmed that the requirements originally set for measuring this parameter were not met throughout the growth season. It was, however, clear that, considering the relation of the plastochron index to shoot parameters, it could be modelled in a similar way than shoot growth, using logistical growth curve analysis. The strategy of using constant plastochron duration estimation is flawed in two ways; firstly, initial shoot growth lagging is not incorporated or accounted for; secondly, the point of shoot growth cessation is arbitrary. Furthermore, useful physiological information is lost if the reduction in shoot growth rate (and therefore increase in PD) is not modelled and incorporated into leaf ageing models.

Depending on the accuracy required, it may be acceptable to simply derive shoot PI from shoot node number, in agreement with Pilar *et al.* (2007), questioning the relevance of measuring leaf vein lengths in order to add decimal accuracy to leaf plastochron index values.

8.2.3 Objective III: Leaf age determination/classification for further studies

A method was proposed to derive leaf age from node number and logistic modelling of the PI:DAB relationship in order to derive the date of leaf formation. The approach was therefore an attempt to incorporate inevitable changes in shoot growth rate and hence plastochron duration throughout the season into leaf age determination.

Based on previous work where leaf age classes were incorporated into physiological studies, these classes were also created for further use in statistical analysis, being as representative as possible of leaf growth transitional phases.

8.2.4 Objective IV: Analysis of leaf chlorophyll and carotenoid profiles during growth

As the canopy age from just before pea size (measurement date B), a decline in total chlorophyll and total carotenoids seemed to be consistent for all leaf ages on primary shoots, with the secondary shoots still showing increases in total chlorophyll content up to date C, just before véraison. The general pigment decrease (on a mass and area basis) from date B is not likely to be in reaction to increased shading conditions in the canopies for two reasons: Firstly, the decrease seemed to be more between dates B and C for the reduced canopies, despite possible higher exposure levels of leaves within the canopy. Secondly, the decrease happened on a mass and area basis for chlorophylls and carotenoids, which are not expected during increased shade conditions. With increased shading, total chlorophyll levels are expected to decrease on an area basis, but increase on a mass basis.

Measurement date C (just prior to véraison) seemed to be a pivotal point with regards to the reaction of chlorophyll a:b ratios, carotenoids and xanthophylls, which could be expected considering the strong increase in water deficit levels in all treatments after measurement date B. While the DEPS ratio, carotenoid:chlorophyll ratio as well as the XPS:chlorophyll ratio reacted to higher exposure levels measured for the reduced canopies on the first two dates, it seemed that only the DEPS ratio seemed responsive to water deficits increasing, especially in young leaves, which probably required more photo-protection at these stages. This effect was especially evident for secondary shoots. The DEPS ratio therefore seems to be a promising indicator, provided that suitable leaves are used as indicators, to assess the effects of water deficits on the xanthophyll de-epoxidation cycle.

8.2.5 Objective V: Leaf structural components and water content during growth

Results from leaf structure and water content confirm the importance of these parameters in integrating the history of the leaf microclimate, as well as its dependence on and relation to the growth of the entire plant. The additive nature of shade and water deficits is well known – the most common and visible phenomenon is a thin, yellow leaf inside a dense canopy of a grapevine experiencing severe water deficits. Once again, the difficulty in separating microclimate and growth limitation-related factors that may affect leaf structural and water content parameters emphasises the importance of either specifying these limitations specifically for each leaf by way of focused measurements or alternatively considering the observed variability (temporal and spatial) in these parameters carefully before interpreting any physiological measurements conducted at leaf level.

The relevance of this is particularly valuable when dealing with “mixed signals”, which can be the case in canopy remote sensing, but also in whole-plant photosynthesis measurements (Edson *et al.*, 1993, 1995a).

8.2.6 Objective VI: Non-destructive assessment of leaf pigment content, specific leaf mass and water content during growth

Leaf structure, water content and age prediction from PCA, PLS and PLS 2 techniques proved effective and also provides methods to develop customised simple ratios, as was illustrated for leaf TSLM.

Pigment predictions were within acceptable error margins for the major pigments in grapevine leaves, but further work is required to improve the modelling of xanthophylls, which probably would also require non-linear multivariate techniques, such as non-linear PLS, spline PLS or artificial neural networks. Data transformation can also be applied to address non-linearity, but this was considered outside the scope of this thesis.

8.3 Major findings: limitations and novelty value – implications

8.3.1 Limitations

In future studies, leaf physiological efficiency should also be probed using photosynthesis, chlorophyll fluorescence and/or stomatal conductance measurements. However, in a targeted approach these parameters could be combined, especially when they are preceded by non-destructive measurements of predicted pigment content, SLM or EWT, which is expected to reduce the potential inter- or intra-leaf variability in the techniques.

To effectively monitor the canopy light regime in response to the canopy manipulations and in response to compensatory growth in different canopy zones, sufficient light measurements should be conducted throughout the season.

Reflectance and transmittance were not separable in measurements, but combined into a single measurement. Although this was done to shorten the time-span of measurements at a particular time, and leaf absorbance spectra still convey most of the relevant information, modelling could potentially have been improved for some parameters (i.e. for those where reflectance does not change, but transmittance does in certain parts of the season) by considering reflectance, transmittance and absorbance of leaves separately.

The node position on primary shoots where secondary shoots emerged was not noted during plastochron measurements on these shoots, which made it impossible to estimate leaf age accurately on these shoots. Therefore, secondary shoot data were mostly excluded in analysis, except where leaf age estimation was not crucial to the interpretation of the data.

The possible practical application of the modelled and predicted parameters was shown for a period around véraison in season two by comparing the reaction of the SR and NSR treatments to developing water deficits. It showed that several parameters, with special mention of the carotenoid:chlorophyll ratio and chlorophyll a:b ratio, can be monitored on selected leaves from leaf age classes two and four to monitor water deficits. Although it did not seem possible to monitor small changes in water deficits, as confirmed by difficult direct prediction of predawn leaf water potentials, leaves may be used to monitor important transitions of water deficits. In this regard, the SLM and EWT parameters may seem irrelevant, but they may be useful to ensure that the selected leaves are representative of a specific leaf class. Alternatively, leaf age prediction can be used alongside these measurements to indicate if a leaf is suitable for measurement or not (i.e. within leaf age classes two or four for a specific time of the season).

8.3.2 Novelty value

The study illustrated the relevance of considering the development of the grapevine along with leaf ageing in the canopy when conducting calibrated non-destructive measurements of leaf pigments, structure and water content. Applications of multivariate techniques in leaf spectroscopy were shown and can be applied and simplified to aid in non-destructive leaf pigment, structure and water content estimation in future studies. It was also the first study, according to our knowledge, that integrated the logistical growth of shoots into leaf age estimation of plants.

It was defined in this study how leaf age and composition developed and what happened during the growth period of each individual leaf in the canopy, in other words the history of each leaf was in fact captured by assessing these parameters at a specific point in time. It may therefore be possible to apply a reversed approach, namely to define the development of the canopy, growth and water deficit conditions of the plant from the composition and age of individual leaves in the canopy. Although this was not evaluated through modelling in the present study, it is a definite

possibility for future studies. Perhaps the models can be calibrated from the data collected in the present study and then validated in a new study.

8.4 Perspectives for future research

This study, along with other national/international collaborative studies that were conducted on grapevine or other crops (Dzikiti *et al.*, 2009; Dzikiti *et al.*, 2010; Delaere *et al.*, 2011; Dzikiti *et al.*, 2011; Van Niekerk *et al.*, 2011), also presented possibilities for follow-up studies on different topics of grapevine remote sensing. The results may be used, possibly along with improvements of the PROSPECT model, to scale up measurements to the canopy level in an approach similar to that followed in the study by Zarco-Tejada *et al.* (2005). Data transformation or non-linear techniques could be investigated to improve non-destructive prediction of xanthophylls and the DEPS ratio.

The HPLC pigment analysis method is currently incorporated into an ultra-performance liquid chromatography (UPLC) method that will allow for shorter sample run-times and increased resolution. It may also be possible to analyse individual carotenoids, along with chlorophylls, using Gauss peak spectra from UV/VIS spectroscopy as indicated by Küpper *et al.* (2007).

Work has been conducted, also as part of an international collaboration, on leaf anthocyanin estimation from non-destructive measurements in grapevine (Delaere *et al.*, 2011), as part of a study on the same vineyard and treatments discussed in this thesis. Some of the aspects mentioned are also worthy of further investigation.

Scanning electron- or X-ray diffraction microscopy can be used to investigate leaf structural adaptations, including stomatal density changes in reaction to leaf microclimate or plant water deficit changes. Future work is planned on investigating leaf adaptation to water deficits and canopy microclimate using these technologies along with the parameters determined in this thesis.

8.5 Final remarks

While studying the interaction of the grapevine and its environment, the ability of the plant to adapt to its environment is striking. While this adaptation was mostly studied on a leaf spectral level, with supporting measurements of pigment content, structure and water content, it may also be relevant in future studies to probe further into the underlying molecular and physiological phenomena that drive these adaptations.

With the availability and cost of irrigation water becoming an increasingly relevant aspect of viticulture in the Western Cape region of South Africa, but also worldwide, the availability of methods to use plant response to schedule irrigation would progressively gain relevance. This study suggests that spectral techniques may be adapted to this end, possibly even without the need to scale up measurements to the aerial or satellite platform level.

Although remote sensing technologies are now sufficiently advanced to detect minor changes in vegetation temperature, biomass or physiological condition, the most challenging aspect is knowledge of the target. In viticulture, the search for relevant spectral features is a more complex issue than merely the levels of leaf variability that were discussed in this thesis, as it may involve differences in, amongst others, soil type and cover, slope, cultivar, rootstock, row orientation, vine spacing, canopy configuration, leaf inclination (training system and canopy management practices). With this in mind, multivariate statistical modelling may be one of the most powerful tools.

8.6 Literature cited

- Delaere, A., Coppin, P., Strever, A.E. & Delvaux, F., 2011. The use of hyperspectral remote sensing for the detection of anthocyanins in grapevine (*Vitis vinifera* L.) leaves. Master in de bio-ingenieurswetenschappen: levensmiddelentechnologie thesis, Katholieke Universiteit Leuven, Leuven, Belgium.
- Dzikiti, A., Verreyne, S., Strever, A., Stuckens, J., Verstraeten, W., Swennen, R. & Coppin, P., 2009. Detecting citrus tree water status by integrating hyperspectral remote sensing with physiological approaches in a water-flow storage model. IGARSS2009.
- Dzikiti, S., Verreyne, J.S., Stuckens, J., Strever, A., Verstraeten, W.W., Swennen, R. & Coppin, P., 2010. Determining the water status of Satsuma mandarin trees [Citrus Unshiu Marcovitch] using spectral indices and by combining hyperspectral and physiological data. *Agricultural and Forest Meteorology* 150, 369-379.
- Dzikiti, S., Verreyne, S.J., Stuckens, J., Strever, A., Verstraeten, W.W., Swennen, R., Theron, K.I. & Coppin, P., 2011. Seasonal variation in canopy reflectance and its application to determine the water status and water use by citrus trees in the Western Cape, South Africa. *Agricultural and Forest Meteorology*.
- Edson, C.E., Howell, G.S. & Flore, J.A., 1993. Influence of Crop Load on Photosynthesis and Dry Matter Partitioning of Seyval Grapevines I. Single Leaf and Whole Vine Response Pre- and Post-harvest. *American Journal of Enology and Viticulture* 44, 139-147.
- Edson, C.E., Howell, G.S. & Flore, J.A., 1995. Influence of Crop Load on Photosynthesis and Dry Matter Partitioning of Seyval Grapevines. II. Seasonal Changes in Single Leaf and Whole Vine Photosynthesis. *American Journal of Enology and Viticulture* 46, 469-477.
- Hunter, J.J. & Visser, J.H., 1990. The effect of partial defoliation on growth characteristics of *Vitis vinifera* L. cv. Cabernet Sauvignon I. Vegetative growth. *South African Journal of Enology and Viticulture* 11, 18-25.
- Küpper, H., Seibert, S. & Parameswaran, A., 2007. Fast, sensitive, and inexpensive alternative to analytical pigment HPLC: Quantification of chlorophylls and carotenoids in crude extracts by fitting with gauss peak spectra. *Analytical chemistry* 79, 7611-7627.
- Pilar, B., Sanchez-de-Miguel, P., Centeno, A., Junquera, P., Linares, R. & Lissarrague, J.R., 2007. Water relations between leaf water potential, photosynthesis and agronomic vine response as a tool for establishing thresholds in irrigation scheduling. *Scientia Horticulturae* 114, 151-158.
- Silvestroni, O., Mattioli, S., Neri, D., Palliotti, A. & Cartechini, A., 2005. Down-regulation of photosynthetic activity for field-grown grapevines. *Acta Hort. (ISHS)* 689, 285-292.
- Van Niekerk, J., Strever, A.E., Du Toit, G.P., Halleen, F. & Fourie, P.H., 2011. Influence of water stress on Botryosphaeriaceae disease expression in grapevines. *Phytopathologia Mediterranea* 50, 151-165.
- Zarco-Tejada, P.J., Berjón, A., López-Lozano, R., Miller, J.R., Martín, P., Cachorro, V., González, M.R. & De Frutos, A., 2005. Assessing vineyard condition with hyperspectral indices: Leaf and canopy reflectance simulation in a row-structured discontinuous canopy. *Remote Sensing of Environment* 99, 271-287.